Technical Publication SJ2019-01

NORTH FLORIDA SOUTHEAST GEORGIA GROUNDWATER MODEL (NFSEG V1.1)

by

Douglas Durden, P.E.
Fatih Gordu, P.E.
Douglas Hearn, P.G.
Tim Cera, P.E.
Tim Desmarais, P.E.
Lanie Meridth
Adam Angel, Ph.D.
Christopher Leahy
Joanna Oseguera
St. Johns River Water Management District
and
Trey Grubbs
Suwannee River Water Management District

St. Johns River Water Management District
Palatka, Florida

2019

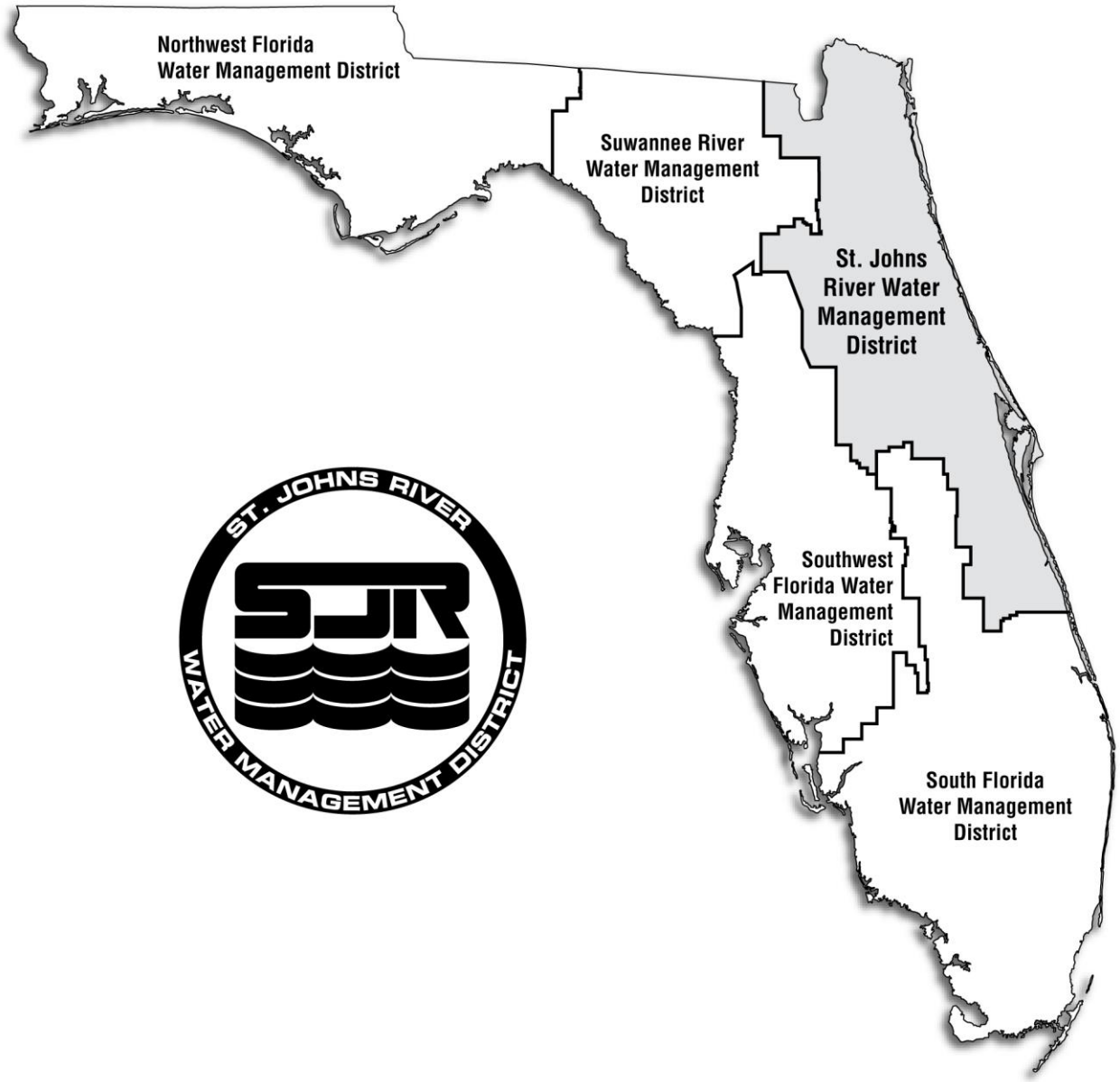

The St. Johns River Water Management District was created in 1972 by passage of the Florida Water Resources Act, which created five regional water management districts. The St. Johns District includes all or part of 18 counties in northeast and east-central Florida. Its mission is to preserve and manage the region's water resources, focusing on core missions of water supply, flood protection, water quality and natural systems protection and improvement. In its daily operations, the district conducts research, collects data, manages land, restores and protects water above and below the ground, and preserves natural areas.

This document is published to disseminate information collected by the district in pursuit of its mission. Electronic copies are available at *www.sjrwmd.com/documents/technical-reports* or by calling the district at the number below.

Scientific Reference Center
St. Johns River Water Management District
4049 Reid Street/P.O. Box 1429
Palatka, FL 32178-1429 (32177 for street deliveries)
386-329-4500

ACKNOWLEDGMENTS

The following people made contributions to this project:

Joanne Chamberlain, P.E.
John Fitzgerald
Qing Sun, Ph.D., P.E.
Tammy Bader-Gibbs
Yassert Gonzalez
Jacy Crosby
James Walters
Joseph Amoah, Ph.D., P.E.
Louis Donnangelo
Gustavo Suarez-Narvaez, P.E.
David Clapp
Yanbing Jia, Ph.D., P.E.
Jill Andrea Stokes
Steve Brown, GISP
Wissam Al-Taliby, Ph.D.
Jeff Davis, P.G.
Don Boniol, P.G.
Lester Williams
Ron Basso, P.E.
Michelle Brown, P.E.
Michelle Tharp
Sherry Brandt-Williams, Ph.D.
Mike Register, P.E.
Kevin Mouyard, P.G., GISP
Dale Jenkins, P.G.
Wei Jin, Ph.D., P.E.
Tim Desmarais, P.E.

We thank our peer reviewers for their constructive and valuable comments on this project and report:

NFSEGv1.1 Technical Peer Review Panel
Louis H. Motz, Ph.D., P.E., D.WRE, Chair
Brian R. Bicknell
J. Hal Davis, P.G.
James Rumbaugh, P.G.
Dann Yobbi, P.G.

We also acknowledge the support and inputs from the NFSEG Technical Team and Steering Committee.

Technical Team Members: Doug Munch, Doug Durden, Patrick Tara, Dale Jenkins, Fatih Gordu, Rick Hutton, George Porter, Del Bottcher, Drew Jackson, Douglas Dufresne, Patrick T. Welsh Peter Schreuder, Jim Kennedy, Cliff Lewis, Camilo Gaitan, Patrick Burger, Robert Knight, Jeff Lehnen,

Steering Team Members: Al Canepa, Carlos Herd, Tony Cunningham, David Richardson, Paul Steinbrecher, Ty Edwards, Staci Braswell, Stan Posey, Katherine Van Zant, Vivian Katz, Mary Lou Hildreth, Jill McGuire, John Sloane, Dana Bryan, Paul Still.

EXECUTIVE SUMMARY

The Northeast Florida-Southeast Georgia (NFSEG) model was developed through a collaborative effort among a technical team of experts from the St. Johns River Water Management District (SJRWMD), Suwannee River Water Management District (SRWMD), Southwest Florida Water Management District (SWFWMD), and stakeholders from water utilities, private industry, governmental organizations, and environmental groups. The model was designed to be a tool that can be used to evaluate inter-district and interstate groundwater pumping effects, as well as effects within an individual district. A primary function of the model is to simulate the regional effects of pumping on groundwater levels, stream baseflows, and spring flows. Intended applications of the model include evaluations of proposed consumptive use permits, support of analyses of minimum flows and levels, and water supply planning.

This report describes version 1.1 of the NFSEG model. Version 1.0 of NFSEG was used to develop the North Florida regional water supply plan for SJRWMD and SRWMD. The NFSEG v1.1 included improvements recommended for version 1.0 by the modeling team, stakeholders, and a peer review panel.

The model covers about 60,000 square miles, encompassing a large area of the Floridan aquifer system in north Florida, Georgia, and South Carolina. The area includes hundreds of streams, rivers, lakes, and more than 300 springs. NFSEG v1.1 is a three-dimensional, steady state model. The model was calibrated to 2001 and 2009 hydrologic conditions and successfully validated using 2010 conditions.

The groundwater model is an application of the MODFLOW-NWT (Niswonger et al. 2011) formulation of the MODFLOW 2005 (Harbaugh 2005) groundwater flow simulation software. MODFLOW-NWT provides enhanced rewetting capabilities in simulations of the water table of unconfined aquifers. Unconfined conditions occur throughout the area corresponding to the domain in the surficial aquifer or in outcrops of the intermediate confining unit or the Upper Floridan aquifer.

Surface water hydrology for all the surface water basins within and flowing into the groundwater model boundary were simulated using the Hydrological Simulation Program—FORTRAN (HSPF) software. HSPF models were used to generate recharge and maximum saturated evapotranspiration for input to the NFSEG groundwater model. HSPF models are comprehensive, interconnected representations of the surface-water and near-surface groundwater flow systems. Calibration constrained estimates of recharge and maximum saturated evapotranspiration developed from the HSPF models are components of a complete and internally consistent water budget. A simpler, much coarser method for recharge estimates often uses the Soil Conservation Service (SCS) curve number (CN) approach; however, SCS CN only represents the runoff component explicitly, leaving maximum saturated evapotranspiration and other water budget components to be estimated by other separate approaches. For this reason, the use of HSPF was preferred over the SCS approach in the development of NFSEG.

The NFSEG model was calibrated using Parameter ESTimation (PEST), a program widely used to facilitate model calibration. The PEST calibration process involved minimizing differences between various types of observations and their model simulated equivalents through adjustment of model parameters within defined ranges. Observation types included groundwater levels, differences in vertical and horizontal groundwater levels, spring flows and baseflows. The NFSEG v1.1 model performed well in matching groundwater level and spring flows in the 2001 and 2009 calibration years, and the 2010 validation year. The percentages of the groundwater level residuals within 2.5 and 5 feet indicate a good match between observed and corresponding simulated values. The results of the calibration with respect to the transmissivity distribution of the Upper Floridan aquifer and leakance of the intermediate confining unit are reasonable and comparable to observations and previous models.

Two significant analyses were performed to estimate certainty about model parameters and model predictions. The parameter and predictive uncertainty analyses together give a powerful evaluation of how useful the model is to answer questions, instead of only focusing on calibration matches to observations.

The analysis showed that the uncertainty estimates of the predicted differences of drawdown and flow reduction between the scenarios are much smaller than the uncertainty estimates of predicted groundwater levels and spring and river flows. This is consistent with the expectation that the model performs better at predicting the differences between scenarios than absolute values of groundwater levels and flows. It should be noted that NFSEG v1.1 will be used in most cases to predict differences between scenarios rather than absolute values.

The NFSEG v1.1 groundwater model and surface water models were independently peer reviewed by an independent panel of modeling experts. The peer review was very positive and identified the model as being appropriate for all intended uses if some recommended additions to documentation were made. These recommended improvements, other less important recommendations by the peer review team, and improvements identified by the modeling team and stakeholders were incorporated into the final NFSEG v1.1.

CHAPTER 1. INTRODUCTION 1-1
PURPOSE AND SCOPE 1-1
DESCRIPTION OF MODEL AREA 1-3
Physiography 1-3
Land Use 1-3
Major Surface Water and Groundwater Basins 1-3
Municipalities and Other Major Pumping Centers 1-9
Climate 1-9

CHAPTER 2. HYDROLOGY OF THE AREA 2-1
SURFACE WATER SYSTEMS 2-1
Rivers 2-2
Lakes 2-3
Swamps/Wetlands 2-4
Atlantic Ocean and Gulf of Mexico 2-4
GROUNDWATER SYSTEMS 2-5
Surficial Aquifer System 2-5
Hydraulic Properties 2-5
Structure 2-8
Water Levels 2-8
Intermediate Confining Unit 2-8
Structure 2-12
Hydraulic Properties 2-13
Vertical Hydraulic Gradient 2-13
Floridan aquifer System 2-17
Gulf Trough 2-17
Southeastern Coastal Plain Aquifer System 2-17
Structure 2-21
Upper Floridan aquifer 2-23
Lower Semi-confining Unit 2-25
Fernandina Permeable Zone 2-26
Hydraulic Properties 2-34
Transmissivity of Zone 1 2-34
Leakance of the Middle Confining Unit 2-34
Transmissivity of the Lower Floridan aquifer 2-38
Water Levels 2-38
Recharge and Evapotranspiration Rates 2-38
Spring Flows 2-44
Baseflows 2-44
Cumulative Baseflow Estimates 2-49
Baseflow Pickup Estimates 2-49
Concentrated Groundwater Inflows 2-53
Groundwater Withdrawals 2-57

CHAPTER 3. Model Configuration 3-1
MODEL CODE SELECTION 3-1
NFSEG GRID 3-4
MODEL LAYERS 3-5

Layer 1 3-13
Layer 2 3-13
Layer 3 3-17
Layer 4 3-23
Layer 5 3-23
Layer 6 3-23
Layer 7 3-23
LATERAL BOUNDARY CONDITIONS 3-31
Layers 1 and 2 3-31
Layer 3 3-31
Northern (N3) 3-31
Eastern, Upper (EU3) 3-35
Eastern, Central (EC3) 3-35
Eastern Lower (EL3) 3-35
Eastern, Seaward (ES3) 3-35
Southern, East (SE3) 3-35
Southern, Central (SC3) 3-37
Southern, West (SW3) 3-37
Western, Seaward (WS3) 3-37
Western, North (WN3) 3-37
Layer 4 3-38
Layer 5 3-38
Layer 6 3-41
Layer 7 3-41
INTERAL BOUNDADRY CONDITIONS 3-41
River Boundaries 3-44
River Stage and Bottom Elevation 3-44
Lake Stage and Bottom Elevation 3-46
Initial Conductance Estimates 3-48
General Head Boundary Conditions 3-48
Drain Boundaries 3-49
Artesian Derived Wetlands 3-49
Ephemeral Stream Reaches 3-50
Recharge and Evapotranspiration 3-50
Well Package 3-56
Time Variant Specified Head Package 3-60
Multiple Assignment of River, Drain, and GHB-Condition Boundaries .. 3-60

CHAPTER 4. MODEL CALIBRATION 4-1
APPROACH 4-1
PEST Facilitated Calibration 4-2
OBSERVATION DATA GROUPS 4-3
Groundwater Levels 4-5
Spring Flow Rates 4-5
Baseflow Rates 4-5
Vertical Head Differences 4-5
Horizontal Head Differences 4-6

Lake Leakage Rates 4-6
Wetting Penalty 4-6
CALIBRATION PARAMETERS GROUPS 4-9
Horizontal and Vertical Hydraulic Conductivity 4-10
Horizontal Hydraulic Conductivity Determination for Layers 1, 3, and 7 and Vertical Hydraulic Conductivity Determination for Layer 6 4-10
Vertical Hydraulic Conductivity of Model Layers 2 and 4, Horizontal Hydraulic Conductivity of Model Layer 5, and Vertical and Horizontal Hydraulic Conductivity Multipliers 4-12
Vertical Anisotropy Ratio 4-18
GHB Conductance for Representation of Spring Discharge 4-22
River Package Conductance Multipliers for Representation of Stream Baseflow 4-23
Drain Package Conductance Multipliers for Representation of Stream Baseflow 4-23
Lake Related Multipliers: River Package Conductance and Lake Zone Multipliers 4-23
Recharge and Maximum Saturated ET Multipliers 4-24
WEIGHTING SCHEME 4-24
Groundwater Levels 4-25
Layer 1 (2001 and 2009) 4-25
Layer 2 (2001 and 2009) 4-25
Layers 3 through 7 (2001 and 2009) 4-26
Groundwater Level Differences 4-26
Vertical groundwater level differences between layers 1 and 3 (2001 and 2009) 4-26
Horizontal groundwater level differences (2001 and 2009) 4-26
Vertical groundwater level differences between layers 3 and 5 (2001 and 2009) 4-26
Flows 4-26
Baseflows and changes in baseflows (2001 and 2009) 4-26
Individual spring flows (2001 and 2009) 4-27
Flows for spring groups (2001 and 2009) 4-27
Other Observations 4-27
Flooding and drying penalties for model cells (2001 and 2009) 4-27
Lake leakage rates (2001 and 2009) 4-28
CALIBRATION RESULTS 4-28
Summary Statistics 4-28
Groundwater Levels (Hydraulic Heads) 4-29
Groundwater-level Residuals of Layer 1 4-29
Observed versus Simulated Groundwater Levels of Layer 1 4-64
Simulated Water Table of the Surficial Aquifer System 4-64
Residuals of Vertical Head Differences between Layers 1 and 3 4-65
Observed versus Simulated Vertical Head Differences between Layers 1 and 3 4-65
Groundwater Level Residuals of Layer 3 4-65
Observed versus Simulated Hydraulic Head of Layer 3 4-66

Residuals of Horizontal Hydraulic Head Difference of Layer 3 4-66
Observed versus Simulated Horizontal Hydraulic Head Differences of Layer 3 4-67
Simulated Potentiometric Surface of Layer 3 4-67
Residuals of Vertical Head Differences between Layers 3 and 5 4-67
Observed versus Simulated Vertical Head Differences between Layers 3 and 5 4-67
Groundwater Level Residuals of Layer 5 4-67
Observed versus Simulated Groundwater Levels of Layer 5 4-68
Simulated Potentiometric Surface of Layer 5 4-68
Flows 4-68
First Magnitude Springs and Spring Groups 4-68
Observed versus Simulated Spring Flows 3 4-68
Observed versus Simulated Spring Group Flows 4-68
Baseflows 4-77
Simulated Net Recharge Rates 4-77
Simulated Downward Leakage Rates of Layer 2 to 3 4-77
Simulated Upward Leakage Rates of Layer 3 to 2 4-77
Simulated Downward Leakage Rates of Layer 4 to 5 4-77
Simulated Downward Leakage Rates of Layer 5 to 4 4-98
Parameters 4-98
Horizontal Hydraulic Conductivity of Layer 1 4-98
Horizontal Hydraulic Conductivity of Layer 3 4-98
Horizontal Hydraulic Conductivity of Layer 5 4-98
Horizontal Hydraulic Conductivity, Layer 7 4-104
Transmissivity of Layer 3 4-104
Transmissivity of Layer 3 in Confined Areas and the Sum of Transmissivities of Layers 1 through 3 in Unconfined Areas 4-104
Observed versus Calibration Derived Transmissivity of the Upper Floridan Aquifer 4-109
Transmissivity, Layer 5 4-109
Vertical Hydraulic Conductivity of Layer 2 4-109
Vertical Hydraulic Conductivity of Layer 4 4-109
Vertical Hydraulic Conductivity, Layer 6 4-109
Leakance of Layer 2 4-109
Leakance of Layer 4 4-116
ADDITIONAL DISCUSSION 4-116
Recharge and Maximum Saturated ET as Calibration Parameters 4-116
Quality of Baseflow Matches 4-118
Spring-Flow Target Uncertainty 4-122
Comparisons of Groundwater-Level Residual Statistics to Other Models 4-124
Statistical and Spatial Trends in NFSEG v1.1 Groundwater-Level Residuals Compared to Trends to Other Groundwater Models 4-130
Calibration-Derived Transmissivity of the Upper Floridan aquifer of NFSEG v1.1 versus Corresponding APT-Derived Values 4-130

Calibration-Derived Transmissivity of the Upper Floridan aquifer in Previous Regional Groundwater Models versus Corresponding APT-Derived Values 4-137
Comparison of NFSEG v1.1 Calibration Statistics in Portions of Model Domain that correspond to the North Florida Water-Supply Planning Areas versus Overall Model Domain 4-142

CHAPTER 5. MODEL SIMULATIONS 5-1
VERIFICATION SIMULATION 5-1
Model Input Files 5-1
Recharge and Maximum Saturated Evapotranspiration 5-4
Drain and River Package 5-4
Well and Multi-Node Well Packages 5-4
General Head Boundary Package 5-12
Lateral Boundaries 5-12
Spring Pool Elevations 5-12
Observation Datasets 5-12
Groundwater Levels 5-13
Springflows 5-13
Baseflows 5-13
Assessment of 2010 Simulation Results 5-13
Residual Statistics 5-15
Groundwater Levels 5-15
Spring Flows 5-15
Estimated Baseflows 5-23
Spatial Distribution of UFA Level Residuals 5-29
Simulated UFA Potentiometric Surface 5-29
Simulated Model Fluxes 5-35
NO-PUMPING SIMULATION 5-35
Groundwater Levels 5-38
Spring Discharges 5-41
Simulated Flooding in Layer 1 5-44
Baseflow Estimates from 1933 through 1942 5-44

CHAPTER 6. WATER BUDGET ANALYSIS 6-1
MODEL-WIDE SUMMARY 6-1
GROUNDWATER BASINS SUMMARY 6-3
GWB 1 6-7
GWB 2 6-9
GWB 3 6-14
GWB 4 6-15
GWB 5 6-21
GWB 6 6-21
GWB 7 6-28
OVERALL SUMMARY 6-33

CHAPTER 7. SENSITIVITY AND UNCERTAINTY ANALYSIS 7-1
PARAMETER SENSITIVITY ANALYSIS 7-1

Traditional Sensitivity Analysis 7-2
Composite-scaled Sensitivity Analysis 7-3
UNCERTAINTY ANALYSIS 7-11
Parameter Uncertainty Analysis Results 7-14
Predictive Uncertainty Analysis Results 7-15

CHAPTER 8. MODEL LIMITATIONS 8-1

CHAPTER 9. DEVELOPMENT AND CALIBRATION OF SURFACE WATER MODELS TO ESTABLISH GROUNDWATER MODEL 9-1
INTRODUCTION 9-1
HYDROLOGICAL SIMULATION PROGRAM—FORTRAN (HSPF) 9-1
Major Water Budget Components of HSPF 9-2
INPUT DATA 9-4
Meteorology 9-4
Precipitation 9-5
NLDAS DATA INTEGRATION AND AVAILABILITY 9-6
COMPARISON AGAINST NEXRAD AND RAIN GAUGES 9-11
Potential Evaporation 9-12
WATER USE 9-12
Agricultural Irrigation 9-12
Urban Irrigation and Septic Fields 9-22
Golf Courses 9-22
Reuse 9-23
SPATIAL DATA 9-23
Watershed and Sub-Watershed Boundaries 9-23
Elevation 9-23
Land Cover 9-25
CALIBRATION DATA 9-25
USGS Flow Observation 9-25
Literature Total Evaporation Estimates 9-31
HSPF MODEL DEVELOPMENT 9-31
Sub-Watershed Delineation 9-33
Closed, Flat, and Frontal Sub-Watersheds 9-33
Closed Basin Representation 9-37
Representation of Springs to Improve HSPF Calibration 9-39
Calibration Process 9-39
MODEL INPUT PARAMETERS 9-43
Common Logic 9-43
Variability of Parameters Across a HSPF Model 9-43
Development of FTABLEs for the Stream Network 9-48
PARAMETER ESTIMATION WITH PEST 9-48
HSPF Special Actions 9-49
Surface FTABLEs 9-53
CALIBRATION RESULTS 9-53

CHAPTER 10. SUMMARY AND CONCLUSIONS 10-1

Table 2-1. Summary of groundwater hydrology system 2-7
Table 2-2. Summary of zones used to define the Floridan aquifer system 2-25
Table 3-1. Represented hydrogeologic units of NFSEG model layers 3-3
Table 3-2. Minimum layer thicknesses 3-6
Table 4-1. NFSEG PEST Observation Groups 4-4
Table 4-2. NFSEG PEST Calibration-Parameter Groups 4-11
Table 4-3. PEST-Generated Anisotropy for Layers other than Layer 3 4-22
Table 4-4. Summary of residual statistics 4-29
Table 4-5. Differences between simulated layer-1 groundwater levels and assigned river-boundary stages, 2001 4-65
Table 4-6. Differences between simulated layer-1 groundwater levels and assigned river-boundary stages, 2009 4-66
Table 4-7. Comparisons of simulated versus estimated spring flows of selected first-magnitude springs and spring groups, 2001 4-75
Table 4-8. Comparisons of simulated versus estimated spring flows of selected first-magnitude springs and spring groups, 2009 4-76
Table 4-9. Model calibration and discretization properties 4-125
Table 4-10. Domain-wide groundwater-level calibration statistics comparison 4-126
Table 4-11. Model overlap groundwater-level calibration statistics comparison 4-127
Table 4-12a. 1-to-1 Model overlap groundwater-level calibration statistics comparison surficial aquifer 4-128
Table 4-12b. 1-to-1 Model overlap groundwater-level calibration statistics comparison upper Floridan aquifer 4-129
Table 4-13. Groundwater-level calibration statistics: overall model domain versus NFWSPA 4-143
Table 5-1. Summary of groundwater withdrawals and influxes 5-12
Table 5-2. Observed and simulated spring flows 5-22
Table 5-3. Range of estimated cumulative baseflow and simulated baseflow 5-24
Table 5-4. Distribution of water level residuals in model layer 1 by GWB 5-30
Table 5-5. Distribution of water level residuals in model layer 3 by GWB 5-30
Table 5-6. Comparison of simulated net fluxes to model for 2001, 2009 and 2010 (all flows in/yr) 5-37
Table 5-7. Simulated 2009 and no-pumping spring discharges and corresponding observations of Stringfield (1936) for selected springs 5-43
Table 5-8. Key USGS stream gauging stations with daily discharge data for the period 1933 through 1942 5-46
Table 5-9. Summary statistics of annual average flow and annual average baseflows, 1933-1942, for USGS Gauge 0223100, ST. MARYS RIVER NEAR MACCLENNY, FL 5-46
Table 5-10. Summary statistics of annual average flow and annual average baseflows, 1933-1942, for USGS Gauge 0224600, NORTH FORK BLACK CREEK NEAR MIDDLEBURG, FL 5-47
Table 5-11. Summary statistics of annual average flow and annual average baseflows, 1933-1942, for USGS Gauge 02315500, SUWANNEE RIVER AT WHITE SPRINGS, FL 5-47

Table 5-12. Summary statistics of annual average flow and annual average baseflows, 1933-1942, for USGS Gauge 02319000, WITHLACOOCHEE RIVER NEAR PINETTA, FL 5-47
Table 5-13. Summary statistics of annual average flow and annual average baseflows, 1933-1942, for USGS Gauge 02319500, SUWANNEE RIVER AT ELLAVILLE, FL 5-48
Table 5-14. Summary statistics of annual average flow and annual average baseflows, 1933-1942, for USGS Gauge 02320500, SUWANNEE RIVER AT BRANFORD, FL 5-48
Table 5-15. Summary statistics of annual average flow and annual average baseflows, 1933-1942, for USGS Gauge 02322500, SANTA FE RIVER NEAR FORT WHITE, FL 5-48
Table 6-1. Simulated model wide mass balance for 2001 (all flows in/yr) 6-6
Table 6-2. Simulated model wide mass balance for 2009 (all flows in/yr) 6-6
Table 6-3. Simulated model wide mass balance for 2010 (all flows in/yr) 6-7
Table 6-4. Simulated model wide mass balance for no-pumping (all flows in/yr) 6-7
Table 6-5. Simulated mass balance of GWB 1 for 2001 (all flows in/yr) 6-10
Table 6-6. Simulated mass balance of GWB 1 for 2009 (all flows in/yr) 6-10
Table 6-7. Simulated mass balance of GWB 1 for 2010 (all flows in/yr) 6-11
Table 6-8. Simulated mass balance of GWB 1 for no-pumping (all flows in/yr) 6-12
Table 6-9. Simulated mass balance of GWB 2 for 2001 (all flows in/yr) 6-15
Table 6-10. Simulated mass balance of GWB 2 for 2009 (all flows in/yr) 6-15
Table 6-11. Simulated mass balance of GWB 2 for 2010 (all flows in/yr) 6-16
Table 6-12. Simulated mass balance of GWB 2 for no-pumping (all flows in/yr) 6-17
Table 6-13. Simulated mass balance of GWB 3 for 2001 (all flows in/yr) 6-19
Table 6-14. Simulated mass balance of GWB 3 for 2009 (all flows in/yr) 6-19
Table 6-15. Simulated mass balance of GWB 3 for 2010 (all flows in/yr) 6-19
Table 6-16. Simulated mass balance of GWB 3 for no-pumping (all flows in/yr) 6-20
Table 6-17. Simulated mass balance of GWB 4 for 2001 (all flows in/yr) 6-23
Table 6-18. Simulated mass balance of GWB 4 for 2009 (all flows in/yr) 6-24
Table 6-19. Simulated mass balance of GWB 4 for 2010 (all flows in/yr) 6-24
Table 6-20. Simulated mass balance of GWB 4 for no-pumping (all flows in/yr) 6-24
Table 6-21. Simulated mass balance of GWB 5 for 2001 (all flows in/yr) 6-27
Table 6-22. Simulated mass balance of GWB 5 for 2009 (all flows in/yr) 6-27
Table 6-23. Simulated mass balance of GWB 5 for 2010 (all flows in/yr) 6-27
Table 6-24. Simulated mass balance of GWB 5 for no-pumping (all flows in/yr) 6-31
Table 6-25. Simulated mass balance of GWB 6 for 2001 (all flows in/yr) 6-31
Table 6-26. Simulated mass balance of GWB 6 for 2009 (all flows in/yr) 6-31
Table 6-27. Simulated mass balance of GWB 6 for 2010 (all flows in/yr) 6-32
Table 6-28. Simulated mass balance of GWB 6 for no-pumping (all flows in/yr) 6-33
Table 6-29. Simulated mass balance of GWB 7 for 2001 (all flows in/yr) 6-36
Table 6-30. Simulated mass balance of GWB 7 for 2009 (all flows in/yr) 6-36
Table 6-31. Simulated mass balance of GWB 7 for 2010 (all flows in/yr) 6-36
Table 6-32. Simulated mass balance of GWB 7 for no-pumping (all flows in/yr) 6-37
Table 7-1. Traditional sensitivity analysis parameter sets 7-2
Table 9-1. Overlapping water balance components between MODFLOW and HSPF ... 9-3
Table 9-2. HSPF meteorological boundary conditions 9-4

Table 9-3. Water use data for HSPF 9-5
Table 9-4. Spatial data 9-5
Table 9-5. NLDAS parameters in forcing file "A" 9-6
Table 9-6. List of datasets used to develop the NLDAS precipitation dataset 9-7
Table 9-7. Comparison of available data from NLDAS, NEXRAD, and rain gauges .. 9-11
Table 9-8. Monthly tensioning factors for NLDAS potential evaporation 9-18
Table 9-9. Irrigation type matched to appropriate part of HSPF water balance 9-22
Table 9-10. NLCD and HSPF land cover classifications 9-27
Table 9-11. Percentage pervious land cover of directly connected impervious area 9-31
Table 9-12. USGS flow data quality categories (Kennedy 1983) 9-33
Table 9-13. Literature total evapotranspiration by land cover 9-35
Table 9-14. Observations and statistics used in the PEST objective function for each USGS station used in the calibration 9-50
Table 9-15. Total Actual ET (TAET) observation groups in the objective function 9-52
Table 9-16. Grading model calibration performance. Adapted from Moriasi et al. (2007) 9-54
Table 9-17. Observed and simulated mean monthly flows, percent differences in flows, and Nash-Sutcliffe coefficients for monthly data 9-55

Figure 1-1. Location of study area 1-4
Figure 1-2. Major physiographic provinces 1-5
Figure 1-3. Geographic features 1-6
Figure 1-4. Land-use coverage 1-7
Figure 1-5. Major groundwater basins 1-8
Figure 1-6. Rainfall totals at various rainfall gauges (2001, 2009, and long-term averages, inches) 1-10
Figure 2-1. NFSEG maximum active model domain and grid extent 2-6
Figure 2-2. Land-surface elevation (and upper limit of the surficial aquifer system; based on USGS 3DEP 10-meter DEM, NAVD88 feet) 2-9
Figure 2-3. Bottom elevation of the surficial aquifer system (NAVD88 feet; after Davis and Boniol, digital communication 2013) 2-10
Figure 2-4. Thickness of the surficial aquifer system (SAS, feet; after Davis and Boniol, in progress) 2-11
Figure 2-5. Top elevation of the intermediate confining unit (NAVD88 feet) 2-14
Figure 2-6. Bottom elevation of the intermediate confining unit (and/or top of the upper Floridan aquifer; Ft NAVD88; after Davis and Boniol, digital communication 2013) 2-15
Figure 2-7. Thickness of the intermediate confining unit (feet; after Davis and Boniol, digital communication 2013) 2-16
Figure 2-8. Estimated leakance distribution of the intermediate confining unit (ICU, per day; after Bush and Johnston 1988) 2-18
Figure 2-9. Intermediate confining unit vertical head difference, 2001 (feet) 2-19
Figure 2-10. Intermediate confining unit vertical head difference, 2009 (feet) 2-20
Figure 2-11. Hydrogeologic relation between the Floridan aquifer system and the Southeastern Coastal Plain aquifer system along a hypothetical dip section in Georgia (after Barker and Pernik 1994) 2-22
Figure 2-12. Elevation of 10,000 milligrams per liter (mg/l) total-dissolved-solids Iso-surface (Williams, digital communication 2013) 2-24
Figure 2-13. Bottom elevation of Zone 1 (and top elevation of Zone 2, feet NAVD88; after Davis and Boniol, digital communication 2013) 2-27
Figure 2-14. Thickness of Zone 1 (feet; after Davis and Boniol, digital communication, 2013) 2-28
Figure 2-15. Bottom elevation Zone 2 (and top elevation of Zone 3, feet NAVD88; after Davis and Boniol, digital communication, 2013; and Williams, digital communication 2013) 2-29
Figure 2-16. Thickness of Zone 2 (feet; after Davis and Boniol, digital communication 2013; and Williams, digital communication 2013) 2-30
Figure 2-17. Bottom elevation of Zone 3 (feet NAVD88; after Davis and Boniol, digital communication 2013; Miller, written communication 1991; and Williams, digital communication, 2013) 2-31
Figure 2-18. Thickness of Zone 3 (feet; after Davis and Boniol, digital communication 2013; Miller, written communication 1991; and Williams, digital communication 2013) 2-32
Figure 2-19. Bottom elevation of the Floridan aquifer system within its freshwater extent (after Miller 1986; Williams, digital communication 2012; and Williams, digital communication 2013) 2-33

Figure 2-20. Top elevation of the lower semi-confining unit (NAVD88 feet; after Miller 1986; Miller, written communication 1991; and Williams, digital communication 2013) 2-35
Figure 2-21. Bottom elevation of the lower semi-confining unit (and top elevation of the Fernandina Permeable Zone, feet NAVD88; after Miller, 1986; Miller, written communication 1991; and Williams, digital communication 2013) 2-36
Figure 2-22. Thickness of the lower semi-confining unit (feet; after Miller, 1986; Miller, written communication 1991; and Williams, digital communication 2013) 2-37
Figure 2-23. Top elevation of the Fernandina Permeable Zone (FPZ; feet NAVD88; after Miller, 1986; Miller, written communication 1991; and Williams, digital communication 2013) 2-39
Figure 2-24. Bottom elevation of the Fernandina Permeable Zone (FPZ, feet NAVD88; after Miller, 1986; Miller, written communication 1991; Williams, digital communication 2012; and Williams, digital communication 2013) 2-40
Figure 2-25. Thickness of the Fernandina Permeable Zone (FPZ, feet; after Miller, 1986; Miller, written communication 1991; and Williams, digital communication 2013) 2-41
Figure 2-26. Aquifer-performance-test transmissivity estimates, Zone 1 (feet squared per day) 2-42
Figure 2-27. Estimated transmissivity, upper Floridan aquifer (feet squared per day; after Bush and Johnston 1988) 2-43
Figure 2-28. Estimated potentiometric surface, upper Floridan aquifer, 2001 (feet NAVD88) 2-45
Figure 2-29. Estimated potentiometric surface, upper Floridan aquifer, 2009 (feet NAVD88) 2-46
Figure 2-30. Middle confining unit vertical head difference, 2001 (feet) 2-47
Figure 2-31. Middle confining unit vertical head difference, 2009 (feet) 2-48
Figure 2-32. Locations and relative discharge rates of springs, 2001 2-50
Figure 2-33. Locations and relative discharge rates of springs, 2009 2-51
Figure 2-34. First-magnitude spring locations and corresponding discharge rates, 2009 2-52
Figure 2-35. USGS gauges used for evaluation of baseflow-estimation approach 2-54
Figure 2-36. Cumulative baseflow estimates at selected USGS gauges, 2001 2-55
Figure 2-37. Cumulative baseflow estimates at selected USGS gauges, 2009 2-56
Figure 2-38. Estimated baseflow pickups, Region A, 2001 2-58
Figure 2-39. Estimated baseflow pickups, Region B, 2001 2-59
Figure 2-40. Estimated baseflow pickups, Region C, 2001 2-60
Figure 2-41. Estimated baseflow pickups, Region A, 2009 2-61
Figure 2-42. Estimated baseflow pickups, Region B, 2009 2-62
Figure 2-43. Estimated baseflow pickups, Region C, 2009 2-63
Figure 2-44. Distribution of total groundwater withdrawals by county (MGD), 2001 2-64
Figure 2-45. Distribution of total groundwater withdrawals by county (MGD), 2009 2-65
Figure 2-46. Groundwater withdrawals by county and use type (MGD), 2001 2-66

Figure 2-47. Groundwater withdrawals by county and use type (MGD), 2009 2-67
Figure 3-1. NFSEG model grid 3-2
Figure 3-2. Locations of hydrogeologic cross sections 3-7
Figure 3-3. Hydrogeologic cross section A-A' 3-8
Figure 3-4. Hydrogeologic cross section B-B' 3-9
Figure 3-5. Hydrogeologic cross section C-C' 3-10
Figure 3-6. Hydrogeologic cross section D-D' 3-11
Figure 3-7. Hydrogeologic cross section E-E' 3-12
Figure 3-8. Top elevation, Layer 1 (feet NAVD88; after Boniol and Davis, digital communication, 2013) 3-14
Figure 3-9. Bottom elevation, Layer 1 (and top elevation, Layer 2; feet NAVD88; after Boniol and Davis, digital communication, 2013) 3-15
Figure 3-10. Thickness, Layer 1 (feet) 3-16
Figure 3-11. Bottom elevation, Layer 2 (and top elevation, Layer 3; after Boniol and Davis, digital communication, 2013) 3-18
Figure 3-12. Thickness, Layer 2 (feet) 3-19
Figure 3-13. Bottom elevation, Layer 3 (and top elevation, Layer 4; feet NAVD88; after Boniol and Davis, digital communication, 2013) 3-20
Figure 3-14. Thickness, Layer 3 (feet) 3-21
Figure 3-15. Bottom elevation, Layer 4 (and top elevation, Layer 5; feet NAVD88; after Boniol and Davis, digital communication, 2013) 3-24
Figure 3-16. Thickness, Layer 4 3-25
Figure 3-17. Bottom elevation, Layer 5 (feet NAVD88; after Miller, 1986; Miller, written communication, 1991; and Williams, digital communication, 2013) 3-26
Figure 3-18. Thickness, Layer 5 (feet) 3-27
Figure 3-19. Top elevation, Layer 6 (feet NAVD88; after Miller, 1986; Miller, written communication, 1991; and Williams and Kuniansky, 2015) 3-28
Figure 3-20. Bottom Elevation, Layer 6 (feet NAVD88; after Miller, 1986; Miller, written communication, 1991; and Williams and Kuniansky, 2015) 3-29
Figure 3-21. Thickness, Layer 6 (feet) 3-30
Figure 3-22. Top Elevation, Layer 7 (feet NAVD88, after Miller 1986; Miller, written communication, 1991; and Williams and Kuniansky, 2015) 3-32
Figure 3-23. Bottom Elevation, Layer 7 feet NAVD88, after Miller, 1986; Miller, written communication, 1991; and Williams and Kuniansky, 2015) 3-33
Figure 3-24. Thickness, Layer 7 (feet) 3-34
Figure 3-25. Model lateral boundaries, Layer 3 3-36
Figure 3-26. Model lateral boundaries, Layer 4 3-39
Figure 3-27. Model lateral boundaries, Layer 5 3-40
Figure 3-28. Model lateral boundaries, Layer 6 3-42
Figure 3-29. Model lateral boundaries, Layer 7 3-43
Figure 3-30. NHDPlusV2 flow-line sub-segments used in river- and drain-package implementations 3-45
Figure 3-31. Portions of NHD flowlines for which river stages were obtained from Existing surface-water models and lake sub-polygons represented in the NFSEG river package 3-47
Figure 3-32. Artesian-derived wetlands represented in the drain package 3-51

Figure 3-33. USGS HUC8 basins for which HSPF models were developed in support of NFSEG development 3-52
Figure 3-34. Simulated flow components--HSPF vs. MODFLOW 3-53
Figure 3-35. HSPF-derived rates of recharge, 2001 (inches per year) 3-54
Figure 3-36. HSPF-derived rates of recharge, 2009 (inches per year) 3-55
Figure 3-37. HSPF-derived rates of maximum saturated ET, 2001 (inches per year) 3-57
Figure 3-38. HSPF-derived rates of maximum saturated ET, 2009 (inches per year)..... 3-58
Figure 3-39. Estimated evapotranspiration extinction depths (feet)..... 3-59
Figure 3-40. Locations of concentrated groundwater influxes..... 3-61
Figure 3-41. Distribution of public-supply, commercial-industrial, and institutional Withdrawals (MGD), 2001 3-62
Figure 3-42. Distribution of public-supply, commercial-industrial, and institutional Withdrawals (MGD), 2009 3-63
Figure 3-43. Distribution of DSS withdrawals (MGD) 3-64
Figure 3-44. Distribution of agricultural withdrawals 3-65
Figure 3-45. Distribution of specified-head grid cells in Layer 1 3-66
Figure 4-1. Estimated horizontal head difference, upper Floridan aquifer, 2001..... 4-7
Figure 4-2. Estimated horizontal head difference, upper Floridan aquifer, 2009..... 4-8
Figure 4-3. Distribution of horizontal hydraulic conductivity pilot Points, Layer 1 4-13
Figure 4-4. Distribution of horizontal hydraulic conductivity pilot Points, Layer 3 4-14
Figure 4-5. Distribution of horizontal hydraulic conductivity pilot Points, Layer 7 4-15
Figure 4-6. Distribution of vertical hydraulic conductivity pilot Points, Layer 6 4-16
Figure 4-7. Distribution of vertical hydraulic conductivity pilot Points and vertical hydraulic conductivity multiplier pilot Points, model Layer 2 4-17
Figure 4-8. Distribution of vertical hydraulic conductivity pilot Points and vertical hydraulic conductivity multiplier pilot Points, model Layer 4 4-19
Figure 4-9. Distribution of horizontal hydraulic conductivity pilot Points and Horizontal hydraulic conductivity multiplier pilot Points, model Layer 5 4-20
Figure 4-10. Distribution of anisotropy pilot points, model Layer 3..... 4-21
Figure 4-11(a).Residuals of hydraulic head (feet), model Layer 1, 2001 4-30
Figure 4-11(b).Relative residuals of hydraulic head (feet), model Layer 1, 2001..... 4-31
Figure 4-12(a).Residuals of hydraulic head (feet), model Layer 1, 2009 4-32
Figure 4-12(b).Relative residuals of hydraulic head (feet), model Layer 1, 2009..... 4-33
Figure 4-13. Observed hydraulic head (feet NAVD88), model Layer 1, 2001 4-34
Figure 4-14. Observed versus simulated hydraulic head (feet NAVD88), model Layer 1, 2009 4-35
Figure 4-15. Simulated water table of model Layer 1 (feet NAVD88), 2001 4-36
Figure 4-16. Simulated water table of model Layer 1 (feet NAVD88), 2009 4-37
Figure 4-17. Residuals of vertical head differences (feet), model Layers 1 and 3, 2001..... 4-38
Figure 4-18. Residuals of vertical head differences (feet), model Layers 1 and 3, 2009..... 4-39
Figure 4-19. Observed versus simulated vertical head differences (feet), model Layers 1 and 3, 2001 4-40
Figure 4-20. Observed versus simulated vertical head differences (feet), model Layers 1 and 3, 2009 4-41

Figure 4-21(a).Residuals of hydraulic head (feet), model Layer 3, 2001 4-42
Figure 4-21(b).Relative residuals of hydraulic head (feet), model Layer 3, 2001..... 4-43
Figure 4-22(a).Residuals of hydraulic head (feet), model Layer 3, 2009..... 4-44
Figure 4-22(b).Relative residuals of hydraulic head (feet), model Layer 3, 2009..... 4-45
Figure 4-23. Observed versus simulated hydraulic head (feet NAVD88), model Layer 3, 2001 4-46
Figure 4-24. Observed versus simulated hydraulic head (feet NAVD88), model Layer 3, 2009 4-47
Figure 4-25. Residuals of horizontal head differences (feet), model Layer 3, 2001 4-48
Figure 4-26. Residuals of horizontal head differences (feet), model Layer 3, 2009 4-49
Figure 4-27. Observed versus simulated horizontal head differences (feet), model Layer 3, 2001 4-50
Figure 4-28. Observed versus simulated horizontal head differences (feet), model Layer 3, 2009 4-51
Figure 4-29. Simulated potentiometric surface, model Layer 3 (feet NAVD88), 2001 ... 4-52
Figure 4-30 Simulated potentiometric surface, model Layer 3 (feet NAVD88), 2009 ... 4-53
Figure 4-31. Residuals of vertical head differences (feet), model Layers 3 and 5, 2001 4-54
Figure 4-32. Residuals of vertical head differences (feet), model Layers 3 and 5, 2009 4-55
Figure 4-33. Observed versus simulated vertical head differences (feet), model Layers 3 and 5, 2001 4-56
Figure 4-34. Observed versus simulated vertical head differences (feet), model Layers 3 and 5, 2009..... 4-57
Figure 4-35. Residuals of hydraulic head (feet), model Layer 5, 2001 4-58
Figure 4-36. Residuals of hydraulic head (feet), model Layer 5, 2009 4-59
Figure 4-37. Observed versus simulated hydraulic head (feet NAVD88), model Layer 5, 2001 4-60
Figure 4-38. Observed versus simulated hydraulic head (feet NAVD88), model Layer 5, 2009 4-61
Figure 4-39. Simulated potentiometric surface, model Layer 5 (feet NAVD88), 2001 4-62
Figure 4-40. Simulated potentiometric surface, model Layer 5 (feet NAVD88), 2009 4-63
Figure 4-41. Magnitude 1 springs and spring groups and corresponding estimated flowrates and Flowrate residuals (cfs), 2001 (sign convention for flows is consistent with that of MODFLOW: negative flows are *from* the aquifer; positive flows are *into* the aquifer.)..... 4-69
Figure 4-42. Magnitude 1 springs and spring groups and corresponding estimated flowrates and Flowrate residuals (cfs), 2009 (sign convention for flows is consistent with that of MODFLOW: negative flows are *from* the aquifer; positive flows are *into* the aquifer.)..... 4-70
Figure 4-43. Observed vs. simulated spring discharges (cfs), 2001 (sign convention for flows is consistent with that of MODFLOW: negative flows are *from* the aquifer; positive flows are *into* the aquifer.) 4-71
Figure 4-44. Observed vs. simulated spring discharges (cfs), 2009 (sign convention for flows is consistent with that of MODFLOW: negative flows are *from* the aquifer; positive flows are *into* the aquifer.) 4-72

Figure 4-45. Observed vs. simulated spring-group discharges (cfs), 2001 (sign convention for flows is consistent with that of MODFLOW: negative flows are *from* the aquifer; positive flows are *into* the aquifer.) 4-73
Figure 4-46. Observed vs. simulated spring-group discharges (cfs), 2009 (sign convention for flows is consistent with that of MODFLOW: negative flows are *from* the aquifer; positive flows are *into* the aquifer.) 4-74
Figure 4-47. Estimated baseflow pickup residuals (cfs), Region A, 2001 (sign convention for flows is consistent with that of MODFLOW: negative flows are *from* the aquifer; positive flows are *into* the aquifer.) 4-78
Figure 4-48. Estimated baseflow pickup residuals (cfs), Region B, 2001 (sign convention for flows is consistent with that of MODFLOW: negative flows are *from* the aquifer; positive flows are *into* the aquifer.) 4-79
Figure 4-49. Estimated baseflow pickup residuals (cfs), Region C, 2001 (sign convention for flows is consistent with that of MODFLOW: negative flows are *from* the aquifer; positive flows are *into* the aquifer.) 4-80
Figure 4-50. Estimated baseflow pickup residuals (cfs), Region A, 2009 (sign convention for flows is consistent with that of MODFLOW: negative flows are *from* the aquifer; positive flows are *into* the aquifer.) 4-81
Figure 4-51. Estimated baseflow pickup residuals (cfs), Region B, 2009 (sign convention for flows is consistent with that of MODFLOW: negative flows are *from* the aquifer; positive flows are *into* the aquifer.) 4-82
Figure 4-52. Estimated baseflow pickup residuals (cfs), Region C, 2009 (sign convention for flows is consistent with that of MODFLOW: negative flows are *from* the aquifer; positive flows are *into* the aquifer.) 4-83
Figure 4-53. Estimated versus simulated baseflow pickups (cfs), 2001 (sign convention for flows is consistent with that of MODFLOW: negative flows are *from* the aquifer; positive flows are *into* the aquifer.) 4-84
Figure 4-54. Estimated versus simulated baseflow pickups (cfs), 2009 (sign convention for flows is consistent with that of MODFLOW: negative flows are *from* the aquifer; positive flows are *into* the aquifer.) 4-85
Figure 4-55. Cumulative baseflow residuals (cfs), 2001 (sign convention for flows is consistent with that of MODFLOW: negative flows are *from* the aquifer; positive flows are *into* the aquifer.) 4-86
Figure 4-56. Estimated vs. simulated cumulative baseflows (cfs), 2009 (sign convention for flows is consistent with that of MODFLOW: negative flows are *from* the aquifer; positive flows are *into* the aquifer.) 4-87
Figure 4-57. Estimated vs. simulated cumulative baseflows (cfs), 2001 (sign convention for flows is consistent with that of MODFLOW: negative flows are *from* the aquifer; positive flows are *into* the aquifer.) 4-88
Figure 4-58. Estimated cumulative baseflow residuals (cfs), 2009 (sign convention for flows is consistent with that of MODFLOW: negative flows are *from* the aquifer; positive flows are *into* the aquifer.) 4-89
Figure 4-59. Simulated net recharge rates (inches/year), 2001 4-90
Figure 4-60. Simulated net recharge rates (inches/year), 2009 4-91
Figure 4-61. Flow through lower face, Layer 2, 2001 (downward leakage rate, Layer 2 to 3, inches/year) 4-92
Figure 4-62. Flow through lower face, Layer 2, 2009 (downward leakage rate, Layer 2 to 3, inches/year) 4-93

Figure 4-63. Flow through lower face, Layer 2, 2001 (upward leakage rate, Layer 3 to 2, inches/year) 4-94
Figure 4-64. Flow through lower face, Layer 2, 2009 (upward leakage rate, Layer 3 to 2, inches/year) 4-95
Figure 4-65. Flow through lower face, Layer 4, 2001 (downward leakage rate, Layer 4 to 5, inches/year) 4-96
Figure 4-66. Flow through lower face, Layer 4, 2009 (downward leakage rate, Layer 4 to 5, inches/year) 4-97
Figure 4-67. Flow through lower face, Layer 4, 2001 (upward leakage rate, Layer 5 to 4, inches/year) 4-99
Figure 4-68. Flow through lower face, Layer 4, 2009 (upward leakage rate, Layer 5 to 4, inches/year) 4-100
Figure 4-69. Modeled distribution of horizontal hydraulic conductivity (feet/day), model Layer 1 4-101
Figure 4-70. Modeled distribution of horizontal hydraulic conductivity (feet/day), model Layer 3 4-102
Figure 4-71. Modeled distribution of horizontal hydraulic conductivity (feet/day), model Layer 5 4-103
Figure 4-72. Modeled distribution of horizontal hydraulic conductivity (feet/day), model Layer 7 4-105
Figure 4-73. Spatial distribution of transmissivity (feet squared/day), model Layer 3 4-106
Figure 4-74. Spatial distribution of transmissivity (feet squared per day), upper Floridan aquifer – Layers 1-3 unconfined region, Layer 1 confined region. 4-107
Figure 4-75. Difference in transmissivity of Layer-3 and upper-Floridan-aquifer transmissivity distributions (feet squared per day) 4-108
Figure 4-76. Multi-well-APT-derived transmissivity versus calibration-derived transmissivity (feet squared per day), upper Floridan aquifer 4-110
Figure 4-77. Spatial distribution of transmissivity (feet squared/day), model Layer 5. NFSEG v1.1 APT database values super imposed 4-111
Figure 4-78. Modeled distribution of vertical hydraulic conductivity (feet/day), model Layer 2 4-112
Figure 4-79. Modeled distribution of vertical hydraulic conductivity (feet/day), model Layer 4 4-113
Figure 4-80. Modeled distribution of vertical hydraulic conductivity (feet/day), model Layer 6 4-114
Figure 4-81. Modeled distribution of Leakance, model Layer 2 4-115
Figure 4-82. Modeled distribution of Leakance, model Layer 4 4-117
Figure 4-83. Residuals of UFA hydraulic head (feet), North Florida model Version 2 and NFSEG Version 1.1 (2009). 4-131
Figure 4-84. Residuals of UFA hydraulic head (feet), Peninsular Florida model Version 2 and NFSEG Version 1.1 (2009) 4-132
Figure 4-85. Scatter plot of NFSEG v1.1 transmissivity vs. NFSEG APT database, confined region 4-134
Figure 4-86. Scatter plot of NFSEG v1.1 transmissivity vs. NFSEG APT database, unconfined region 4-135

Figure 4-87. Locations and results of APTs used for comparisons to calibration-derived transmissivities 4-136
Figure 4-88. Scatter plot of NF v2 UFA transmissivity vs. NFSEG APT database, confined region 4-138
Figure 4-89. Scatter plot of NF v2 UFA transmissivity vs. NFSEG APT database, unconfined region 139
Figure 4-90. Scatter plot of PF v2 UFA transmissivity vs. NFSEG APT database, confined region 4-140
Figure 4-91. Scatter plot of PF v2 UFA transmissivity vs. NFSEG APT database, unconfined region 4-141
Figure 4-92. Map of North Florida regional water supply Planning Area 4-144
Figure 5-1. Map of annual average precipitation in 2010, and bar charts of 2001, 2009 and 2010 average annual precipitation by groundwater basin. 5-2
Figure 5-2. Difference in precipitation rate between 2010 and 2001 (left) and 2010 and 2009 (right) 5-3
Figure 5-3. Map of annual average MSET in 2010, and bar charts of 2001, 2009 and 2010 average annual MSET by groundwater basin. 5-5
Figure 5-4. Difference in MSET rate between 2010 and 2001 (left) and 2010 and 2009 5-6
Figure 5-5. Map of annual average recharge rate in 2010, and bar charts of 2001, 2009 and 2010 average annual recharge rate by groundwater basin. 5-7
Figure 5-6. Difference in recharge rate between 2010 and 2001 (left) and 2010 and 2009 5-8
Figure 5-7. Distribution of public-supply, commercial-industrial and institutional withdrawals (MGD), 2010. 5-9
Figure 5-8. Distribution of Total groundwater withdrawals by County (MGD), 2010 5-10
Figure 5-9. Distribution of Multi-aquifer wells in 2010. 5-11
Figure 5-10. Distribution of Observation wells, 2010. 5-14
Figure 5-11. Simulated vs. observed groundwater levels (feet NAVD88), model Layer 1, 2010. 5-16
Figure 5-12. Simulated vs. observed groundwater levels (feet NAVD88), model Layer 3, 2010. 5-17
Figure 5-13. Simulated vs. observed groundwater levels (feet NAVD88), model Layer 5, 2010. 5-18
Figure 5-14. Residual groundwater level Statistics comparison for model Layers 1, 3 and 5. 5-19
Figure 5-15. Simulated vs. observed spring discharges (cfs), 2010 5-20
Figure 5-16. Residual spring discharge Statistics comparison. 5-21
Figure 5-17. Simulated vs. estimated baseflow pickups (cfs), 2010. 5-25
Figure 5-18. Residual baseflow pickup Statistics comparison. 5-26
Figure 5-19. Simulated vs. estimated Range of cumulative baseflow estimates in 2010 5-27
Figure 5-20. Residual cumulative baseflow Statistics comparison. 5-28
Figure 5-21. 2010 groundwater level residuals, model Layer 1 5-31
Figure 5-22. 2010 groundwater level residuals, model Layer 3. 5-32
Figure 5-23. Simulated UFA potentiometric surface, 2010. 5-33
Figure 5-24. Observed UFA potentiometric surface, 2010. 5-34

Figure 5-25. Model-wide mass balance summary, 2010 5-36
Figure 5-26. USGS estimated predevelopment potentiometric surface of the Floridan aquifer system within the NFSEG domain (after Johnston et al. 1980) 5-39
Figure 5-27. NFSEG simulated no-pumping Layer 3 potentiometric surface and USGS estimated predevelopment potentiometric surface of the Floridan aquifer system (after Johnston et al. 1980) 5-40
Figure 5-28. Differences between the USGS estimated predevelopment potentiometric surface of the Floridan aquifer system (after Johnston et al. 1980) and the NFSEG simulated no-pumping Layer 3 potentiometric surface within the area of interest 5-42
Figure 5-29. Increases in depth of flooding of NFSEG Layer 1 between the NFSEG 2009 and no-pumping simulations within the area of interest 5-45
Figure 6-1 Map of all groundwater basins (GWB) within the model boundary 6-2
Figure 6-2 Simulated model wide mass balance for 2001 6-4
Figure 6-3 Simulated model wide mass balance for 2009 6-4
Figure 6-4. Simulated model wide mass balance for 2010 6-5
Figure 6-5. Simulated model wide mass balance for no-pumping 6-5
Figure 6-6. Simulated mass balance of GWB 1 for 2001 6-8
Figure 6-7. Simulated mass balance of GWB 1 for 2009 6-8
Figure 6-8. Simulated mass balance of GWB 1 for 2010 6-9
Figure 6-9. Simulated mass balance of GWB 1 for no-pumping 6-11
Figure 6-10. Simulated mass balance of GWB 2 for 2001 6-12
Figure 6-11. Simulated mass balance of GWB 2 for 2009 6-13
Figure 6-12. Simulated mass balance of GWB 2 for 2010 6-13
Figure 6-13. Simulated mass balance of GWB 2 for no-pumping 6-16
Figure 6-14. Simulated mass balance of GWB 3 for 2001 6-17
Figure 6-15. Simulated mass balance of GWB 3 for 2009 6-18
Figure 6-16. Simulated mass balance of GWB 3 for 2010 6-18
Figure 6-17. Simulated mass balance of GWB 3 for no-pumping 6-20
Figure 6-18. Simulated mass balance of GWB 4 for 2001 6-22
Figure 6-19. Simulated mass balance of GWB 4 for 2009 6-22
Figure 6-20. Simulated mass balance of GWB 4 for 2010 6-23
Figure 6-21. Simulated mass balance of GWB 4 for no-pumping 6-25
Figure 6-22. Simulated mass balance of GWB 5 for 2001 6-25
Figure 6-23. Simulated mass balance of GWB 5 for 2009 6-26
Figure 6-24. Simulated mass balance of GWB 5 for 2010 6-26
Figure 6-25. Simulated mass balance of GWB 5 for no-pumping 6-29
Figure 6-26. Simulated mass balance of GWB 6 for 2001 6-29
Figure 6-27. Simulated mass balance of GWB 6 for 2009 6-30
Figure 6-28. Simulated mass balance of GWB 6 for 2010 6-30
Figure 6-29. Simulated mass balance of GWB 6 for no-pumping 6-32
Figure 6-30. Simulated mass balance of GWB 7 for 2001 6-34
Figure 6-31. Simulated mass balance of GWB 7 for 2009 6-35
Figure 6-32. Simulated mass balance of GWB 7 for 2010 6-35
Figure 6-33. Simulated mass balance of GWB 7 for no-pumping 6-37
Figure 6-34. Inflows and outflows of simulated model wide mass balance for 2001 6-38
Figure 6-35. Inflows and outflows of simulated model wide mass balance for 2009 6-38
Figure 6-36. Inflows and outflows of simulated model wide mass balance for 2010 6-39

Figure 6-37. Inflows and outflows of simulated model wide mass balance for no-pumping 6-39
Figure 7-1. Sensitivity of simulated groundwater levels to changes in aquifer parameters and boundary conditions.....7-4
Figure 7-2. Sensitivity of simulated baseflows to changes in aquifer parameters and boundary conditions 7-5
Figure 7-3. Sensitivity of simulated spring flows to changes in aquifer parameters and boundary conditions 7-6
Figure 7-4. Sensitivity of simulated groundwater levels to changes in lateral boundary heads 7-7
Figure 7-5. Sensitivity of simulated baseflows to changes in lateral boundary heads 7-8
Figure 7-6. Sensitivity of simulated spring flows to changes in lateral boundary heads 7-9
Figure 7-7. Composite-scaled sensitivities for all observations. Parameter group IDs are defined in Table 7-1 7-12
Figure 7-8. Composite-scaled sensitivities for groundwater-level observations. Parameter group IDs are defined in Table 7-1 7-12
Figure 7-9. Composite-scaled sensitivities for baseflow observations. Parameter group IDs are defined in Table 7-1 7-13
Figure 7-10. Composite-scaled sensitivities for spring-flow observations. Parameter group IDs are defined in Table 7-1 7-13
Figure 7-11. Coefficient of Variations for all parameter groups. Parameter group IDs are defined in Table 7-1 7-17
Figure 7-12. Location evaluated in the prediction uncertainty analysis 7-17
Figure 7-13. Histogram for the predicted change in flow in the upper Floridan aquifer groundwater level near Lake Brooklyn from 2009 to the 2035 hypothetical withdrawal scenario based on 522 sets of parameters 7-18
Figure 7-14. Histogram for the predicted flow reduction in the Santa Fe River near Fort White from 2009 to the 2035 hypothetical withdrawal scenario based on 522 sets of parameters..... 7-19
Figure 9-1. Legend for HSPF model simulation graphics in Figure 2 and Figure 3 9-3
Figure 9-2. Illustration of water storage and movement in HSPF PERvious LaND (PERLND) 9-8
Figure 9-3. Illustration of water storage and movement in the HSPF model impervious land element (IMPLND) 9-9
Figure 9-4. Water collection and movement in a HSPF reach/reservoir element (RCHRES) 9-10
Figure 9-5. Average annual difference between NEXRAD and NLDAS precipitation. 9-13
Figure 9-6. NLDAS annual precipitation for 2001 in inches..... 9-14
Figure 9-7. NLDAS annual precipitation for 2009 in inches..... 9-15
Figure 9-8. NLDAS annual precipitation for 2010 in inches..... 9-16
Figure 9-9. Comparison of NLDAS potential evaporation to USGS potential evaporation at several locations. 9-17
Figure 9-10. Potential evaporation for 2001 from NLDAS tensioned to USGS. 9-19
Figure 9-11. Potential evaporation for 2009 from NLDAS tensioned to USGS. 9-20
Figure 9-12. Potential evaporation for 2010 from NLDAS tensioned to USGS. 9-21
Figure 9-13. USGS HUC8 watersheds. 9-24

Figure 9-14. Elevation from the National Elevation Dataset (NED), now 3DEP 9-26
Figure 9-15. National Land Cover database, land cover for 2001..... 9-30
Figure 9-16. USGS Flow Observation Gauges..... 9-32
Figure 9-17. USGS quality assessment of flow data for water year 2009..... 9-34
Figure 9-18. Map of closed basins within the NFSEG model. 9-38
Figure 9-19. Conventional representation of a sub-watershed for a tributary basin. 9-40
Figure 9-20. Closed basin representation of a sink to replace outflow, where surface flow Q = 0. 9-41
Figure 9-21. Sink and drainage wells within NFSEG domain. 9-42
Figure 9-22. Conceptual framework for the IGWO representation of springs. 9-44
Figure 9-23. UFA potentiometric surface and springsheds in the Suwannee River Basin. 9-45
Figure 9-24. Identified sub-watersheds that were used as springshed outlets. 9-46
Figure 9-25. Overview of calibration process. 9-47
Figure 9-26. Map showing Nash-Sutcliffe values for model calibrations at individual gauges over the NFSEG model domain. 9-70
Figure 9-27. Nash-Sutcliffe efficiency values plotted against USGS data quality evaluation 9-71
Figure 9-28. Percent bias chart plotted against USGS data quality evaluation. 9-72

List of Acronyms

3DEP: 3D Elevation Program

AFSIRS: Agricultural Field-Scale Irrigation Requirements Simulation

AGWET: Active Groundwater ET

AGWI: Active Groundwater Inflow

AGWO: Active Groundwater Outflow

AGWS: Active Groundwater Storage

AGWT: Active Groundwater Flow

APT: Aquifer Performance Test

BASET: Baseflow ET

BASINS: Better Assessment Science Integrating point & Non-point Sources

BFI: Baseflow Index

CEPE: Interception Evaporation

CEPS: Interception Storage

cfs: Cubic Feet per Second

CRF: Calibration Results Flows

CRH: Calibration Results Heads

CRP: Calibration Results Parameters

CUAHSI: Consortium of Universities for the Advancement of Hydrologic Science

DCIA: Directly Connected Impervious Area

DEEPFR: A portmanteau for DEEP FRaction, a HSPF parameter that defines how much of the infiltration is lost to deep recharge, called IGWI (Inactive GroundWater Inflow)

DEM: Digital Elevation Model

EC3: Eastern Central Lateral Boundary of Layer 3

EC4: Eastern Central Lateral Boundary of Layer 4

EC5: Eastern Central Lateral Boundary of Layer 5

ECFT: East-Central Florida Transient

EL3: Eastern Lower Lateral Boundary of Layer 3

ES3: Eastern Seaward Lateral Boundary of Layer 3

ES4: Eastern Seaward Lateral Boundary of Layer 4

ES4: Southern East Lateral Boundary of Layer 4

ES5: Southern East Lateral Boundary of Layer 5

ET: evapotranspiration

EU3: Eastern Upper of Lateral Boundary of Layer 3

EU4: Eastern Upper of Lateral Boundary of Layer 4

EU5: Eastern Upper of Lateral Boundary of Layer 5

EVTRMUL: Evapotranspiration Rate Multiplier

FGS: Florida Geological Survey

FTABLE: Function Table

FWSW6: Lateral boundary in which top of model layer 6 Intersects the 10,000 mg/l TDS concentration iso-surface

FWSW7: Lateral boundary in which top of model layer 7 Intersects the 10,000 mg/l TDS concentration iso-surface

GDP: Geo Data Portal

GHB: General Head Boundary

GW: Groundwater

GWB: Groundwater Basins

HDR: High Density Residential

HEC-RAS: Hydrological Engineering Centre - River Analysis System

HGL6: Lateral boundary that approximates the line pinch-out for the lower semi-confining unit of Layer 6

HGL7: Lateral boundary that approximates the line pinch-out for the lower semi-confining unit of Layer 7

HSPF: Hydrological Simulation Program – FORTRAN

HUC12: Hydrologic Unit Code 12

HUC16: Hydrologic Unit Code 16

HUC4: Hydrologic Unit Code 4

HUC8: Hydrologic Unit Code 8

HYSEP: Hydrograph Separation

ICU: Intermediate Confining Unit

IFWI: Interflow Inflow

IFWO: Interflow Outflow

IGWI: Inactive Ground Water Inflow

IGWI: Inactive Groundwater Flow

IGWO: Inactive Ground Water Outflow (interpretation of model feature added to represent springs in several of the models)

IMPLND: Impervious Land Element

in/yr: Inches per Year

IND: Industrial

INTB: Integrated Northern Tampa Bay

LDR: Low Density Residential

LZET: Lower Zone Evapotranspiration

LZLI: Lower Zone Lateral Inflow

LZS: Lower Zone Storage

MCU: Middle Confining Unit

MDR: Medium Density Residential

MNW2 Package: Multi-Node Well Package

MODFLOW NWT: A Newton Formulation for MODFLOW-2005

MODFLOW: Modular Three-Dimensional Finite-Difference Groundwater Flow Model

MSET: Maximum Saturated Evapotranspiration

N3: Northern Lateral Boundary of Layer 3

N4: Northern Lateral Boundary of Layer 4

N5: Northern Lateral Boundary of Layer 5

NDCIA: Non Directly Connected Impervious Area

NED: National Elevation Model

NEF: Northeast Florida

NEXRAD: Next-Generation Radar

NFSEG: North Florida South East Georgia Groundwater Flow Model

NLCD: National Land Cover Database

NLCD: National Land Cover Database

NLDAS: National Land Data Assimilation Systems

NURF: Nutrient Reduction Facility

NWFWMD: Northwest Florida Water Management District

PART: Name of computer program which uses streamflow partitioning to estimate a daily record of groundwater discharge under the streamflow record

PERLND: Pervious Land Element

PEST: Parameter Estimation

POR: Period of Record

RCH: Reach

RCHRES: Reach Module
RIBS: Rapid Infiltration Basins
SC: Spring-Conductance
SC3: Southern Central Lateral Boundary of Layer 3
SC4: Southern Central Lateral Boundary of Layer 4
SC5: Southern Central Lateral Boundary of Layer 5
SCPE: Single Continuum Porous Equivalent
SCS: Soil Conservation Service
SE3: Southern East Lateral Boundary of Layer 3
SE4: Southern East Lateral Boundary of Layer 4
SE5: Southern East Lateral Boundary of Layer 5
SJRWMD: St. Johns River Water Management District
SRWMD: Suwannee River Water Management District
SSW: Simple Subset Wizard
SUPY: Water supply to land element (if not modeling ice/snow equal to precipitation)
SURET: Surface Storage Evapotranspiration
SURLI: Surface Lateral Inflow
SURO: Surface Outflow
SURS: Surface Detention Storage
SW3: Southern West Lateral Boundary of Layer 3
SW4: Southern West Lateral Boundary of Layer 4
SW5: Southern West Lateral Boundary of Layer 5
SWFWMD: Southwest Florida Water Management District
TDS: Total dissolved solids
UFA: Upper Floridan Aquifer
UFWI: University of Florida Water Institute
USEPA: United States Environmental Protection Agency
USGS: United States Geological Survey
UZET: Upper Zone Evapotranspiration
UZS: Upper Zone Storage
WAFR: Wastewater Facility Regulation
WBD: Watershed Boundary Dataset
WN3: Western North Lateral Boundary of Layer 3

WN4: Western North Lateral Boundary of Layer 4

WN5: Western North Lateral Boundary of Layer 4

WS3: Western Seaward Lateral Boundary of Layer 3

WS5: Western Seaward Lateral Boundary of Layer 5

CHAPTER 1. INTRODUCTION

The St. Johns River Water Management District (SJRWMD) develops and applies groundwater models to facilitate decision making regarding water resources and groundwater uses. An application of the SJRWMD's Northeast Florida Groundwater Flow Model (NEF, Russo 2011) indicated the potential for significant water resource related impacts in areas of both the Suwannee River Water Management District (SRWMD) and SJRWMD due to projected groundwater withdrawals within the NEF model domain. In 2009, a groundwater modeling group was assembled to discuss issues regarding the NEF model. The meetings of the groundwater modeling group, which were facilitated by the University of Florida Water Institute (UFWI), occurred between August 2009 and February 2010 and enabled all stakeholders to come together for a series of meetings where issues regarding the SJRWMD NEF model development and application were investigated. The stakeholders included a variety of groups, including water utilities, private industry, governmental organizations and environmental groups.

A summary report on groundwater modeling was prepared by Dr. Wendy Graham and Lisette Staal of the UFWI (Graham and Staal, 2010) summarizing the outcome of these meetings. Several recommendations for further groundwater model development were included as part of the report. One of the recommendations stated that "More time should be spent 'up-front' with stakeholders providing input on methods and model evaluation criteria than on defending and/or critiquing the end-product. Given the sensitive hydrologic and ecological conditions at the boundary between the SJRWMD and SRWMD, the two Districts should work toward developing a common North Florida model." Because of these recommendations, the SJRWMD and SRWMD undertook the joint creation of the North Florida Southeast Georgia regional groundwater flow model (NFSEG). The Districts agreed that the use of one model would enhance efficiency and effectiveness and provide consistency in planning and permitting decisions.

PURPOSE AND SCOPE

A technical team of experts from SJRWMD, SRWMD and stakeholders from water utilities, private industries, governmental organizations and environmental groups initiated development of the NFSEG model in 2012. The technical team's directive was to ensure appropriate science was applied to the modeling and data analysis to support decision making and that the work completed was defensible, understood by the team and collaboratively developed, as described in the NFSEG project charter, available at northfloridawater.com. The primary purpose of the NFSEG model was to enable improved evaluations of within-district, inter-district (e.g., SJRWMD/SRWMD) and interstate (e.g., Florida/Georgia) water level changes in the surficial and Floridan aquifer systems and

changes in spring flows and river and stream base flows resulting from groundwater use over the model domain.

The technical team completed an interim version of NFSEG (NFSEG v1.0) in 2016. NFSEG v1.0 was utilized to support the North Florida Regional Water Supply Plan (2015-2035). Several documents resulted from the development of version 1.0 and include the following three reports:

1. Data Availability for Development of the North Florida Southeast Georgia (NFSEG) Regional Groundwater Flow Model in the Area of its Potential Domain (Durden 2012);

2. North Florida Southeast Georgia (NFSEG) Groundwater Flow Model Conceptualization (Durden, Cera and Johnson 2013); and

3. Development and Calibration of the North Florida Southeast Georgia Groundwater Model V1.0 - Draft (Gordu, Durden and Grubbs 2016).

The Data Availability report (item 1 above) includes a brief description of the study area, a general description of the groundwater flow system of the area, the types and expected availability of data required for construction of the NFSEG groundwater model and potential boundaries of the model domain. The Conceptualization report (item 2) details the plan for construction of the NFSEG groundwater flow model, including model extent, configuration and lateral and internal boundary conditions, an analysis and interpretation of data needed for determination of the model calibration years, a plan for determination of groundwater recharge and maximum saturated evapotranspiration rates, and proposed NFSEG model calibration objectives. The third report describes the construction and calibration of version 1.0 of the NFSEG groundwater model.

The purpose of this report is to describe the development of the next version of the groundwater flow model, NFSEG v1.1. Some important changes that were implemented in development of NFSEG v1.1 included the following items:

1. Multiple river and drain boundaries within grid cells were aggregated within grid cells so that a maximum of one river and one drain boundary was assigned in most cases.

2. Baseflow targets were revised.

3. Estimated surficial aquifer system and Upper Floridan aquifer groundwater levels for use as “synthetic targets” in areas for which improved simulated groundwater levels were deemed needed but groundwater-level observations were unavailable or sparse.

4. The representation of multi-zone production wells with assigned zero flows was discontinued.

5. Additional drain boundaries were added to represent previously unrepresented surface water flow features.

6. Spring flow estimates were updated to reflect more recent data collection.

7. A non-linear parameter and predictive uncertainty of NFSEG v1.1 was completed .

DESCRIPTION OF MODEL AREA

The approximately 60,000 square mile model domain encompasses a large area of the Floridian aquifer system in north Florida, Georgia and South Carolina (Figure 1-1). Land surface elevations range from sea level to more than 450 feet, NAVD88 in northern Georgia.

Physiography

The model area lies within the Coastal Plain physiographic province of Florida, Georgia and South Carolina. This area has been subdivided into the Sea Island, East Gulf Coastal Plain and Floridian Sections (Fenneman and Johnson 1946; Figure 1-2). The Coastal Plain extends from the Fall Line, the line of outcrop of the igneous and metamorphic rocks of the Piedmont region, southward towards the Atlantic and Gulf coasts. The topography of the Coastal Plain varies from low-lying flat plains to rounded foothills of the Piedmont region. Karstic landscapes prevail in areas where limestone is near land surface. Low-lying coastal terraces occupy much of the area and reflect changes in Pleistocene sea-level stands (Renken 1996). Other geographic features are shown in Figure 1-3.

Land Use

According to the National Land Cover Database (NLCD) land use coverage in 2001, excluding the ocean, forested areas covered a significant portion of the model area (36.5%; Figure 1-4). Wetlands, agricultural lands and urban areas constituted 23%, 16.5% and 9% of land uses, respectively.

Major Surface Water and Groundwater Basins

Major surface water basins that are partially or fully encompassed by the study area include the St. Johns, Suwannee, Altamaha, Satilla and Savannah River basins. Smaller basins include those of the Flint, Ochlocknee, Aucilla, Steinhatchee, Wacissa, St. Marks, St. Marys and Ocklawaha Rivers.

For this study, seven major groundwater basins were delineated based on the Upper Floridan aquifer (UFA) potentiometric surface (Figure 1.5). The potentiometric surface

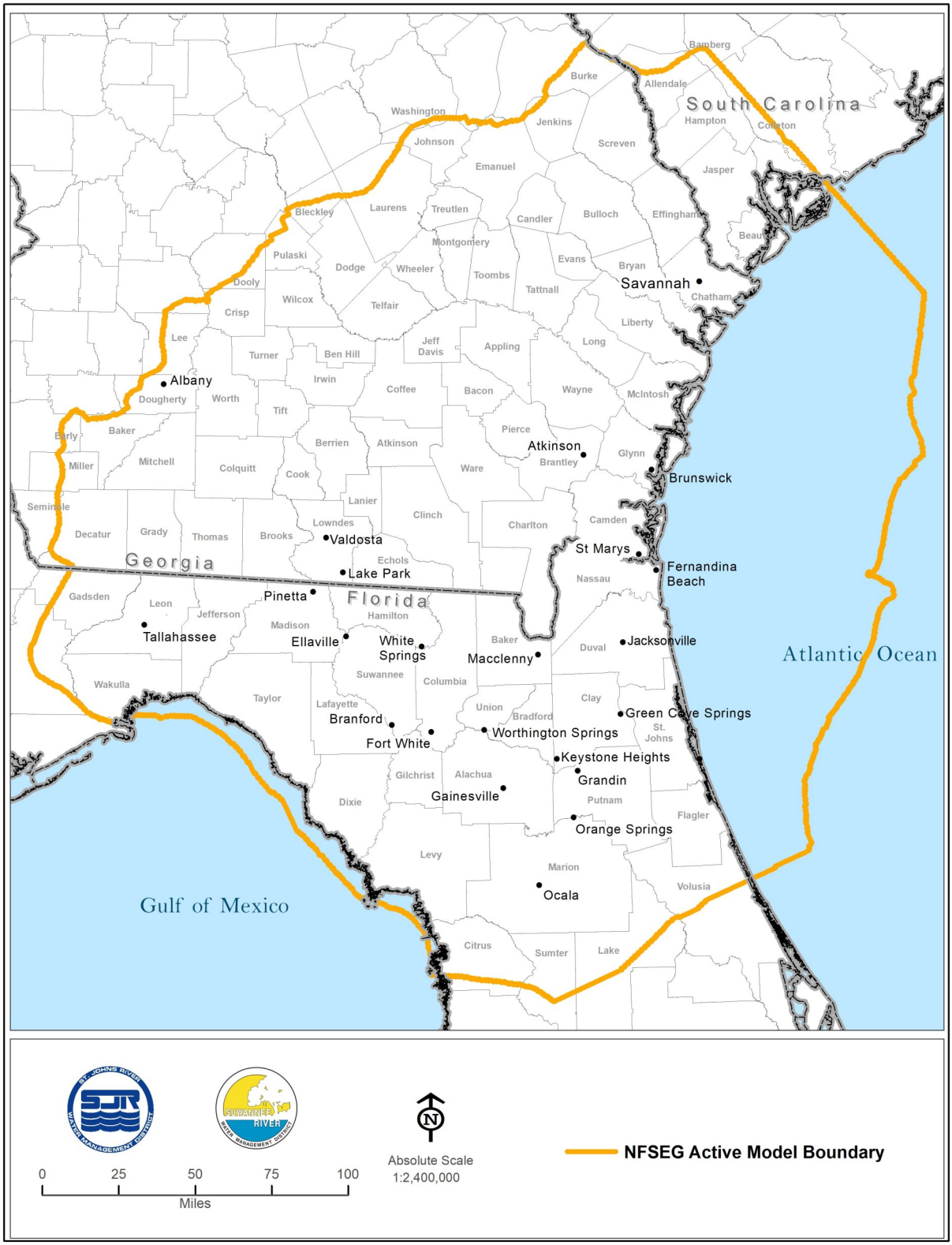

Figure 1-1. Location of study area

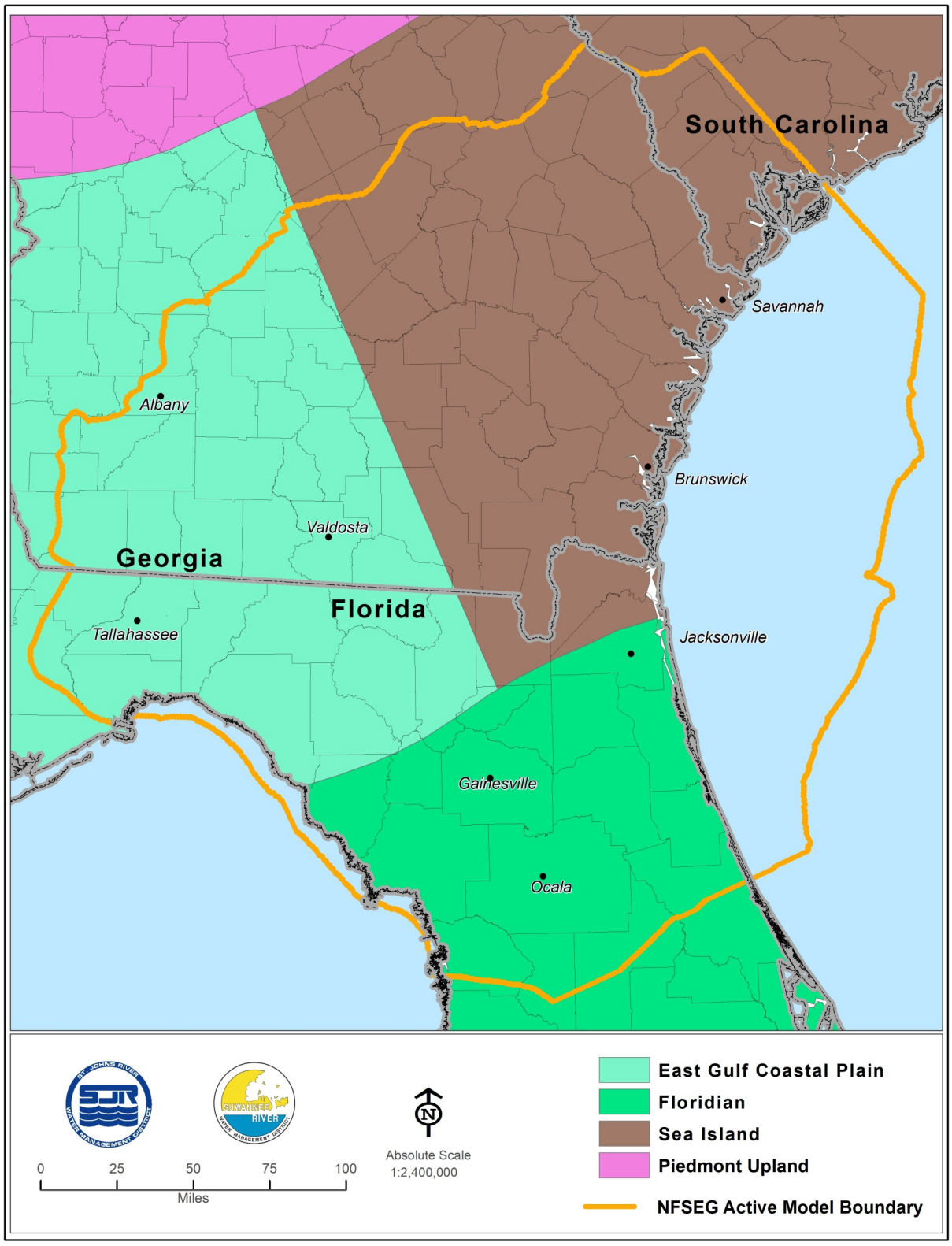

Figure 1-2. Major physiographic provinces

Figure 1-3. Geographic features

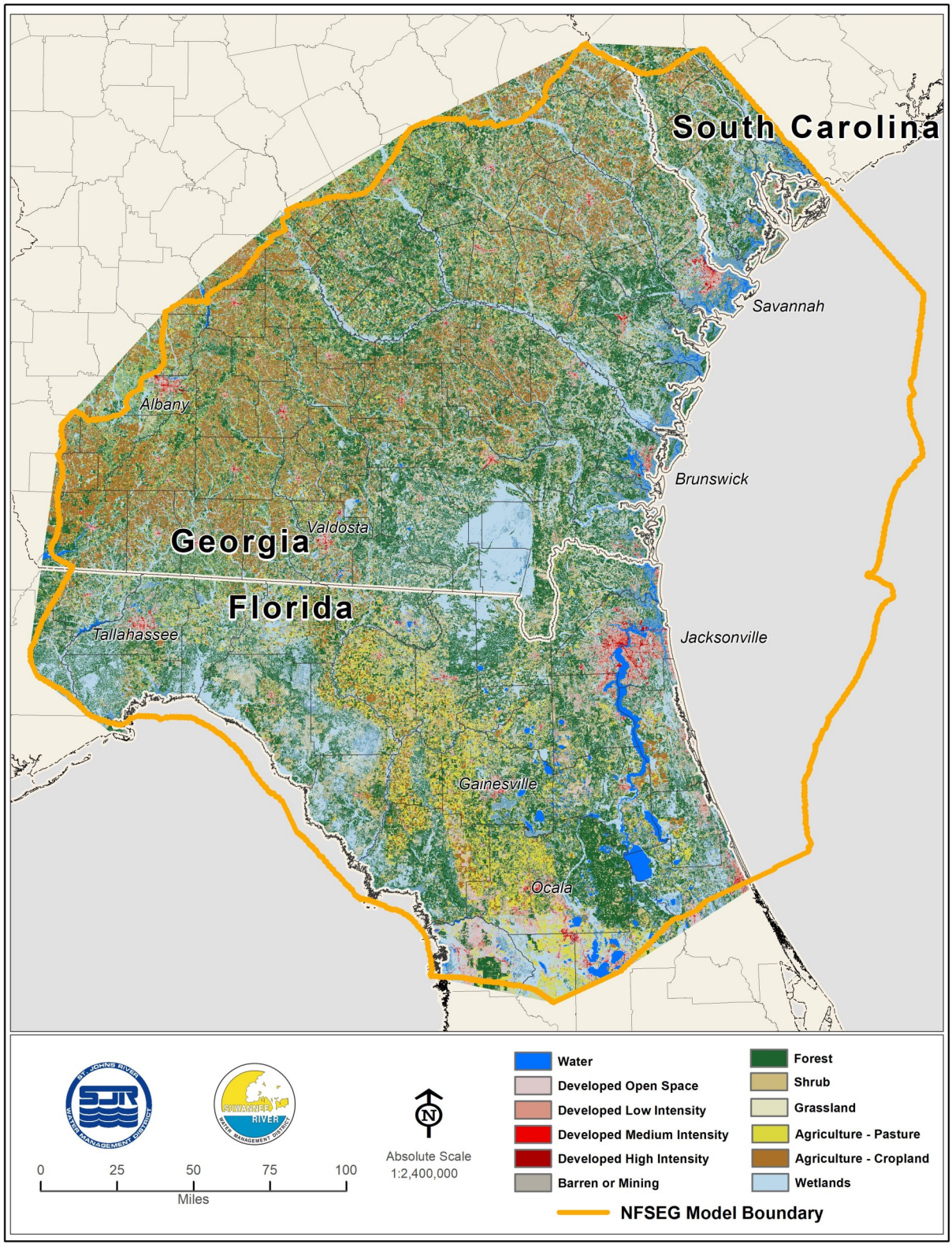

Figure 1-4. Land-Use coverage

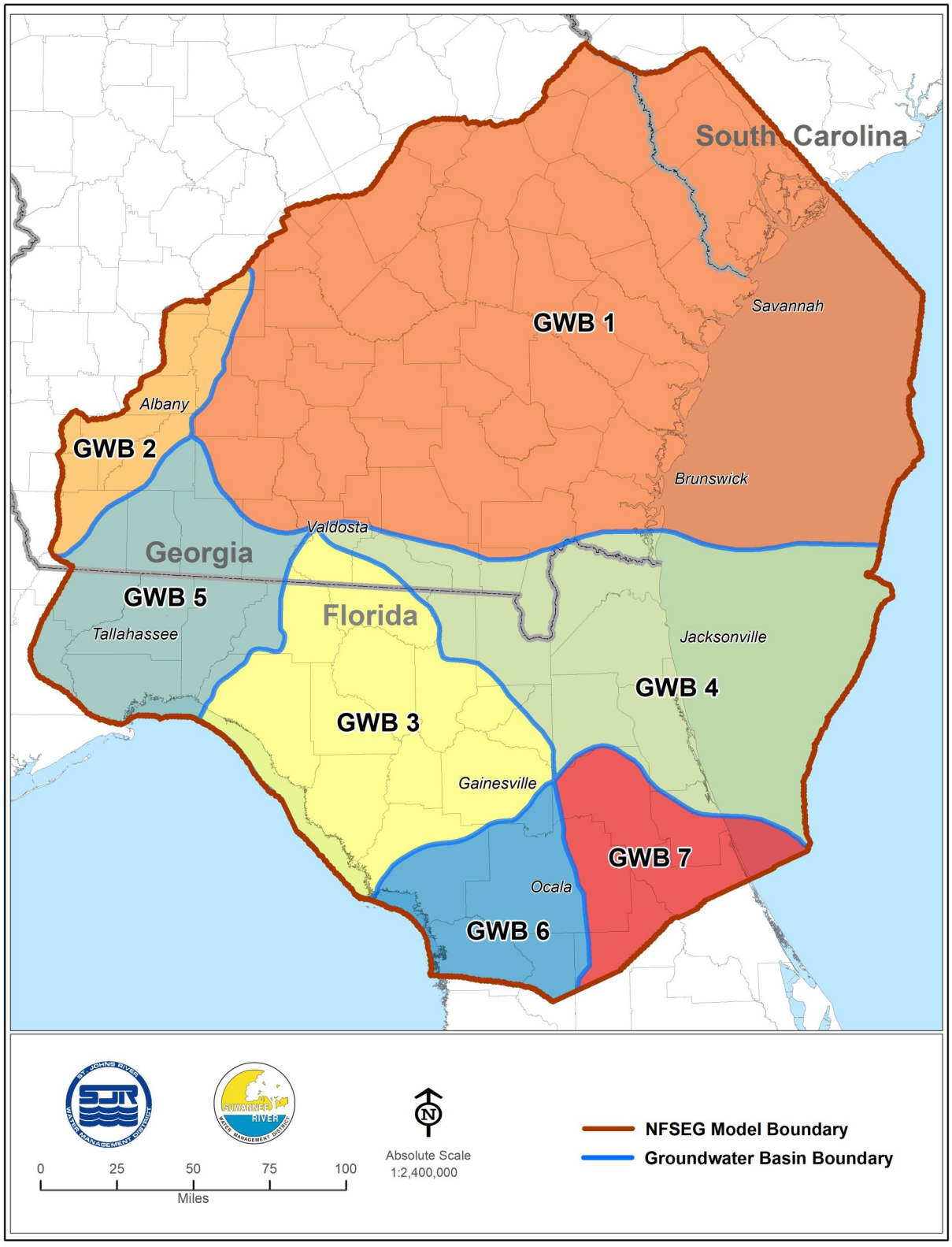

Figure 1-5. Major groundwater basins

highs in southeast Clay County, Florida, the Keystone Heights area of north-central Florida and Valdosta, Georgia are the major features that divide major groundwater basins in north Florida. These groundwater basins are similar to those mapped by Bush and Johnston (1988).

Municipalities and Other Major Pumping Centers

Major pumping centers are generally located in large cities, where municipal, commercial and industrial water requirements are concentrated. In Florida, these cities include Jacksonville, Gainesville, Fernandina Beach and Tallahassee. In Georgia, the cities include Savannah, Brunswick and Albany. Areas of notable agricultural withdrawals include southwest Georgia, eastern Putnam, southern St. Johns and Flagler counties, Florida and the Suwannee River basin in Florida.

Climate

The climate of the area is characterized as subtropical, with hot, humid summers and mild winters. On average, temperatures in the summer range typically from the low 70's to the low 90's Fahrenheit and in the winter typically range from the low 30's to the low 70's Fahrenheit (Climate of Florida, 2012, Climate of Georgia, 2012). Winter rainfall patterns tend towards widespread frontal activity, while summer rainfall patterns tend towards afternoon thundershowers (Climate of Florida, 2012, Climate of Georgia, 2012)**.** Long-term average rainfall within the model domain from 2001 to 2010 is approximately 50 inches per year. Figure 1-6 provides the 2001-2010 long-term annual averages as well as 2001 and 2009 annual rainfall totals for several locations within the model area.

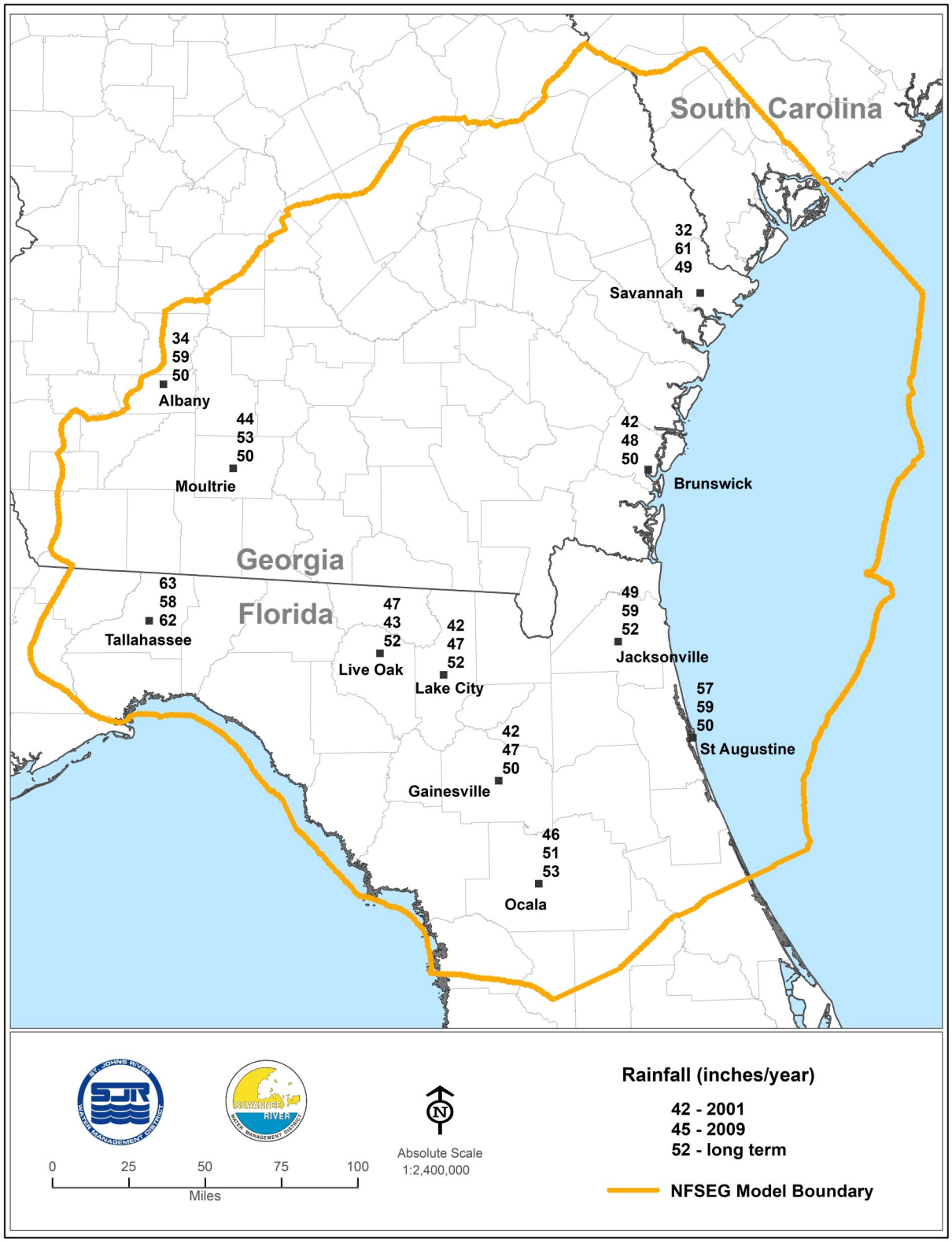

Figure 1-6. Rainfall totals at various rainfall gauges (2001, 2009, and long-term averages, inches)

CHAPTER 2. HYDROLOGY OF THE AREA

The hydrology within the NFSEG model domain is comprised of surface water and groundwater systems. The groundwater system is comprised of the Floridan aquifer system and, where present, the overlying intermediate confining unit and surficial aquifer system. The surface water systems are of concern because of the interactions with the groundwater flow system. A brief description of surface water systems within the NFSEG domain is provided, followed by a detailed description of the groundwater flow system.

SURFACE WATER SYSTEMS

Surface water systems of the area include streams, lakes, wetlands, estuaries, the Atlantic Ocean and the Gulf of Mexico. Hundreds of streams and rivers and more than 300 lakes are represented in the NFSEG model. Hydraulically, surface water bodies are of interest because of their potential for water exchange and for influencing water levels of adjacent groundwater systems. The rate of exchange between a surface water body and surrounding groundwater system depends on the level of resistance to flow of the materials connecting the two systems and the head gradient between them. The head gradient is the difference in water level between the surface water body and the aquifer with which it is in hydraulic contact divided by the distance over which the decline in water level occurs. Where resistance to flow is greater, a larger head gradient between a given surface water body and surrounding aquifer is required to realize the same rate of exchange. Less resistance to flow requires a smaller head gradient to drive flows, so water levels of surface water bodies and groundwater systems to which they are connected hydraulically tend towards similarity under conditions of low flow resistance. The manner of representing surface water bodies in the NFSEG model is discussed in detail in later sections of the report that describe the model lateral and internal boundary conditions, including the descriptions of implementation of the MODFLOW River, Drain, General Head Boundary and Basic Packages.

The following discussion includes brief descriptions of selected rivers, lakes, wetlands and the Atlantic Ocean and Gulf of Mexico, focusing primarily on the interaction of these bodies with the groundwater system. The types of interactions that occur between surface water bodies and groundwater flow system within the NFSEG model depend on various conditions, including the degree of confinement of the Floridan aquifer system and relative water levels of a given surface water body and aquifer(s) with which it interacts hydraulically. In addition to the two ocean bodies, the selected surface water bodies include rivers, lakes and wetlands, thus encompassing the range of types of surface water bodies that occur within the NFSEG model domain, given that estuaries are treated as extension of oceans.

Rivers

Major rivers in the NFSEG model domain include the Suwannee River and Santa Fe River, a tributary to the Suwannee River. The Suwannee and Santa Fe rivers, in their respective upper reaches, correspond to areas in which the Floridan aquifer system is confined or semiconfined. Hence, in their respective upper reaches, these rivers are in hydraulic contact with the surficial aquifer system. However, these rivers down cut progressively through underlying sediments in their respective down gradient courses. Each river first down cuts into the intermediate confining unit and eventually into the Floridan aquifer system. Hence, baseflow in these rivers is ultimately derived from all three aquifer systems, although the Floridan aquifer system becomes the dominant source of baseflow once they are incised into it, as evidenced by numerous, large springs that contribute to the flows of the two rivers along those respective portions of their courses.

Two other important tributaries to the Suwannee River are the Alapaha and Withlacoochee rivers. Most of the respective basins of these two rivers are in Georgia. Their respective confluences with the Suwannee River occur just south of the Florida-Georgia state line. Baseflows in these rivers are derived from the surficial aquifer system, intermediate confining unit and Floridan aquifer system, as contact with all three aquifer/confining unit systems occurs along their respective courses, depending on location.

Under low flow conditions, all flow in the lower reaches of the Alapaha River is captured by the Floridan aquifer system by a series of sinks just upstream of and at the end of a small distributary known as the Dead River. The flow reemerges from the Floridan aquifer system at the Alapaha Rise and Holton Creek, from which the reemergent Alapaha River flows through short spring runs to their confluences with the Suwannee River. The intermediate confining unit is absent in the general areas of the Dead River and Alapaha Rise, so the Floridan aquifer system in this area is unconfined.

The Withlacoochee River also loses water to the Floridan aquifer system in areas in which the intermediate confining unit is absent or has been breached by karst features. North of Valdosta, Georgia, a portion of the river flow is diverted to sinks during high flows and all of it is during low flows. Direct recharge to the Floridan aquifer system contributes greatly to the formation of the Valdosta potentiometric high, a regionally important feature of the potentiometric surface of the Floridan aquifer system. Discharge to the river via springs emanating from the Floridan aquifer system begins near the Florida-Georgia state line (Krause 1979).

Located east of the Suwannee River near the Atlantic coast, the St. Johns River flows northward from its headwaters, which are south of the southern extent of the model domain. The St. Johns River is in close hydraulic contact with the Floridan aquifer system in the southern area of its occurrence within the model domain. Discharge from the Floridan aquifer system to the St. Johns River at Lake George, a large lake that occurs along the course of the St. Johns River in northwestern Volusia, eastern Marion and southeastern Putnam counties, contributes to a noticeable low in the potentiometric surface of the Floridan aquifer system in the area. Discharge from several springs in this area, including Silver Glen and Salt springs, also contribute. The runs of these springs form tributaries to the St. Johns River, as they discharge to Lake George. North of

Lake George, the thickness of the intermediate confining unit increases along the course of the St. Johns River. At the town of Green Cove Springs, Florida, Green Cove Springs emanates from the Floridan aquifer system and the discharge travels via a short run to the St. Johns River. This occurs despite significant confinement of the Floridan aquifer system by the intermediate confining unit, which is approximately 250 feet thick at this location. Further to the north, in Jacksonville, Florida, significant hydraulic contact with the St. Johns River is limited to the surficial aquifer system, as the Floridan aquifer system in this area is heavily confined, the intermediate confining unit being on the order of 400 feet thick.

The Ocmulgee River is a major river system in Georgia that is in close hydraulic contact with the Floridan aquifer system near the northern extent of the model domain. The Ocmulgee River is the principal tributary to the Altamaha River, which is formed by the confluence of the Ocmulgee and Oconee rivers. The Oconee River is also in close hydraulic contact with the Floridan aquifer system near its intersection with the northern boundary of the model domain. These rivers derive baseflow from the surficial aquifer system, the intermediate confining unit and the Floridan aquifer system.

The rivers mentioned in the preceding discussion are a small, albeit important, sampling of rivers within the vast model domain. Other rivers are present, many of which are in close contact with the Floridan aquifer system over significant portions of their runs due to prevailing unconfined conditions in the Floridan aquifer system. Such rivers include the Flint River in southwestern Georgia and the Steinhatchee River of Lafayette, Dixie and Taylor counties, Florida. Others lack close contact with the Floridan aquifer system due to confinement. Those rivers are in contact with the surficial aquifer system and/or intermediate confining unit.

Lakes

Many naturally formed lakes in the model domain are sinkhole lakes, which are formed in depressions that occur due to the collapse of cavities in the limestone of the underlying Floridan aquifer system. Resistance to downward vertical leakage due to the presence of the intermediate aquifer system aids in the retention of water in the resulting depressions, thus helping to form lakes. Large numbers of sinkhole lakes are found in Keystone Heights, Florida and surrounding areas. Lakes Brooklyn and Geneva are examples of such lakes. These lakes are part of the Upper Etonia Creek basin chain of lakes, which has been the subject numerous hydrological assessments. A similar group of lakes occurs in Lowndes County near Lake Park, Georgia and surrounding areas.

Sinkhole lakes can act as sources of relatively concentrated recharge to the underlying Floridan aquifer system in recharge areas. Leakage rates beneath them to the Floridan aquifer system is often enhanced by disturbances that occurred in the intermediate confining unit during the collapse(s) within the Floridan aquifer system that resulted in their formation. In and surrounding the town of Keystone Heights, Florida, rates of recharge, which are enhanced by downward leakage from numerous sinkhole lakes, are large enough to result in the formation of the Keystone Heights potentiometric high, a prominent, hydrologically important feature of the potentiometric surface of the Flori-

dan aquifer system. The Keystone Heights potentiometric high is centered approximately on the Upper Etonia Creek basin chain of lakes, which includes Lake Brooklyn, as mentioned previously. A strong correlation exists between the water levels of Lake Brooklyn and the Floridan aquifer system (Motz et al. 1991).

Other lakes occur in areas in which the Floridan aquifer system is unconfined. The water levels of such lakes usually are close to the level of the potentiometric surface of the Floridan aquifer system. An example of such a lake is Lake Grandin in Putnam County, Florida.

Swamps/Wetlands

Wetlands within the NFSEG model domain are related to the hydrogeology of the system in several ways. Of course, in recharge areas, confinement of the Floridan aquifer system in flat terrain can impede leakage to the Floridan aquifer system, while the flatness of the terrain impedes runoff. The Okefenokee Swamp in southeast Georgia is an example of such a swamp. Other swamps occur in recharge areas in which the Floridan aquifer system is generally unconfined due to the absence or thinness of the intermediate confining unit, but, due to lower horizontal and vertical hydraulic conductivity within the Floridan aquifer system, potential recharge to the Floridan aquifer system spills over to land surface, thus forming wetland areas. Mallory Swamp, which is centered on the boundary between Lafayette and Dixie counties, Florida, is an example of this type of swamp. A third type of wetland occurs in coastal discharge zones in which the Floridan aquifer system is unconfined and in which its potentiometric surface is above land surface, thus enabling artesian discharge to relatively flat land. This results in pooling of the discharged water on the land surface, i.e. swamp formation. Wetlands resulting from this type of exchange occur extensively along the coast of the Gulf of Mexico.

Atlantic Ocean and Gulf of Mexico

The Atlantic Ocean and Gulf of Mexico are the ultimate catchments of whatever water remains within the Floridan aquifer system seaward of their respective coasts. Horizontal gradients in the surficial aquifer system and Floridan aquifer system at either coast are generally towards the coast. Water levels in the Floridan aquifer system along the coasts of both the Atlantic Ocean and Gulf of Mexico generally exceed sea level, except locally along the Atlantic coast where intense pumping occurs, so vertical gradients are generally directed upwardly. Remaining fresh groundwater within the surficial aquifer discharges at the coast. Along the Gulf coast, the Floridan aquifer system is generally unconfined, so the water remaining within it likely discharges within a very short distance of the coast, probably within 5 miles in most areas. Heavy confinement exists along the Atlantic coast of southeast Georgia and northeast Florida, between Savannah, Georgia, south to the Duval/St. Johns county line. The heavy confinement enables freshwater within the Floridan aquifer system to extend offshore for many miles, perhaps up to 50 miles along parts of this coast. South of the general area of St. Augustine, Florida, however, confinement lessens. This enables increasing dis-

charge to nearby offshore areas and water levels within the Floridan aquifer system decline markedly from St. Augustine, Florida, to areas south of it within the model domain. Crescent Beach Springs is located about two and a half miles offshore of Crescent Beach, Florida. The rate of discharge of this spring is unknown, but it creates a noticeable "boil" at the water surface. The decline in the water levels of the Floridan aquifer system from St. Augustine south parallels increasing concentrations of relict seawater in the same direction. Municipal water supplies obtained from the Floridan aquifer system in this area are mixed with freshwater obtained from the surficial aquifer system and/or subjected to treatment processes to reduce total dissolved concentrations to levels prescribed by drinking water standards.

GROUNDWATER SYSTEM

The domain of the NFSEG model includes large areas of both Florida and Georgia and a portion of South Carolina (Figure 2-1). Major aquifer systems in this area include the Floridan aquifer system and, where present, the intermediate confining unit and surficial aquifer system. The Southeastern Coastal Plain aquifer system underlies the entire area (Miller 1990; Figure 2-1), but its influence on flow in the Floridan aquifer system is only in the northern extent of the model domain, primarily north of the Gulf Trough. The following sections provide more detailed descriptions of these aquifer systems.

Surficial Aquifer System

The surficial aquifer system is the uppermost aquifer system within the domain of the NFSEG model. The surficial aquifer system occupies a large portion of the model domain (Miller 1990; Davis and Boniol, digital communication). The surficial aquifer system is unconfined generally and is comprised primarily of unconsolidated beds of sand, shelly sand, shell and clay of post-Miocene age (Miller 1986; Table 2-1).

In some areas, the surficial aquifer system is divided between an upper unconfined and lower semiconfined zone by beds of relatively low permeability. An example is the surficial aquifer system of Volusia County, Florida, where the surficial aquifer system is comprised of an upper unconfined zone consisting primarily of sand separated by clay or silt layers from a lower semiconfined zone consisting primarily of sand and shell (Phelps 1990).

Hydraulic Properties

Generalized regional maps of the hydraulic properties of the surficial aquifer system are not available, as the surficial aquifer system has been characterized in most cases on a localized basis or, in more recent modeling studies, on a subregional basis. The surficial aquifer system has been the subject of aquifer performance tests (e.g., Hayes 1981 and Annable et al. 1996). The transmissivity of the surficial aquifer system has been estimated as ranging from 1,000 to 10,000 square feet per day (ft^2/d) with a maximum range of 25,000 to 50,000 ft^2/d (Miller 1990).

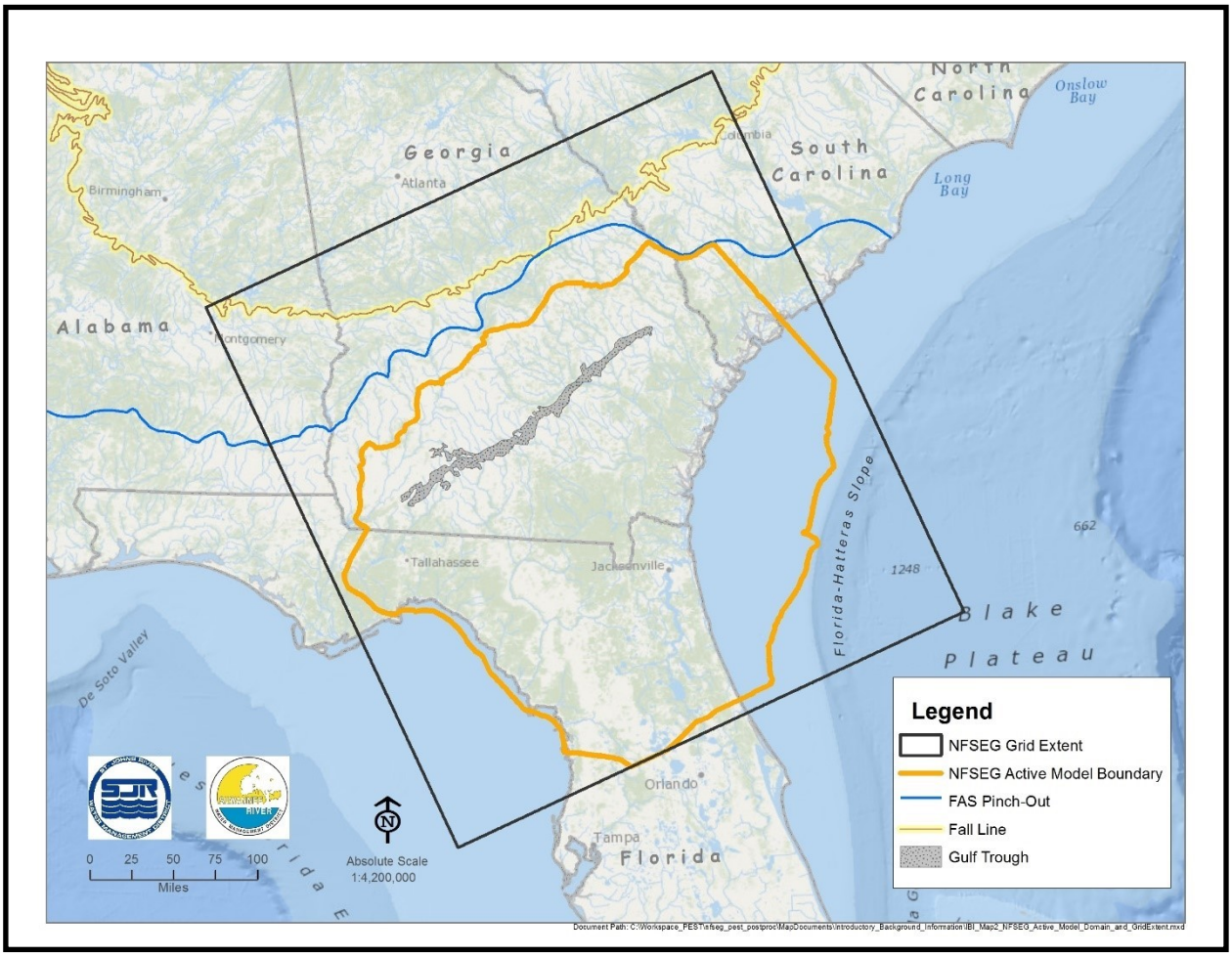

Figure 2-1. NFSEG maximum active model domain and grid extent

Table 2-1. Summary of groundwater hydrology system

<table>
<tr><th colspan="3">Downdip of Gulf Trough</th><th colspan="3">Updip of Gulf Trough</th></tr>
<tr><th>Series</th><th colspan="2">Hydrogeologic Unit</th><th>Series</th><th colspan="2">Hydrogeologic Unit</th></tr>
<tr><td>Post-Miocene</td><td colspan="2">Surficial Aquifer System</td><td>Post-Miocene</td><td colspan="2">Surficial Aquifer System[1]</td></tr>
<tr><td>Miocene</td><td colspan="2">Intermediate Aquifer System/Intermediate Confining Unit</td><td>Miocene</td><td colspan="2">Intermediate Aquifer System/Intermediate Confining Unit[1]</td></tr>
<tr><td>Oligocene</td><td rowspan="2">Upper Floridan Aquifer</td><td rowspan="6">Floridan Aquifer System</td><td>Oligocene</td><td colspan="2" rowspan="2">Upper Floridan Aquifer</td></tr>
<tr><td>Upper Eocene</td><td>Upper Eocene</td></tr>
<tr><td rowspan="2">Middle Eocene</td><td rowspan="2">Middle Semiconfining Unit; East: Lower Permeability; West: Higher Permeability or part of the transmissive system</td><td rowspan="2">Middle Eocene</td><td rowspan="3">Pearl River Aquifer</td><td rowspan="6">Southeastern Coastal Plain Aquifer System</td></tr>
<tr><td rowspan="2">Lower Floridan Aquifer (Upper Zone)</td></tr>
<tr><td rowspan="2">Lower Eocene</td><td rowspan="2">Lower Eocene</td></tr>
<tr><td>Lower Semiconfining Unit</td></tr>
<tr><td rowspan="2">Paleocene</td><td rowspan="2">Lower Floridan Aquifer (Fernandina Permeable Zone)</td><td rowspan="2">Paleocene</td><td>Chattahoochee River Aquifer Confining Unit</td></tr>
<tr><td rowspan="2">Upper Cretaceous</td><td colspan="2" rowspan="2">Sub-Floridan Confining Unit</td><td rowspan="2">Upper Cretaceous</td><td rowspan="2">Chattahoochee River Aquifer</td></tr>
</table>

*Where the middle confining unit is absent, the entire Floridan aquifer system is comprised of the Upper Floridan aquifer

In St. Johns County, Florida, estimates of the transmissivity of the lower permeable zone of the surficial aquifer system ranged from 6,500 to 7,000 ft^2/d (Hayes 1981). Other investigations resulted in values ranging from 1,300 ft^2/d to as high as 25,500 ft^2/d, the upper end value representing a shell bed of 60 feet or more in thickness (Spechler and Hampson 1984). In Volusia County, Florida, the transmissivity of the surficial aquifer system was determined to range from 100 to 9,300 ft^2/d (Phelps 1990).

An aquifer performance test at Halfmoon Lake in Putnam County, Florida, resulted in estimates of horizontal hydraulic conductivity that range as high as 62 feet/day (ft/d; Annable et al. 1996).

Structure

The top of the surficial aquifer system coincides with land surface (Figure 2-2). The bottom of the surficial aquifer system coincides with the top of the intermediate confining unit, where it is present (Miller 1990; Davis and Boniol, digital communication 2013; Figure 2-3). The thickness of the surficial aquifer system is generally less than 100 feet (ft; Miller 1990), but ranges upwardly to nearly 300 feet (e.g., areas near Brunswick, Georgia; Figure 2-4).

Water Levels

Generally, the water table of the surficial aquifer system is a subdued reflection of land surface (Miller 1986). Currently, a domain-wide map of the water table is not available, due to a lack of available water level data in many areas. Nevertheless, the water level of the surficial aquifer system is known at the locations of numerous monitoring wells within the model domain (Appendix A).

The water levels of the surficial aquifer system relative to those of the underlying Floridan aquifer system determine the direction of leakage to or from the Floridan aquifer system in semiconfined to confined regions of the Floridan aquifer system. Interactions of the surficial aquifer system with surface water bodies that are in hydraulic contact with it can influence the water levels of the surficial aquifer system to a large degree locally. Partly for this reason, the surficial aquifer system is generally not viewed as a regional flow system, despite its large extent within the model domain. Another factor in this is the potential for strong localized influences of the Floridan aquifer system in semiconfined regions of the Floridan aquifer system.

Intermediate Confining Unit

Throughout most of its extent, the Floridan aquifer system is overlain by middle Miocene age (i.e., Hawthorn Group) to post-Miocene age clay rich units, which function as the intermediate confining unit (Miller 1986; Bush and Johnston 1988; Table 2-1). Depending on location, the clays of the intermediate confining unit are interbedded with sand, shell and or carbonate lenses that are adequately extensive and permeable as to constitute aquifers of limited lateral and vertical extent (Miller 1986). Perhaps the most notable and well known of such aquifers is the Brunswick aquifer system in the Bruns-

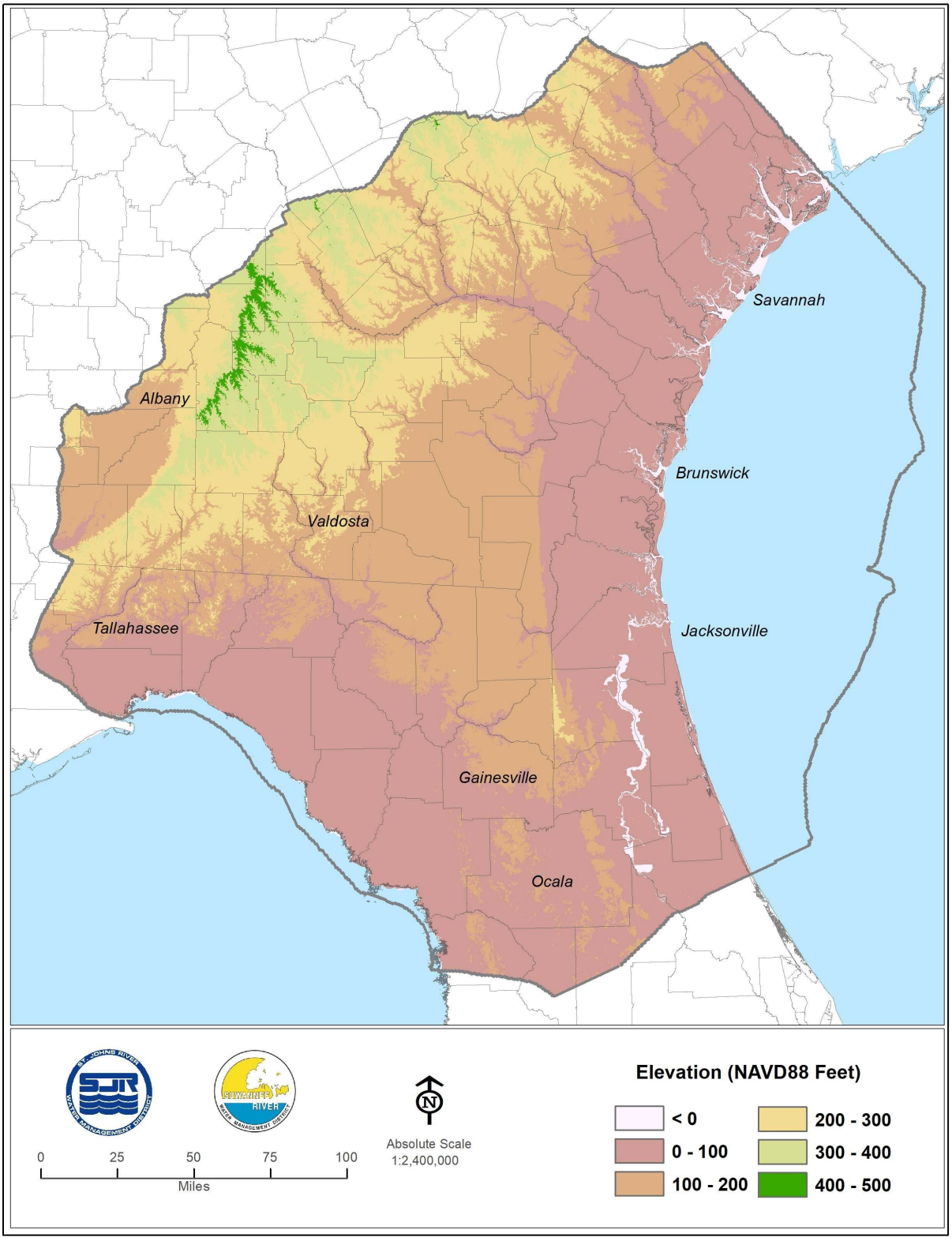

Figure 2-2. Land-surface elevation (and upper limit of the surficial aquifer system; based on USGS 3DEP 10-meter DEM, NAVD88 feet)

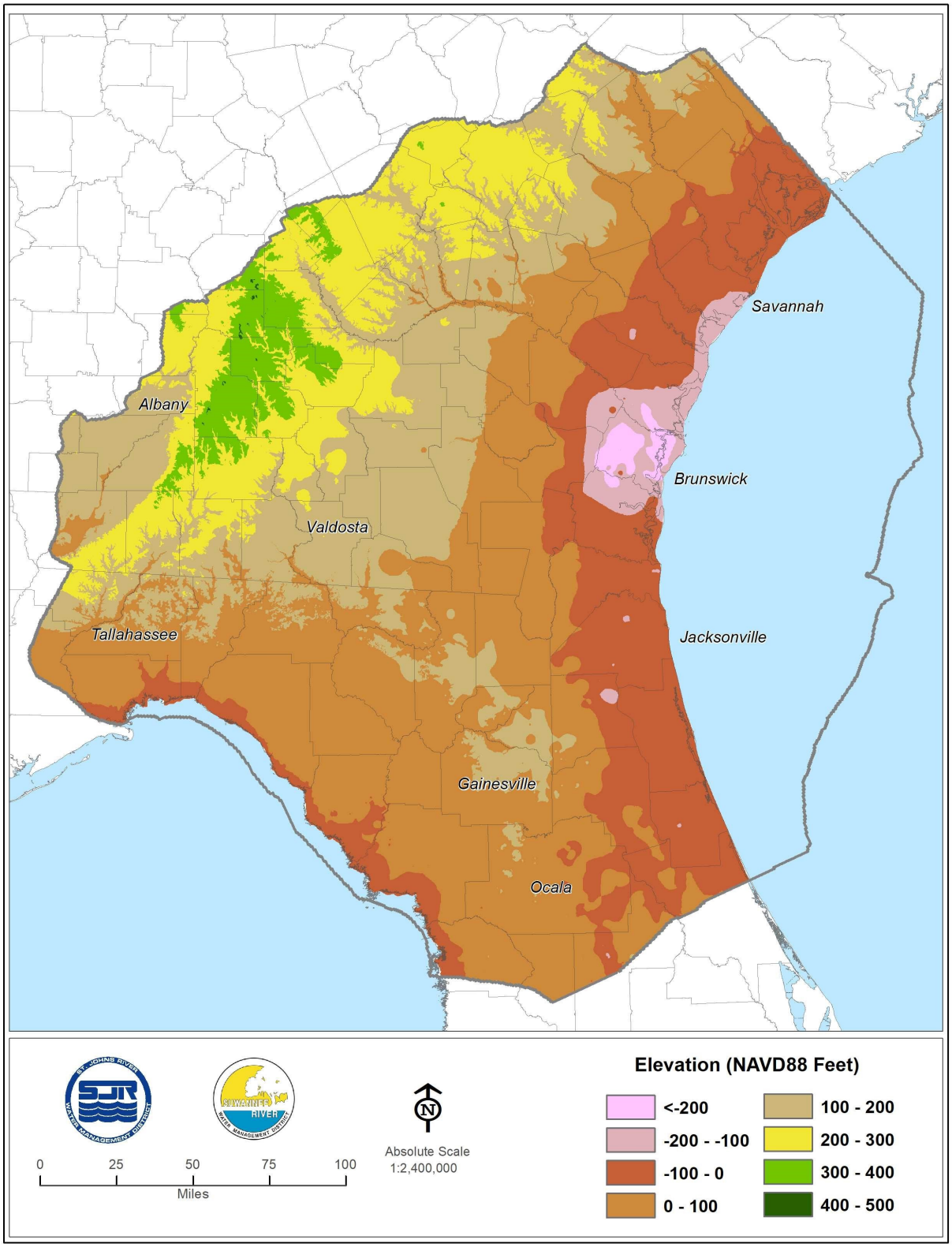

Figure 2-3. Bottom elevation of the surficial aquifer system (NAVD88 feet; after Davis and Boniol, digital communication 2013)

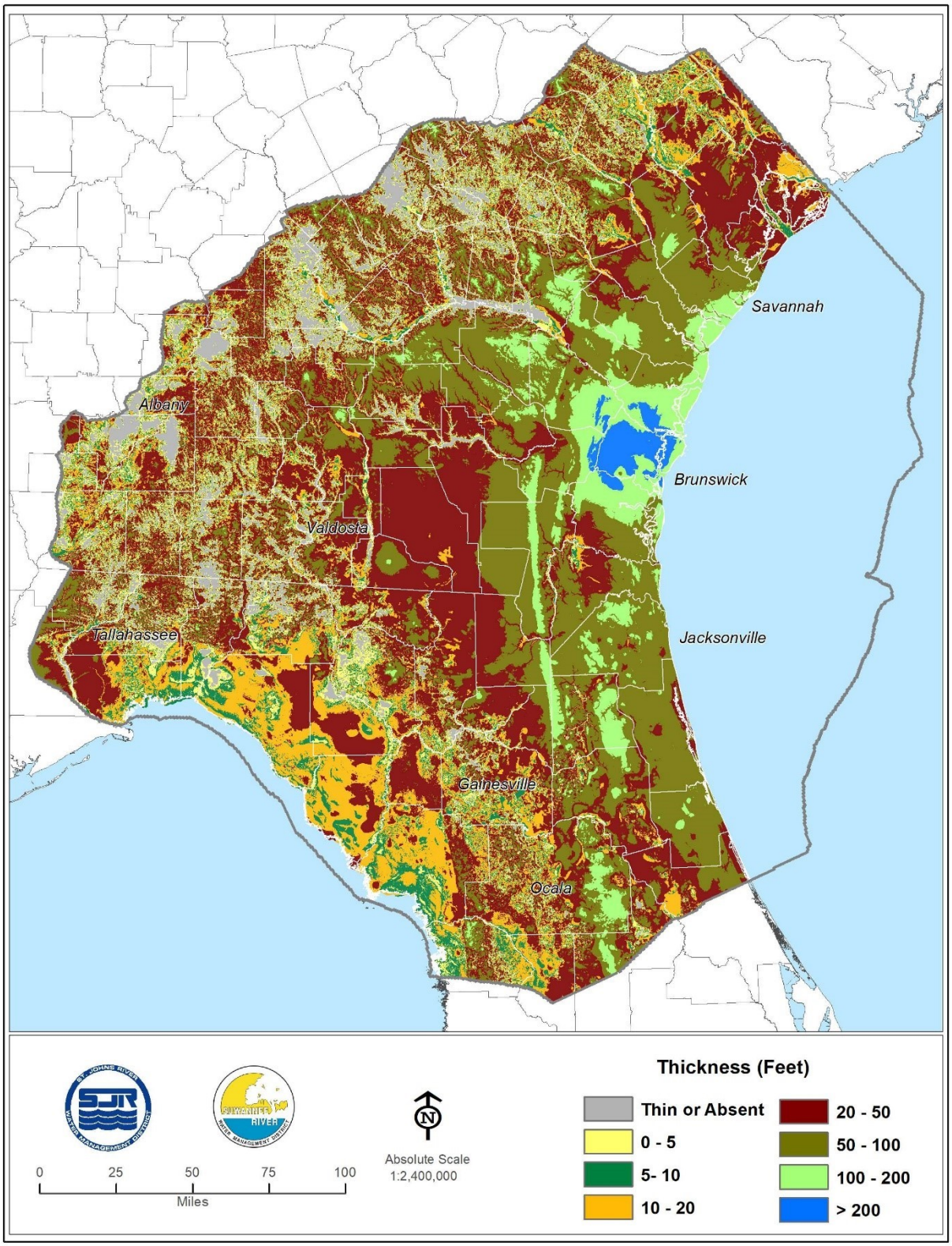

Figure 2-4. Thickness of the surficial aquifer system (SAS, feet; after Davis and Boniol, in progress)

wick area of southeast Georgia (Steele and McDowell 1998). Because of the presence of internal aquifers, the intermediate confining unit is often referred to alternatively as the intermediate aquifer system (Florida Geological Survey 1986).

The intermediate confining unit separates the underlying Floridan aquifer system from the overlying surficial aquifer system throughout a large portion of the NFSEG model domain. In some areas, the Floridan aquifer system is unconfined due to the absence of the intermediate confining unit. Examples are the area of the lower Suwannee River basin in the SRWMD and the Flint River basin of southwest Georgia (Bush and Johnston 1988). In other areas within the model domain, the intermediate confining unit is quite thick. In Duval and Nassau counties, Florida and Camden and Glynn counties, Georgia, for instance, its thickness is in the hundreds of feet.

A primary controlling factor on flow within the Floridan aquifer system is the degree to which it is confined by the intermediate confining unit. Conditions in this regard range from unconfined to heavily confined within the model domain, as mentioned previously. In confined areas, the leakance of the intermediate confining unit in conjunction with the water level difference between the underlying Floridan aquifer system and overlying surficial aquifer system determine the rate and direction of leakage to or from the Floridan aquifer system.

Diffuse recharge to the Floridan aquifer system in confined areas must first pass through the surficial aquifer system and intermediate confining unit. Of the amount that makes its way to the surficial aquifer system in confined areas, a smaller amount generally ends up in the Floridan aquifer system due to diversions incurred in the surficial aquifer system and intermediate confining unit. Additionally, surface water runoff is generally higher in confined areas, making less recharge available to the surficial aquifer system at the start. In unconfined areas, net recharge to the Floridan aquifer system is generally higher because diversions of potential recharge to the Floridan aquifer system are typically less. Surface water runoff, for instance, is often relatively small to nonexistent in unconfined areas. Potential diversions that occur in the surficial aquifer system and intermediate confining unit are not a factor, as recharge occurs directly to the Floridan aquifer system. In many unconfined areas with thick overburden above the Floridan aquifer system, rates of evapotranspiration are often relatively low because depth to water table (i.e., depth to the potentiometric surface of the Floridan aquifer system) is often relatively large.

Structure

The top of the intermediate confining unit (Davis and Boniol, digital communication 2013) coincides with the bottom of the surficial aquifer system, where the surficial aquifer system is present (Figure 2-5). The bottom of the intermediate confining unit coincides with the top of the Floridan aquifer system (Figure 2-6). Within the NFSEG model, the thickness of the intermediate confining unit ranges from 0 ft in areas in which the Floridan aquifer system is unconfined to more than 600 ft in parts of Georgia (Davis and Boniol, digital communication 2013; Figures 2-7).

In unconfined areas, discontinuous outliers of the intermediate confining unit are numerous and scattered throughout (Davis and Boniol, digital communication 2013; Figure 2-6), as are outliers of the surficial aquifer system (Davis and Boniol, digital com-

munication 2013; Figure 2-4). The complexity of occurrence of the surficial aquifer system and intermediate confining unit in unconfined regions of the model domain led to simplification of their respective representations in the NFSEG model, as will be discussed in a later section of this report.

In past studies (e.g., Miller 1990), the areal extent of the surficial aquifer system was represented as somewhat smaller than that of the intermediate confining unit, but much additional data have been collected and analyzed since then. Currently, a distinct line of pinch-out of the surficial aquifer system is difficult to specify. For the intermediate confining unit, this somewhat easier but still difficult. Current results (i.e., those of Davis and Boniol, digital communication 2013) indicate a much more complex distribution of the surficial aquifer system and intermediate confining unit sediments than representations of past studies (Figures 2-4 and 2-7).

Hydraulic Properties

The leakance of the intermediate confining unit has been estimated based on aquifer performance tests and the results of previous modeling studies (e.g., Bush and Johnston 1988). Estimates vary widely depending on location. However, leakance estimates are generally lower in areas of greater intermediate confining unit thickness. In areas in which the intermediate confining unit is thick, intermediate confining unit leakance may be on the order of 10^{-6} per day or lower (Bush and Johnston 1988; Figure 2-8). In areas in which the intermediate confining unit is thin, intermediate confining unit leakance may be on the order of 10^{-4} per day or higher (Bush and Johnston 1988; Figure 2-8). Locally higher leakance values, on the order of 10^{-3} to 10^{-2} per day occur beneath occur some of the karstic lakes in the Keystone Heights area and have been used to simulate leakage from these lakes to the subsurface (Merritt 2000). The clay content of the intermediate confining unit affects leakance also, with greater clay content tending towards lower leakance. In some areas, relatively thin but continuous clay layers can effectively confine the Floridan aquifer system (Bush and Johnston 1988).

The horizontal hydraulic conductivity of the intermediate confining unit is generally low, ranging between 10^{-6} to 10^{-2} ft/d in most areas, except in areas in which aquifers of significant size and permeability are present, such as the Brunswick aquifer system. Aquifer performance tests of the Lower Brunswick aquifer at Colonel's Island in Glynn County, Georgia, indicate transmissivities of 2,000 to 4,700 ft^2/d with corresponding hydraulic conductivities of 20 to 57 ft/d (Clarke et al. 1990).

Vertical Hydraulic Gradient

The water level difference across the intermediate confining unit, estimated as the difference in water level between the overlying surficial aquifer system and underlying Floridan aquifer system, is referred to herein as the intermediate confining unit vertical head difference. The ratio of the intermediate confining unit vertical head difference to the thickness of the intermediate confining unit approximates the vertical hydraulic gradient across the intermediate confining unit. The vertical hydraulic gradient can be indicative of the degree of confinement provided by the intermediate confining unit (Figures 2-9 and 2-10).

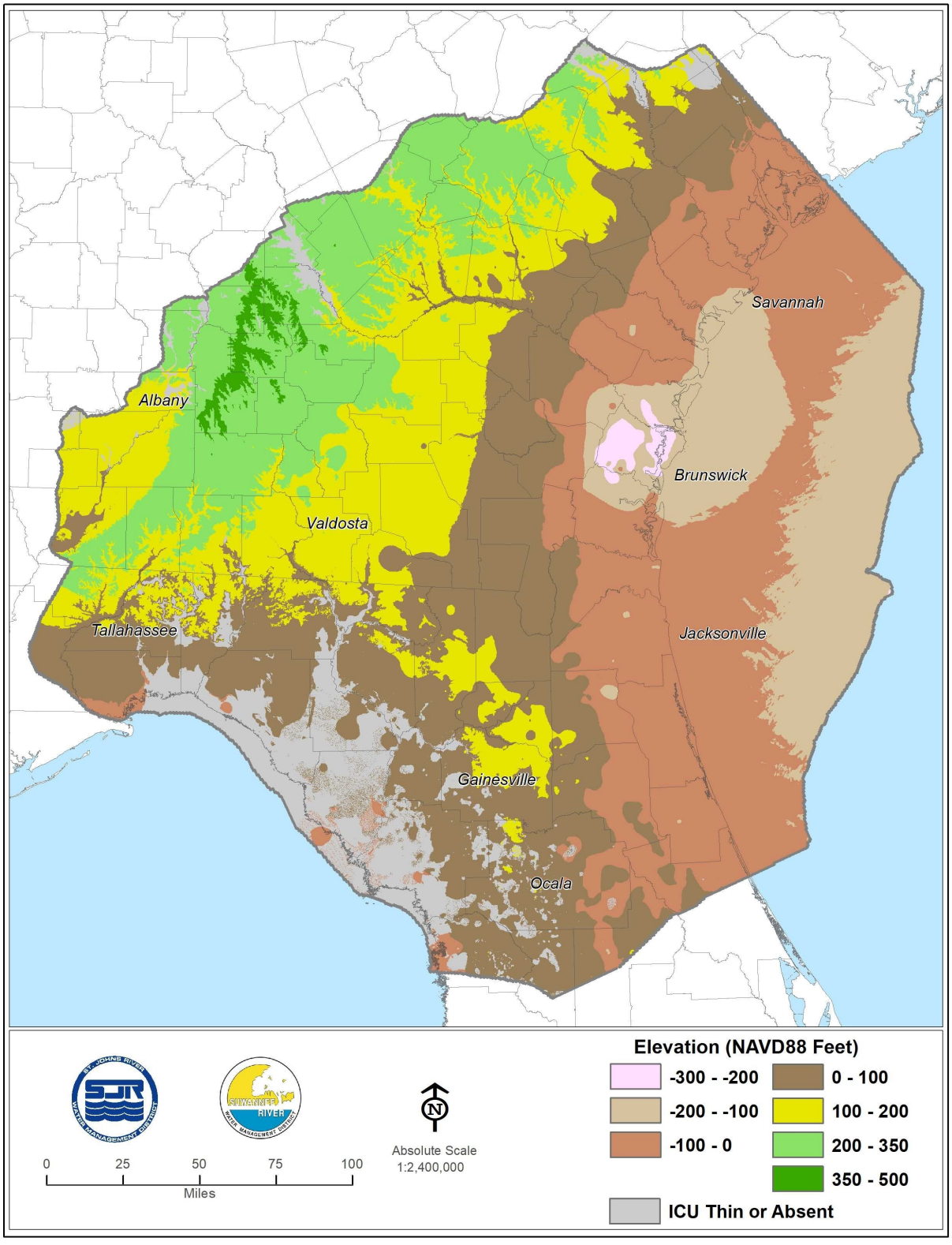

Figure 2-5. Top elevation of the intermediate confining unit (NAVD88 feet)

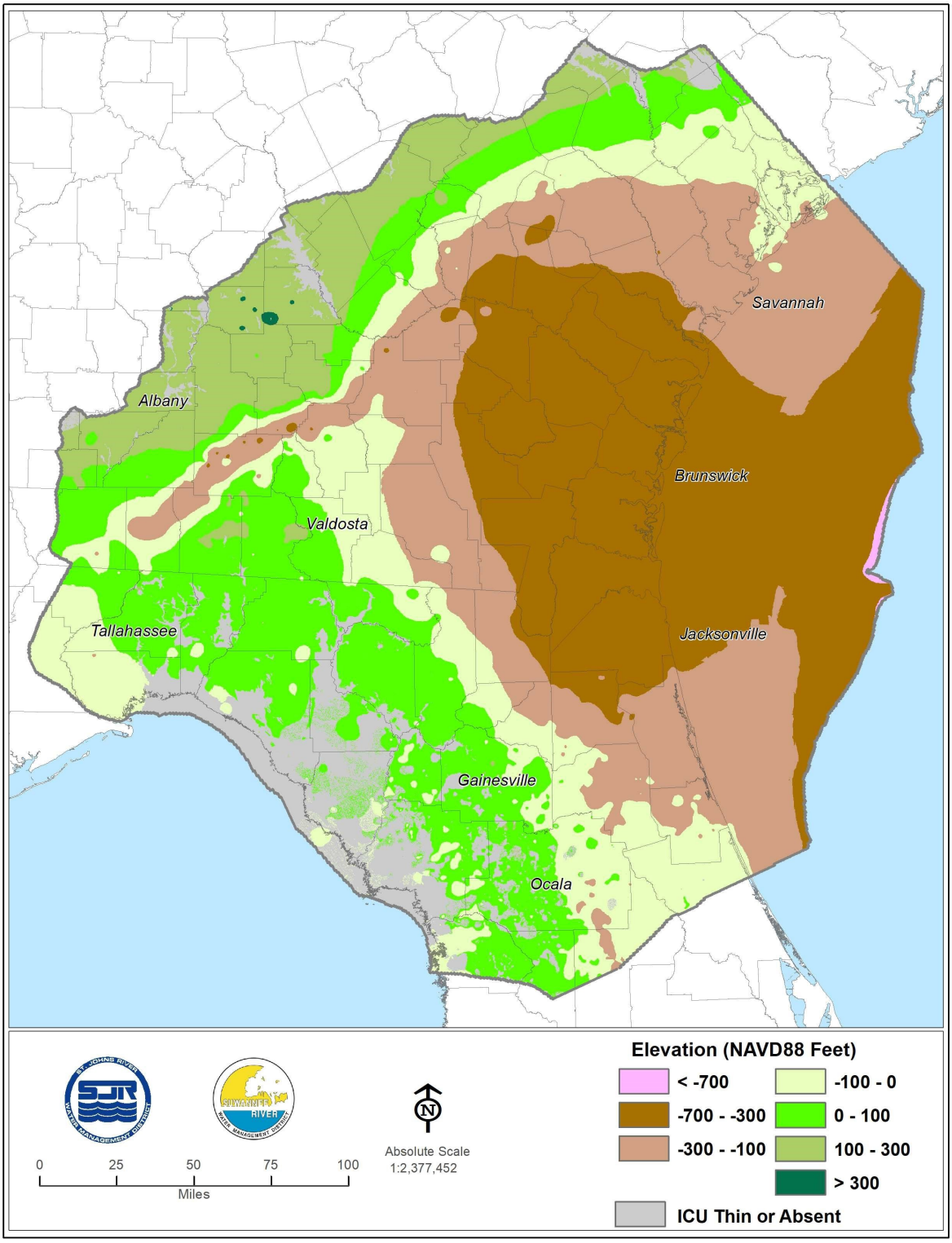

Figure 2-6. Bottom Elevation of the intermediate confining unit (and/or top of the upper Floridan aquifer; Feet NAVD88; after Davis and Boniol, digital communication 2013)

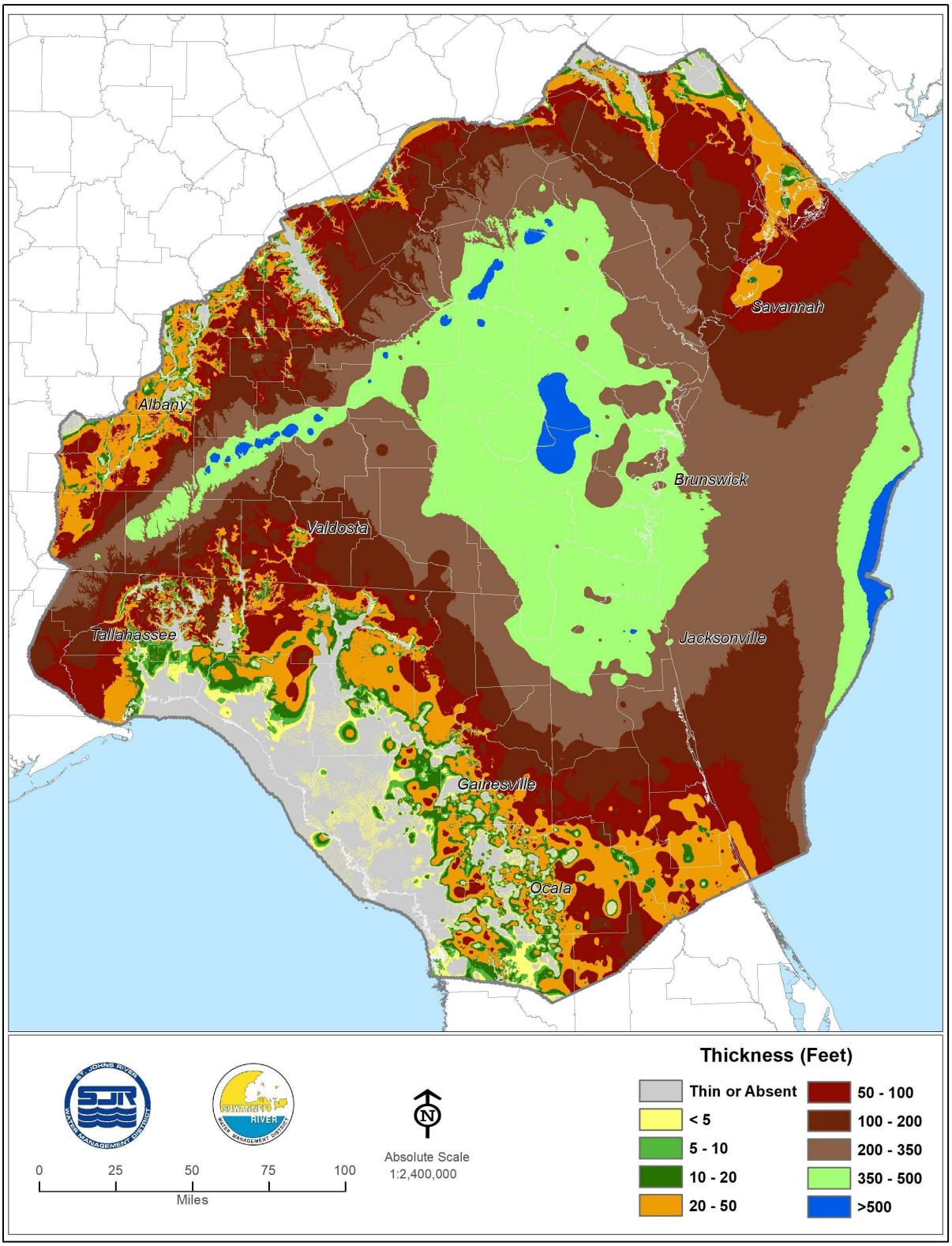

Figure 2-7. Thickness of the intermediate confining unit (feet; after Davis and Boniol, digital communication 2013)

Observations of the intermediate confining unit water level are sensitive to the position of the open interval of intermediate confining unit monitoring wells. For this reason, these observations were not utilized to the same degree as estimates of vertical head difference in the present study.

Floridan aquifer System

The Floridan aquifer system within the NFSEG model domain is comprised primarily of carbonate rocks of Upper Cretaceous to Early Miocene age (Table 2-1). The Floridan aquifer system underlies the entire state of Florida, southeastern Georgia and parts of Alabama and South Carolina (Miller 1990). In many areas, water within the Floridan aquifer system is brackish or saline (Miller 1990). However, the Floridan aquifer system is highly productive and has become an essential source of water wherever water quality permits (Miller 1990). In much of its extent, the Floridan aquifer system is comprised of an upper aquifer, the Upper Floridan aquifer and lower aquifer, the Lower Floridan aquifer (Miller 1986). The two aquifers are separated by a semi-confining unit referred to hereon as the middle confining unit. Regionally, the middle confining unit varies in lithologic composition and hydraulic characteristics and the degree of confinement of the middle confining unit can vary significantly (Miller 1986). Where the middle confining unit is not present, the Floridan aquifer system is a single aquifer, referred to as the Upper Floridan aquifer (Miller 1986). In northeast Florida and southeast Georgia, the Lower Floridan aquifer is further subdivided into an upper zone, referred to as the upper zone of the Lower Floridan aquifer herein and a lower zone, the Fernandina permeable zone (Miller 1986; Falls et al. 2005). The upper zone of the Lower Floridan aquifer is separated from the Fernandina permeable zone by a confining unit, referred to hereon as the lower semi-confining unit (Miller 1986; Falls et al. 2005; Table 2-1).

Gulf Trough

A geological feature that causes notable resistance to lateral flow within the Floridan aquifer system is the Gulf Trough in Georgia (Kellam and Gorday 1990; Figure 2-1), also known as the Suwannee Straits. The Gulf Trough is hypothesized as a system of fault-induced grabens into which lower permeability Miocene sediments have downdropped (Miller 1986). This feature is linear in shape and is oriented generally along a southwesterly-northeasterly alignment (Figure 2-1). The increased resistance to lateral flow within the Gulf Trough manifests in the form of bunched potentiometric contours along its length on maps of the potentiometric surface of the Floridan aquifer system (i.e., a linear feature characterized by high horizontal hydraulic gradients).

Southeastern Coastal Plain Aquifer System

The Southeastern Coastal Plain aquifer system within the NFSEG model domain is comprised of several regionally mapped aquifers, including from top to bottom, the Pearl River aquifer, the Chattahoochee River aquifer and the Black Warrior River aquifer, separated by regionally extensive confining units (Barker and Pernik 1994; Renken 1996; Figure 2-11; Table 2-1). The thickness of the Southeastern Coastal Plain aquifer

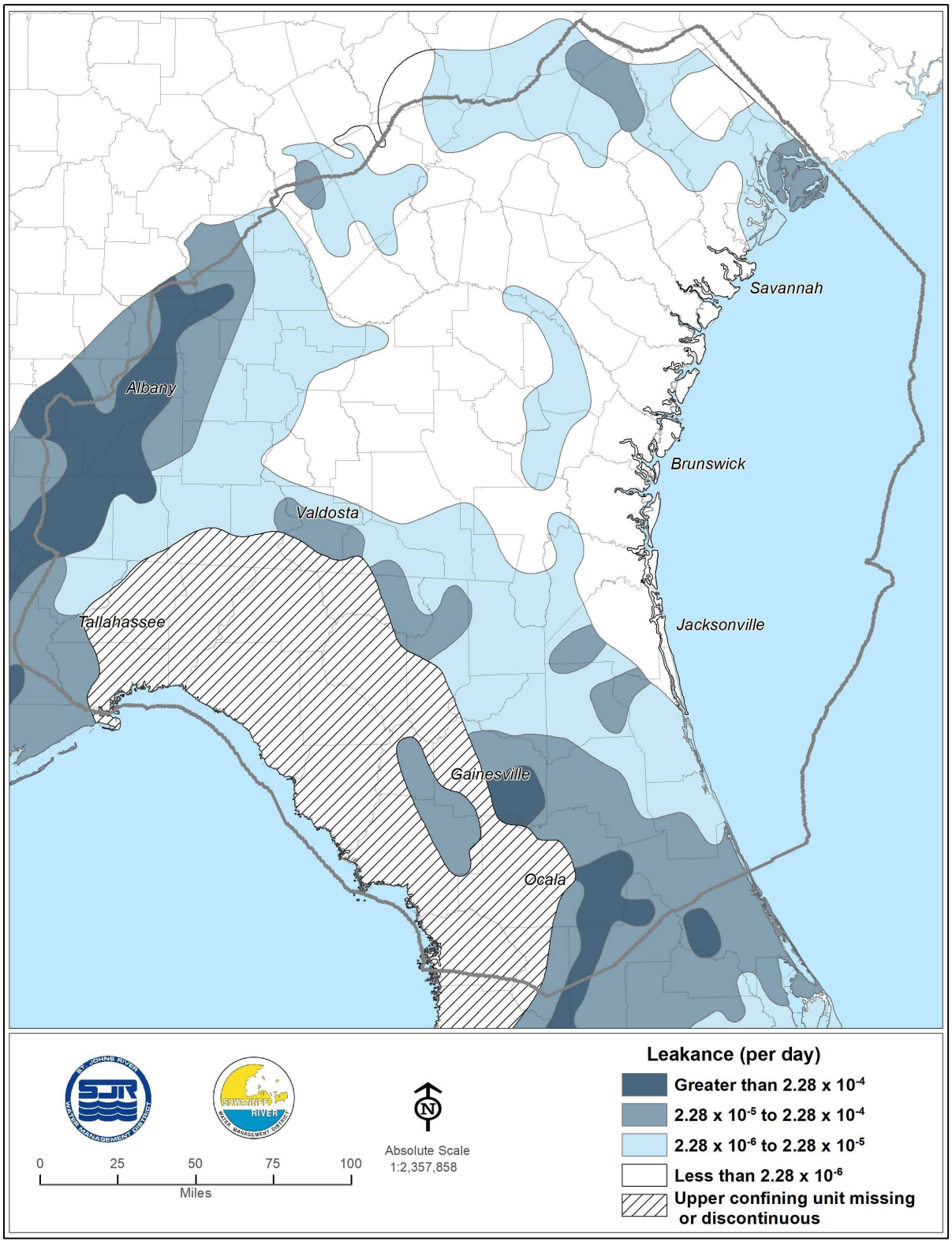

Figure 2-8. Estimated leakance distribution of the intermediate confining unit (ICU, per day; after Bush and Johnston 1988)

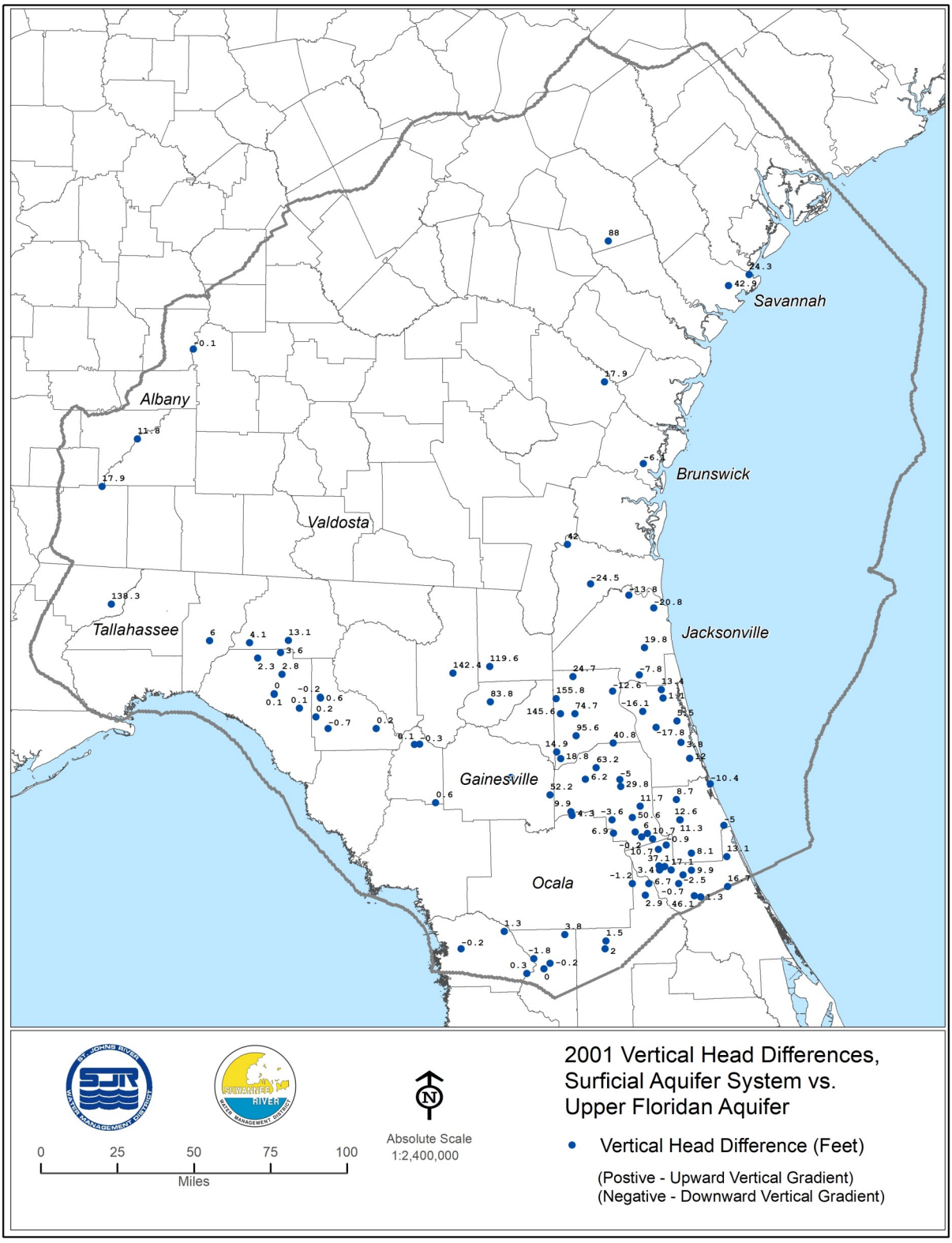

Figure 2-9. Intermediate confining unit vertical head difference, 2001 (feet)

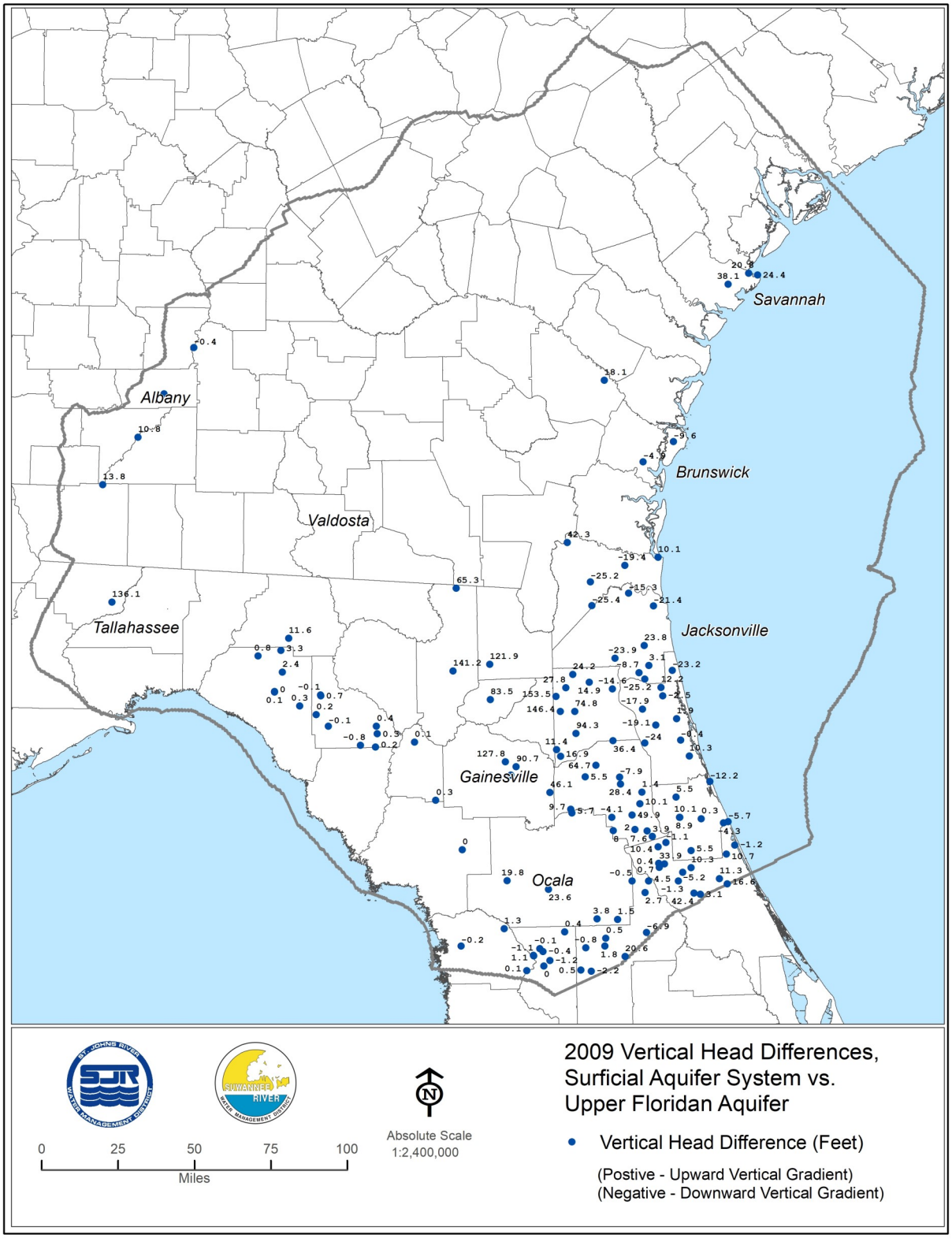

Figure 2-10. Intermediate confining unit vertical head difference, 2009 (feet)

system increases from its line of pinch-out, the Fall Line, towards the Gulf of Mexico and the Atlantic Ocean. The clastic rocks of the Southeastern Coastal Plain aquifer system grade both laterally and vertically into the carbonate rocks of the Floridan aquifer system in western South Carolina, southern Georgia and southeastern Alabama, resulting in a direct hydraulic connection between the two aquifer systems at such boundaries (Barker and Pernik 1994). Downgradient of such boundaries, the hydraulic connection between the Southeastern Coastal Plain aquifer system and the Floridan aquifer system manifests in the form of diffuse leakage across the semi-confining units that separate the Southeastern Coastal Plain aquifer system from the overlying Floridan aquifer system (McFadden and Perriello 1983). Although leakage between the Floridan aquifer system and Southeastern Coastal Plain aquifer system occurs, the amounts represent a relatively small proportion of the total flux of the Floridan aquifer system (Barker and Pernik 1994).

The Pearl River aquifer is the Southeastern Coastal Plain aquifer system equivalent of the Lower Floridan aquifer and the two aquifers are in direct hydraulic connection at their boundaries (Barker and Pernik 1994). In Georgia, the Pearl River aquifer is known subregionally as the Claiborne aquifer in its western area of occurrence and as the Gordon aquifer in its eastern area of occurrence (McFadden and Perriello 1983; Brooks et al. 1985; Long 1989; Lee et al. 1997). The Pearl River aquifer and Lower Floridan aquifer are treated as a single aquifer in the present study, consistent with previous groundwater modeling studies of the Floridan aquifer system that encompass parts of Georgia and Florida (e.g., Krause and Randolph 1989 and Payne et al. 2005).

Structure

A complicating factor related to the stratigraphy of the Floridan aquifer system involves the presence of saline water within the Floridan aquifer system. The onset of saline water is determined herein by comparison to a surface that represents the approximate onset of groundwater within the Floridan aquifer system of total dissolved solids (TDS) concentration greater than 10,000 milligrams per liter (mg/l; Williams, digital communication 2013; Figure 2-12). Groundwater below this surface is treated as being outside the zone of freshwater flow. The presence of saline water limits the lateral and vertical extents of the model representations of all aquifers and semi-confining units comprising the Floridan aquifer system within the NFSEG model domain, as the model is limited in representation to the freshwater flow system.

The maps shown herein are limited to the respective estimated lateral and vertical extents of freshwater flow within the various subject hydrogeologic units. This means that where the estimated onset of saline water is above the bottom of a unit, the "bottom" of the unit as shown is the estimated elevation of the onset of saline water. Where the estimated onset of saline water is below the bottom, then the bottom as shown is an estimate of the elevation of the actual bottom. A sparsity of data regarding the hydrostratigraphic extents of the Fernandina permeable zone and its overlying semi-confining unit does not enable an alternative representation regarding these two units. More details regarding the process of mapping these two units is provided below.

The accuracy of the maps lessens with increasing distance from the Atlantic coast, due to sparsity of data. The representation of the surficial aquifer and intermediate confin-

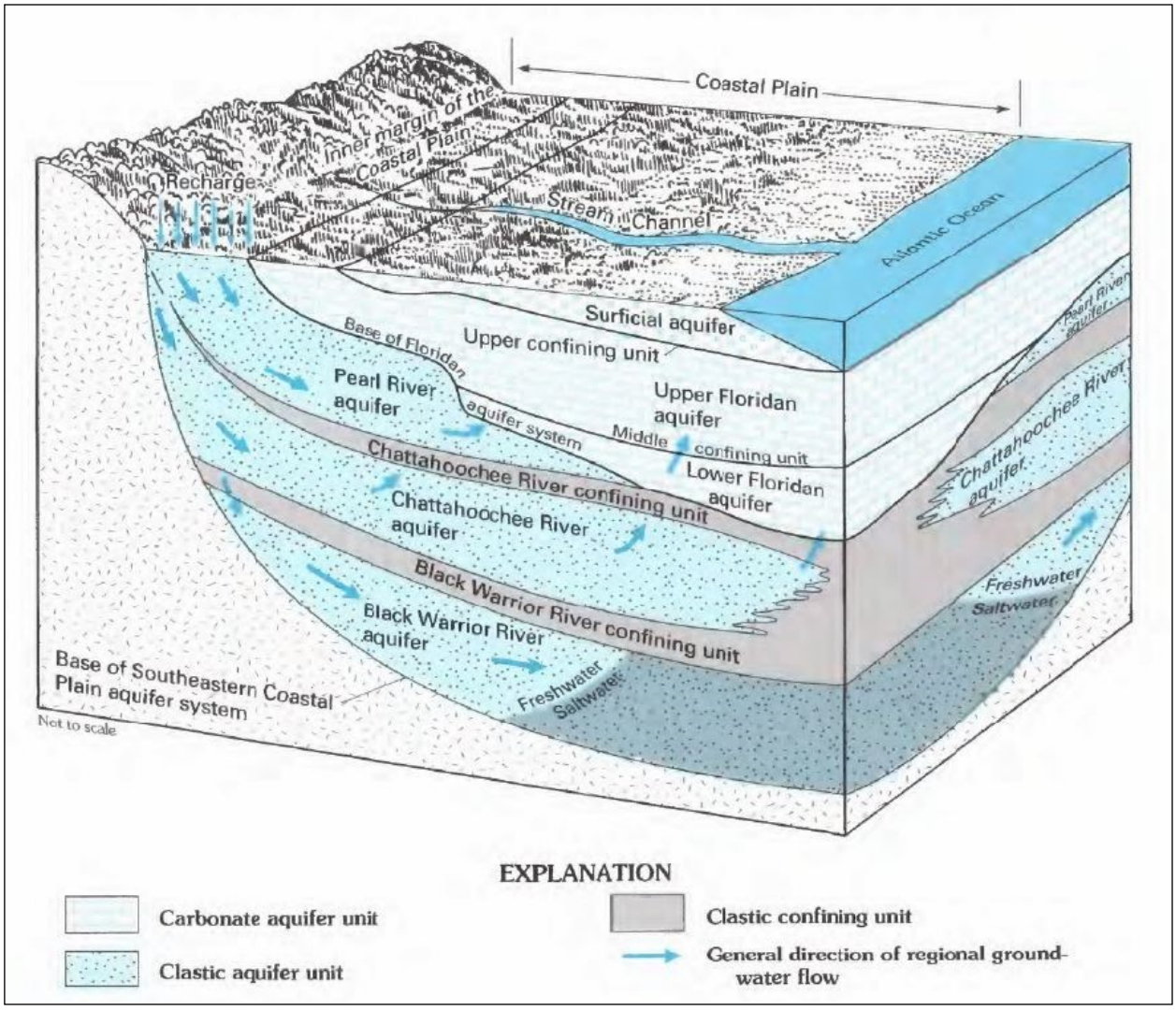

Figure 2-11. Hydrogeologic relation between the Floridan aquifer system and the Southeastern Coastal Plain aquifer system along a hypothetical dip section in Georgia (after Barker and Pernik 1994)

ing unit indicate a high level of complexity in their respective sediment distribution, contiguity and thickness, more so than can be represented in the NFSEG model. Comparisons of the maps of the surficial aquifer system and intermediate confining unit to maps of corresponding model layers indicates the degree of generalization that was implemented in the respective model representations. The maps of the hydrogeologic units of the Floridan aquifer system are nearly identical to those of the corresponding model layers.

Another complication is related to the discontinuous nature of the middle confining unit. Miller (1986) mapped four different middle confining units in the model domain (numbers 1, 2, 3 and 7). In more recent studies, the tops and bottoms of these units were found to coincide with the corresponding top and bottom of a marker unit, which is generally present throughout the model domain (Jeff Davis, personal communication), although data needed to characterize the hydraulic properties of this unit are not. Within the lateral extents of the middle confining units mapped by Miller (1986), this marker unit was interpreted, based on current geophysical and stratigraphic information, to represent the top and bottom elevations of the middle confining units.

In the regions that lie beyond the middle confining units of Miller (1986), the marker unit was used to vertically divide the Upper Floridan aquifer (i.e., the Floridan aquifer system in areas in which Miller ([1986] did not map middle confining units) into three separate (upper, middle and lower) layers. This vertical discretization of the Upper Floridan aquifer was facilitated by use of the marker unit to represent the middle confining units of Miller (1986) within their respective extents. It also allowed for continuity of model layering with areas where Miller (1986) had not mapped the presence of a middle confining unit, thus resulting in the definition of three continuous layers representing the Floridan aquifer system throughout the model domain, referred to hereafter as Zones 1, 2 and 3 in the present report (Table 2-2). Zone 1 is comprised only of the upper layer of the Upper Floridan aquifer in areas in which Miller (1986) did not map a middle confining unit and of the entire Upper Floridan aquifer elsewhere. Zone 2 is comprised only of the middle layer of the Upper Floridan aquifer in areas in which Miller (1986) did not map a middle confining unit and of the middle confining unit elsewhere. Zone 3 is comprised only of the lower layer of the Upper Floridan aquifer in areas in which Miller (1986) did not map a middle confining unit and of the Lower Floridan aquifer elsewhere. Within the extent of the Fernandina permeable zone, it includes only the upper zone of the Lower Floridan aquifer (i.e., the portion of the Lower Floridan aquifer that is above the lower semi-confining unit of the Fernandina permeable zone). The definition of Zones 1, 2 and 3 facilitated subsequent model development in a way that recognized more recent stratigraphic analyses, as well as uncertainties arising from a lack of hydraulic data to correlate with these analyses.

Upper Floridan aquifer

The top of the Upper Floridan aquifer ranges in elevation from less than -750 feet, North American Datum 1988 (ft NAVD88), in southeast Georgia to nearly 375 ft NAVD88 near the northern extent of the model domain (Davis and Boniol, digital communication 2013; Figure 2-6).

The bottom of Zone 1 ranges in elevation from approximately -1,000 ft NAVD88 in

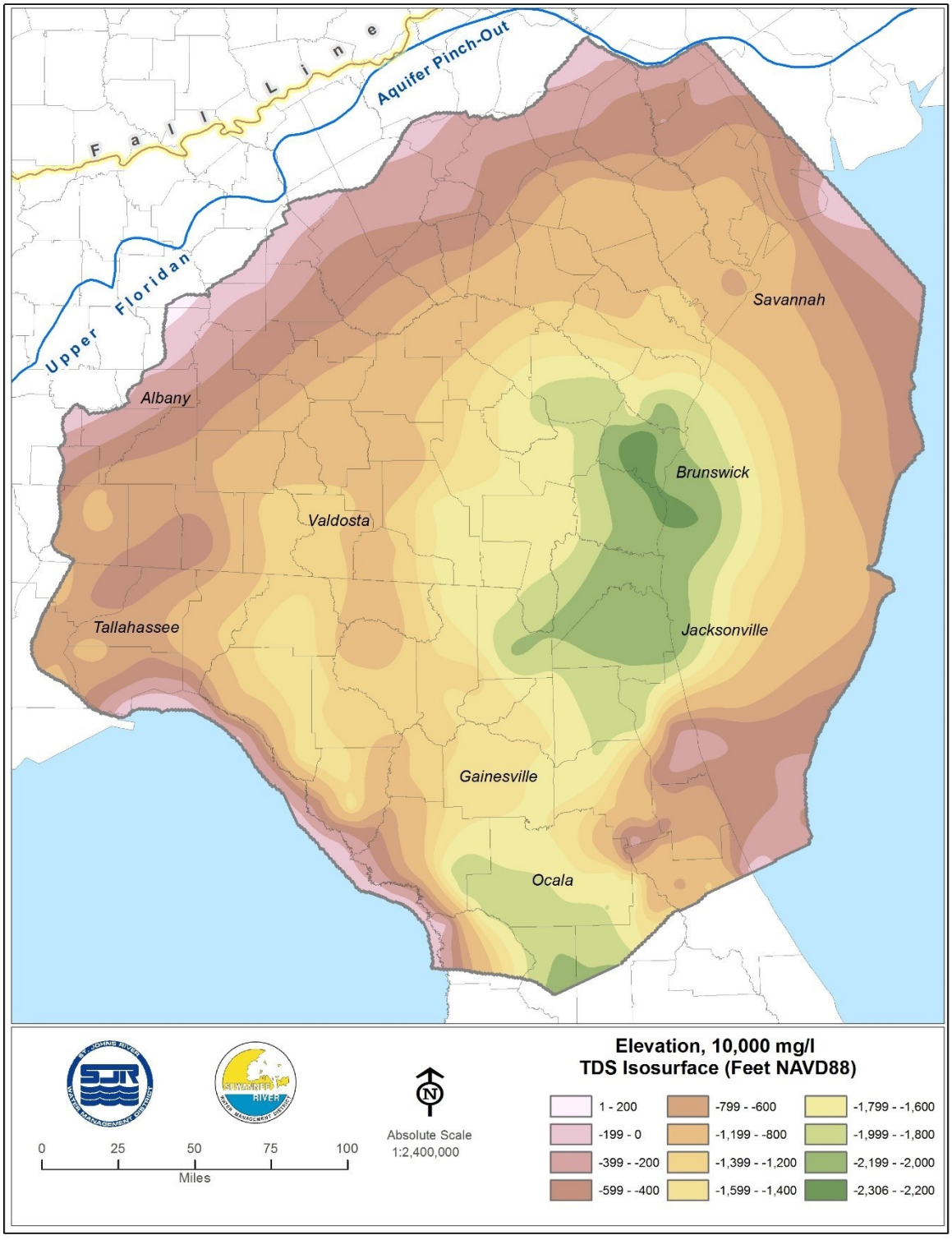

Figure 2-12. Elevation of 10,000 milligrams per liter (mg/l) total-dissolved-solids iso-surface (Williams, digital communication 2013)

southeast Georgia to approximately 225 ft NAVD88 near the northern extent of model domain (Davis and Boniol, digital communication 2013; Figure 2-13). The thickness of the Upper Floridan aquifer ranges from near 0 ft in outcrop areas of the northern extent of the model domain and in a limited area of the Gulf Trough in Georgia to nearly 1,000 ft in the northwest region of the model domain (Figure 2-14).

The top of Zone 2 coincides with the bottom of Zone 1 (Figure 2-13). The bottom of Zone 2 coincides with the top of Zone 3 (Figure 2-15). Onshore, it ranges in elevation from approximately -1,000 ft NAVD88 in southeast Georgia to approximately 500 ft NAVD88 near the northern extent of the model domain (Davis and Boniol, digital communication 2013). The thickness of Zone 2 ranges from less than 75 ft throughout numerous large areas of the NFSEG model domain to more than 700 ft in Marion County, Florida (Figure 2-16).

The bottom of Zone 3 ranges from -2,100 ft NAVD88 in Glynn County, Georgia, to more than 160 ft NAVD88 near the northern extent of the model domain (2-17). Where the lower semi-confining unit that lies atop the Fernandina permeable zone is present, the bottom of Zone 3 coincides with the estimated top of the lower semi-confining unit. The thickness of Zone 3 ranges from 0 to more than 1,500 ft within its freshwater extent (Figure 2-18).

The bottom of the Floridan aquifer system within the model domain ranges from approximately -2,300 ft NAVD88 in Glynn County, Georgia, to around 165 ft NAVD88 near the northern extent of the model domain (Figure 2-19). As with all other reported bottom elevations herein, these elevations refer to the elevation of the onset of saline water where the onset is above the estimated actual bottom of the Floridan aquifer system. This surface was based on data obtained from Williams (digital communication 2012) and partly on Miller (1986).

Lower Semi-confining Unit

The lateral extent of the lower semi-confining unit was not available to the present study via a previous study. Its western boundary was assumed to coincide with the western boundary of the Fernandina permeable zone as shown in Miller (1986). Its *freshwater* extent to the north and south and to the east beneath the Atlantic Ocean was determined by intersecting its estimated top and bottom surfaces with the estimated 10,000 milligrams per liter (mg/l) total dissolved solids (TDS) concentration iso-

Table 2-2. Summary of zones used to define the Floridan aquifer system

Areas Outside Limits of Miller (1986) Middle Confining Units	Areas Within Limits of Miller (1986) Middle Confining Units	Present Study
Upper Floridan aquifer – Upper Layer	Upper Floridan aquifer	Zone 1
Upper Floridan aquifer – Middle Layer	Middle Confining Unit	Zone 2
Upper Floridan aquifer – Lower Layer	Lower Floridan aquifer	Zone 3

surface of Williams, digital communication (2013; Figure 2-12). The discussion below regards the freshwater extent of the lower semi-confining unit.

The top of the lower semi-confining unit is based partly on thickness data of the lower semi-confining unit obtained from Miller (written communication 1991). A thickness layer was created in ArcGIS based on these data. The thickness layer incorporated the western extent of the Fernandina permeable zone as depicted by Miller (1986), along which the lower semi-confining unit thickness was assumed to be zero. The resulting thickness layer was intersected with the 10,000 mg/l TDS concentration iso-surface (Williams, digital communication 2013; Figure 2-12) to determine the freshwater extent of the lower semi-confining unit. The resulting freshwater thickness distribution of the lower semi-confining unit was then added to the top surface of the Fernandina permeable zone, described below, to obtain the top surface of the lower semi-confining unit (Figure 2-20). It is constrained to intersect with the bottom of the Floridan aquifer system along its western boundary, as is the bottom of the lower semi-confining unit and the top and bottom of the Fernandina permeable zone, which implies a coincident line of pinch-out of the lower semi-confining unit and Fernandina permeable zone along the western boundary. This treatment is consistent with the representation of the Fernandina permeable zone in Miller (1986). The top of the lower semi-confining unit, which coincides with the bottom of the upper zone of the Lower Floridan aquifer within its extent, ranges from about -1,300 ft NAVD88 in northeast Alachua County, Florida, to about -2,100 ft NAVD88 in Glynn County, Georgia to (Figure 2-20).

The bottom of the lower semi-confining unit coincides with the top of the Fernandina permeable zone within its area of extent. The top of the Fernandina permeable zone is described below. However, the extent of the lower semi-confining unit is different from that of the Fernandina permeable zone, so it is shown here as a separate map. Its elevations range from -2,200 ft NAVD88 to -1,400 ft NAVD88 (Figure 2-21).

The freshwater thickness of the lower semi-confining unit was estimated primarily on data obtained from Miller (written communication 1991) but also on other sources of information and assumptions, as noted above in the description of the lower semi-confining unit top. The freshwater thickness of the lower semi-confining unit ranges from zero to approximately 325 feet (Figure 2-22).

Fernandina Permeable Zone

The top of the Fernandina permeable zone was based primarily on Miller (1986) and Miller (written communication 1991; Figure 2-23). The surface is assumed to coincide with the bottom of the Floridan aquifer system along the western extent of the Fernandina permeable zone, where Miller (1986) indicated that the Fernandina permeable zone pinches out. Elsewhere, the freshwater extent of the top of the Fernandina permeable zone was determined by intersecting the top surface with the 10,000 mg/l TDS iso-surface of Williams, digital communication 2013; Figure 2-12). The resulting surface ranges in elevation from more than -2,000 ft NAVD88 in Glynn County, Georgia, to approximately -1,200 ft NAVD88 in northeastern Alachua County, Florida, (Figure 2-23).

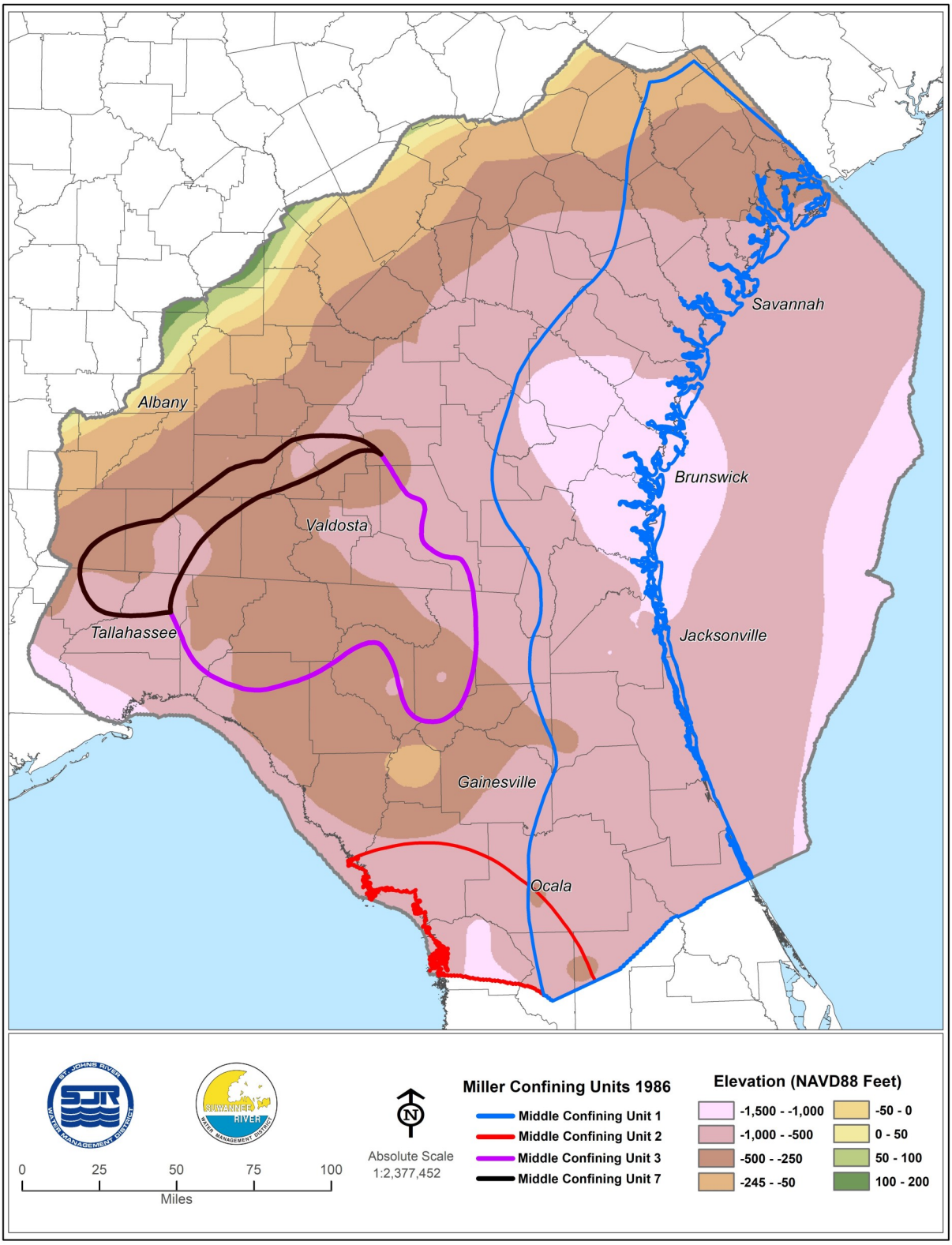

Figure 2-13. Bottom elevation of Zone 1 (and top elevation of Zone 2, feet NAVD88; after Davis and Boniol, digital communication 2013)

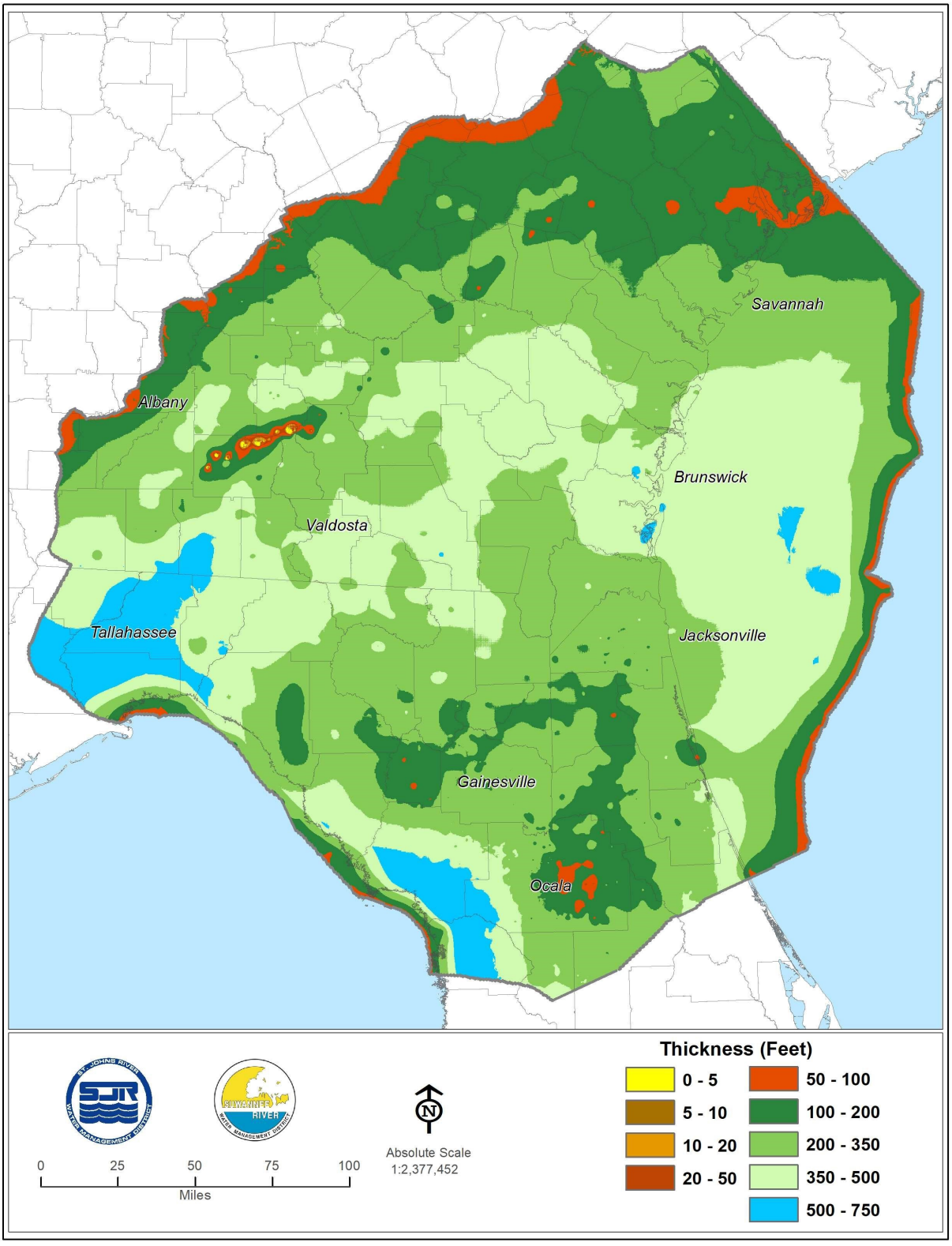

Figure 2-14. Thickness of Zone 1 (Feet; after Davis and Boniol, digital communication, 2013)

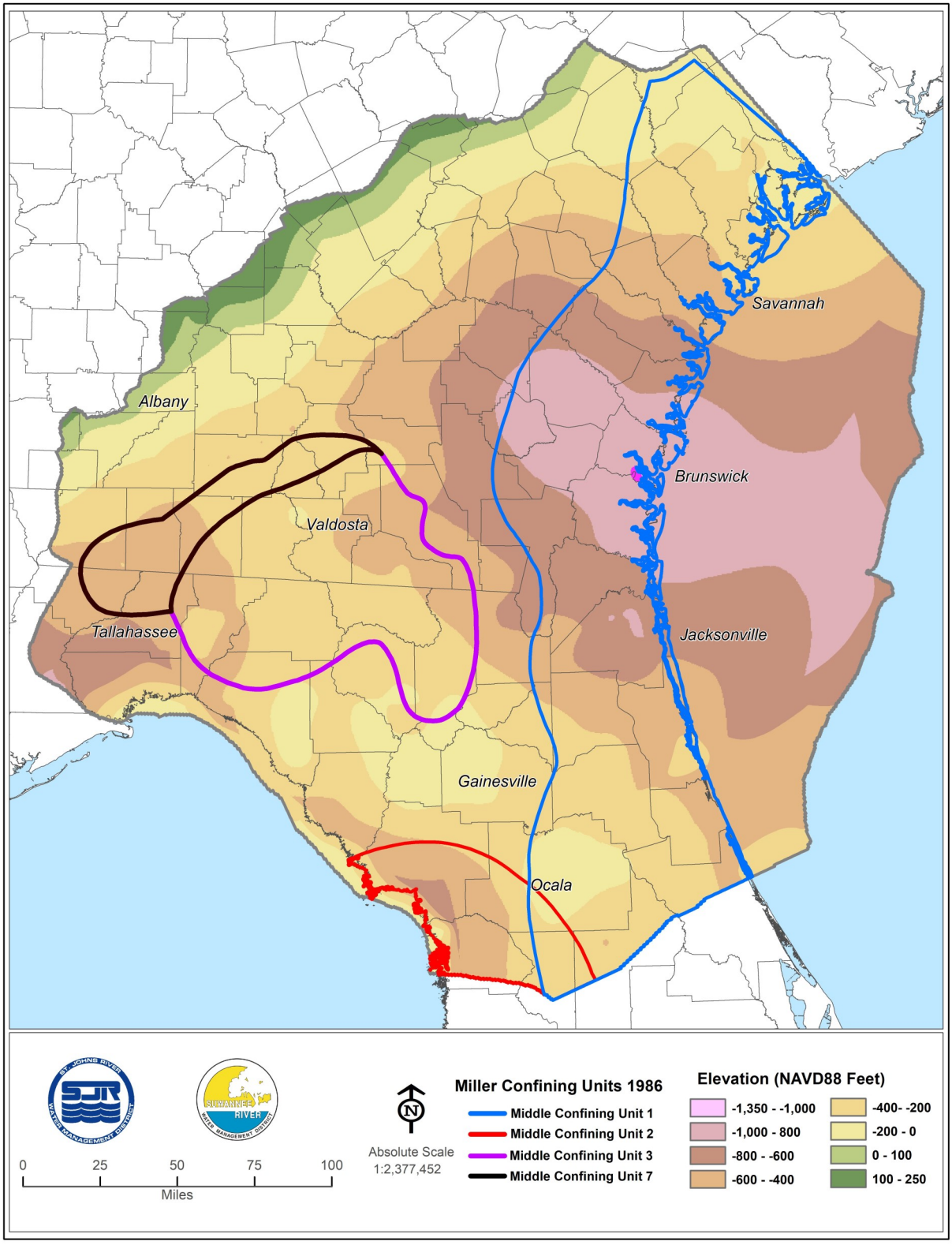

Figure 2-15. Bottom elevation Zone 2 (and top elevation of Zone 3, feet NAVD88; after Davis and Boniol, digital communication, 2013; and Williams, digital communication 2013)

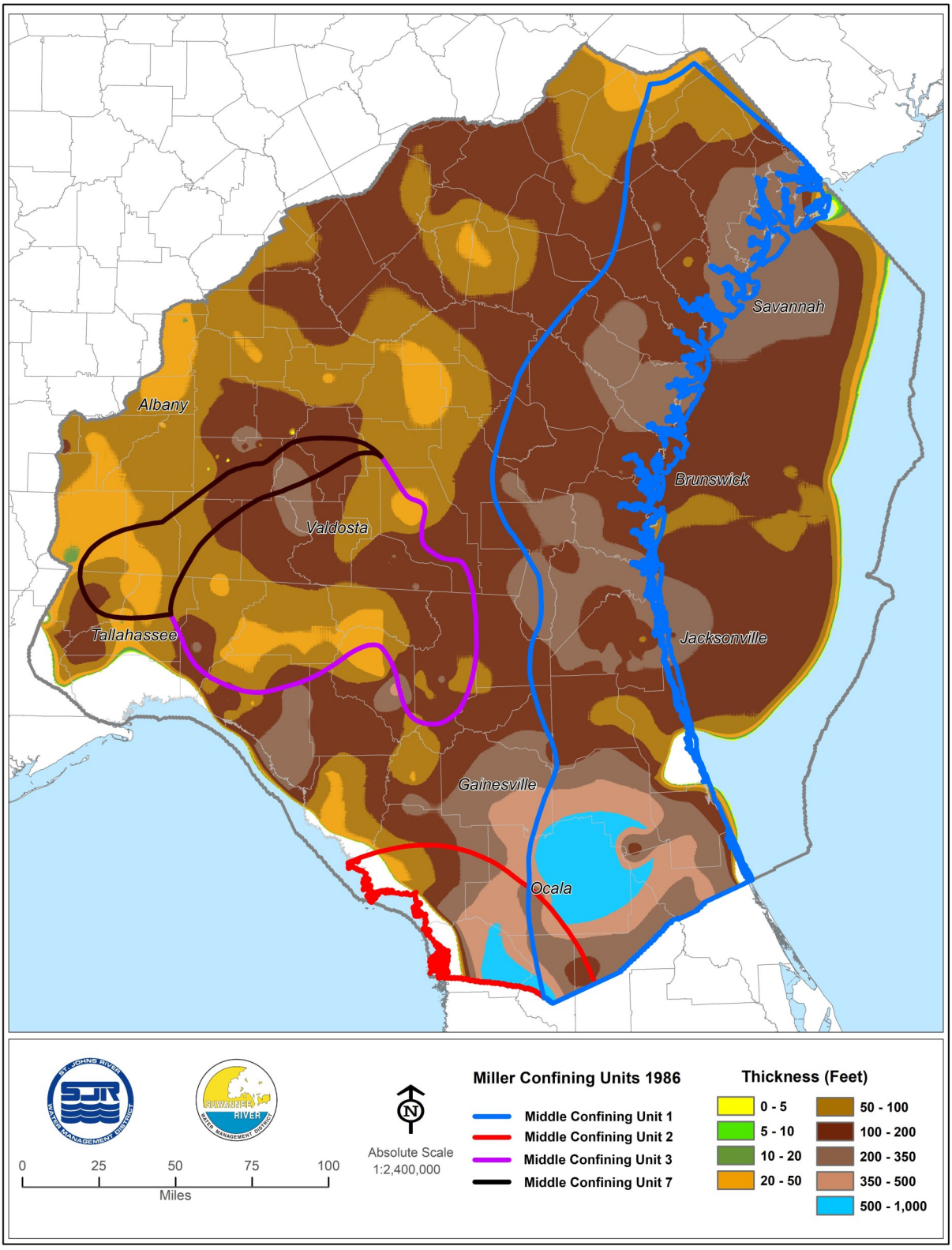

Figure 2-16. Thickness of Zone 2 (Feet; after Davis and Boniol, digital communication 2013; and Williams, digital communication 2013)

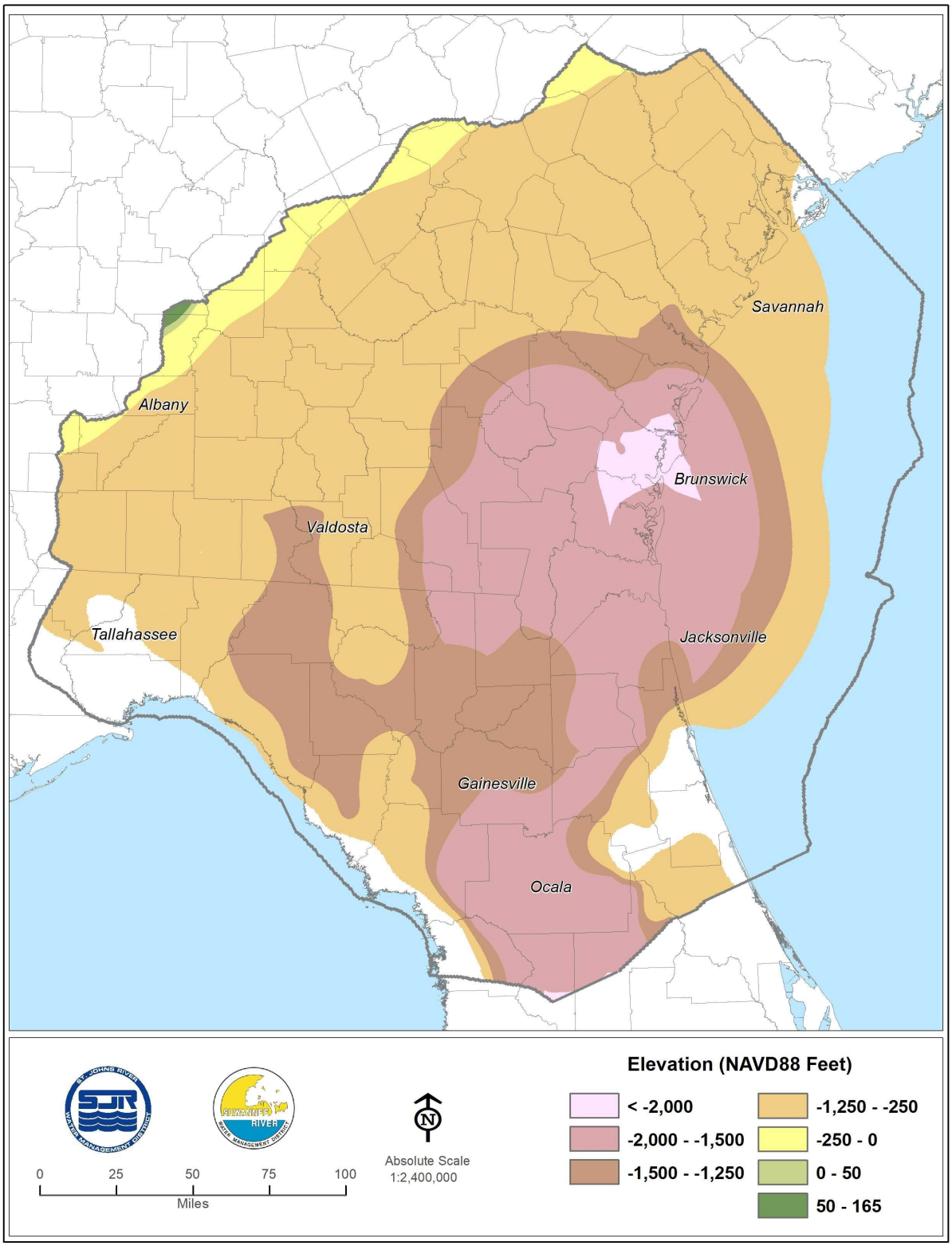

Figure 2-17. Bottom elevation of Zone 3 (Feet NAVD88; after Davis and Boniol, digital communication 2013; Miller, written communication 1991; and Williams, digital communication, 2013)

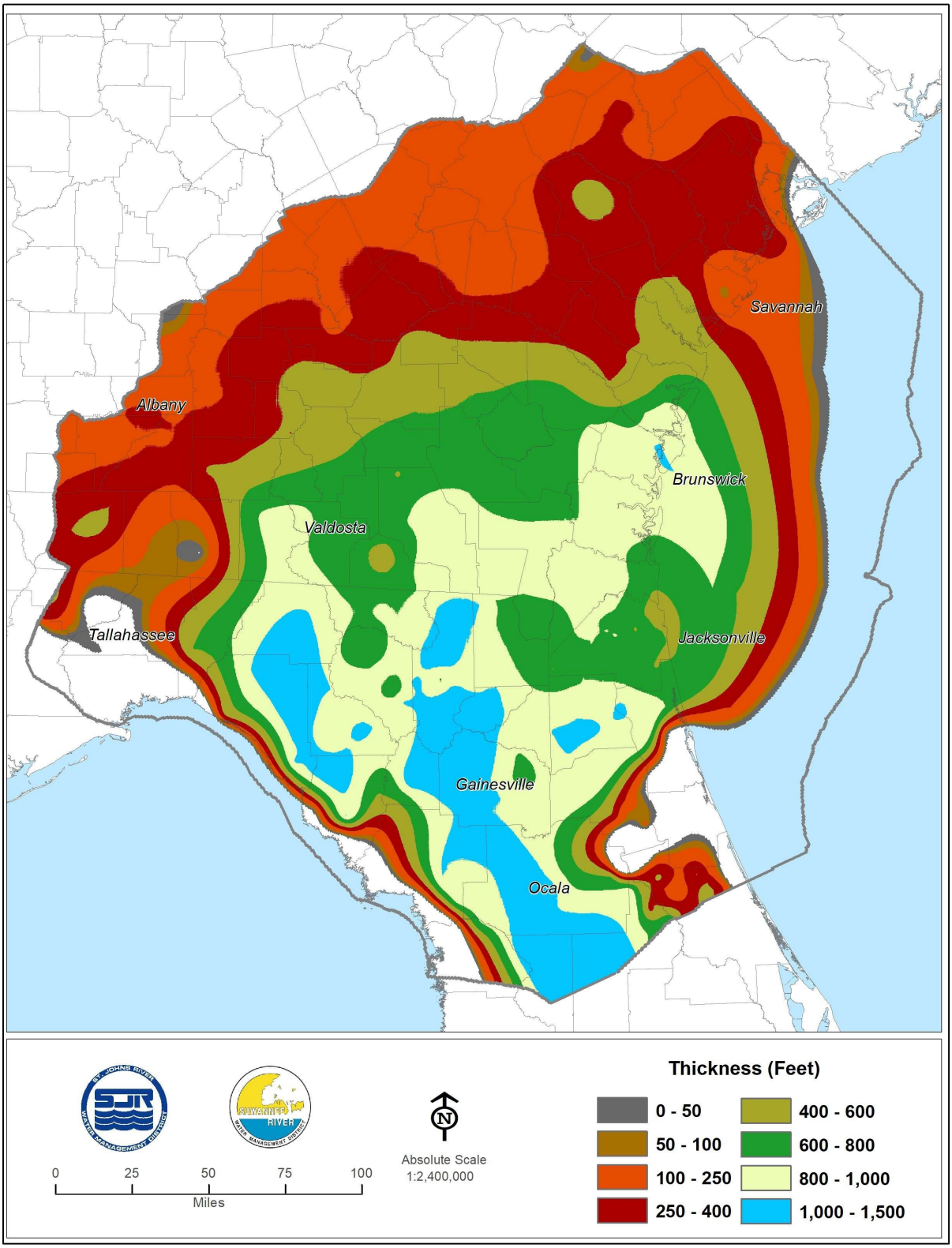

Figure 2-18. Thickness of Zone 3 (Feet; after Davis and Boniol, digital communication 2013; Miller, written communication 1991; and Williams, digital communication 2013)

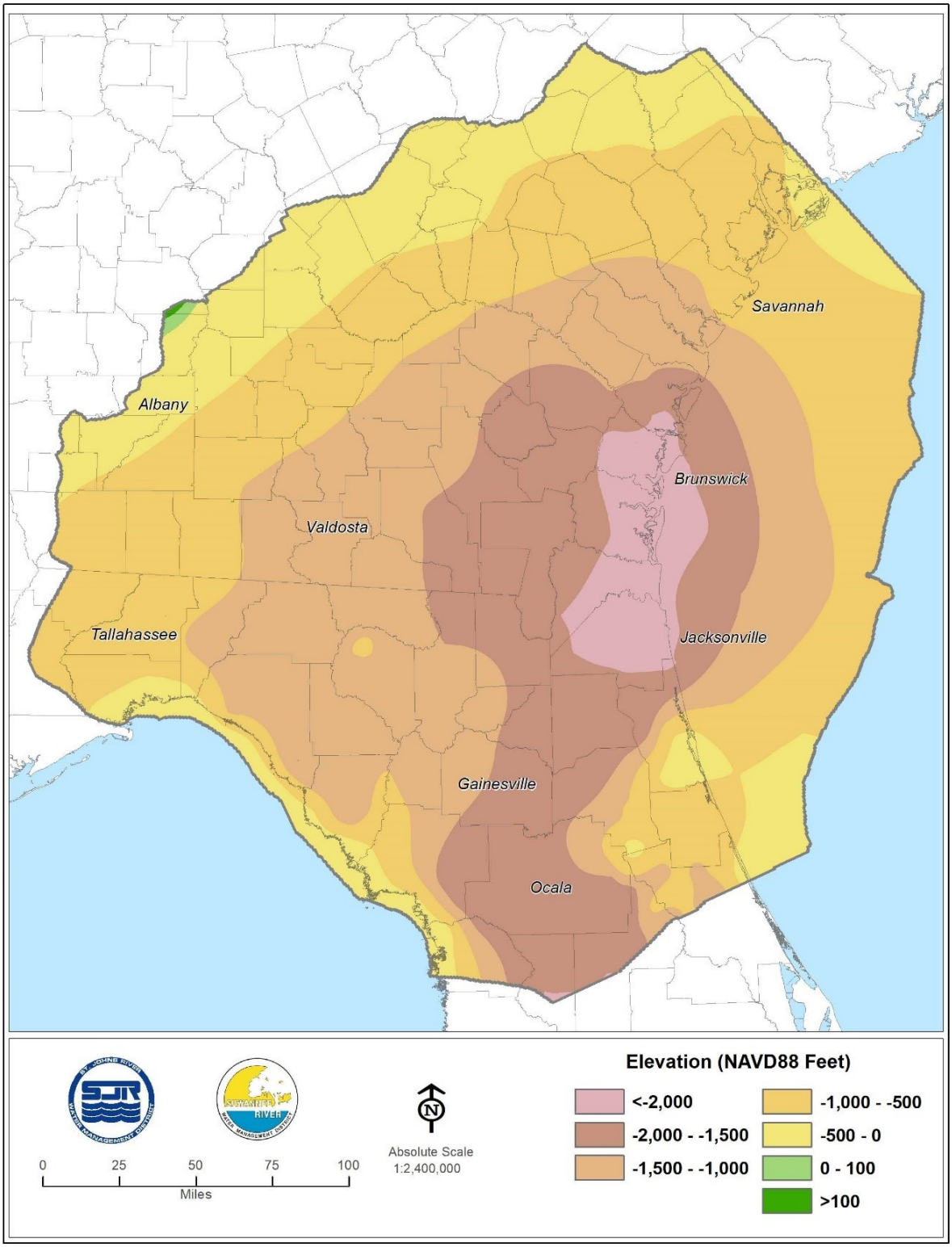

Figure 2-19. Bottom elevation of the Floridan aquifer system within its freshwater extent (after Miller 1986; Williams, digital communication 2012; and Williams, digital communication 2013)

The bottom of the Fernandina permeable zone coincides with the bottom of the Floridan aquifer system, described below. It ranges in elevation from approximately -2,300 ft NAVD88 in Glynn County, Georgia, to approximately -1,450 ft NAVD88 in northeastern Alachua County, Florida (Figure 2-24).

The freshwater thickness of the Fernandina permeable zone ranges from zero feet along its western boundary, a line of pinch-out, to approximately 450 ft in southeast Duval County, Florida (Figure 2-25).

Hydraulic Properties

Transmissivity of Zone 1

Estimates of the transmissivity of Zone 1 within the NFSEG model domain are based largely on aquifer performance tests (Figure 2-26) and the results of previous groundwater modeling studies (for example Johnston and others, 1988). Bush and Johnston (1988) mapped the transmissivity of the Upper Floridan aquifer. Their map shows low to moderate transmissivity along the corridor of and west of the Ochlockonee river in the Florida panhandle and into Georgia along the general path of the Gulf Trough (10,000 to 100,000 ft^2/d). Between the Aucilla and Ochlockonee rivers, the transmissivity is generally high (>1,000,000 ft^2/d). In the Suwannee River Basin, extending northeast into Georgia, transmissivity is moderately high (250,000 to 1,000,000 ft^2/d). In coastal areas of Georgia and northeast Florida, transmissivity is low to moderate (10,000 to 100,000 ft^2/d; Figure 2-27).

Using flow-net analysis, Faulkner (1973) determined the transmissivity of the Upper Floridan aquifer near Silver Springs to be greater than 1,000,000 ft^2/d in areas surrounding Silver Springs. The maximum transmissivity estimate resulting from the analysis was 25,500,000 ft^2/d. The average transmissivity over the entire flow net was 2,090,000 ft^2/d.

Kuniansky and others (2012) mapped the results of numerous aquifer performance tests of the Upper Floridan aquifer. Based on their map, the transmissivity of the Upper Floridan aquifer tends to be lower in east-central and northeast Florida and north and west of the Gulf Trough (< 50,000 ft^2/d generally) and higher in the unconfined areas of the Suwannee River basin and Gulf Coast (>50,000 ft^2/d). The areas of highest transmissivity are in southeast Georgia, parts of the Suwannee River basin and Silver and Rainbow springs basins (>100,000 ft^2/d; Kuniansky and others, 2012).

Leakance of the Middle Confining Unit

Other than results of modeling studies, the leakance of the middle confining unit is not well known in Florida. A recent aquifer performance test of the middle confining unit near Ocala, Florida, resulted in a leakance estimate of 1.05×10^{-2} per day (CDM Smith 2017). In Georgia, the vertical hydraulic conductivity of the middle confining unit in Brunswick is reported to be 4×10^{-6} ft/d (Clarke and others, 2004). At Savannah, Georgia, the vertical hydraulic conductivity is reported to be 6.7×10^{-4} ft/d (Clarke and others, 2004).

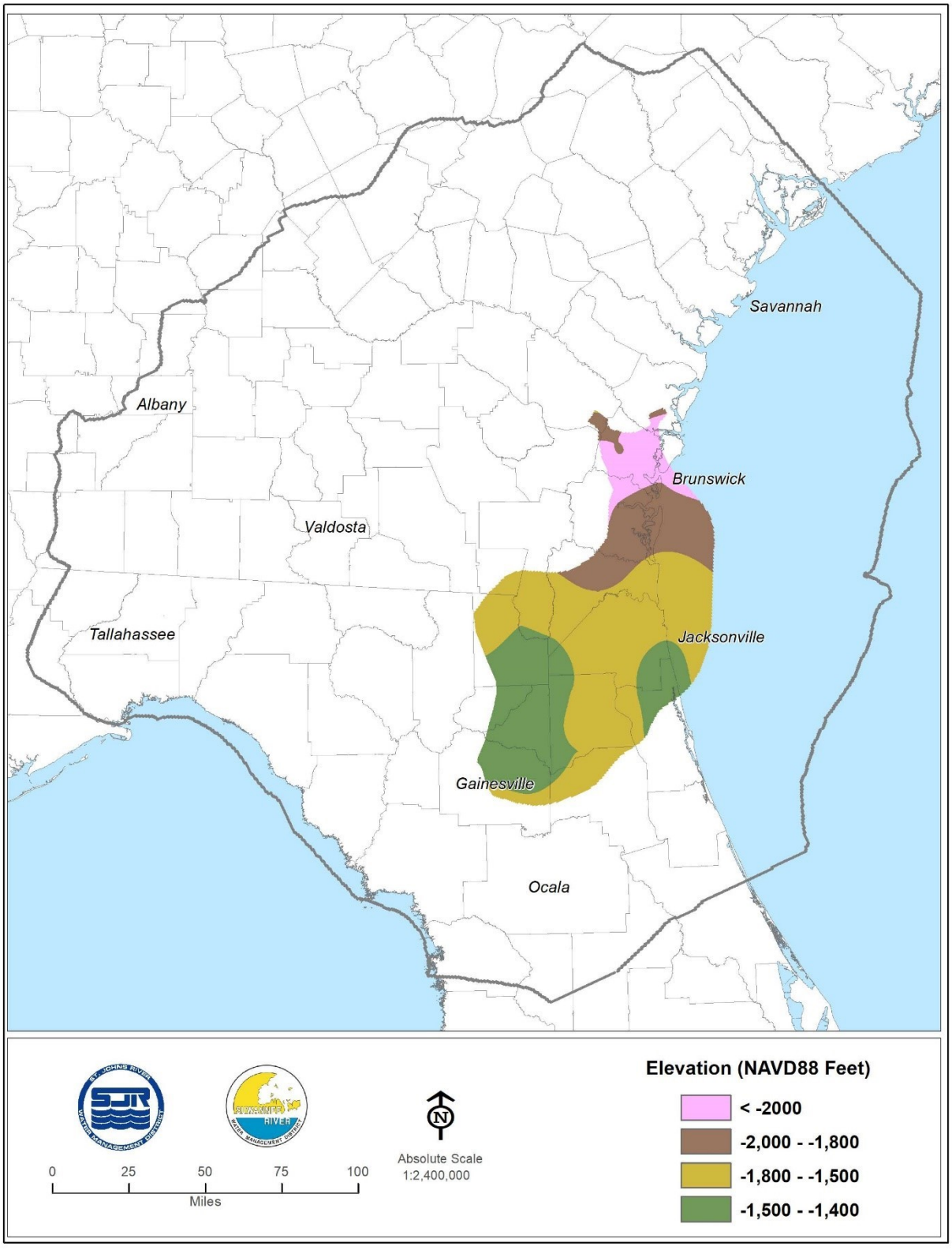

Figure 2-20. Top elevation of the lower semi-confining unit (NAVD88 Feet; after Miller 1986; Miller, written communication 1991; and Williams, digital communication 2013)

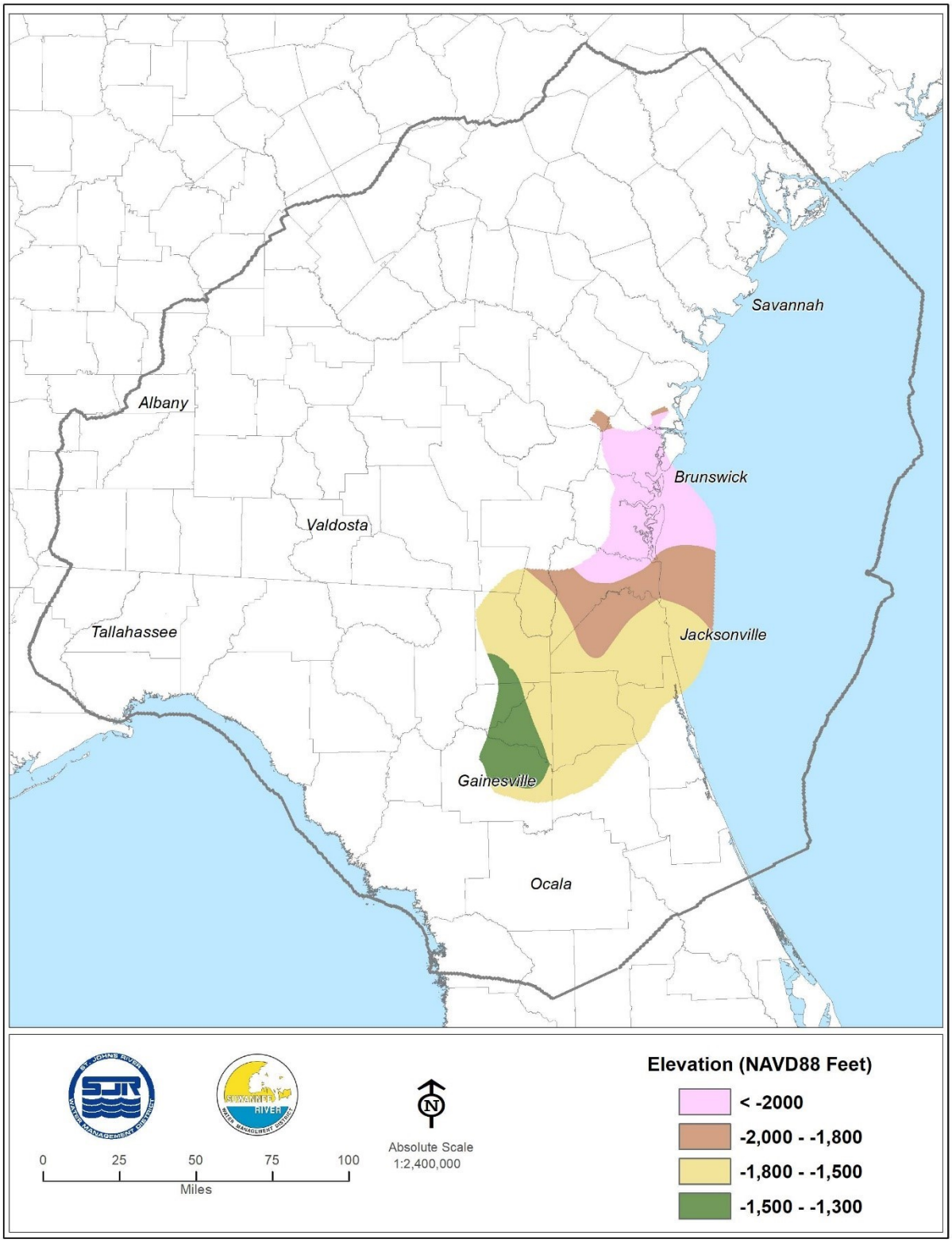

Figure 2-21. Bottom elevation of the lower semi-confining unit (and top elevation of the Fernandina Permeable Zone, feet NAVD88; after Miller, 1986; Miller, written communication 1991; and Williams, digital communication 2013)

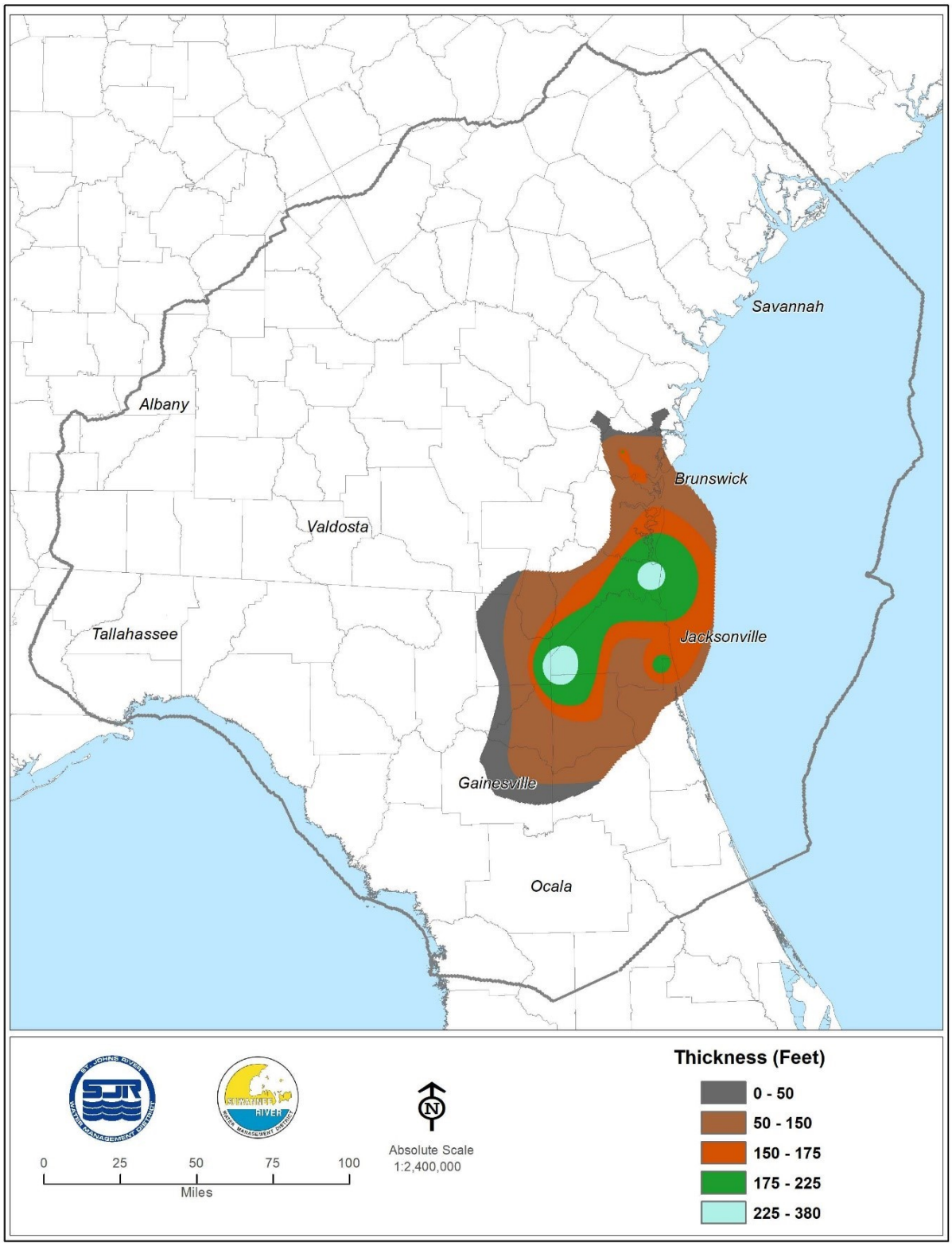

Figure 2-22. Thickness of the lower semi-confining unit (feet; after Miller, 1986; Miller, written communication 1991; and Williams, digital communication 2013)

Transmissivity of the Lower Floridan aquifer

The transmissivity of the Lower Floridan aquifer is not as well-known as that of the Upper Floridan aquifer. Only three aquifer performance tests of the Lower Floridan aquifer in the Florida portion of the NFSEG model domain are known to have been performed. These tests were performed near Keystone Heights (Connect Consulting, Inc. 2009), Grandin (Kleinfelder 2017) and Ocala (CDM Smith 2017), Florida and resulted in estimated Lower Floridan aquifer transmissivity values of 60,000; 57,000; and 3,500,000 ft^2/d, respectively.

In Georgia, transmissivity values of the Lower Floridan aquifer range from 170 to 15,000 ft^2/d with a median of 3,500 ft^2/d in areas in which the Lower Floridan aquifer is primarily clastic and from 500 to 43,000 ft^2/d with a median of 2,900 ft^2/d in areas in which it is primarily carbonate (Clarke and others, 2004).

In Duval County, Florida, tests performed using multi-aquifer wells (wells open to the Upper Floridan aquifer and an upper portion of the Lower Floridan aquifer) have resulted in transmissivity values of 2,100 ft^2/d at well D-168 and 200,000 ft^2/d at well M503 (Clarke and others, 2004).

Water Levels

The water level of the Upper Floridan aquifer is known at numerous monitoring wells that are cased to and penetrate the Upper Floridan aquifer (Appendix A). In the present study, medians of these water levels were determined for the years 2001 and 2009 and, along with estimated river stages in unconfined areas, contoured to create maps of the median potentiometric surface of the Upper Floridan aquifer in the years 2001 and 2009 (Figures 2-28 and 2-29). In some cases, statistical methods were used to augment the number and quality of water-level observations in areas of limited water-level data availability (Appendix B).

As with the intermediate confining unit, the middle confining unit vertical head difference can be indicative of the degree of confinement of the middle confining unit. The absolute value of the middle confining unit vertical head difference is typically less than 10 ft (Figures 2-30 and 2-31).

The water levels of the Lower Floridan aquifer are known at many monitoring wells (Appendix A). Fresh water levels in the Fernandina Permeable zone are known at two monitoring wells in the years of interest (Appendix A).

Recharge and Evapotranspiration Rates

Bush and Johnston (1988) estimated net recharge to the predevelopment Upper Floridan aquifer throughout the extent of the Upper Floridan aquifer. Estimates in the unconfined regions of the NFSEG model domain range from 5 to 20 inches/year (in/yr) over a large proportion of the area. Bush and Johnston (1988) did not indicate any significant change in recharge rates in these areas since predevelopment.

Using a water budget analysis, Knowles (1996) estimated total annual net recharge to

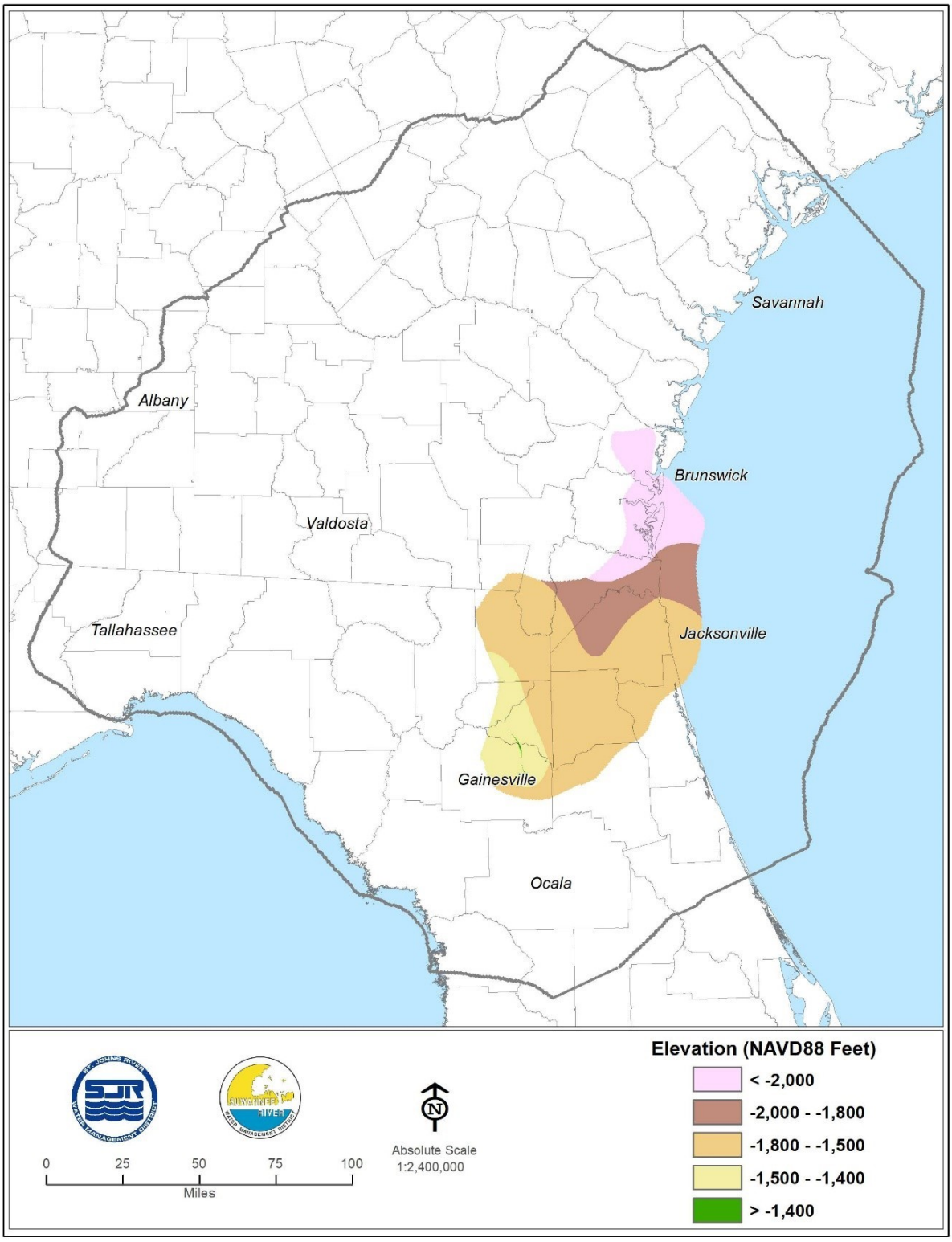

Figure 2-23. Top elevation of the Fernandina Permeable Zone (FPZ; feet NAVD88; after Miller, 1986; Miller, written communication 1991; and Williams, digital communication 2013)

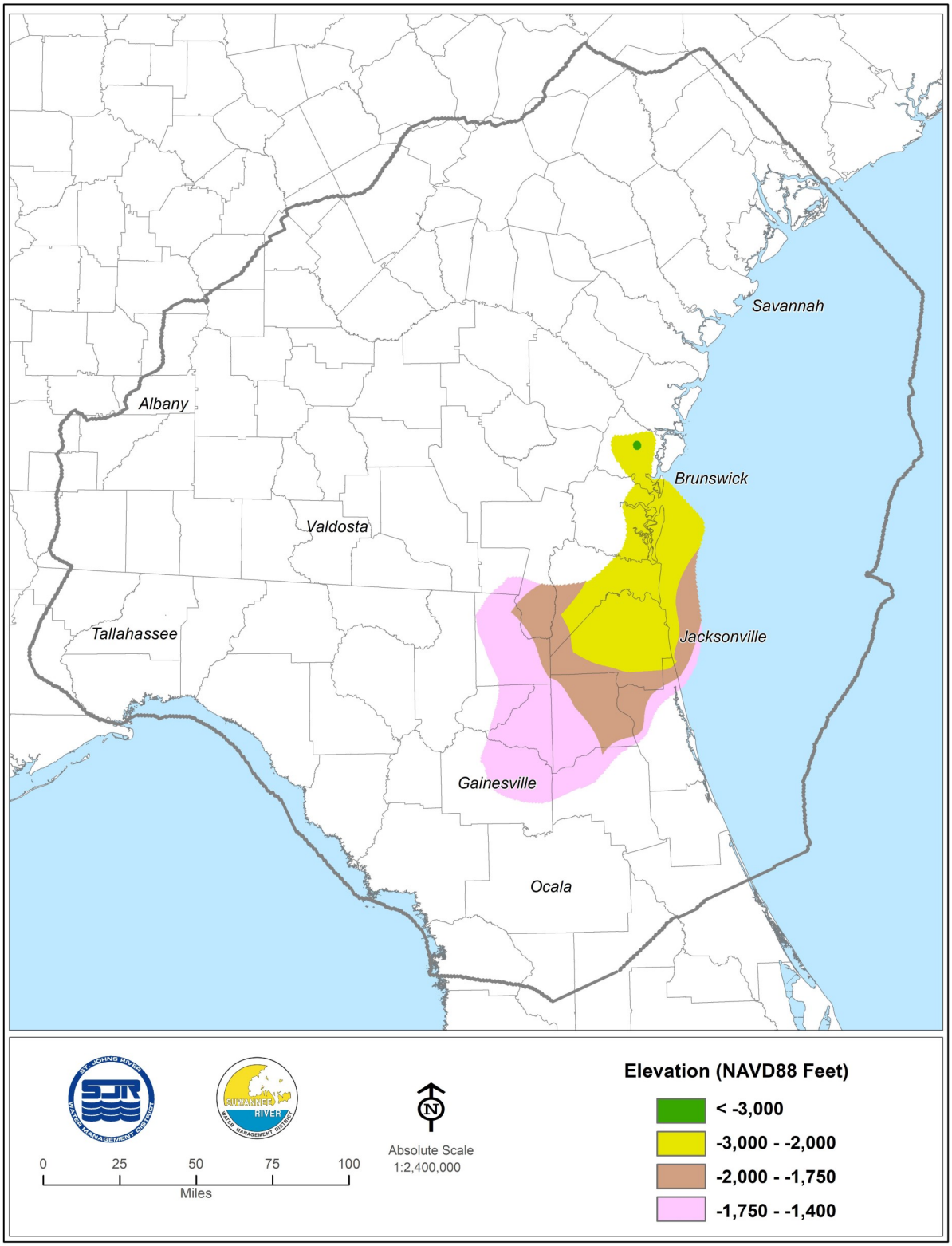

Figure 2-24. Bottom elevation of the Fernandina Permeable Zone (FPZ, feet NAVD88; after Miller, 1986; Miller, written communication 1991; Williams, digital communication 2012; and Williams, digital communication 2013)

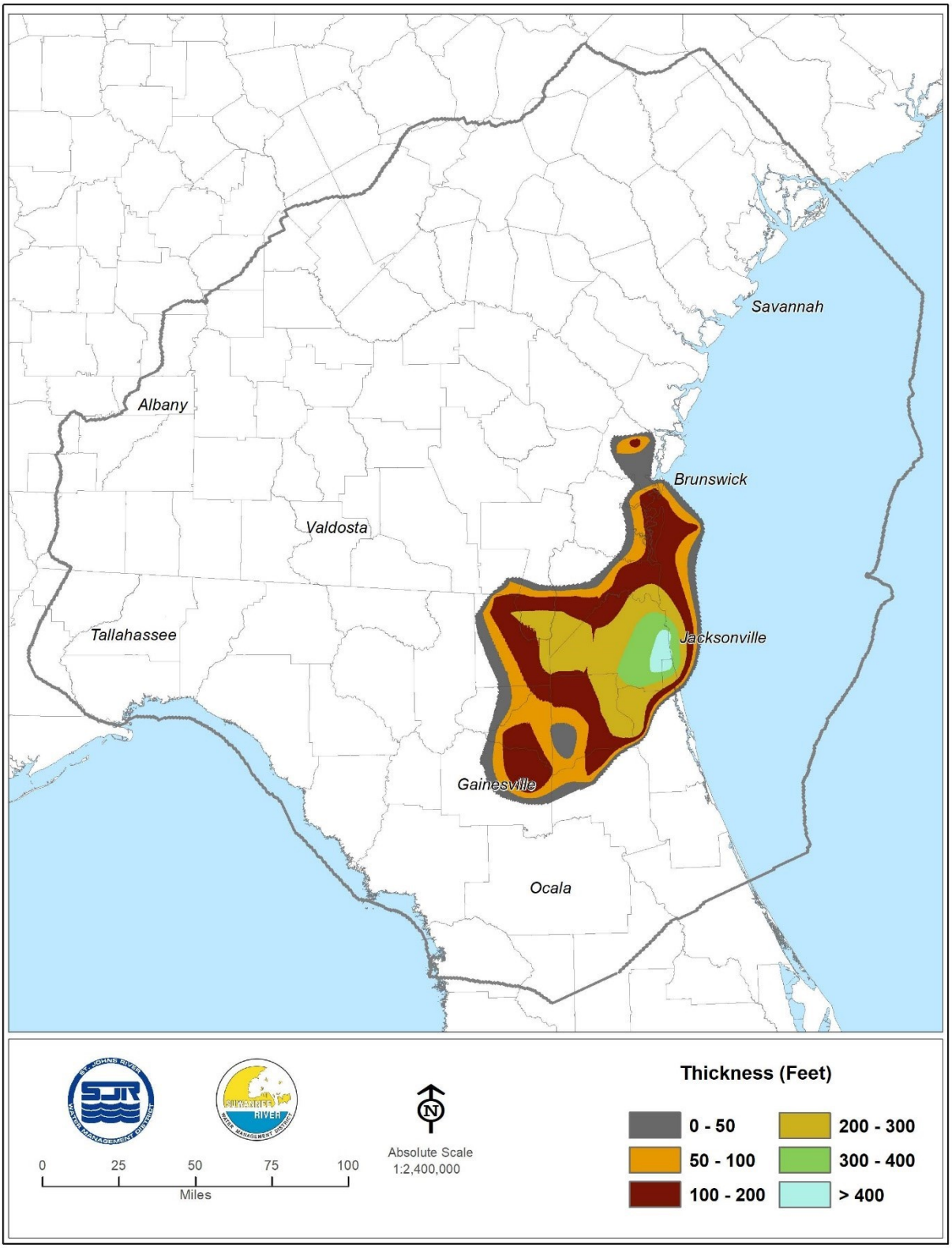

Figure 2-25. Thickness of the Fernandina Permeable Zone (FPZ, feet; after Miller, 1986; Miller, written communication 1991; and Williams, digital communication 2013)

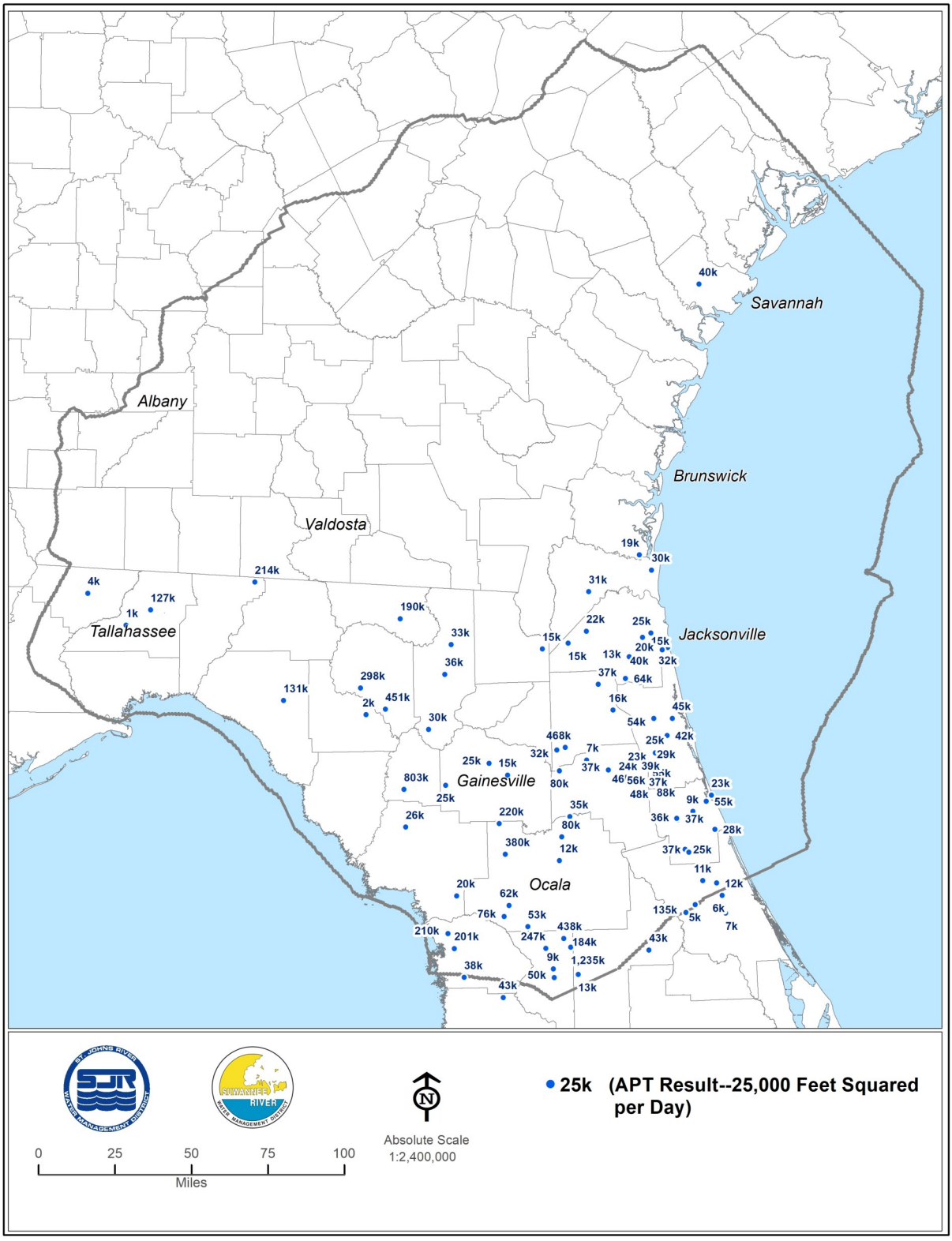

Figure 2-26. Aquifer-performance-test transmissivity estimates, Zone 1 (feet squared per day)

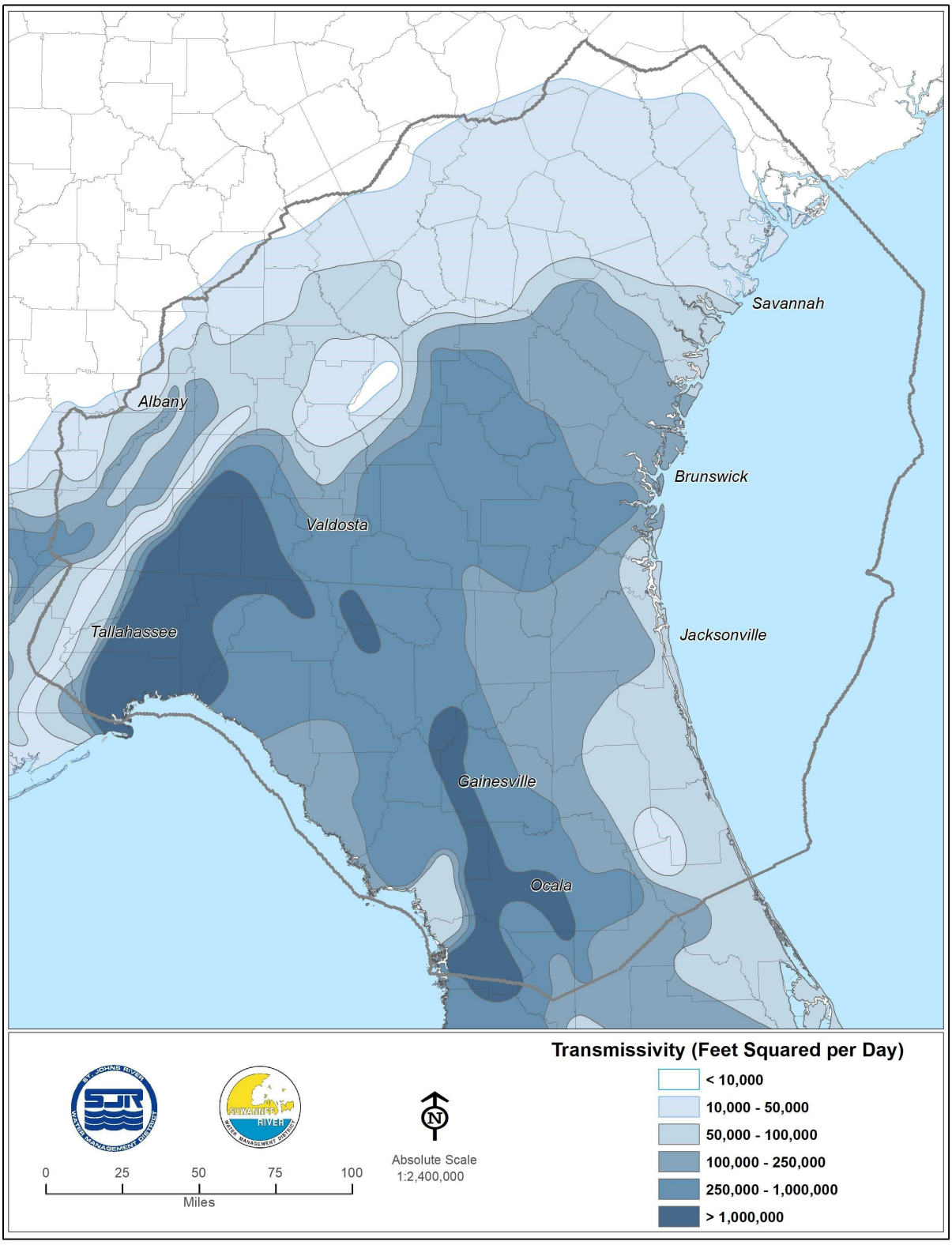

Figure 2-27. Estimated transmissivity, upper Floridan aquifer (feet squared per day; after Bush and Johnston 1988)

the springshed areas of Rainbow and Silver springs as 15.2 in/yr and 11.6 in/yr, respectively, for the period of 1965 through 1994. These basins are unconfined, so net recharge to these springs was assumed to be equivalent to discharge from the springs.

Bush and Johnston (1988) estimated total rates of ET (sum of saturated and unsaturated ET rates) as ranging from 31 in/yr in the northern extent of the model domain in Georgia to 41 in/yr parts in parts of the Steinhatchee and lower Suwannee river basins. An average value appears to be on the order of 35 in/yr for the NFSEG model domain-wide. Based on water budget analyses of the period of 1965 through 1994, Knowles (1996) estimated total average annual evapotranspiration from the combined springshed areas of Rainbow and Silver springs to be 38 in/yr.

Spring Flows

Spring flows are a major mode of discharge from the groundwater system in the model domain. More than 300 springs are represented in the NFSEG model, most of which are in areas in which the ICU is thin or absent. Spring discharge totaled approximately 6,029 cubic feet per second (cfs) in 2001 and 7,911 cfs in 2009. All but five springs within the NFSEG model domain emanate from the Upper Floridan aquifer, with the remaining five emanating from the ICU (Figures 2-32 and 2-33).

A unique type of spring that occurs in karstic terrains, which are found within NFSEG model domain, is the river rise. River rises are upwellings that occur downgradient of sinks into which part or all the flow in a river or stream is captured. Upon entering the sink, the river flow may mix with groundwater flow before emerging at the rise location. The exact proportion of surface water versus groundwater at river rises is not well defined. Major river rises in the model domain include the Alapaha River Rise, St. Marks River Rise, Santa Fe River Rise, Steinhatchee River Rise and Holton Creek Rise.

Springs with discharge rates that are greater than or equal to 100 cfs on average are classified as first magnitude springs. There are 18 first magnitude springs in the NFSEG model, not counting major river rises. The estimated total discharge of first magnitude springs was 2,932 cfs in 2001 and 5,234 cfs in 2009 (Figure 2-34).

Baseflows

Baseflows were determined by averaging the results of four different hydrograph separation techniques and a fifth approach that utilizes flow duration curves. Three of the four hydrograph separation techniques were implemented using the United States Geological Survey (USGS) computer program *Groundwater Toolbox* (Barlow et al. 2015; https://water.usgs.gov/ogw/gwtoolbox/#over). These three methods are the BFI standard and modified technique (Institute of Hydrology 1980a, b) and the HYSEP local minimum technique (Sloto and Crouse 1996). The fourth hydrograph separation technique is that of Perry (1995; also known as the "USF method"), a low pass filter method that utilizes a moving window of 121 days. The fifth method utilizes flow duration curves and is based partly on empirical results of previous investigations (e.g., Stricker 1983). In the implementation of the current study, baseflow discharges for the years

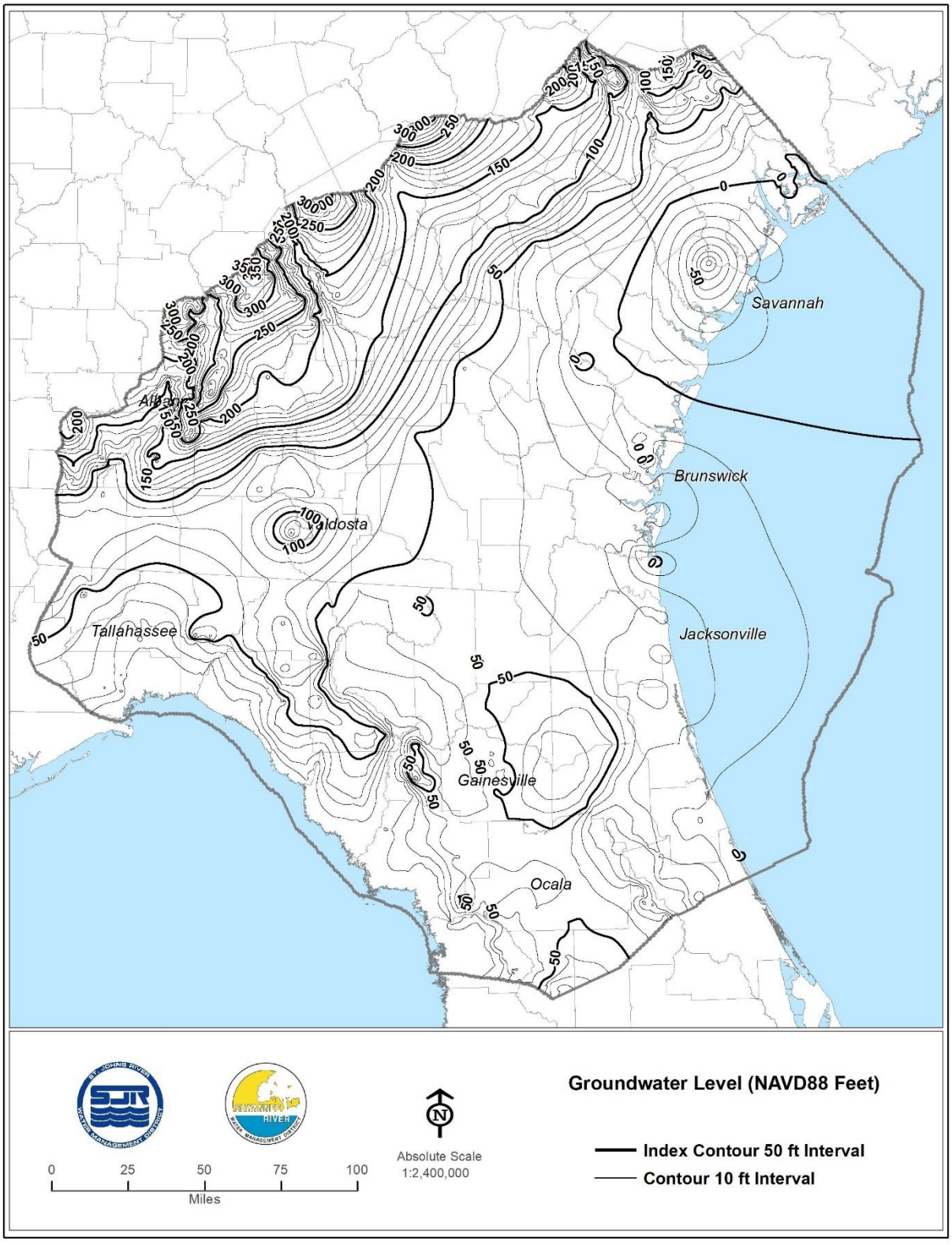

Figure 2-28. Estimated potentiometric surface, upper Floridan aquifer, 2001 (Feet NAVD88)

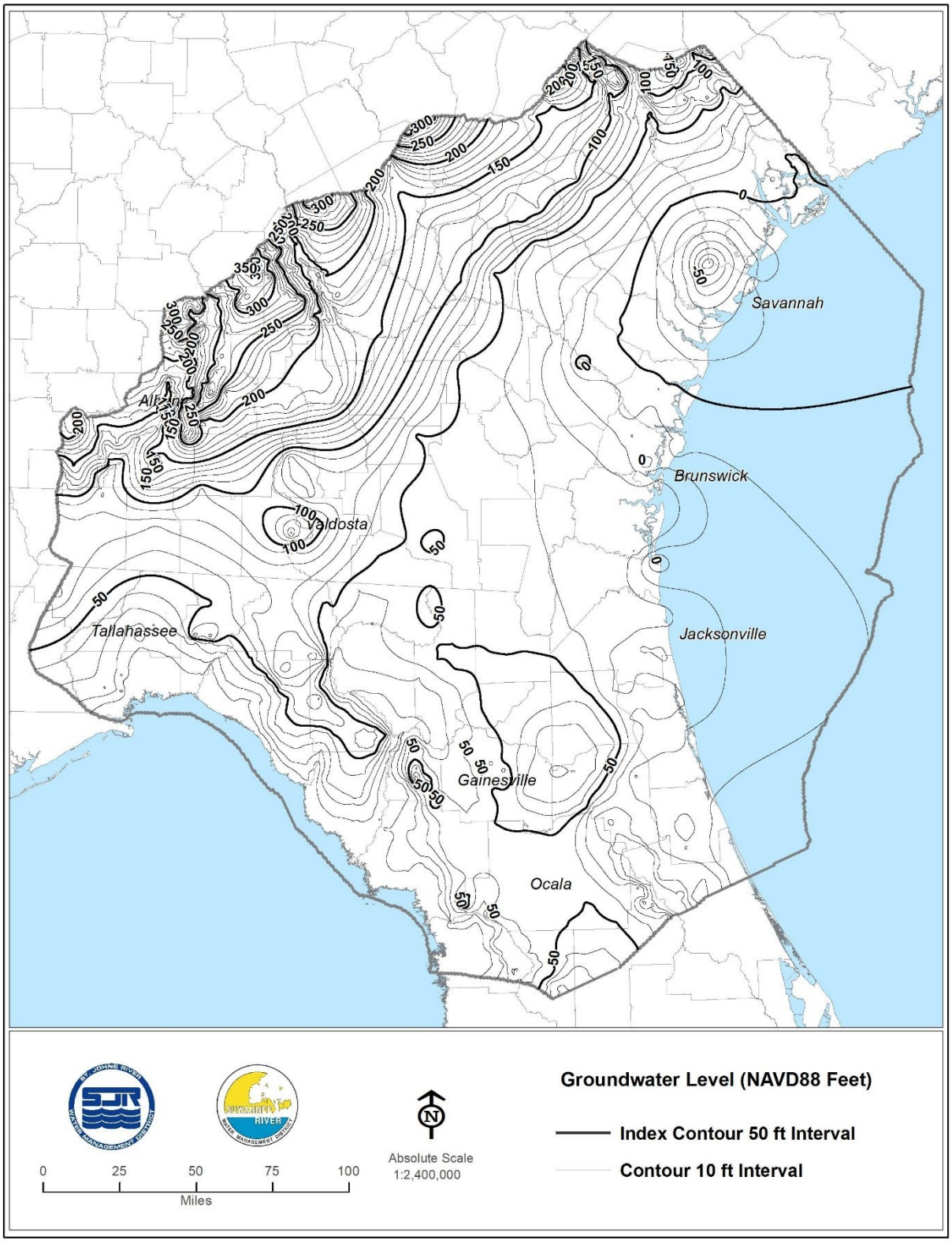

Figure 2-29. Estimated potentiometric surface, upper Floridan aquifer, 2009 (Feet NAVD88)

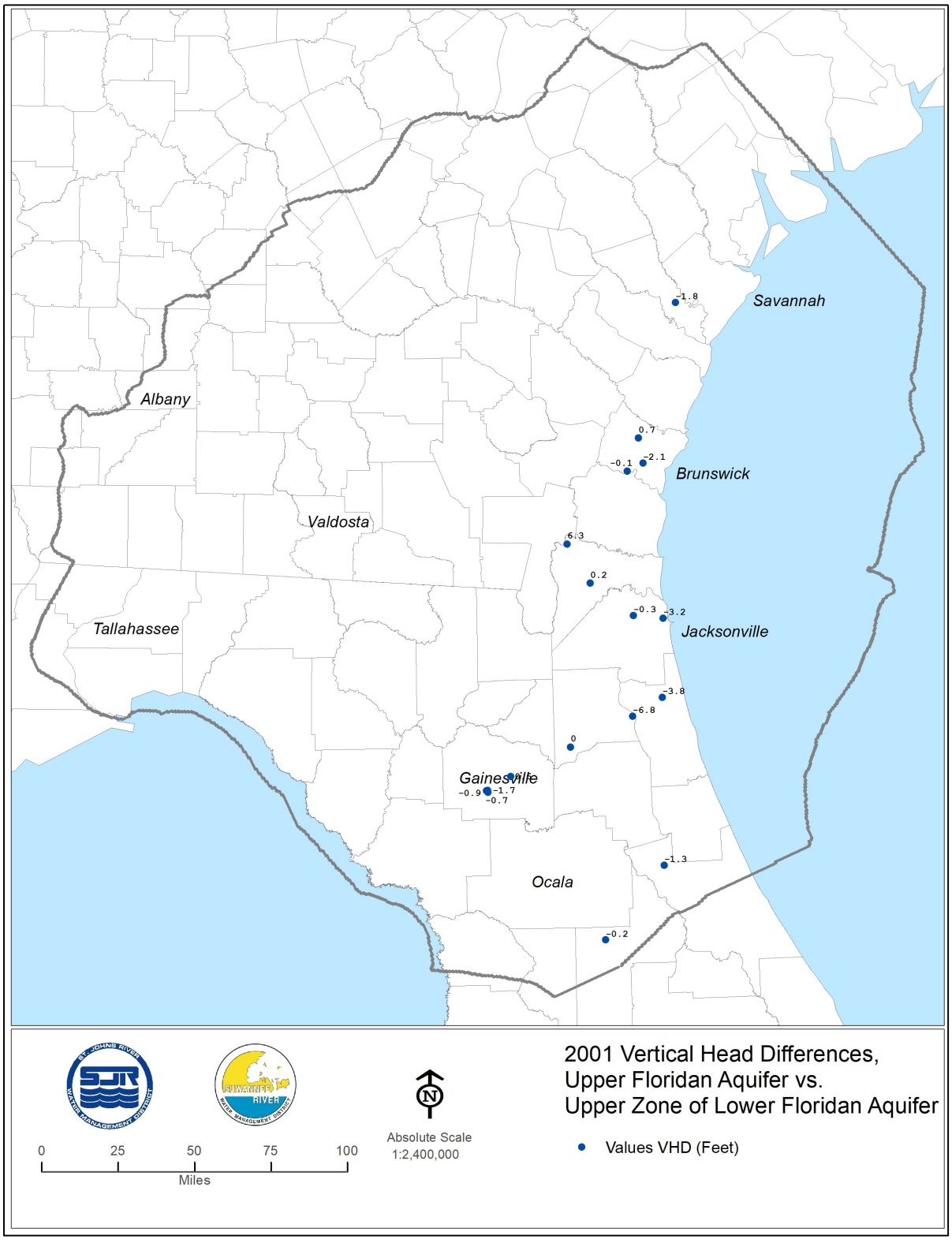

Figure 2-30. Middle confining unit vertical head difference, 2001 (Feet)

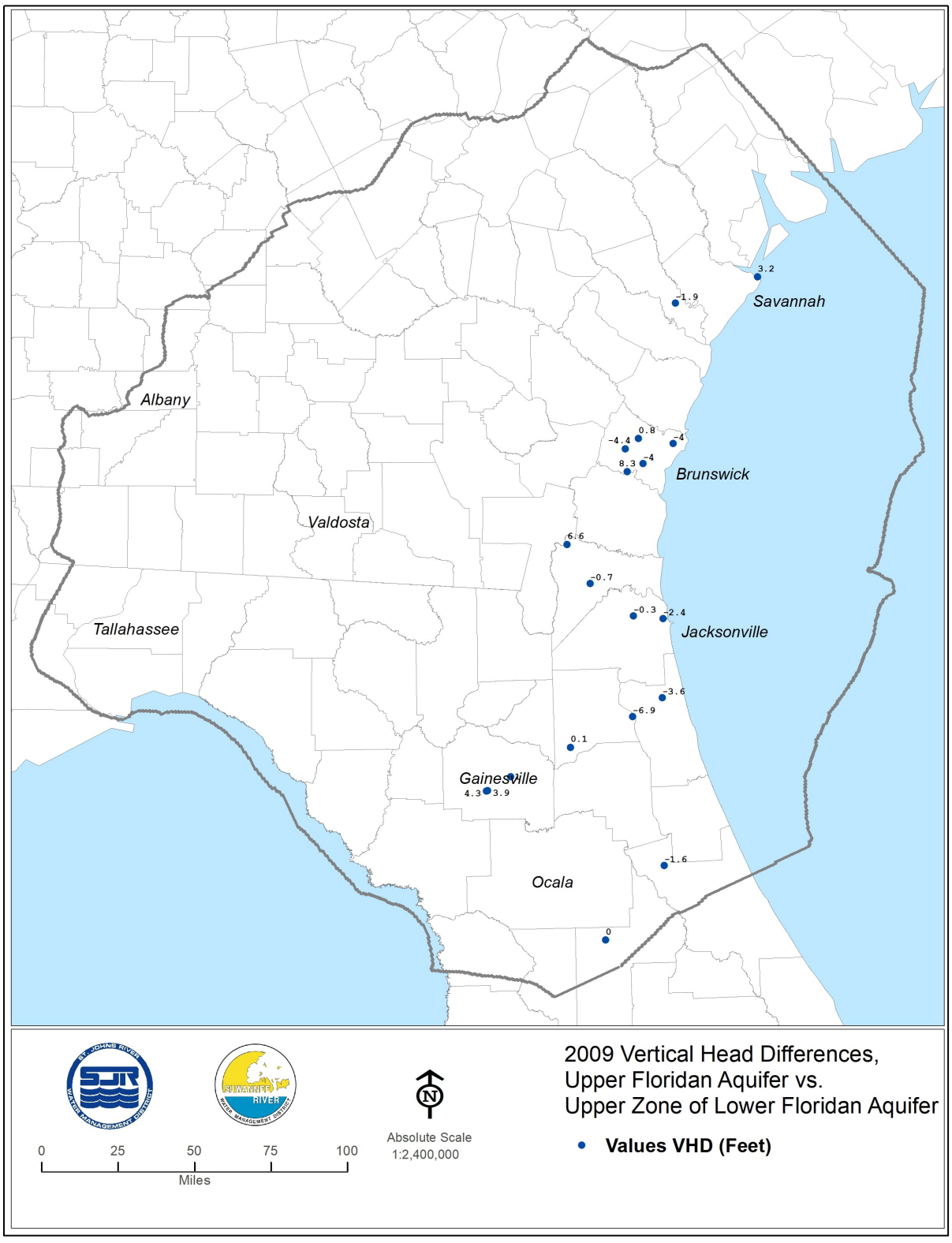

Figure 2-31. Middle confining unit vertical head difference, 2009 (Feet)

2001 and 2009 were estimated as corresponding to a probability of exceedance of 70 percent on annualized flow duration curves of the years 2001 and 2009, respectively.

Estimates derived from the HYSEP fixed interval and sliding interval methods and the PART method (Rutledge 1998) were considered also, as these approaches are also implemented in *Groundwater Toolbox* (Barlow et al. 2015). However, these methods resulted in baseflow hydrographs that mimic too closely the respective total flow hydrographs from which they were derived, resulting in overestimated baseflows. This conclusion was based on inspection of the results of analyses of the total flow hydrographs of 14 USGS streamflow gauges within the NFSEG model domain (Figure 2-35).

The baseflow estimates derived from the BFI standard and modified methods and HYSEP Local Minimum method tend to cluster at the high end of a range, while the estimates resulting from the USF Method (Perry 1995) and exceedance plot-based approach tend to cluster at the low end. Using this approach, average annual baseflow rates were determined at 92 USGS gauges for 2001 and 77 USGS gauges for 2009. Estimates were not determined for tidally affected sites, sites located immediately downstream of dams, or sites missing more than a few average daily flows in 2001 or 2009. Determining baseflow rates based on the averages of five widely accepted methods presumably moderates potential eccentricities of any one of the approaches and thus helps attain better all-around estimates.

Cumulative Baseflow Estimates

Cumulative baseflows are defined herein as the total of all baseflows above a given USGS gauge location in a stream. Cumulative baseflows determined using the averaging techniques discussed above are shown in Figures 2-36 and 2-37 for the years 2001 and 2009, respectively. They were determined primarily for gauges located in the middle to lower reaches of major systems, including the Suwannee, Alapaha, Withlacoochee, Santa Fe, St. Marys, Ochlocknee and Satilla rivers and Orange Creek. These cumulative baseflows represent averages over relatively large proportions of the respective stream basins and are therefore applicable to evaluation of large areas of the NFSEG model domain. The cumulative baseflow rates for 2001 range from 5.7 cfs at Orange Creek at Orange Springs to approximately 3,000 cfs at Suwannee River at Branford. For 2009, estimates range from approximately 8.4 cfs at Orange Creek at Orange Springs to 3,320 cfs at Suwannee River at Branford (Figures 2-36 and 2-37).

Baseflow Pickup Estimates

A baseflow pickup is a measure of the contribution of the groundwater system to the flow of a stream between a downstream point and one or more upstream points. In the current study, baseflow pickups were determined generally as differences in baseflow between a downstream gauge (i.e., a “to” gauge) and the sum of baseflows of one or more upstream gauges (i.e., the “from” gauges). In some cases, however, a “from” gauge is not available. In these cases, the “to” gauge baseflow pickup estimate is, strictly speaking, a cumulative baseflow. The “to” gauge in these cases is generally in the upper reaches of the stream basin in which it is located, however, so these

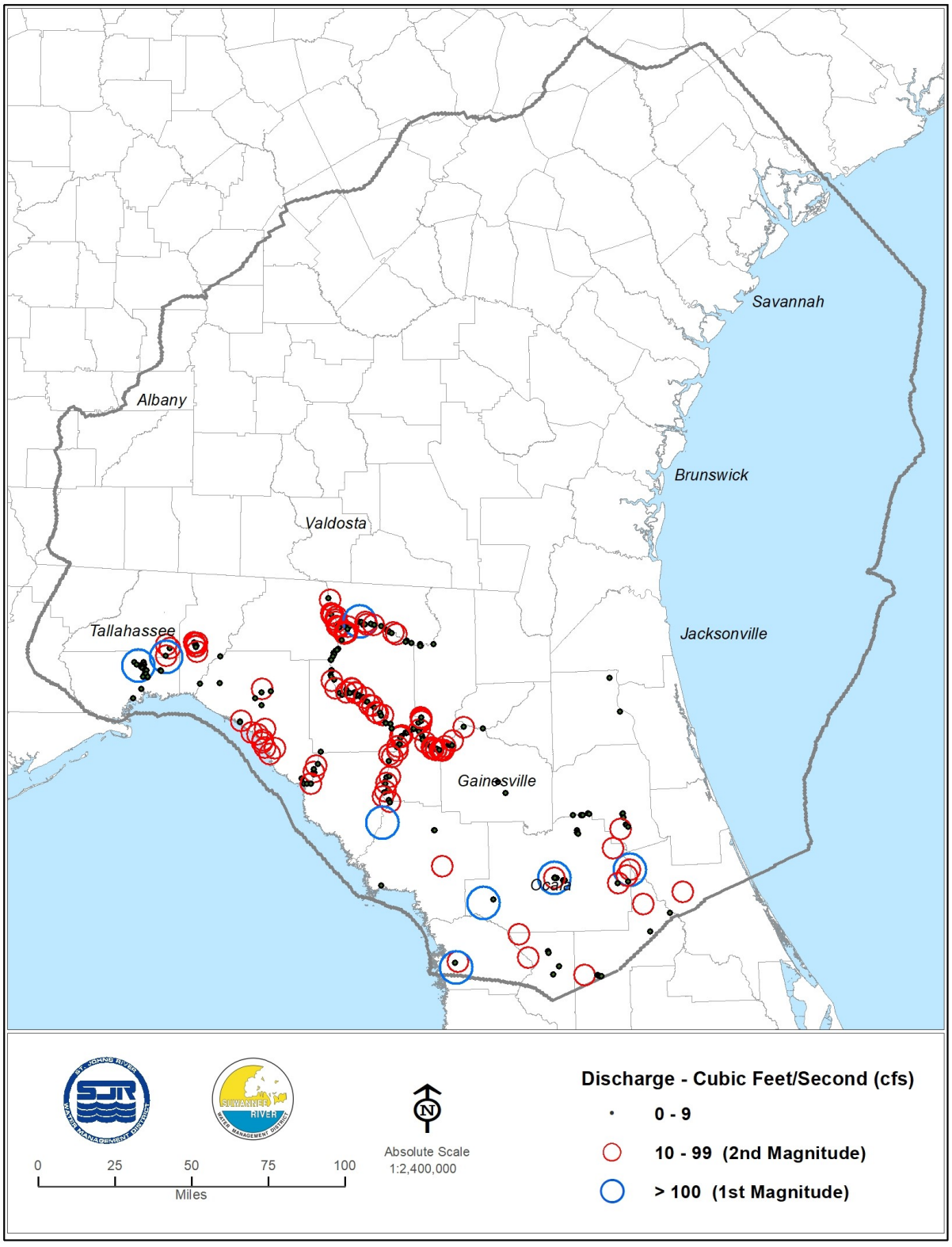

Figure 2-32. Locations and relative discharge rates of springs, 2001

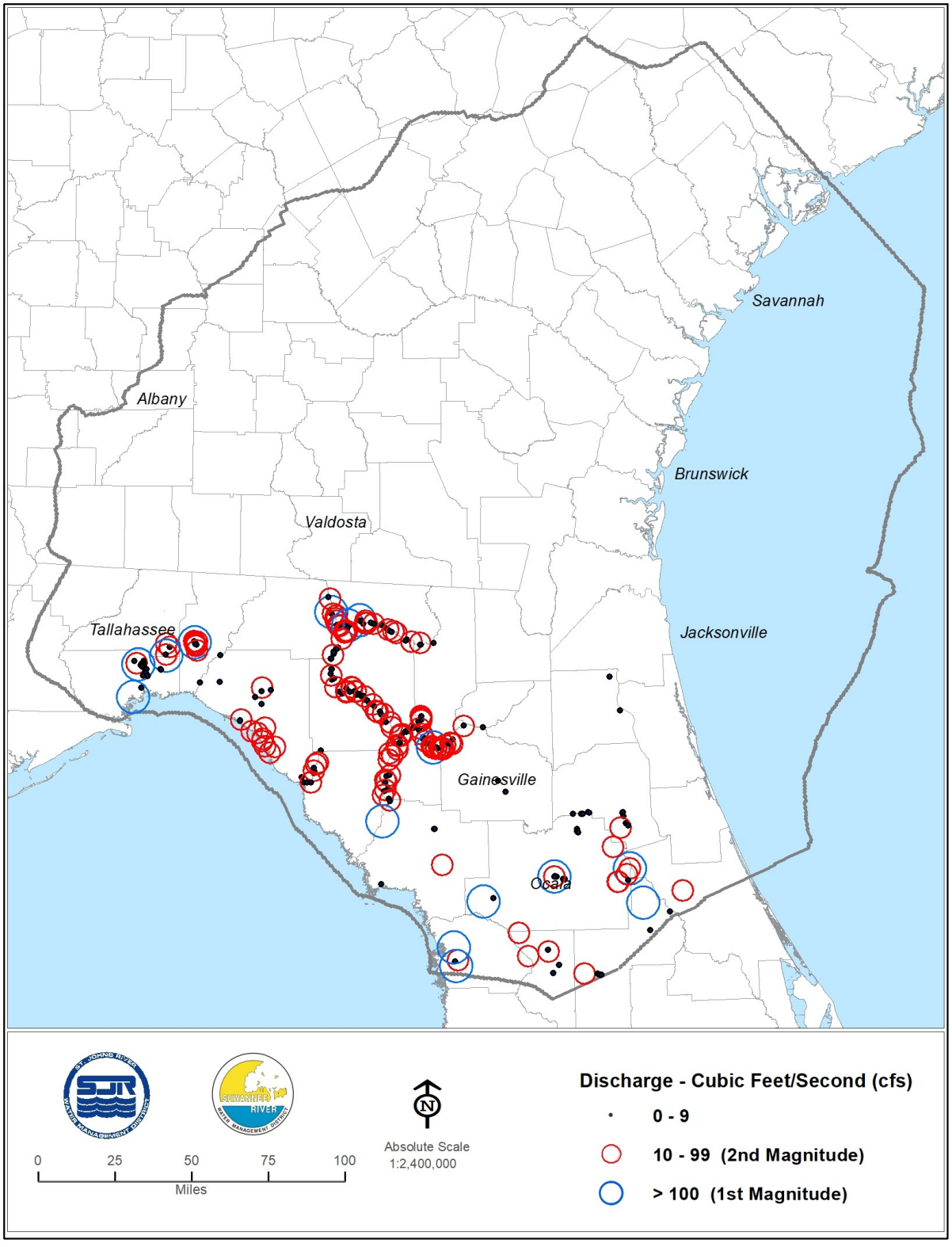

Figure 2-33. Locations and relative discharge rates of springs, 2009

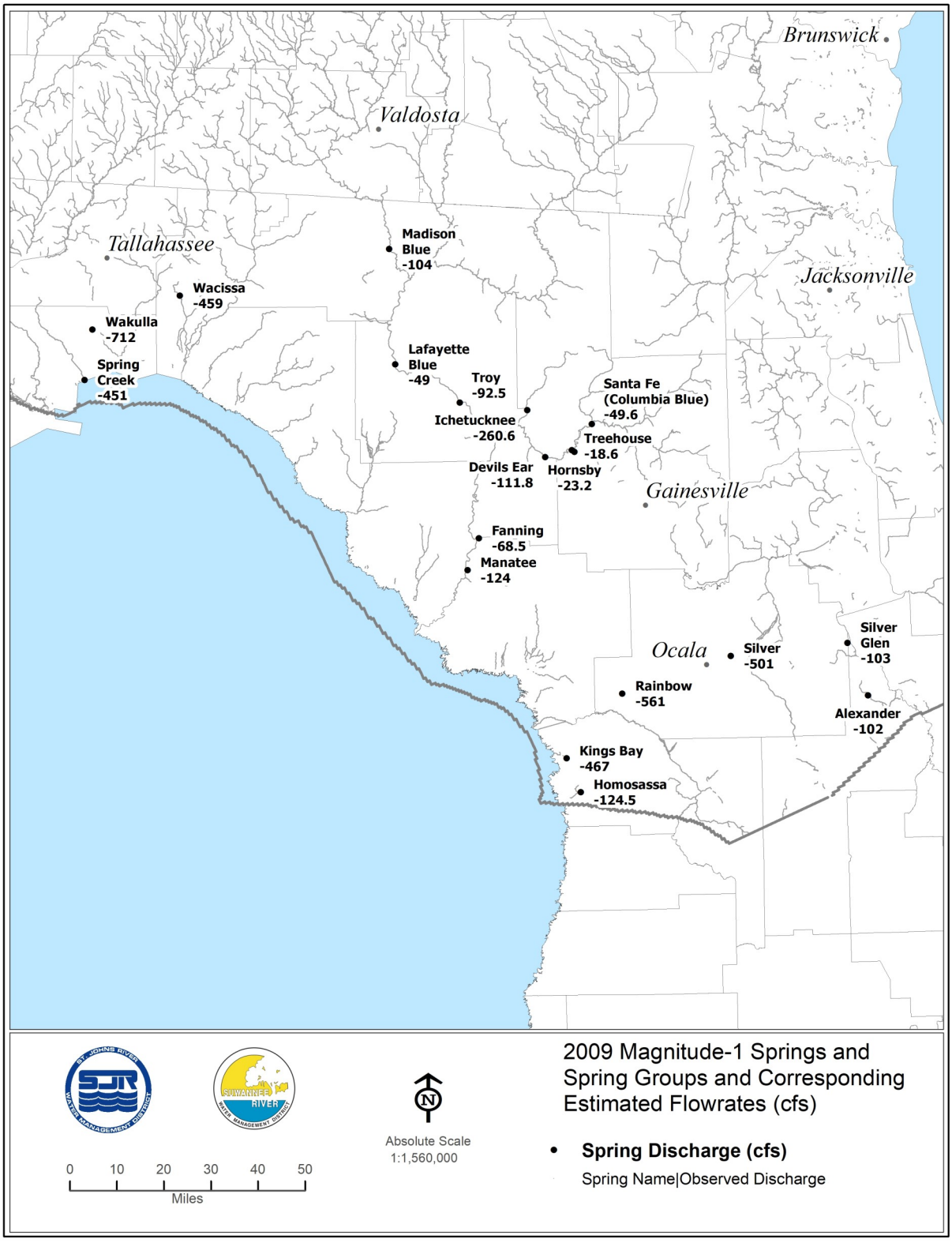

Figure 2-34. First-magnitude spring locations and corresponding discharge rates, 2009

baseflows are comparable to other baseflow pickups.

The baseflows used in the baseflow pickup determinations were derived mostly using the averaging technique discussed above. An alternative approach was utilized for determining baseflow pickups between adjacent gauges that defined a river reach adjacent to unconfined karst areas and which lacked a well-developed, channelized surface drainage network. In this approach, baseflow pickup was determined by taking the difference in the total observed flows of the upstream and downstream bounding gauges, based on the assumption that overland runoff is negligible in areas in which the Upper Floridan aquifer is unconfined. The resulting baseflow pickup estimates range from less than 5 cfs to more than 500 cfs for 2001 and from less than 5 cfs to more than 1,000 cfs for 2009 (Figures 2-38 through 2-43).

In selected cases, because of unique circumstances regarding available data or hydrologic characteristics of the reach, variations on the above methods were used. These are discussed below:

1. Suwannee River between gaging stations at Ellaville and at Dowling Park: negative values (decreasing) change in flow along the reach during calendar year 2001 indicated that rated flows may not have been sufficiently accurate to estimate the change in baseflow. The target value used in the calibration was based on the sum of the aggregate spring flow within the reach and an estimate of the diffuse pickup within the reach. The estimated diffuse pickup within the reach was determined by multiplying the estimated diffuse leakage between the Ellaville and Branford gauges by the ratio of aggregate spring flow within the reach to the aggregate spring flow within the reach between the Ellaville and Branford gauges. The same process was used to estimate the baseflow pickup in 2001 in the reach immediately downstream between the gauges at Dowling Park and at Luraville.
2. Reach upstream of the gauge on the Suwannee River near Wilcox and downstream of the gauges Suwannee River at Branford and Santa Fe River near Hildreth: difference between baseflow estimates at the Wilcox gauge and the two upstream gauges was negative, indicating that the baseflow estimate at the Wilcox gauge that was derived from the five baseflow separation methods could be too low. Therefore, baseflow was estimated as the sum of the baseflows of the two upstream gauges plus the change in total flow from the upstream gauges to the gauge at Wilcox.

Concentrated Groundwater Inflows

Concentrated groundwater inflows represent a significant form of recharge to the groundwater flow system within the NFSEG model domain. They are both human induced and naturally occurring. Human induced inflows occur via rapid infiltration basins (RIBs), drainage wells and injection wells. Naturally occurring inflows occur via sinks. In RIBs water is applied to land surface so inflow due to them is usually directed to the surficial aquifer system. Drainage wells are constructed into the Upper Floridan aquifer and the injection wells located in the NFSEG model domain are constructed into the Lower Floridan aquifer. Inflow via sinks is to the Upper Floridan aquifer. Rates of inflow to drainage wells and sinks have been approximated in the present study as runoff to closed basins in HSPF. For sinks, measured flows are available in some cases.

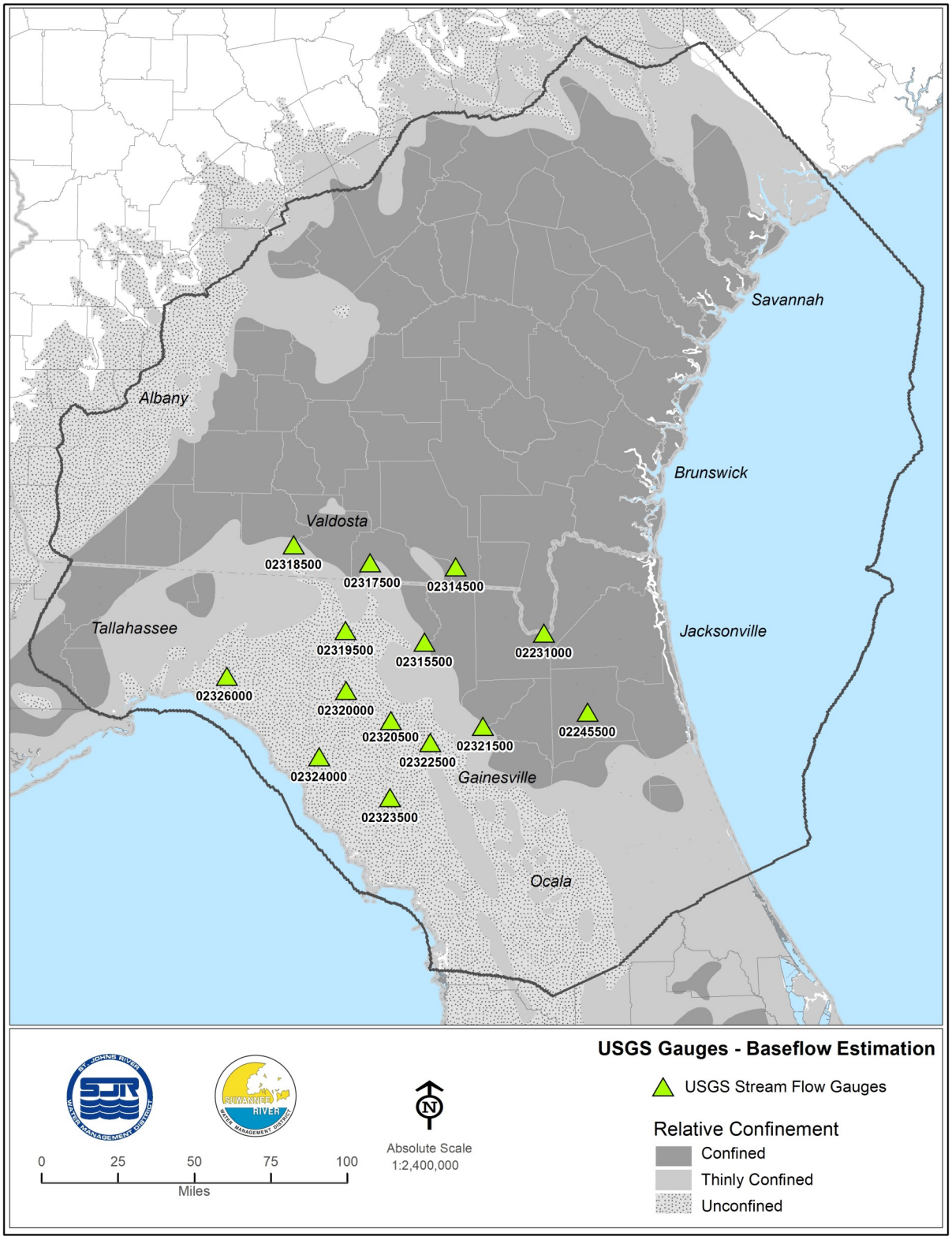

Figure 2-35. USGS gauges used for evaluation of baseflow-estimation approach

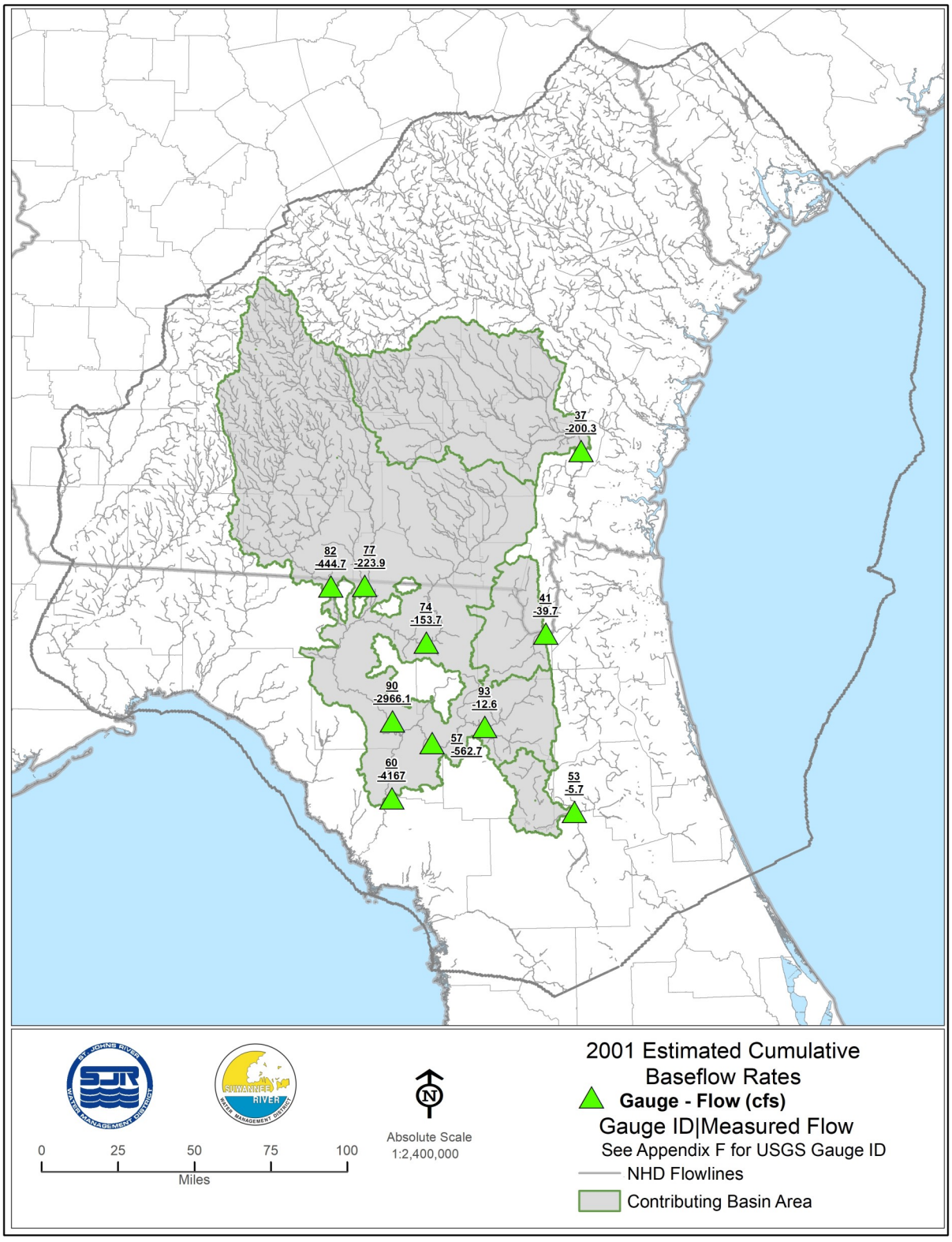

Figure 2-36. Cumulative baseflow estimates at selected USGS gauges, 2001

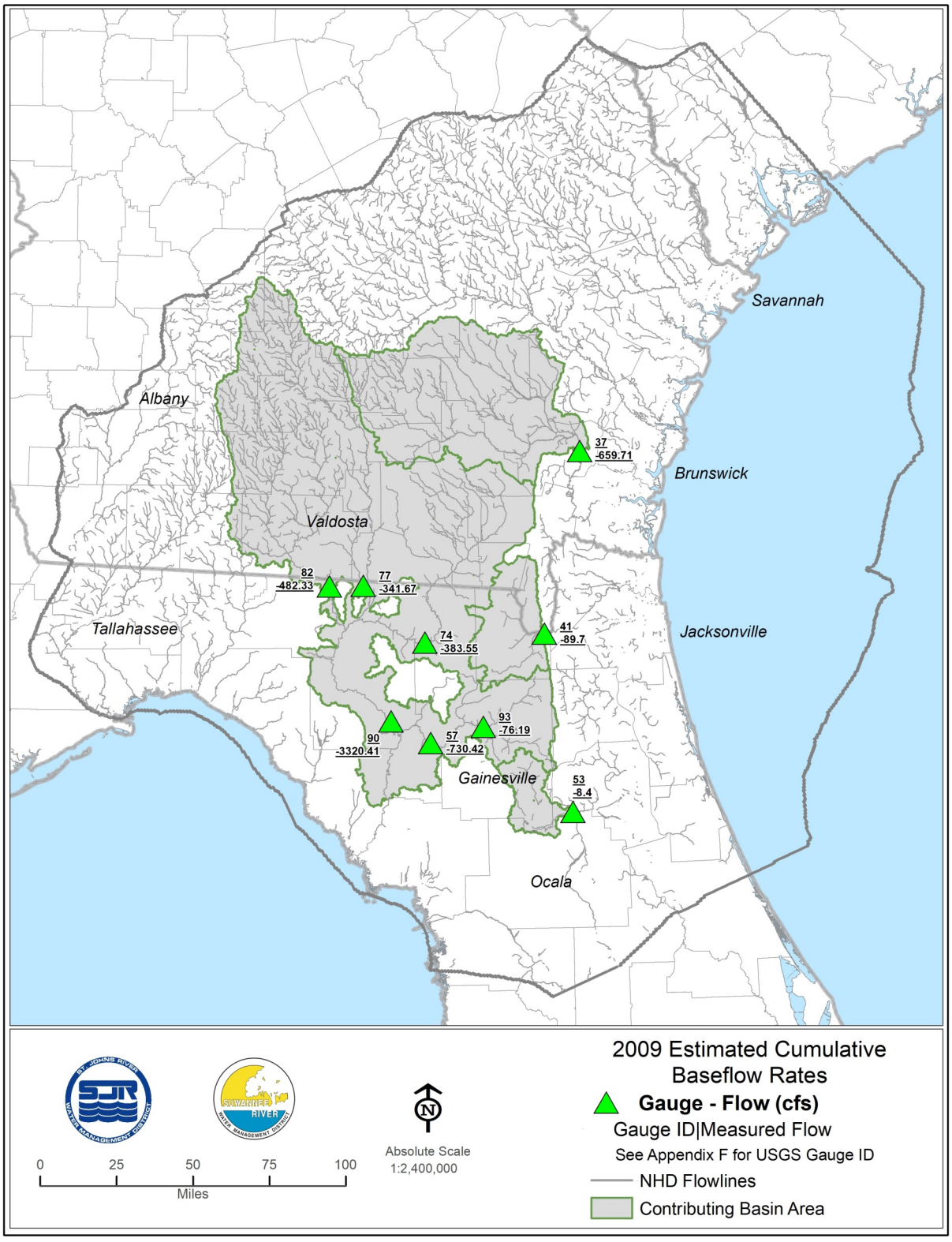

Figure 2-37. Cumulative baseflow estimates at selected USGS gauges, 2009

Groundwater Withdrawals

Groundwater withdrawals in the NFSEG model domain include withdrawals for purposes of public/commercial/industrial/institutional supply; agricultural irrigation supply; recreational irrigation supply (e.g., golf courses); and domestic self supply. Most large withdrawals take place from the Upper Floridan aquifer, but significant amounts of water are also withdrawn from the Lower Floridan aquifer using wells that are open to both the Upper and Lower Floridan aquifers. In areas in which the Floridan aquifer system water quality requires extensive treatment, the surficial aquifer system is utilized as an alternative source for enhancement of supplies obtained from the Floridan aquifer system (Figures 2-44 through 2-47).

Single aquifer wells cased to and open to the Upper Floridan aquifer are the primary mode of major withdrawals within the model domain. Multi-aquifer wells are wells that are open to more than one aquifer. In the case of the NFSEG model domain, the open interval of these wells extends from the Upper Floridan aquifer into the Lower Floridan aquifer. These wells are used extensively in Duval and Clay counties, Florida, for major withdrawals and can be found less extensively in other parts of the model domain. The actual distribution of withdrawals between the Upper and Lower Floridan aquifers in these wells is not well defined.

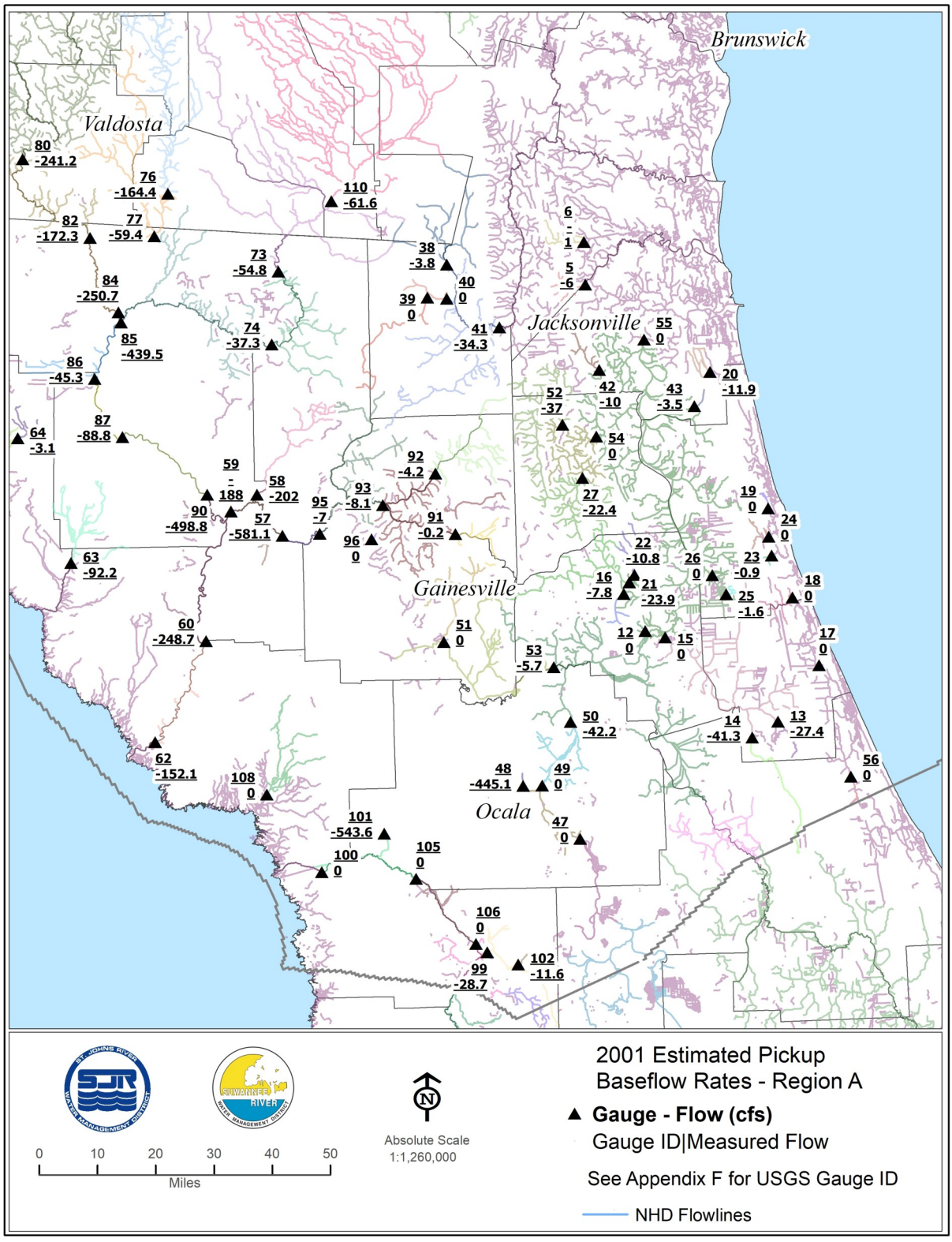

Figure 2-38. Estimated baseflow pickups, Region A, 2001

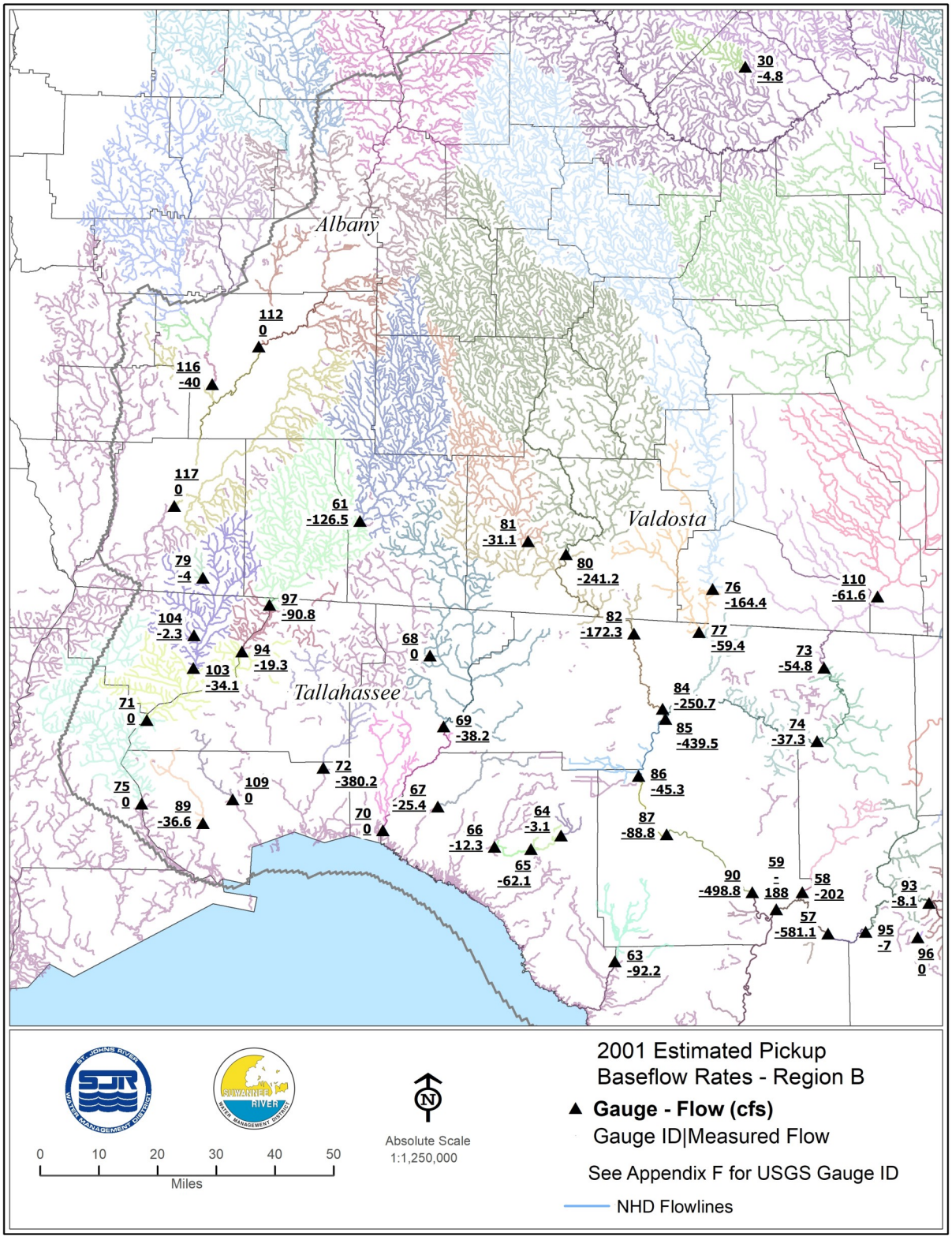

Figure 2-39. Estimated baseflow pickups, Region B, 2001

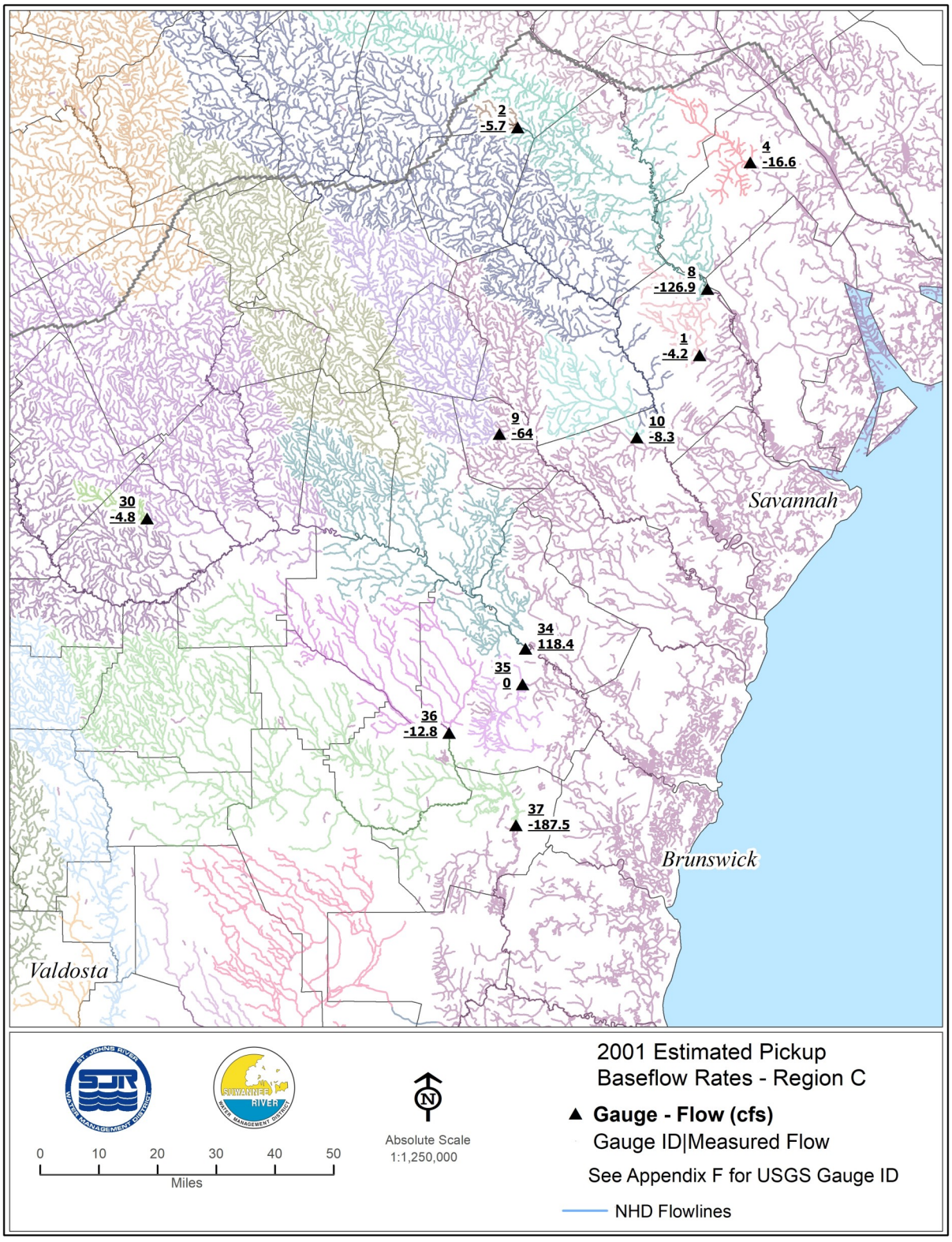

Figure 2-40. Estimated baseflow pickups, Region C, 2001

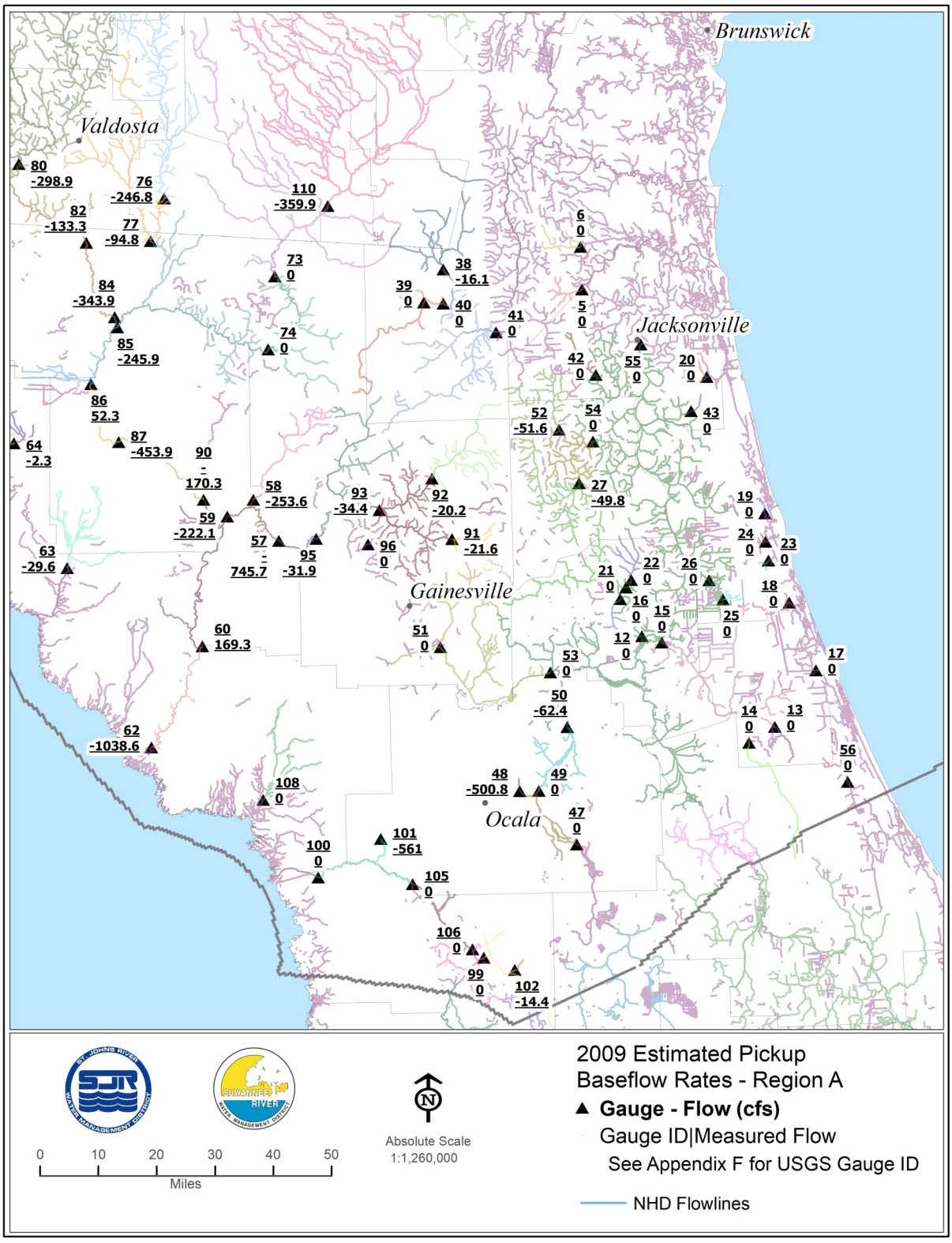

Figure 2-41. Estimated baseflow pickups, Region A, 2009

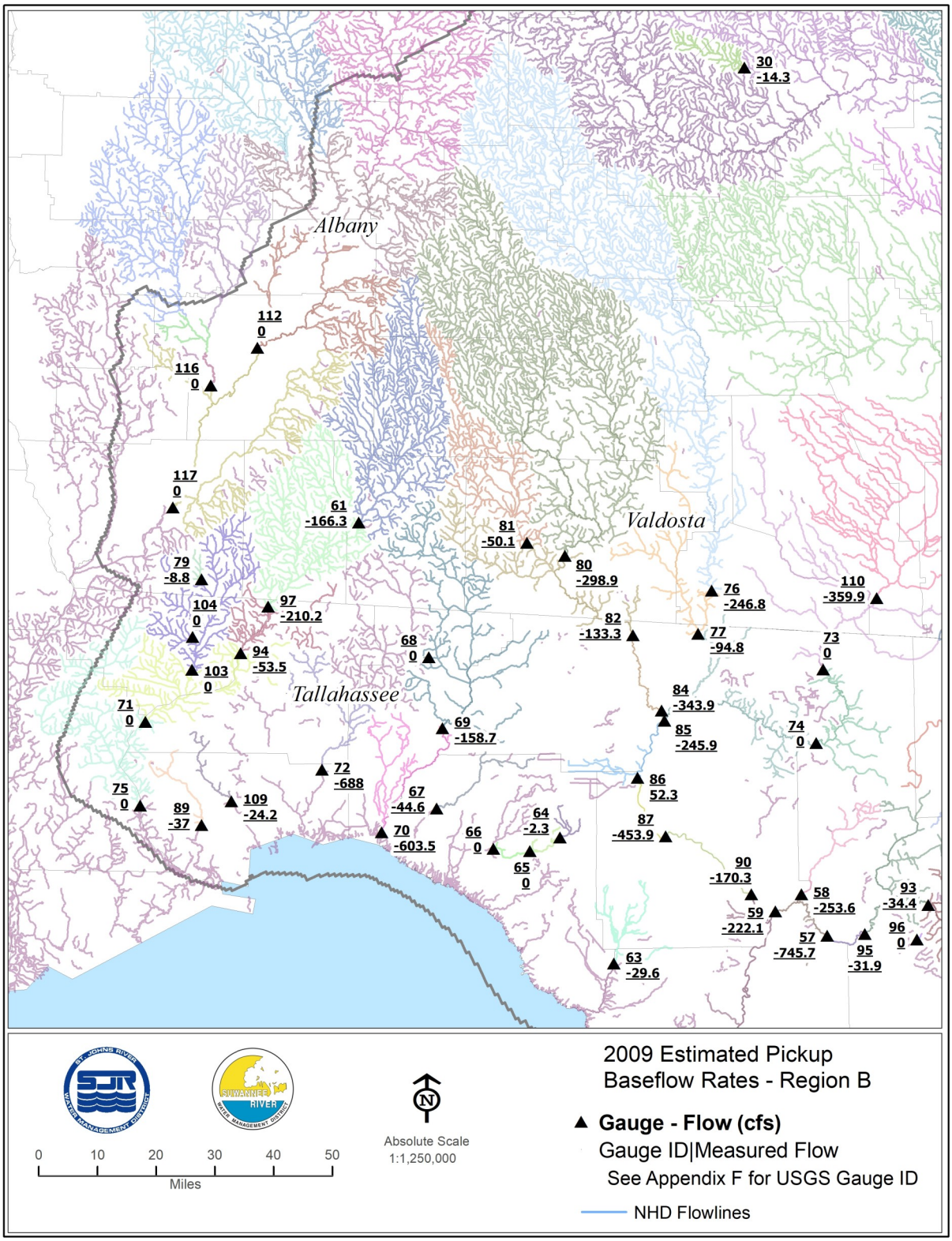

Figure 2-42. Estimated baseflow pickups, Region B, 2009

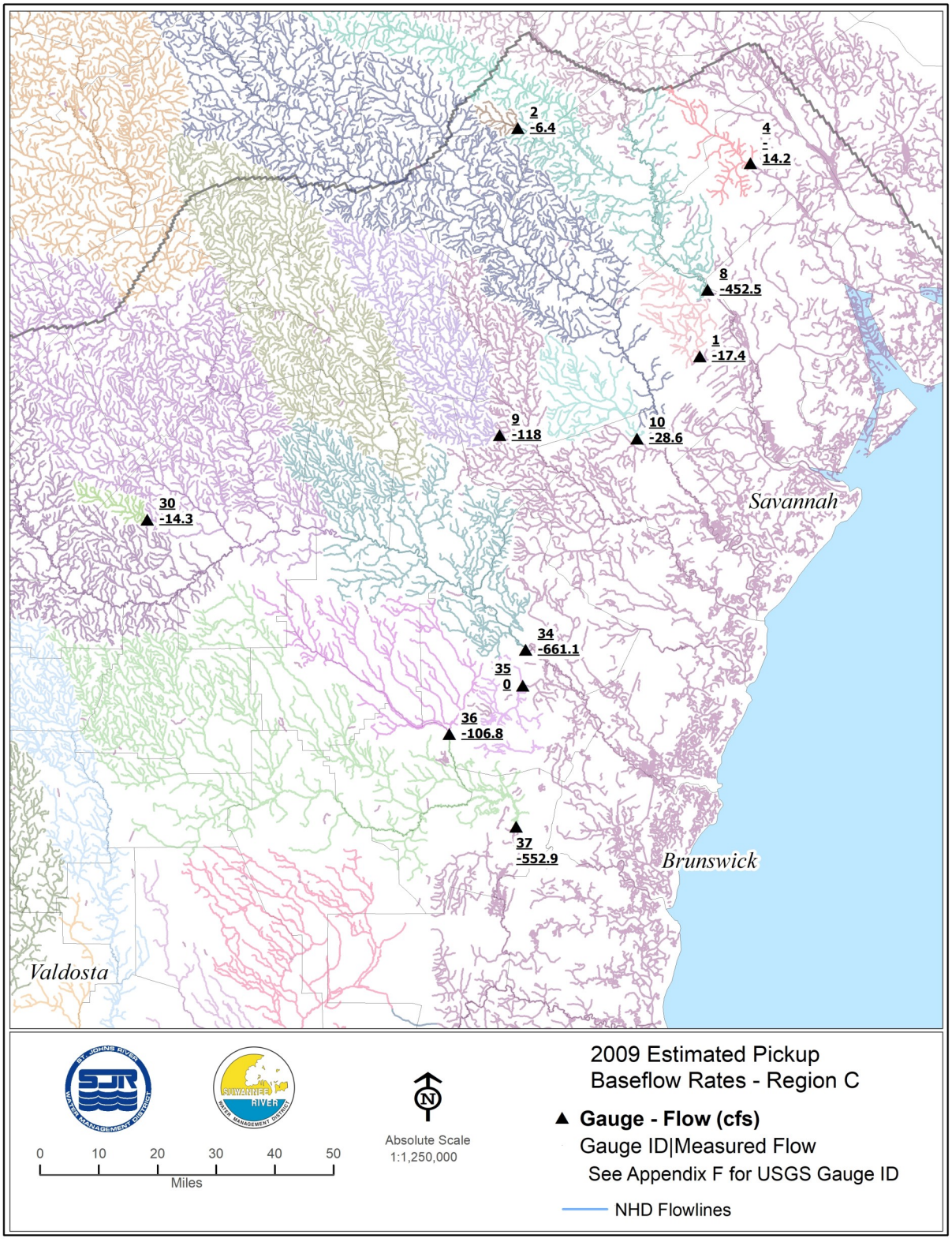

Figure 2-43. Estimated baseflow pickups, Region C, 2009

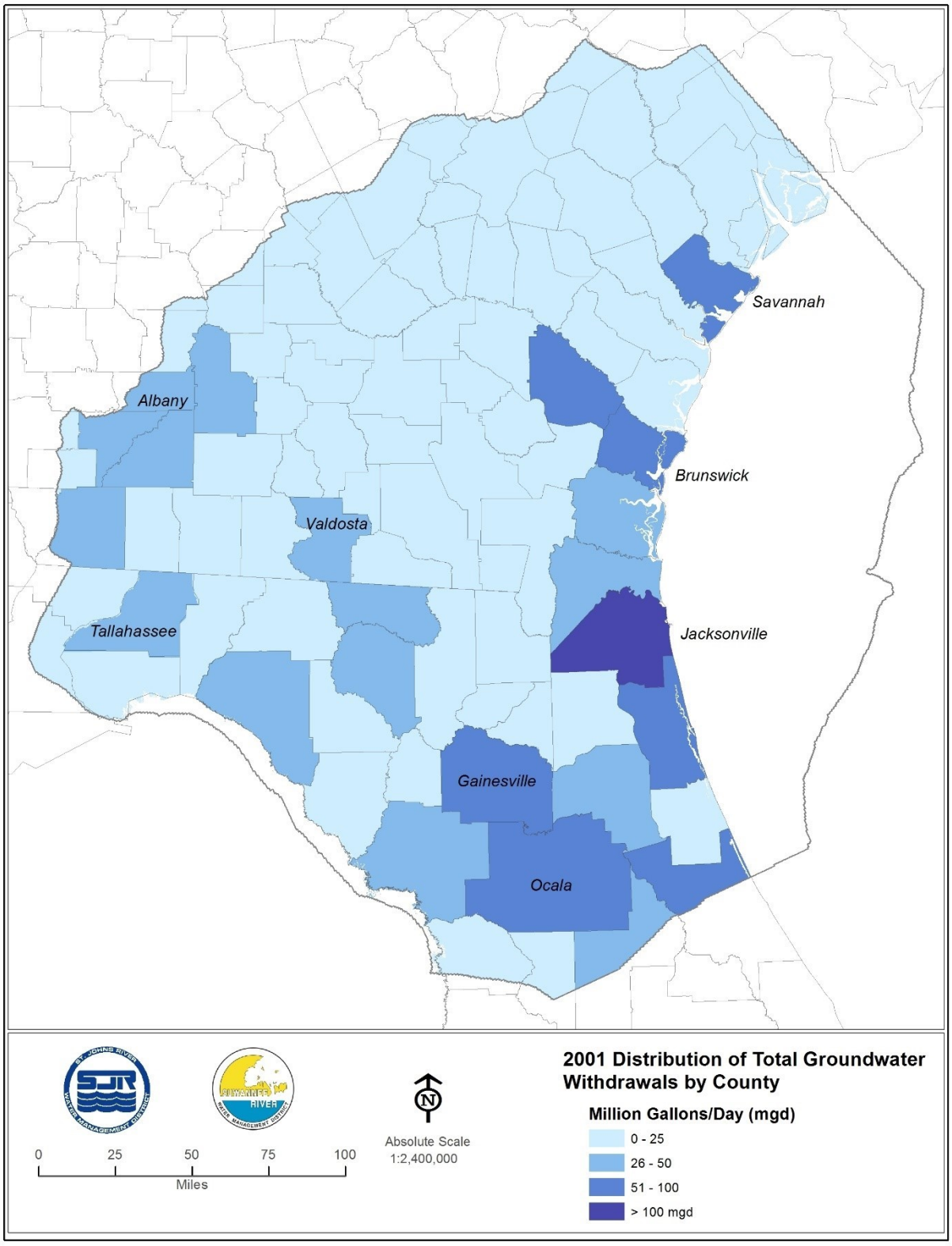

Figure 2-44. Distribution of total groundwater withdrawals by county (MGD), 2001

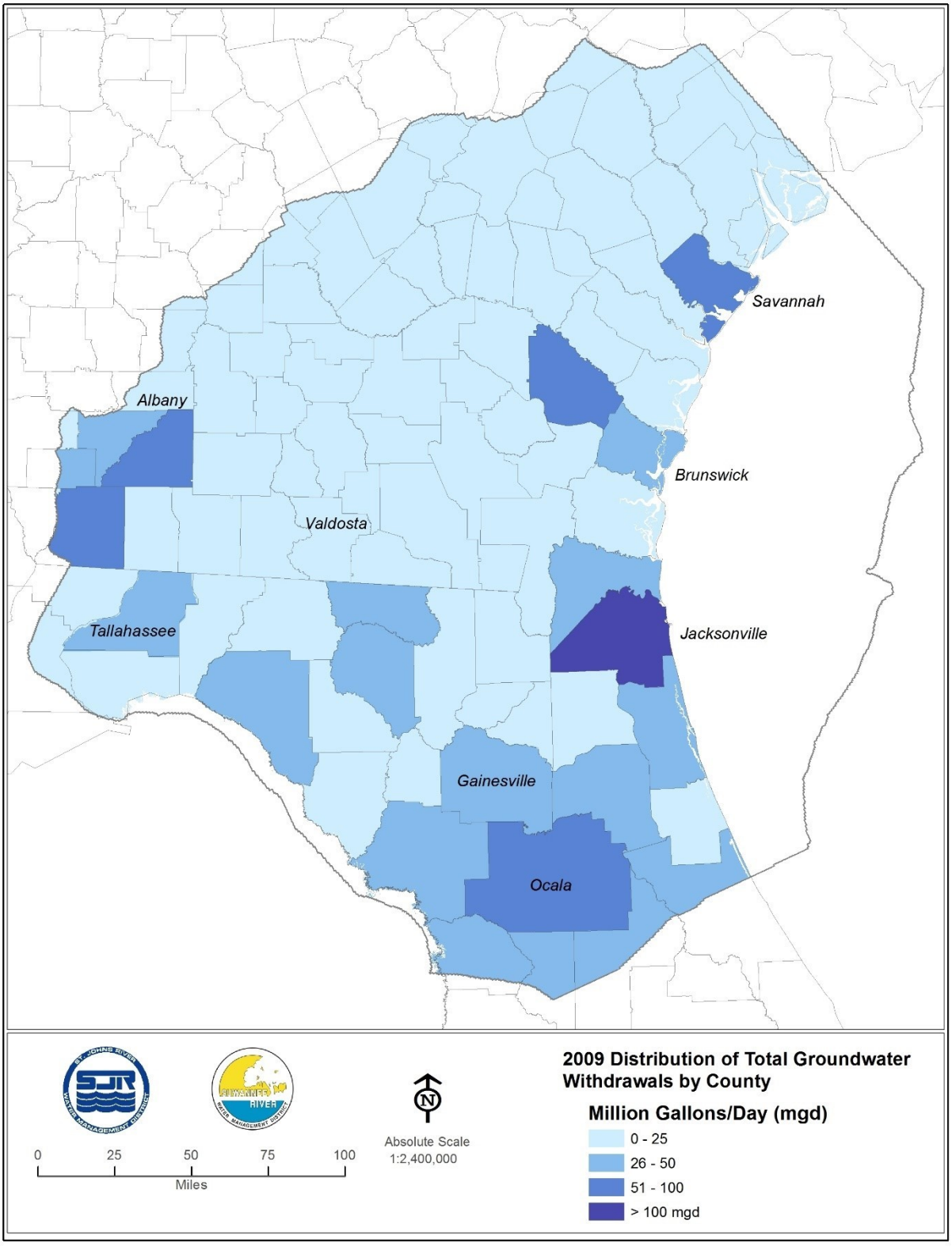

Figure 2-45. Distribution of total groundwater withdrawals by county (MGD), 2009

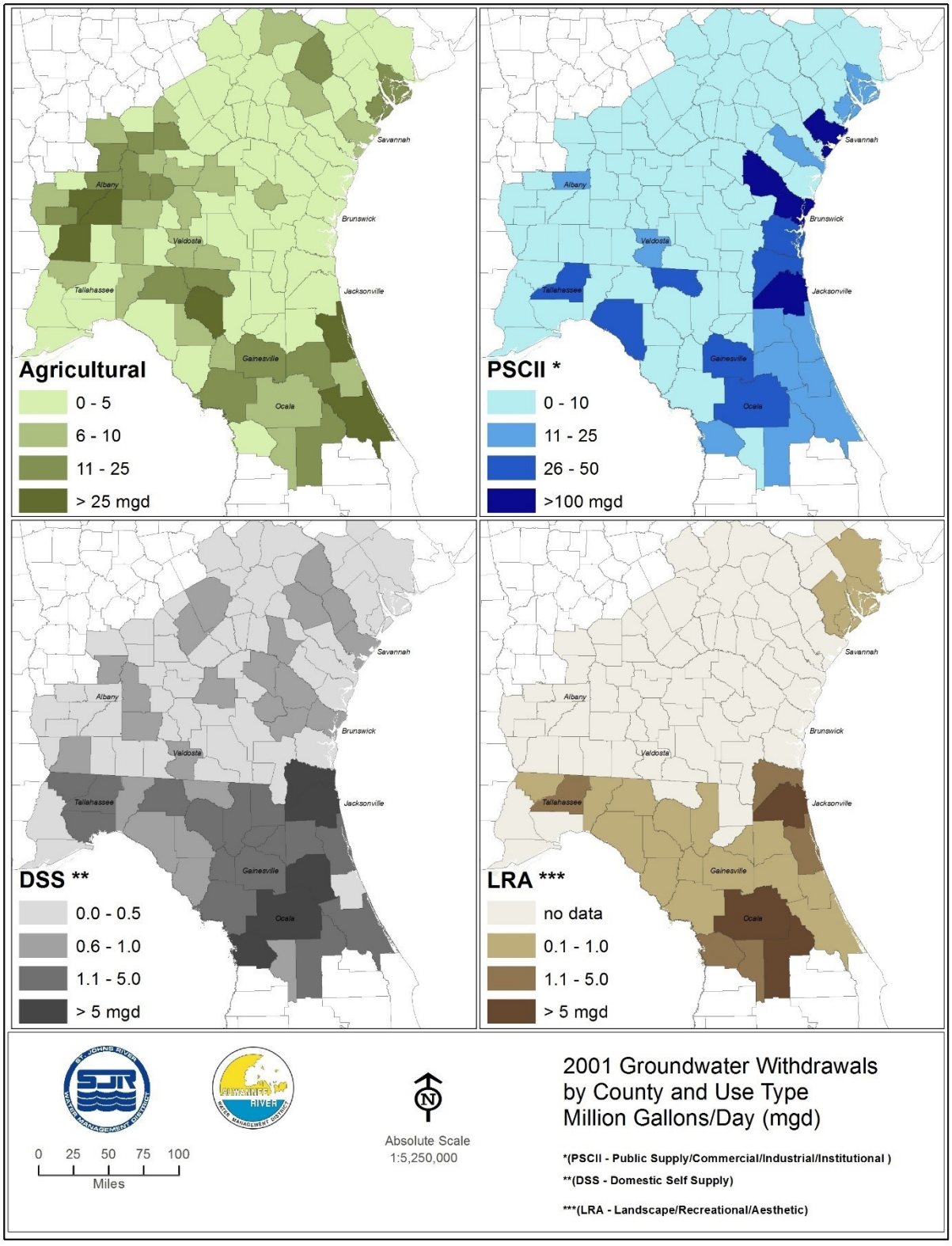

Figure 2-46. Groundwater withdrawals by county and use type (MGD), 2001

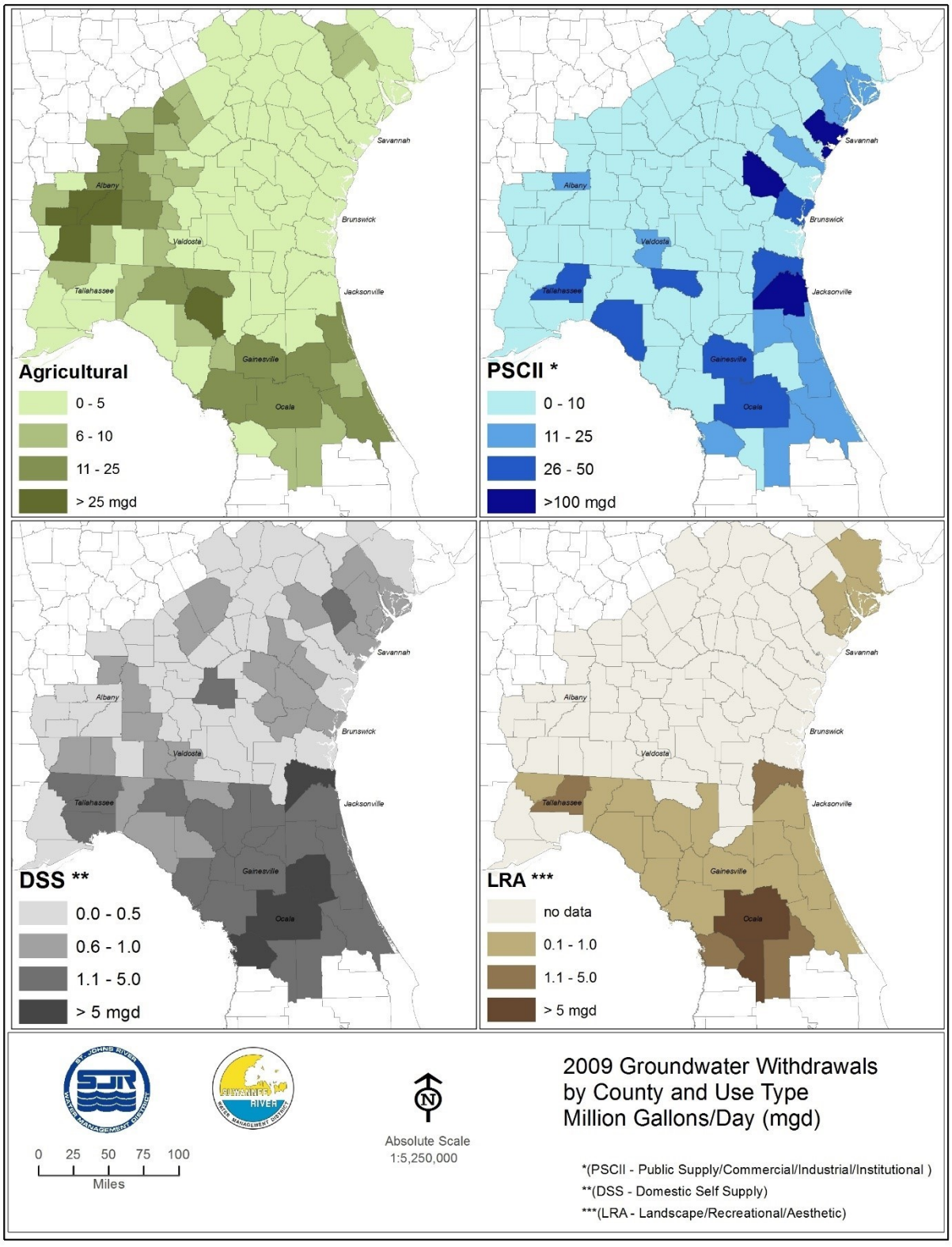

Figure 2-47. Groundwater withdrawals by county and use type (MGD), 2009

CHAPTER 3. MODEL CONFIGURATION

At its maximum extent, the active domain of the NFSEG model corresponds to portions of three states - Florida, Georgia, and South Carolina, and portions of the Atlantic Ocean and the Gulf of Mexico - an area of approximately 60,000 square miles (Figure 3-1). In its present form, the model is fully three dimensional and steady state and has been calibrated to hydrologic conditions of years 2001 and 2009. The model consists of seven active layers that represent, from top to bottom, the surficial aquifer (where present, or the unconsolidated sediments overlying the Upper Floridan aquifer otherwise), the intermediate aquifer or intermediate confining unit (where present, Upper Floridan aquifer otherwise), the Upper Floridan aquifer, the middle confining unit (MCU) or the Upper Floridan aquifer where the MCU is absent, the Lower Floridan aquifer (or the Upper Floridan aquifer where the MCU is absent or the upper zone of the Lower Floridan aquifer within the extent of the Fernandina Permeable zone), the lower semi-confining unit and the Fernandina Permeable zone of the Lower Floridan aquifer, where these hydrogeologic units are present (Table 3-1).

MODEL CODE SELECTION

The NFSEG model is an application of the MODFLOW-NWT (Niswonger et al. 2011) formulation of the MODFLOW 2005 (Harbaugh 2005) groundwater flow simulation software. MODFLOW-NWT was developed to provide an improved method for addressing numerical difficulties that result from the nonlinearity of the unconfined groundwater flow equation. More specifically, as compared to other versions of MODFLOW, MODFLOW-NWT provides enhanced rewetting capabilities in simulations of the water table of unconfined aquifers. Unconfined conditions occur throughout the area corresponding to the NFSEG model domain in the surficial aquifer or in outcrops of the intermediate confining unit or the Upper Floridan aquifer.

The ability of MODFLOW-NWT to represent drying and rewetting processes effectively was the primary consideration in its selection for use in the NFSEG model development. Other important considerations were the ability of MODFLOW-NWT to represent aquifer systems in a fully three-dimensional manner under both steady state and transient conditions. In addition, as a product of the U.S. Geological Survey, MODFLOW-NWT is recognized worldwide, resides in the public domain, and is available for download as executable and source code at no cost to the user.

The geometries and locations of conduits providing preferential flow to springs within the Floridan aquifer are unknown or poorly known in most cases. An exception to this within the NFSEG model domain is Wakulla Springs, a first order magnitude spring with a mean flow rate exceeding 400 cubic feet per second (cfs). An extensive network

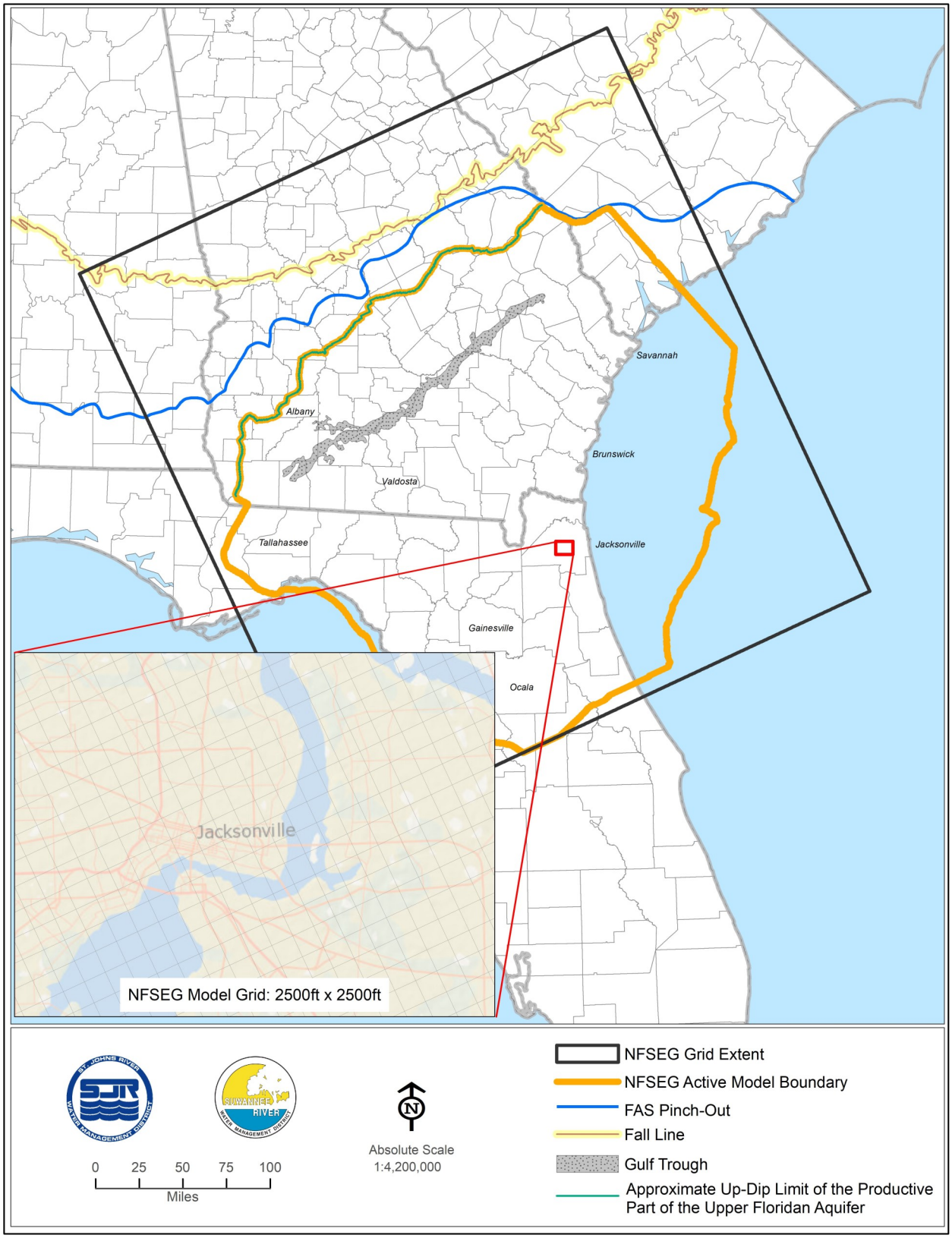

Figure 3-1. NFSEG model grid

Table 3-1. Represented hydrogeologic units of NFSEG model layers

<table>
<tr><th rowspan="2">Series</th><th colspan="2">Downdip of Gulf Trough</th><th colspan="2">Updip of Gulf Trough</th></tr>
<tr><th>Hydrogeologic Unit</th><th>Model Layer</th><th>Hydrogeologic Unit</th><th>Model Layer</th></tr>
<tr><td>Post-Miocene</td><td>Surficial Aquifer System</td><td>Layer 1</td><td>Surficial Aquifer System</td><td>Layer 1</td></tr>
<tr><td>Miocene</td><td>Intermediate Aquifer System/Intermediate Confining Unit</td><td>Layer 2</td><td>Intermediate Aquifer System/Intermediate Confining Unit</td><td>Layer 2</td></tr>
<tr><td>Oligocene</td><td rowspan="2">Upper Floridan Aquifer</td><td rowspan="2">Layer 3</td><td>Upper Floridan Aquifer</td><td rowspan="2">Layer 3</td></tr>
<tr><td>Upper Eocene</td><td>Pearl River Aquifer Confining Unit</td></tr>
<tr><td rowspan="3">Middle Eocene</td><td>Middle Semiconfining Unit; East: Lower Permeability; West: Higher Permeability or part of the transmissive system</td><td>Layer 4</td><td rowspan="4">Pearl River Aquifer</td><td>Layer 4</td></tr>
<tr><td rowspan="2">Lower Floridan Aquifer (Upper Zone)</td><td rowspan="2">Layer 5</td><td rowspan="2">Layer 5</td></tr>
<tr><td rowspan="2">Lower Eocene</td></tr>
<tr><td>Lower Semiconfining Unit</td><td>Layer 6</td><td>Layer 6*</td></tr>
<tr><td>Paleocene</td><td rowspan="2">Lower Floridan Aquifer (Fernandina Permeable Zone)</td><td rowspan="2">Layer 7</td><td>Chattahoochee River Aquifer Confining Unit</td><td rowspan="2">Layer 7*</td></tr>
<tr><td>Upper Cretaceous</td><td>Sub-Floridan Confining Unit</td><td>Inactive</td><td>Chattahoochee River Aquifer</td></tr>
<tr><td colspan="4">*Layer not represented</td><td>Inactive</td></tr>
</table>

of conduits supplying preferential flow to Wakulla Springs has been mapped through underwater cave exploration (Rupert 1988; Lane 2001; http://www.usdct.org/wakulla2.php; http://www.gue.com; http://www.wkpp.org). An additional network of conduits has been inferred through knowledge of the hydrological system, evaluation of solute travel times, and calibration of existing groundwater models (Davis 1996; Davis and Katz 2007; and Davis and others 2010). The simulation of groundwater flow within the Floridan aquifer and the surrounding area, including Wakulla Springs and its network of mapped and inferred conduits, using the standard MODFLOW approach (i.e., with simulated groundwater flow represented as Darcian flow), was shown by Kuniansky (2016) to compare well to that of an alternative MODFLOW model. Conduit flow, in the alternative MODFLOW model, to Wakulla Springs was represented more rigorously using the MODFLOW Conduit Flow Package (Shoemaker et al. 2008). The results of the study indicated that the presence of conduits, even an extensive network of relatively large conduits such as that of Wakulla Springs, should not necessarily preclude application of the standard Darcian flow approach for simulation of flows that are averaged over a month or longer or flows that are simulated on a regional to subregional scale (Kuniansky 2016). Based on these results and given the large extent of the Wakulla Springs conduit system and the relatively large sizes of its mapped and inferred conduits, the standard MODFLOW approach is assumed to be applicable throughout the NFSEG model domain

NFSEG GRID

The NFSEG model grid consists of 752 rows and 704 columns. The grid cells are uniformly 2,500 feet (ft) by 2,500 ft in dimension horizontally (Figure 3-1). The NFSEG model grid is nested within that of an early version of the grid of the U.S. Geological Survey system-wide groundwater flow model (http://fl.water.usgs.gov/floridan/numerical-model.html), which has since been revised. The size of the grid cells relative to the extent of the active model domain provides a high degree of resolution in the representation of the regional groundwater system without overburdening the NWT solver routine. Grid uniformity lends towards simplicity of design and supports the potential for equally good representation of all major regions within the area corresponding to the model domain.

The grid-cell size employed in NFSEG (2,500 feet by 2,500 feet) is consistent with that of most other regional-scale models employed by the Districts for regulatory and/or planning purposes in areas that overlap significantly with its domain. Examples include the North Florida version 2 model (NF v2; Intera Inc. 2014), the Northeast Florida version 3 model (NEF v3; Russo 2011), the North-Central Florida version 2 model (NCF v2; Motz and Dogan 2004), the Volusia model (Williams 2006), and the East-Central Florida model (ECF; McGurk and Presley 2002). All these models have uniform grids that are comprised of grid cells that are 2,500 by 2,500 feet in dimension. The NEF v3, NCF v2, Volusia, and ECF grids nest within that of the Peninsular Florida version 2 (PF v2; Intera, Inc. 2011) model, also known as the "Mega-Model," which has a uniform grid-cell size of 5,000 by 5,000 feet. The East-Central Florida Transient (ECFT) model has a somewhat smaller uniform grid-cell size of 1,250 by 1,250 feet. Nevertheless, precedent for uniform grids comprised of grid cells with dimensions of 2,500 feet by

2,500 feet is well established within the domain of NFSEG and in nearby areas.

The NFSEG model was constructed using an Albers Equal Area Map Projection, with the following specifications:

Projection: Albers
False_Easting: 0.0
False_Northing: 0.0
Central_Meridian: -84.0
Standard_Parallel_1: 29.5
Standard_Parallel_2: 45.5
Latitude_Of_Origin: 23.0
Linear Unit: Meter (1.0)

Geographic Coordinate System: GCS_North_American_1983
Angular Unit: Degree (0.0174532925199433)
Prime Meridian: Greenwich (0.0)
Datum: D_North_American_1983
Spheroid: GRS_1980
Semimajor Axis: 6378137.0
Semiminor Axis: 6356752.314140356
Inverse Flattening: 298.257222101

The above specifications are referred to as NAD83 Albers, meters, horizontal coordinate system. This custom projection was provided early in the model development by the USGS (Jason Bellino, personal communication 2011). The vertical datum used for all elevation data in this study is feet above the North American Vertical Datum of 1988 (NAVD 1988).

MODEL LAYERS

Each of the seven NFSEG model layers generally represents a single hydrogeologic unit, although there are some important exceptions (Table 3-1). In areas in which the estimated thickness of a given hydrogeologic unit is less than a layer specified minimum, the corresponding grid cells of the layer are assigned the minimum thickness of that layer in place of the estimated thickness (Tables 3-1 and Table 3-2; Figures 3-2 through 3-7). The hydraulic properties assigned to these grid cells, which are calibration derived, represent vertically averaged composite values of the primarily represented hydrogeologic unit, assuming it is present, and the included portions of the hydrogeologic units that bound it above and/or below. This approach is implemented in the representations of all primarily represented hydrogeologic units (Tables 3-1 and 3-2). It is referred to hereafter as the "minimum thickness approach."

Although the minimum thickness approach is used in the representations of all hydrogeologic units represented in NFSEG, it is used most widely in respect to the surficial aquifer system and intermediate confining unit, which are represented primarily by model

Layers 1 and 2, respectively (Tables 3-1 and 3-2; Figures 3-2 through 3-7). Relatively small and isolated (laterally discontinuous) areas of both hydrogeologic units can occur within portions of the unconfined region of the model domain (Figures 2-4 and 2-7), and their geographic distributions can be quite complex. They range in area from less than that of a single grid cell (0.22 square miles) to collective areas of many grid cells (Figures 2-4 and 2-7). For either unit, where the estimated thickness is less than 30 feet (ft), a minimum thickness of 30 ft is assigned, and the top and bottom elevations of underlying model layers are adjusted as needed to also maintain their respective minimum thicknesses. This means that no grid cells are designated as inactive within the active extents of Layers 1 and 2, regardless of whether the surficial aquifer system or intermediate confining unit is present. The same also applies to the representations of all primarily represented hydrogeologic units in the other respective model layers. Unconsolidated sediments make up Layers 1 and 2 as well as in the regionally unconfined area. They are typically unsaturated, seasonally saturated, or saturated but without a discernible vertical head difference between them and the Floridan aquifer system.

It is presumed in the calibration process that in the unconfined zones of the Floridan aquifer system, the uppermost 30 feet of hydrogeologic material resembles the surficial aquifer system more closely than the Floridan aquifer system in its hydraulic properties. Therefore, Layer 1 horizontal hydraulic conductivities in the unconfined zones of the Floridan aquifer system are limited to 50 ft/d, as they are in the remaining part of the model domain (as a maximum hydraulic conductivity value for sand, silts, and clayey sand). In Layer 2, the value of vertical hydraulic conductivity assigned to a given Layer 2 grid cell in an unconfined zone (where the intermediate confining unit was mapped as having a thickness of less than 30 feet), the hydraulic properties are assumed to be equal to the value assigned to the Layer 3 grid cell of the same vertical column of grid cells. This is because Layer 2 is presumed to correspond more closely to the Floridan aquifer system than to the surficial aquifer system or the intermediate confining unit because of its depth, keeping in mind that depth to the top of the Floridan aquifer system in unconfined regions is usually small (less than 30 ft). The decrease in

Table 3-2. Minimum layer thicknesses

NFSEG Model Layer	MODFLOW-NWT UPW Layer-Type Designation	Applied Minimum Thickness (Feet)
1	Unconfined	30
2	Confined	30
3	Confined	50
4	Confined	30
5	Confined	50
6	Confined	10
7	Confined	10

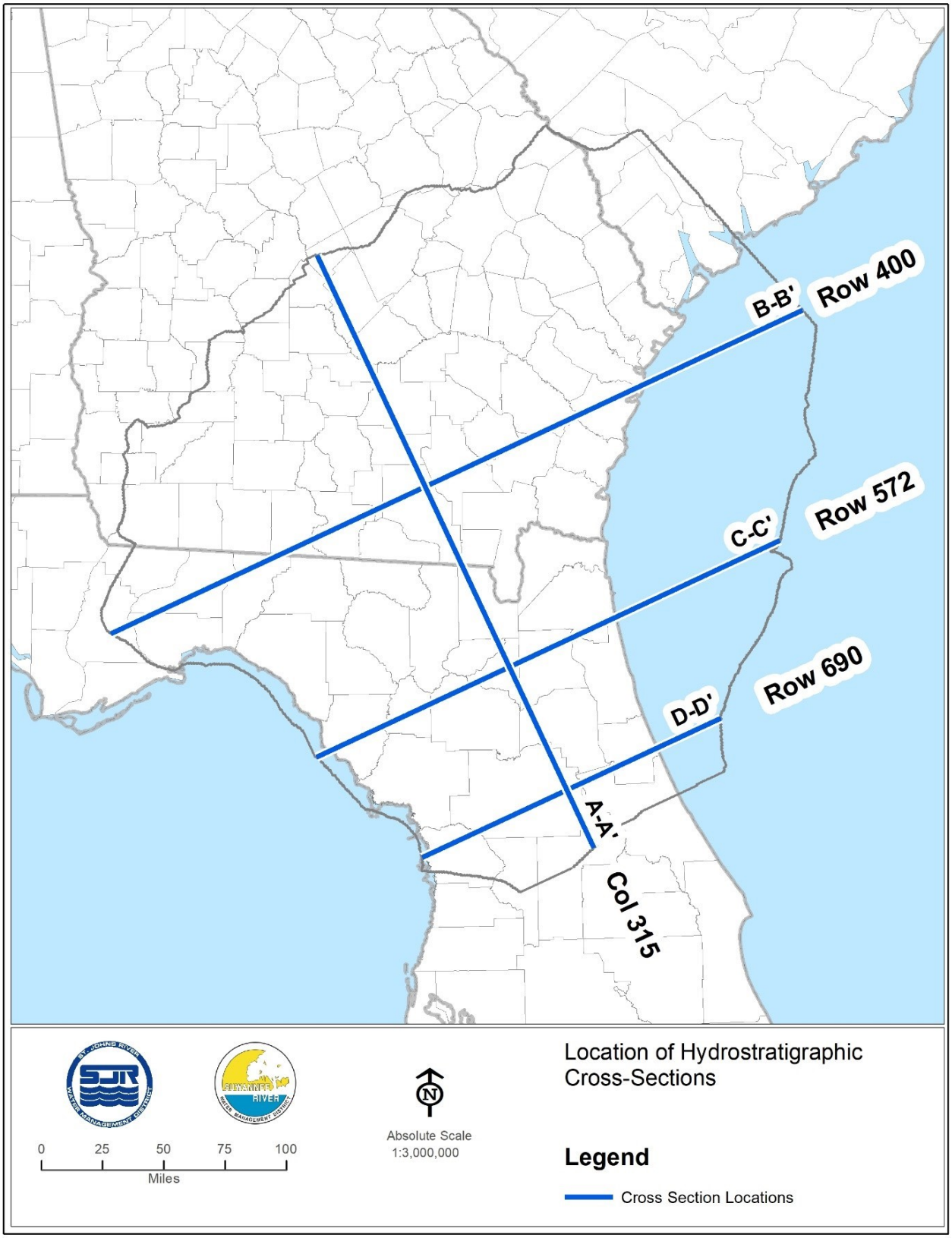

Figure 3-2. Locations of hydrogeologic cross sections

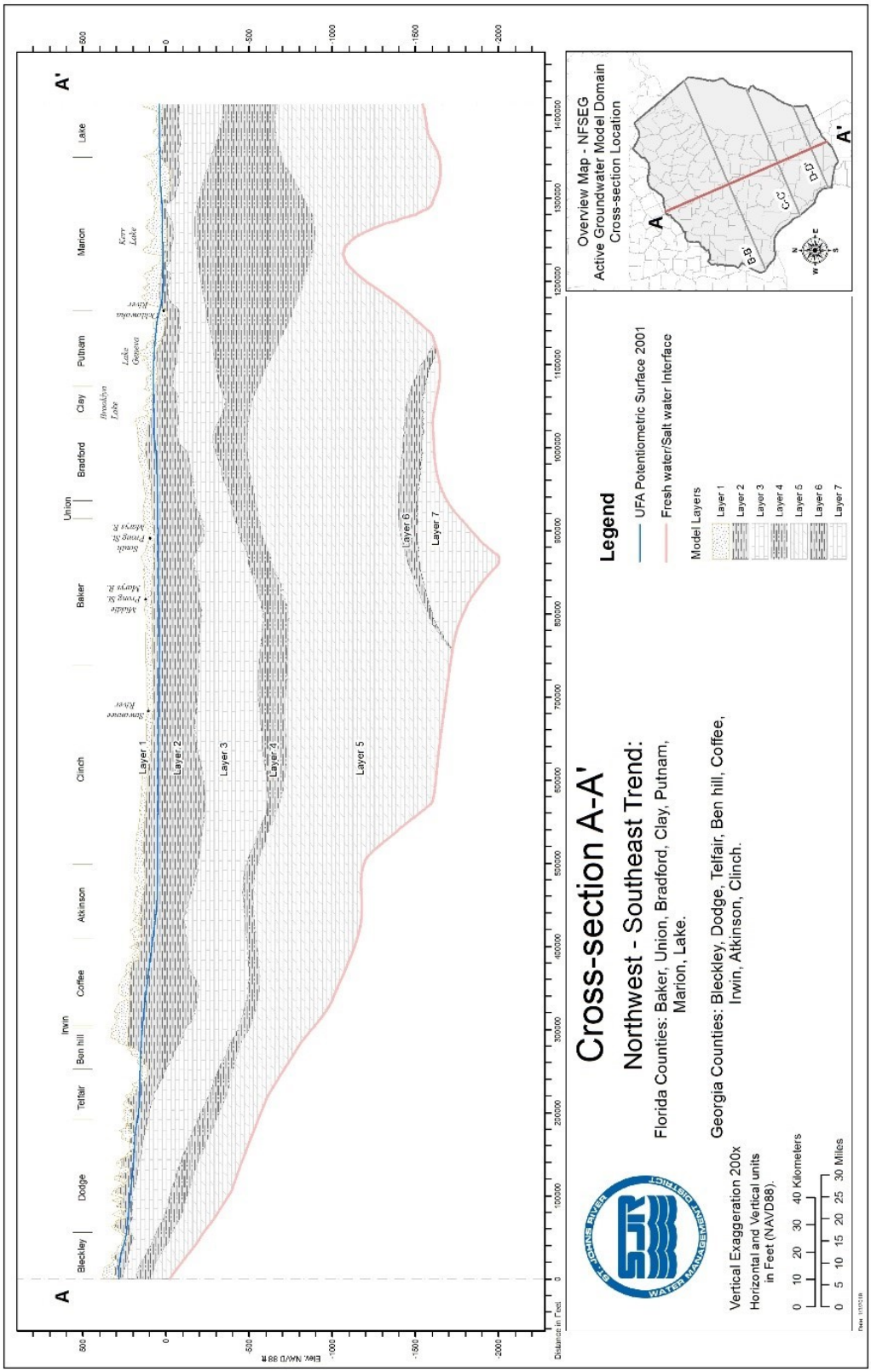

Figure 3-3. Hydrogeologic cross section A-A'

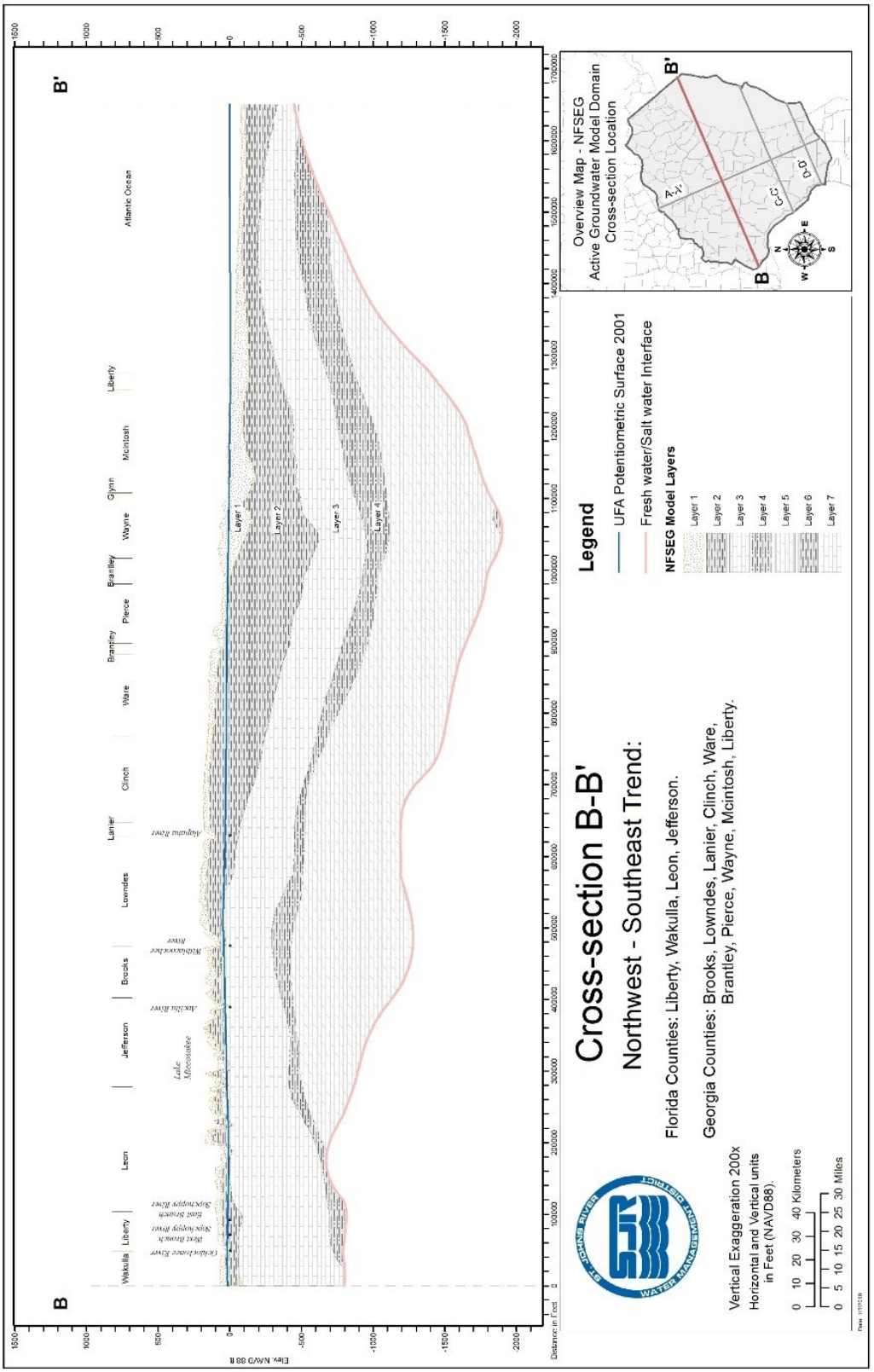

Figure 3-4. Hydrogeologic cross section B-B'

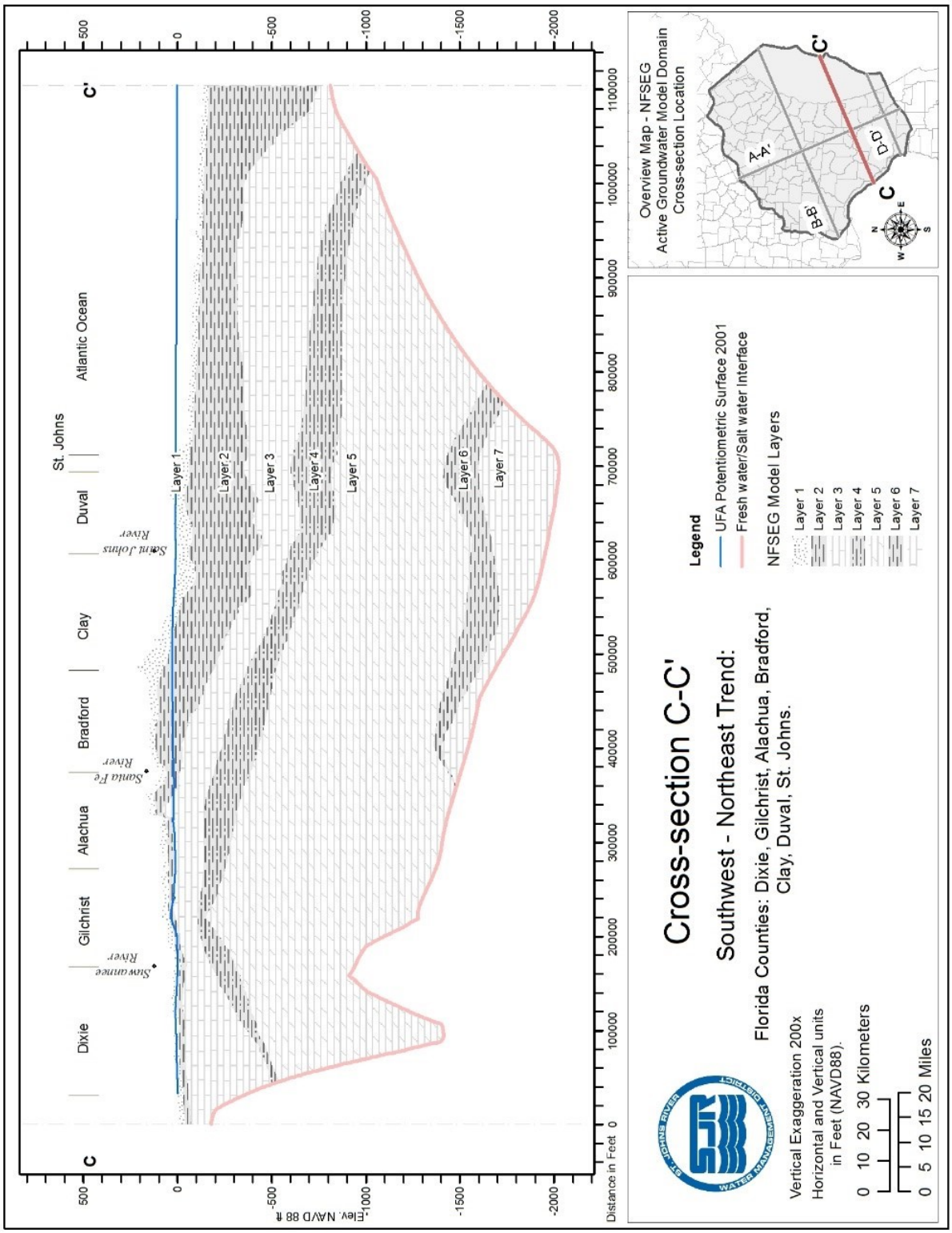

Figure 3-5. Hydrogeologic cross section C-C'

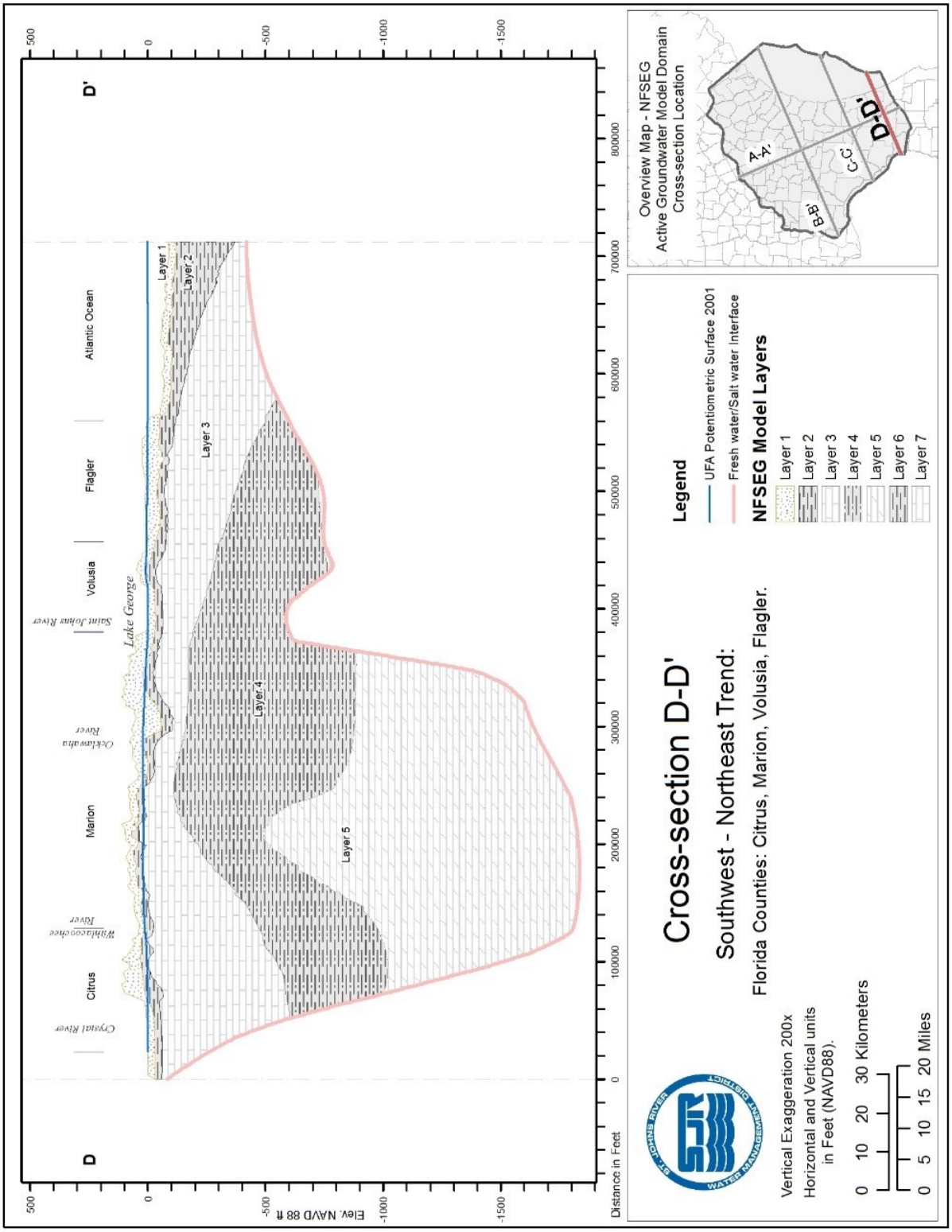

Figure 3-6. Hydrogeologic cross section D-D’

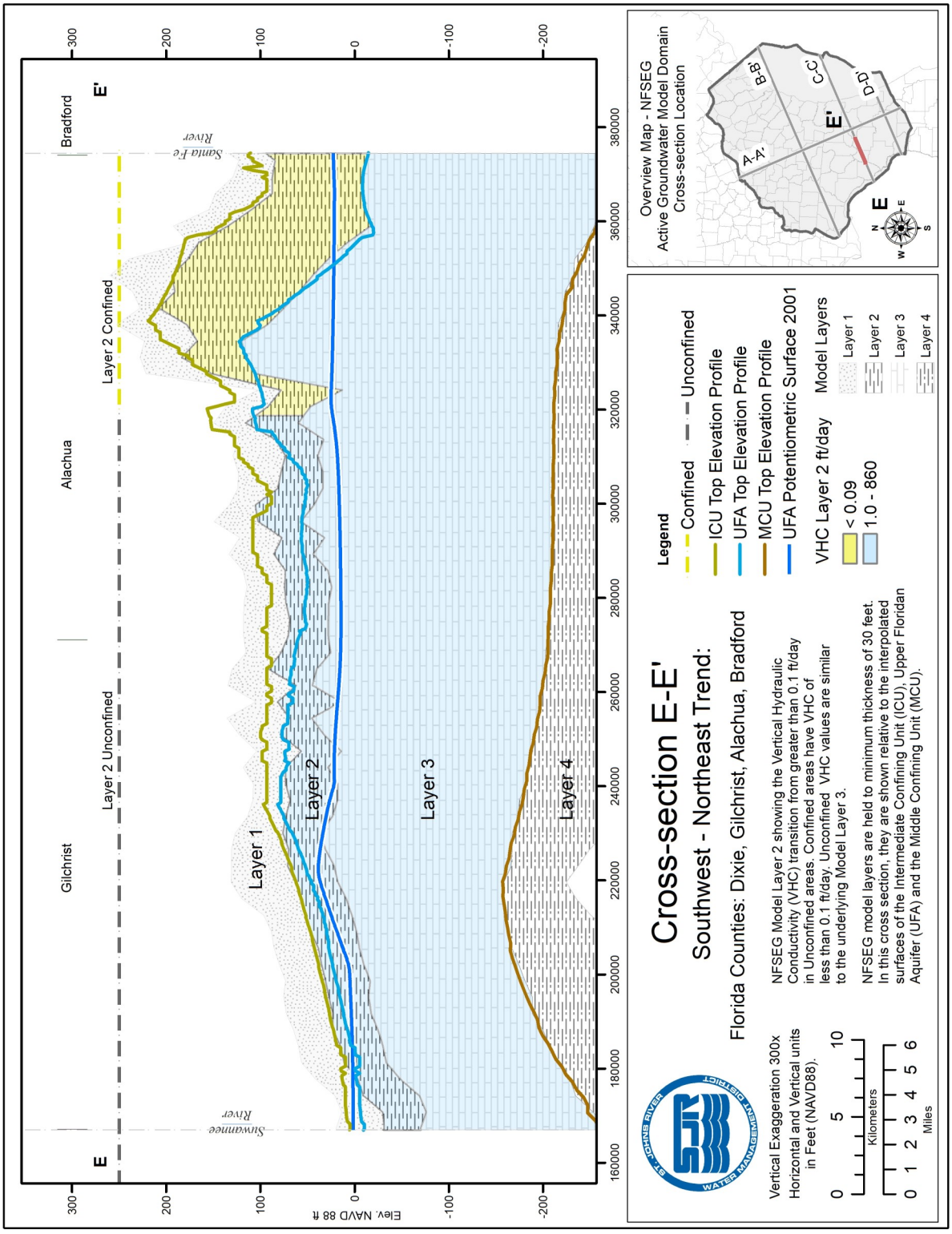

Figure 3-7. Hydrogeologic cross section E-E'

layer thickness of model Layer 3 required to implement minimum layer thicknesses for Layers 1 and 2 is relatively small in most instances, so effects on transmissivity calculations are small. Nevertheless, separate maps of the transmissivity of Layer 3 versus estimates for the entire thickness of upper Floridan aquifer, both resulting from model calibration, are provided in section 4, which contains the description of the model calibration process.

Limiting correspondence of layer grid cells to the representation of only one hydrogeologic unit is feasible in a large portion of the NFSEG active model domain, and where this is the case, model grid cells of a given layer correspond entirely to one hydrogeologic unit only. Restricting grid cell representation of large regions within a layer is often desirable, because it can facilitate aspects of the model development, such as simplifying the pre- and postprocessing necessary to implement model calibration. However, in the unconfined zones of the Floridan aquifer system, this approach is impractical because of system complexity and, furthermore, would likely contribute to numerical instability.

An additional advantage of the minimum thickness approach lies in the relative simplicity afforded by it in implementing internal boundary conditions, such as the MODFLOW River and Drain Packages. In all but a few cases, river boundaries are assigned to Layer 1 or 2, and in all cases, drain boundaries are assigned to Layer 1. In all cases, maximum saturated evapotranspiration is assigned to Layer 1, as all extinction depths are contained within Layer 1. This is all possible because of the minimum thickness of 30 ft assigned to Layers 1 and 2. The minimum thickness approach also allows for refining the assignment of hydraulic properties described above through the calibration process. Thus, unnecessarily detailed representations of complex distributions of surficial aquifer system and intermediate confining unit outliers (whose locations and properties may not be well defined) are avoided, and whose portrayal as scattered "islands" of active grid cells would likely undermine model stability.

Layer 1

Layer 1 is used primarily to represent the surficial aquifer system, as discussed above (Tables 3-1 and 3-2). Outside the contiguous extent of the surficial aquifer system, individual grid cells of Layer 1 represent a composite of the surficial aquifer system, the intermediate confining unit, and/or the Upper Floridan aquifer. The active areal extent of Layer 1 was made equivalent to that of Layer 3. The top, bottom, and thickness of Layer 1 are depicted on Figures 3-8, 3-9, and 3-10, respectively. Details regarding the determination of the active areal extent of Layer 3 are provided in the discussion of Layer 3 below.

Layer 2

Layer 2 is used primarily to represent the intermediate confining unit (Tables 3-1 and 3 -2). Outside the contiguous extent of the intermediate confining unit, individual grid cells of Layer 2 are assumed to represent the intermediate confining unit or the Upper

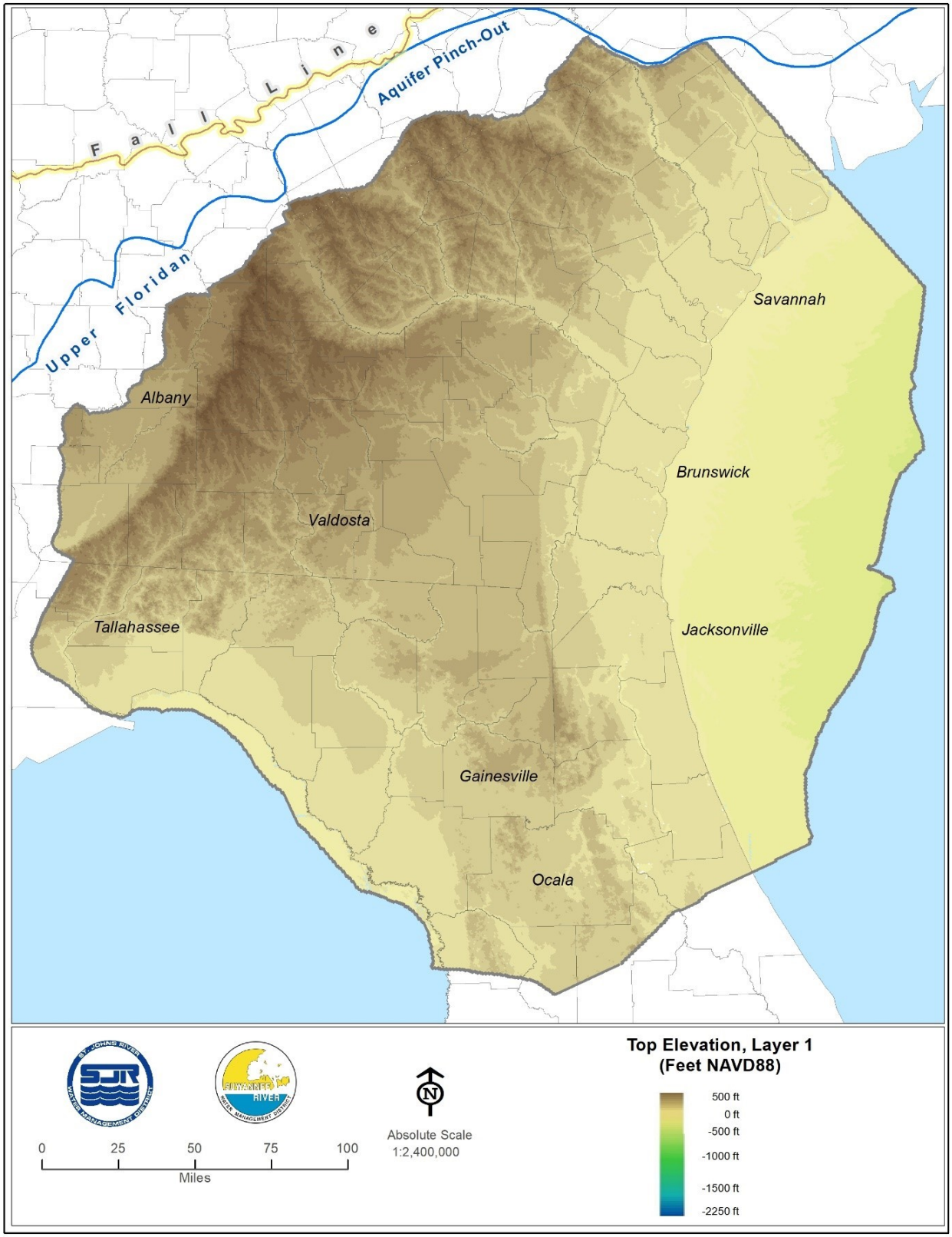

Figure 3-8. Top elevation, Layer 1 (Feet NAVD88; after Boniol and Davis, digital communi cation, 2013)

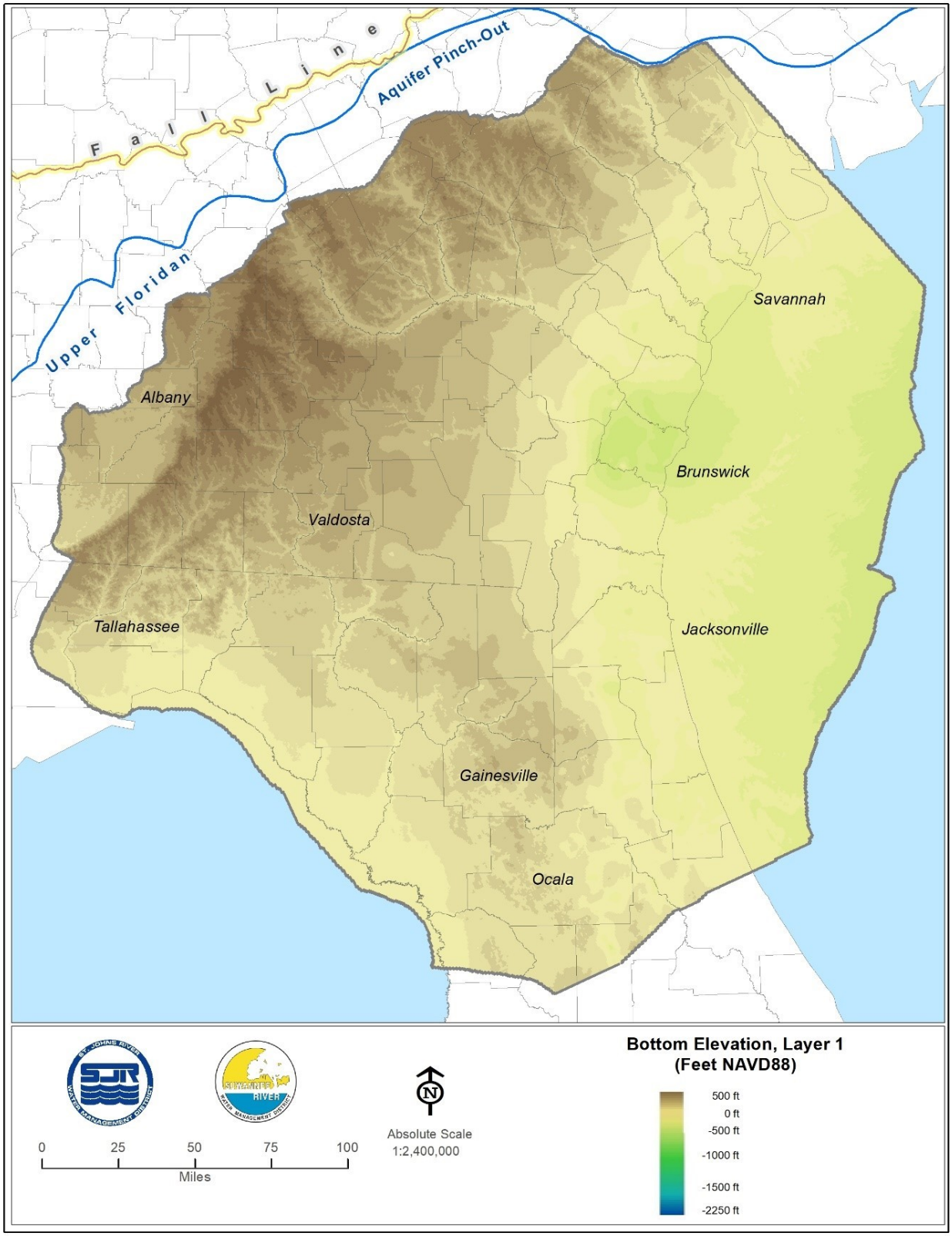

Figure 3-9. Bottom elevation, Layer 1 (and Top Elevation, Layer 2; Feet NAVD88; after Bo niol and Davis, digital communication, 2013)

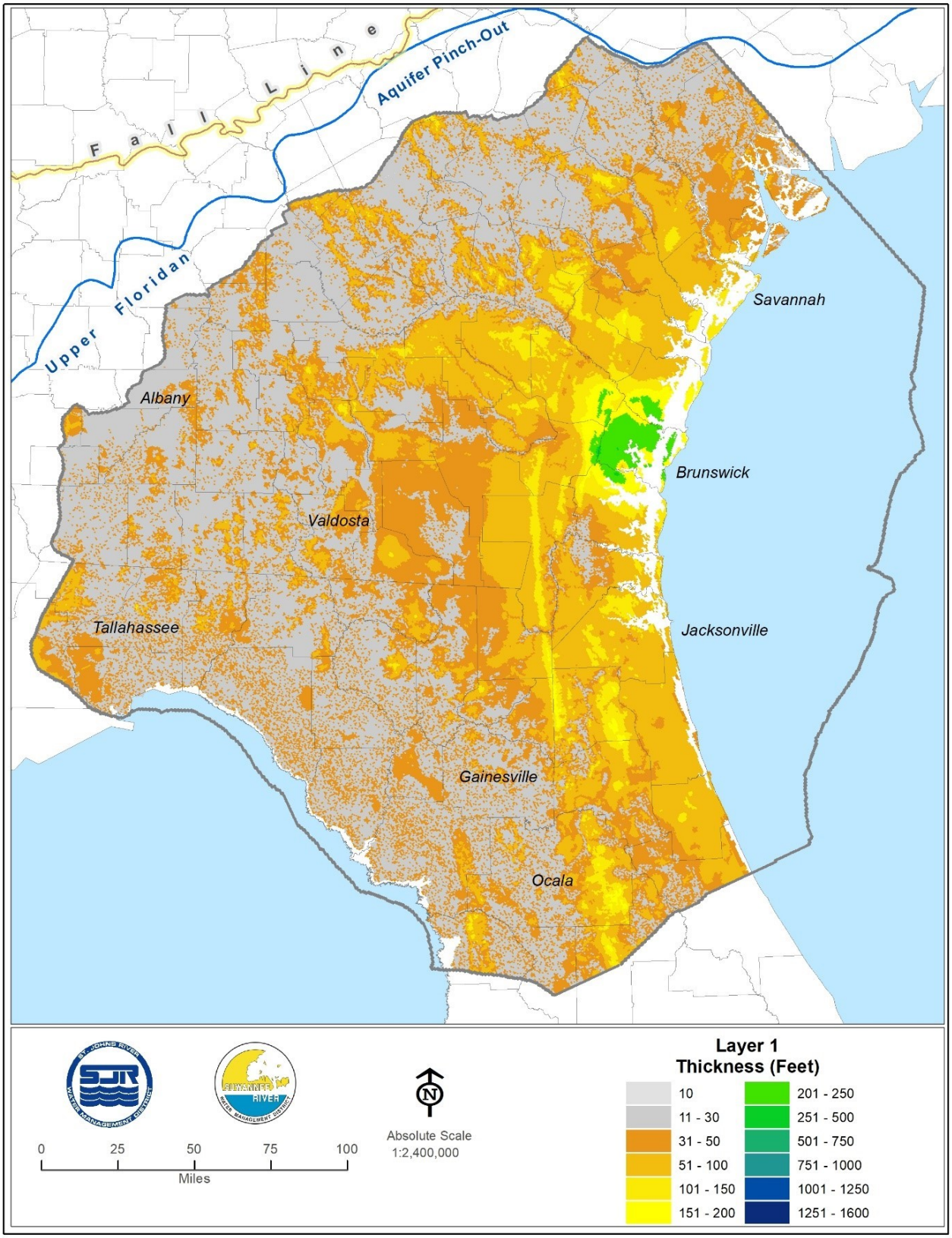

Figure 3-10. Thickness, Layer 1 (Feet)

Floridan aquifer. Although Layer 2 represents the intermediate confining unit, or the Upper Floridan aquifer in the noncontiguous extent of the intermediate confining unit, it is assumed in the model calibration process, described in detail in section 4, that the hydraulic properties of Layer 2 resemble those of the Floridan aquifer system more closely than those of the intermediate confining unit in these areas. For this reason, calibration determined vertical hydraulic conductivity values assigned to grid cells in the noncontiguous areas of the intermediate confining unit are biased towards the values assigned to corresponding Layer 3 grid cells. The areal extent of Layer 2 was made equivalent to that of Layer 3. The top, bottom, and thickness of Layer 2 are depicted on Figures 3-9, 3-11, and 3-12, respectively. Details regarding the determination of the areal extent of Layer 3 are provided in the discussion of Layer 3 below.

Layer 3

Layer 3 is used primarily to represent the Upper Floridan aquifer. Where the Upper Floridan aquifer is not present as a separate hydrogeologic unit (i.e., where the middle confining unit is effectively absent), Layer 3 represents a shallower section of the Floridan aquifer system (Zone 1 of the present study, as noted in Table 2.2). The assigned minimum layer thickness of model Layer 3 is 60 ft (Tables 3-1 and 3-2; Figures 3-11, 3 -13, and 3-14).

The primary consideration in specifying the locations of the lateral boundaries of Layer 3 was to eliminate or at least minimize their influences on critical portions of the active model domain. The approach for achieving this was to place the lateral boundaries, as much as feasible, at locations that correspond approximately to the physical boundaries of the Floridan aquifer system or the boundaries of freshwater flow therein. Where placement at physical boundaries was infeasible, placement was made at locations that are as far as feasible from areas of critical concern.

The domain of the NFSEG model is oriented along southwest-northeast and northwest-southeast alignments (Figure 3-1). Hence, the lateral limits of the model are defined by a northwest facing lateral boundary, a northeast facing lateral boundary, a southeast facing lateral boundary and a southwest facing lateral boundary. For simplicity, these are referred to hereafter as the northern, eastern, southern and western lateral boundaries, respectively. As stated previously, the general approach in specifying the locations of the lateral boundaries was to place them at the physical boundaries of the Upper Floridan aquifer or the limits of the freshwater flow system therein to the extent that such placement was feasible.

As model development proceeded, however, additional criteria were applied to enhance numerical stability. The implementation of these criteria resulted in changes in the northern, eastern, and western lateral boundaries and a corresponding reduction in the active areal extent of Layer 3 due to removal from the active model domain of grid cells that failed to meet the additional criteria. The additional criteria are as follows: (1) the freshwater thickness of the Upper Floridan aquifer was required to be at least 50 feet (prior to introduction of the minimum thickness); and (2) the height of the 2010 potentiometric surface as depicted by Kinnaman and Dixon (2011) was required to be

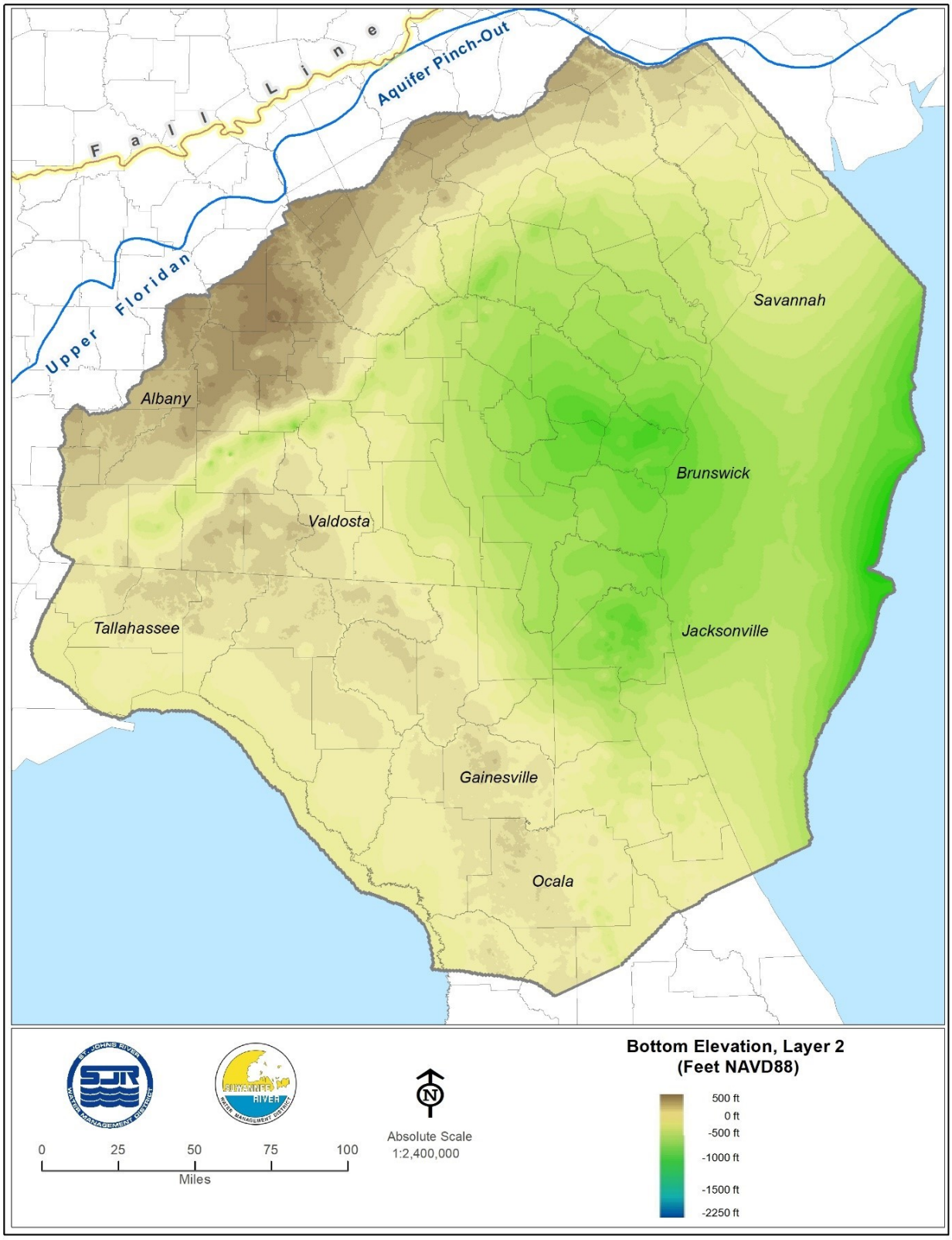

Figure 3-11. Bottom elevation, Layer 2 (and top elevation, Layer 3; after Boniol and Davis, digital communication, 2013)

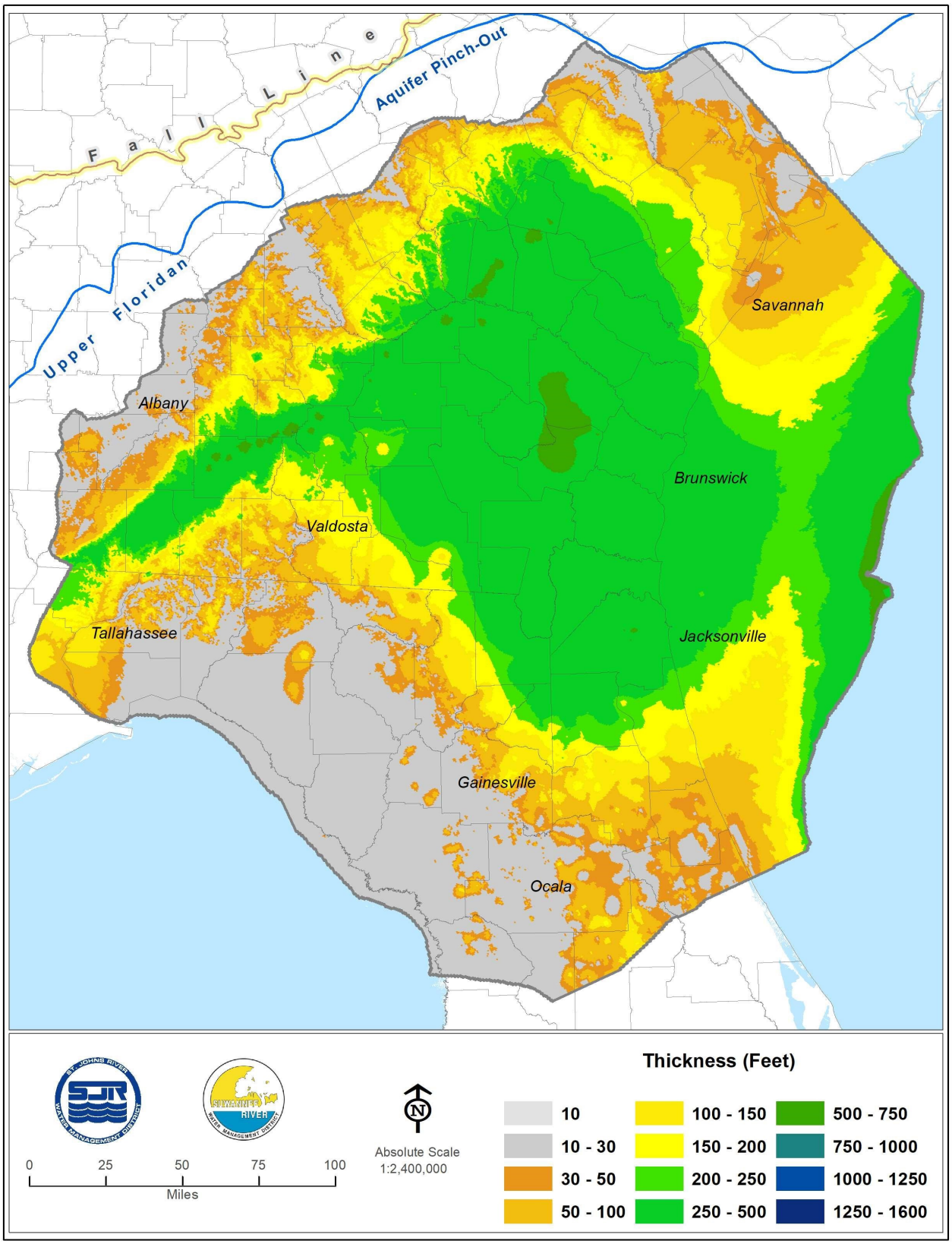

Figure 3-12. Thickness, Layer 2 (Feet)

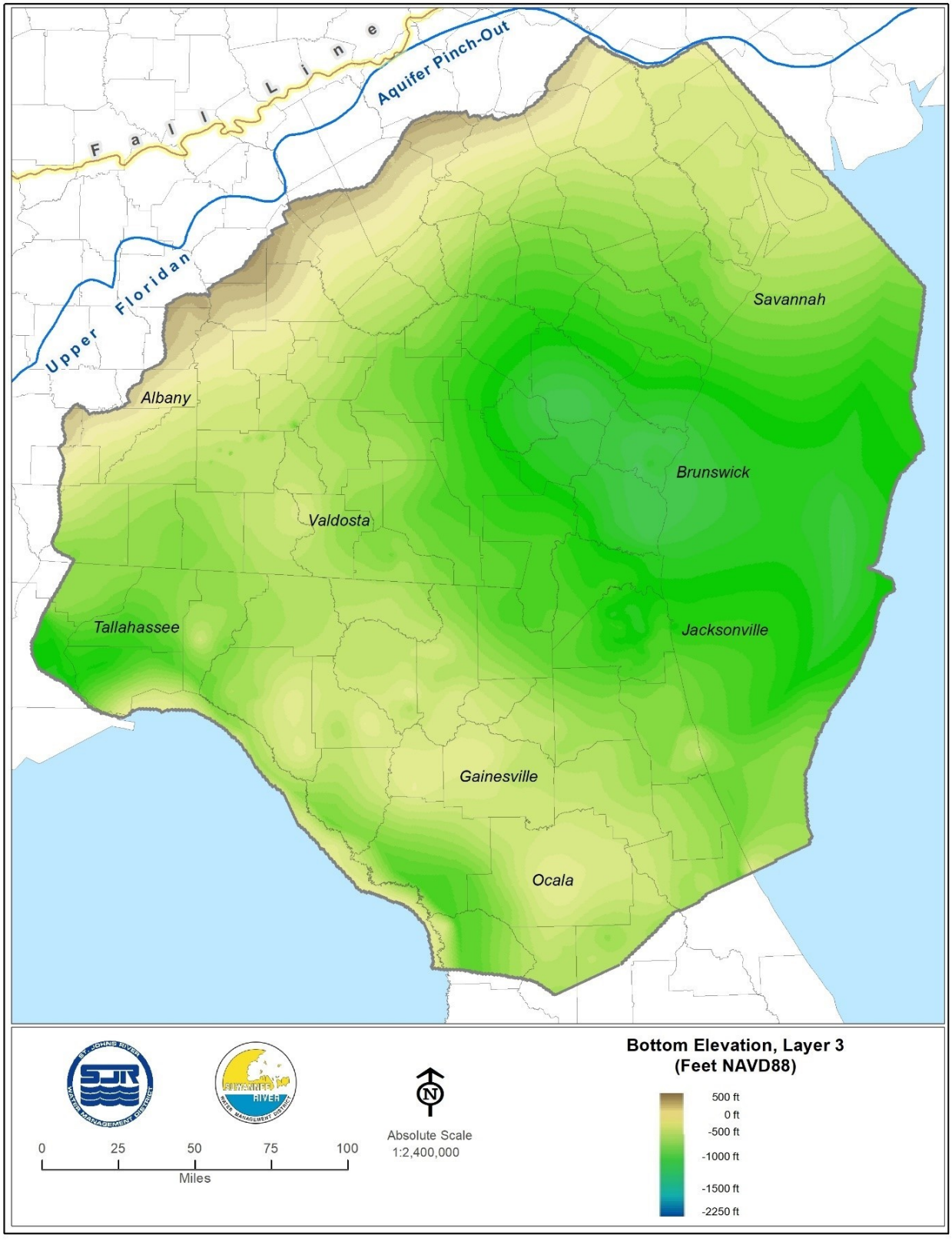

Figure 3-13. Bottom elevation, Layer 3 (and top elevation, Layer 4; feet NAVD88; after Bo niol and Davis, digital communication, 2013)

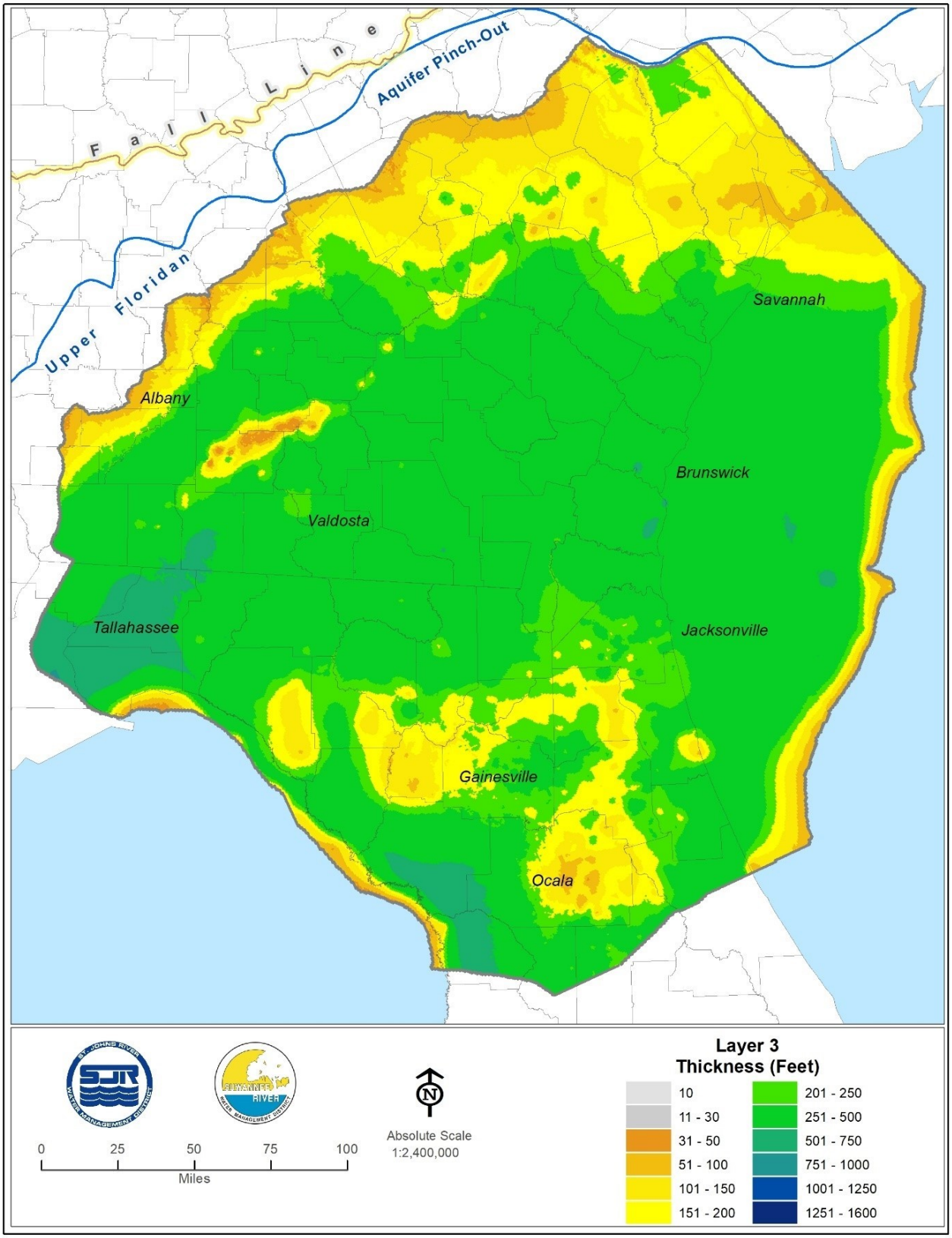

Figure 3-14. Thickness, Layer 3 (Feet)

at least 100 feet above the tops of the grid cells of Layer 4. The purpose of these criteria was to reduce or eliminate the tendency of grid cells located near the original northern and eastern lateral boundaries of Layers 3, 4 and 5 to desaturate due to numerical instability.

The physical boundary of the Upper Floridan aquifer north of the Gulf Trough in Georgia is its line of pinch-out, approximated by Williams and Kuniansky 2015 (Figure 2-1). Accordingly, prior to implementation of the additional criteria described above, the northern boundary of Layer 3 was set to coincide with this line. The active domain of Layer 3 in areas representative of portions of the Floridan aquifer system that lie beneath the Gulf of Mexico and the Atlantic Ocean extends to the approximate limits of freshwater flow within the Floridan aquifer system. In the case of the Atlantic Ocean, the seaward limit of freshwater flow in the Floridan aquifer system was assumed initially to be coincident with the onset of the Florida-Hatteras slope, a transition in depth that connects the relatively shallow waters of the continental shelf to the deeper waters of the Blake Plateau off the southeast coast of the United States (Milliman 1972). Accordingly, prior to implementation of the first of the two additional criteria listed above, the eastern seaward limit of model Layer 3 was set to correspond with the onset of the Florida-Hatteras slope.

Along the portions of the Gulf Coast that correspond in location to portions of the active model domain, the Floridan aquifer system is unconfined, and with aquifer hydraulic heads exceeding sea level by only a few feet. Therefore, it was assumed that the limit of freshwater flow in the Upper Floridan aquifer is within a relatively short distance seaward of the coast. Consequently, the lateral boundary of Layer 3 was made to correspond to locations that are within approximately five to 10 miles of the Gulf Coast, a distance that should be sufficient to include the limits of fresh groundwater flow in an unconfined, highly transmissive system.

Placement of the southern lateral boundary was designed to be of sufficient distance from critical areas to the north, such as the Keystone Heights potentiometric high and the Lower Suwannee River basin, so that influences of the southern lateral boundary would be negligible. The Silver and Rainbow springs complexes are highly influential features of the Floridan aquifer system within their respective springsheds. These springsheds, as delineated by Faulkner 1973 and Knowles 1996, are encompassed fully within the area corresponding to the NFSEG active model domain. The southern lateral boundary is delineated based on persistent features of the Upper Floridan aquifer potentiometric surface (e.g., Kinnaman and Dixon 2011), as discussed in greater detail below.

The implementation of the additional criteria stated above, resulted in a decrease in the size of the active model domain of Layer 3. The intersection of the estimated 10,000 mg/l TDS concentration iso-surface with the top of Layer 3 along the seaward most portion of the eastern lateral boundary, which is the result of implementing additional criterion 1 above, represents an improvement over the initial assumption for the location of this boundary, i.e., coincidence with the Florida-Hatteras slope. The southern lateral boundary was unaffected, and the western lateral boundary was minimally affected. The northern lateral boundary was affected the most. It now falls roughly along a line referred to by the U.S. Geological Survey as the “approximate up-dip limit

of (the) productive part of Upper Floridan aquifer" (Williams and Kuniansky 2015). This change is due to the implementation of criterion 1, stated above.

Layer 4

The specified minimum thickness for Layer 4 is 30 feet (Tables 3-1 and 3-2; Figures 3-13, 3-15, and 3-16). The western and eastern lateral boundaries of Layer 4 were determined primarily by intersecting the estimated 10,000 mg/l TDS concentration isosurface with the estimated top of Layer 4. The northern boundary and the portions of the western and southern lateral boundaries within the freshwater flow system coincide with the respective corresponding lateral boundaries of Layer 3. Where the middle confining unit is assumed to be absent, due to relatively high vertical conductivity, Layer 4 represents a subdivision (discretization) within the Floridan aquifer system (Zone 2 of the present study).

Layer 5

The specified minimum thickness of model Layer 5 is 50 feet (Tables 3-1 and 3-2; Figures 3-15, 3-17, and 3-18). The western and eastern lateral boundaries of Layer 5 were determined primarily by intersecting the estimated 10,000 mg/l TDS concentration isosurface with the estimated top of model Layer 5. The northern boundary and portions of the western and southern lateral boundaries within the freshwater flow system coincide with the respective corresponding lateral boundaries of model Layer 3. Where the middle confining unit is assumed to be absent, due to relatively high vertical conductivity, Layer 5 represents a deeper segment of the Floridan aquifer system (Zone 3 of the present study).

Layer 6

The specified minimum thickness of model Layer 6 is 10 feet (Tables 3-1 and 3-2; Figures 3-19 through 3-21). The areal extent of model Layer 6 was determined primarily by intersecting the estimated 10,000 mg/l TDS concentration isosurface with the estimated top and bottom of Layer 6 (Figures 2-12, 3-19, and 3-20). The top of Layer 6 is based on data obtained from Miller (written communication, 1991). The bottom of Layer 6 (and top of Layer 7) is based on data provided in Miller (1986) and other data obtained from Miller (written communication, 1991). A portion of the western lateral boundary coincides with the approximate pinch-out of the lower semi-confining unit, as detailed below in the description of the model lateral boundaries.

Layer 7

The specified minimum thickness of model Layer 7 is 10 feet (Tables 3-1 and 3-2; Figures 3-22 through 3-24). The areal extent of model Layer 7 was determined primarily

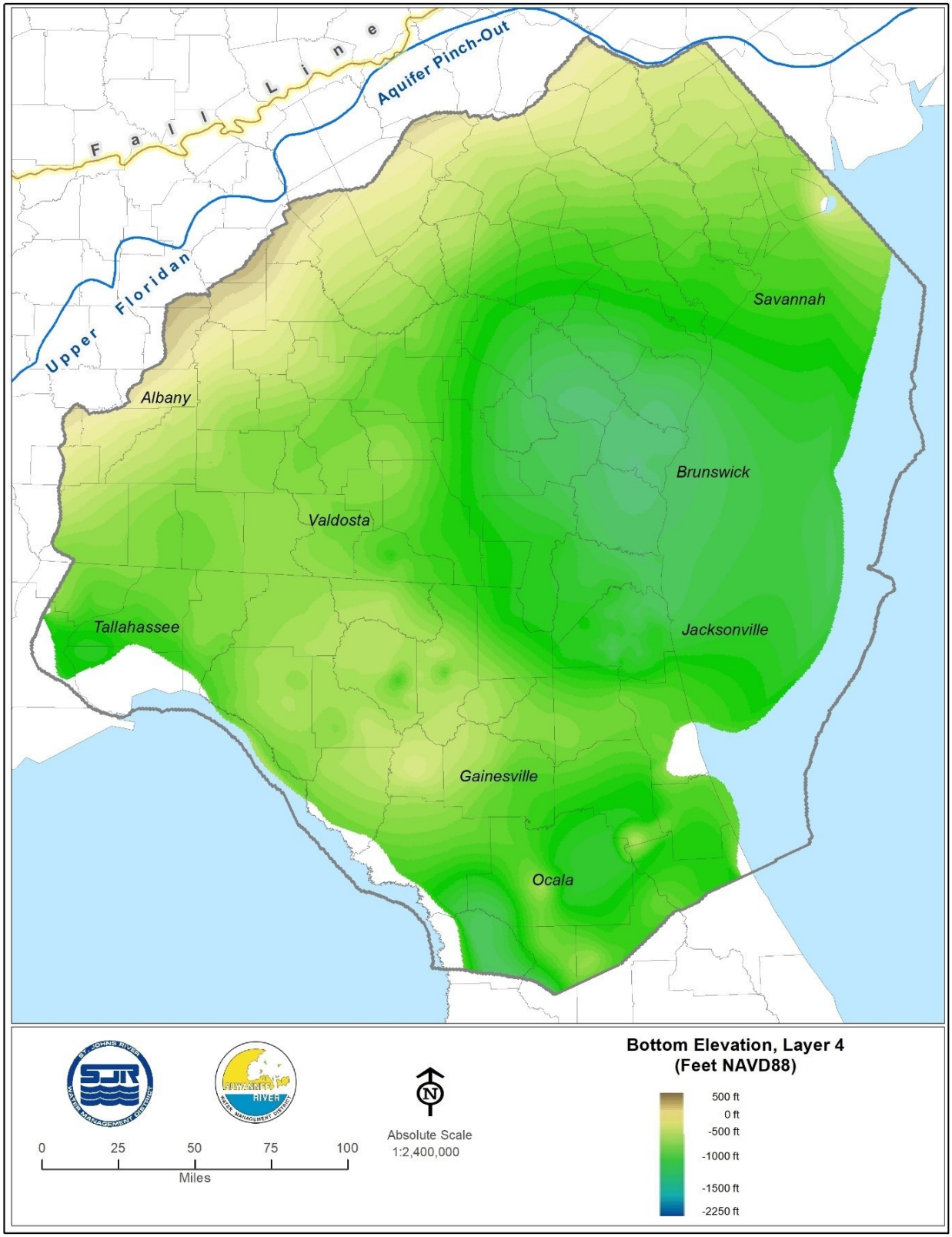

Figure 3-15. Bottom elevation, Layer 4 (and top elevation, Layer 5; feet NAVD88; after Bo niol and Davis, digital communication, 2013)

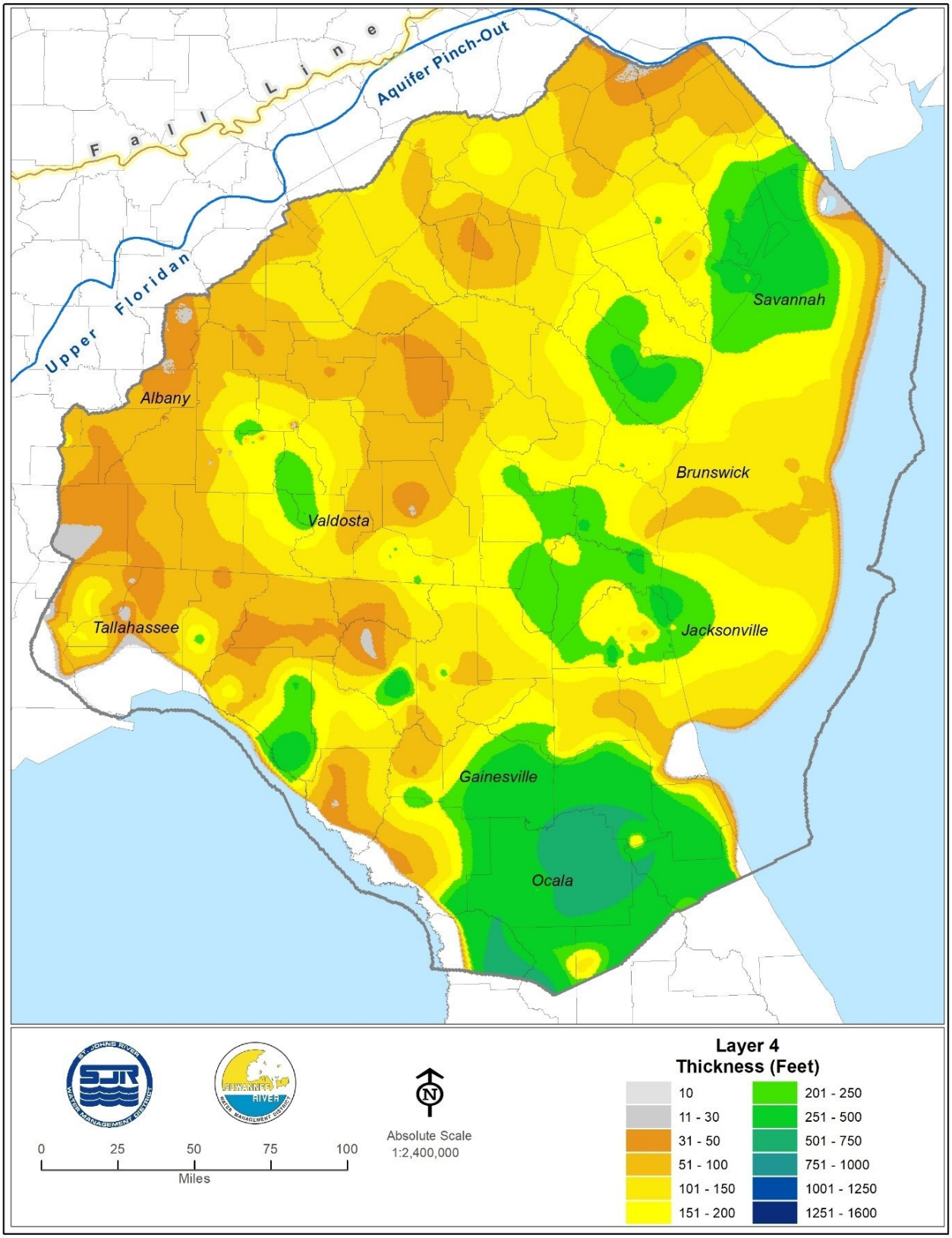

Figure 3-16. Thickness, Layer 4

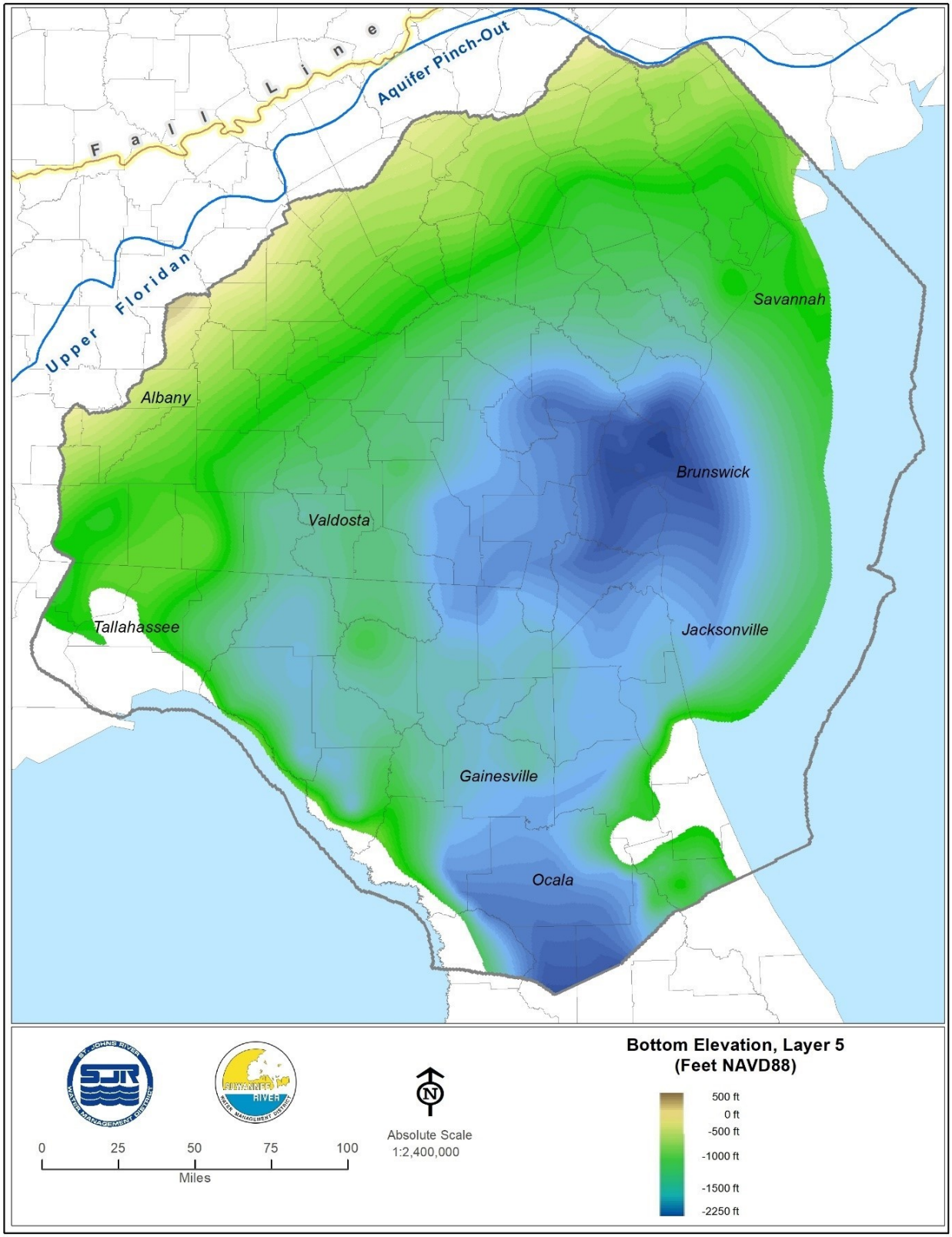

Figure 3-17. Bottom elevation, Layer 5 (feet NAVD88; after Miller, 1986; Miller, written com munication, 1991; and Williams, digital communication, 2013)

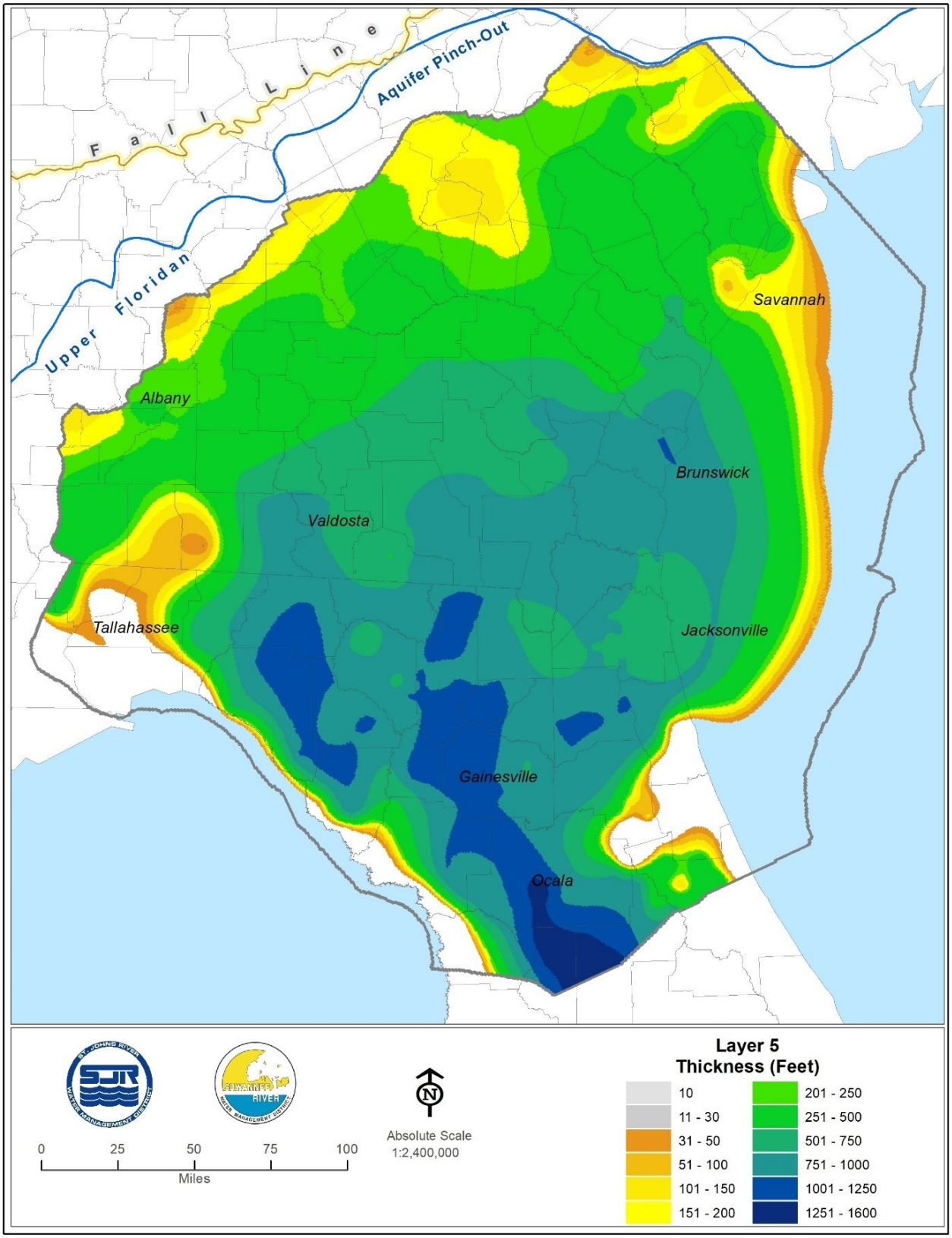

Figure 3-18. Thickness, Layer 5 (Feet)

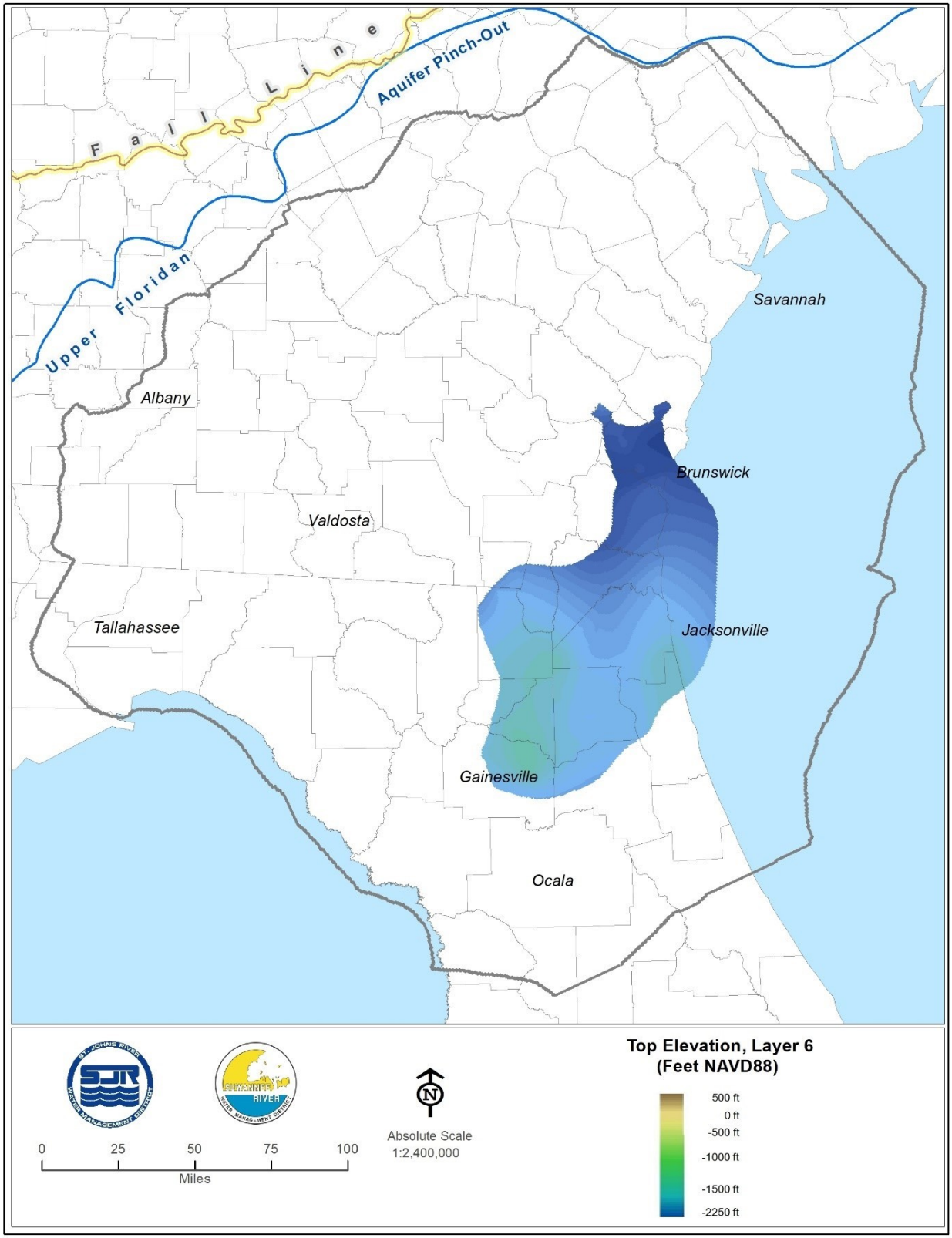

Figure 3-19. Top elevation, Layer 6 (feet NAVD88; after Miller, 1986; Miller, written commu nication, 1991; and Williams and Kuniansky, 2015)

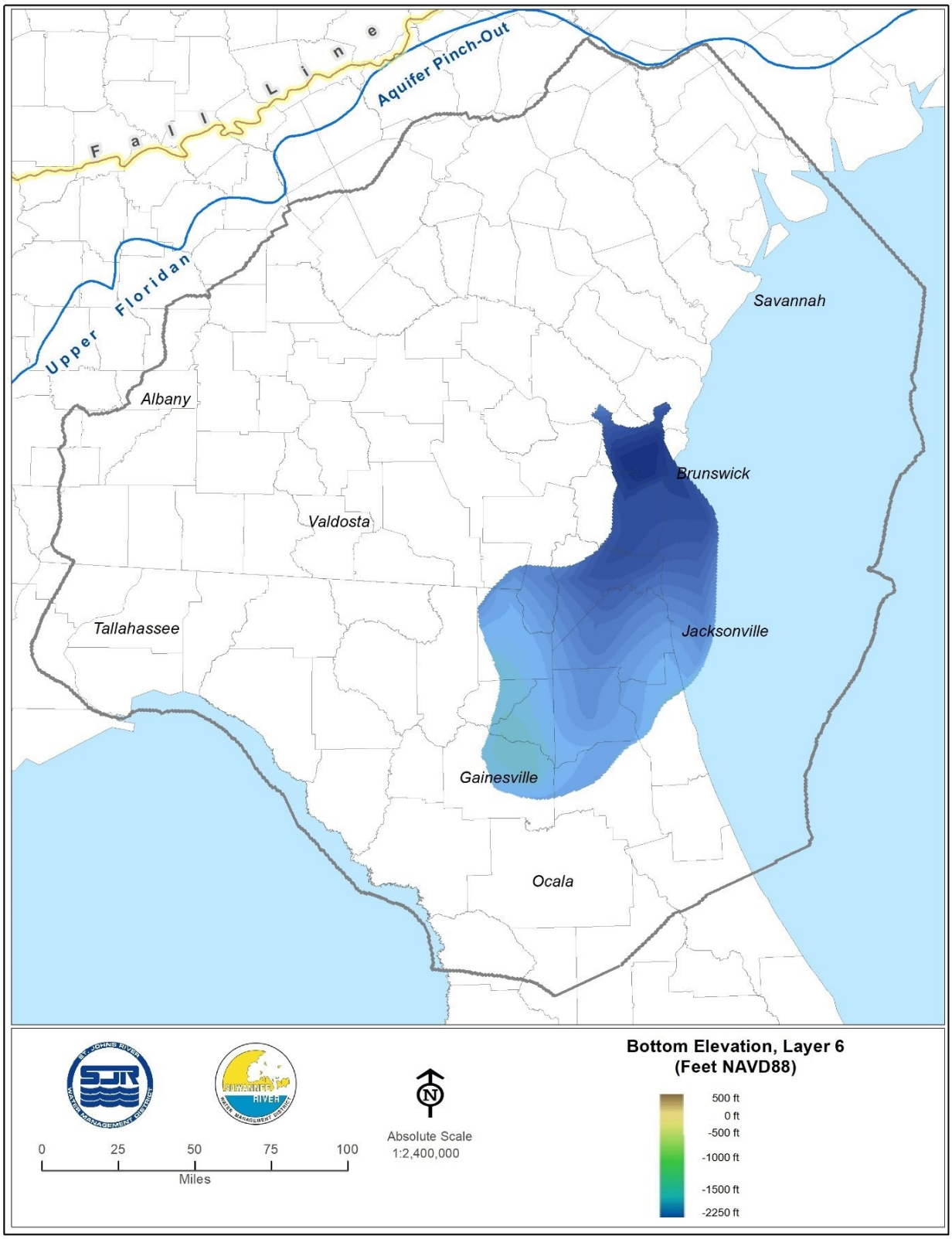

Figure 3-20. Bottom elevation, Layer 6 (Feet NAVD88; after Miller, 1986; Miller, written communication, 1991; and Williams and Kuniansky, 2015)

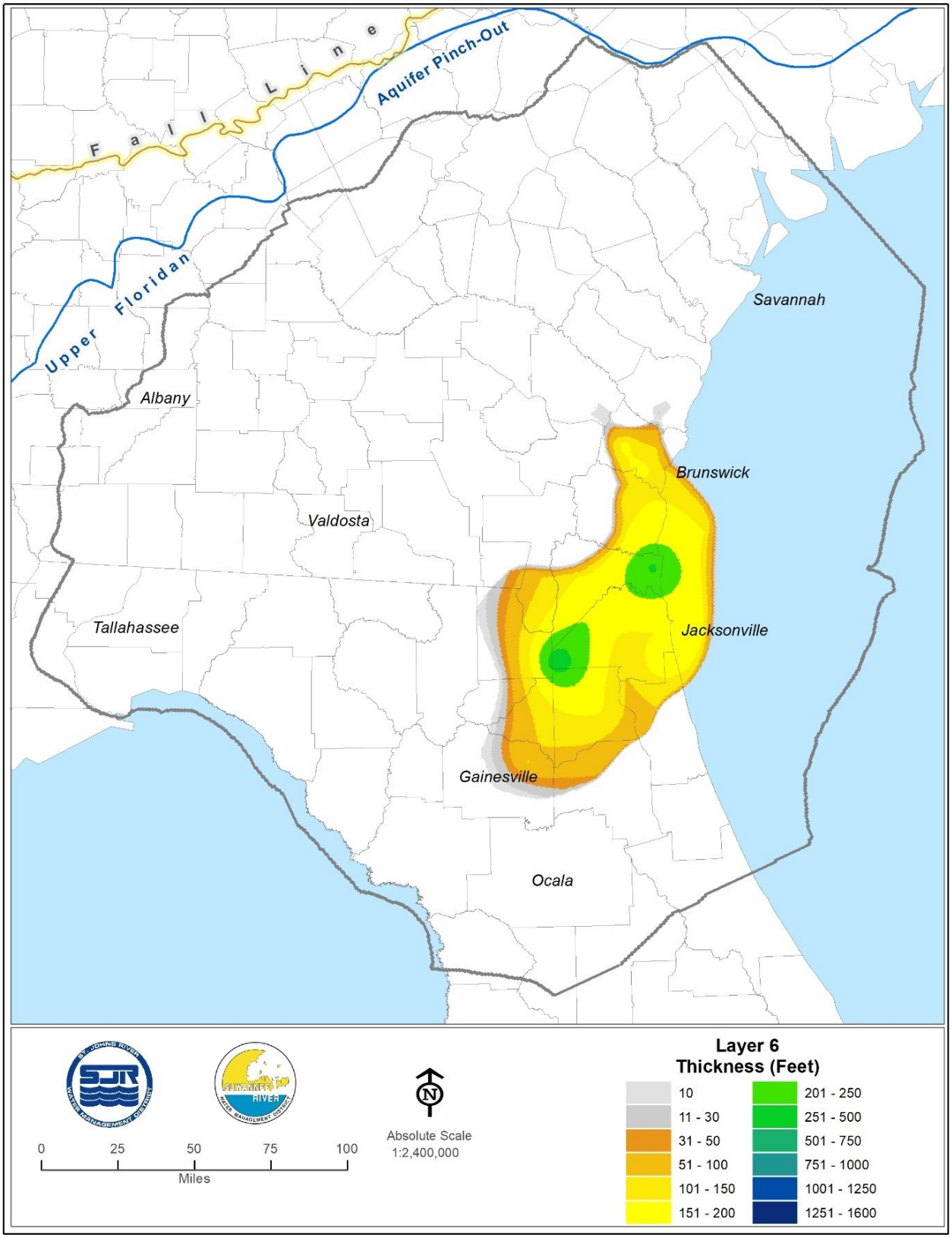

Figure 3-21. Thickness, Layer 6 (Feet)

by intersecting the estimated 10,000 mg/l TDS concentration isosurface with the estimated top of model Layer 7 (Figures 2-12 and 3-22). The top of model Layer 7 was based on Miller (1986) and Miller (written communication, 1991). A portion of the western lateral boundary coincides with the approximate pinch-out of the Fernandina permeable zone, as detailed below in the description of the lateral boundaries.

LATERAL BOUNDARY CONDITIONS

The model lateral boundary conditions represent prevailing flow conditions at locations corresponding to the edges of the active domains of the model layers. In some cases, lateral boundaries coincide approximately with the pinch-out of a hydrogeologic unit or the freshwater flow system. In other cases, lateral boundaries are oriented parallel to the direction of groundwater flow, as inferred from the configuration of the potentiometric surface of the Floridan aquifer system. Conditions at lateral boundaries in these cases are specified as no-flow because no flow is assumed to occur across the model lateral boundaries. Where flux across lateral boundaries is inferred based on the configuration of the potentiometric surface of the Upper Floridan aquifer, general head boundary (GHB) conditions are specified. To facilitate the following discussion of the model lateral boundary conditions, the lateral boundaries of model Layers 3 through 5 are subdivided into northern, eastern, southern, and western segments and subsegments. The lateral boundaries of model Layers 6 and 7 are subdivided into two subsegments, respectively, also for this purpose.

Layers 1 and 2

Layers 1 and 2 represent primarily the surficial aquifer system or the intermediate confining unit, respectively, although the hydraulic properties of Layer 2 are assumed to represent those of Zone 1 of the Floridan aquifer system (present study nomenclature) in areas where the intermediate confining unit doesn't exist or is less than a minimum thickness. Flow in the surficial aquifer system and intermediate confining unit is typically local in nature in the case of the surficial aquifer system or dominated by vertical gradients in the case of the intermediate confining unit, and therefore, generally isn't driven by regionally significant lateral gradients. Therefore, the lateral boundaries of model Layers 1 and 2 are specified as no-flow boundaries.

Layer 3

Northern (N3)

Although the northern lateral boundary of Layer 3, referred to hereafter as "N3," was relocated somewhat to the south of the estimated line of pinch-out of the Floridan aquifer system as delineated by Williams and Kuniansky 2015 (Figure 2-1), it is still assumed to approximate conditions of zero lateral flux. Hence, no-flow lateral boundary conditions are specified for the entire length of N3 (Figure 3-25).

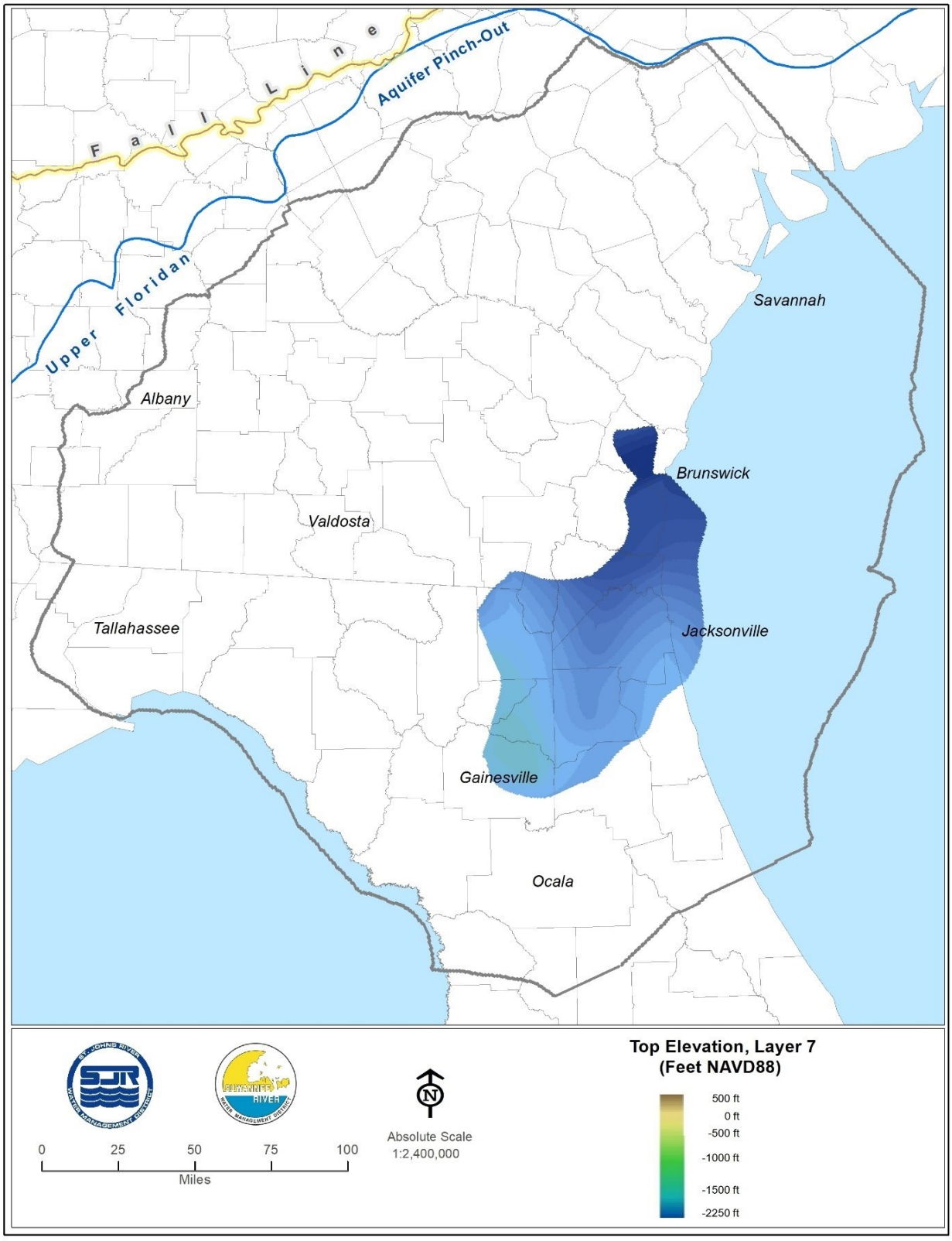

Figure 3-22. Top elevation, Layer 7 (feet NAVD88, after Miller 1986; Miller, written commu nication, 1991; and Williams and Kuniansky, 2015)

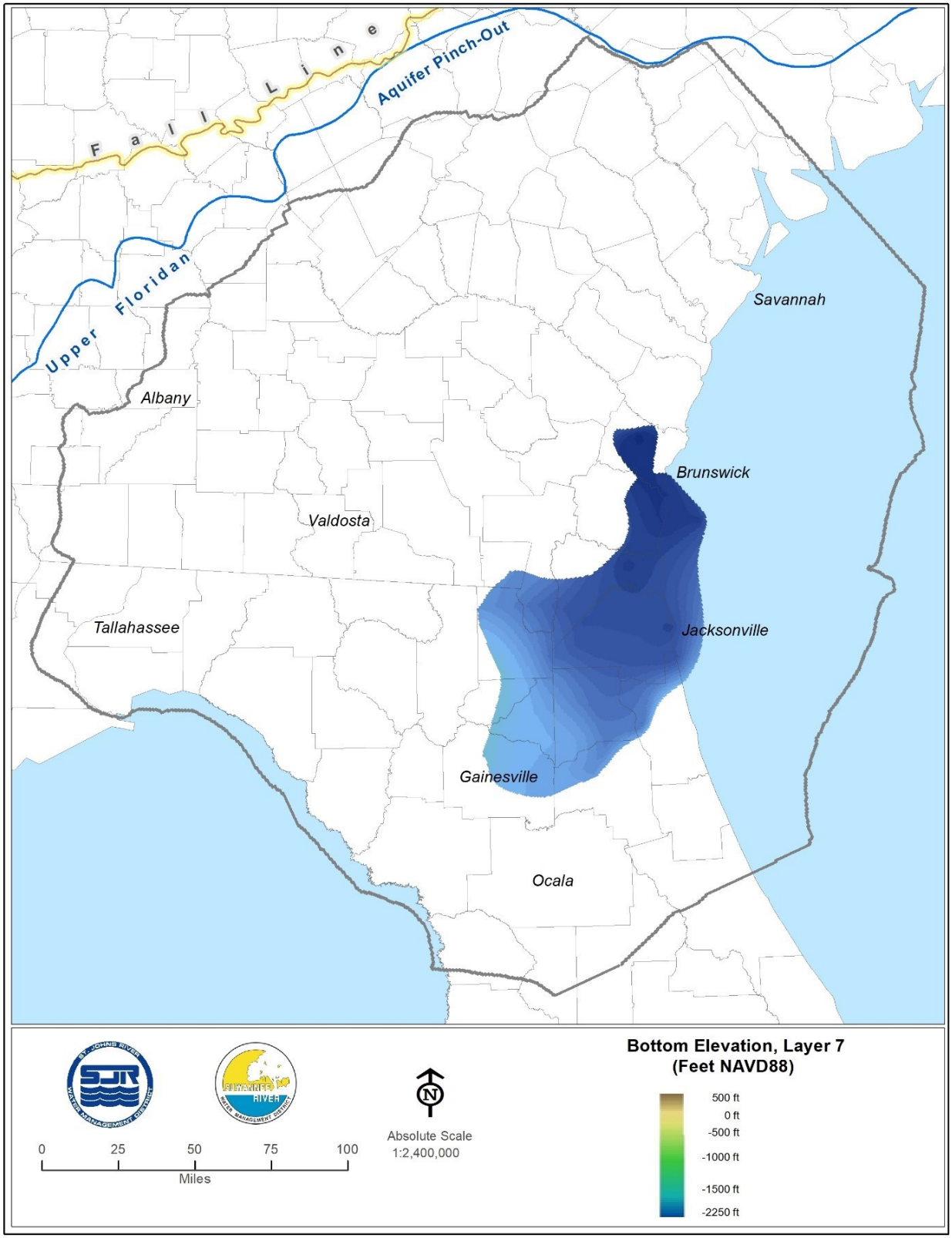

Figure 3-23. Bottom elevation, Layer 7 feet NAVD88, after Miller, 1986; Miller, written com munication, 1991; and Williams and Kuniansky, 2015)

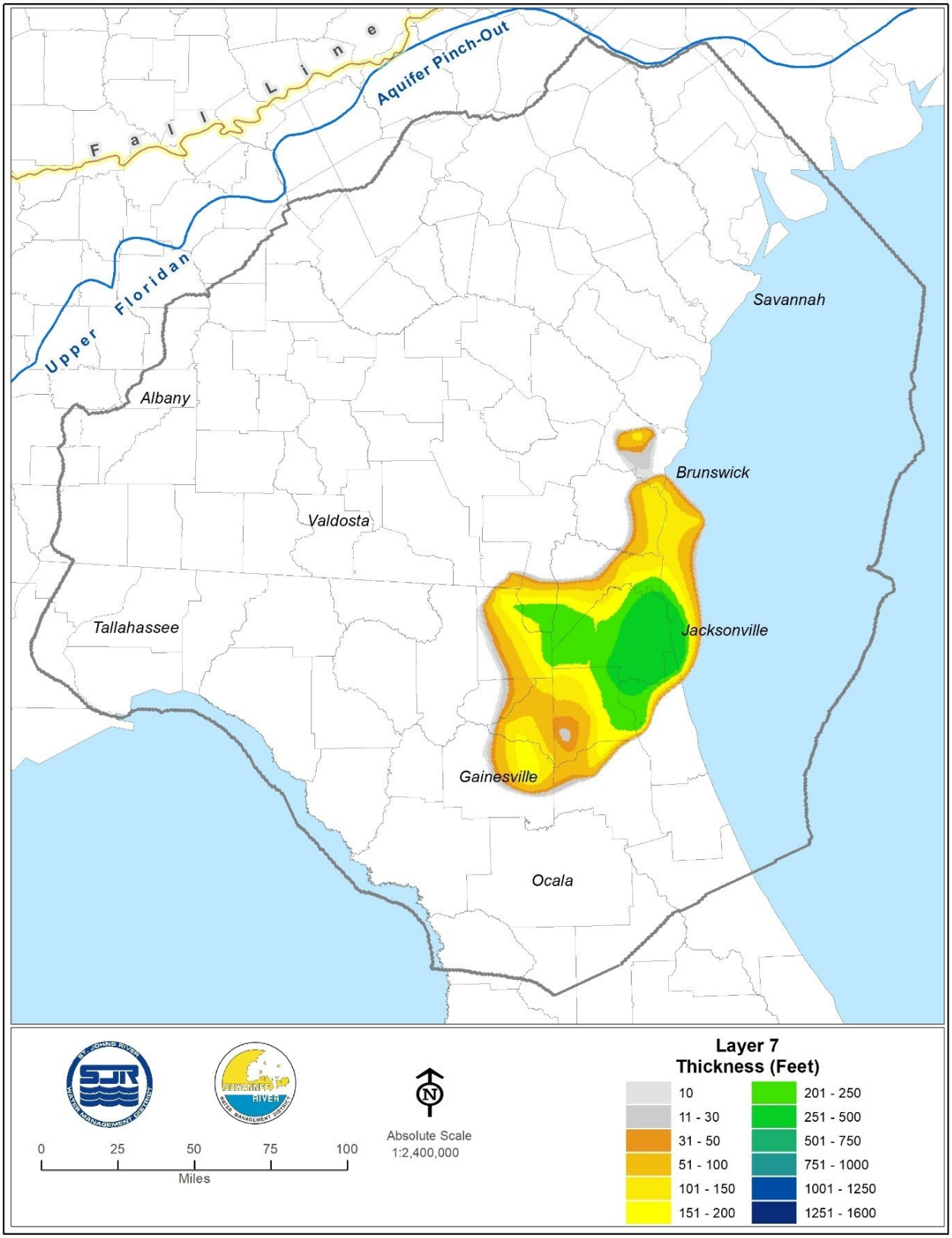

Figure 3-24. Thickness, Layer 7 (Feet)

Eastern, Upper (EU3)

The eastern lateral boundary of Layer 3 is subdivided into three subsegments, to facilitate the present discussion. The northernmost subsegment is labeled "eastern, upper" and is referred to hereafter as "EU3" (Figure 3-25). This subsegment is oriented parallel to the direction of groundwater flow, as inferred from the configuration of the 2010 potentiometric surface of the Upper Floridan aquifer (Kinnaman and Dixon 2011). Conditions along EU3 are accordingly represented as no-flow.

Eastern, Central (EC3)

The middle eastern lateral boundary subsegment is labeled "eastern, central" and referred to hereafter as "EC3." EC3 passes through an area of induced lateral influx to Layer 3. The lateral influx is induced by a large cone of depression in the potentiometric surface of the Floridan aquifer system that results from groundwater withdrawals near Savannah, Georgia. EC3 is accordingly represented with GHB lateral boundary conditions along its length (Figure 3-25). The source heads of the GHB conditions were interpolated from the May-June 2010 map of the potentiometric surface of the Floridan aquifer system (Kinnaman and Dixon 2011).

Eastern, Lower (EL3)

Moving clockwise, generally, the southernmost lateral boundary subsegment of the first three eastern lateral boundary subsegments is labeled "eastern, lower" and is referred to hereafter as "EL3" (Figure 3-25). EL3 corresponds in location to areas of the Floridan aquifer system that lie beneath the Atlantic Ocean. Groundwater flow in this area is assumed to be unaffected by onshore pumping and therefore in the same general direction as groundwater flow along EU3. Conditions along EL3 are designated accordingly as no-flow.

Eastern, Seaward (ES3)

The "eastern, seaward" (Figure 3-25) lateral boundary subsegment is the most seaward of the eastern lateral boundary subsegments. It is referred to hereafter as "ES3." ES3 represents the approximate line of pinch-out of freshwater flow in the Floridan aquifer system beneath the Atlantic Ocean. Conditions along ES3 are therefore designated as no-flow.

Southern, East (SE3)

The southern lateral boundary of Layer 3 is subdivided into three subsegments, the easternmost of which is labeled "southern, east" and referred to hereafter as "SE3" (Figure 3-25). SE3 is oriented parallel to the general direction of groundwater flow. Conditions along SE3 are designated therefore as no-flow.

Southern, Central (SC3)

The Polk City (Green Swamp) potentiometric high, which occurs mainly to the south of

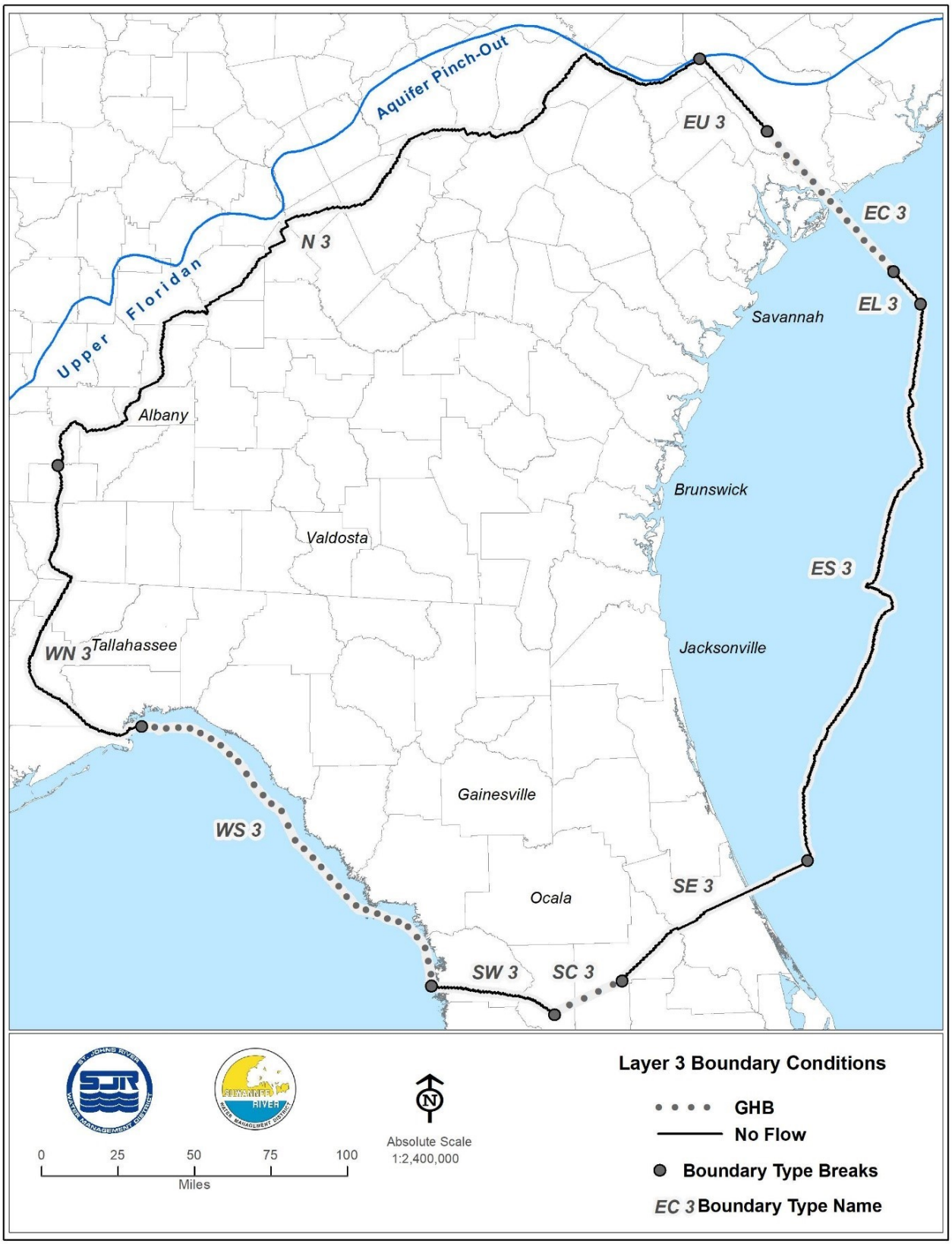

Figure 3-25. Model lateral boundaries, Layer 3

the NFSEG model domain, intersects the NFSEG model domain along the "southern, central" subsegment of the southern lateral boundary, referred to hereafter as "SC3" (Figure 3-25). SC3 is represented accordingly with GHB conditions. The source heads of the GHB conditions were interpolated from maps of the potentiometric surface of the Floridan aquifer system. For 2001, a map representing the average of water levels observed in May and September of 2001 was derived from the maps of Knowles (2001) and Knowles and Kinnaman (2001) and was utilized for this purpose. A similar map of 2009 average water levels, based on the maps of Kinnaman and Dixon (2009) and Boniol (digital communication 2013), was utilized for interpolation of 2009 source heads.

Southern, West (SW3)

The westernmost subsegment of the southern lateral boundary of Layer 3 is labeled "southern, west" and referred to hereafter as "SW3" (Figure 3-25). SW3 is oriented parallel to the general direction of groundwater flow. Conditions along SW3 are designated therefore as no-flow.

Western, Seaward (WS3)

The western lateral boundary of Layer 3 is subdivided into two subsegments. The more southerly is the "western, seaward," referred to hereafter as "WS3" (Figure 3-25). WS3 represents an approximation of the maximum seaward limit of freshwater flow in the Upper Floridan aquifer beneath the Gulf of Mexico. GHB conditions were specified along WS3 to allow for the possibility that freshwater flow in the Floridan aquifer system might, in places, extend farther seaward than the position of WS3. The source heads of all GHB conditions used for WS3 are equivalent freshwater heads of the Gulf of Mexico.

Western, North (WN3)

The more northerly subsegment of the western lateral boundary is the "western, north," referred to hereafter as "WN3" (Figure 3-25). In Florida, WN3 is oriented parallel to the general direction of groundwater flow and is therefore designated as a no-flow condition. In Georgia, WN3 is coincident with the path of Spring Creek, the smallest of three tributaries whose confluence forms the Apalachicola River. Spring Creek is in close hydraulic connection with the Floridan aquifer system, as evidenced by the configuration of the 2010 potentiometric surface of the Floridan aquifer system along its path (Kinnaman and Dixon 2011), so groundwater flow is assumed to be converging on it from opposing directions. Spring Creek therefore approximates a line of stagnation within the Floridan aquifer system, a no-flow condition for lateral flux within Layer 3. Accordingly, conditions along the entire length of WN3 are designated as no-flow.

Layer 4

As compared to Layer 3 lateral boundaries, the corresponding lateral boundary subsegments in model Layer 4 are referred to as "N4," "EU4," "EC4," "ES4", "SE4," "SC4,"

"SW4," "WS4," and "WN4" (Figure 3-26). Because of the way the 10,000 mg/l TDS concentration iso-surface intersects the top of Layer 4, these subsegments differ in exact shape and/or length as compared to the respective, corresponding Layer 3 subsegments. Also for this reason, a Layer 4 subsegment corresponding to EL3 does not exist.

Conditions at WS4, which corresponds to the Gulf coastal region, are designated as no-flow, in contrast with those of WS3, which were designated as GHB. The intersection of the 10,000 mg/l TDS concentration iso-surface with the top of Layer 4 occurs more to landward because Layer 4 represents a deeper section of the Floridan aquifer system in an area in which the onset of saline water is relatively shallow. Hence, WS4 is considered a reasonable approximation of the maximum seaward limit of freshwater flow in Layer 4 in the region of the Gulf Coast and is designated accordingly as a no-flow boundary.

Conditions at EU4, EC4, ES4, SE4, SC4, SW4, and WN4 are assumed to be similar in nature to those of corresponding subsegments of Layer 3. The source heads of GHB conditions assigned to EC4 are identical to those of the corresponding GHB conditions of EC3. The source heads of GHB conditions assigned to SC4 are identical to those of the corresponding GHB conditions of SC3.

Conditions along N4 are designated as GHB, in contrast with the no-flow designation of N3. No-flow conditions are specified along N3 because the northern lateral boundary approximates the line of pinch-out of the Floridan aquifer system. The lines of pinch-out of hydrogeologic units beneath the Floridan aquifer system are farther to the north, however. Use of GHB conditions to represent conditions along N4 enables simulation of lateral fluxes via N4 without having to extend the active model domain of Layer 4 northward beyond that of Layer 3. The source heads of GHB conditions specified along N4 are interpolated from the May-June 2010 map of the potentiometric surface of the Floridan aquifer system (Kinnaman and Dixon 2011).

Layer 5

The corresponding lateral boundary subsegments in Layer 5 are "N5," "EU5," "EC5," "ES5," "SE5," "SC5," "SW5," "WS5," and "WN5" (Figure 3-27). Because of the way the 10,000 mg/l TDS concentration iso-surface (Figure 2-12) intersects the top of Layer 5, Layer 5 subsegments differ in exact shape and/or length with respect to corresponding Layer3 and Layer 4 subsegments.

Conditions along WS5, which corresponds to the Gulf coastal region, are designated as no-flow, in contrast with those of WS3, which were designated as GHB. The intersection of the 10,000 mg/l TDS concentration iso-surface with the top of Layer 5 occurs more to landward because Layer 5 represents a deeper section of the Floridan aquifer system in an area in which the onset of saline water is relatively shallow. Therefore, it is considered a reasonable approximation of the seaward boundary of freshwater flow in model Layer 5 along the Gulf Coast and is designated accordingly as a no-flow boundary.

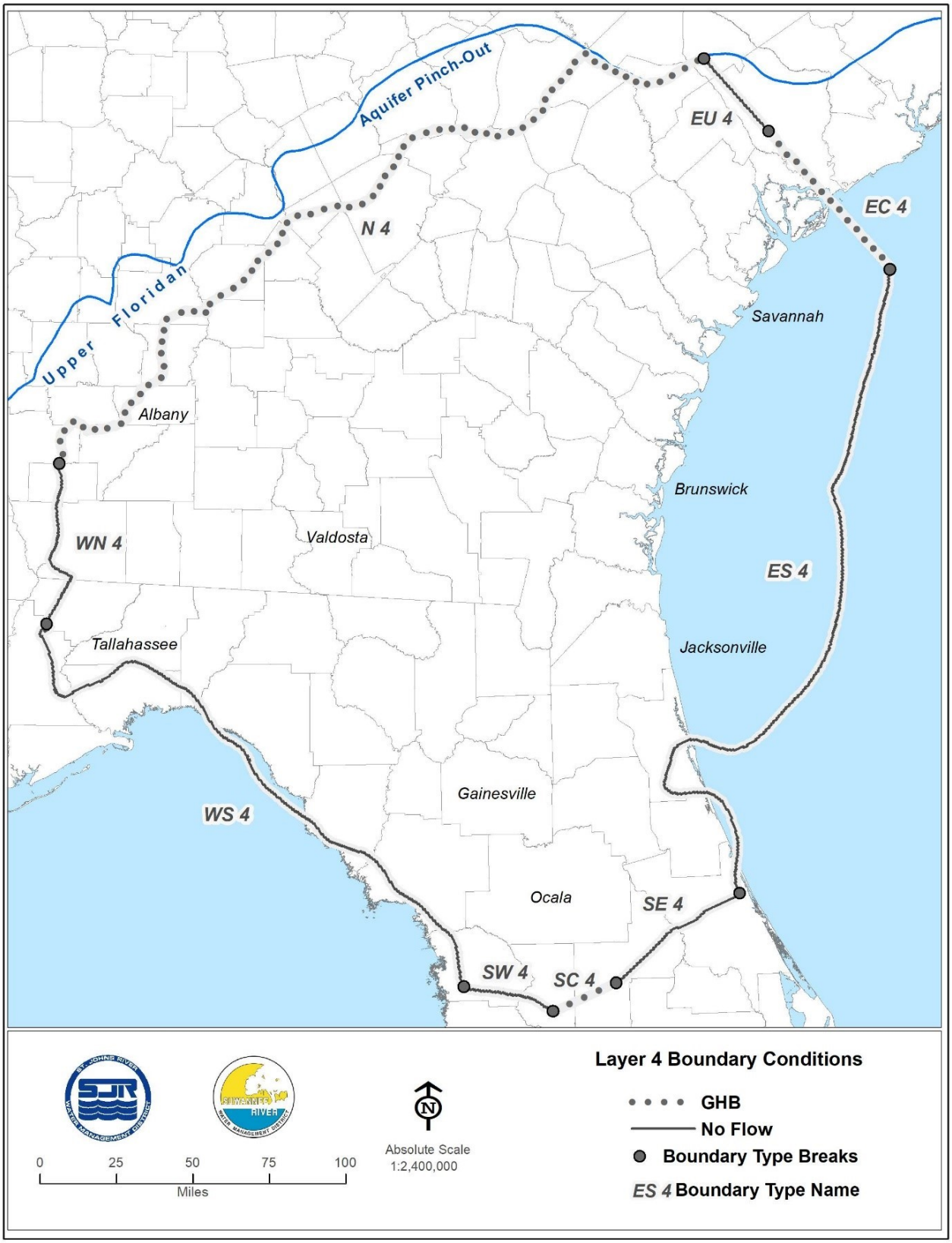

Figure 3-26. Model lateral boundaries, Layer 4

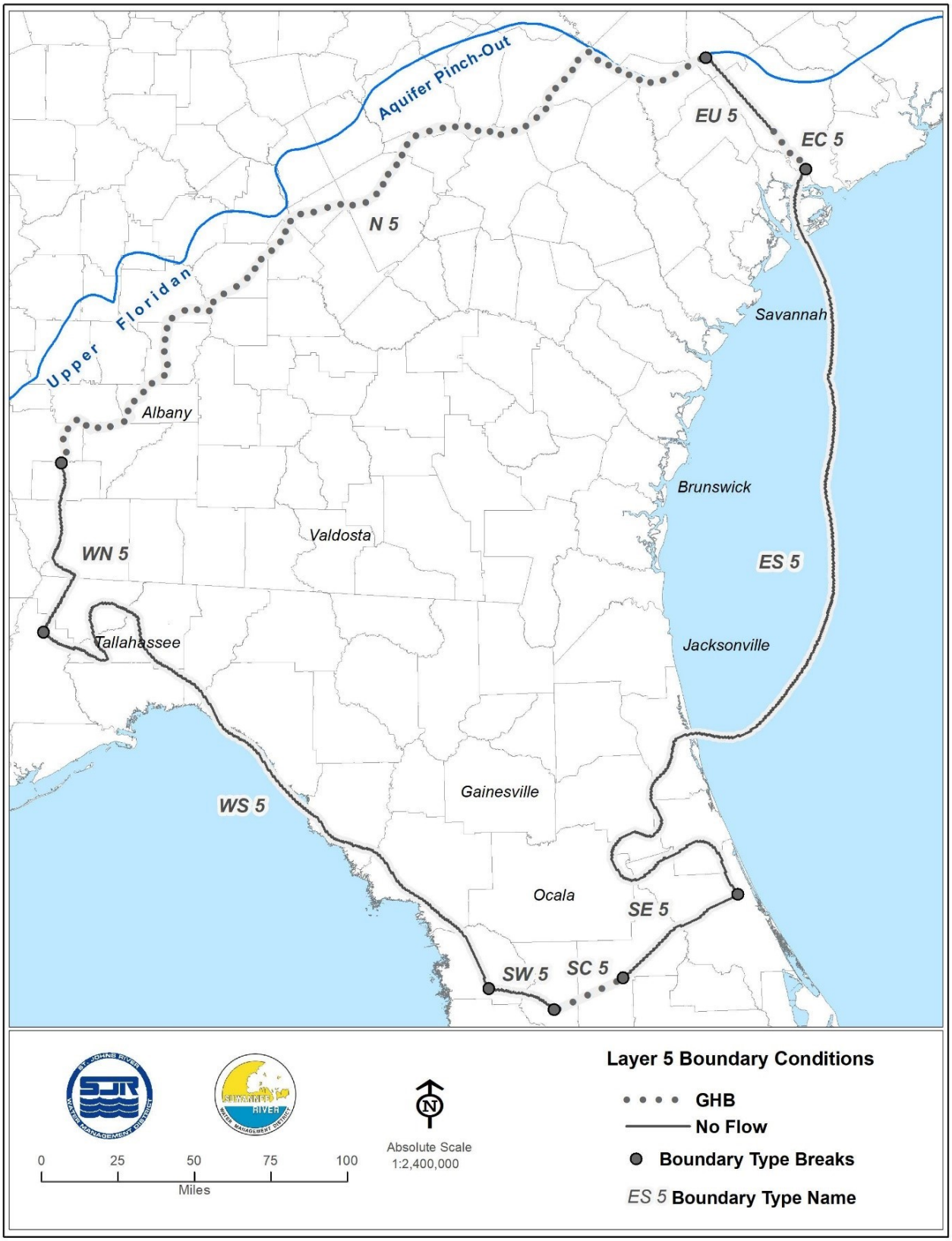

Figure 3-27. Model lateral boundaries, Layer 5

Conditions at EU5, EC5, ES5, SE5, SC5, SW5, WS5, and WN5 are assumed to be similar in nature to those of corresponding subsegments of Layer 3. The source heads of GHB conditions assigned to EC5 are identical to those of the corresponding GHB conditions of EC3. The source heads of GHB conditions assigned to SC5 are identical to those of the corresponding GHB conditions of subsegment SC3.

Conditions along N5 are designated as GHB, in contrast with the no-flow designation of N3. No-flow conditions are specified along N3 because the northern lateral boundary approximates the line of pinch-out of the Floridan aquifer system. The lines of pinch -out of the middle semi-confining unit and the Lower Floridan aquifer (or equivalent hydrogeologic units in this area) are farther north, however. Use of GHB conditions to represent conditions along N5 enables simulation of lateral fluxes across N5 without having to extend the active domain of model Layer 5 northward beyond that of Layer 3. The source heads of GHB conditions specified along N5 are interpolated from the map of the May-June 2010 potentiometric surface of the Floridan aquifer system (Kinnaman and Dixon 2011).

Layer 6

The lateral boundary of model Layer 6 is comprised of two subsegments, one that is the result of the intersection of the 10,000 mg/l TDS concentration iso-surface (Figure 2-12) with the top of model Layer 6, referred to as “FWSW6” (Figure 3-28) and another that approximates the line of pinch-out of the lower semi-confining unit, referred to as “HGL6” (Figure 3-28). Conditions along FWSW6 and HGL6 are designated accordingly as no-flow.

Layer 7

The lateral boundary of model Layer 7 is comprised of two subsegments, one that is the result of the intersection of the 10,000 mg/l TDS concentration isosurface (Figure 2-12) with the top of model Layer 7, referred to as “FWSW7” (Figure 3-29), and another that approximates the line of pinch-out of the lower semi-confining unit, referred to as “HGL7” (Figure 3-29). Conditions along FWSW7 and HGL7 are designated accordingly as no-flow.

Internal Boundary Conditions

Internal boundary conditions enable the representation of interaction with features, such as streams, lakes, springs, and the ocean, that are hydraulically connected to the groundwater flow system. In the NFSEG model, internal boundary conditions are utilized to represent the following flow phenomena: groundwater flux to and from perennial streams and lakes; groundwater discharge to ephemeral streams; discharge to springs; artesian discharge to land surface; discharge to single zone wells; discharge to multi-zone wells; recharge to the groundwater system; discharge to the atmosphere via evapotranspiration, and discharge to oceans. These processes are represented through

Figure 3-28. Model lateral boundaries, Layer 6

Figure 3-29. Model lateral boundaries, Layer 7

implementation of various MODFLOW packages, described as follows.

River Boundaries

Discharge between the groundwater flow system and perennial streams and lakes are represented in the NFSEG model by implementation of the MODFLOW River Package. An estimate of stage, conductance, and bottom elevation is required for each River Package boundary condition.

For layer assignment, the assigned stages and bottom elevations of river boundaries were compared to the assigned top and bottom elevations of the model layers. In most cases, assignment to Layers 1 and/or 2 was the result of this comparison, although assignments to Layer 3 were made also.

River Stage and Bottom Elevation

The paths of streams were represented using flowlines of the National Hydrography Dataset Plus, Version 2 (NHDPlusV2; McKay et al. 2013; http://www.horizon-systems.com/NHDPlus/NHDPlusV2_documentation.php). This data set includes Strahler order classifications for stream and river reaches. Stream reaches classified as Strahler order 2 and above were included in the NFSEG model implementation of the MODFLOW River Package as perennial streams. Stream reaches classified as Strahler order 1 were included in the implementation of the MODFLOW Drain Package as ephemeral streams (Figure 3-30), described in greater detail below in the section on the Drain Package implementation.

The estimation of stream stages involved first intersecting NHDPlusV2 flowlines with the NFSEG model grid in ArcGIS, thereby breaking the NHDPlusV2 flowlines into flowline subsegments (Figure 2-25, Appendix B). Within each grid cell, a bank elevation for each of the resulting subsegments was computed by averaging the United States Geological Survey 3DEP 10-meter digital elevation model (USGS 3DEP 10m DEM; http://nationalmap.gov/3DEP/index.html) elevation values over the length of each subsegment.

The mean depth of the stream was calculated according to the following formula, obtained from Moore (2007):

$$Ym = 0.28Q^{0.22}$$

where

Ym = mean channel depth (meter [m]), and
Q = mean channel discharge (m3/second [s]).

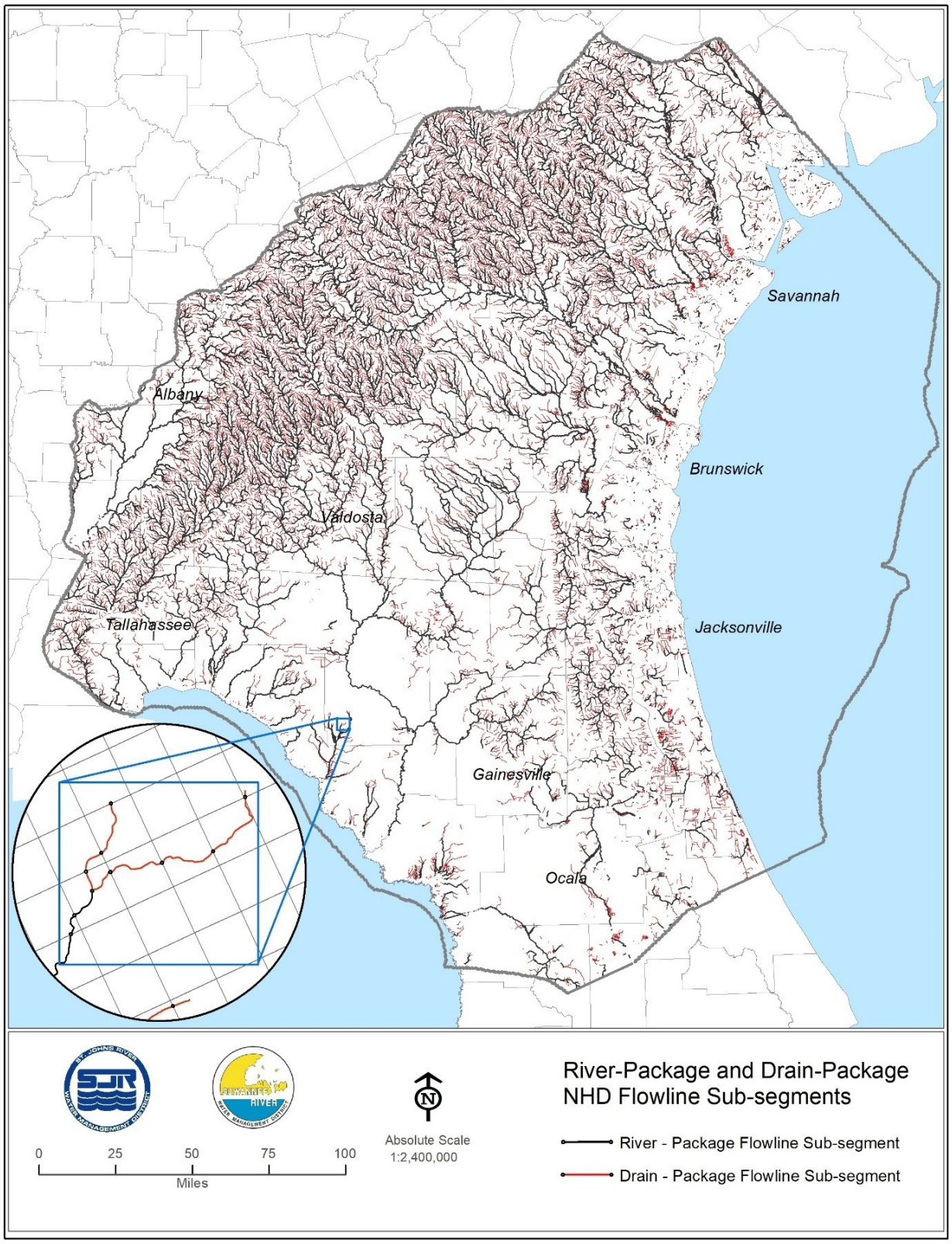

Figure 3-30. NHDPlusV2 flow-line sub-segments used in river- and drain-package imple mentations

The value of Q was approximated as the flow parameter Q0001E (m3/s) of the NHDPlusV2 dataset (McKay et al. 2013).

The "incised" depth of the stream, i.e., the distance from bank to stream bottom, was assumed to be 1.25 times the mean depth, as suggested by Moore (2007). The incised depth was then subtracted from the USGS 3DEP 10m DEM derived bank elevation to yield an estimate of the stream bottom elevation. The mean depth of the stream was then added to the bottom elevation to obtain an estimate of the stream stage. Stages so derived were implemented throughout the model domain initially except in the cases of portions of the St. Johns and Suwannee Rivers (and selected reaches of their major tributaries) for which stages were derived using existing surface water models and river stages measured at gaging stations.

Later, many of the USGS 3DEP 10m DEM derived stages and corresponding bottom elevations were altered to address a tendency in the derived elevations to increase in the downstream direction along portions of some NHDPlusV2 flowlines, rather than decline consistently. These alterations were affected through use of an interpolation process carried out in ArcGIS. The interpolation process resulted in smooth, steady declines in stage from the uppermost flowline subsegments to as far downstream as necessary. Stages for "flow-through" lakes, which were estimated through a process described below, were honored in this process. Additional details concerning these processes are described by Desmarais (written communication, 2016; Appendix H).

Stages and river bottom elevations for portions of the Suwannee River and its tributaries that are incised into the Floridan aquifer system, and portions of the St. Johns River and its tributaries were not estimated using the approach outlined by Desmarais (written communication 2016; Figure 3-31). In the case of the Suwannee River and selected reaches of the contributing Withlacoochee, Santa Fe, and Ichetucknee Rivers, River Package stages were estimated by using simulated water surface profiles from HEC-RAS surface water models of these rivers to interpolate stage data from stream gauges. Channel thalweg data from these models were also used to estimate river bottom elevations that are specified in the River Package (Environmental Consulting and Technology 2014). In the case of the St. Johns River, stages and bottom elevations were obtained from a hydrodynamic model of the St. Johns River created by the St. Johns River Water Management District (SJRWMD; Suscy et al. 2012).

Lake Stage and Bottom Elevation

Representations of lake areas were obtained from the National Land Cover Database (NLCD; http://www.mrlc.gov). The lake areas were converted to lake polygons in ArcGIS and then intersected with the NFSEG model grid, resulting in the formation of lake sub-polygons. Elevations were extracted from the 10-meter DEM at the centroid location of each sub-polygon for use as an approximate lake stage, unless actual stage data were available. Sources of actual lake stage data included the SJRWMD, the Northwest Florida Water Management District, and the U.S. Geological Survey. Lake bottom elevations were based on an assumed average depth, usually eight feet. Where lake sub-polygons coincided with river boundary subsegments, river boundary subsegments were removed. Likewise, river boundary subsegments were also removed wherever specified head boundary conditions were assigned to represent the Atlantic Ocean

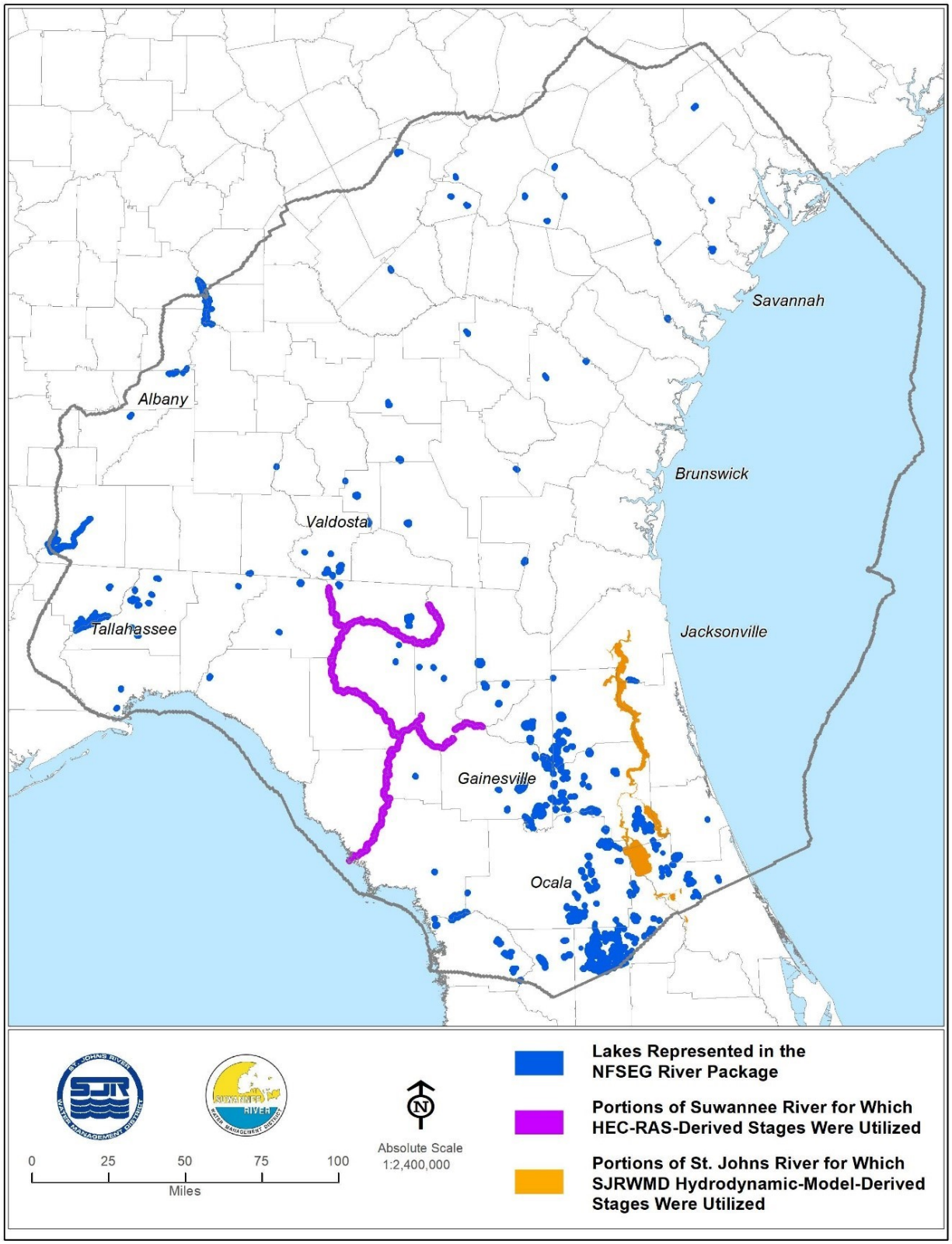

Figure 3-31. Portions of NHD flowlines for which river stages were obtained from existing surface-water models and Lake sub-polygons represented in the NFSEG river package

or Gulf of Mexico. Only lakes covering more than 50% of the grid cell area were modeled using the River Package.

Initial Conductance Estimates

Initial River Package conductance values were estimated based on assumed horizontal and vertical hydraulic conductivities, corresponding total hydraulic areas, and assumed flow-path lengths. The bottom areas of stream subsegments were determined as the products of subsegment lengths and mean widths, with the length determined by ArcGIS and the mean width determined according to the following formula, obtained from Moore (2007), as follows:

$$W = 11.95Q^{0.47}$$

where

W = mean width (m), and
Q = mean channel discharge (m3/s).

The value of Q was approximated as the flow parameter Q0001E (m3/s) of the NHDPlusV2 dataset (McKay et al. 2013). The total hydraulic area is determined as the sum of the bottom area and the side area of a given stream subsegment. The side area is determined as the subsegment length multiplied by the estimated depth times 2.

General Head Boundary Conditions

In addition to representing fluxes via lateral boundaries, GHB conditions were used also to represent springs in the NFSEG model. In this application, the value of the GHB condition source head represents the elevation of the surface of the receiving body of water into which a spring discharges (i.e., the "spring pool elevation"). Use of the GHB package as opposed to the drain package to represent springs enables the simulation of reverse spring flow. This occurs when the spring pool elevation exceeds the aquifer head at a spring and is typically the result of seasonally high surface water.

Most springs within the NFSEG model domain emanate from the Floridan aquifer system. A smaller number emanate from the intermediate aquifer system. Accordingly, most GHB conditions used to represent springs are assigned to Layer 3, with the remaining ones being assigned to aquifer Layer 2 (Appendix E). Spring pool elevations were obtained from observation data, stage estimates, estimated from topographic maps, or the USGS 3DEP 10m DEM representation.

Springs that emanate from the Upper Floridan aquifer were assigned to model Layer 3 because Layer 3 is representative of most or nearly all the vertical extent of the Upper Floridan aquifer (or Zone 1 as defined in Chapter 2) throughout the model domain. In unconfined areas of the model, the elevation of the boundary between the consolidated sediments that comprise the Upper Floridan aquifer (or Zone 1) and the overlying, relatively thin, unconsolidated sediments that comprise the surficial aquifer system and/or

remnants of the intermediate confining unit is typically not known precisely at specific locations. Thus, in many cases, the top of the Upper Floridan aquifer (or Zone 1) in unconfined areas corresponds to somewhere within model Layer 1 or 2. In unconfined areas, therefore, a relatively small portion of the vertical extent of the Upper Floridan aquifer (or Zone 1)--less than 60 feet of it--may be included in the representations of model Layers 1 and/or 2. However, the opposite never occurs, which is to say that model Layer 3 is restricted in its representation to most or nearly all the vertical extent of the Upper Floridan aquifer (or Zone 1) and is never representative of any portion of the unconsolidated sediments that lie atop the Upper Floridan aquifer (or Zone 1).

In the unconfined areas of the model domain, the assignments of relatively large values of Layer 2 vertical hydraulic conductivity results in simulated water levels in Layers 1, 2, and 3 that are typically very similar or nearly the same. However, differences may exist, with larger differences between the three layers generally occurring where differences in hydraulic conductivity are greater. Although Layer 1 or 2 would be expected to serve as well as Layer 3 for assignment of Upper-Florida-aquifer springs in areas in which water levels are essentially the same in all three layers, this may not be the case in areas in which water levels do not match as closely. An approach that applies to both conditions was therefore selected (i.e., assignment of springs to Layer 3). An additional consideration is that springsheds typically include both confined and unconfined areas, with the spring head usually located in the unconfined area. In this situation, assignment to Layer 1 or 2 might serve equally as well as assignment to Layer 3 for determination of water levels and flows in unconfined areas, but this approach might not work as well in confined areas. Such problems are easily avoided by assignment of springs that emanate from the Upper Floridan aquifer (or Zone 1) to Layer 3.

In summary, then, Layer 3 is representative of most or all the vertical extent of the Upper Floridan aquifer (or Zone 1) throughout the model domain, whereas Layers 1 and/or 2 may or may not represent portions of the vertical extent of the Upper Floridan aquifer (or Zone 1). Furthermore, in cases in which Layers 1 and/or 2 do represent portions of the vertical extent of the Upper Floridan aquifer (or Zone 1), the portion so represented is typically only a relatively small portion of the vertical extent (less than 60 feet at most). In view of these considerations, Layer 3 was determined to be the most appropriate layer for assignment of springs that emanate from the Upper Floridan aquifer (or Zone 1).

Drain Boundaries

Artesian Derived Wetlands

The MODFLOW Drain Package is used in the NFSEG model to represent discharge from the Floridan aquifer system to land surface in relatively flat, low-lying, unconfined areas along the coast of the Gulf of Mexico and other areas in which the Floridan aquifer system water level exceeds the land surface elevation. Under such conditions, discharge from the Floridan aquifer system tends to pool on the ground, forming artesian derived wetlands. To represent the discharge from the Floridan aquifer system that results from this process, drain boundaries were assigned to grid cells in parts of the

model domain that correspond to such areas (Figure 3-32). The grid cells were selected based on the following criteria:

1. Wetland areas as shown on the U.S. Fish and Wildlife Service Wetlands Inventory map (https://www.fws.gov/wetlands/data/NSDI-Wetlands-Layer.html) are present;
2. Upper Floridan aquifer water levels as shown on the map of the Upper Floridan aquifer potentiometric of 2010 (Kinnaman and Dixon 2011) exceed average land surface elevation as derived from the USGS 3DEP 10m DEM; and
3. Unconfined conditions prevail, based on mapping of the ICU thickness (Figure 2-10).

The conductance of the assigned drain boundaries was initially estimated based on the estimated vertical hydraulic conductivity of Layer 1 and the area of the wetlands contained within the affected grid cells. The assigned drain elevation was the average land surface elevation of the affected grid cells.

Ephemeral Stream Reaches

The Drain Package was used also to represent ephemeral portions of streams. The portion of a stream represented by a given drain boundary condition flows only when the elevation of the simulated water table of the grid cell to which it is assigned exceeds the elevation of the drain boundary. Ephemeral portions of streams were identified in this process as the portions of the NHDPlusV2 flowlines with a Strahler order designation of 1. The portions of streams with Strahler order greater than 1 are represented using the NFSEG model river package implementation (Figure 3-30). Additional drain features were later added to areas where excessive flooding occurred in the model. These additional drain features represented surface water canals and sloughs determined to be present based on a review of available information including aerial photographs, USGS topographic maps, etc.

Recharge and Evapotranspiration

As stated above, recharge rates were obtained from 55 different HSPF models developed specifically for supplying surface water related data to the NFSEG model (Figure 3-33). Implementation of these data in the Recharge Package requires determining weighted averages of the sums of the "AGWI" (i.e., active groundwater inflow) and "IGWI" (i.e., inactive groundwater inflow) parameters of the HSPF models (Figure 3-34). Separate recharge arrays were developed using this approach for the years 2001 and 2009 (Figures 3-35 and 3-36).

During model simulations, a specified recharge rate is applied to the uppermost active grid cell of each vertical column of grid cells. In the usual situation, all NFSEG model layers are active. However, in some cases, the grid cells of Layer 1 or Layers 1 and 2 are simulated as being dry. Such grid cells are treated as inactive by the model in the application of recharge rates. Dry cells occur in areas of the model domain in which the

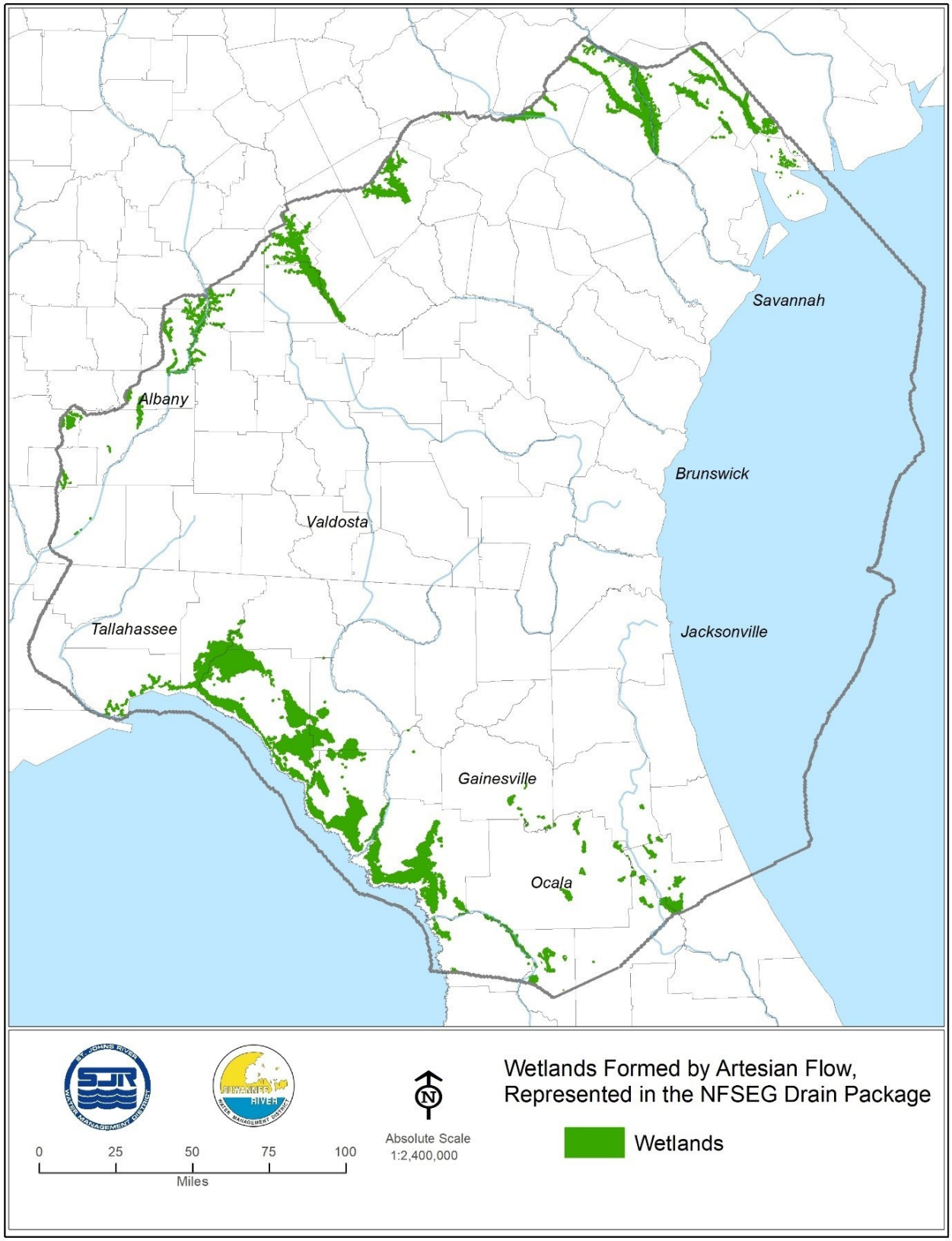

Figure 3-32. Artesian-derived wetlands represented in the drain package

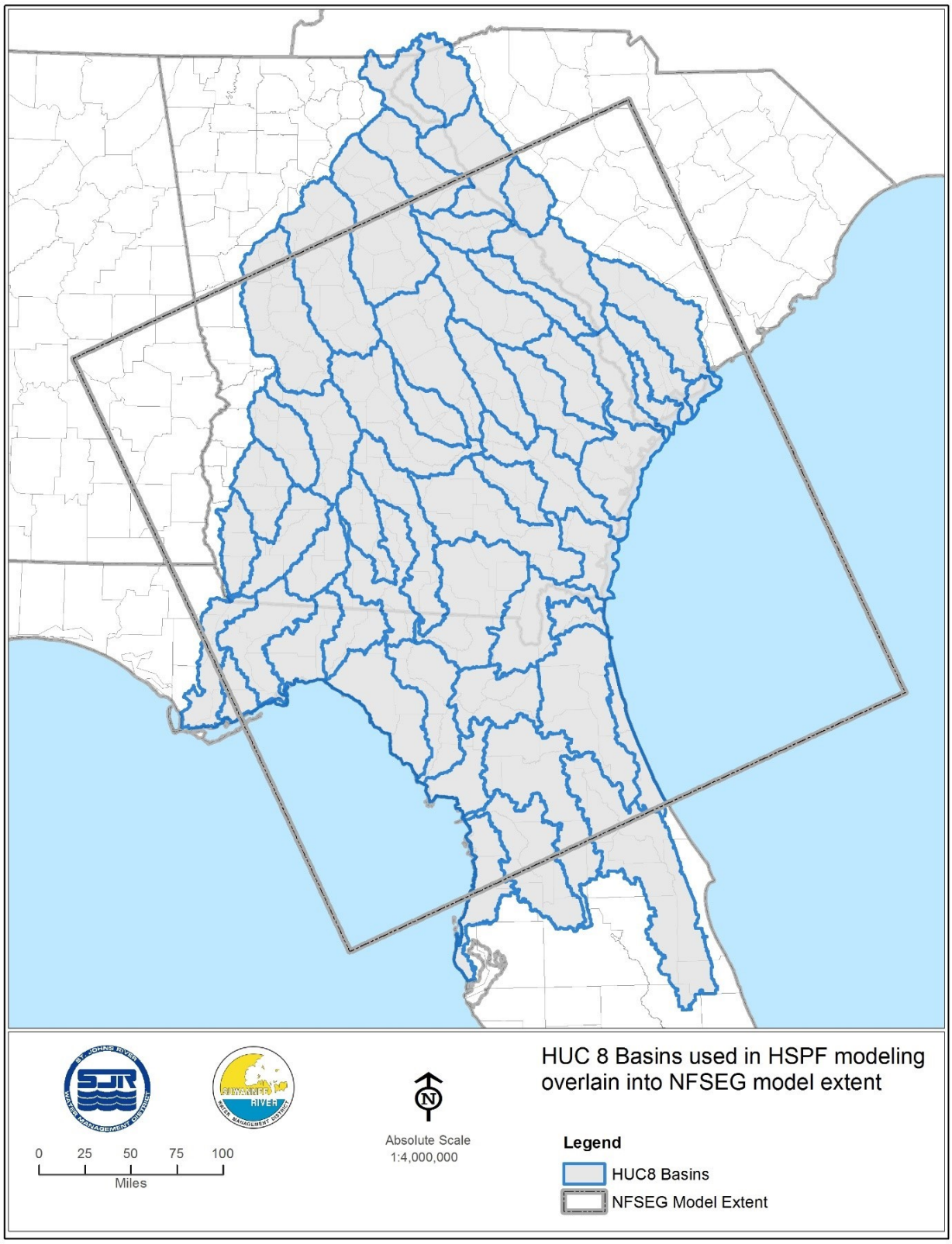

Figure 3-33. USGS HUC8 basins for which HSPF models were developed in support of NFSEG development

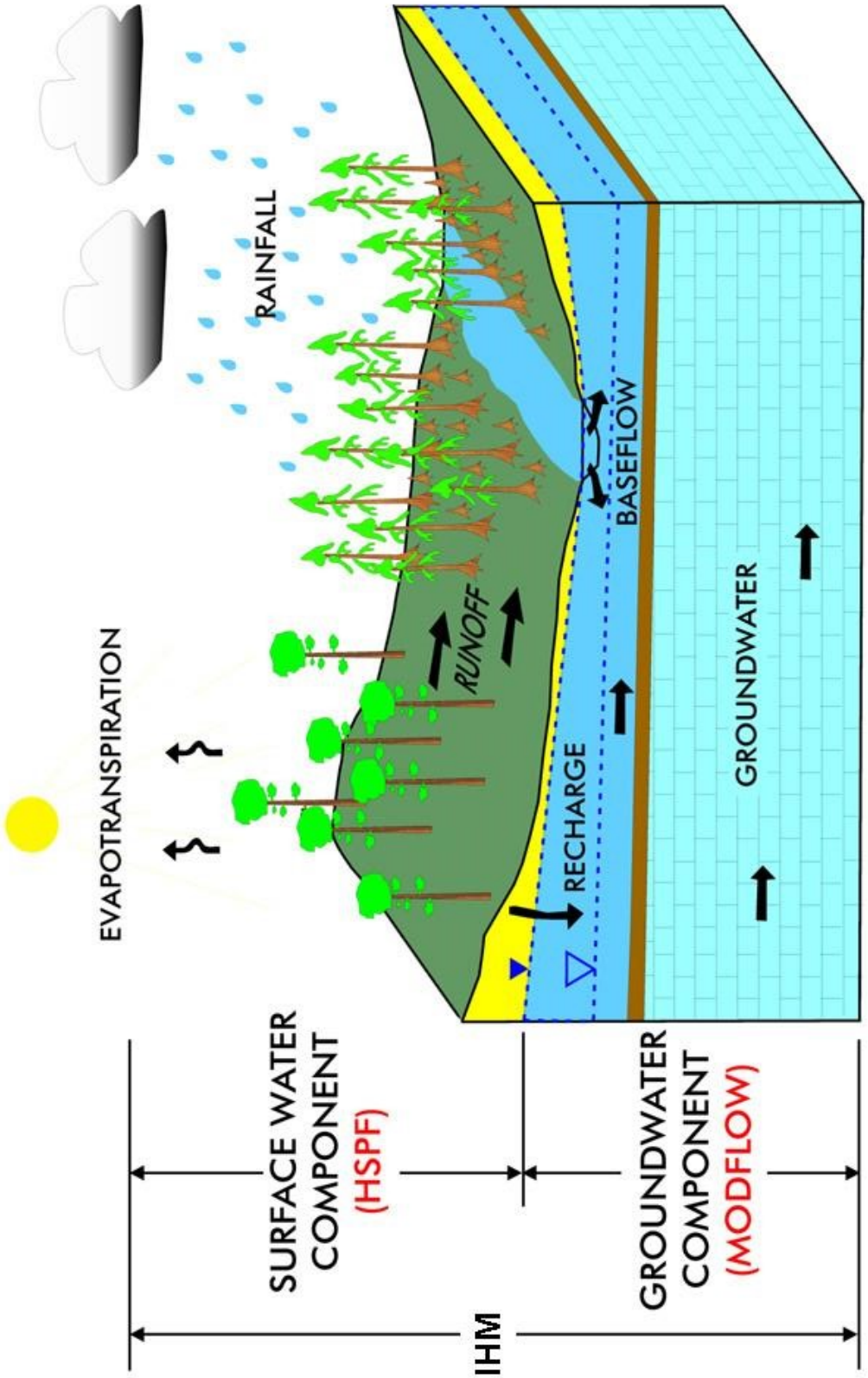

Figure 3-34. Simulated flow components--HSPF vs. MODFLOW

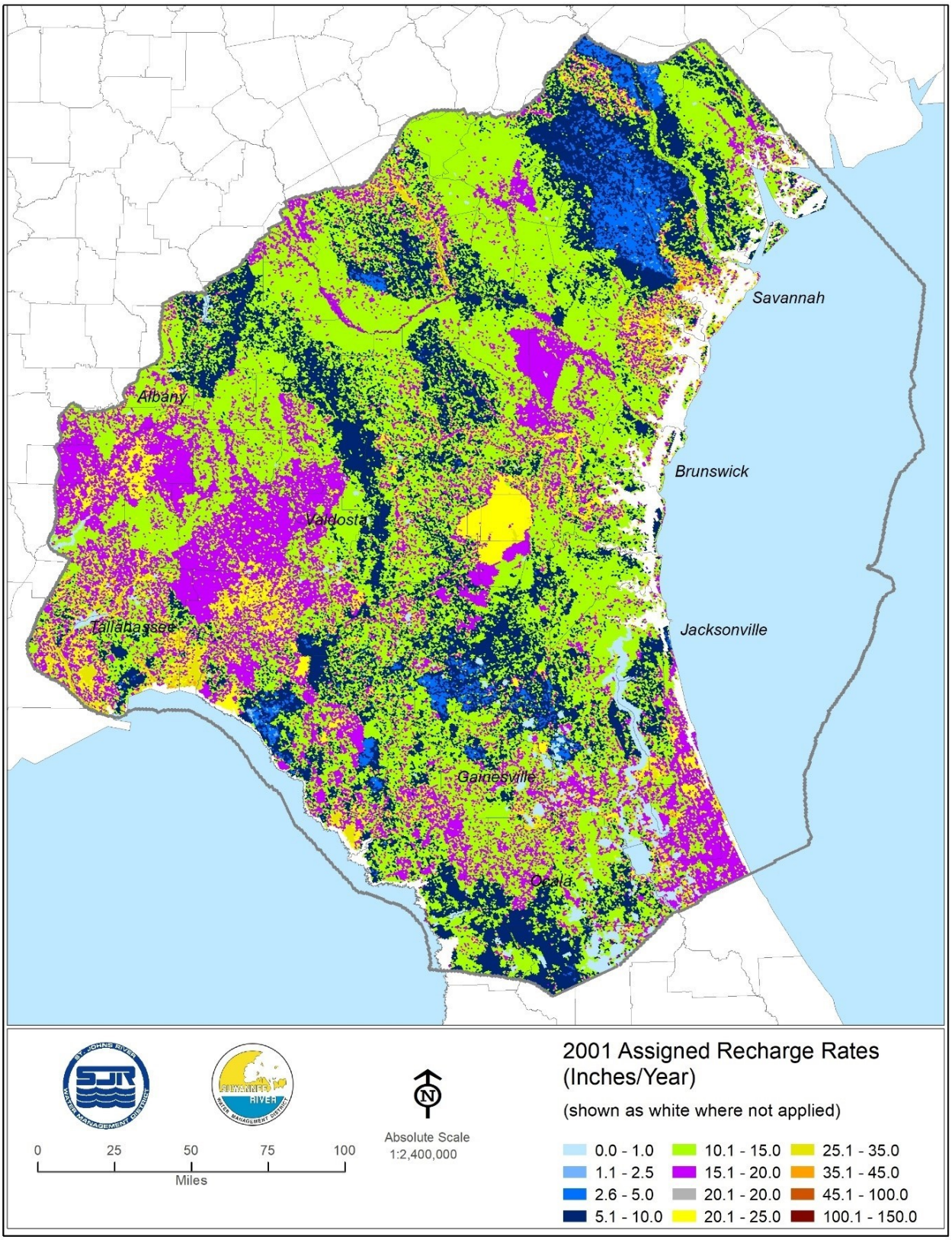

Figure 3-35. HSPF-derived rates of recharge, 2001 (inches per year)

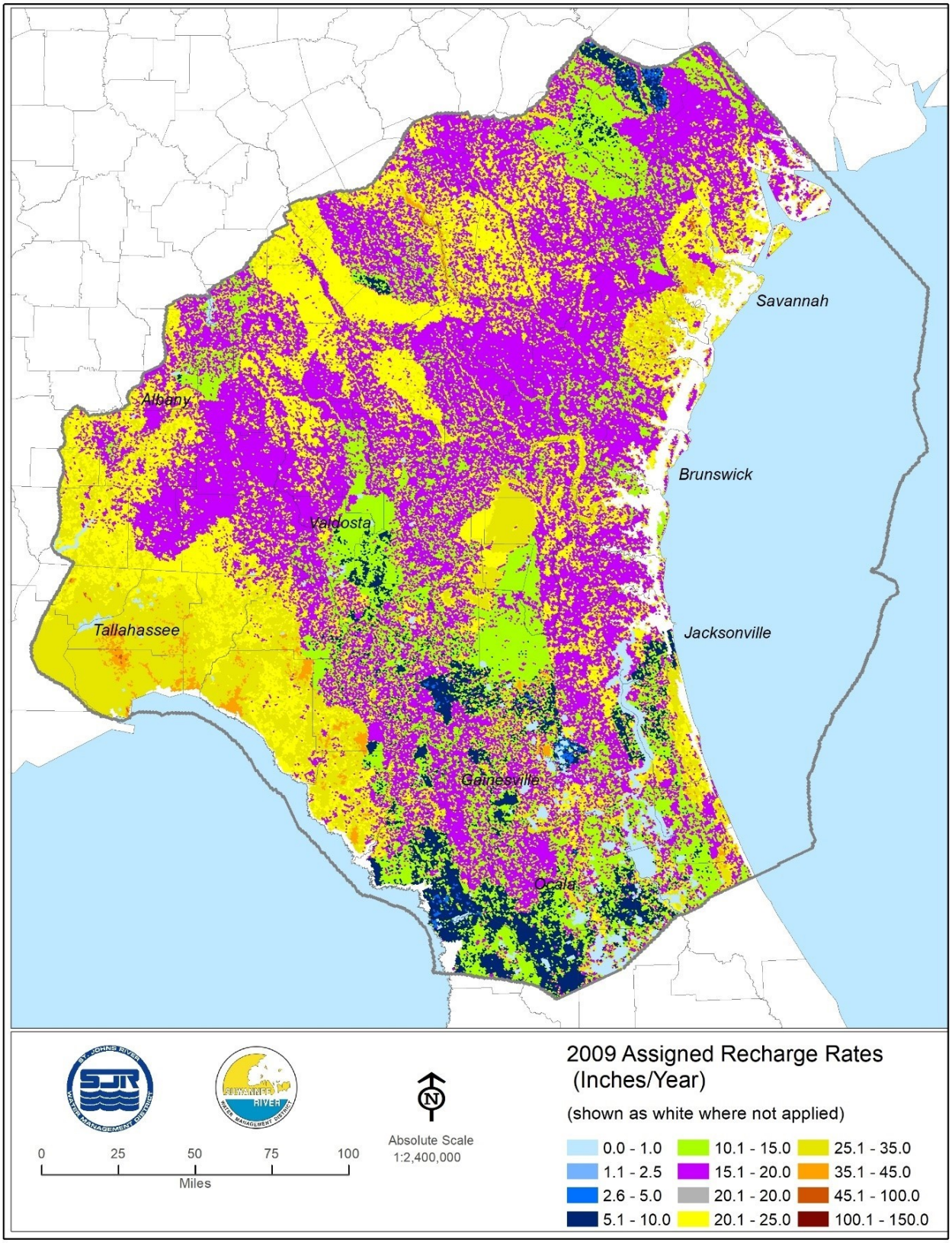

Figure 3-36. HSPF-derived rates of recharge, 2009 (inches per year)

water table is simulated as lying beneath the bottom of Layer 1 or bottoms of Layers 1 and 2. Areas in which Layer 1 or Layers 1 and 2 are dry correspond generally to those in which the surficial aquifer system and/or intermediate confining unit are thin to non-existent. In cases in which Layer 1 is active, recharge is applied to Layer 1. For cases in which Layer 1 is dry but Layer 2 is not, recharge is applied to Layer 2. For cases in which Layers 1 and 2 are both dry, recharge is applied to Layer 3.

The Evapotranspiration (ET) Package simulates evapotranspiration from the saturated groundwater flow system. This package requires arrays of the maximum rate of saturated evapotranspiration (MSET), the ET surface elevation (the water table elevation at which the maximum rate of ET is realized—specified as land surface elevation in the NFSEG model), and the ET extinction depth (the depth at which the ET rate declines to zero). As stated above, arrays of MSET for the years 2001, 2009, and 2010 were estimated using HSPF models (Figure 3-37 and 3-38). The approach used for estimating ET extinction depths (Figure 3-39) was based on an adaptation of the approach of Shah et al. (2007). The adaptation was developed by Freese (Appendix D) and implemented in ArcGIS by Stokes and Finer (digital communication 2014).

Regarding the accuracies of the recharge and maximum saturated ET values used in the NFSEG model, recharge and maximum saturated ET multiplier parameters were assessed in the NFSEG non-linear uncertainty analysis (see Chapter 7 and Appendix L). The results provided a measure of uncertainty of the HSPF-generated recharge and maximum saturated ET estimates. The coefficients of variation associated with the recharge and maximum saturated ET parameter groups were among the lowest, as shown in the boxplots of these coefficients of variation in Figure 7-11.

The HSPF models are calibration-constrained and based on internal mass balances of represented surface-water and groundwater flow components. Therefore, use of HSPF models to estimate recharge and maximum saturated ET was favored over other approaches, such as implementation of the SCS curve-number approach, that are not calibration-constrained. The use of HSPF for determination of recharge and maximum saturated ET was decided upon prior to initiation of NFSEG model development by the NFSEG Technical Tea

Well Package

The MODFLOW Well Package was used to represent single aquifer withdrawal wells. Single aquifer withdrawals are from wells that are open to only one aquifer or model layer. The MNW2 Package was used to represent “dual-zone” withdrawal wells. Dual -zone wells have open intervals that intersect the Upper Floridan aquifer, the middle confining unit, and the Lower Floridan aquifer and thus potentially extract water from both the Upper and Lower Floridan aquifers.

The MNW2 package calculates the contributions to the total well withdrawal of the various aquifers intersected by the open interval of a multi-aquifer well. In the implementation of MNW2, the distribution of the total discharge from a represented multi-aquifer well is based on the respective aquifer water levels and assigned horizontal hydraulic conductivities of the Upper Floridan aquifer, the middle confining unit, and up-

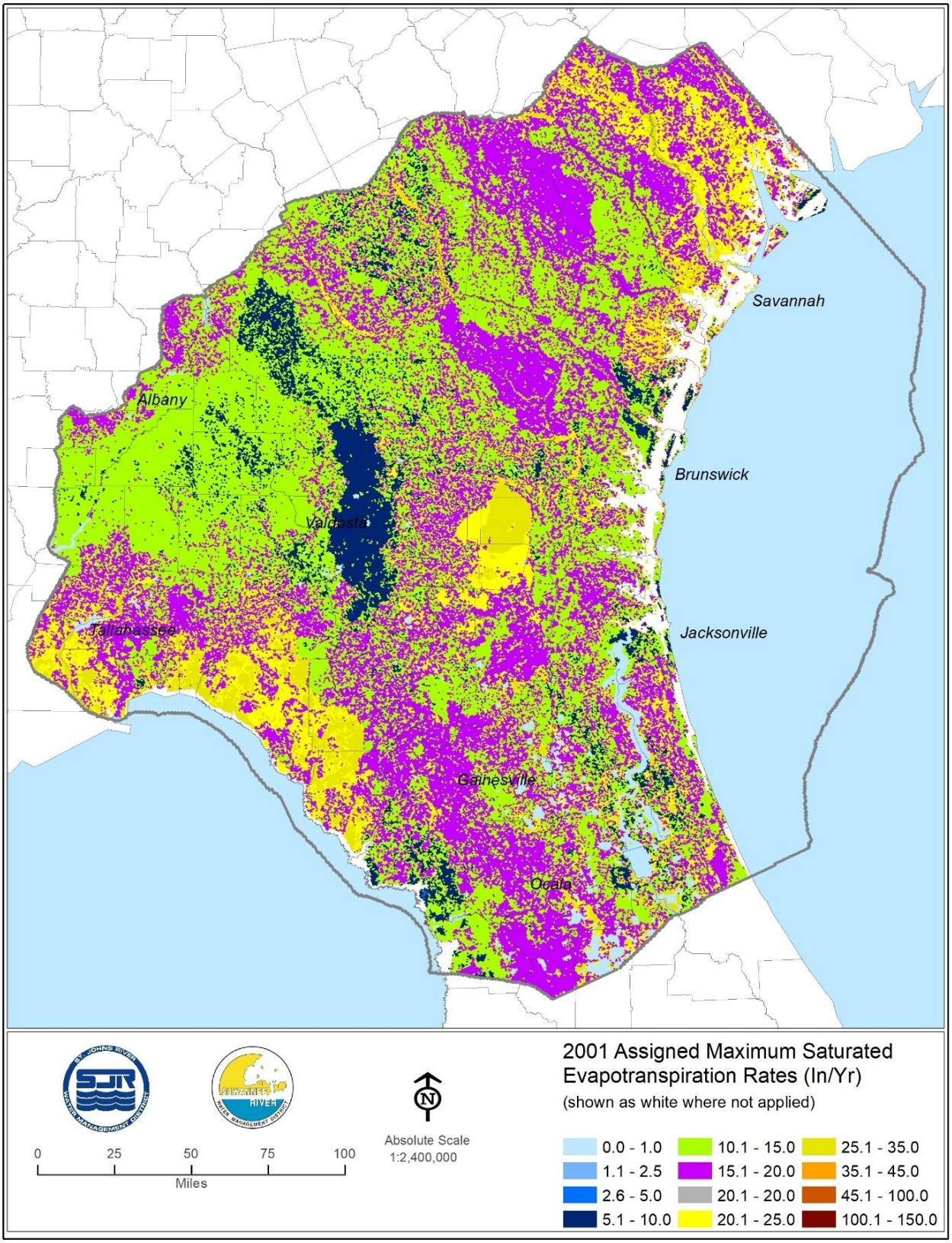

Figure 3-37. HSPF-derived rates of maximum saturated ET, 2001 (inches per year)

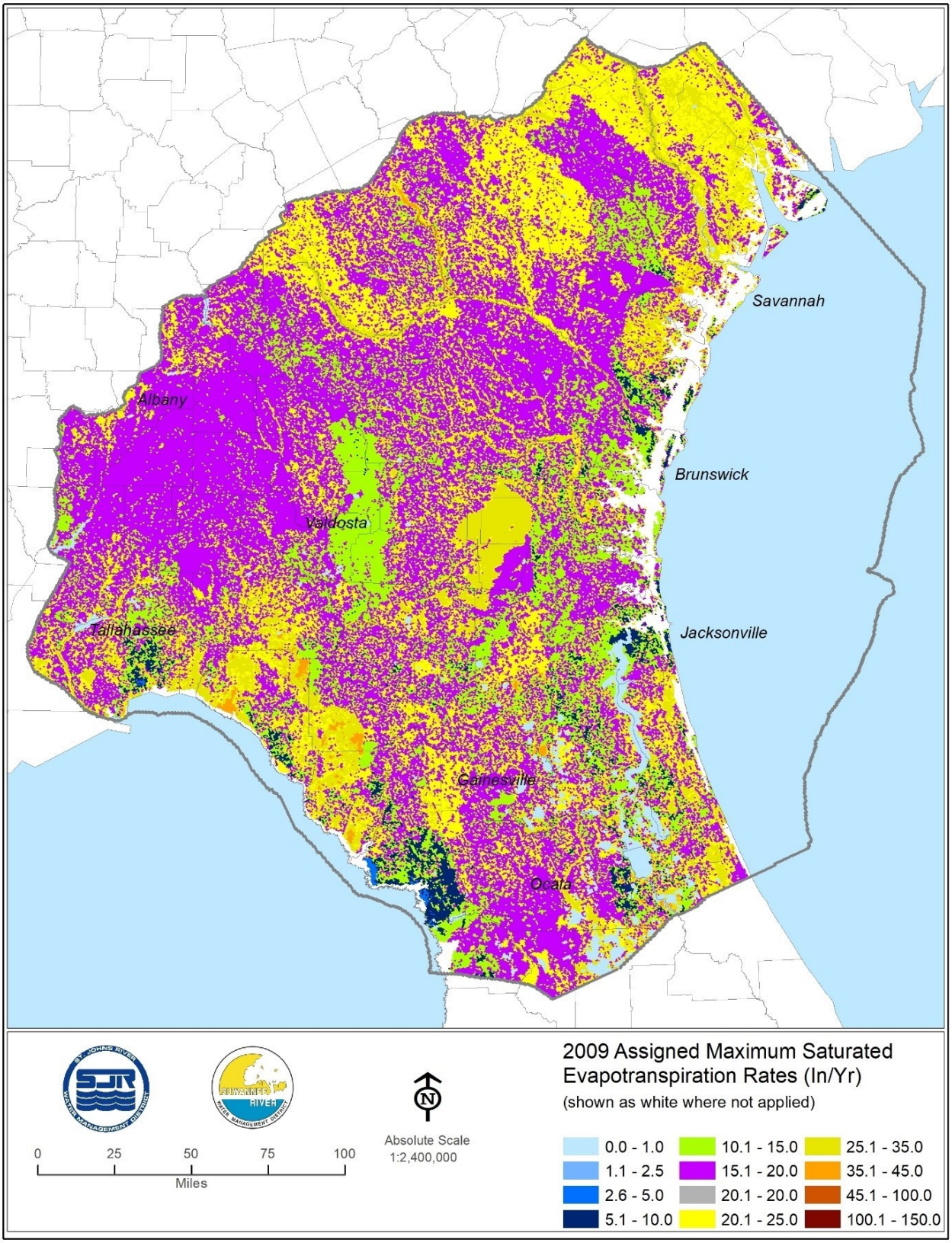

Figure 3-38. HSPF-derived rates of maximum saturated ET, 2009 (inches per year)

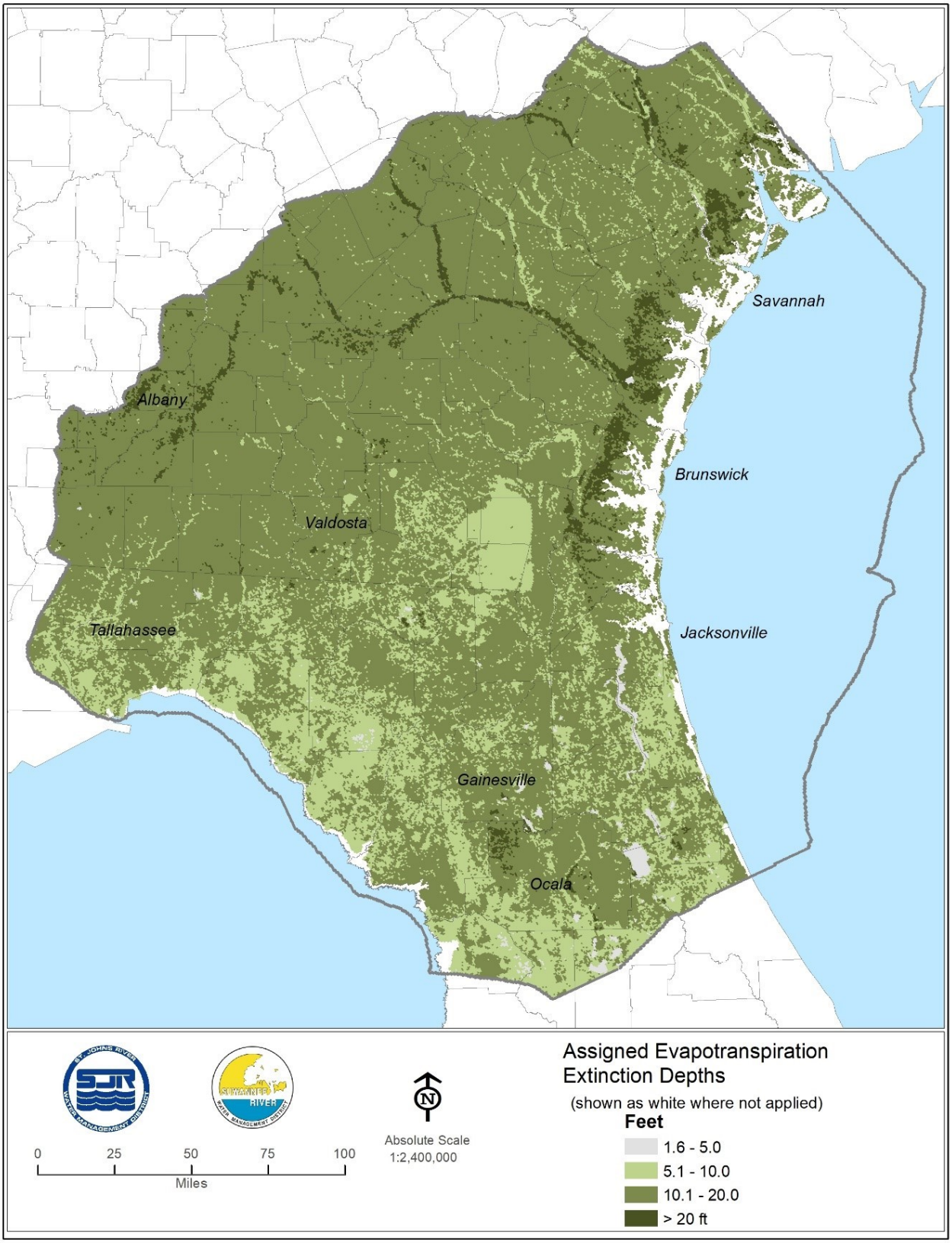

Figure 3-39. Estimated evapotranspiration extinction depths (feet)

per zone of the Lower Floridan aquifer at the location of the well. Because NFSEG is a regional model with a relatively large grid size, friction loss in the well bore was not simulated.

Most wells represented in the NFSEG model are single aquifer wells and are thus represented in the Well Package. Multi-aquifer wells, however, tend to be larger and deeper and therefore extract a disproportionate share of total groundwater withdrawals. Figures 3-40 through 3-44 depict locations of fluxes into and out of the model domain that were simulated with the Well and MNW2 packages.

Time Variant Specified Head Package

The Time Variant Specified Head Package was used to implement the assignment of specified head boundaries. Specified head boundaries were used in the model primarily to represent water levels of the Atlantic Ocean and the Gulf of Mexico. These levels were represented as equivalent freshwater heads (Figure 3-45). They are assigned to grid cells of Layer 1 that correspond to offshore locations and nearshore locations.

As applied in the current study, equivalent freshwater head is determined based on the following formula and was determined at the centroid of each grid cell that corresponds in location to the offshore region:

$$Hef = d(\Upsilon s/\Upsilon f-1)$$

where

Hef = equivalent freshwater head (feet NAVD88);
d = depth of ocean (feet);
Υs = the specific weight of seawater (pounds per cubic foot)
Υf = specific weight of fresh water (pounds per cubic foot).
$\Upsilon s/\Upsilon f$ = specific gravity of seawater (1.025 in the NFSEG application).

The depth d above was based on land surface and bottom elevation data provided in the USGS 3DEP 10m DEM.

Multiple Assignment of River, Drain, and GHB-Condition Boundaries

In many cases, more than one internal boundary condition must be assigned to a single grid cell to properly reflect conditions in the field. In the cases of river, drain, and GHB-condition boundaries under this circumstance, which are head-dependent flux-type boundaries that require specification of a conductance value and stage, the same simulated groundwater level is of course used by MODFLOW in determining the various simulated discharges of the various boundaries. Conductance, being scale-dependent in nature, adjusts for this implicitly, however, which is to say that, with all else being equal, different values of conductance must be utilized to simulate the same

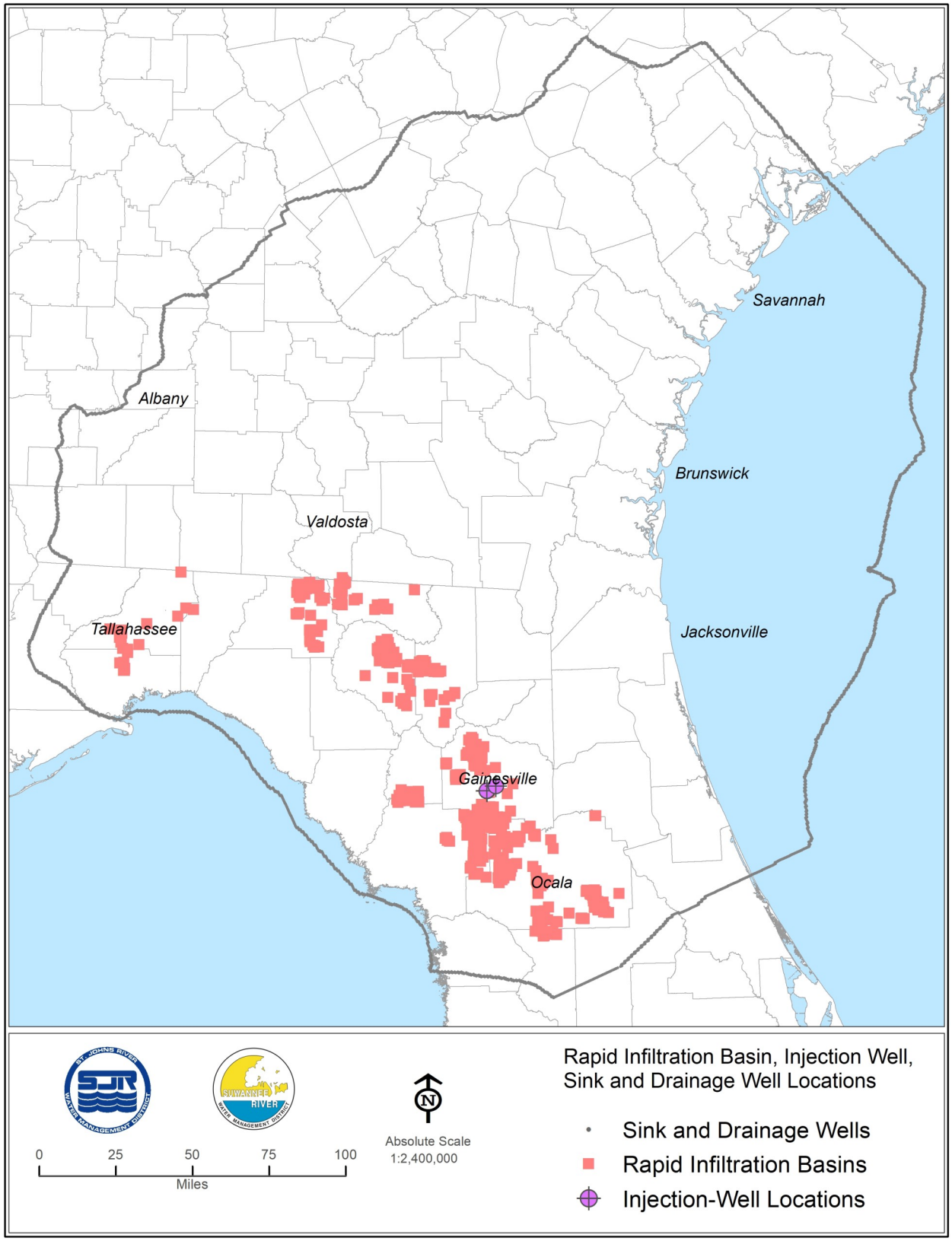

Figure 3-40. Locations of concentrated groundwater influxes

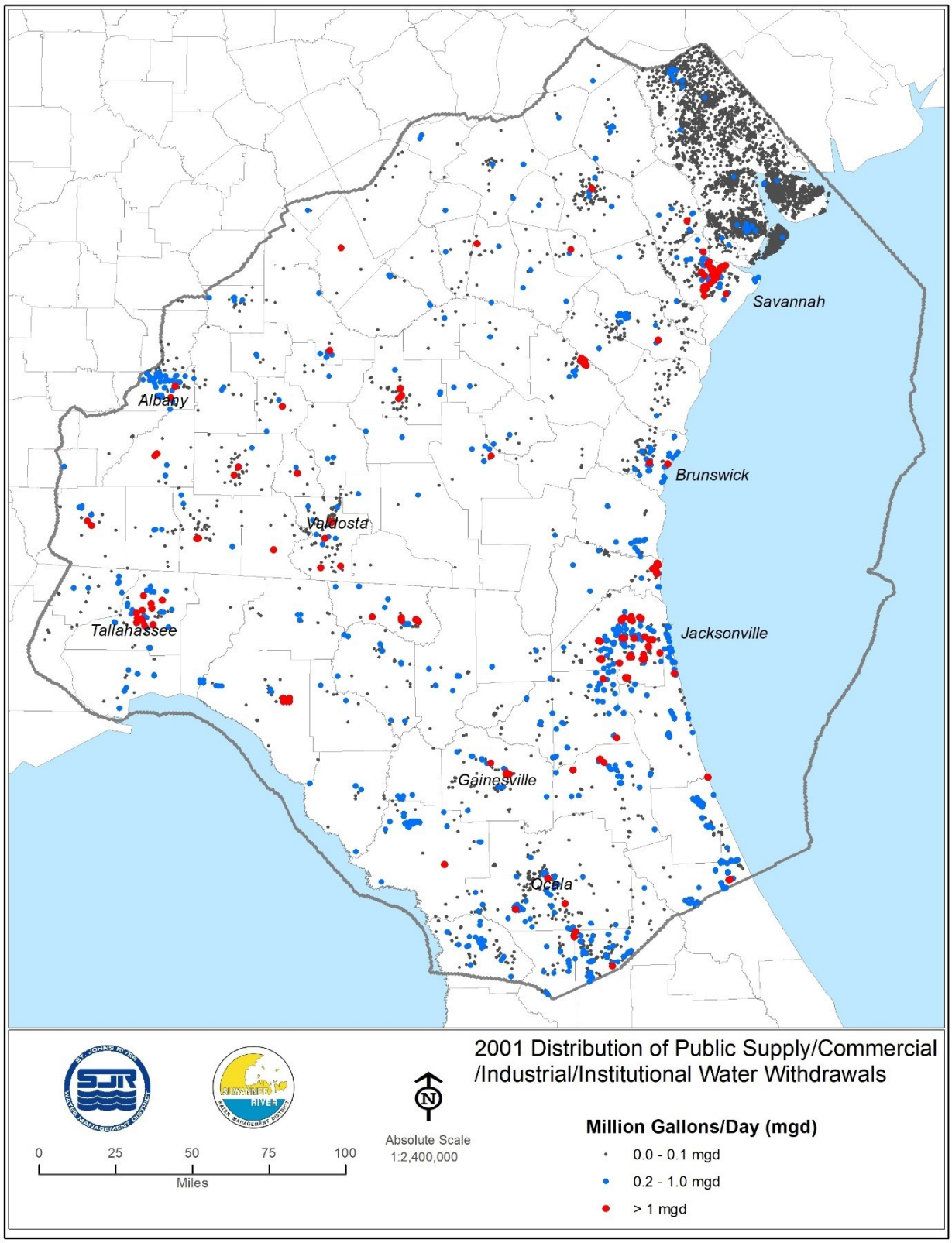

Figure 3-41. Distribution of public-supply, commercial-industrial, and institutional withdrawals (MGD), 2001

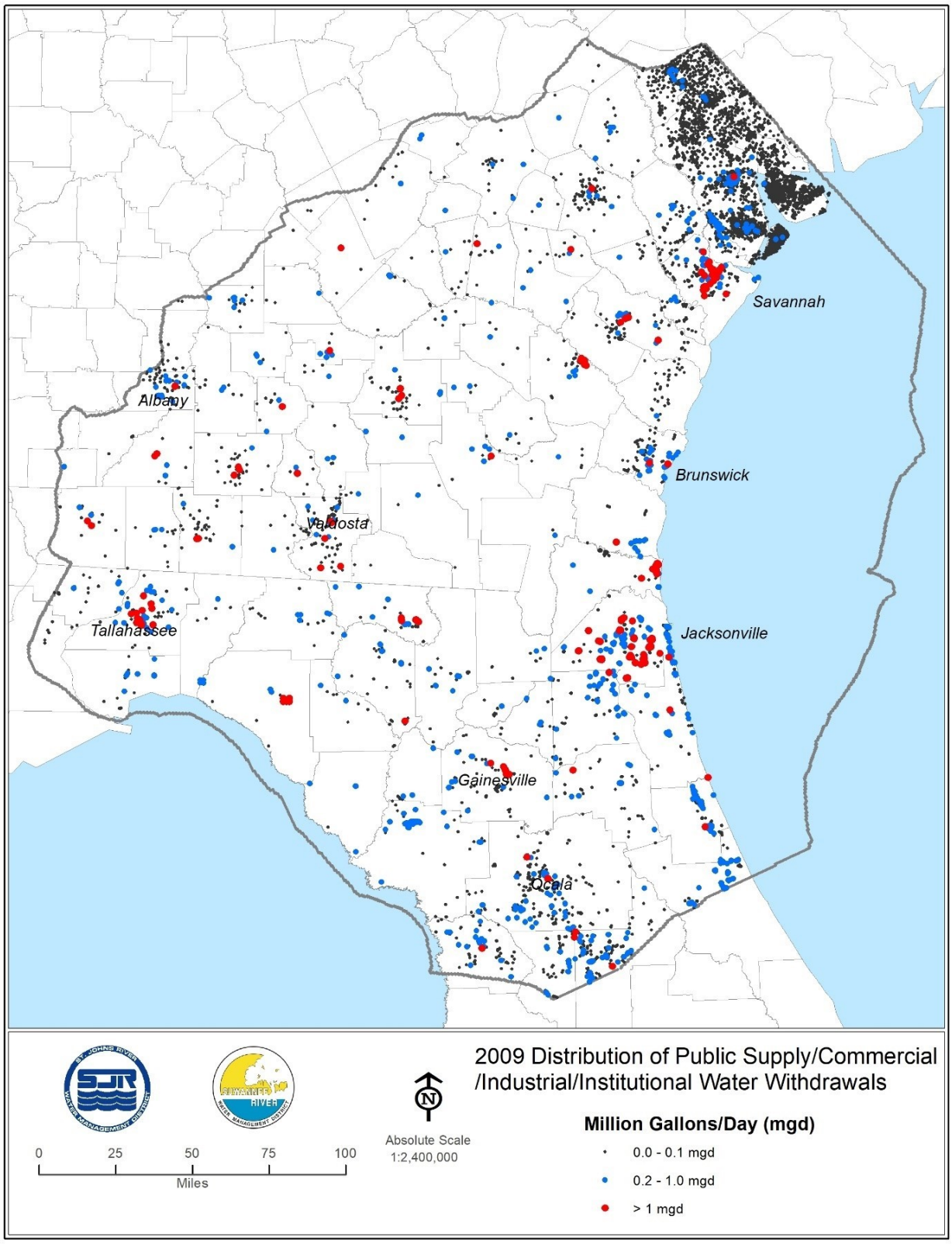

Figure 3-42. Distribution of public-supply, commercial-industrial, and institutional withdrawals (MGD), 2009

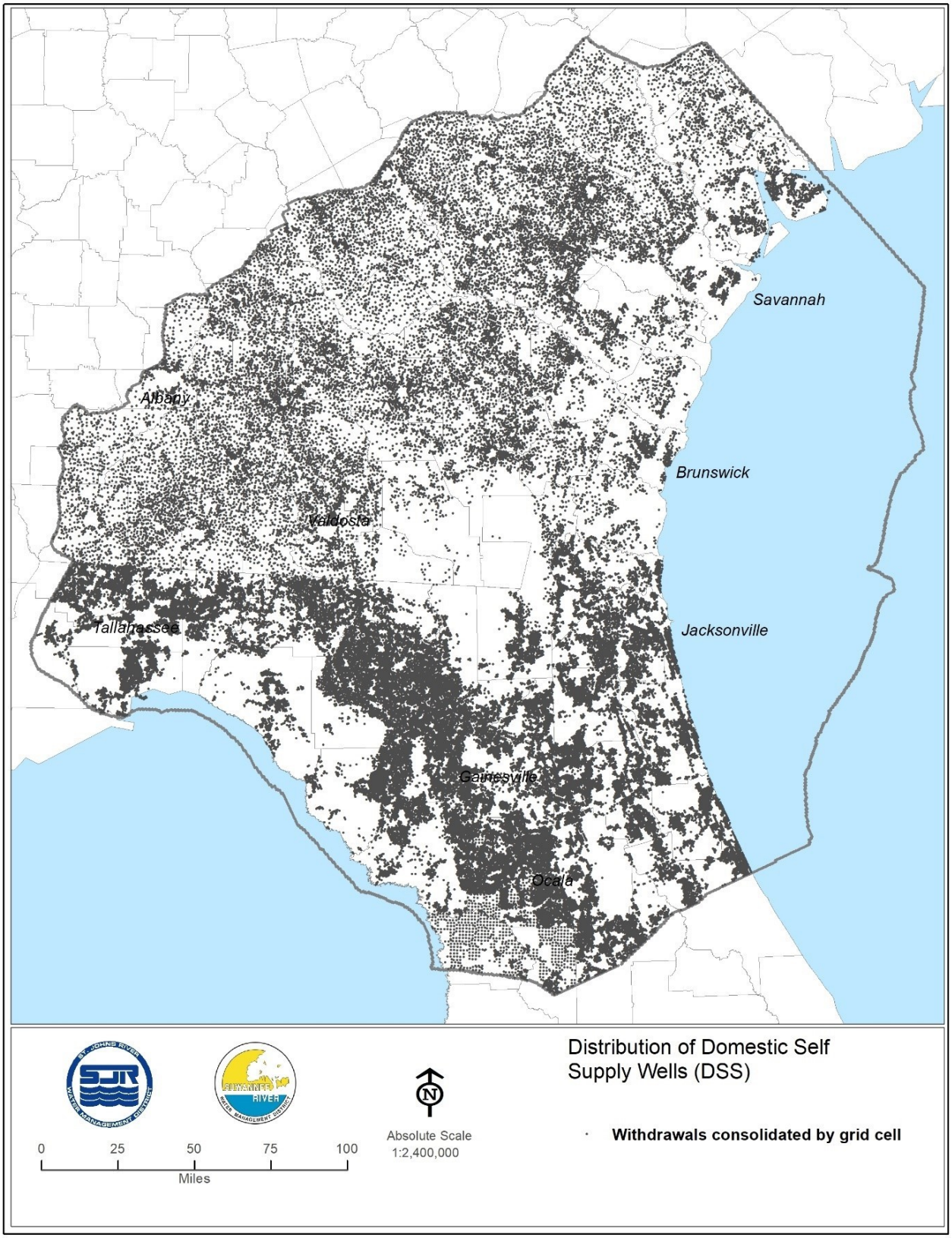

Figure 3-43. Distribution of DSS withdrawals (MGD)

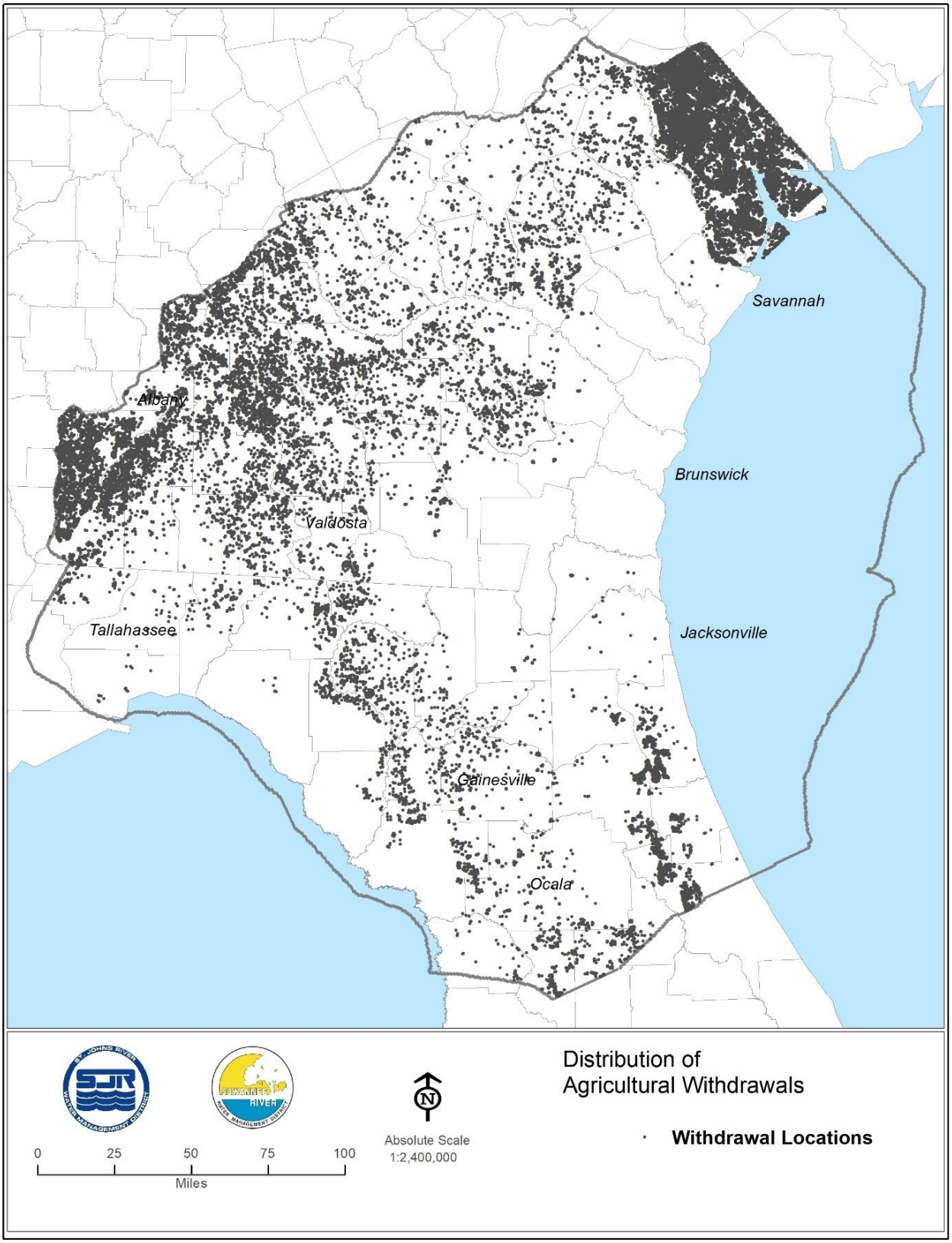

Figure 3-44. Distribution of agricultural withdrawals

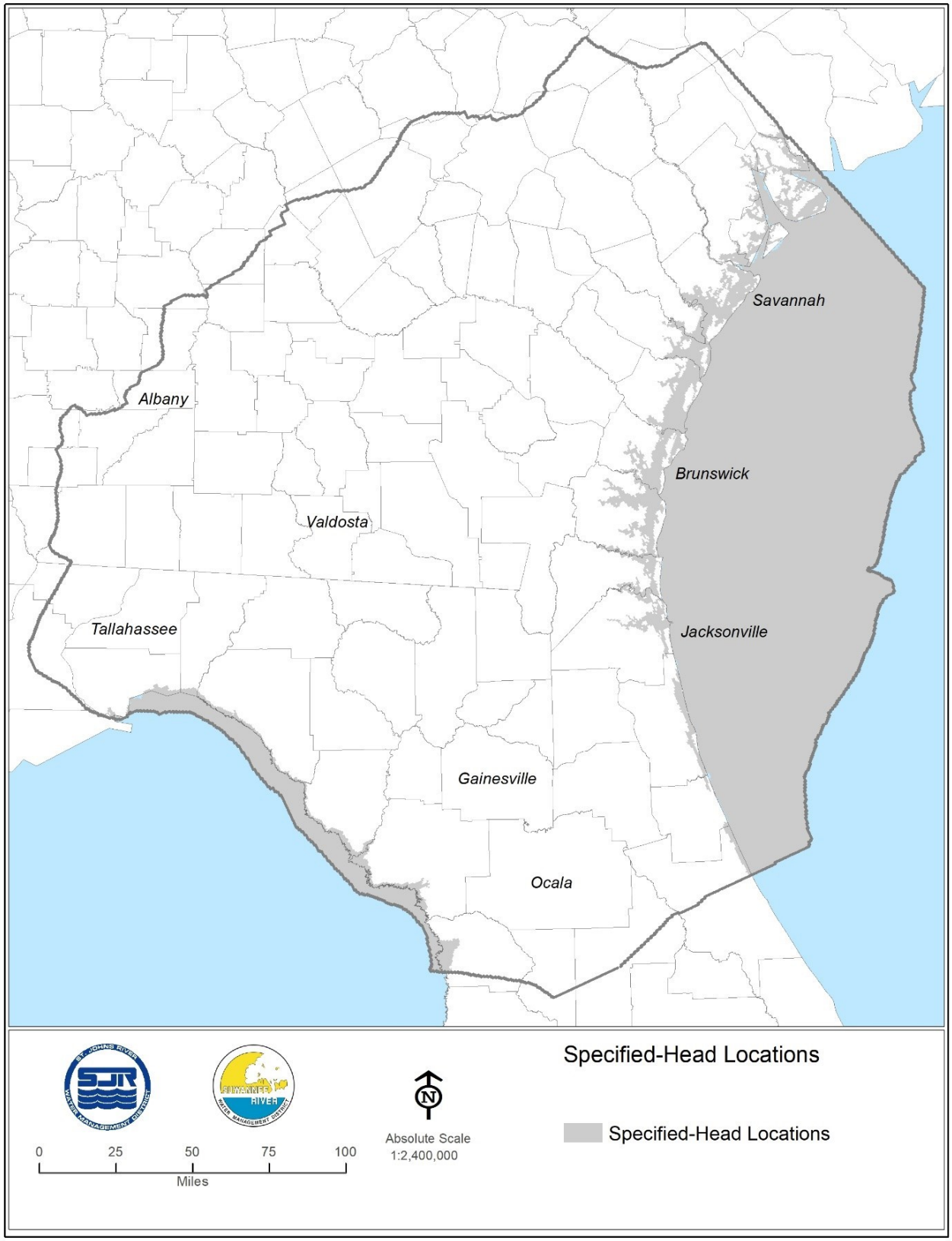

Figure 3-45. Distribution of specified-head grid cells in Layer 1

discharge under different levels of discretization. This is a characteristic of the finite-difference approach employed in MODFLOW and is not unique to NFSEG.

Regarding the representation of springs, the need to assign multiple GHB-condition boundaries to a given grid cell for representation of multiple springs would likely arise under any practical level of uniform discretization given the number and distribution of springs within the NFSEG model domain, which includes representation of more than 300 springs. Each NFSEG spring representation is assigned its own pool elevation in addition to its own conductance. In the case of river boundaries, only one boundary is assigned per grid cell in most cases. The same applies to drain boundaries. Regardless, each boundary is assigned its own conductance and pool elevation/stage, at least in cases in which different assignments are warranted, although assignment of a separate pool elevation of GHB conditions assigned to a given grid cell was not warranted in most instances. This allows for independent determinations of discharge in all cases, whether the boundary is the only one assigned to a given grid cell or shares assignment with other head-dependent flux-type boundaries.

CHAPTER 4. MODEL CALIBRATION

APPROACH

The NFSEG model calibration process included the selection of two calibration years. The primary considerations in the selection of the years were steadiness of groundwater levels and the degree to which rainfall could be characterized as average with respect to annual totals and monthly distributions. An additional requirement was that the years should be recent to increase the likelihood that needed data, such as water use, water level, and flow data, would be accessible and available. Due to this requirement, the selection period was limited to the years 2000 through 2010. As part of the resulting selection process, groundwater hydrographs and rainfall records were obtained and analyzed (Durden et 2013). The analyses included principal component analyses of groundwater hydrographs and analyses of departures from long-term monthly averages of rainfall amounts at various stations (Durden et al. 2013). Based on the results of the analyses, the NFSEG Technical Team concluded that 2001 and 2009 exhibited adequately constant groundwater levels and rainfall amounts that are acceptably close to long-term averages. An additional consideration was that 2001 was relatively dry while 2009 was relatively wet, thus providing the calibration process with a challenging range of climatic conditions.

The model was calibrated through implementation of Parameter ESTimation (PEST; Doherty 2015; Doherty 2016a; and Doherty 2016b). Prior to the PEST facilitated calibration, an initial calibration process was undertaken with the following objectives:

- To develop an improved understanding of the hydrological system;
- To develop improved understanding of model sensitivity to changes in hydraulic conductivity and other parameters;
- To develop improved understanding of potential ranges of horizontal and vertical hydraulic conductivity within model layers;
- To develop improved understanding of model numerical requirements, resulting in improved numerical stability and performance through implementation of MODFLOW-NWT; and
- To identify and implement needed improvements and/or corrections in model features.

The initial calibration process involved matching model simulated water levels and spring discharges to corresponding observed or estimated values throughout the model domain. The groundwater flow system was approximated as steady state in this analysis. Matching was carried out to 2001 and 2009 median observed conditions. The initial calibration culminated in a high level of consistency between simulated and observed

water levels and spring discharges throughout the model domain for both 2001 and 2009. Insights and results obtained from the initial calibration process were used to guide the PEST facilitated calibration process.

PEST Facilitated Calibration

The following description provides a general outline of the process used to calibrate the NFSEG groundwater model through implementation of PEST. PEST calibration is organized around two primary groups of data, observation groups and calibration parameter groups. Observation groups are comprised of water level and flow rate observations. Enablement of adequate simulation of the observations that comprise the observation groups is the primary objective of the calibration process. PEST facilitates calibration through a process of systematic adjustment of the various model parameters that constitute the calibration parameter groups. In the context of the NFSEG model, parameters are model representations of physical aspects of the hydrological system that control groundwater levels and flow rates.

PEST runs a model many times through numerous optimization iterations. For each of these iterations, and prior to estimating a set of parameter values, PEST constructs a Jacobian matrix, which contains the derivative of each observation with respect to each model parameter. PEST uses the resulting Jacobian matrix to arrive at an improved parameter data set by adjusting parameter values at the beginning of an iteration within ranges established by the PEST user. The quality of a parameter set is encapsulated in the PEST objective function, a measure of the goodness of fit between the observations that comprise the observation groups and model simulated counterparts. In its simplest form, the PEST objective function is defined as follows:

$$\Phi = \sum_{i=1}^{n} (w_i r_i)^2$$

where

Φ is the value of the PEST objective function resulting from a given PEST iteration, equal to the summation of the squares of the products of w_i and corresponding value of r_i, summed over n observations;
w_i is the weight assigned to the residual of observation i;
r_i is the difference between the value of observation i and its model simulated counterpart (i.e., the residual of observation i); and
n is the number of all observations comprising the various observation groups.

Through multiple iterations, PEST determines numerous parameter data sets, resulting in numerous objective function values. The objective of the process is to minimize the value of the objective function while maintaining the values of the various calibration parameters within user specified ranges.

PEST calibration requires detailed design, oversight, and analysis of the results of the calibration process and thus is not an automated process. The process can be influenced using pre and postprocessing programs that control the interpretation of PEST determined parameters, an approach that was utilized extensively in the NFSEG calibration.

PEST users influence the calibration process through specification of initial, maximum, and minimum values of calibration parameters (i.e., starting values and acceptable ranges of parameters). PEST users also influence the calibration process through specification of weights assigned to residuals of observations (i.e., the relative influence of a residual).

An additional component of the PEST objective function is often utilized, in addition to the one discussed above. That component is based on the difference between the initial value of a given calibration parameter and the corresponding PEST determined value. The process of implementation of the additional objective function component is called regularization. In the application of PEST, however, this component was deemphasized due to time constraints and difficulties in implementation. Therefore, in the NFSEG model application, the PEST objective function is represented nearly entirely by the value of Φ as stated above.

OBSERVATION DATA GROUPS

Through implementation of PEST, the NFSEG model was calibrated simultaneously to median observed water levels and flow rates for the years 2001 and 2009, with conditions for both years represented as steady state. Table 4-1 provides a detailed listing of the observation groups utilized in the PEST calibration process. The observation groups listed there may be categorized generally as follows:

- Groundwater levels;
- Spring discharge rates;
- Baseflow rates (as total baseflow accumulation for specific gauges, i.e., "cumulative baseflows," and as the difference in baseflow between gauges, i.e., "pickups");
- Vertical head differences, i.e., between corresponding observed groundwater levels in the surficial aquifer system and Upper Floridan aquifer (model Layers 1 and 3) or between the Upper Floridan aquifer and Lower Floridan aquifer (model Layers 3 and 5);
- Horizontal head differences within the Upper Floridan aquifer (i.e., Layer 3); and
- Estimated lake leakage rates.

A wetting penalty function that incorporated observations of maximum water table elevations was also implemented in limited areas to help prevent excessive simulated flooding in Layer 1. This function was based on assumed maximum heights of the water table above land surface in wetlands and uplands.
Temporal head difference targets were also employed in the earlier stages of the calibration process of NFSEG v1.1. These targets were computed as the difference in the head observation (target value) between the two calibration years (2001 and 2009) at a given observation well and then assigned to one of six temporal head difference groups corresponding to model Layers 1, 2, 3, 4, 5 and 6. These temporal observation groups were zero weighted during the development of NFSEG v1.1 because recharge and maximum saturated ET were not being adjusted.

Table 4-1. NFSEG PEST Observation Groups

Observation Group Name	Description
h2001_lay1 , h2001_lay2 … h2001_lay7	Heads in Layers 1 through 7 in 2001
h2009_lay1 , h2009_lay2 … h2009_lay7	Heads in Layers 1 through 7 in 2009
hd2001_lay3	Lateral head differences in Layer 3: 2001
hd2009_lay3	Lateral head differences in Layer 3: 2009
td_lay1 … td_lay7	Temporal head differences in Layers1 through 7
wp_dry_2001, wp_dry_2009	'penalty function' for minimizing the occurrence of dry cells areas in wetland areas: 2001 and 2009
wp_wet_2001 , wp_wet_2009	'penalty function' for minimizing the occurrence of 'flooded cells': 2001, 2009
vd_1to3_01, vd_1to3_09	Vertical head differences: Layer 1 to 3 in 2001, 2009
vd_3to5_01 , vd_3to5_09	Vertical head differences: Layer 3 to 5 in 2001, 2009
qr01 , qr09	Inflow to river reaches bounded by one or more gauges: 2001 , 2009
qspring01 , qspring09	Inflow to springs: 2001, 2009
qs_spring01 , qs_spring09	Inflow to spring groups: 2001, 2009
qs01 , qs09	Cumulative inflow to collections of river reaches: 2001, 2009
qlake01 , qlake09	Flow to/from lakes: 2001, 2009

Groundwater Levels

The groundwater level observation groups contain data obtained from various sources, including USGS, SJRWMD, SRWMD, SWFWMD and NWFWMD. Statistical methods were used to augment the number and quality of water level observations in areas of limited water level data availability, as detailed in Appendix A.

Spring Flow Rates

Spring flow rates for the years 2001 and 2009 were estimated from available field measurements (Figures 2-33 through 2-35; Appendix E). Generally, for springs with field measurements specific to 2001 and/or 2009, the medians of the available field measurements were utilized. For cases in which data specific to 2001 and/or 2009 were not available, period of record (POR) estimates were used. Outside of the SRWMD, POR estimates were utilized directly. Within the SRWMD, POR estimates were reduced by approximately 25 percent and 5 percent in the years 2001 and 2009, respectively. This was done to reflect more closely the hydrologic conditions of the two calibration years. For some cases in which regression relations between spring flows and concurrent groundwater levels or other data were available, improved estimates of the 2001 and 2009 spring flow targets were computed based on the regression relations. In addition, differences between upstream and downstream flow estimates or geochemical data were used to estimate flows from selected river rises. Sources of data included the USGS, SJRWMD, SRWMD, SWFWMD and NWFWMD.

Baseflow Rates

Baseflow estimates to reaches bounded by one or more gauges and baseflow estimates from collections of these reaches were used as calibration targets, as discussed in Chapter 2 (Figures 2-36 through 2-44; Appendix F). Baseflow rates are generally estimated through baseflow separation analysis, as detailed in Chapter 2.

Vertical Head Differences

Vertical head differences were computed from observations obtained in the same year from two wells that are open to different aquifers at or near the same geographical location. Vertical head differences between the surficial aquifer system and Zone 1 (between model Layers 1 and 3; see Chapter 2 for definitions of Zones 1, 2, and 3) and between Zones 1 and 3 (between model Layers 3 and 5) were computed (Figures 2-9 and 2-10; Figures 2-31 and 2-32; Appendix B). The main purpose of this group is to provide information for calibration of the vertical hydraulic conductivity of model Layers 2 and 4.

Horizontal Head Differences

Horizontal head differences are based on observations obtained in the same year from two wells that are open to the same aquifer at different geographical locations and that are typically aligned along the path of a groundwater streamline as inferred from a map of the potentiometric surface of the Upper Floridan aquifer. This observation group is based solely on lateral water level differences in Zone 1 (Figures 4-1 and 4-2; Appendix H; see Chapter 2 for definitions of Zones 1, 2 and 3). The purpose of this group was to improve estimation of horizontal hydraulic conductivity of Layer 3 through improved simulation of horizontal head gradients in Layer 3.

Lake Leakage Rates

The purpose of the lake leakage observation groups is to prevent the simulation of unrealistically high lake leakage rates. During calibration, unrealistically high simulated lake leakage rates can compensate for other processes or parameters that are poorly represented in the model and thus mask underlying calibration issues with respect to those processes or parameters as well as lake leakage rates. Including limits on lake leakage rates helped to constrain leakage rates to reasonable values and prevent masking of other calibration issues as well. The lakes represented with the MODFLOW River Package represent a small fraction of the active NFSEG domain, which minimizes the potential for errors in estimating lake leakage rates from adversely affecting calibration derived estimates of parameter values.

Except for some lakes in the Keystone Heights region in southeast Clay County and lakes in the Orange Creek Basin in Alachua County, Florida, lake leakage rates were estimated as the difference between rainfall and potential evapotranspiration. The leakage rates of lakes Brooklyn and Geneva of the Upper Etonia Creek basin chain of lakes as well as lakes Orange and Lochloosa in the Orange Creek Basin were estimated based on values cited in previous studies (Clark et al. 1963; Deevey 1988; Dykehouse 1998; Hirsch and Randazzo 2000; Annable et al. 1996; Merritt 2001; Motz et al. 1994; and Lin 2011).

Wetting Penalty

The wetting penalty is a special observation data group created for purposes of reducing the occurrence of excessive simulated flooding. In the wetting penalty implementation, the NFSEG model grid is subdivided into grid cell blocks of 10 rows by 10 columns. Each active grid cell of each grid cell block is designated as wetland or upland, depending on prevailing conditions within the grid cell. A wetting penalty is then determined for each active grid cell, depending on its designation. The wetting penalty is a contribution to the PEST objective function that depends on the grid cell designation and the height of the simulated water table above land surface within the grid cell.

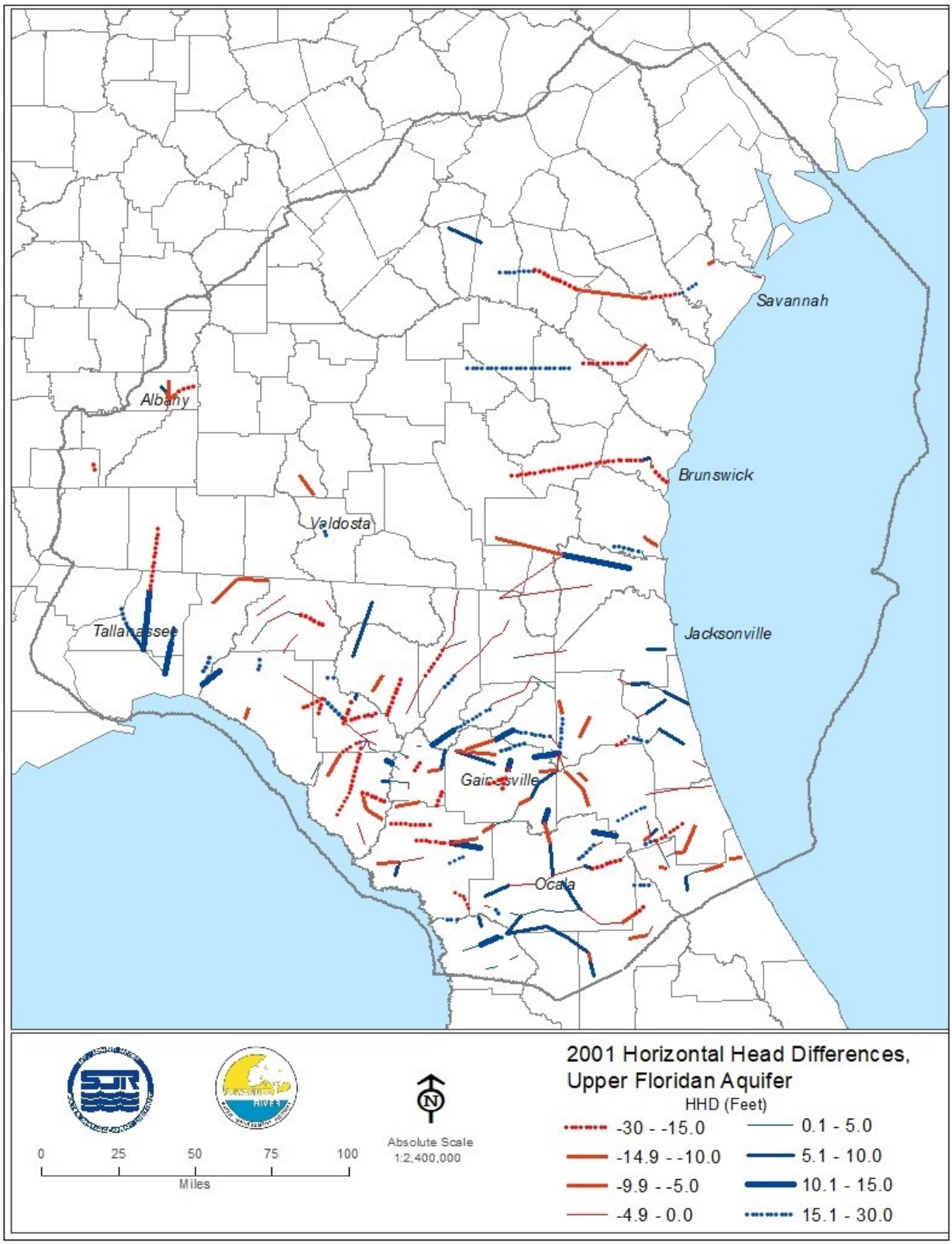

Figure 4-1. Estimated horizontal head difference, upper Floridan aquifer, 2001

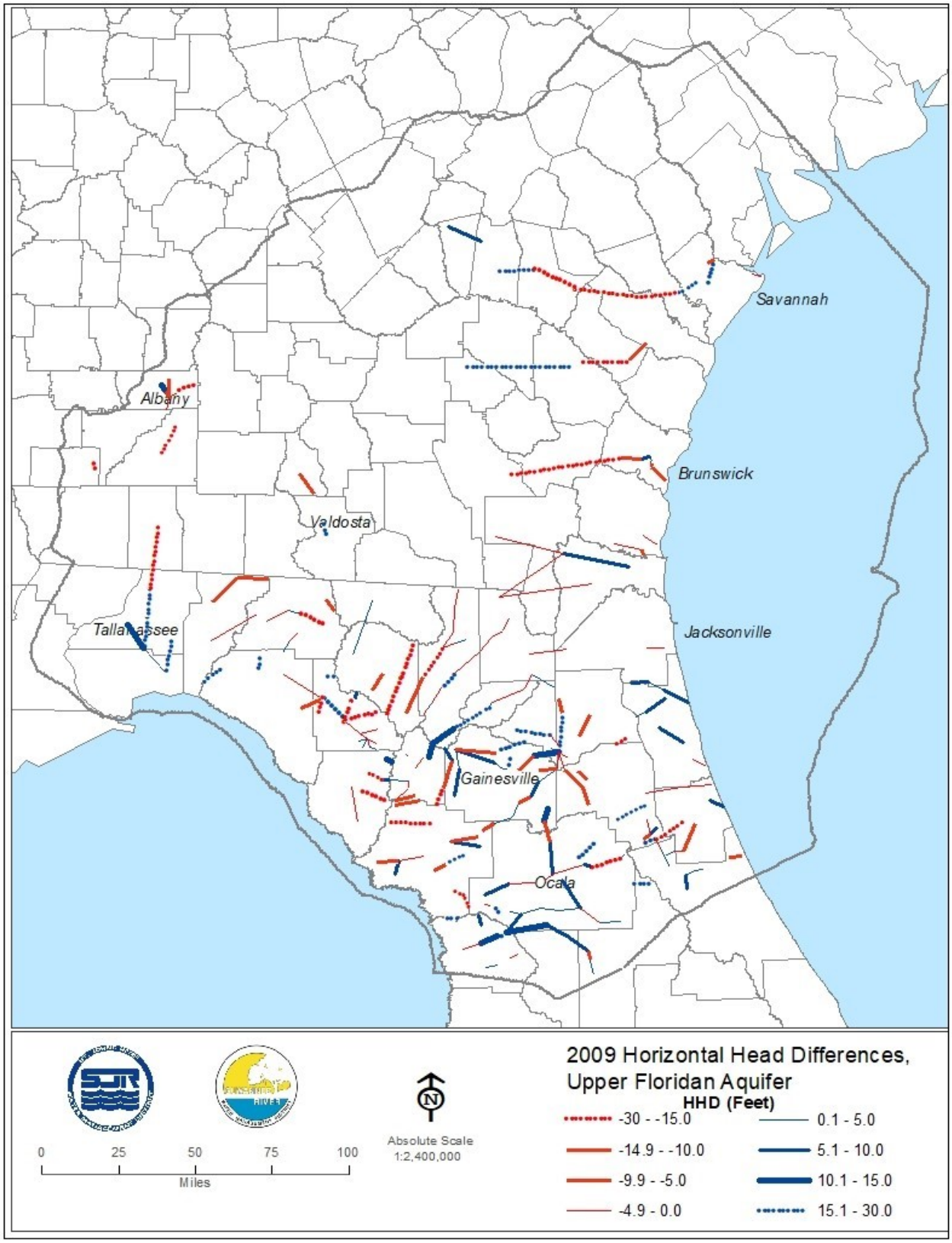

Figure 4-2. Estimated horizontal head difference, upper Floridan aquifer, 2009

For each wetland designated grid cell given grid cell block *p*, the wetting penalty is determined according to the following formula:

$$л = w_p(m\text{-}1) \text{ for } m \geq 1 \text{ foot and}$$
$$л = 0 \quad \text{for } m < 1 \text{ foot}$$

where

л = wetting penalty contribution to the PEST objective function of the grid cell in question,

w_p = the weight assigned to all grid cells contained within grid cell block *p*; and

m = height of the simulated water table above the average land surface elevation of the grid cell (feet).

For each upland designated grid cell of grid cell block *p*, the wetting penalty is

$$л = w_p(m) \text{ for } m \geq 0 \text{ foot and}$$
$$л = 0 \quad \text{for } m < 1 \text{ foot}$$

The wetting penalty can be emphasized to a lesser or greater degree over an entire grid cell block through adjustment of the assigned wetting penalty weight, as the same weight is used for all grid cells within a grid cell block. By setting the weight to zero, the contribution to the value of the objective function of a cumulative wetting penalty of an entire grid cell block can be eliminated.

As the calibration phase of the NFSEG model development progressed, flooding issues were determined to be due to the lack of representation of surface water drainage features in most cases. In most of such instances, the omitted surface water feature was in the form of sloughs, which are indicated on U.S. Geological Survey 1: 24,000 scale quadrangle maps, aerial photography and/or the USGS 3DEP 10m DEM. These data were used to determine the appropriate flow paths of the omitted streams or sloughs and to implement their representation in the NFSEG model Drain Package as ephemeral reaches within larger stream networks, the simulated flows of which are constrained in the calibration process through comparisons to estimated baseflows. Implementation of the wetting penalty was not required in such cases. During the development of NFSEG v1.0, application of the wetting penalty was eliminated from nearly all of the model domain to minimize to potential for convergence instability during the calibration process, except for a region of southern Alachua and northern Marion counties.

CALIBRATION PARAMETER GROUPS

Table 4-2 provides a detailed listing of the calibration parameter groups utilized in the NFSEG PEST calibration process. The calibration parameter groups listed there may be categorized generally as follows:

1. Hydraulic conductivity (horizontal and vertical), horizontal and vertical hydraulic conductivity multipliers, and anisotropy ratio;
2. GHB conductance for spring representation;

3. River Package conductance multipliers for determination of river package conductance in representation of perennial stream reaches;
4. Drain Package conductance multipliers for determination of drain package conductance in representation of ephemeral stream reaches and selected wetlands;
5. River Package conductance multipliers for lake representation;
6. Lake zone multipliers for adjustment of model Layer 2 vertical hydraulic conductivity beneath lakes to constrain lake leakage rates;
7. Recharge multipliers; and
8. Maximum saturated ET multipliers.

PEST calibration requires specification of an initial value and an upper and lower bound for each parameter member of the calibration parameter groups. Additional information concerning the calibration parameter groups follows.

Interpolation is utilized to assign parameter values to model cells between pilot points. PEST interpolation was performed with the "calc_kriging_factors_auto_2d" function from John Doherty's PLPROC program (Doherty 2016), which was implemented with the default, ordinary kriging option. This function employs an exponential variogram in which the parameter, ***a***, that is used to characterize the range of the variogram varies spatially and is a function of the distance between pilot points (Doherty 2016).

Horizontal and Vertical Hydraulic Conductivity

Horizontal Hydraulic Conductivity Determination for Layers 1, 3, and 7 and Vertical Hydraulic Conductivity Determination for Layer 6

Horizontal hydraulic conductivity is determined in the NFSEG PEST calibration process directly for Layers 1, 3 and 7 at the locations of "pilot points." Vertical hydraulic conductivity is likewise determined directly for Layer 6 at pilot points. Pilot points are user specified points at which the values of calibration parameters are determined in the PEST calibration process. After the determination of hydraulic conductivity at pilot points, PEST is used to determine values of hydraulic conductivity at individual grid cells by interpolating between pilot points using kriging.

In the calibration process, the determination of pilot point locations was initialized through application of *Groundwater Vistas* (http://www.groundwatermodels.com/), a program that facilitates the processing of input and output data for MODFLOW and for MODFLOW related applications of PEST. Implementation of this feature of *Groundwater Vistas* resulted in the creation of pilot point meshes comprised of triangular patterns formed around observation wells. Gaps in a mesh, which can occur due to localized sparseness in the observation well network, were filled with pilot points spaced at regular intervals of 25,000 to 125,000 feet (varies by layer). Thus, localized, rectilinear patterns of pilot points were interspersed within the triangular mesh that was generated initially by *Groundwater Vistas*. As a final step, individual or small groups of pilot points were added at specific locations as deemed necessary or desirable.

Table 4-2. NFSEG PEST Calibration-Parameter Groups

Parameter Group Name	Parameterization Device	Description
k1x	pilot points	horizontal hydraulic conductivity – Layer 1
k3x	pilot points	horizontal hydraulic conductivity – Layer 3
k5xk3x	pilot points	horizontal hydraulic conductivity multiplier outside MCU – Layer 5
k5x	pilot points	horizontal hydraulic conductivity – Layer 5
k7x	pilot points	horizontal hydraulic conductivity – Layer 7
k2z	pilot points	vertical hydraulic conductivity – Layer 2
k2zk3z	pilot points	vertical hydraulic conductivity multiplier outside ICU – Layer 2
k4zk3z	pilot points	vertical hydraulic conductivity multiplier outside MCU – Layer 4
k4z	pilot points	vertical hydraulic conductivity – Layer 4
k6z	pilot points	vertical hydraulic conductivity – Layer 6
vanis1	entire layer	vertical anisotropy – Layer 1
vanis2	zoned according to presence/ absence of ICU	vertical anisotropy – Layer 2
vanis3	pilot points	vertical anisotropy – Layer 3
vanis4	zoned according to presence/ absence of MCU	vertical anisotropy – Layer 4
vanis5	zoned according to presence/ absence of MCU	vertical anisotropy – Layer 5
vanis6	entire layer	vertical anisotropy – Layer 6
vanis7	entire layer	vertical anisotropy – Layer 7
lcm	zoned according to lakes	multiplier applied to lakebed conductance
rcm	zoned according based on HUC10 hydrologic basin boundaries	multiplier applied to river reach conductance
sc	1 parameter per spring	GHB conductance at springs
rechmul	zoned according based on HUC10 hydrologic basin boundaries	multiplier applied to recharge rates
evtrmul	zoned according based on HUC10 hydrologic basin boundaries	multiplier applied to maximum EVT rates
lkzmul	zoned according to lakes	vertical conductivity multiplier under lakes

Such points usually corresponded to places within the model domain for which additional information was needed from the calibration process or at which additional information was available for application to it. Examples of such places include areas of steep gradients in the potentiometric surface of the Upper Floridan aquifer and near springs (Figures 4-3 through 4-6).

Vertical Hydraulic Conductivity of Model Layers 2 and 4, Horizontal Hydraulic Conductivity of Model Layer 5, and Vertical and Horizontal Hydraulic Conductivity Multipliers

For Layer 2, vertical hydraulic conductivity is determined directly in the NFSEG PEST calibration process at pilot points in the parts of the model domain that correspond to areas in which the intermediate confining unit is contiguous (Figure 4-7). This is the same approach as described above regarding the determinations of horizontal hydraulic conductivity in Layers 1, 3 and 7 and vertical hydraulic conductivity in Layer 6. Likewise, after the determination of the vertical hydraulic conductivity of Layer 2 at pilot points, PEST was used to determine vertical hydraulic conductivity at individual grid cells by interpolating between the pilot points using kriging.

For portions of the model domain that corresponded to areas in which the intermediate confining unit is thin or absent, i.e., unconfined regions, a slightly more complicated approach, referred to hereafter as "the multistep approach," was used for determining the vertical hydraulic conductivity of model Layer 2. The multistep approach is designed to address the possibility that areas of local confinement may exist within areas that are broadly classified as unconfined. In this approach, the hydraulic properties of Layer 2 were assumed to be the same as the Upper Floridan aquifer unless calibration data indicated that a degree of local confinement existed.

For areas in which the intermediate confining unit was generally absent, Layer 2 vertical hydraulic conductivity at a particular cell was equated to the product of the vertical hydraulic conductivity of the underlying Layer 3 grid cell and a multiplier assigned by PEST. Prior to assigning multipliers to individual grid cells, PEST was first used to determine multipliers at pilot points located in parts of the model domain that corresponded to noncontiguous areas of the intermediate confining unit. The values assigned to individual grid cells were determined by interpolating between pilot points (Figure 4-7).

This approach tends towards similarity between the distributions of Layer 2 and Layer 3 vertical hydraulic conductivity in parts of the model domain that correspond to areas in which the intermediate confining unit is generally absent. Layer 2 is thus assumed to be generally more representative of the hydraulic characteristics of the Floridan aquifer system than the intermediate confining unit in such areas, due to the general absence of the intermediate confining unit and thinness of the overburden above the Floridan aquifer system. Nevertheless, the approach provides for the possibility of deviation of the vertical hydraulic conductivity of Layer 2 from that of Layer 3, to a significant degree if needed, to match observed data.

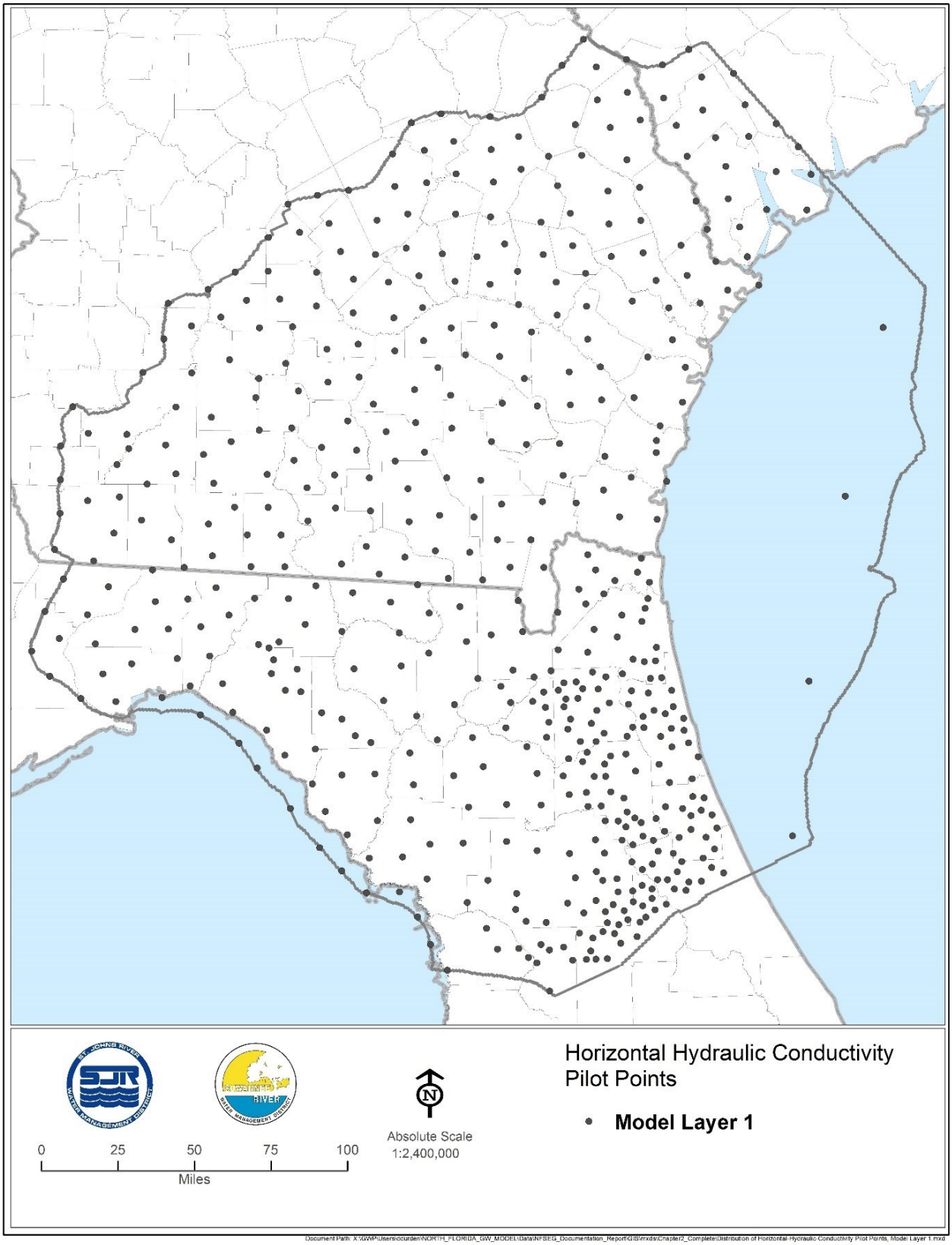

Figure 4-3. Distribution of horizontal hydraulic conductivity pilot points, Layer 1

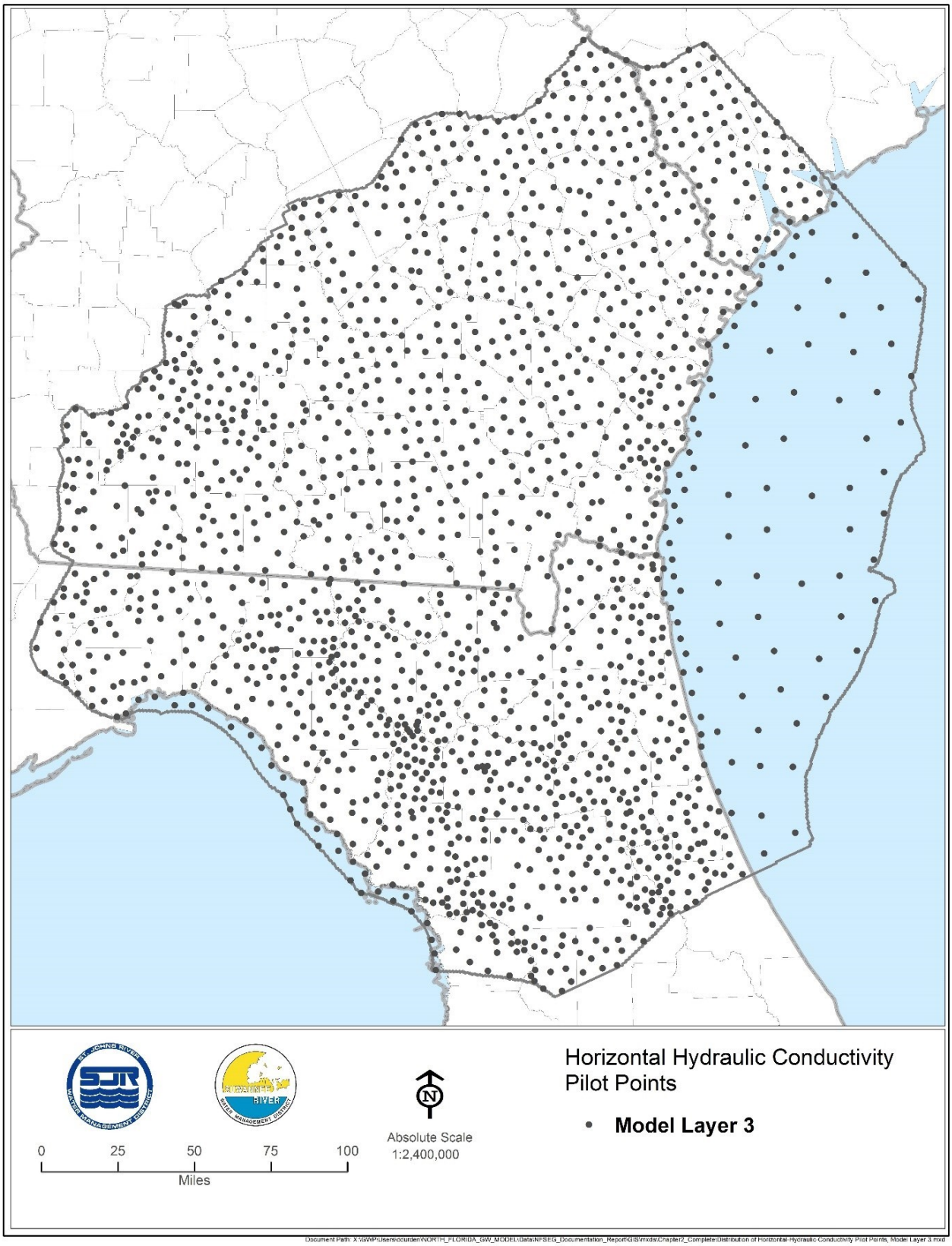

Figure 4-4. Distribution of horizontal hydraulic conductivity pilot points, Layer 3

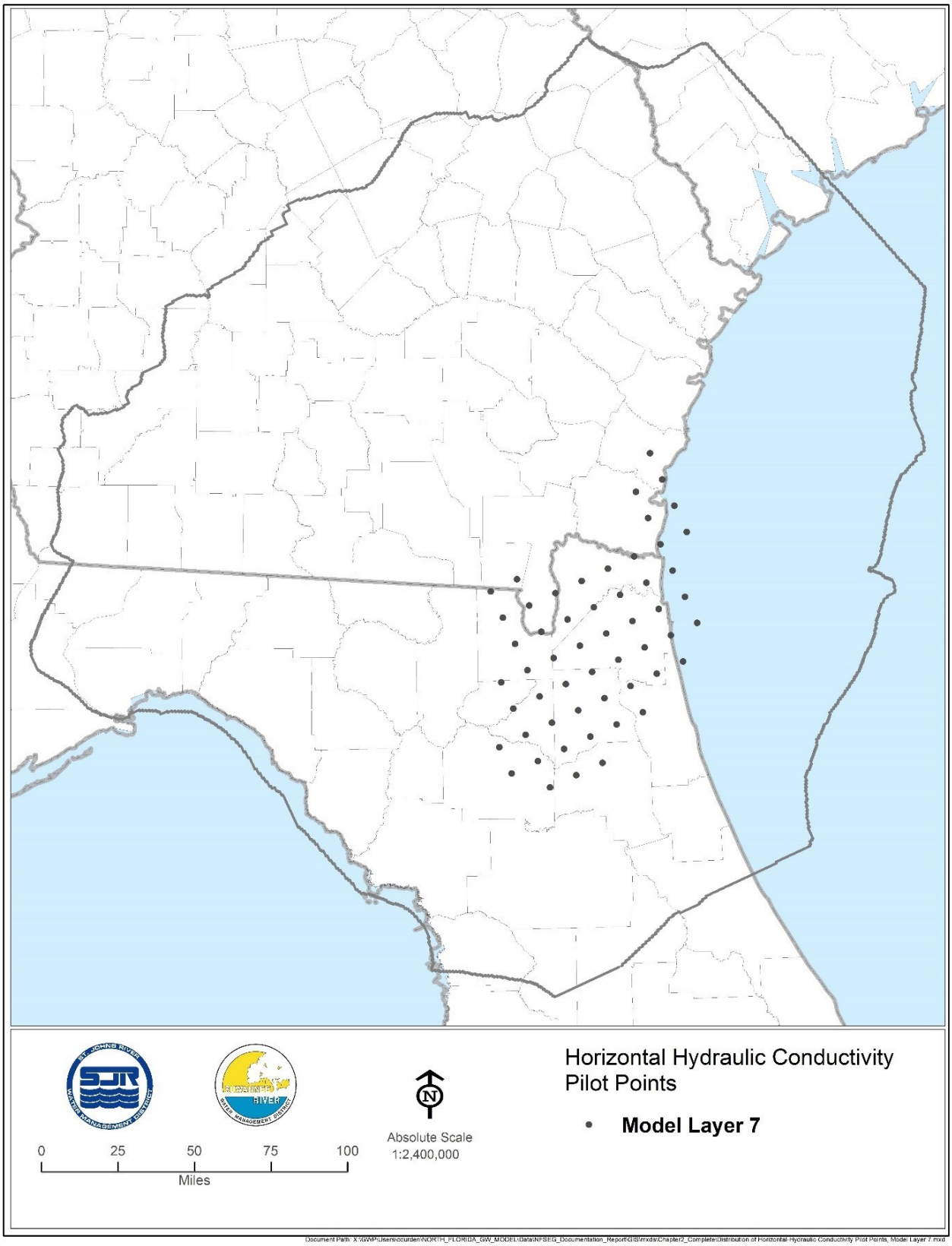

Figure 4-5. Distribution of horizontal hydraulic conductivity pilot points, Layer 7

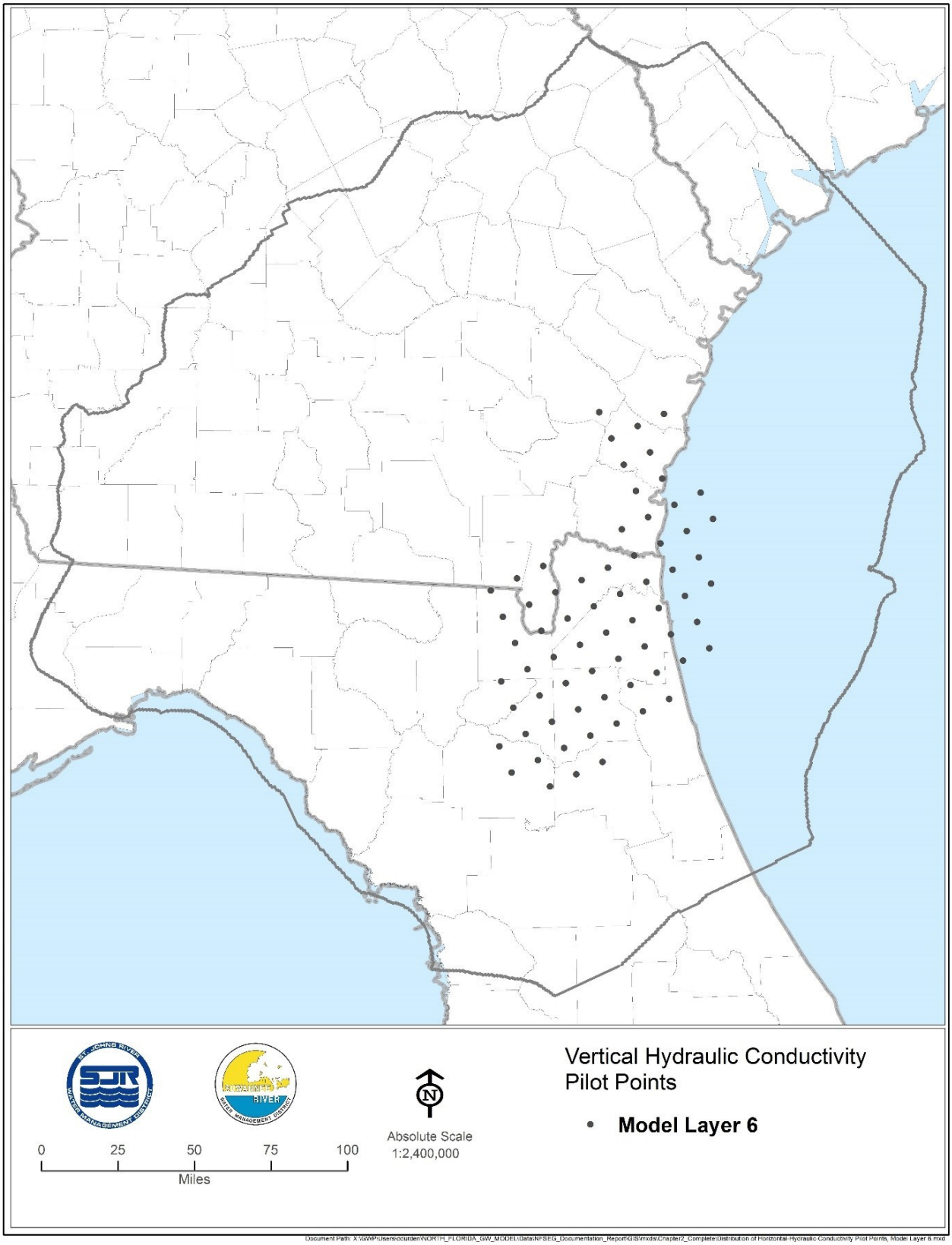

Figure 4-6. Distribution of vertical hydraulic conductivity pilot points, Layer 6

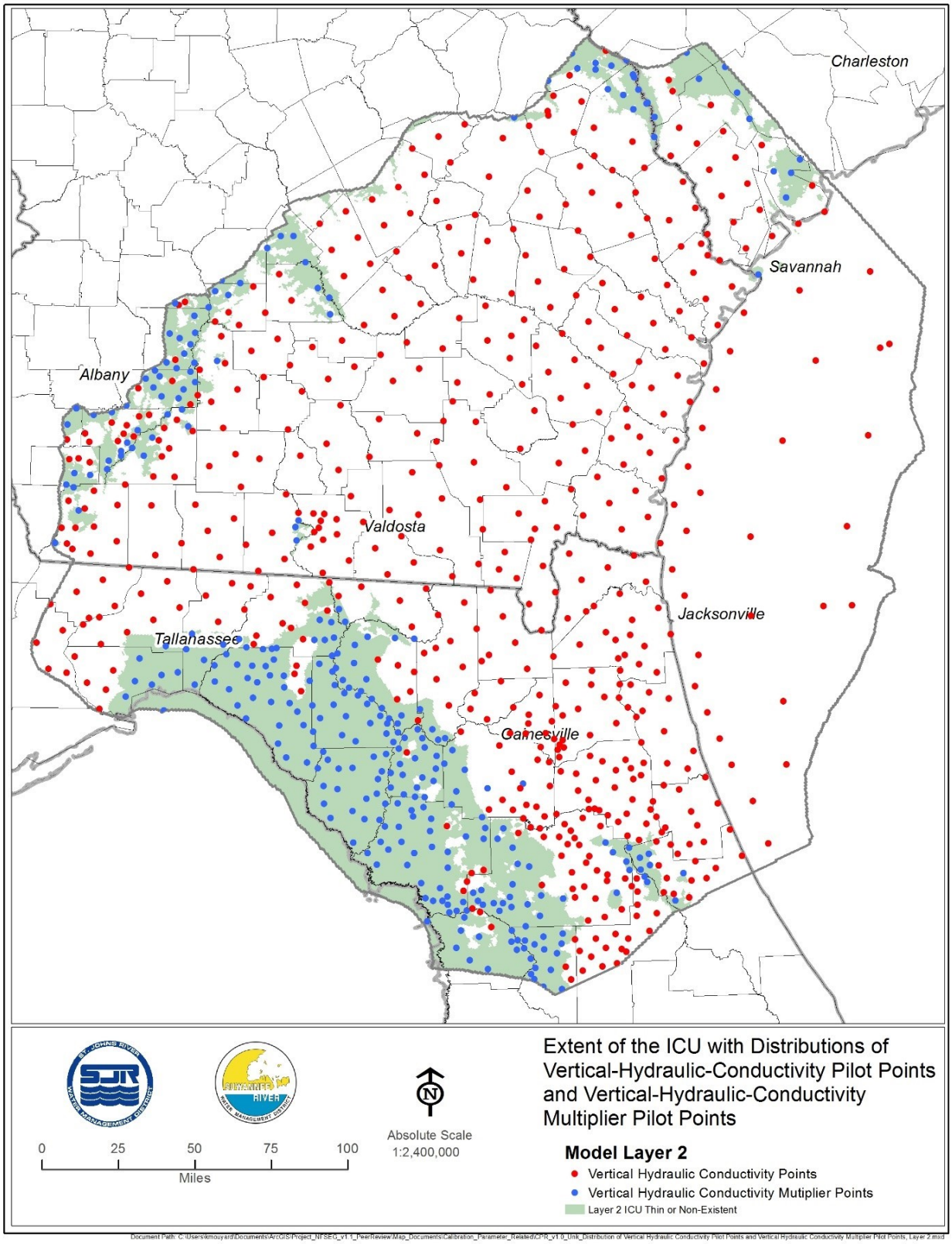

Figure 4-7. Distribution of vertical hydraulic conductivity pilot points and vertical hydraulic conductivity multiplier pilot points, model Layer 2

A similar approach is used for Layers 4 and 5 due to the discontinuous nature of the middle confining unit. Vertical hydraulic conductivity values for Layer 4 and horizontal hydraulic conductivity values for Layer 5 were determined directly using PEST in portions of the model domain that corresponded to areas in which the middle semiconfining unit is present according to Miller (1986). These values are determined for respective arrays of pilot points in Layers 4 and 5. Values of vertical hydraulic conductivity of Layer 4 and horizontal hydraulic conductivity of Layer 5 were determined at grid cells of Layers 4 and 5, respectively, by interpolating between the respective arrays of pilot points (Figures 4-8 and 4-9).

In the parts of the model domain that corresponded to areas in which the middle semiconfining unit is not present according to Miller (1986) (noted shaded region on Figures 4-8 and 4-9), PEST was used to determine the vertical hydraulic conductivity of Layer 4 and horizontal hydraulic conductivity of Layer 5 using a multistep approach similar to the one described above regarding the vertical hydraulic conductivity of Layer 2. As in that case, the multistep approach was implemented to address the possibility that areas of local confinement may exist within areas that are broadly classified as unconfined. In this approach, the hydraulic properties of Layers 4 and 5 were assumed to be the same as those of Layer 3 unless calibration data indicated that a degree of local confinement existed.

In the portions of Layer 4 that correspond to areas in which the middle semiconfining unit is not present according to Miller (1986), the vertical hydraulic conductivity of a given grid cell was equated to the product of the vertical hydraulic conductivity multiplier as interpolated by PEST for the grid cell in question and the vertical hydraulic conductivity of the overlying grid cell of Layer 3. With respect to portions of Layer 5 that correspond to this area, the horizontal hydraulic conductivity of a given grid cell of Layer 5 was equated to the product of the horizontal hydraulic conductivity multiplier as interpolated by PEST at the grid cell in question and the horizontal hydraulic conductivity of the overlying grid cell of Layer 3. For both layers, PEST bases its respective interpolations on values assigned to the respective distributions of pilot points of Layers 4 and 5 (Figures 4-8 and 4-9).

Vertical Anisotropy Ratio

The ratio of vertical anisotropy as applied in the calibration process is defined as the ratio of horizontal hydraulic conductivity to vertical hydraulic conductivity. PEST was used to determine values of the vertical anisotropy ratio through the calibration process. For Layer 3, values of vertical anisotropy are determined by PEST at pilot points and then determined for individual grid cells through kriging (Figure 4-10). Thus, each active grid cell of Layer 3 was assigned a separate value of vertical anisotropy.

Layer 2 has two anisotropy values, one for the area in which the intermediate confining unit is present and another for areas in which the intermediate confining unit is thin or absent (Table 4-3). Layers 4 and 5, similarly, have two values each, one for areas in which the middle confining unit is present according to Miller (1986) and another for areas in which it is not. Layers 6 and 7 each have only one value of anisotropy ratio.

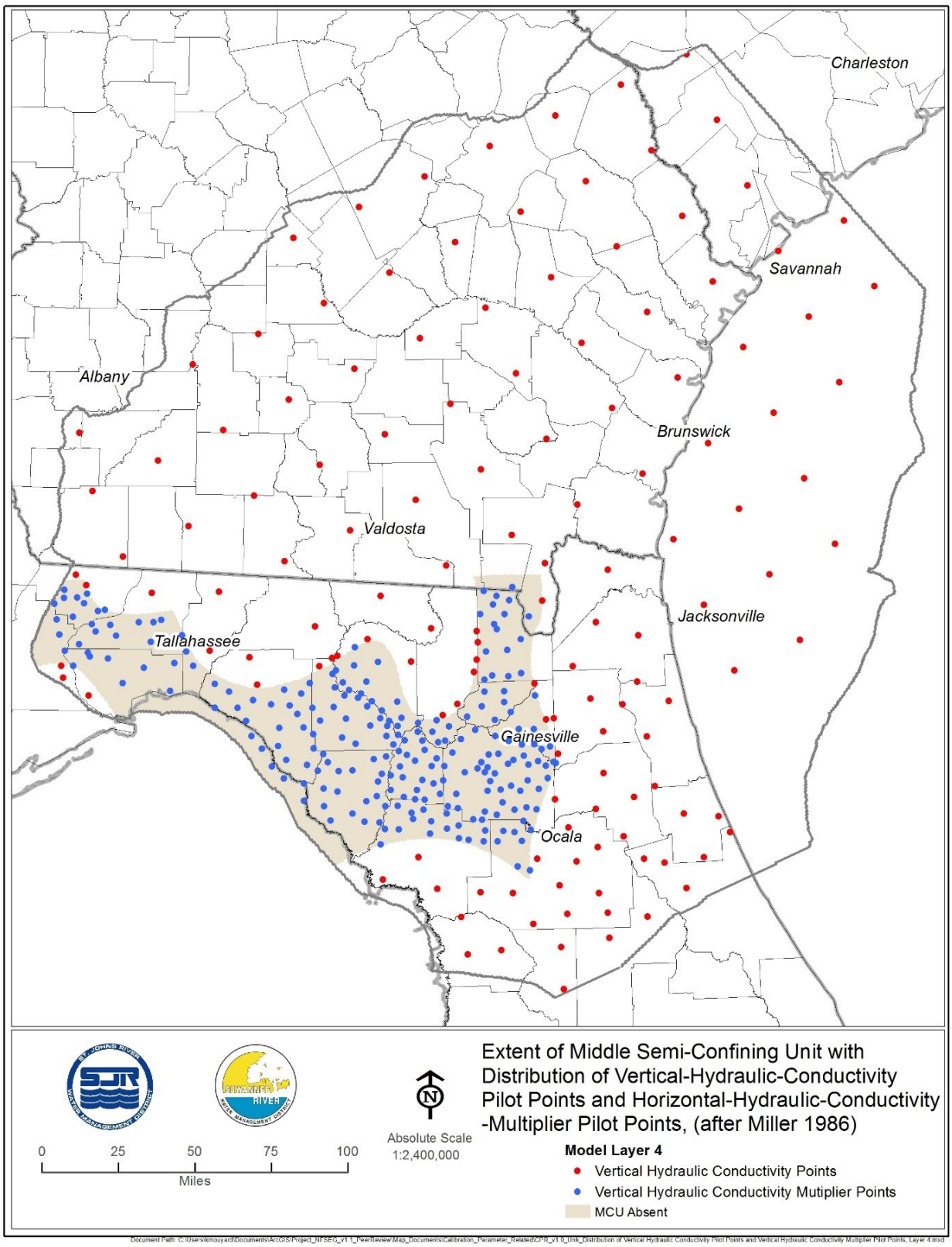

Figure 4-8. Distribution of vertical hydraulic conductivity pilot points and vertical hydraulic conductivity multiplier pilot points, model Layer 4

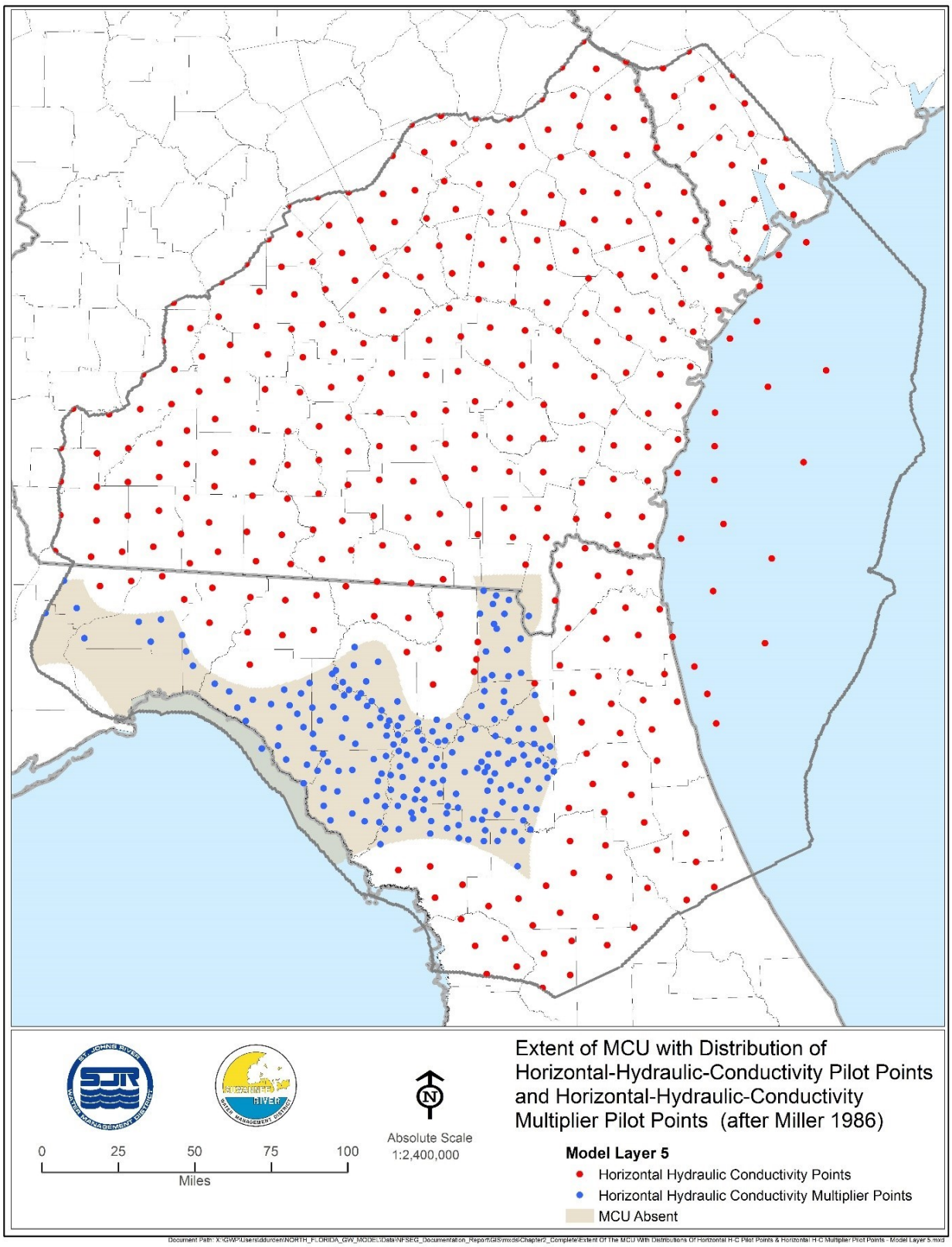

Figure 4-9. Distribution of horizontal hydraulic conductivity pilot points and horizontal hydraulic conductivity multiplier pilot points, model Layer 5

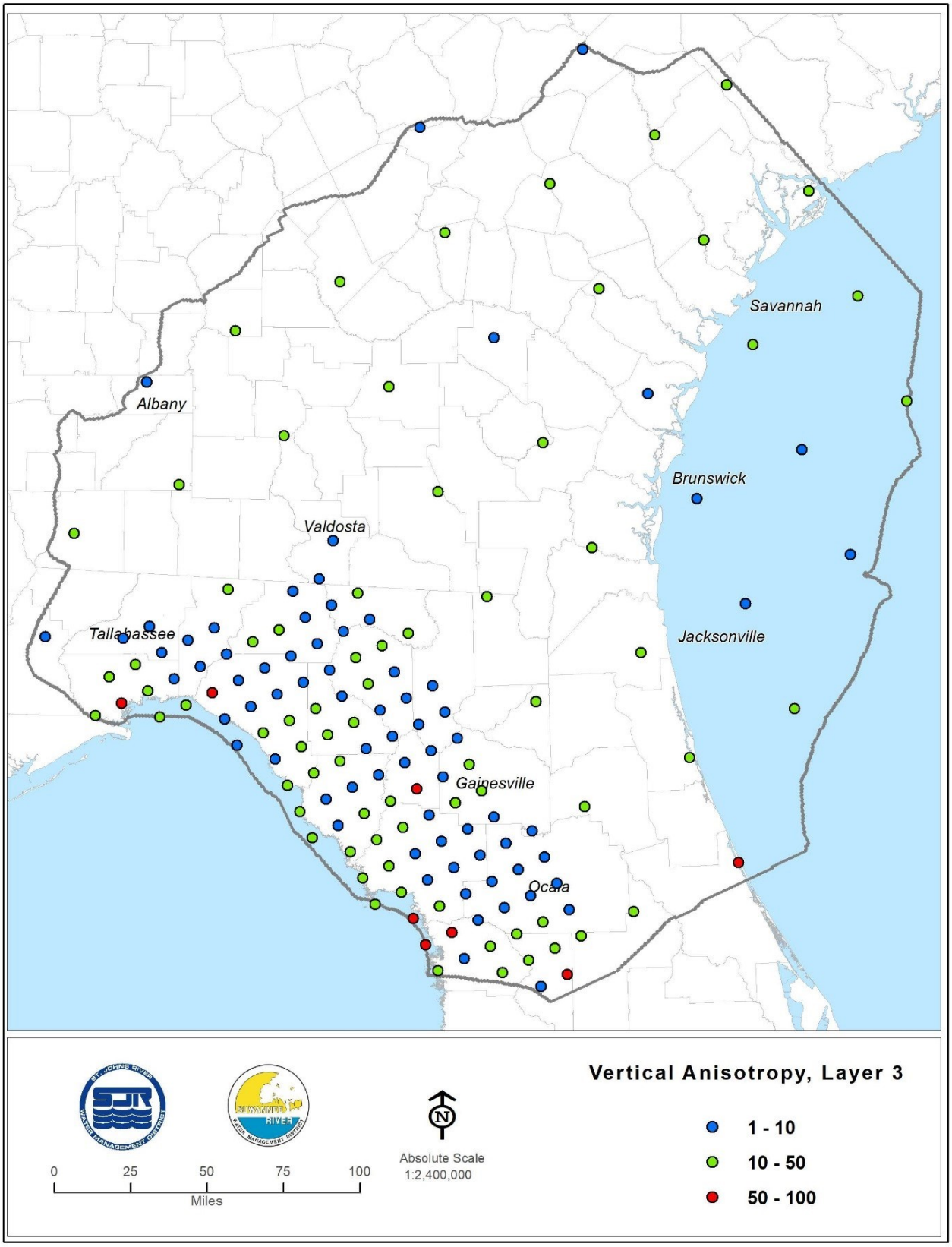

Figure 4-10. Distribution of anisotropy pilot points, model Layer 3

As described above, horizontal hydraulic conductivity was determined for Layers 1, 3, 5 and 7, either directly or through a multistep approach that utilized multipliers. For Layers 2, 4 and 6, vertical hydraulic conductivity was determined likewise. To obtain corresponding values of vertical hydraulic conductivity for Layers 1, 3, 5 and 7, the already determined horizontal hydraulic conductivity values were divided by the applicable anisotropy ratio (Figure 4-8 and Table 4-3). Similarly, to obtain corresponding horizontal hydraulic conductivity values for Layers 2, 4 and 6, the already determined vertical hydraulic conductivity values were multiplied by the applicable anisotropy ratio (Figure 4-8 and Table 4-3).

GHB Conductance for Representation of Spring Discharge

As stated previously, GHB conditions were used in the representation of springs (Figures 2-33 through 2-35; Appendix E). GHB conductance is an important factor in the simulation of spring flows. GHB conductance is scale dependent and is not readily observable. Therefore, it must be determined through the calibration process. The set of GHB conductance values used in the representation of springs is therefore included in the calibration process as a calibration parameter group.

The primary objective of the calibration process with respect to the determination of spring conductance was to enable the model to simulate spring flow rates adequately. In general, a greater emphasis was placed on matching the flows of larger springs and the total flows of spring groups, as the estimates of such flows are generally more relia-

Table 4-3. PEST-Generated Anisotropy for Layers other than Layer 3

Area of Application	PEST-Generated Anisotropy
Model Layer 1	7.0
Model Layer 2, ICU Present	8.2
Model Layer 2, ICU Not Present	26.0
Model Layer 4, MSCU Present	9.5
Model Layer 4, MSCU Not Present	10.3
Model Layer 5, MSCU Present	10.0
Model Layer 5, MSCU Not Present	9.2
Model Layer 6	10.0
Model Layer 7	10.0

ble due to greater data availability. They are more significant in terms of their effects on the flow system as well and therefore more critical to the overall representation of the groundwater system.

River Package Conductance Multipliers for Representation of Stream Baseflow

As stated previously, the River Package was used in the representation of perennial stream reaches. The primary objective of the calibration process in this regard was adequate simulation of stream baseflow rates. As detailed in Chapter 2, baseflow rates were estimated at stream gauges within the model domain (Figure 2-36 through 2-44). River package conductance was an important factor in the simulation of stream baseflow rates.

The conductance of River Package boundaries was determined in the calibration process as the product of a multiplier determined by PEST for the HSPF subwatershed to which the boundary corresponds in location and the area of the stream segment that it represented. The same multiplier was assigned to all River Package boundaries that correspond to a given HSPF subwatershed.

Drain Package Conductance Multipliers for Representation of Stream Baseflow

The Drain Package was used in the representation of ephemeral stream reaches, as previously stated. As with the River Package implementation, the conductance of a given Drain Package boundary was determined in the calibration process as the product of a multiplier of the HSPF subwatershed to which the Drain Package boundary corresponds in location and the area of the stream segment that it represents. The same multiplier was assigned to all Drain Package boundaries that correspond to a given HSPF subwatershed.

Lake Related Multipliers: River Package Conductance and Lake Zone Multipliers

Two sets of multipliers were associated with lakes represented in the NFSEG model. The first of these was used in the calculation of the conductance values of the River Package boundaries used to represent a given lake. For lake representation, this value was a primary controlling factor in the determination of rates of exchange between the lake and the aquifer that bounds it, usually the surficial aquifer system. The conductance of River Package boundaries used to represent lakes were determined in the same manner as for any other river Package boundary, as the product of a multiplier determined by PEST for the HSPF subwatershed to which the boundary corresponded in location and the area of the stream segment that it represented.

The second type of multiplier was used to help constrain the rate of leakage between a given lake and the underlying Floridan aquifer system. This was accomplished with lake “zones” for which “lake zone” multipliers were estimated for application to the

vertical hydraulic conductivity of Layer 2. A lake zone was defined in this process as a specified group of Layer 2 grid cells that underlie a given lake, with a single lake zone multiplier for each lake.

Recharge and Maximum Saturated ET Multipliers

Multipliers for recharge and maximum saturated ET were also included in the set of parameters available for calibration to adjust the HSPF derived recharge and maximum saturated ET by subwatershed. The purpose of these multipliers was to allow for the adjustment of the HSPF derived recharge and maximum saturated ET rates during the calibration, if needed.

To date, however, this feature of the calibration process has not been activated, except as part of the parameter and prediction analysis, which is discussed in Chapter 9.

WEIGHTING SCHEME

As previously described, weights are multiplied by residuals (observed minus simulated values) to estimate the contribution of each observation to the objective function, which is the sum of the squared weighted residuals. Weights therefore help to determine the relative influence of each observation on the value of the objective function. The objective function is minimized by PEST during model calibration for determination of optimal parameter estimates to enable adequate simulation of groundwater flows and levels. Ideally, weights should account for measurement errors of observation data used in model calibration and structural errors that result from the inevitable differences between a model and represented groundwater flow system. Structural errors are typically the dominant source of error in models, but, unfortunately, they are difficult or impossible to quantify (Doherty J., et al, 2010). Weights also help to equalize differences in the relative influences of observation groups that result merely from differences in their general range of magnitude as expressed in their units of measure (groundwater flows vs. levels, for instance). In the calibration process, weights were initially assigned uniform values or were based on an assumed constant ratio of the standard deviation of the observation error and the value of an observation. As the calibration process proceeded, the initial values of the weights were modified in some cases based on information gained from simulation results. The final weighting scheme used to calibrate the NFSEG v1.1 model is summarized below.

For groundwater level targets, weights were initially assigned uniform values, and, for baseflow and spring flow targets, weights were initially based on an assumed constant ratio of the standard deviation of the observation error and the value of an observation. As the calibration process proceeded, the initial values of the weights were modified in some cases based on information gained from the initial calibration and knowledge of local and regional hydrogeology, either to heighten the visibility of certain observation

groups for PEST or perhaps to de-emphasize them. Weights for baseflow observations were determined as the reciprocal of 10 percent of a given estimated baseflow. This approach was designed to help ensure that smaller baseflows were given as much visibility in the calibration process as larger baseflows. For spring flows, final weights consisted of a tiered weighting structure based on the magnitude of the springs. Larger weights were assigned to larger individual spring flows and thus helped to ensure better matches to larger springs. First and second magnitude springs capture flow from larger areas of the groundwater flow system and typically receive higher protection priority and have more available data.

One of the main purposes of weights is to provide a means of incorporating knowledge of the system into the PEST calibration process. Weights of some of the groundwater level targets were modified during calibration to improve the simulation of known features of the Upper Floridan aquifer potentiometric surface in terms of both groundwater levels and gradients in areas.

Groundwater Levels

Layer 1 (2001 and 2009)

A uniform weight of 1 was assigned for all observations except for selected observations for which weights were reduced for one of the following reasons:

- Observed water levels of some of the monitoring wells were higher than Layer 1 top elevations. This occurs because Layer 1 top elevations represent land surface elevation averaged over the area of model grid cells (2,500 feet by 2,500 feet).
- The surveyed top elevations of some of the monitoring wells were more than 10 feet above the model Layer 1 top elevations.
- Some of the water levels were estimated from USGS topographic quadrangle maps, rather than from groundwater level measurements. This was done, for example, in some areas where wetlands occurred, based on the assumption that the groundwater level in Layer 1 should be at or near land surface.

Layer 2 (2001 and 2009)

A uniform weight of 0.1 was assigned to all observations. Observed water level elevations in the intermediate confining unit, which is represented by Layer 2, can be strongly dependent on casing depths and positions of open intervals of monitoring wells in many locations because of large vertical hydraulic gradients across the intermediate confining unit. Since the NFSEG model was not designed to simulate vertical heterogeneity of the intermediate confining unit, Layer 2 observations were not considered important targets for the model calibration. Instead, estimated groundwater level differences between the surficial aquifer system and Upper Floridan aquifer (i.e., vertical head differences between Layers 1 and 3) were the primary targets utilized for estimating the degree of confinement of Layer 2 in the calibration. However, because the number of these targets was limited, observations of water levels within the intermedi-

ate confining unit were included in the model calibration process also, although their importance was deemphasized by assignment of the relatively low weight of 0.1.

Layers 3 through 7 (2001 and 2009)

A uniform weight of 1 was initially assigned to all groundwater level observations in Layers 3 through 7. During model calibration, weights of some observations in Layer 3 were increased to improve calibration in certain critical areas in north Florida. In some instances, zero valued weights were also assigned to some targets because it was discovered that the groundwater levels were not representative. Examples include wells in Layer 2 that were dry or wells in Layer 7 that were affected by saline water.

Groundwater Level Differences

Vertical groundwater level differences between Layers 1 and 3 (2001 and 2009)

A weight of 2 was assigned to the observations of vertical head differences between Layers 1 and 3 (observation groups vd_1to3_01 and vd_1to3_09) if a vertical groundwater level difference was calculated using a Layer 1 observation having a weight of 1. Otherwise, a weight of 0.1 was assigned. The higher weight of 2 was applied to increase the visibility of these observations since their magnitudes were relatively smaller than the water level observations.

Horizontal groundwater level differences (2001 and 2009)

A uniform weight of 1 was assigned to all observations (observation groups hd2001_lay3 and hd2009_lay3).

Vertical groundwater level differences between Layers 3 and 5 (2001 and 2009)

A uniform weight of 10 was assigned to observations of vertical groundwater level differences between Layers 3 and 5. The larger weight utilized for these observation groups was intended to make them relatively more visible to PEST since they are generally small as compared to other water level difference observations.

Flows

Baseflows and changes in baseflows (2001 and 2009)

For observations of baseflows or changes in baseflows along river reaches (observation groups qr01, qr09, qs01, and qs09), weights were calculated as the inverse of ten percent of the estimated flows, thus resulting in weighted flows of 10 cfs. For example, for a baseflow estimate of 50 cfs, a weight of 0.2 was used. Weights of zero were applied in instances of unreliable baseflow estimates, which can result from missing hydrograph data, tidal effects, proximity to reservoirs, or generally poor data quality. Assignment of zero weights effectively eliminated these baseflow estimates from the calibration process.

Individual spring flows (2001 and 2009)

For observations of flows at individual springs (observation groups qspring01 and qspring09), the general approach was to apply larger weights to springs of greater magnitude, in accordance with the following:

- If the spring flow is 10 cfs or less, the weight was calculated as the inverse of 10 percent of the observed flow, thus resulting in a weighted spring discharge of 10 cfs;
- If the spring flow is greater than 10 or less than 100 cfs, a weight was applied so that the weighted spring flow would be 50 cfs;
- If the spring flow is greater than 100 or less than 500 cfs, a weight was applied so that weighted spring flow would be 250 cfs; and
- If the spring flow is greater than 500 cfs, a weight was applied so that weighted spring flow would be 500 cfs.

As compared to baseflows, which are generally based on hydrograph separation techniques and stage discharge rating curves, spring discharges are largely based on actual measurements. Generally, therefore, estimates of spring discharge are more reliable than estimates of baseflow and thus merit more weight in the calibration process.

Flows for spring groups (2001 and 2009)

For observations of flows of collection of springs (observation groups qs_spring01 and qs_spring09), a uniform weight of 1 was assigned to all observations except for the 2001 flows of Wakulla Springs, to which zero weight was assigned due to lack of confidence in the data.

Other Observations

Flooding and drying penalties for model cells (2001 and 2009)

Nonzero weights were also assigned to the flooded and dry cell observation groups, as well as the lake leakage observation groups. Only twelve observations in the flooded and dry cell observation groups (wp_wet_2001, wp_wet_2009, wp_wet_2001, and wp_wet_2009) received nonzero weights, and all were assigned a weight of 2. These penalties were developed to prevent excessive flooding and drying and were used for only a few areas, which were decided upon during the calibration process.

The areas to which flooding penalties were applied were small, generally corresponding in extent to only one or two grid cells. These areas are generally subject to significant inflow but lack nearby surficial aquifer system water level observations that could be used to guide the calibration process. The number of these observations with nonzero weights was limited to mitigate against potential numerical instabilities that might arise due to the nonlinear nature of this observation class.

Lake leakage rates (2001 and 2009)

The lake leakage observation groups (qlake01 and qlake09) were implemented to minimize the likelihood of individual lakes becoming infinite sources or sinks for water. A uniform weight of 1 was assigned to all observations except for a few lakes of critical concern to the districts for which estimates of leakage were available in the literature. The weights for these lakes were adjusted as needed during calibration process to improve calibration.

CALIBRATION RESULTS

As described previously, a primary objective of the calibration process was to minimize differences between various observations and their simulated counterparts. Accordingly, the following description of the calibration results is presented largely in terms of comparisons of simulated groundwater levels, groundwater level differences, and groundwater flows to corresponding observations. The differences between observed values of groundwater levels and their simulated counterparts (groundwater level residuals) are summarized statistically. In addition, an extensive set of maps and graphs of groundwater level and flow residuals, calibration determined parameters, and simulated water level and flow related data are presented. Collectively, the statistical summaries, maps, and graphs are intended to facilitate assessment of the quality of the calibration. The maps and graphs are categorized further as follows: calibration results heads (CRH), calibration results flows (CRF), and calibration results parameters (CRP). The various components of the objective function, which are described in a previous section of this chapter entitled "PEST Facilitated Calibration," are listed for 2001 and 2009 in Appendix M.

Summary Statistics

Table 4-4 summarizes statistical goals for the NFSEG model calibration and various statistics of groundwater level residuals, aggregated across the model domain. Statistical summaries were determined for the overall model and Layer 3 only for both calibration years, 2001 and 2009. The statistical goals were specified prior to construction and calibration of the NFSEG model in the conceptualization report (Durden et al. 2013). As indicated in the model conceptualization report, the calibration goals were not intended as hard and fast requirements.

In many areas, groundwater levels within the ICU vary vertically to such a degree that observed ICU groundwater levels are not representative of the full vertical extent of the ICU, the observed values being representative only of the relatively limited extent of observation well open intervals. As NFSEG v1.1 simulates the average of the entire vertical extent of the ICU, close agreement between observed and simulated groundwater levels should not be expected in such cases. For this reason, Layer 2 residuals were not factored into the statistics of Table 4-4. Layer 2 observed groundwater levels were utilized in the calibration process mainly as "system information," which is to say as a means of providing general guidance to PEST. The purpose was to help ensure a reasonable range of simulated results, not specific values.

Table 4-4. Summary of residual statistics

Statistical Criterion	Proposed Target	All Target Wells Except Layer-2 Wells*		Layer 3 Only	
		2001	2009	2001	2009
-5 feet < Residual < 5 feet	80%	74%	76%	76%	76%
-2.5 feet < Residual < 2.5 feet	50%	43%	49%	43%	49%
Mean of Residuals	-	-0.3	-0.7	-0.4	-0.9
Standard Deviation of Residuals	-	5.4	5.0	4.8	4.6
Mean of Absolute Residuals	-	3.9	3.5	3.6	3.4
Number of Targets	-	1263	1284	977	993

*See main report for explanation on omitting Layer 2 residuals.

Groundwater Levels (Hydraulic Heads)

The CRH group is a set of maps and graphs that provide comparisons of observed versus corresponding simulated groundwater levels (i.e., hydraulic heads). These include maps of groundwater level residuals of Layers 1, 3 and 5; graphs of observed versus simulated hydraulic head; and maps of the simulated water table of Layer 1 and simulated potentiometric surfaces of Layers 3 and 5 (Figures 4-11 through 4-40).

Groundwater Level Residuals of Layer 1

Maps of residuals of the groundwater levels of Layer 1 show the difference between observed groundwater levels of Layer 1 at various observation wells in 2001 and 2009 and their model simulated counterparts (Figures 4-11a and b, 4-12a and b; Appendix A). The water levels of Layer 1 represent the water table of the surficial aquifer system where it is present.

The Layer 1 2009 groundwater level observation data set includes estimates, as opposed to observations, of the water table elevation, primarily in wetland areas, that were based on USGS 1: 24,000 scale topographic maps and elevations of the USGS 3DEP DEM. In upland areas, the stages of nearby lakes were used to estimate the water table elevation at some locations. These estimates were obtained at locations for which water table estimates were needed to provide additional constraint to the calibration but for which observations were not available.

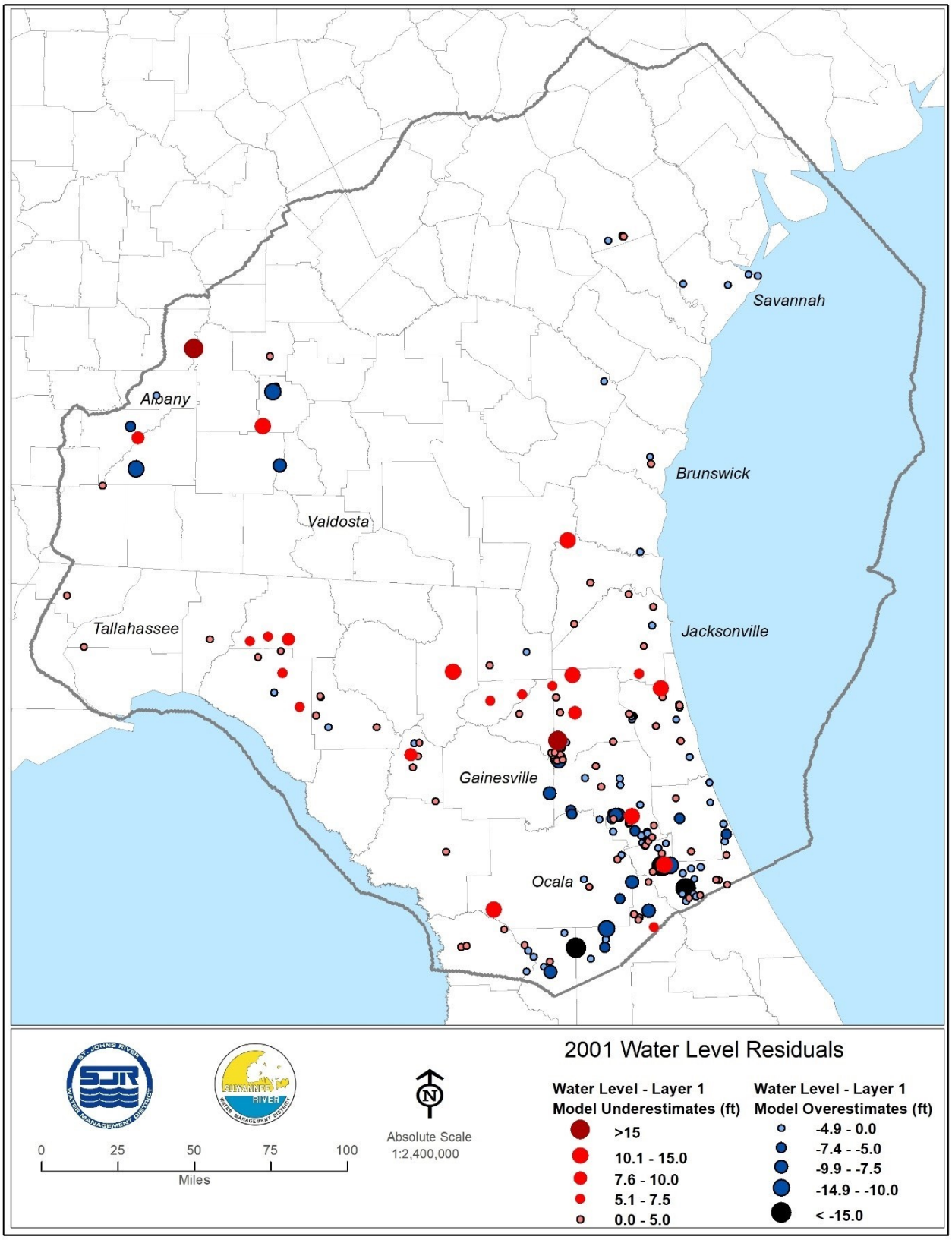

Figure 4-11 (a). Residuals of hydraulic head (feet), model Layer 1, 2001

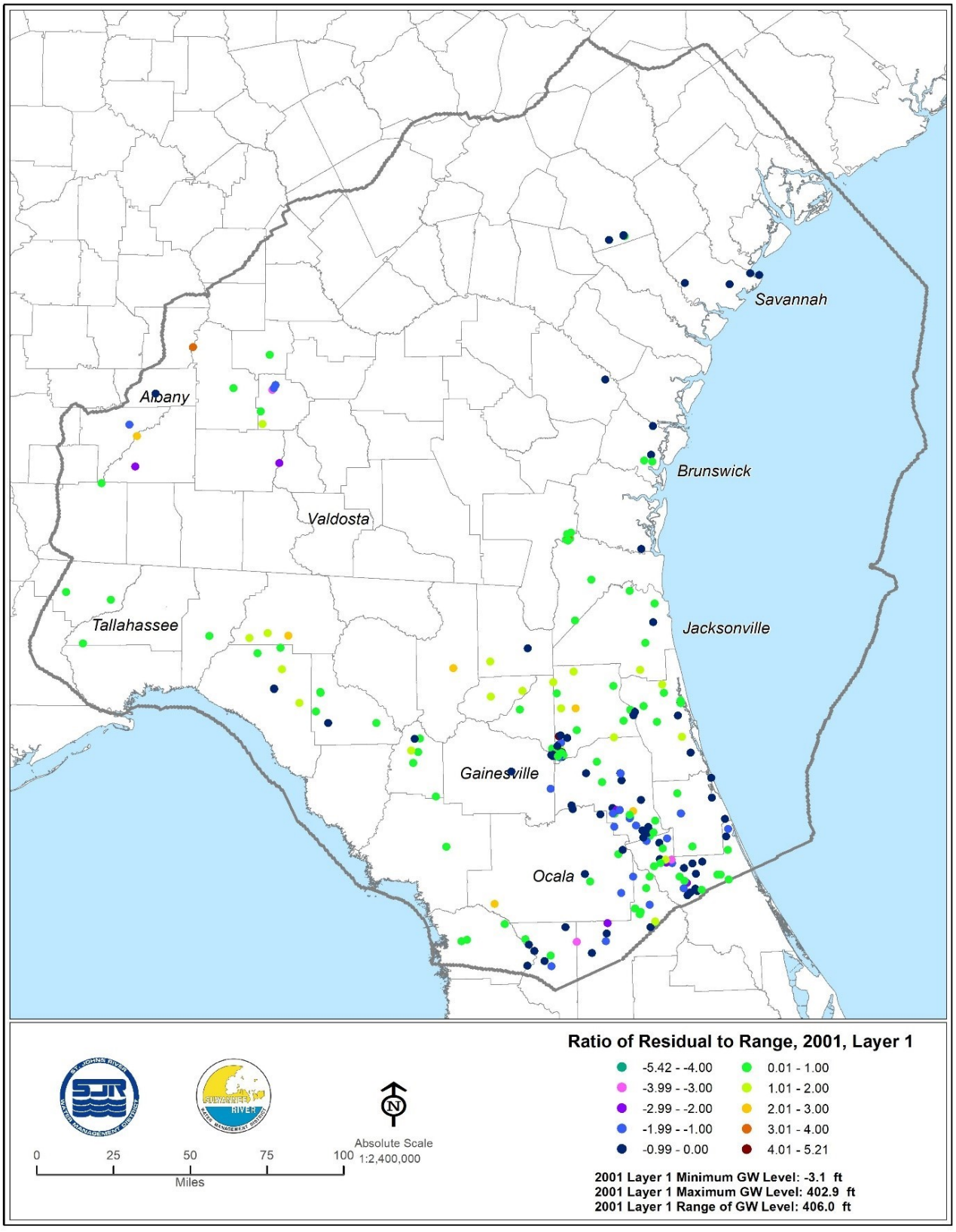

Figure 4-11 (b). Relative residuals of hydraulic head (feet), model Layer 1, 2001

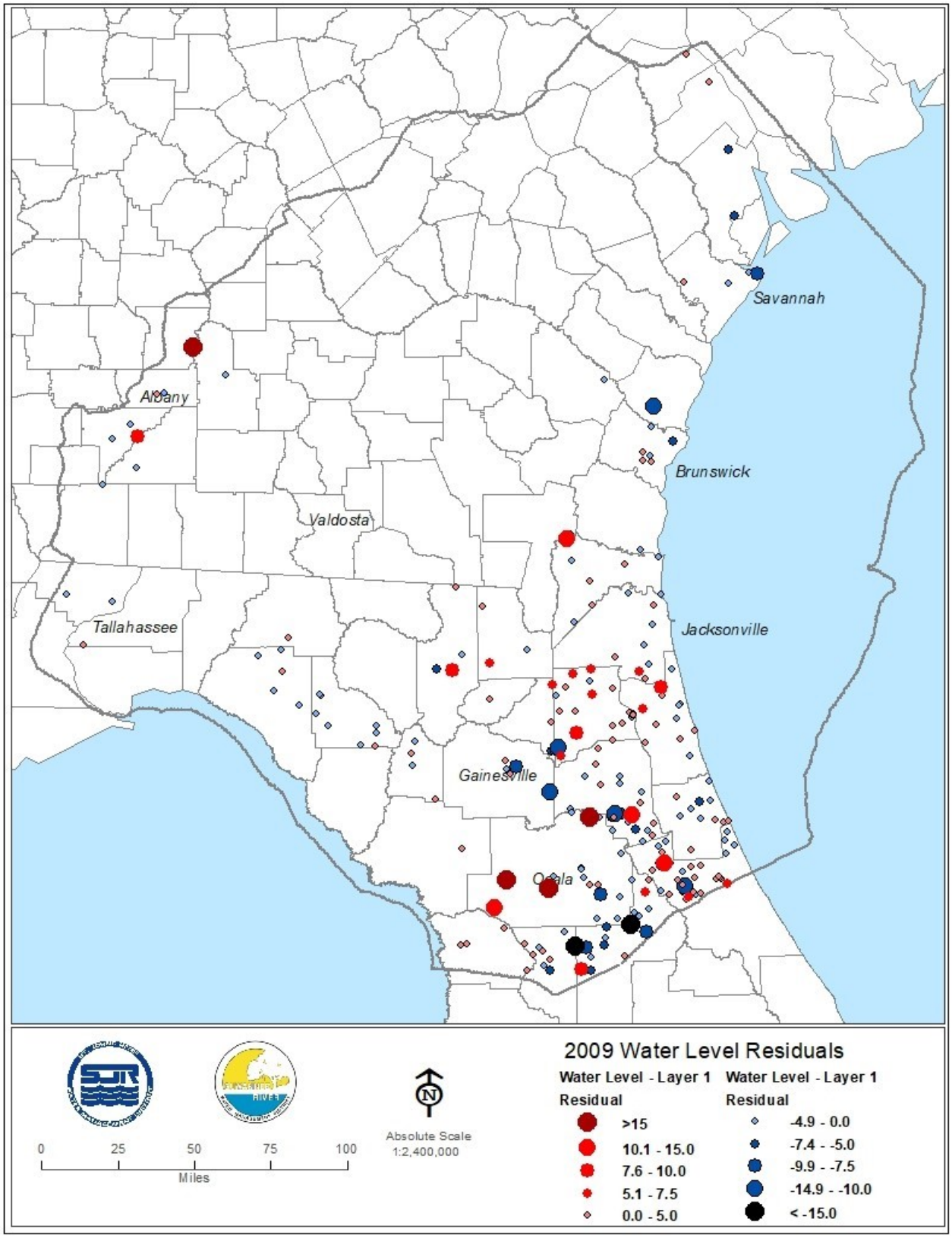

Figure 4-12 (a). Residuals of hydraulic head (feet), model Layer 1, 2009

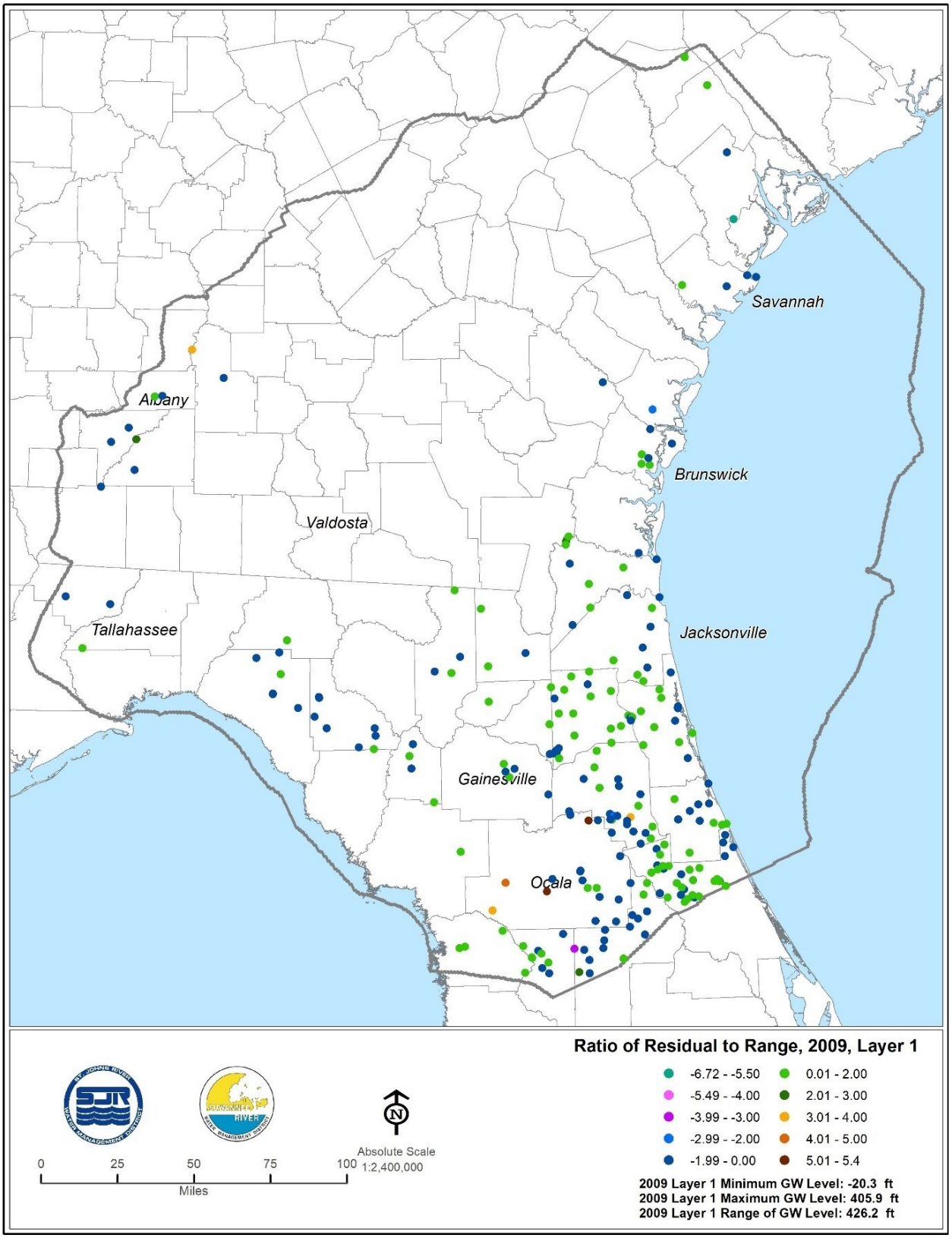

Figure 4-12 (b). Relative residuals of hydraulic head (feet), model Layer 1, 2009

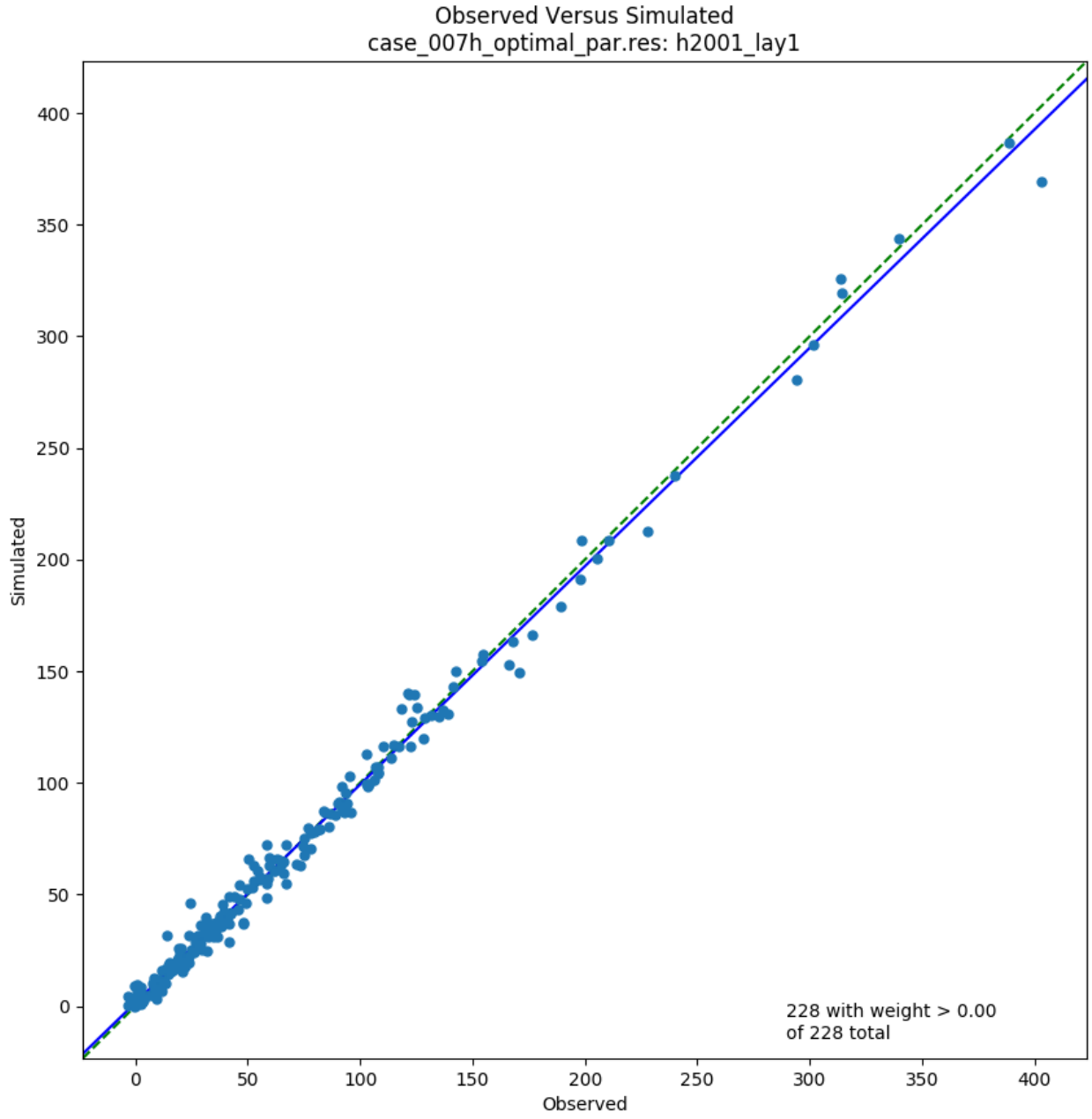

Figure 4-13. Observed hydraulic head (feet NAVD88), model Layer 1, 2001

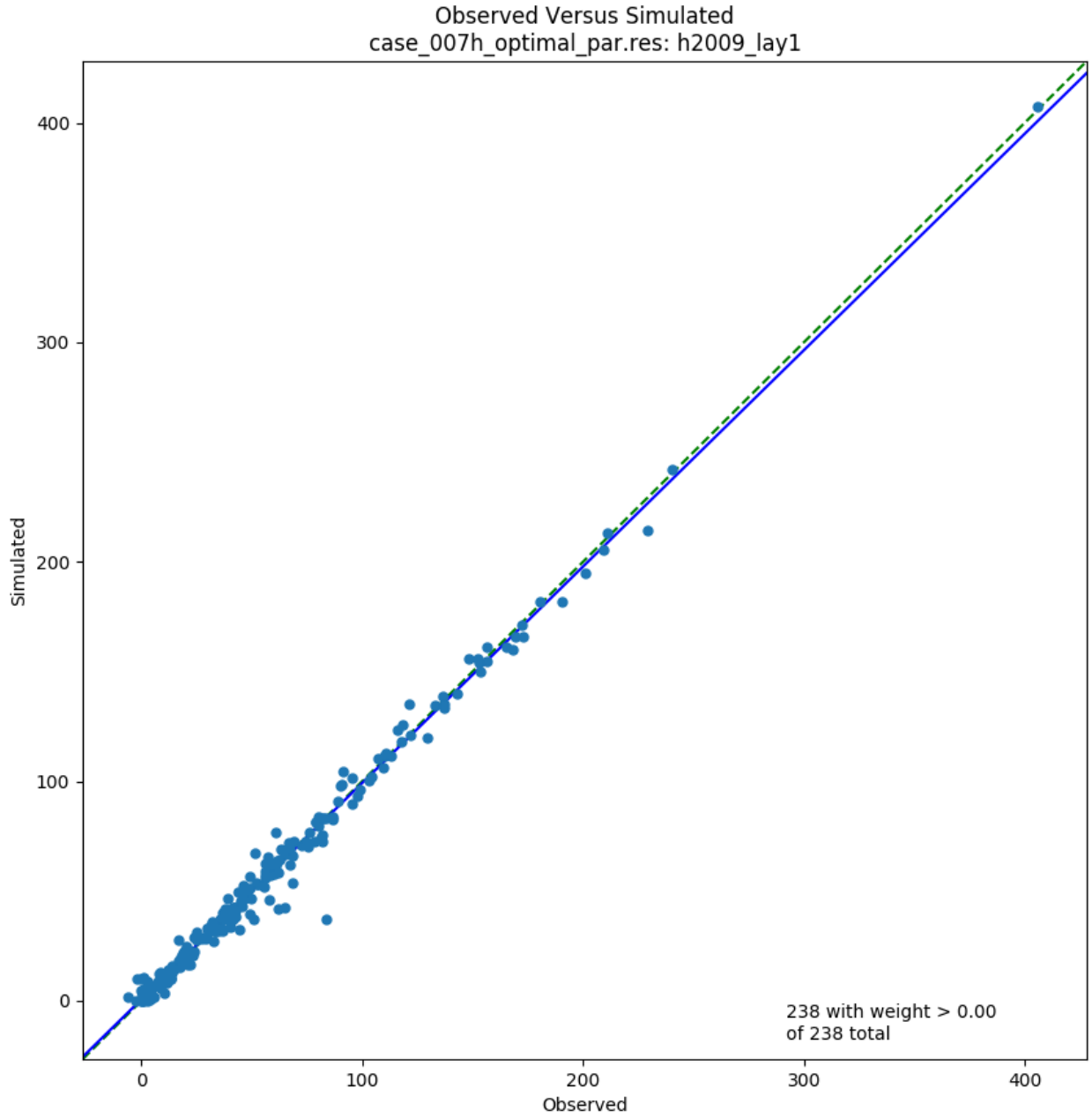

Figure 4-14. Observed versus simulated hydraulic head (feet NAVD88), model Layer 1, 2009

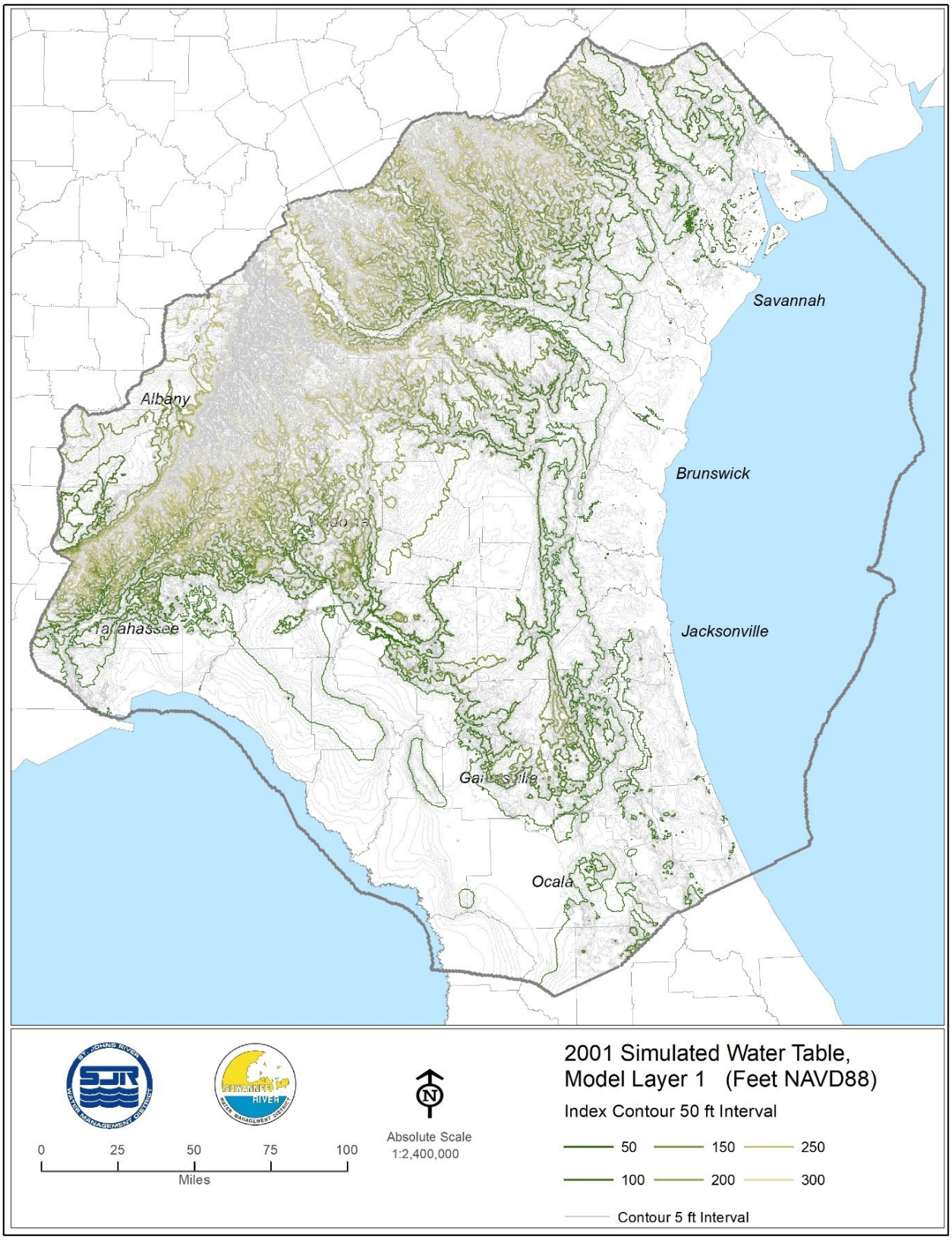

Figure 4-15. Simulated water table of model Layer 1 (feet NAVD88), 2001

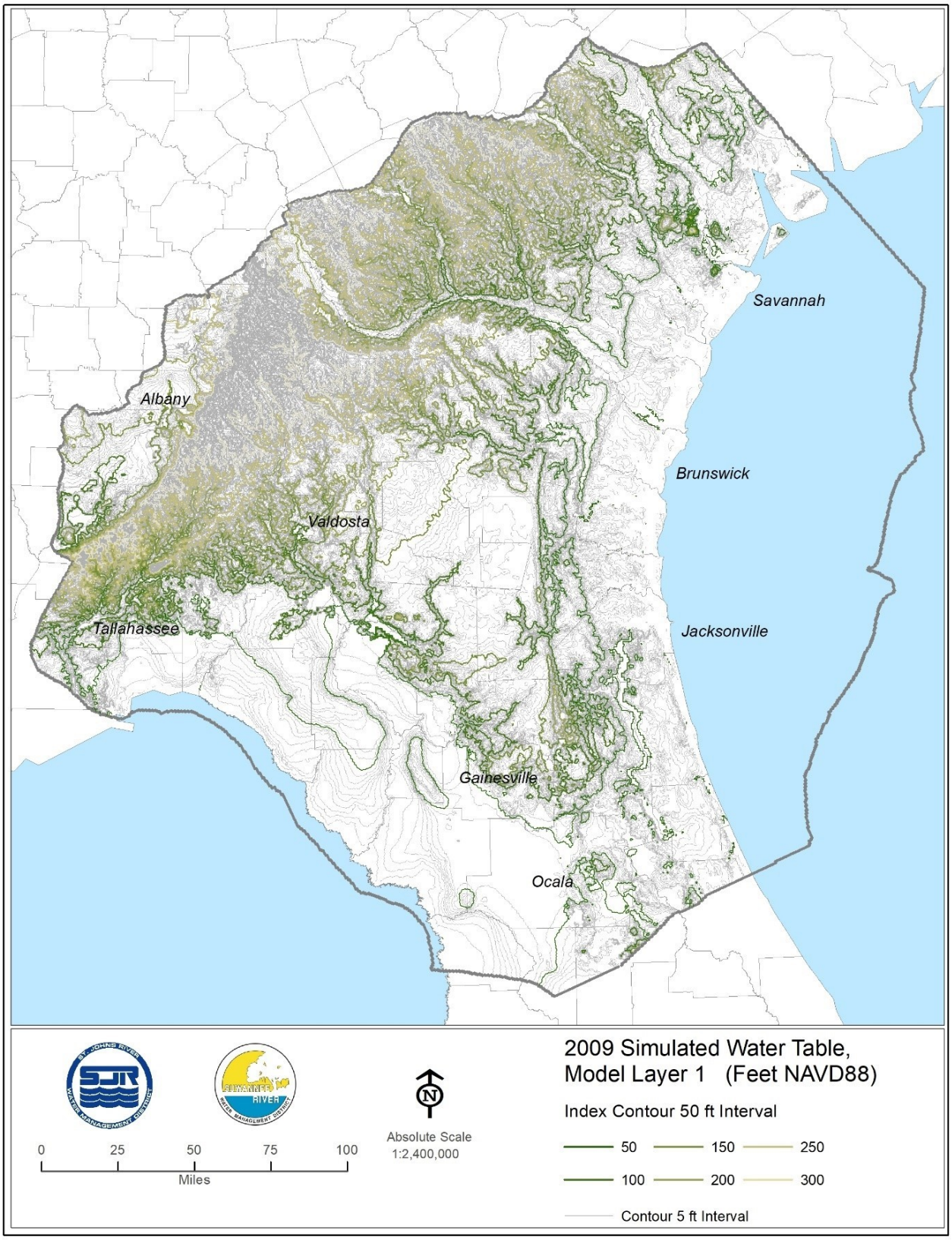

Figure 4-16. Simulated water table of model Layer 1 (feet NAVD88), 2009

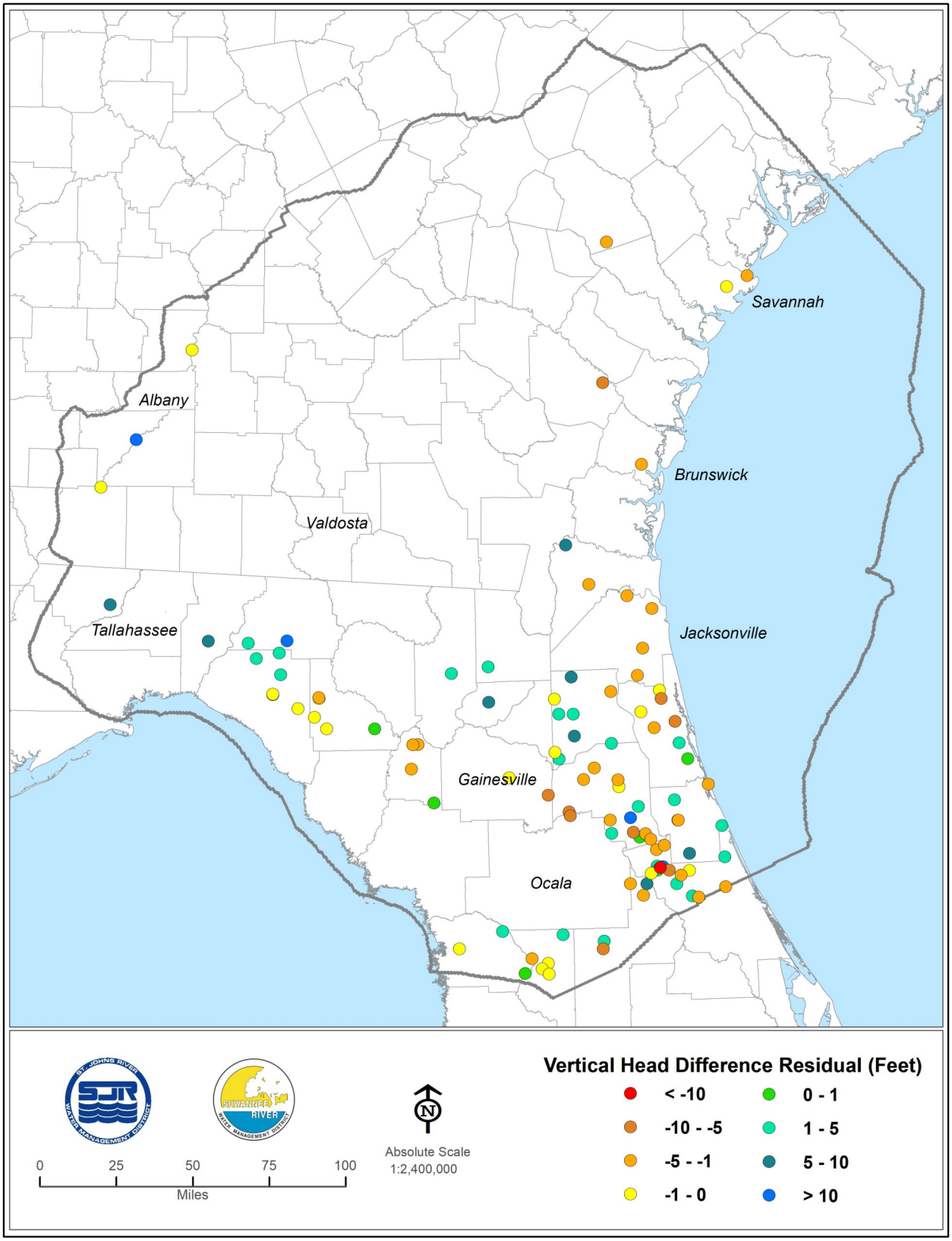

Figure 4-17. Residuals of vertical head differences (feet), model Layers 1 and 3, 2001

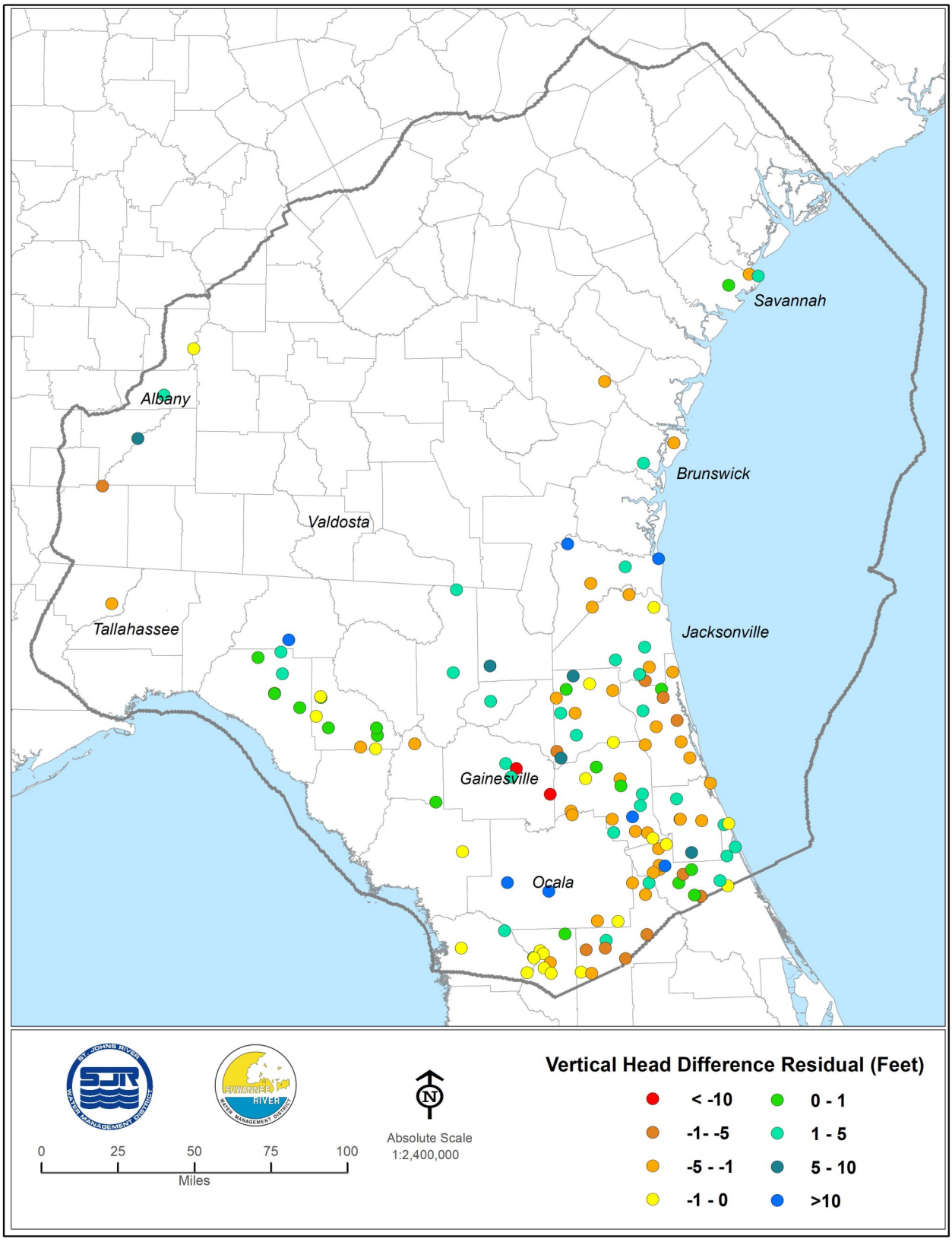

Figure 4-18. Residuals of vertical head differences (feet), model Layers 1 and 3, 2009

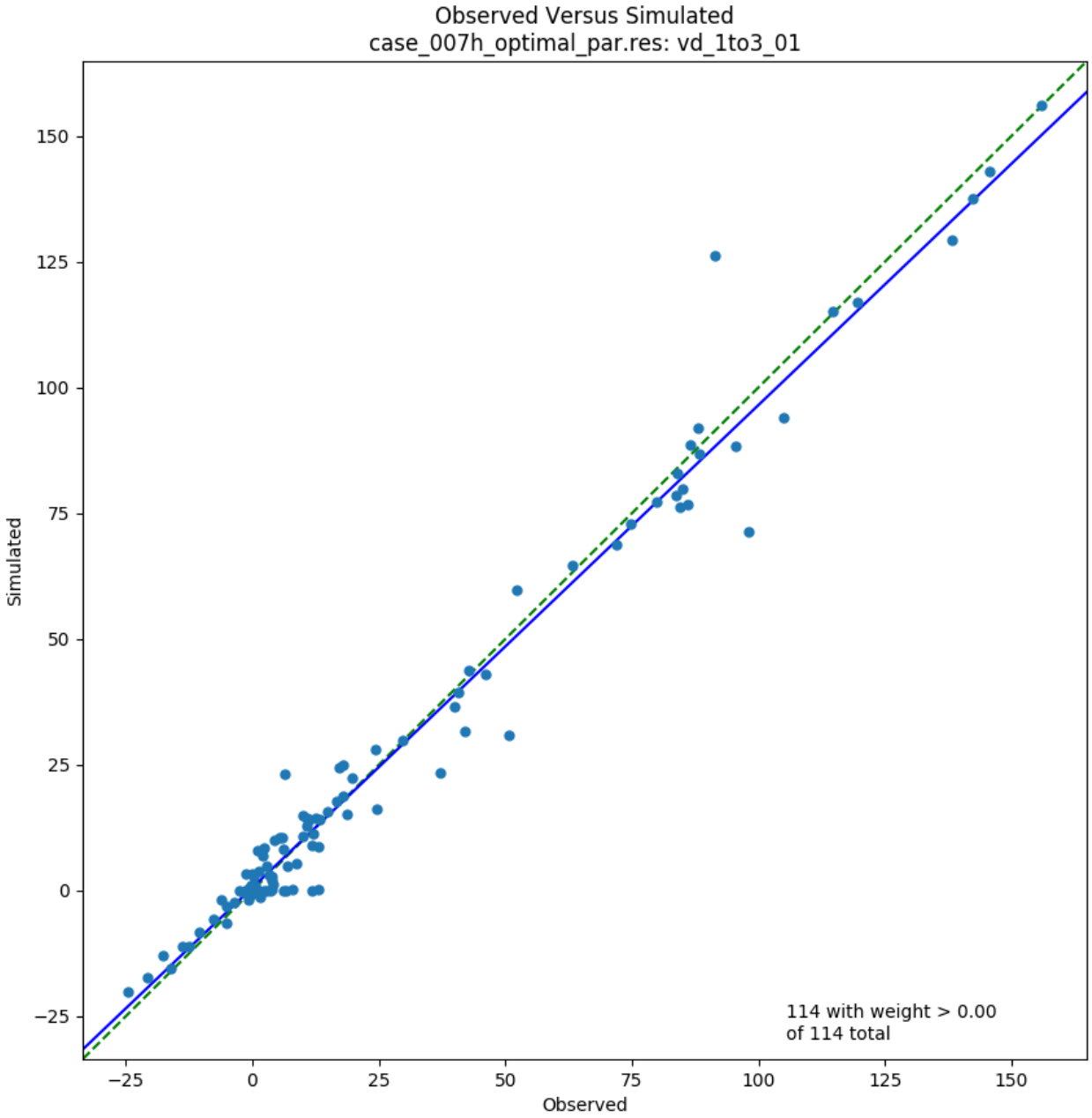

Figure 4-19. Observed versus simulated vertical head differences (feet), model Layers 1 and 3, 2001

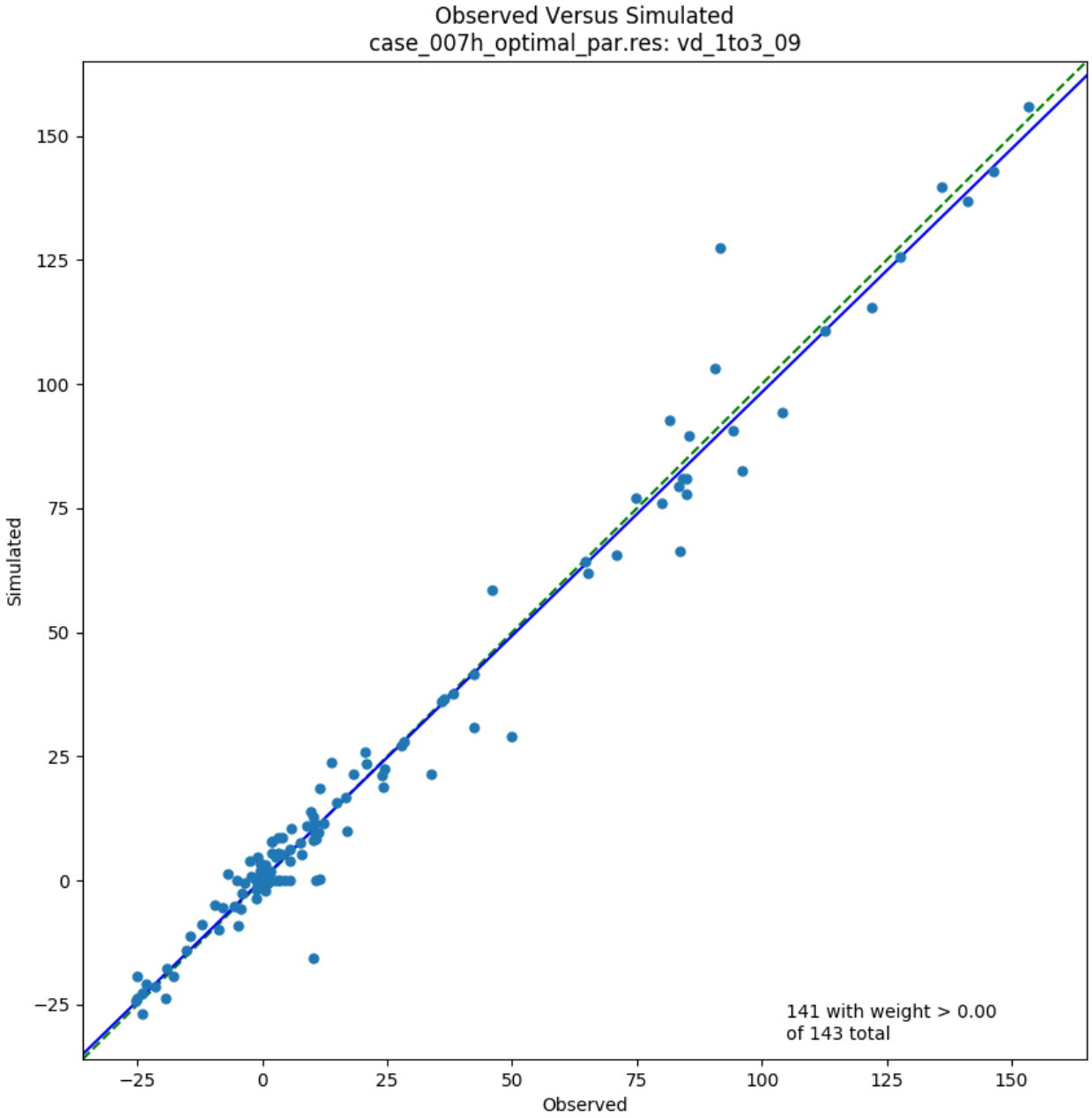

Figure 4-20. Observed versus S=simulated vertical head differences (feet), model Layers 1 and 3, 2009

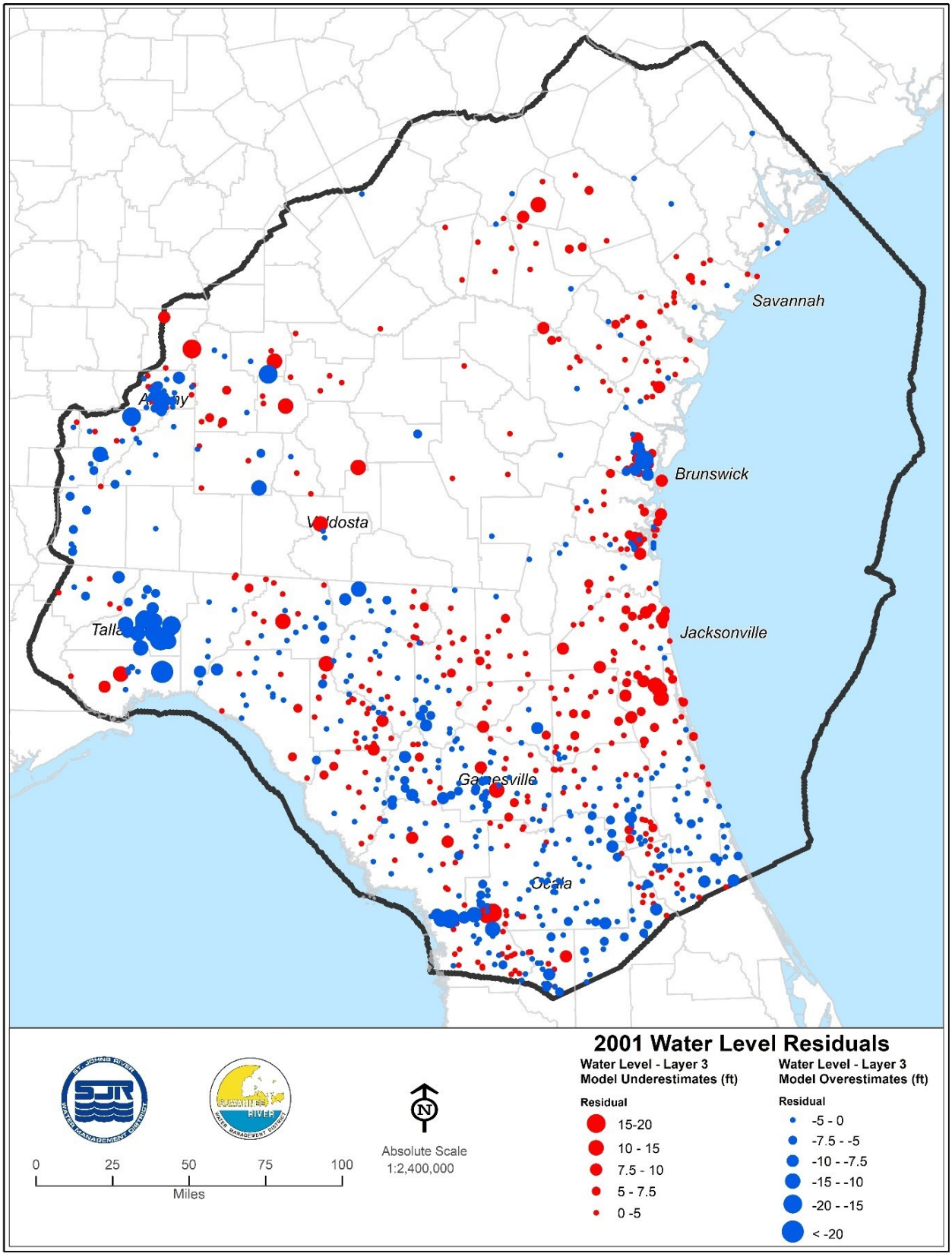

Figure 4-21 (a). Residuals of hydraulic head (feet), model Layer 3, 2001

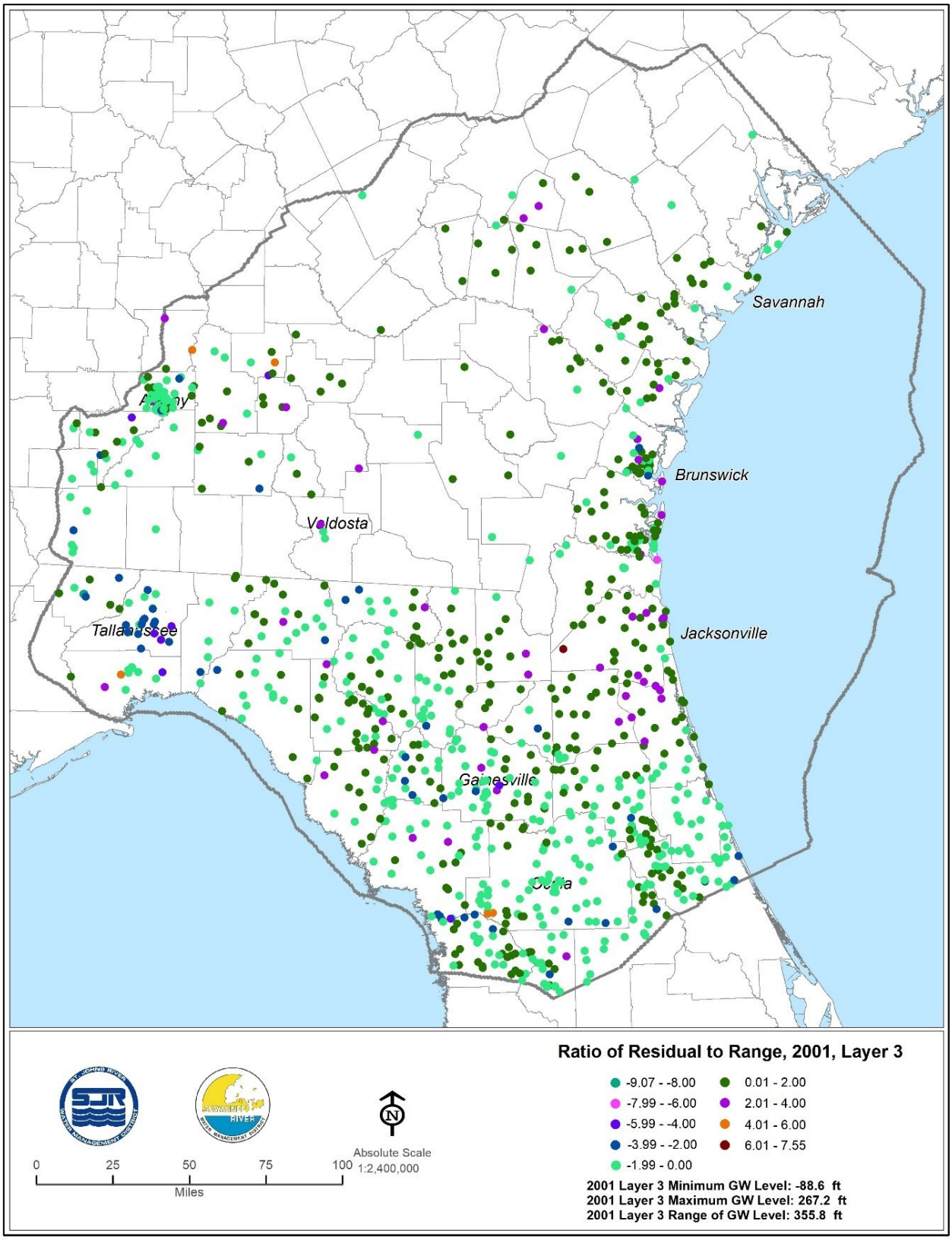

Figure 4-21 (b). Relative Residuals of Hydraulic Head (Feet), Model Layer 3, 2001

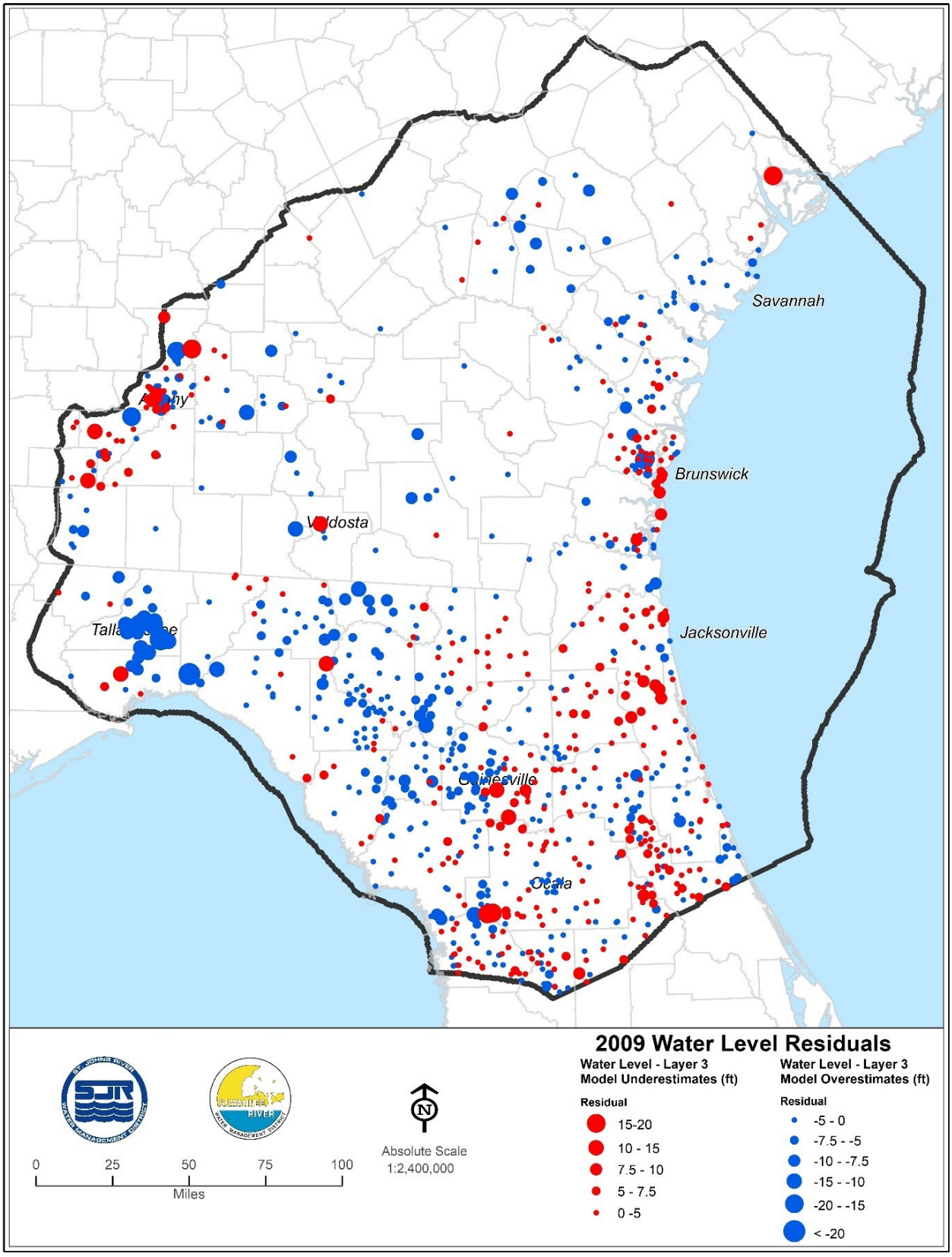

Figure 4-22 (a). Residuals of Hydraulic Head (Feet), Model Layer 3, 2009

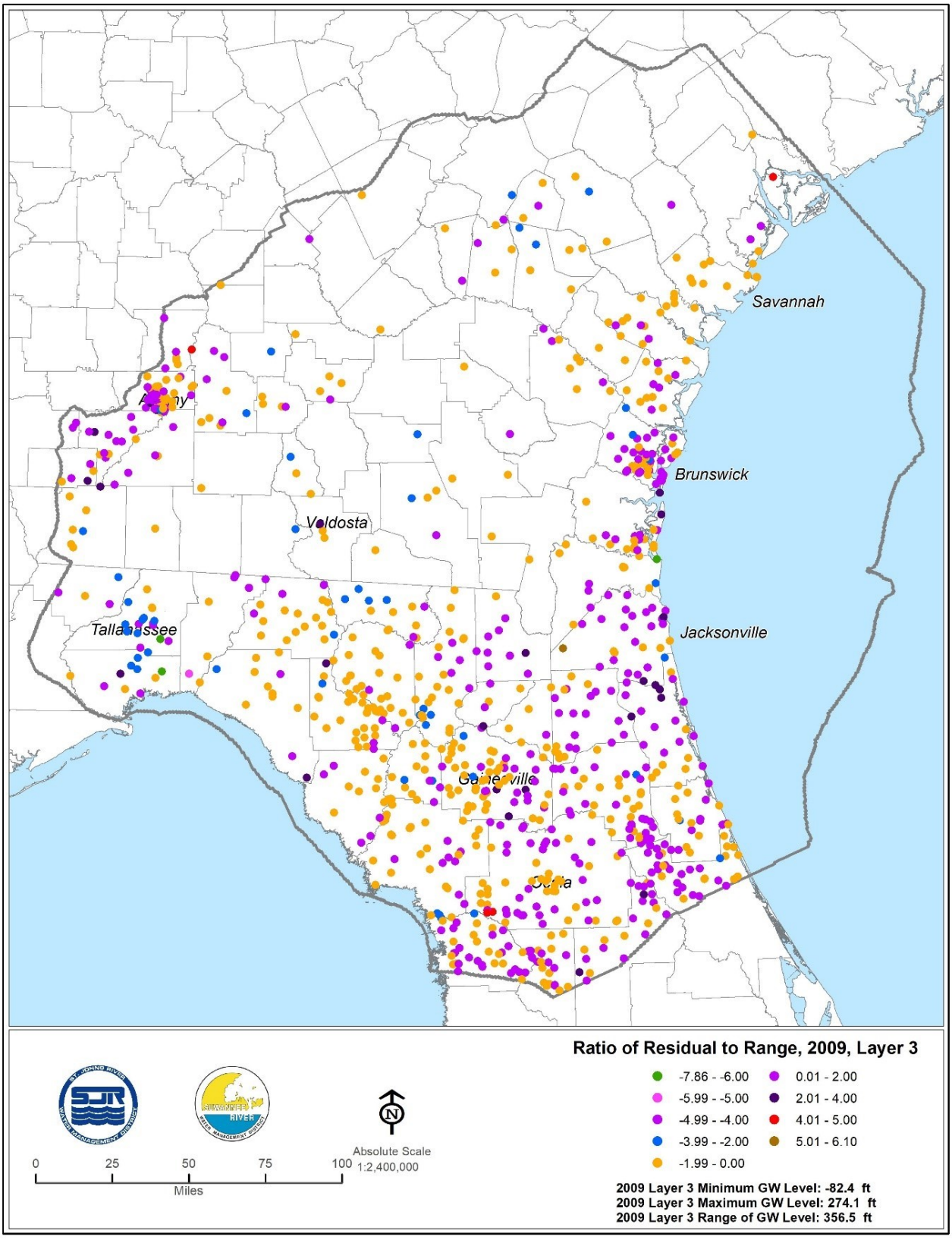

Figure 4-22 (b). Relative Residuals of Hydraulic Head (Feet), Model Layer 3, 2009

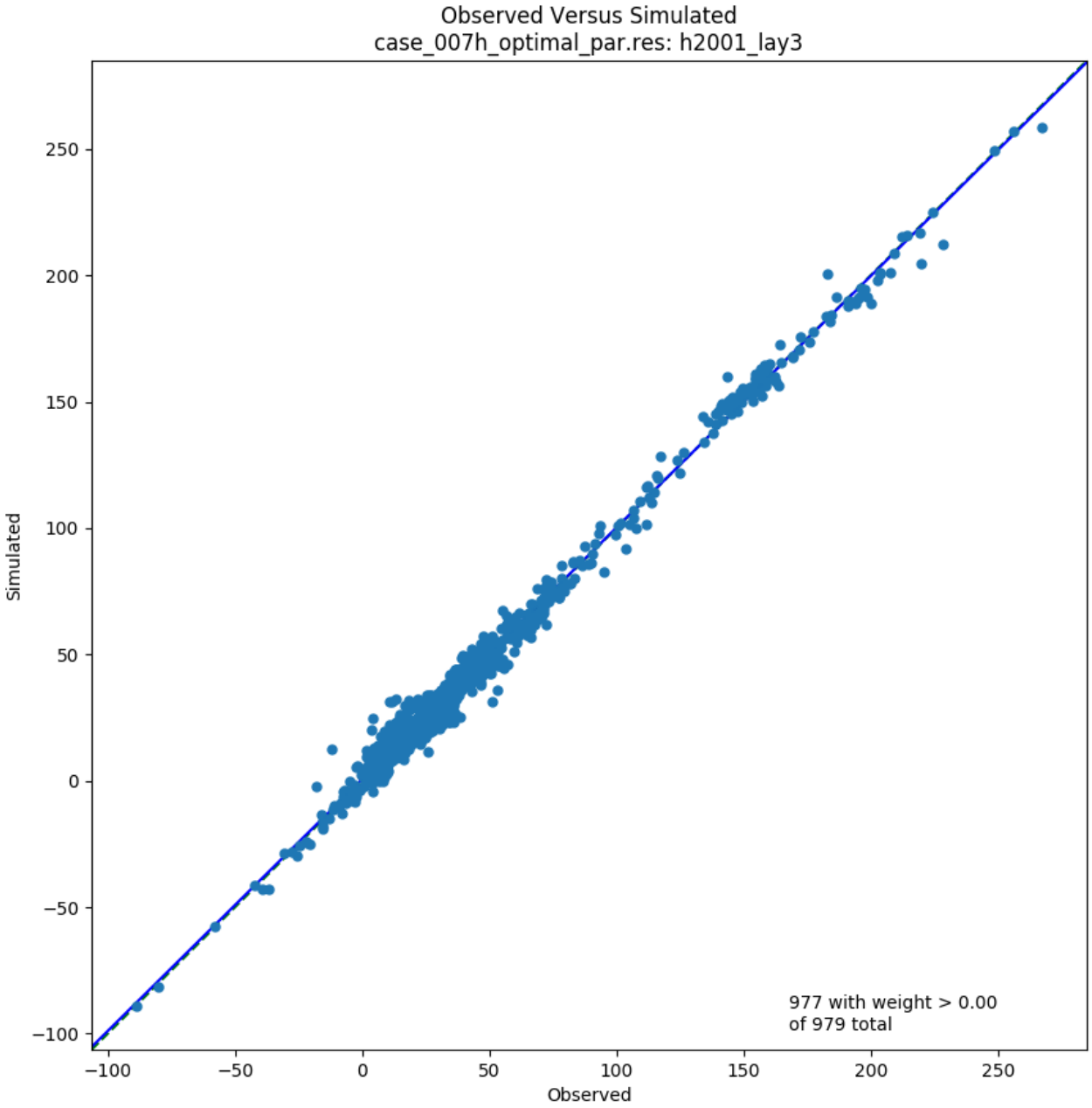

Figure 4-23. Observed versus simulated hydraulic head (feet NAVD88), model Layer 3, 2001

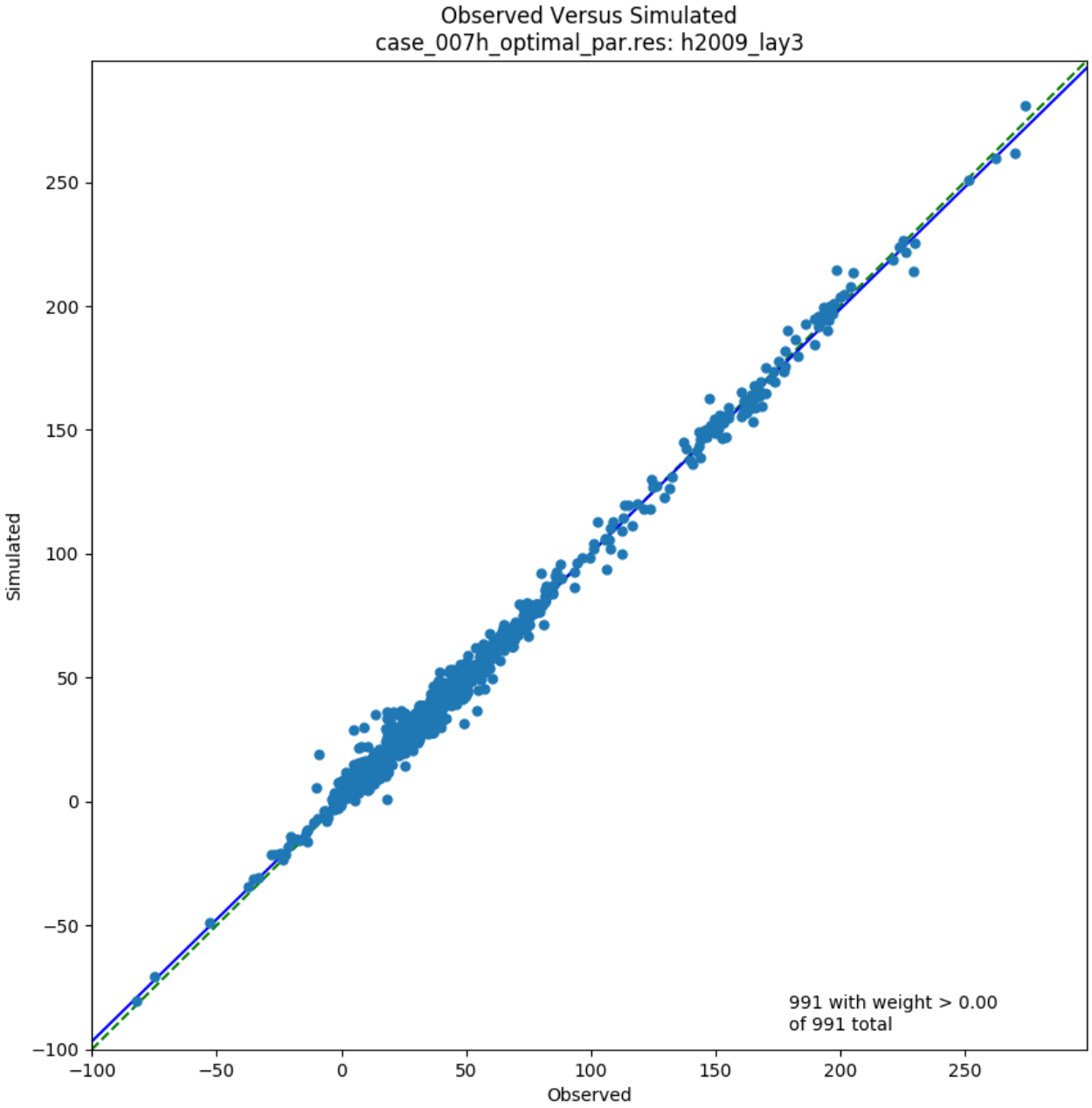

Figure 4-24. Observed versus simulated hydraulic head (Feet NAVD88), model Layer 3, 2009

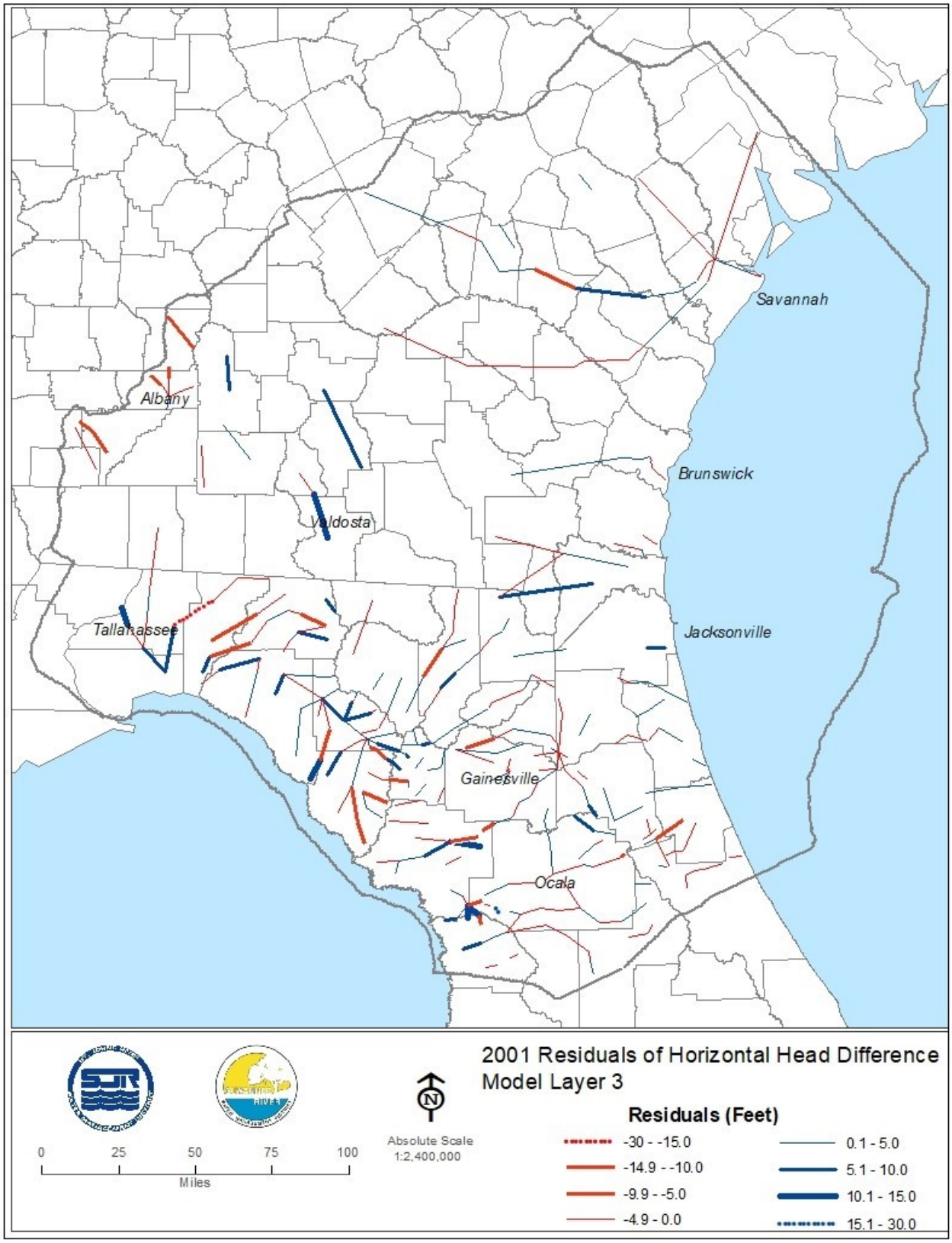

Figure 4-25. Residuals of horizontal head differences (feet), model Layer 3, 2001

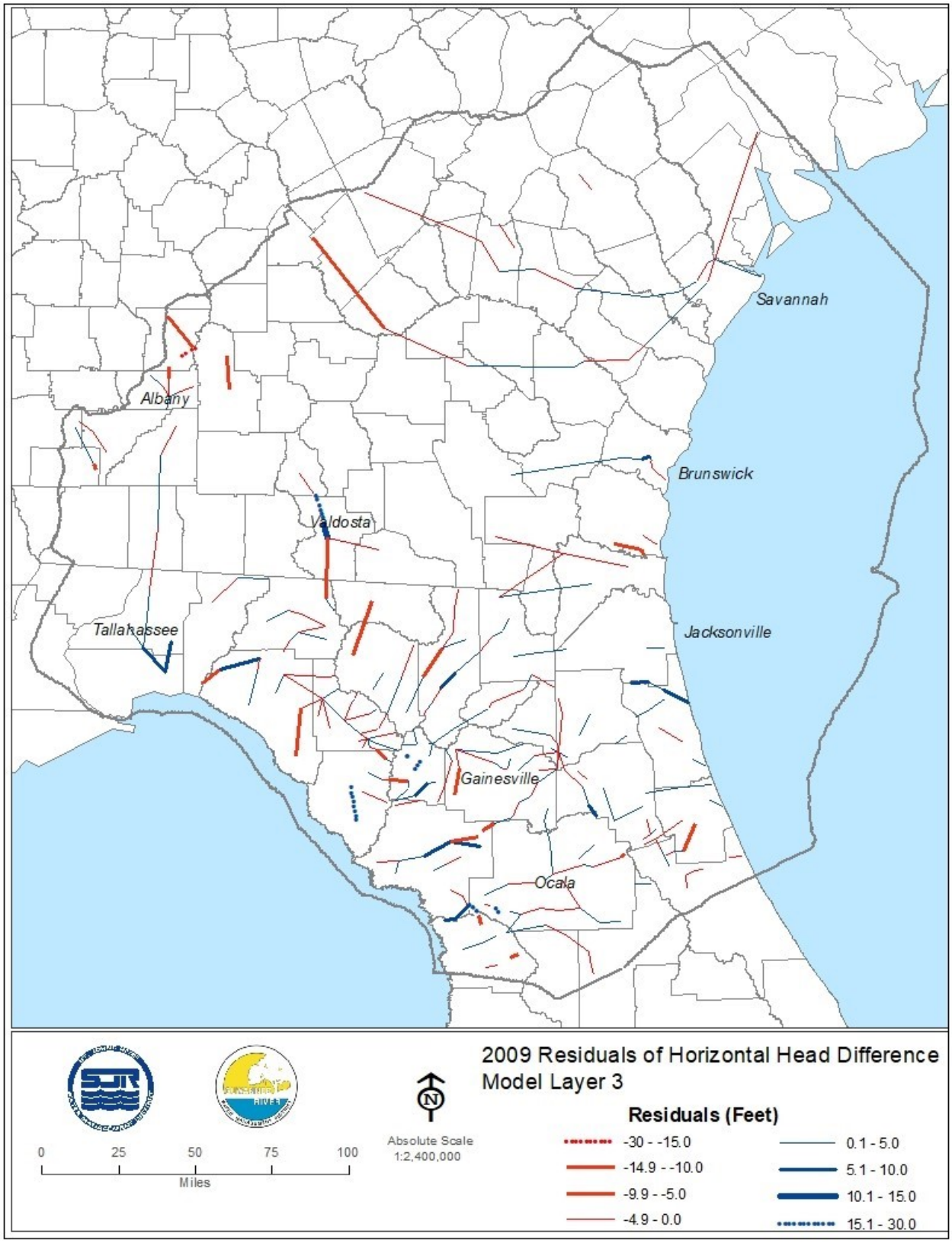

Figure 4-26. Residuals of horizontal head differences (feet), model Layer 3, 2009

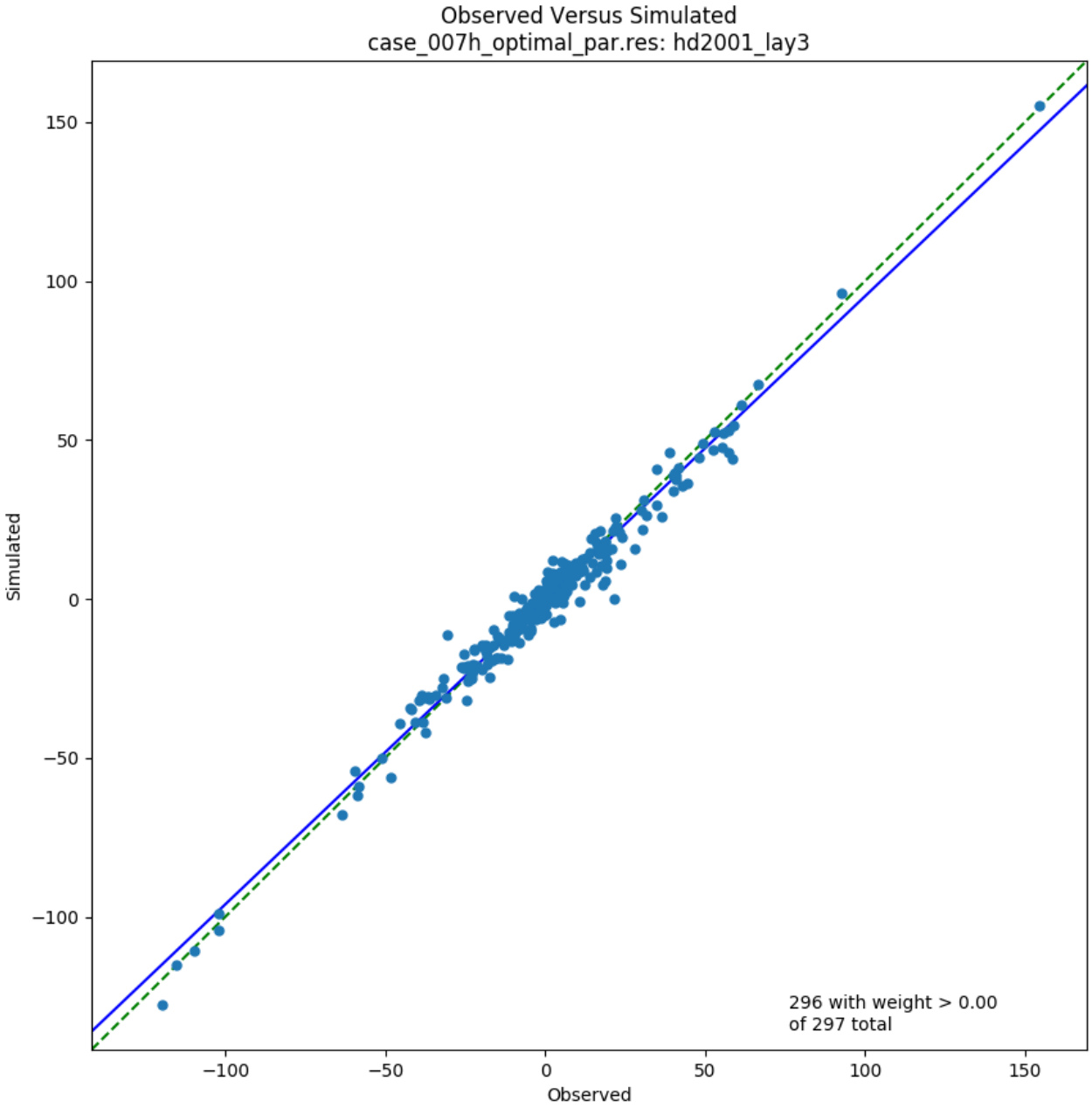

Figure 4-27. Observed versus simulated horizontal head differences (feet), model Layer 3, 2001

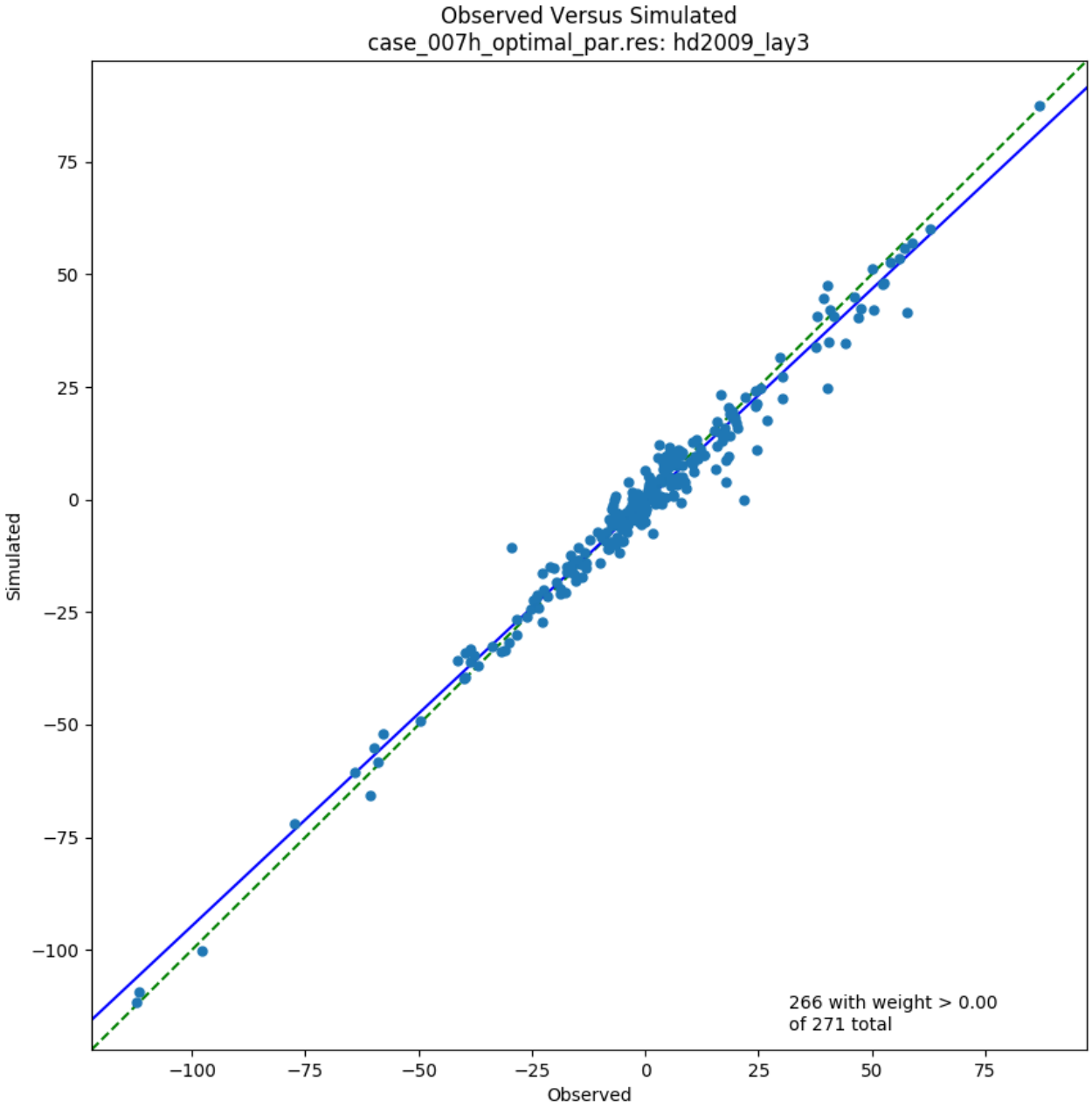

Figure 4-28. Observed versus simulated horizontal head differences (feet), model Layer 3, 2009

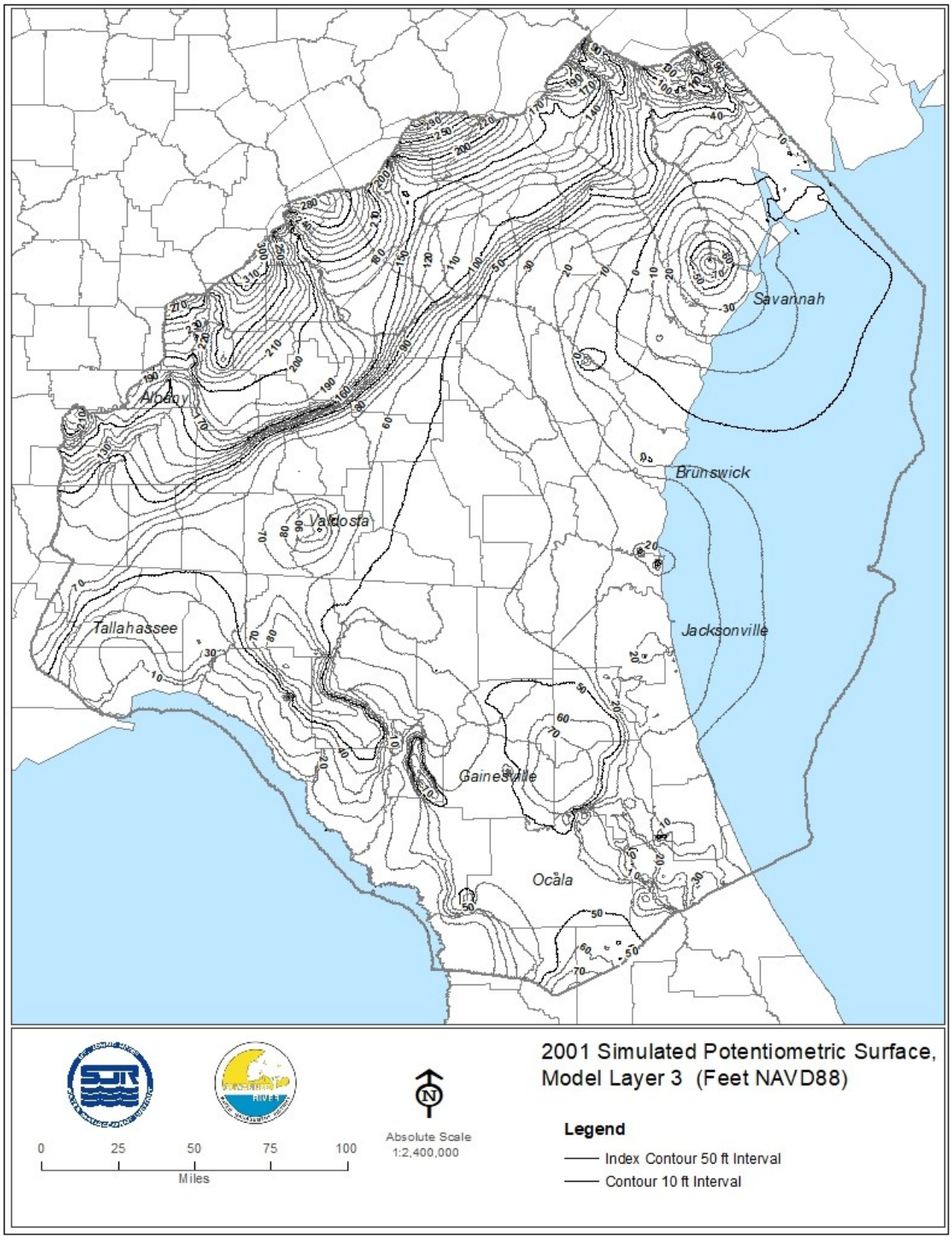

Figure 4-29. Simulated potentiometric surface, model Layer 3 (Feet NAVD88), 2001

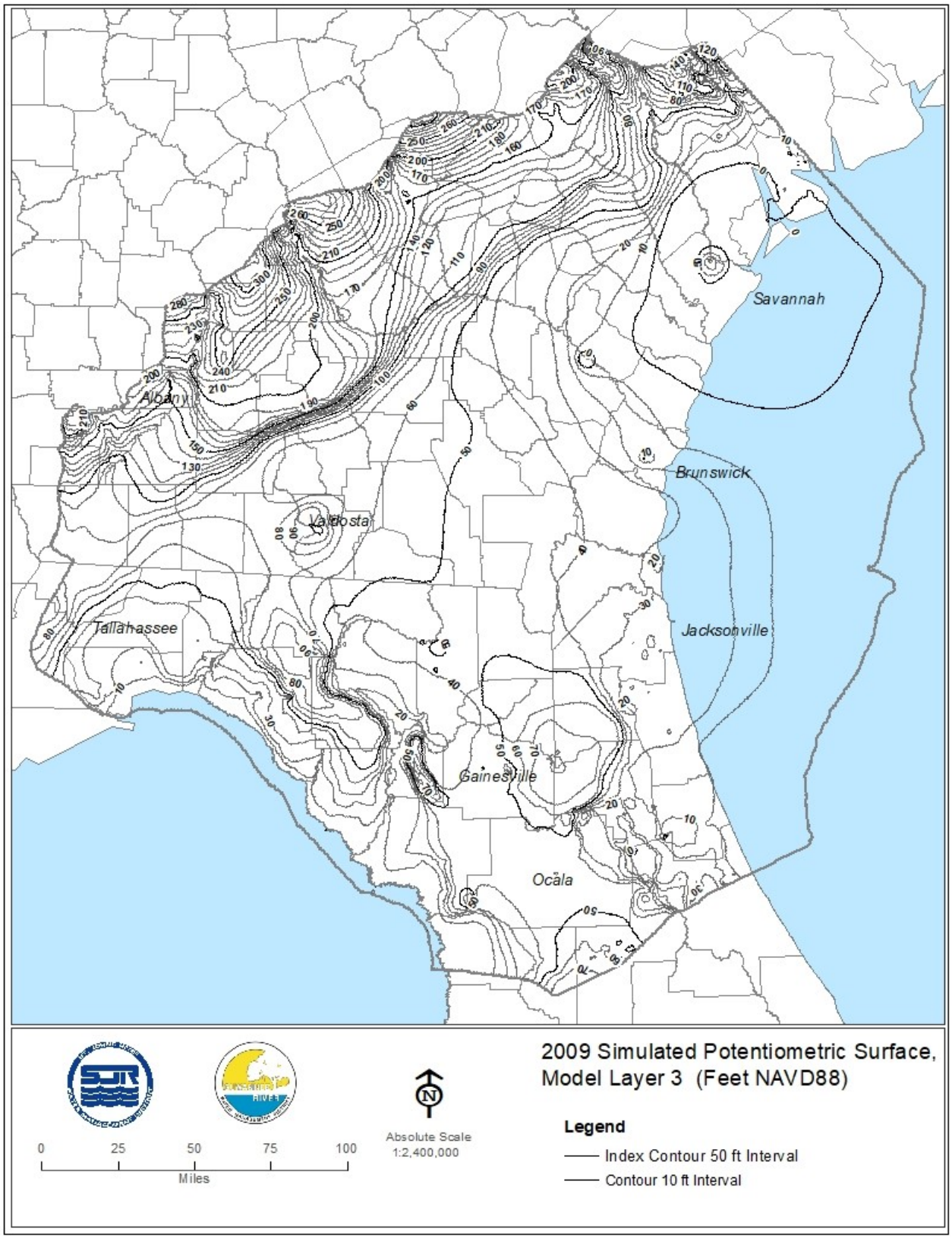

Figure 4-30. Simulated potentiometric surface, model Layer 3 (Feet NAVD88), 2009

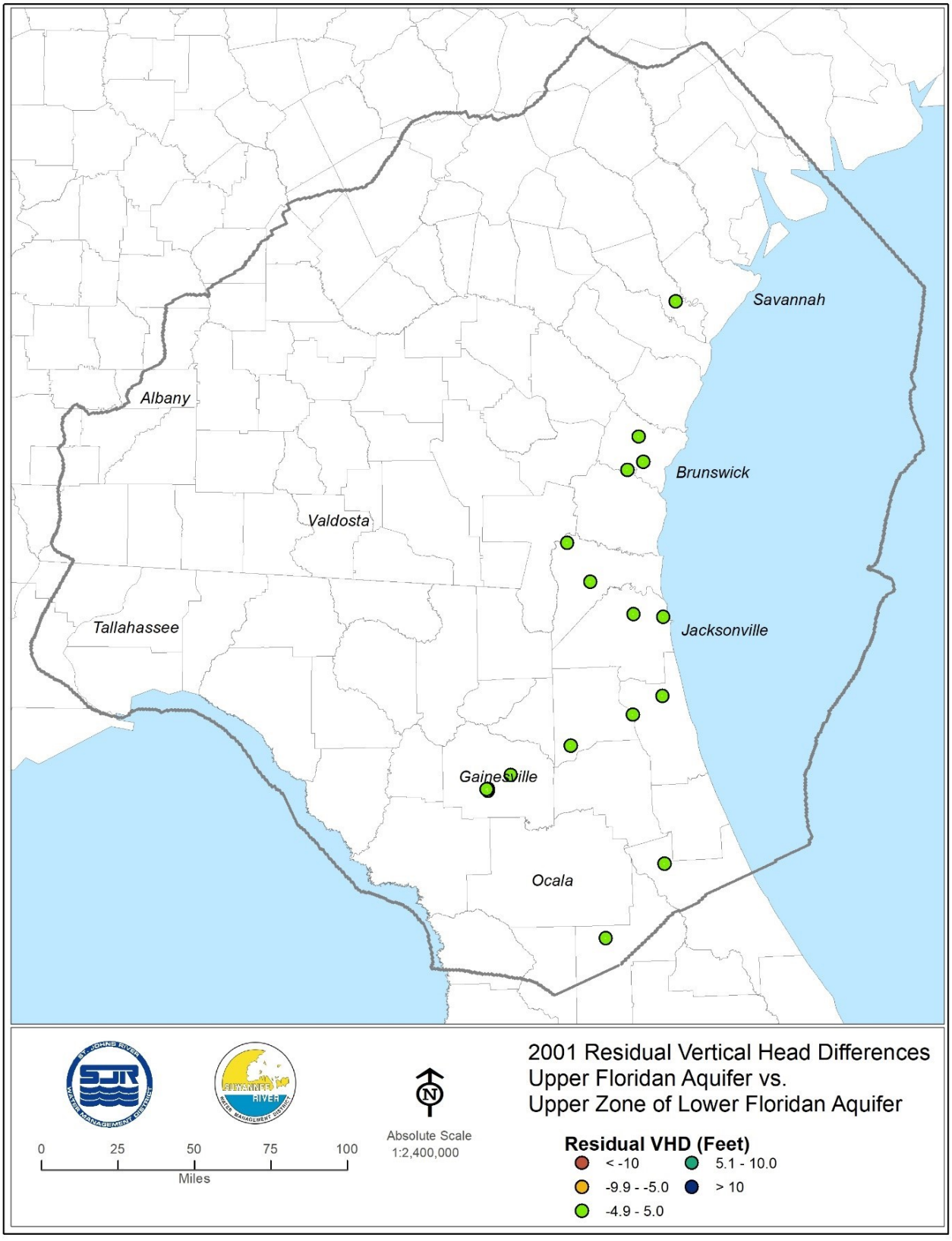

Figure 4-31. Residuals of vertical head differences (feet), model Layers 3 and 5, 2001

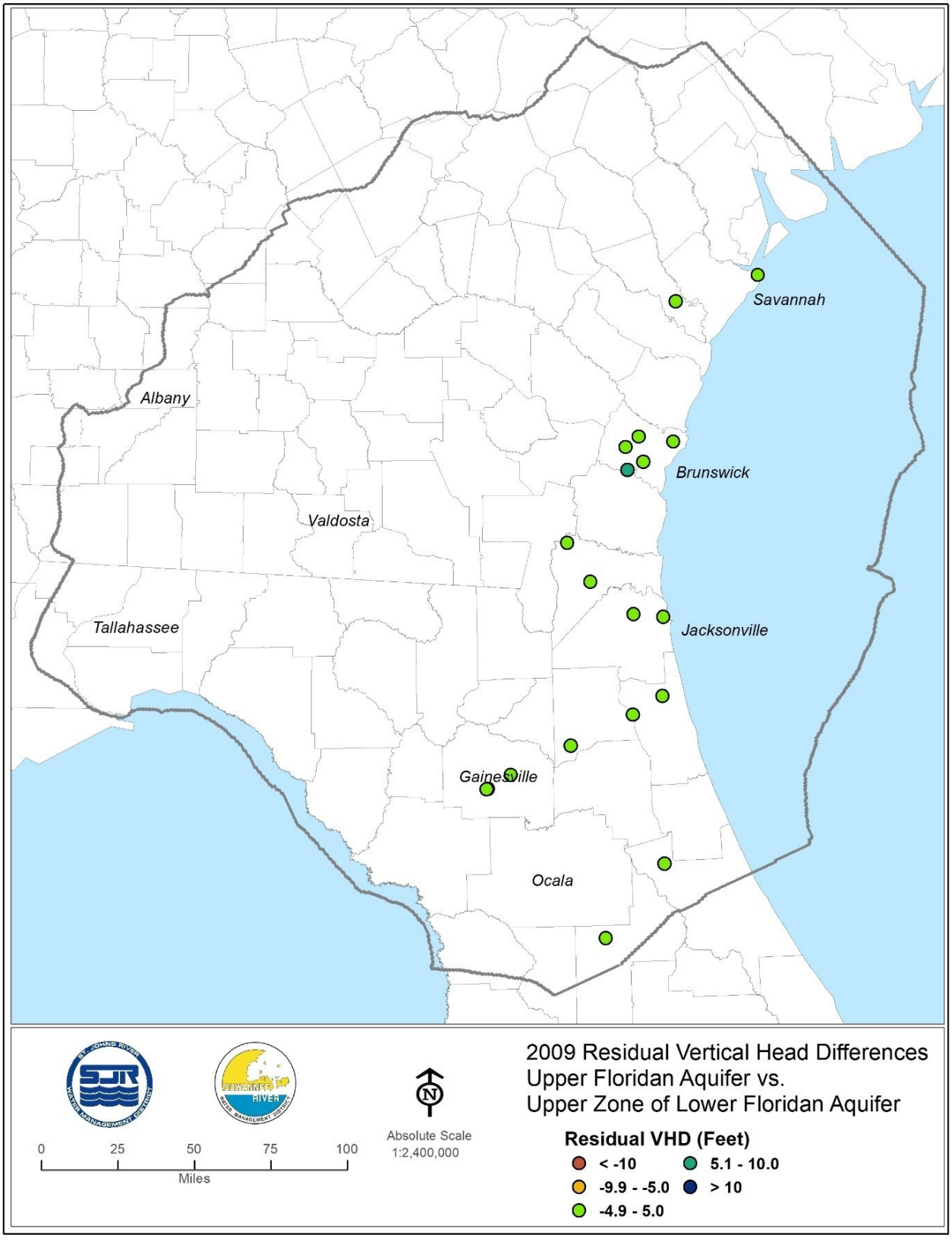

Figure 4-32. Residuals of vertical head differences (feet), model Layers 3 and 5, 2009

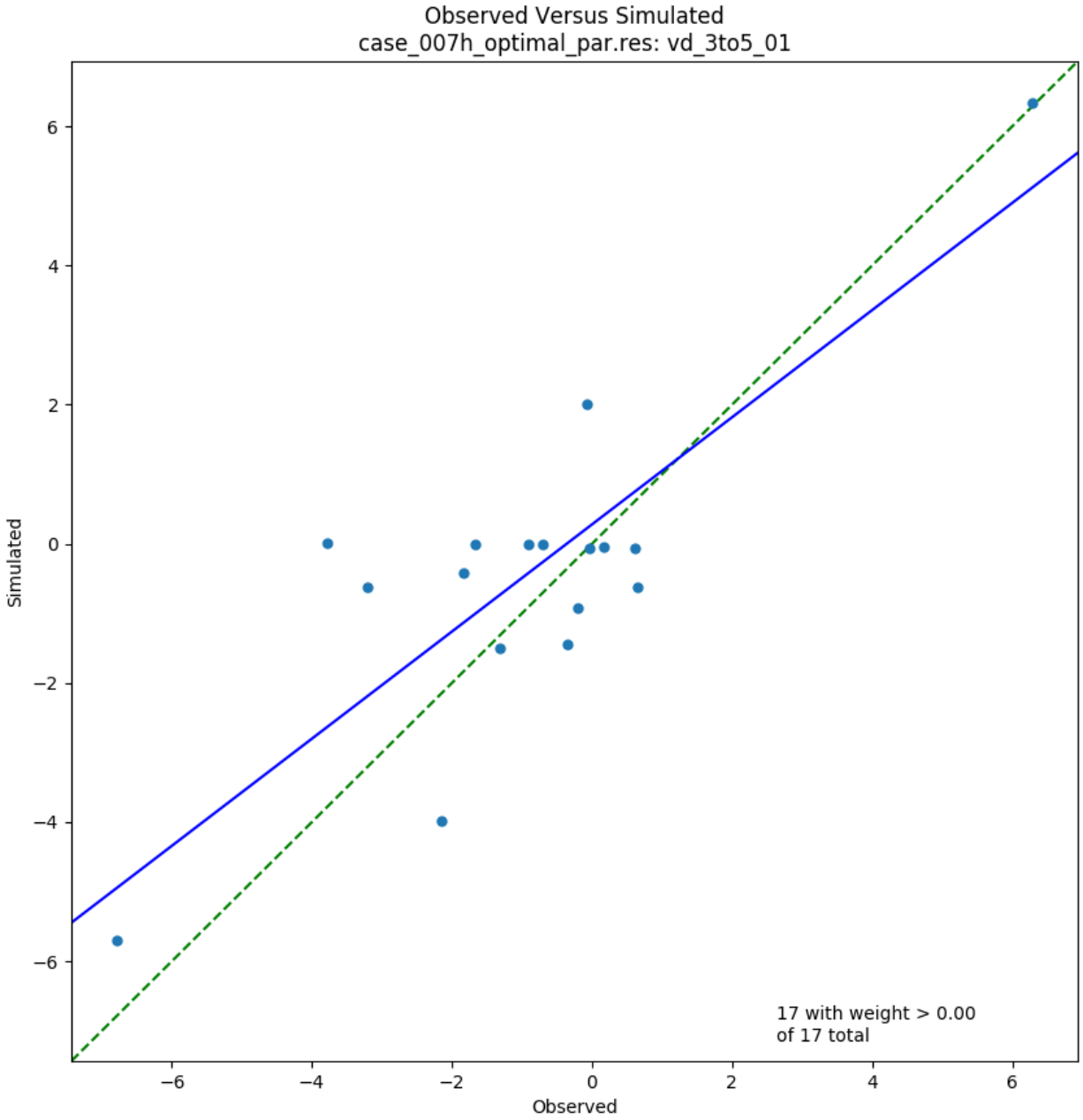

Figure 4-33. Observed versus simulated vertical head differences (feet), model Layers 3 and 5, 2001

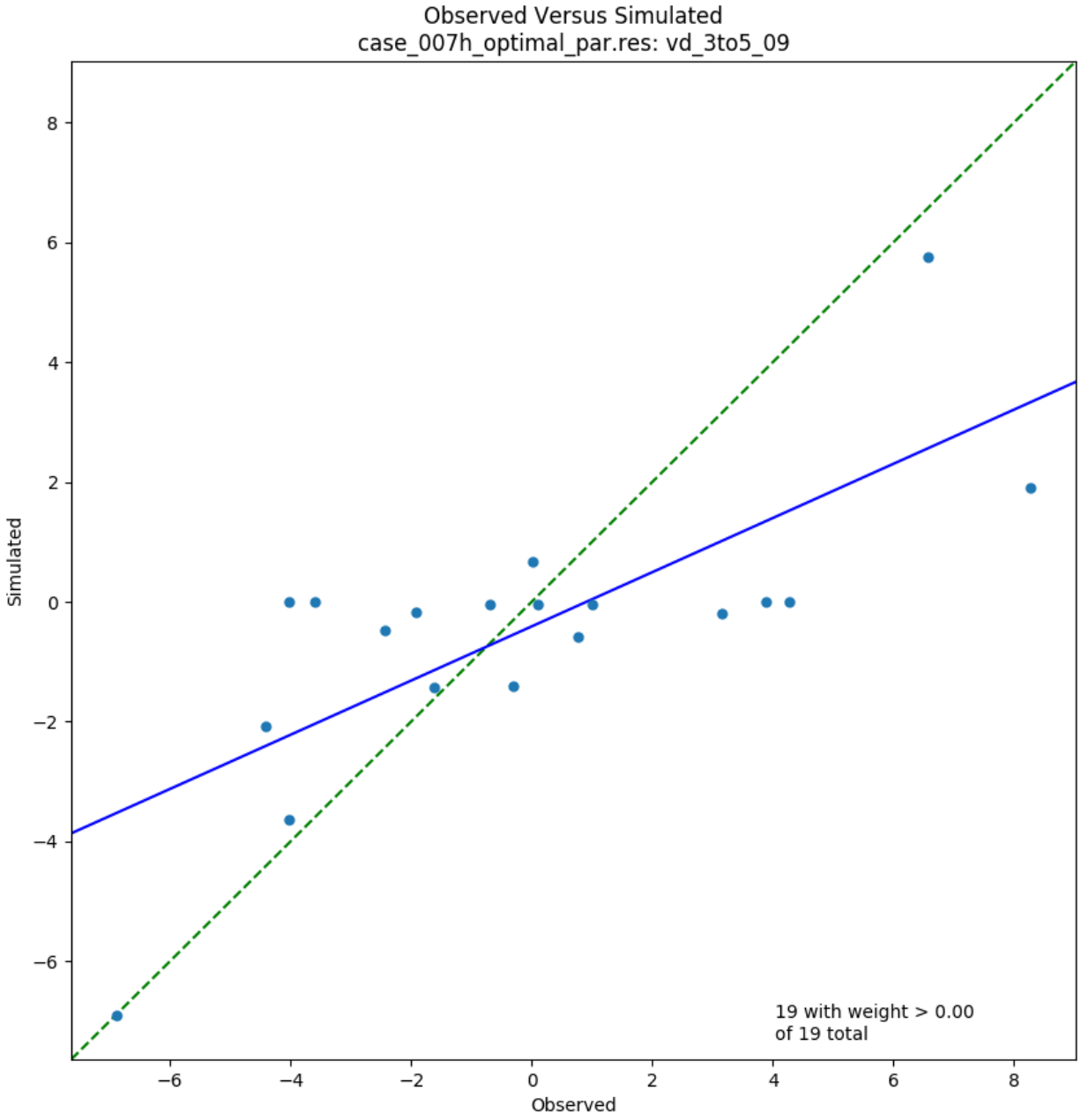

Figure 4-34. Observed versus simulated vertical head differences (feet), model Layers 3 and 5, 2009

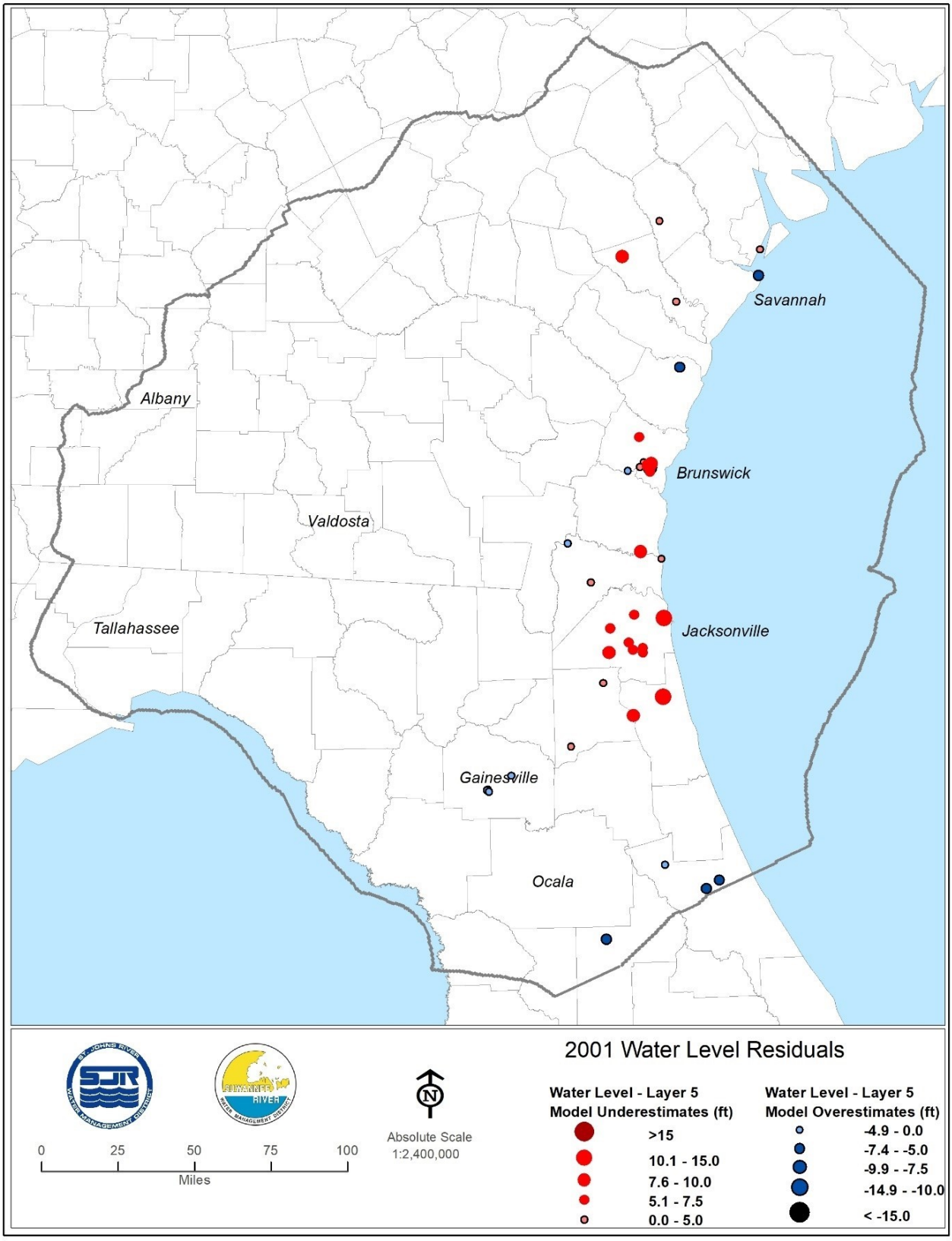

Figure 4-35. Residuals of hydraulic head (feet), model Layer 5, 2001

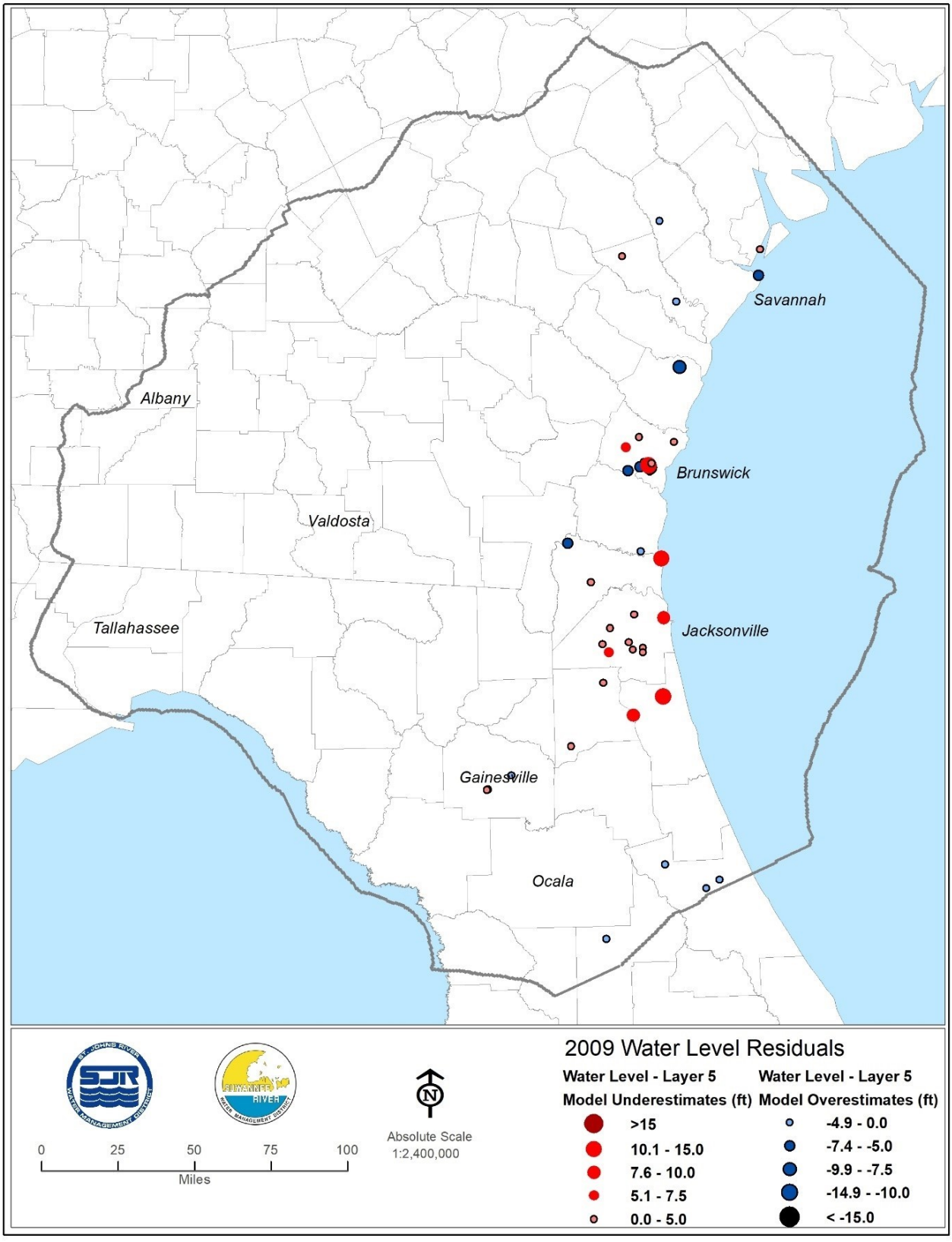

Figure 4-36. Residuals of hydraulic head (feet), model Layer 5, 2009

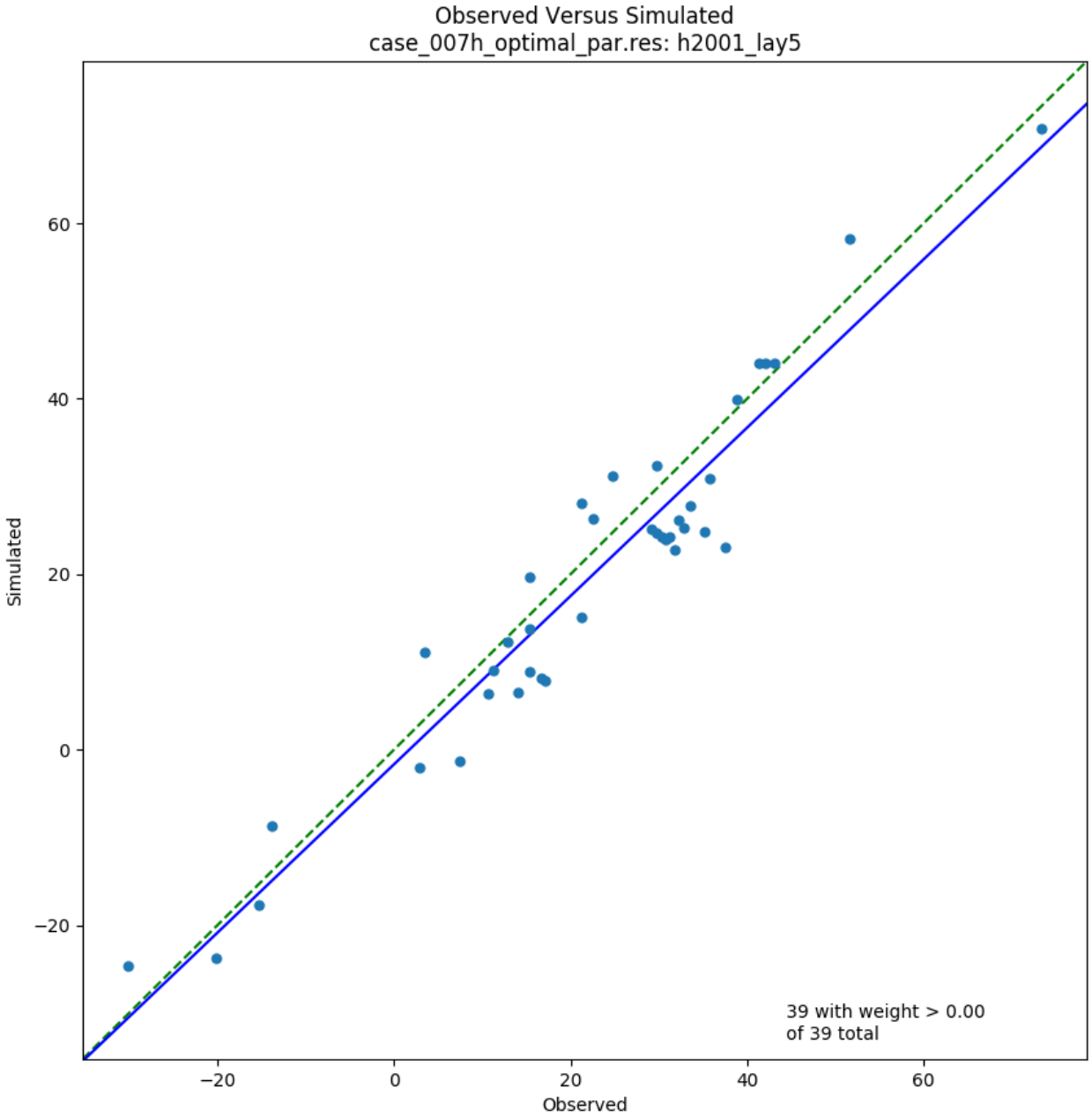

Figure 4-37. Observed versus simulated hydraulic head (feet NAVD88), model Layer 5, 2001

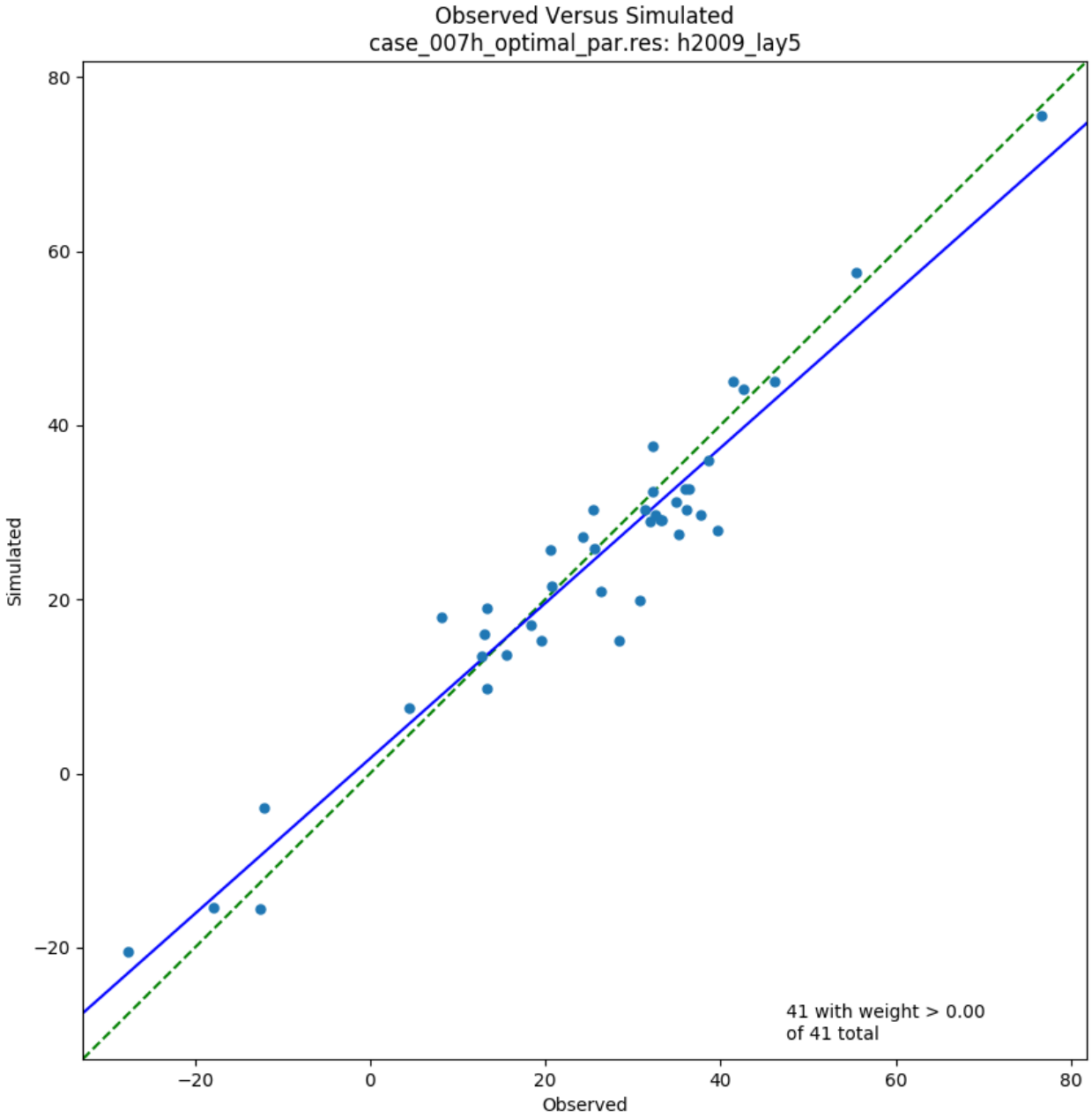

Figure 4-38. Observed versus simulated hydraulic head (feet NAVD88), model Layer 5, 2009

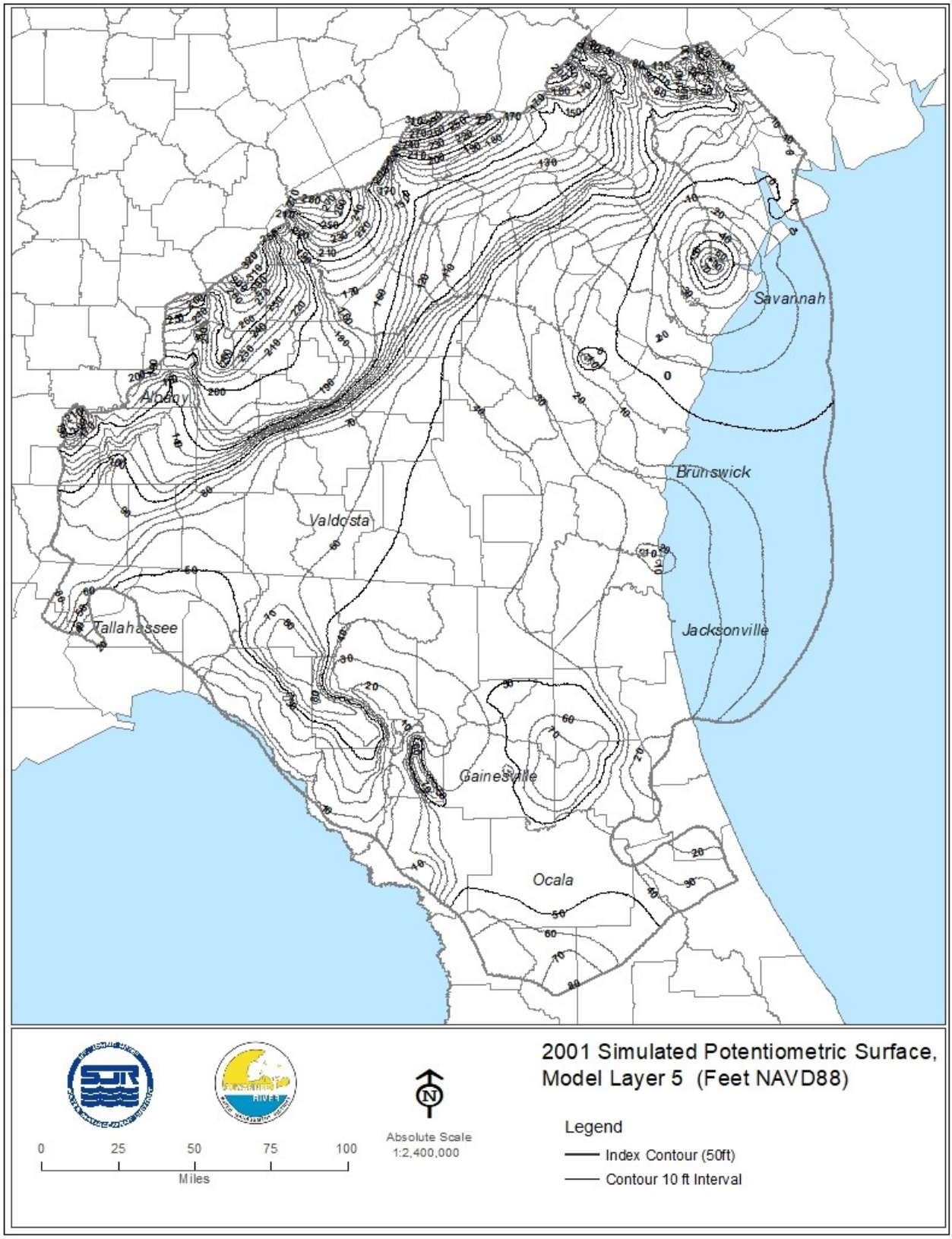

Figure 4-39. Simulated potentiometric surface, model Layer 5 (feet NAVD88), 2001

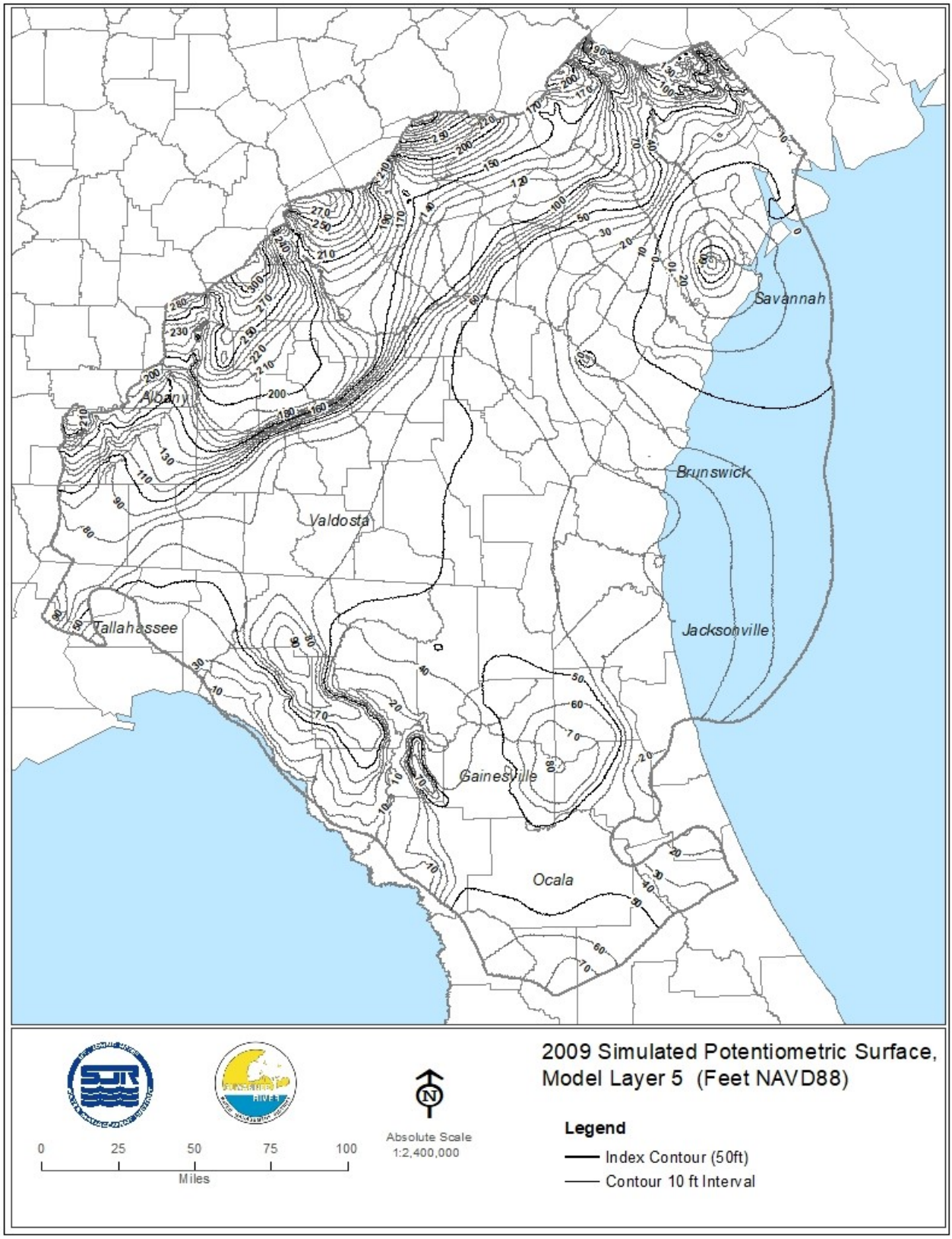

Figure 4-40. Simulated potentiometric surface, model Layer 5 (feet NAVD88), 2009

As these estimates are not observations, they were assigned a lower weight in the calibration process, so differences between them and corresponding simulated values tend to be larger than average for Layer 1. A large proportion of these points are positioned in the general region of pinch out of the intermediate confining unit (the Cody Escarpment). This may point to the need for additional surficial aquifer system monitoring wells in these areas. As the synthetic groundwater levels are not observations but estimates that were utilized to impart system knowledge to PEST in areas of scarce groundwater level observations, their residuals are not included in Figures 4-12 or 4-14.

Water levels of the surficial aquifer system are sensitive to local conditions. It is therefore more difficult to match at the regional scale, as variations of water levels across the area corresponding to a model grid cell, which can be considerable in the case of the water table, are represented by a single average value. This results in larger residuals in many cases.

Layer 1 simulated groundwater levels were compared to river boundary condition assigned stages to further evaluate their reasonableness. Tables 4-5 and 4-6 below summarize the differences for 2001 and 2009. As seen in Tables 4-5 and 4-6, in about 85 percent of cases, the differences are relatively small (less than five feet), as would be expected. In most cases, the simulated groundwater levels of Layer 1 are higher than corresponding river boundary stages, which is also expected, as most streams within the model domain are gaining streams at most locations. In some cases, the differences are large, which can indicate calibration error, though not necessarily. Instances in which large differences would not necessarily indicate calibration error are cases of a high degree of topographic relief. In such cases, the stream stage tends to be much lower than the simulated groundwater level, which is higher because it is averaged over the area of the grid cell.

Observed versus Simulated Groundwater Levels of Layer 1

Scatter plots of observed versus simulated hydraulic head provide a graphical comparison of observed and simulated hydraulic heads of Layer 1 in 2001 and 2009 (Figures 4-13 and 4-14). As with the maps of Layer 1 groundwater level residuals discussed in the previous section, scatter plots of 2009 Layer 1 groundwater levels did not include representation of synthetic groundwater levels. As is the case with all scatter plots of observed vs. simulated values shown in the report and as noted on the plots, observations with assigned weights below the minimum value shown on the plots were not represented in the plots.

Simulated Water Table of the Surficial Aquifer System

The 2001 and 2009 simulated water levels of Layer 1 represent the water table of the surficial aquifer system in 2001 and 2009, respectively, where the surficial aquifer system is present (Figures 4-15 and 4-16). The simulated water table is similar in appearance and general configuration for both years. In confined regions, it is reflective of the topography of the land surface but also reflects the influence of various rivers and streams in the form of v-shaped distortions in the contours of the water table that occur where the contours cross streams and that point upstream. In unconfined regions, the

simulated water table resembles more closely the Upper Floridan aquifer potentiometric surface, with differences likely being attributable to represented effects of the overburden above the Floridan aquifer system. As expected, the simulated water table approaches sea level with increasing proximity to the Atlantic Ocean and the Gulf of Mexico.

Residuals of Vertical Head Differences between Layers 1 and 3

In the most cases, the match between estimated and corresponding simulated vertical head differences between Layers 1 and 3 is within 5 feet (Figures 4-17 and 4-18; Appendix B). This comparison can be indicative of the degree to which the confining properties of the intermediate confining unit are represented in the model, although numerous other factors can also influence the value of a vertical head residual at any given location.

Observed versus Simulated Vertical Head Differences between Layers 1 and 3

Scatter plots of observed versus simulated vertical head differences between Layers 1 and 3 are shown in Figures 4-19 and 4-20, and a listing is provided in Appendix B. Scatter in these plots may be indicative of a lack of precision in knowledge of the confining properties of the intermediate confining unit at specific locations. As noted on the plots, observations with assigned weights below the minimum value shown on the plots were not represented.

Groundwater Level Residuals of Layer 3

Maps of residuals of the groundwater levels of Layer 3 for 2001 and 2009 show the match between observed and corresponding simulated water levels of the Upper Floridan aquifer (Figures 4-21a and b, 4-22a and b; Appendix A). The absolute value of groundwater level residuals were generally less than 5 feet within the model domain, with larger residuals occurring in some areas. Additional discussion of Layer 3 groundwater level residuals is provided in the section that follows entitled "Additional Discussion."

Table 4-5. Differences between simulated Layer-1 groundwater levels and assigned river boundary stages, 2001

Year 2001								
Mean Difference (Feet)	Standard Deviation (Feet)	Mean Absolute Value (Feet)	Maximum (Feet)	Minimum (Feet)	Percentage with Absolute Difference Greater than			
					2.5 Ft	5 Ft	15 Ft	50 Ft
-0.9	7.3	2.7	98.7	-78.9	21.5	14.8	4.6	0.4

Table 4-6. Differences between simulated Layer-1 groundwater levels and assigned river boundary stages, 2009

Year 2009								
Mean Difference (Feet)	Standard Deviation (Feet)	Mean Absolute Value (Feet)	Maximum (Feet)	Minimum (Feet)	Percentage with Absolute Difference Greater than			
					2.5 Ft	5 Ft	15 Ft	50 Ft
-1.6	8.1	3.1	93	-	23	16	5	0.4

As seen on the Figures 4-21 and 4-22, Upper Floridan aquifer groundwater level residuals in much of Duval, Clay, and St. Johns counties, Florida, and Camden County, Georgia, reflect widespread under simulation by the model. Conversely, in much of Columbia, Hamilton, Suwannee, Madison, and Gilchrist counties, Florida, they reflect widespread over simulation by the model. A pre-dominance of positive or negative residuals within a subregion is indicative of "trends" in groundwater level residuals. This and other aspects of the calibration results are discussed in greater detail in the section of the report entitled "Additional Discussion," which follows the current section.

Observed versus Simulated Hydraulic Head of Layer 3

The scatter plots of observed versus simulated hydraulic head of Layer 3 for 2001 and 2009 are shown in Figures 4-23 and 4-24. As noted on the plots, observations with assigned weights below the minimum value shown on the plots were not represented.

Residuals of Horizontal Head Difference of Layer 3

The maps of residuals of horizontal head differences of Layer 3 are shown in Figures 4-25 and 4-26, and a listing is provided in Appendix H. The ability of the model to simulate the horizontal gradients of the Upper Floridan aquifer potentiometric surface that are relatively steep or flat is indicated by these maps. Relatively large horizontal gradients can be more critical and difficult to simulate. The results show general adherence of simulated to observed gradients.

Note that the horizontal distance between the well pair associated with a given horizontal head difference is implicitly represented when the simulated value of the difference is simulated. Therefore, simulated horizontal head differences that correspond well to their observed counterparts also indicate a good correspondence between simulated and observed horizontal gradients.

Observed versus Simulated Horizontal Hydraulic Head Differences of Layer 3

Scatter plots of observed versus simulated horizontal head differences of Layer 3 in 2001 and 2009 are shown in Figures 4-27 and 4-28, and a listing is provided in Appendix H. As noted on the plots, observations with assigned weights below the minimum value shown on the plots were not represented.

Simulated Potentiometric Surface of Layer 3

The model generated water levels of Layer 3 represent the simulated potentiometric surface of the Upper Floridan aquifer (Figures 4-29 and 4-30). Water levels and gradients seen on the estimated 2001 and 2009 potentiometric surfaces of the Upper Floridan aquifer (Figures 2-29 and 2-30, respectively) are similar, and major features are comparable in extent, orientation, and location (Figures 2-29 and 2-30). Such features include the Keystone Heights potentiometric high, the Waccasassa Flats potentiometric high, the Mallory Swamp potentiometric high, the Valdosta potentiometric high, the zone of high horizontal gradient across the Gulf Trough, the area of low horizontal gradient within the Silver and Rainbow springsheds, and pumping induced cones of depression at Fernandina Beach, Florida, and St. Marys (in 2001), Brunswick, and Savannah, Georgia.

Residuals of Vertical Head Differences between Layers 3 and 5

The maps of the residuals of vertical head differences between Layers 3 and 5 frequently reflect the ability of the model to represent the degree of confinement provided by the middle confining unit. The observed values of vertical head differences between Layers 3 and 5 are generally small (less than a few feet), as are corresponding simulated values. Thus, both sets of values are consistent with a generally leaky middle confining unit (Figures 4-31 and 4-32; Appendix B).

Observed versus Simulated Vertical Head Differences between Layers 3 and 5

Scatter plots of observed versus simulated vertical head differences between Layers 3 and 5 are shown on Figures 4-33 and 4-34, and a listing of vertical head differences between Layers 3 and 5 is provided in Appendix B. As noted on the plots, observations with assigned weights below the minimum value shown on the plots were not represented.

Groundwater Level Residuals of Layer 5

The residuals of groundwater levels of Layer 5 are concentrated along the Atlantic coastal region, where most Lower Floridan aquifer monitoring wells are located. Residuals in Duval and St. Johns counties indicate a trend of under simulation of observed groundwater levels, more so in the 2001 results than the 2009 results (Figures 4-35 and 4-36; Appendix A). Most matches throughout the domain are within 10 feet in the 2001 simulation and 5 feet in the 2009 simulation.

Observed versus Simulated Groundwater Levels of Layer 5

The scatter plots of observed versus simulated groundwater levels of Layer 5 are shown in Figures 4-37 and 4-38. More scatter is seen in these plots than in the corresponding plots of Layer 3. As noted on the plots, observations with assigned weights below the minimum value shown on the plots were not represented.

Simulated Potentiometric Surface of Layer 5

The simulated water levels of Layer 5 represent the simulated potentiometric surface of Zone 3 (see Chapter 2 for definitions of Zones 1, 2, and 3). This surface resembles closely that of Layer 3 (Figures 4-39 and 4-40).

Flows

The CRF group is a set of maps and graphs that provide comparisons of observed versus corresponding simulated flows. These include graphs of observed versus simulated spring discharge and estimated versus simulated baseflow rates. The CRF group also includes maps of simulated net recharge rates and simulated downward leakage rates to Layer 3 and upward leakage rates from Layer 3.

First Magnitude Springs and Spring Groups

Maps of observed spring flows for first magnitude springs and spring groups with corresponding flow residuals (differences between observed and simulated flow rates) were created for the 2001 and 2009 simulations (Figures 4-41 and 4-42). These are springs and spring groups with average flows of 100 cfs or more. Comparisons of simulated versus estimated flow of several first magnitude springs and spring groups are also provided in Tables 4-7 and 4-8.

Observed versus Simulated Spring Flows

Plots of observed versus simulated spring flows for 2001 and 2009 are shown in Figures 4-43 and 4-44. Comparisons of simulated versus estimated flow of springs and other information are provided in Appendix E. Percent differences of simulated versus estimated spring flows of springs with estimated flows of 10 cfs or more are provided in Appendix N.

Observed versus Simulated Spring Group Flows

Spring groups are collections of springs associated with a given river reach. Spring group flow is the combined flow of all springs that constitute a spring group. Spring groups in the NFSEG model include the Crystal River, Silver River, Wacissa River, Ichetucknee River, and Lower Santa Fe River spring groups. The flows of these spring groups are relatively large, so matching them closely in the calibration process was considered important. Plots of observed versus simulated spring group flows for 2001 and 2009 are shown in Figures 4-45 and 4-46. These plots show close matches between the estimated and simulated spring group flows, as shown by R square values of 1.0 in both the 2001 and 2009 calibrations.

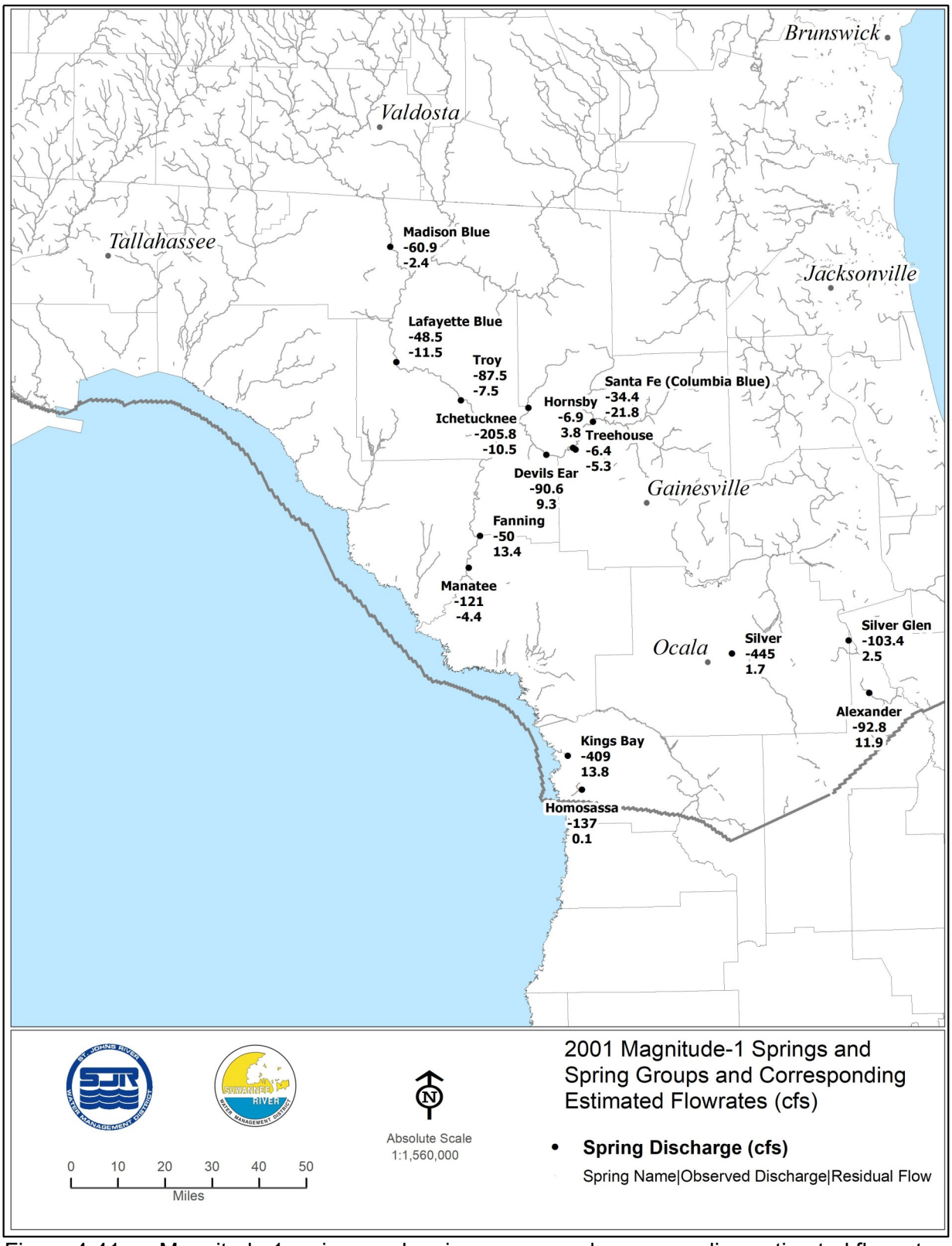

Figure 4-41. Magnitude 1 springs and spring groups and corresponding estimated flowrates and flowrate residuals (cfs), 2001 (sign convention for flows is consistent with that of MODFLOW: negative flows are *from* the aquifer; positive flows are *into* the aquifer.)

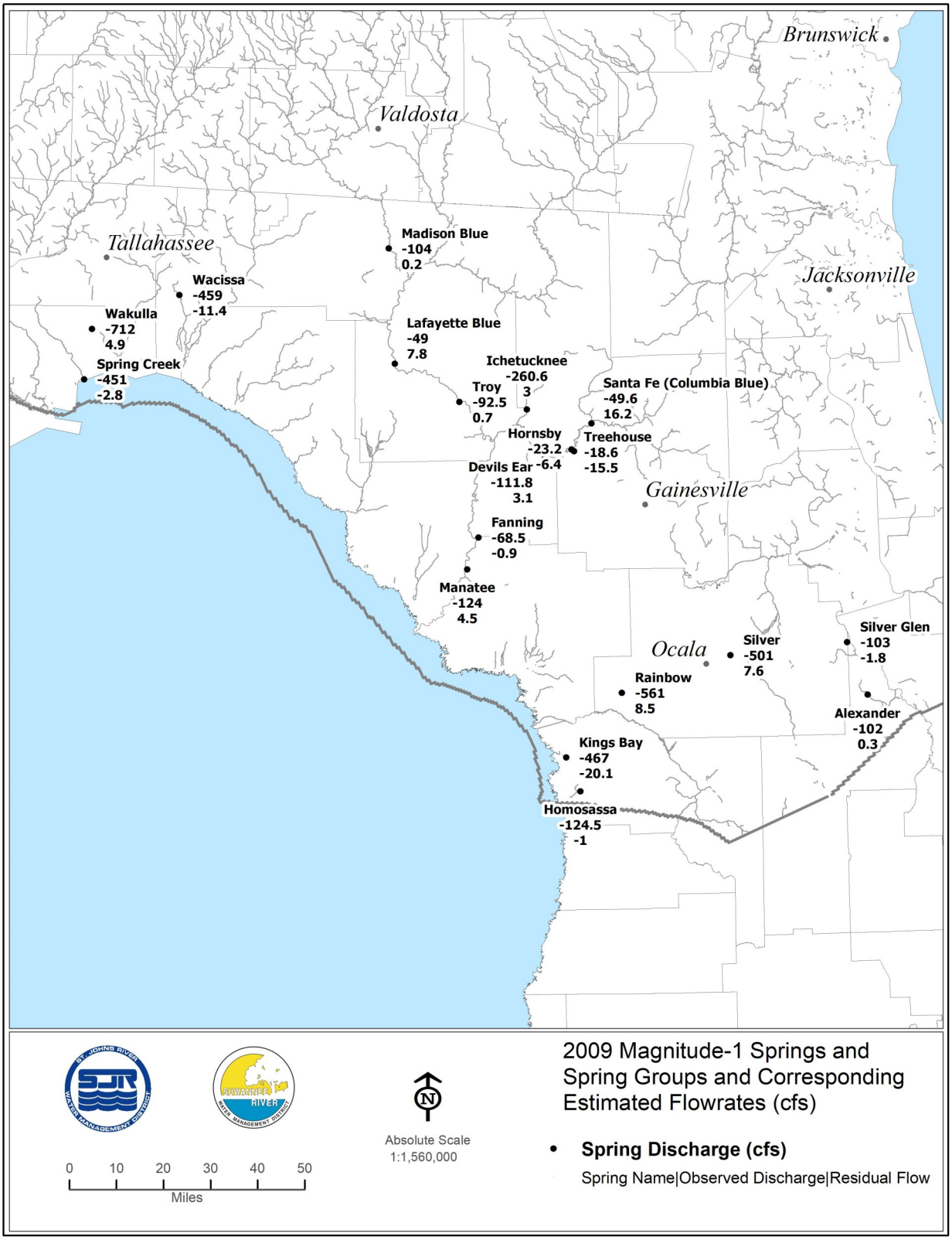

Figure 4-42. Magnitude 1 springs and spring groups and corresponding estimated flowrates and flowrate residuals (cfs), 2009 (sign convention for flows is consistent with that of MOD-FLOW: negative flows are *from* the aquifer; positive flows are *into* the aquifer.)

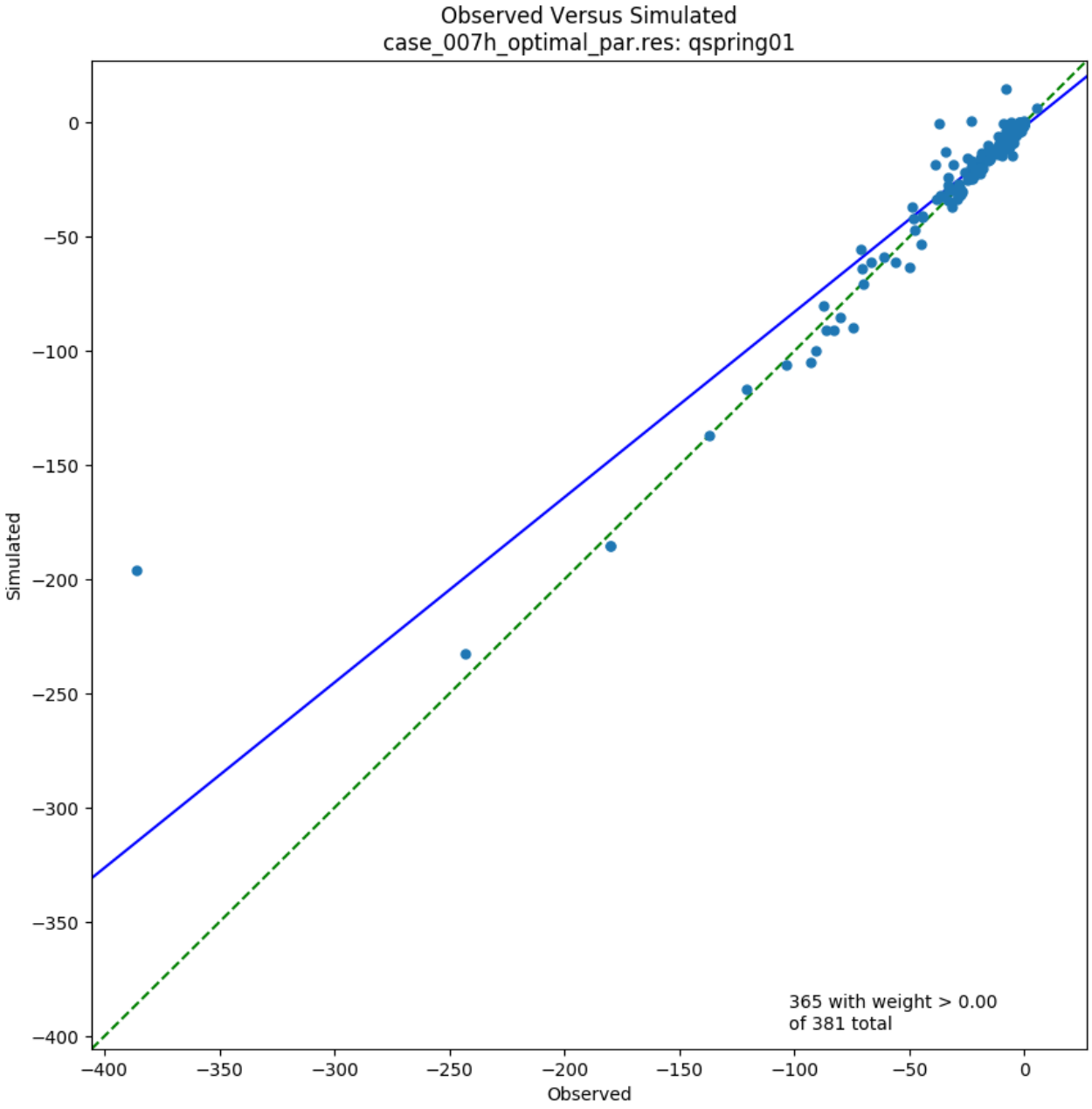

Figure 4-43. Observed vs. simulated spring discharges (cfs), 2001 (sign convention for flows is consistent with that of MODFLOW: negative flows are *from* the aquifer; positive flows are *into* the aquifer.)

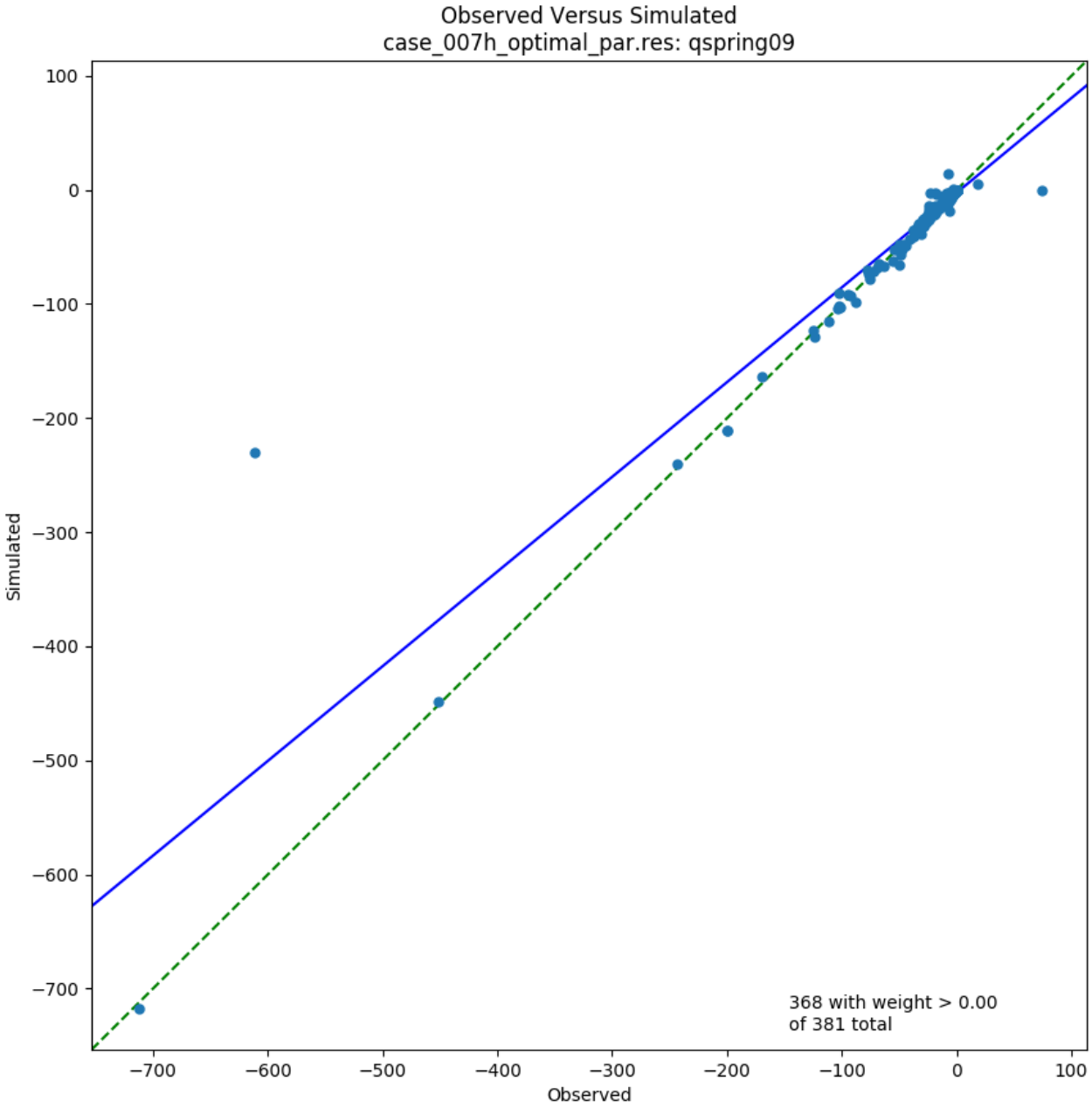

Figure 4-44. Observed vs. simulated spring discharges (cfs), 2009 (sign convention for flows is consistent with that of MODFLOW: negative flows are *from* the aquifer; positive flows are *into* the aquifer.)

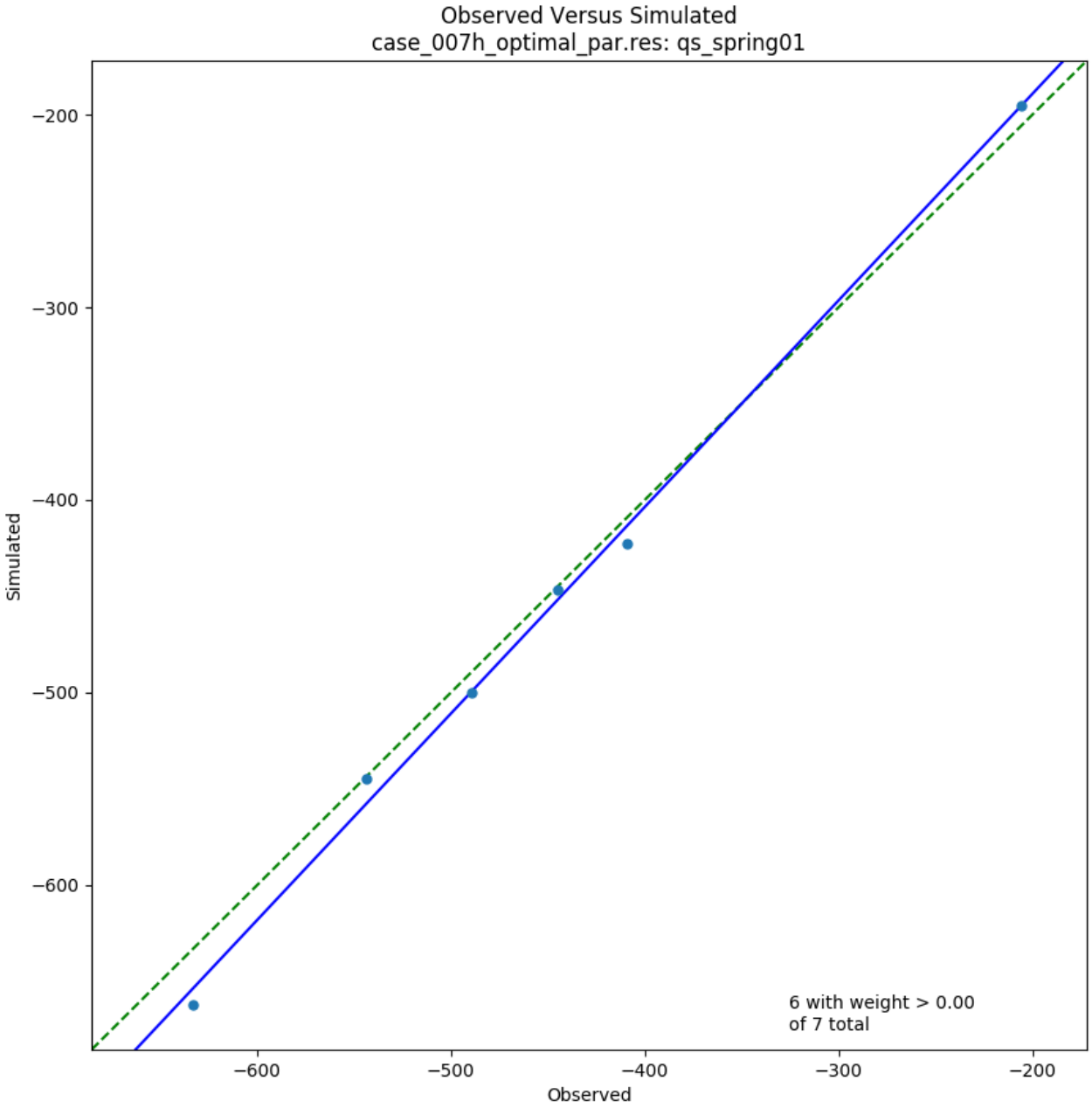

Figure 4-45. Observed vs. simulated spring-group discharges (cfs), 2001 (sign convention for flows is consistent with that of MODFLOW: negative flows are *from* the aquifer; positive flows are *into* the aquifer.)

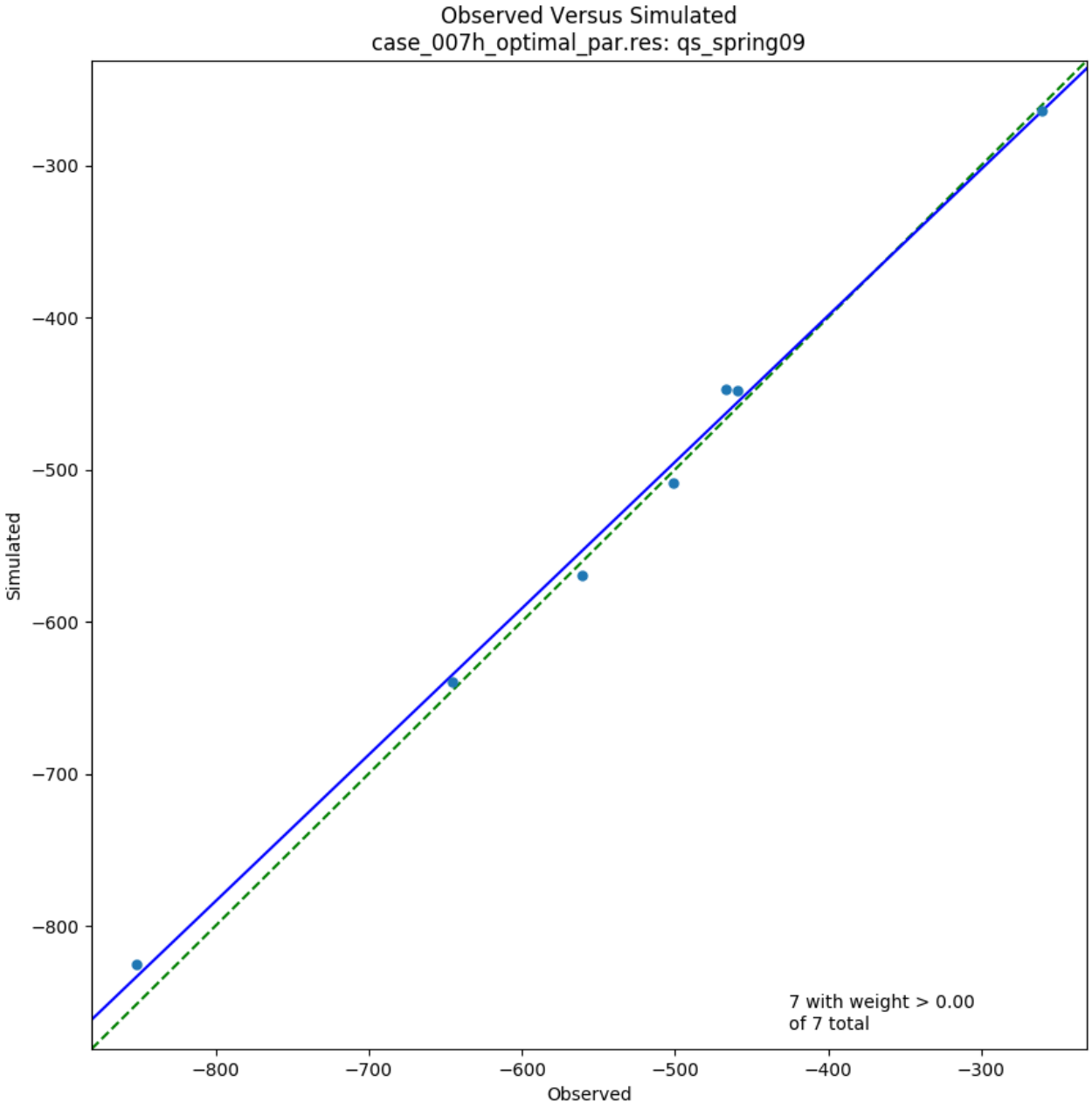

Figure 4-46. Observed vs. simulated spring-group discharges (cfs), 2009 (sign convention for flows is consistent with that of MODFLOW: negative flows are *from* the aquifer; positive flows are *into* the aquifer.)

Table 4-7. Comparisons of simulated versus estimated spring flows of selected first-magnitude springs and spring groups, 2001

Important first magnitude springs and spring groups	Water Management District	Estimated Discharge (cfs)	Simulated Discharge (cfs)	Residual Discharge (cfs)	Percent Error
Wacissa Springs Group	SR	N/A	N/A	N/A	N/A
Ichetucknee Springs Group	SR	206	195	11	5%
Crystal River Springs Group	SWF	409	423	-14	3%
Rainbow Springs	SWF	543	544	-1	0%
Springs on the Santa Fe River between Worthington Springs and Fort White	SR	489	501	-12	2%
Silver Springs Group	SJR	445	447	-2	0%
Lower Santa Fe Springs Group	SR	633	662	-29	5%
Wakulla Spring Main Vent	NWF	N/A	N/A	N/A	N/A
Wacissa Head Spring	SR	94	87	8	8%
Madison Blue Spring	SR	61	59	2	4%
Alexander Spring	SJR	93	105	-12	13%
Silver Glen Spring	SJR	103	106	-3	2%
St. Marks River Rise	NWF	386	196	196	51%
Spring Creek Springs Group	NWF	N/A	N/A	N/A	N/A

Table 4-8. Comparisons of simulated versus estimated spring flows of selected first-magnitude springs and spring groups, 2009

Important first magnitude springs and spring groups	Water Management District	Estimated Discharge (cfs)	Simulated Discharge (cfs)	Residual Discharge (cfs)	Percent Error
Wacissa Springs Group	SR	459	448	11	2%
Ichetucknee Springs Group	SR	260	264	-4	1%
Crystal River Springs Group	SWF	467	447	20	4%
Rainbow Springs	SWF	561	570	-9	2%
Springs on the Santa Fe River between Worthington Springs and Fort White	SR	645	640	-5	1%
Silver Springs Group	SJR	501	509	-8	2%
Lower Santa Fe Springs Group	SR	851	826	25	3%
Wakulla Spring Main Vent	NWF	712	717	-5	1%
Wacissa Head Spring	SR	170	164	6	4%
Madison Blue Spring	SR	104	104	0	0%
Alexander Spring	SJR	102	102	0	0%
Silver Glen Spring	SJR	103	101	2	2%
St. Marks River Rise	NWF	612	230	382	62%
Spring Creek Springs Group	NWF	451	448	3	1%

Baseflows

As detailed in Chapter 2, the baseflow estimates were derived from applications of baseflow separation techniques, with exceptions for reaches along certain rivers. Therefore, more uncertainty exists regarding these estimates than for the other members of the flow observation groups. Potential errors in baseflow estimates may be an important contributing factor in poor comparisons between estimated and simulated values. Additional discussion and interpretation of the comparisons between simulated baseflows and corresponding baseflow targets are provided below in the section entitled "Additional Discussion."

Maps of estimated baseflow pickup rates and corresponding residuals for 2001 and 2009 are shown in Figures 4-47 through 4-52 and are listed in Appendix F. Scatter plots of baseflow pickup rates are shown in Figures 4-53 and 4-54._Maps of cumulative baseflow rates and corresponding residuals for 2001 and 2009 are shown in Figures 4-55 and 4-56. Scatter plots of estimated versus simulated cumulative baseflow rates for 2001 and 2009 are shown in Figures 4-57 and 4-58.

Simulated Net Recharge Rates

Maps of net recharge rates (differences between inflow rates specified in the MODFLOW recharge package and simulated rates of evapotranspiration) are shown in Figures 4-59 and 4-60. Simulated net recharge rates are generally higher in areas in which the depth to water table is greater and where runoff is less due to greater internal drainage. Simulated rates are generally lower in areas in which evapotranspiration rates are relatively high due to the presence of a shallow water table. The range of simulated net recharge rates is similar to that of Bush and Johnston (1988).

Simulated Downward Leakage Rates of Layer 2 to 3

Maps of simulated downward leakage rates from Layer 2 to 3 for 2001 and 2009 show wide expanses within the model domain of downward leakage into the Upper Floridan aquifer (Figures 4-61 and 4-62). In most of the model domain, simulated rates are less than 5 inches/year (in/yr). In unconfined regions, simulated rates are generally higher, ranging in many areas from 10 to 50 in/yr.

Simulated Upward Leakage Rates of Layer 3 to 2

Maps of simulated upward leakage rates from Layer 3 to 2 for 2001 and 2009 show extensive areas of discharge from the Upper Floridan aquifer (Figures 4-63 and 4-64). Discharge areas are concentrated along the coasts of the Gulf of Mexico and the Atlantic Ocean, except in areas surrounding Savannah, Georgia, where drawdowns due to groundwater withdrawals have reversed the natural upward vertical gradient between the surficial aquifer system and Upper Floridan aquifer. Simulated discharge areas also occur along some river corridors, particularly in unconfined areas.

Simulated Downward Leakage Rates of Layer 4 to 5

Maps of simulated downward leakage rates from Layer 4 to 5 for 2001 and 2009 show downward leakage into Layer 5 (Figure 4-65 and 4-66) within a large proportion of the overall area. The patterns of downward leakage are much more complex than corresponding 2001 and 2009 patterns from Layer 2 to Layer 3. The highest rates of downward leakage generally occur in the unconfined zones of the Upper Floridan aquifer.

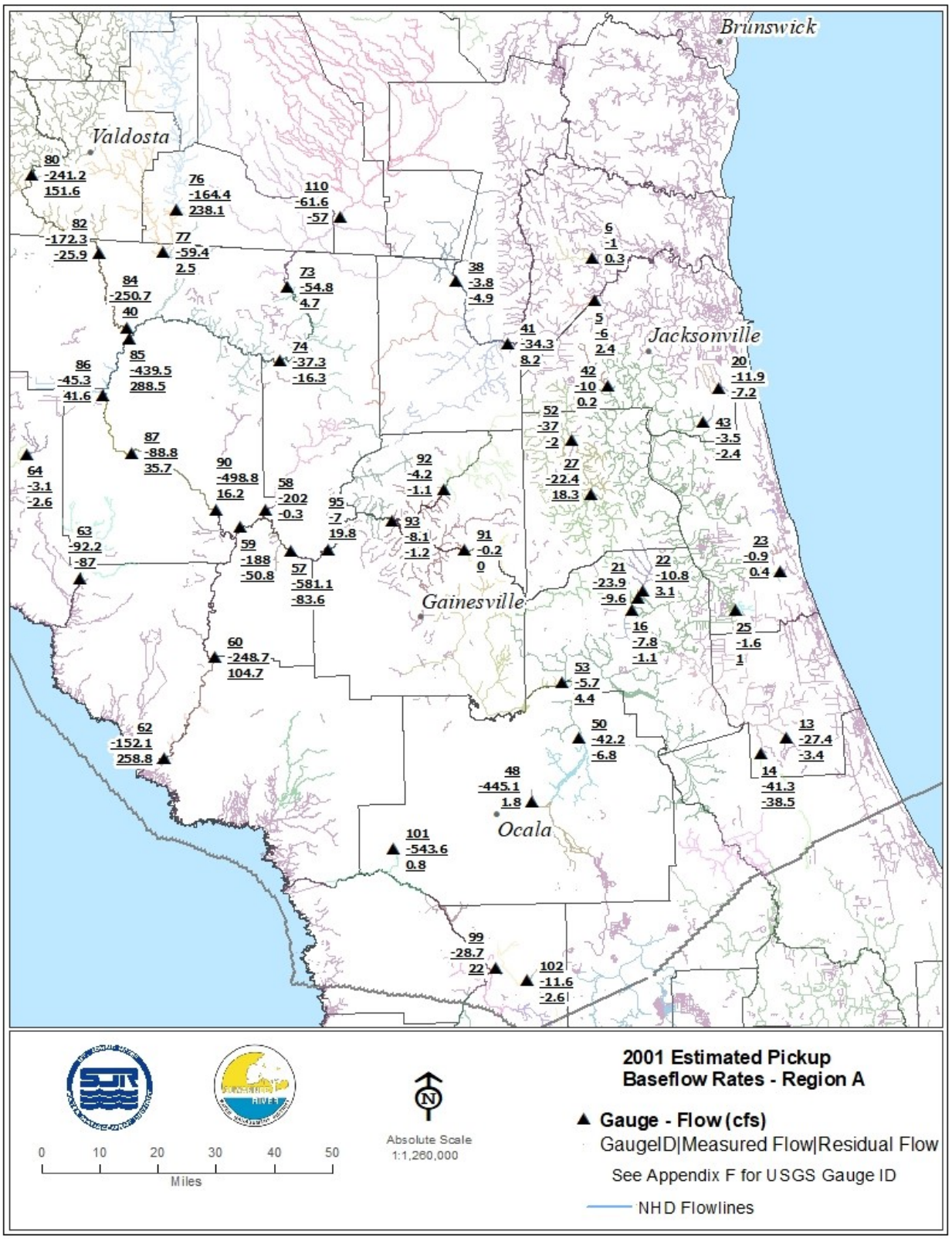

Figure 4-47. Estimated baseflow pickup residuals (cfs), Region A, 2001 (sign convention for flows is consistent with that of MODFLOW: negative flows are *from* the aquifer; positive flows are *into* the aquifer.)

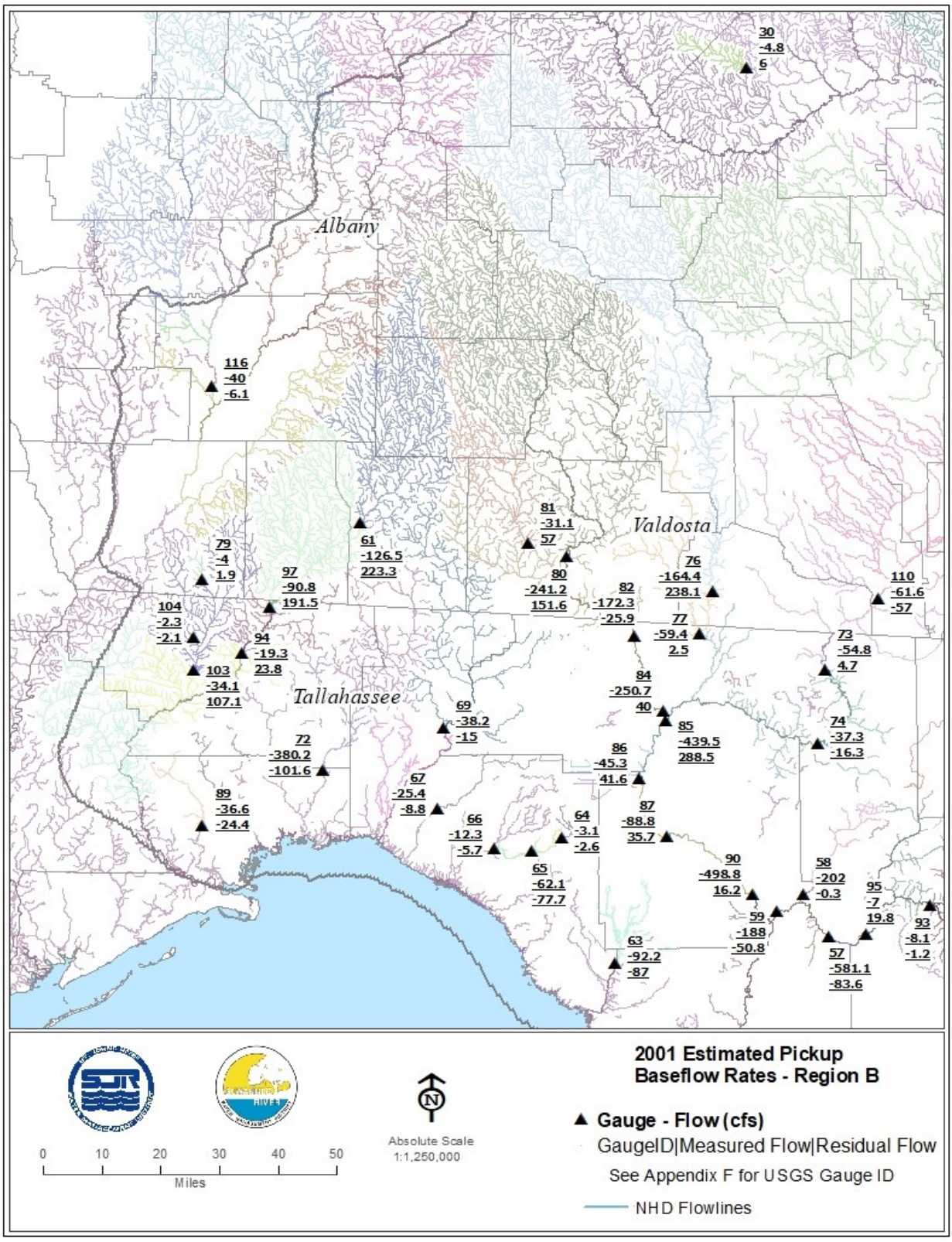

Figure 4-48. Estimated baseflow pickup residuals (cfs), Region B, 2001 (sign convention for flows is consistent with that of MODFLOW: negative flows are *from* the aquifer; positive flows are *into* the aquifer.)

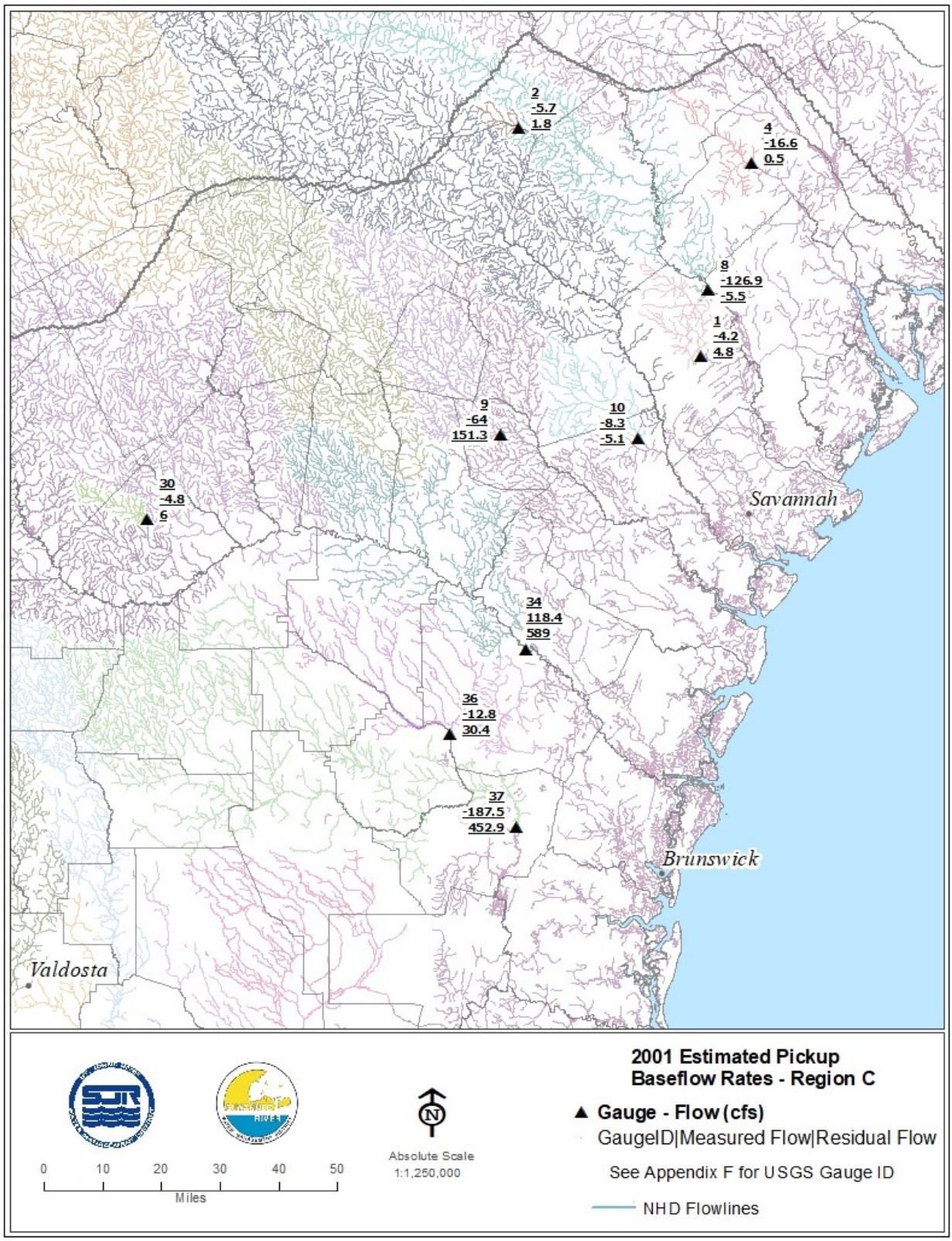

Figure 4-49. Estimated baseflow pickup residuals (cfs), Region C, 2001 (sign convention for flows is consistent with that of MODFLOW: negative flows are *from* the aquifer; positive flows are *into* the aquifer.)

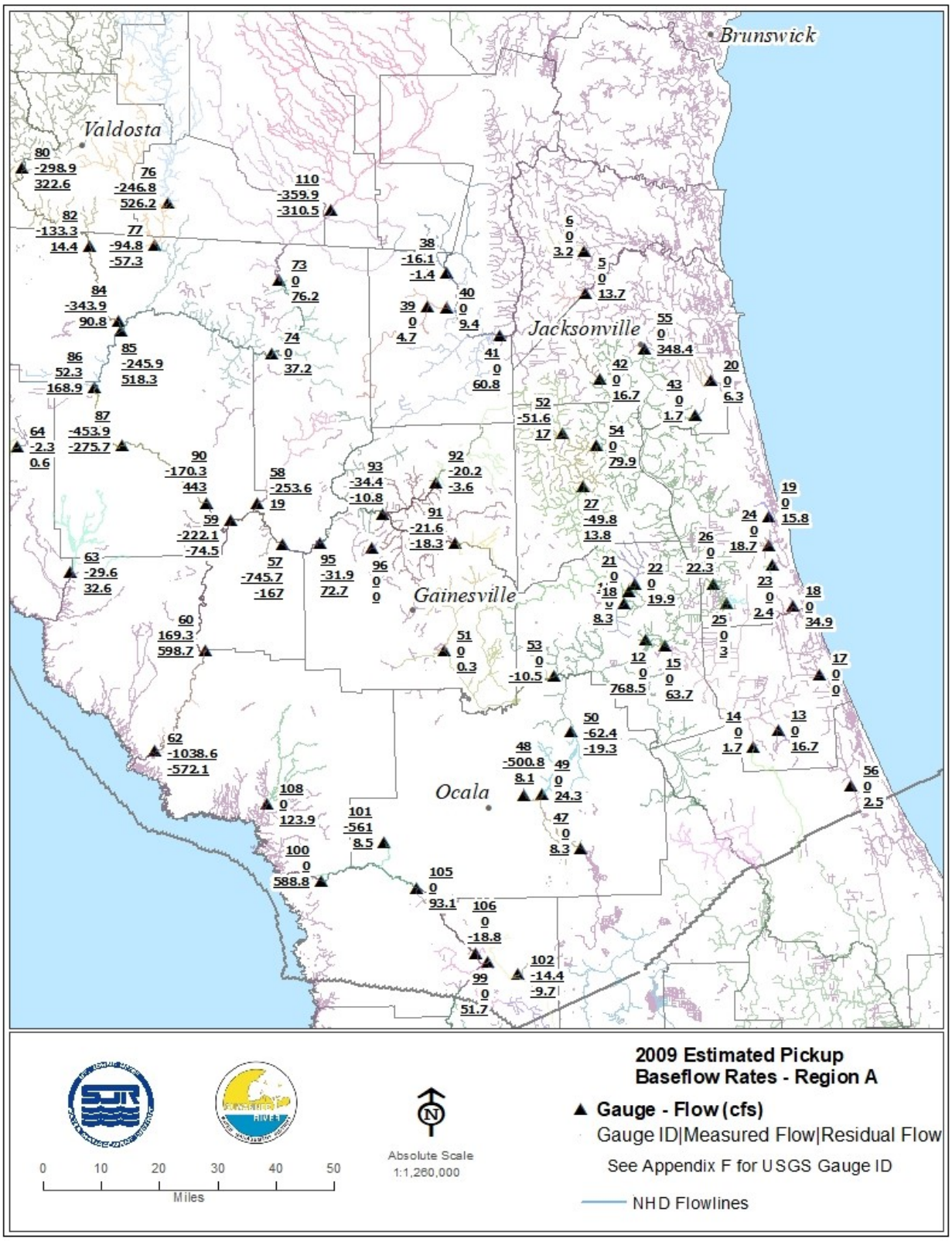

Figure 4-50. Estimated baseflow pickup residuals (cfs), Region A, 2009 (sign convention for flows is consistent with that of MODFLOW: negative flows are *from* the aquifer; positive flows are *into* the aquifer.)

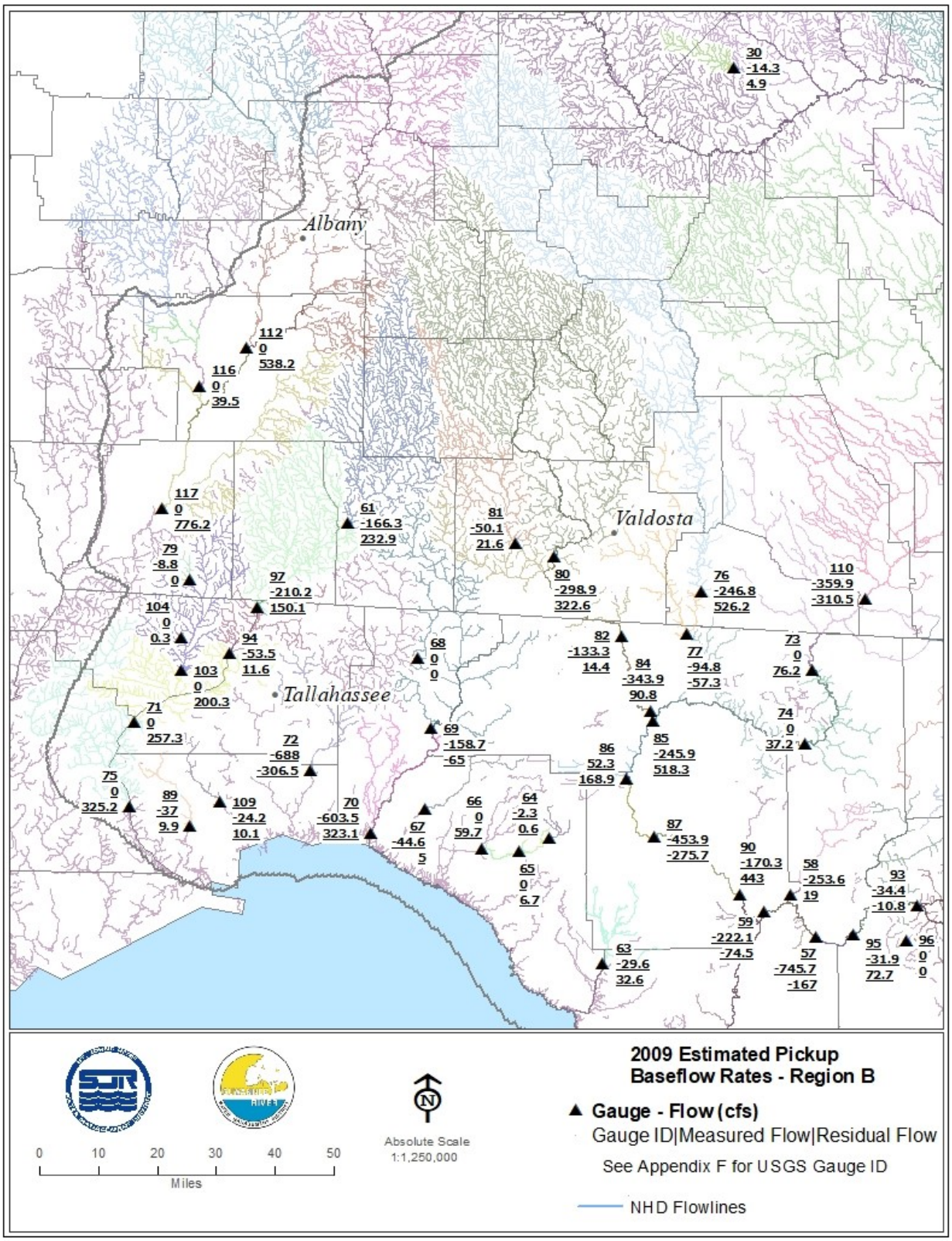

Figure 4-51. Estimated baseflow pickup residuals (cfs), Region B, 2009 (sign convention for flows is consistent with that of MODFLOW: negative flows are *from* the aquifer; positive flows are *into* the aquifer.)

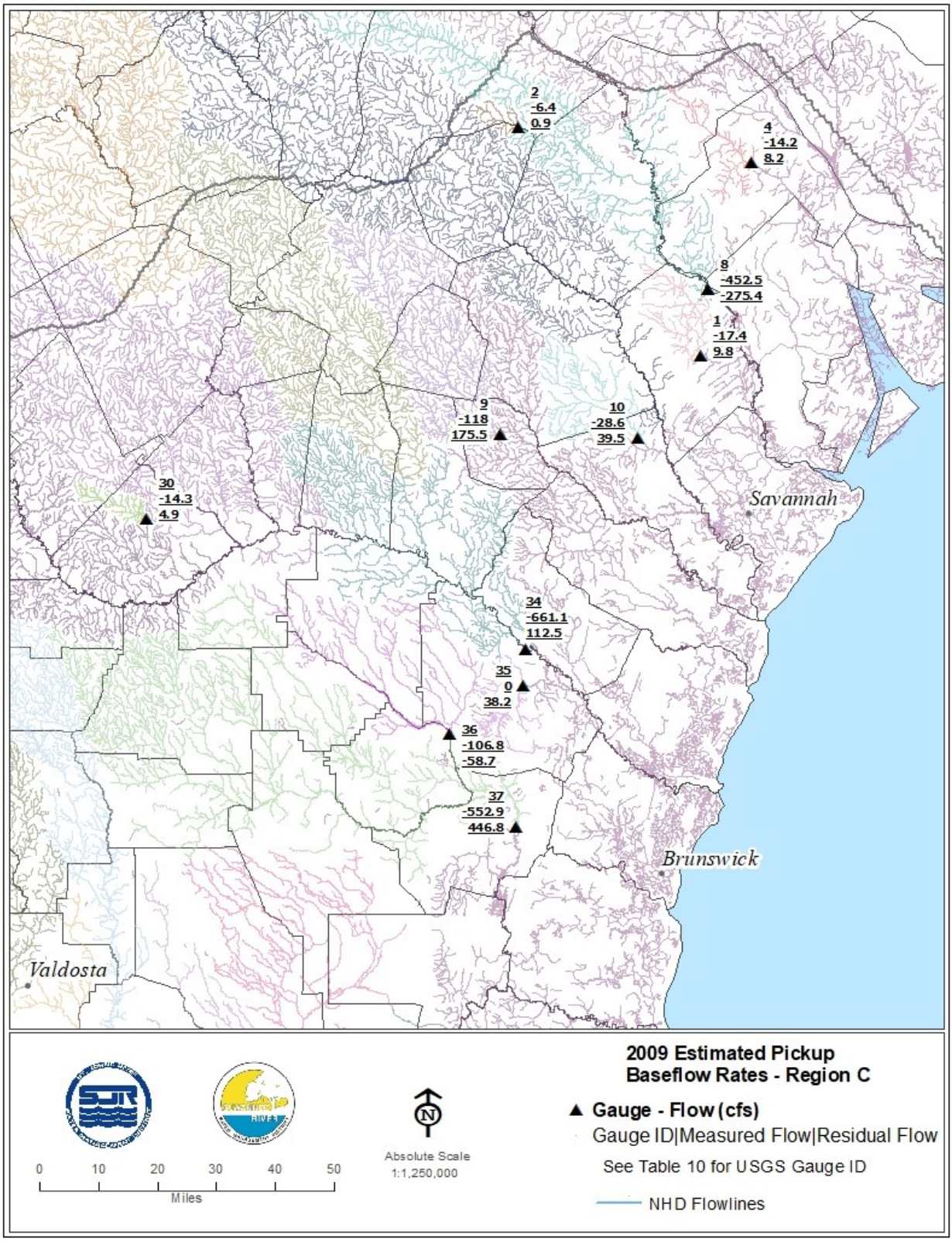

Figure 4-52. Estimated baseflow pickup residuals (cfs), Region C, 2009 (sign convention for flows is consistent with that of MODFLOW: negative flows are *from* the aquifer; positive flows are *into* the aquifer.)

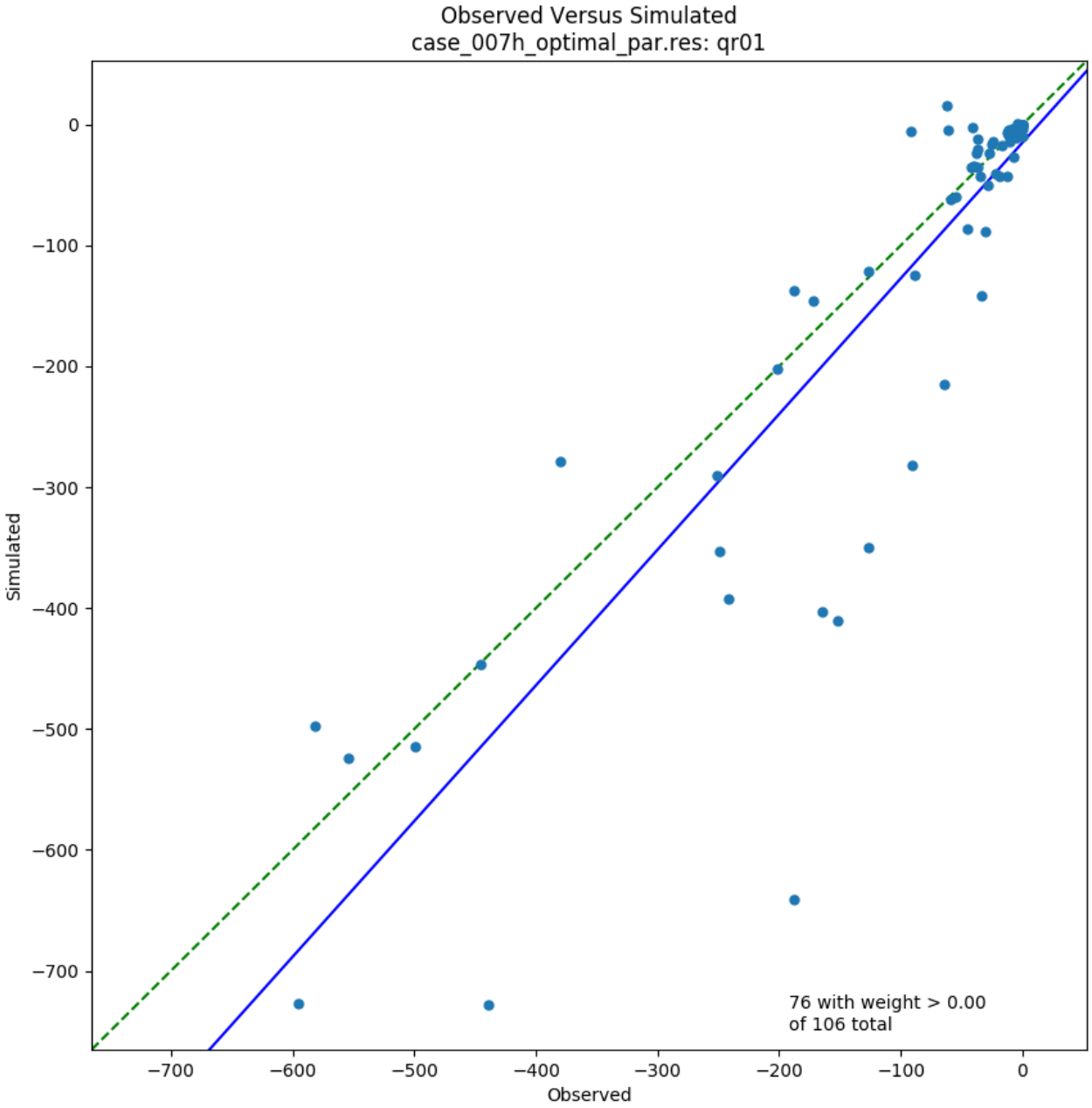

Figure 4-53. Estimated versus simulated baseflow pickups (cfs), 2001 (sign convention for flows is consistent with that of MODFLOW: negative flows are *from* the aquifer; positive flows are *into* the aquifer.)

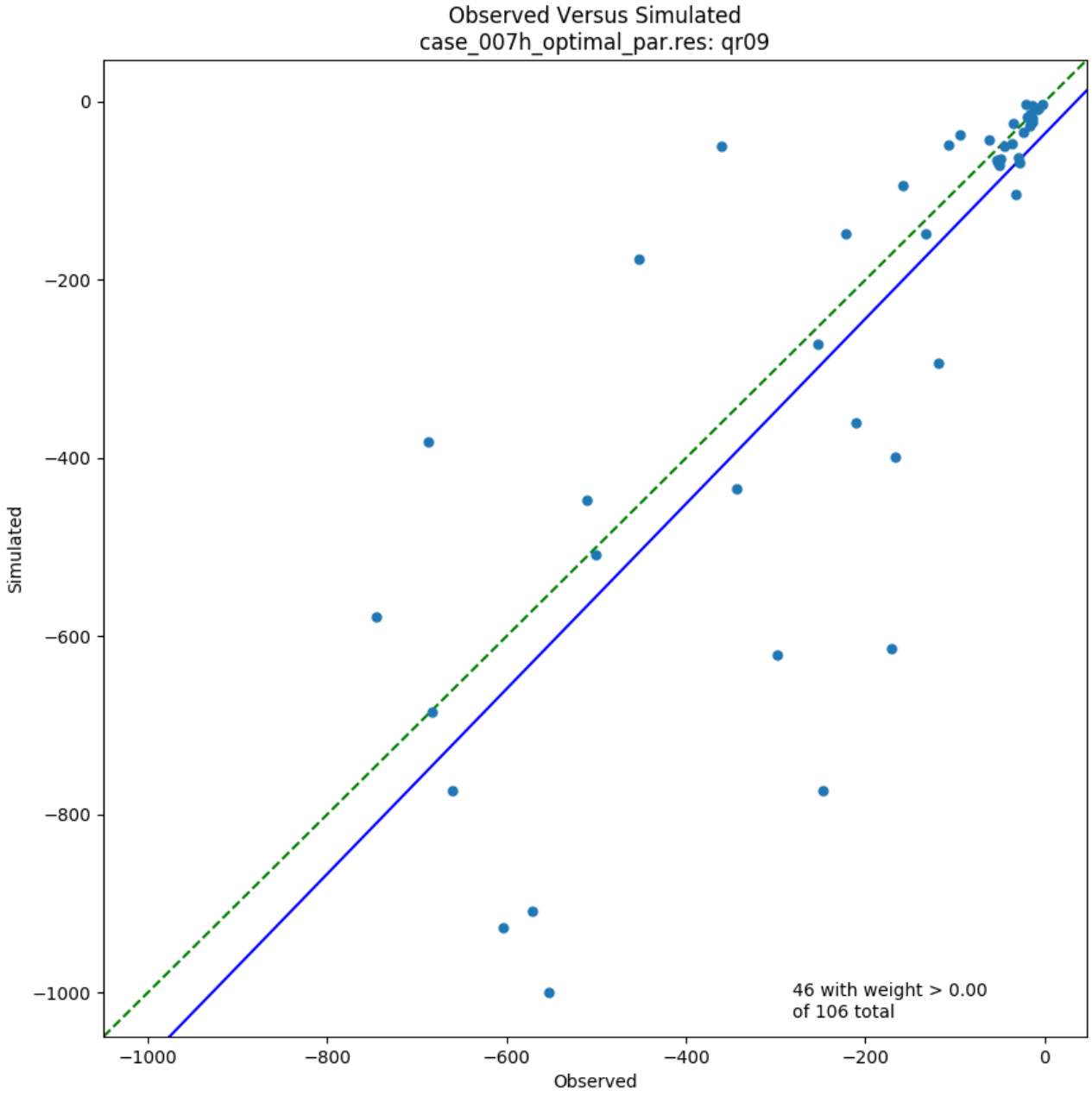

Figure 4-54. Estimated versus simulated baseflow pickups (cfs), 2009 (sign convention for flows is consistent with that of MODFLOW: negative flows are *from* the aquifer; positive flows are *into* the aquifer.)

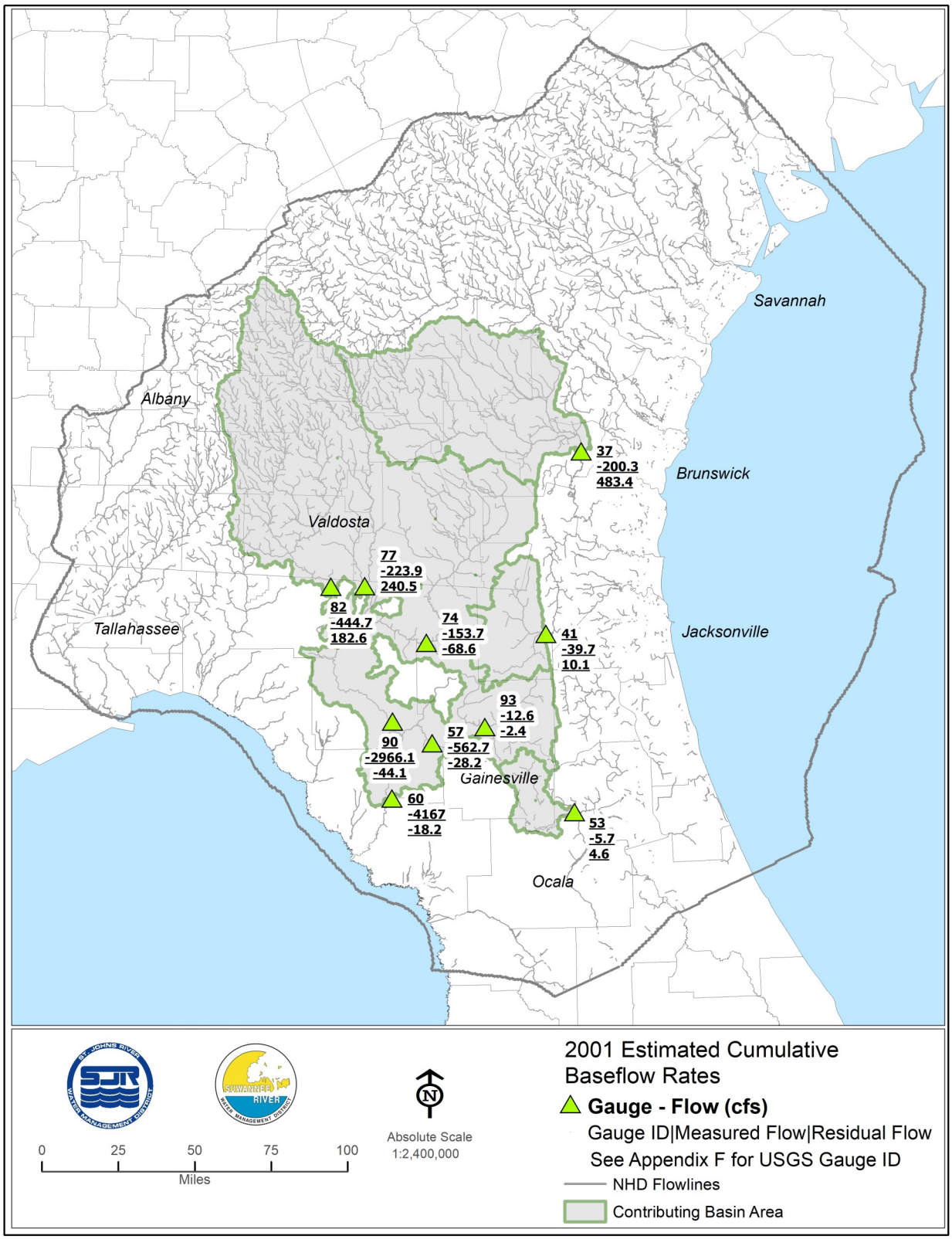

Figure 4-55. Cumulative baseflow residuals (cfs), 2001 (sign convention for flows is consistent with that of MODFLOW: negative flows are *from* the aquifer; positive flows are *into* the aquifer.)

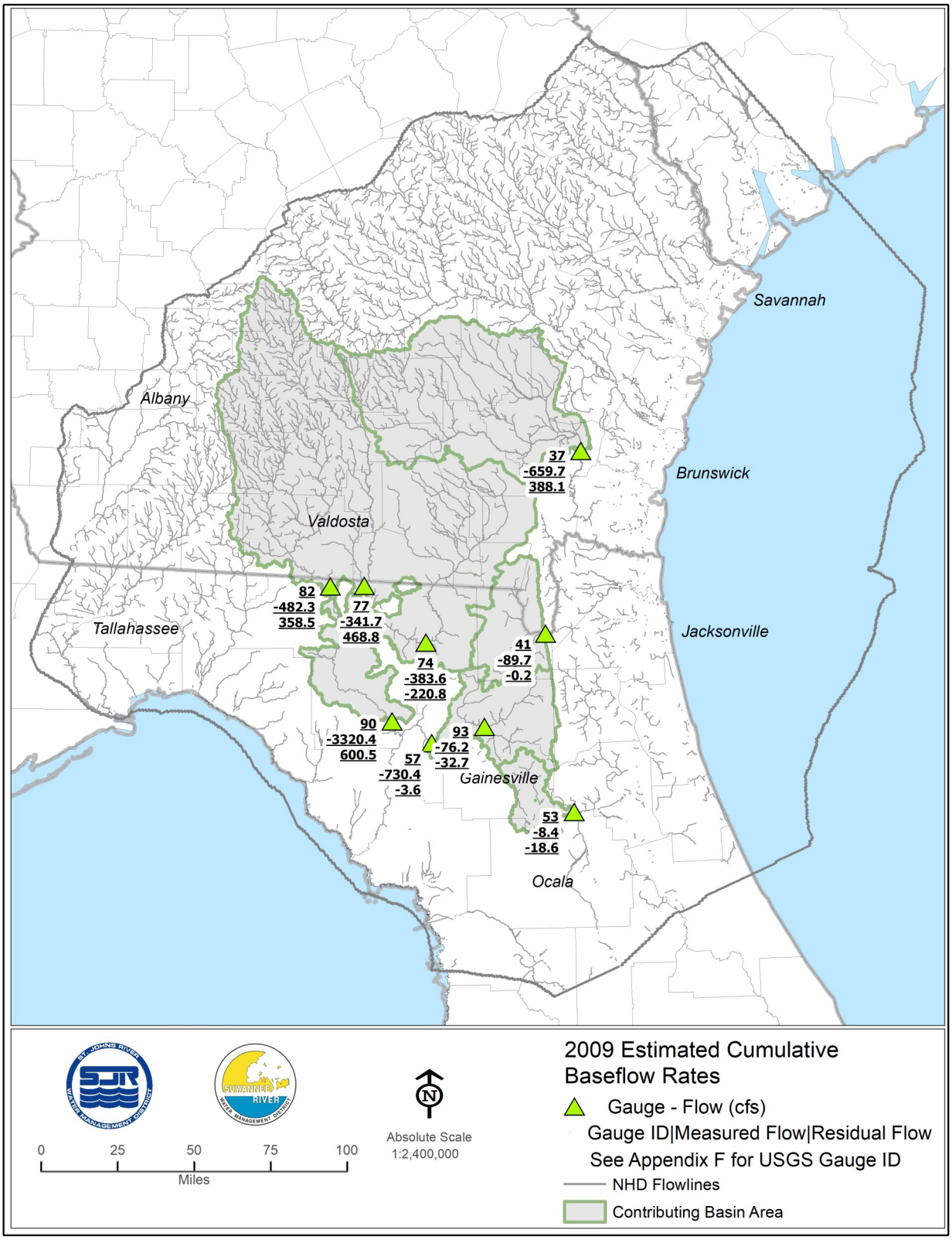

Figure 4-56. Estimated vs. simulated cumulative baseflows (cfs), 2009 (sign convention for flows is consistent with that of MODFLOW: negative flows are *from* the aquifer; positive flows are *into* the aquifer.)

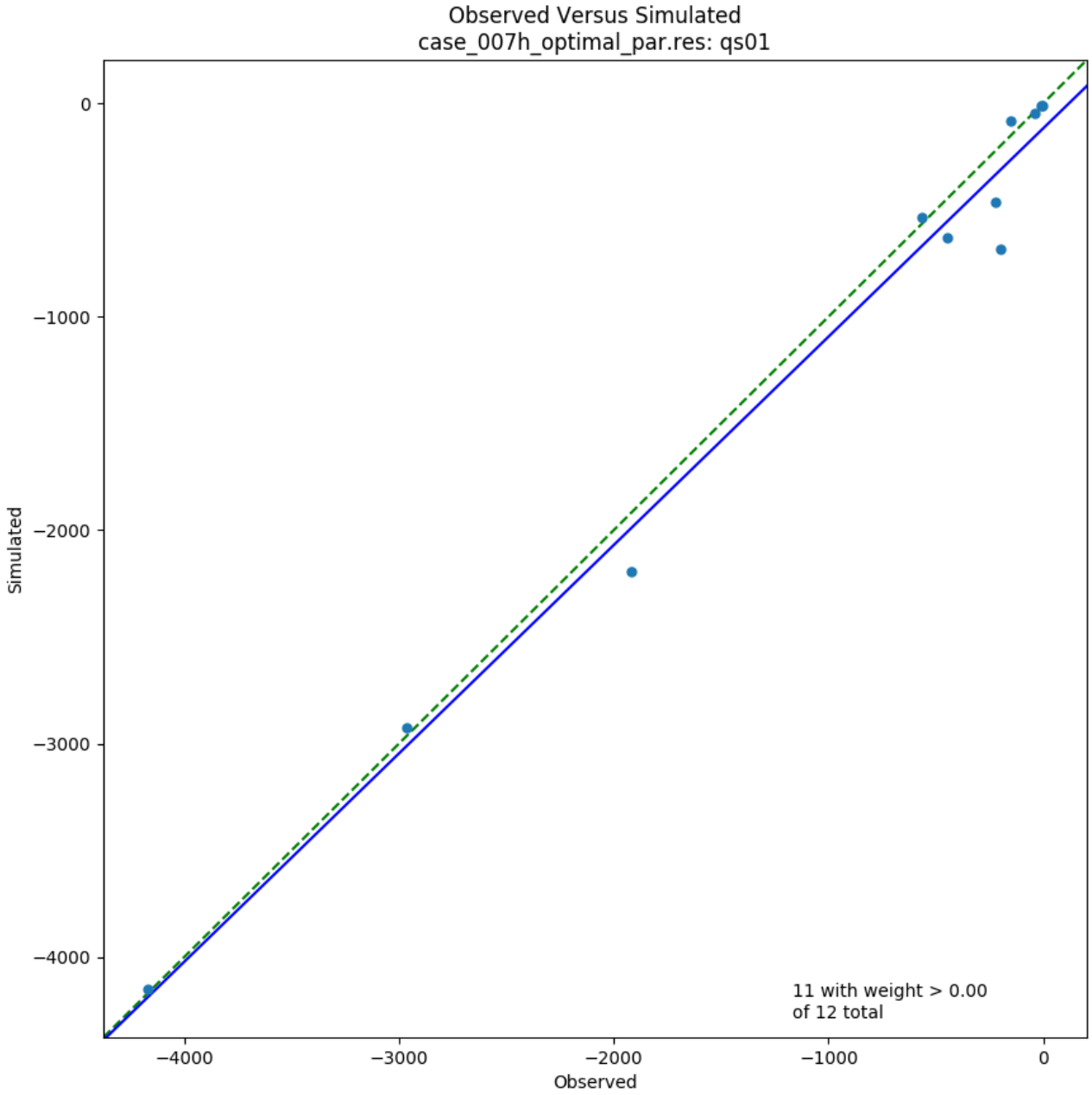

Figure 4-57. Estimated vs. simulated cumulative baseflows (cfs), 2001 (sign convention for flows is consistent with that of MODFLOW: negative flows are *from* the aquifer; positive flows are *into* the aquifer.)

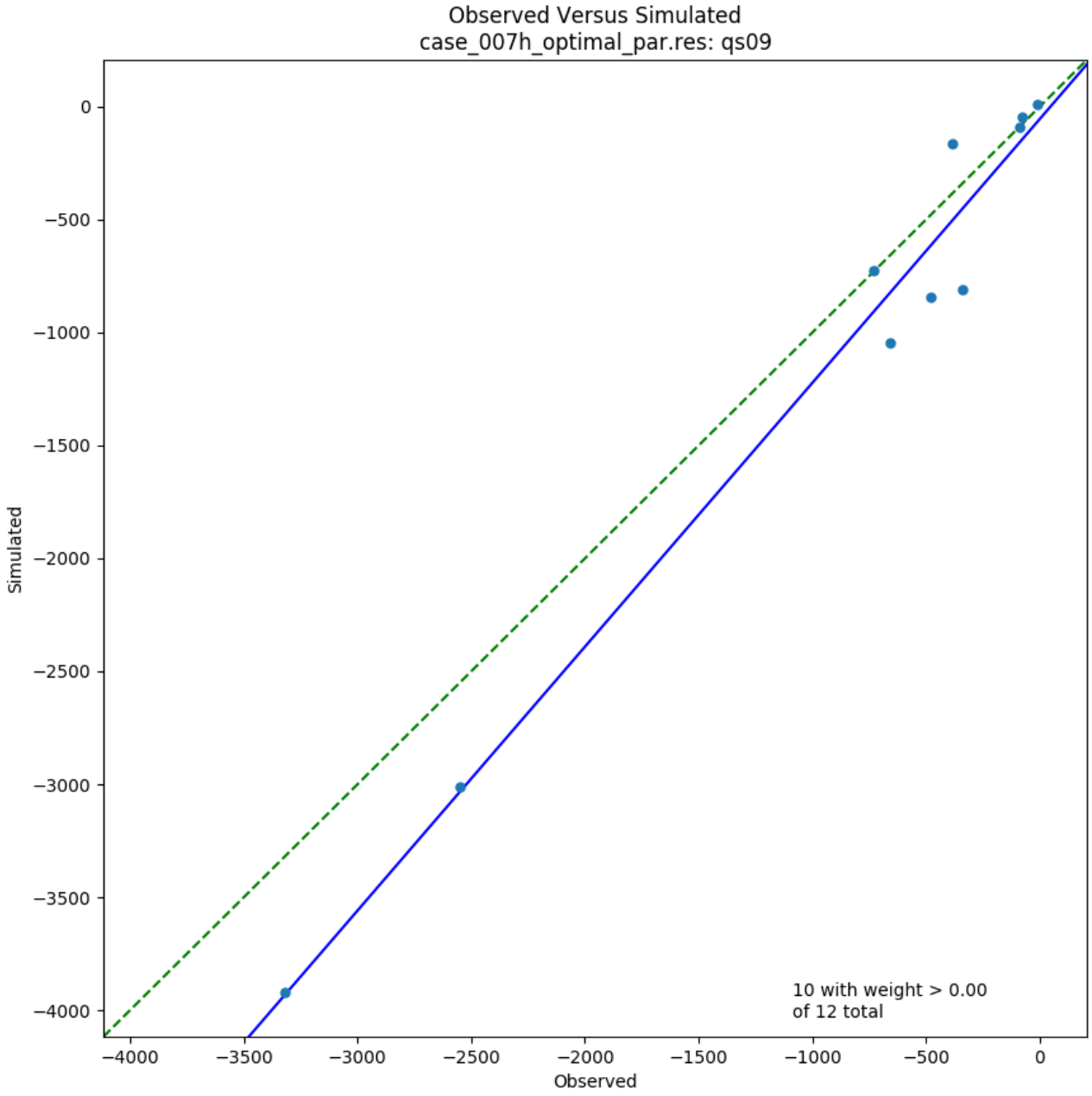

Figure 4-58. Estimated cumulative baseflow residuals (cfs), 2009 (sign convention for flows is consistent with that of MODFLOW: negative flows are *from* the aquifer; positive flows are *into* the aquifer.)

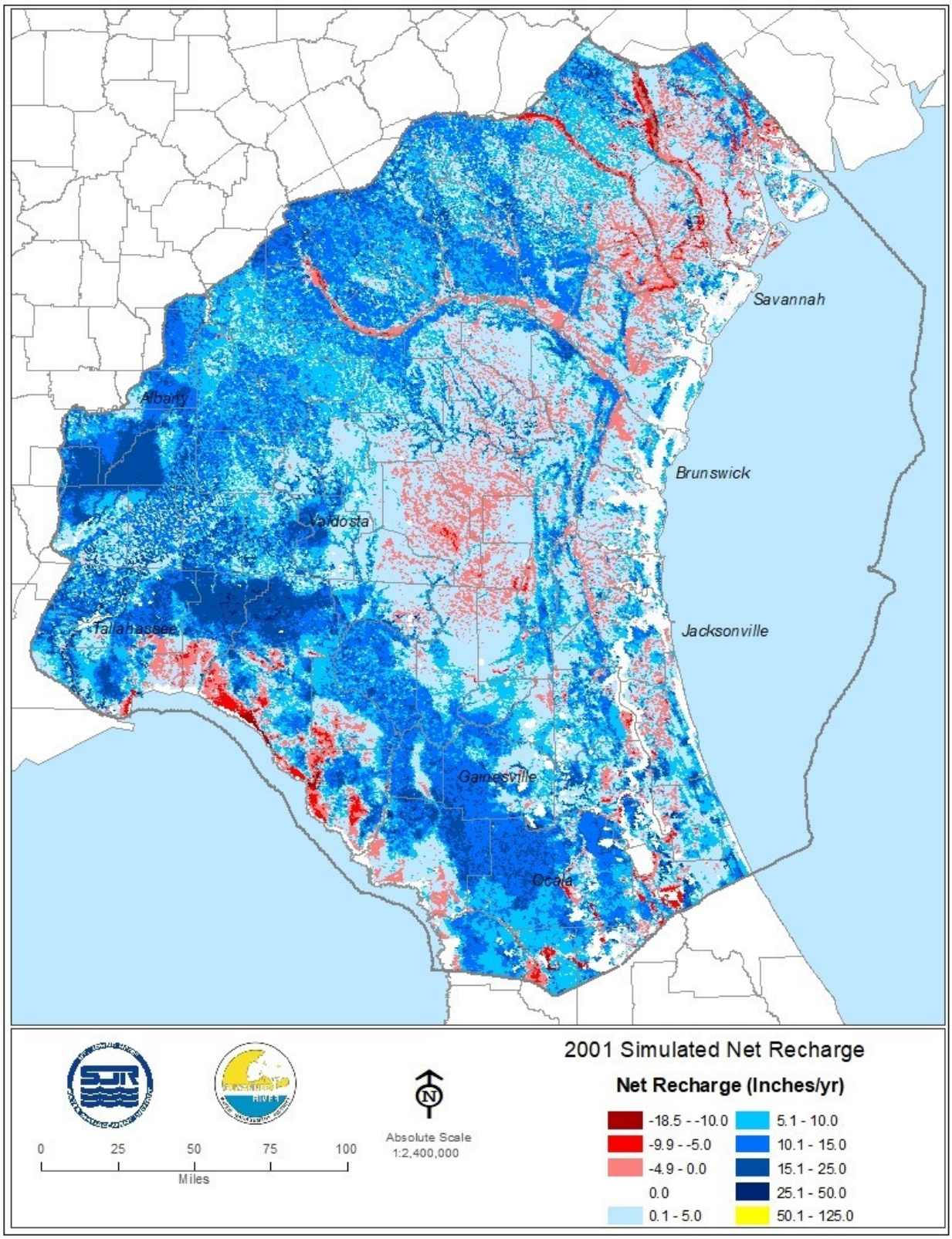

Figure 4-59. Simulated net recharge rates (inches/year), 2001

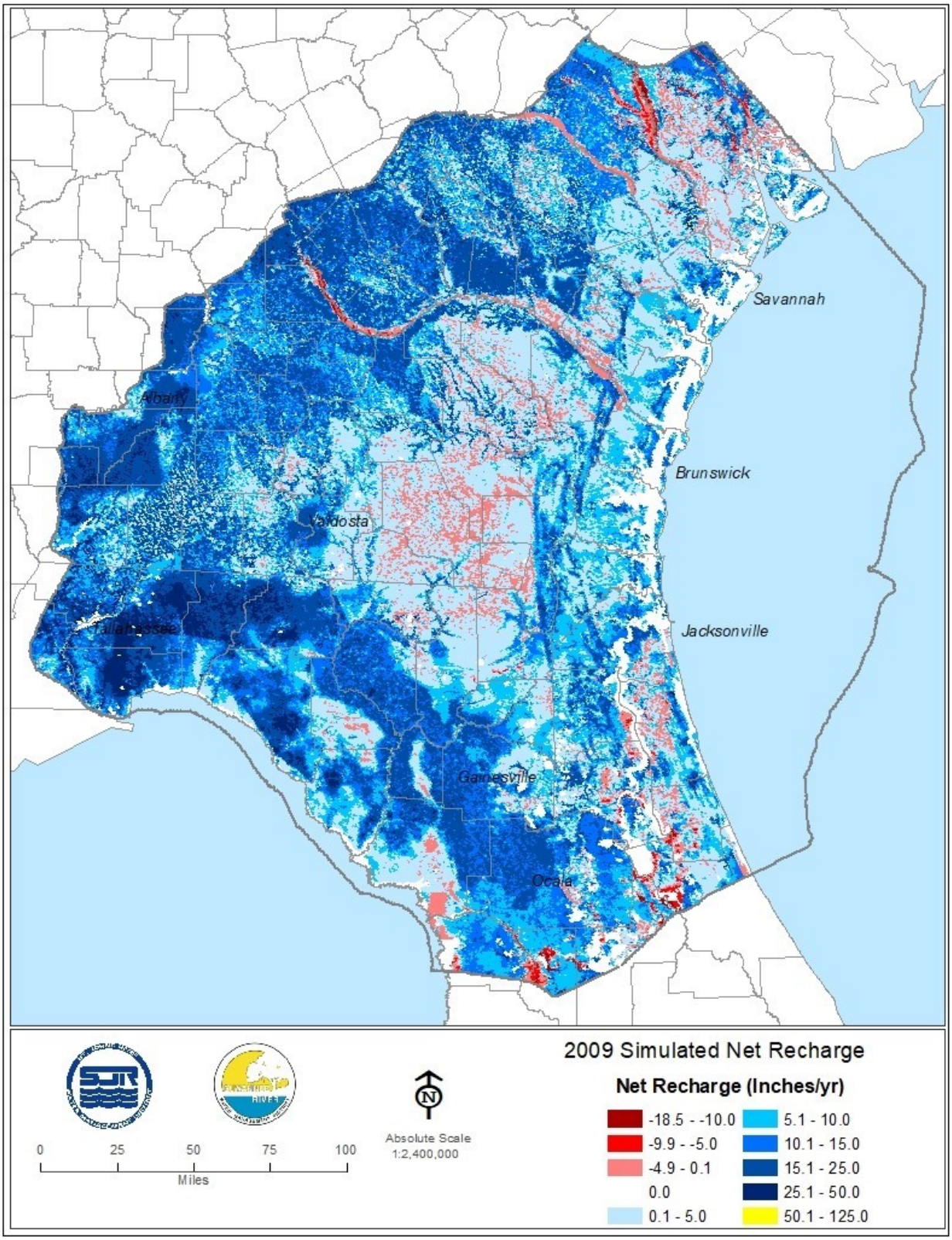

Figure 4-60. Simulated net recharge rates (inches/year), 2009

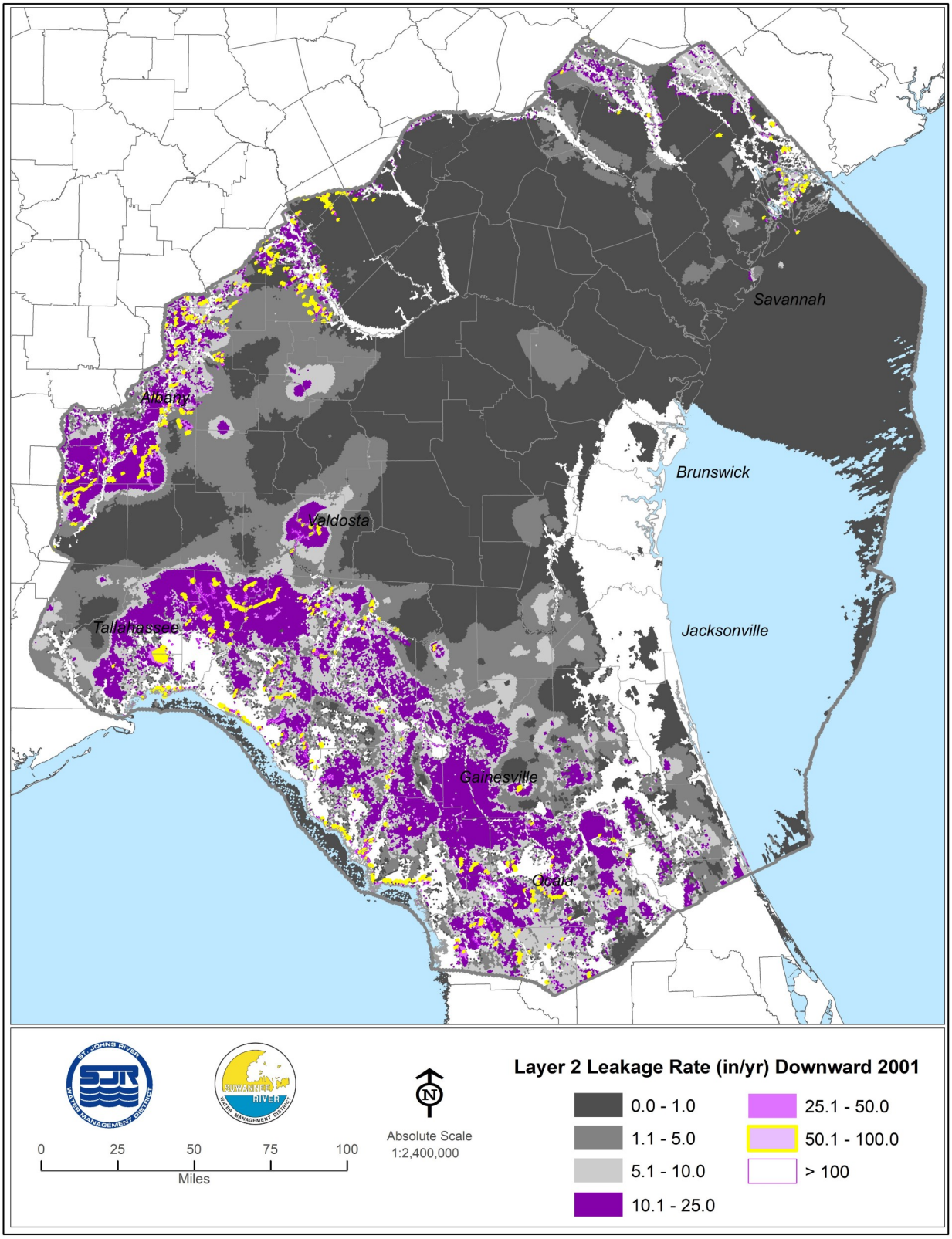

Figure 4-61. Flow through lower face, Layer 2, 2001 (downward leakage rate, Layer 2 to 3, inches/year)

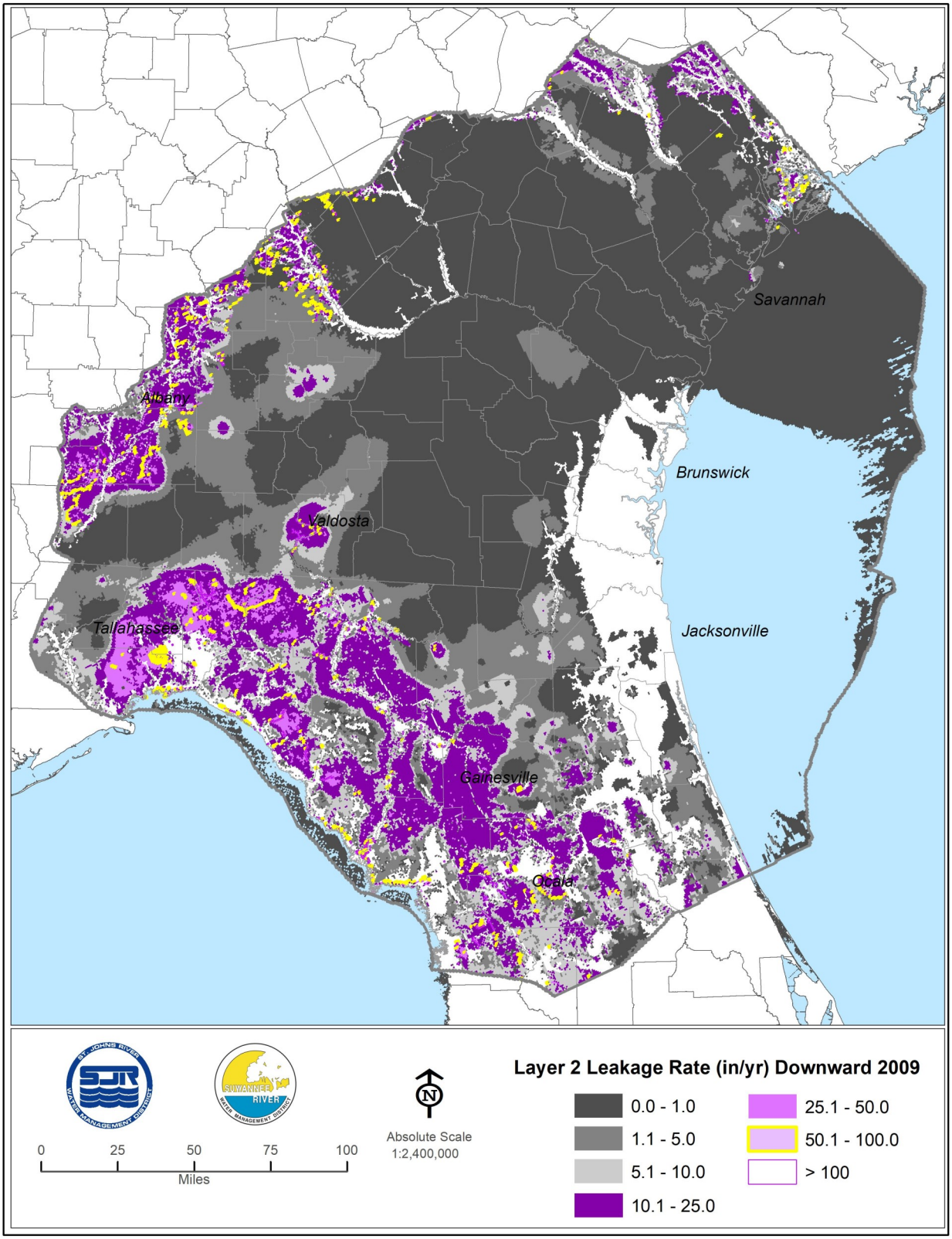

Figure 4-62. Flow through lower face, Layer 2, 2009 (downward leakage rate, Layer 2 to 3, inches/year)

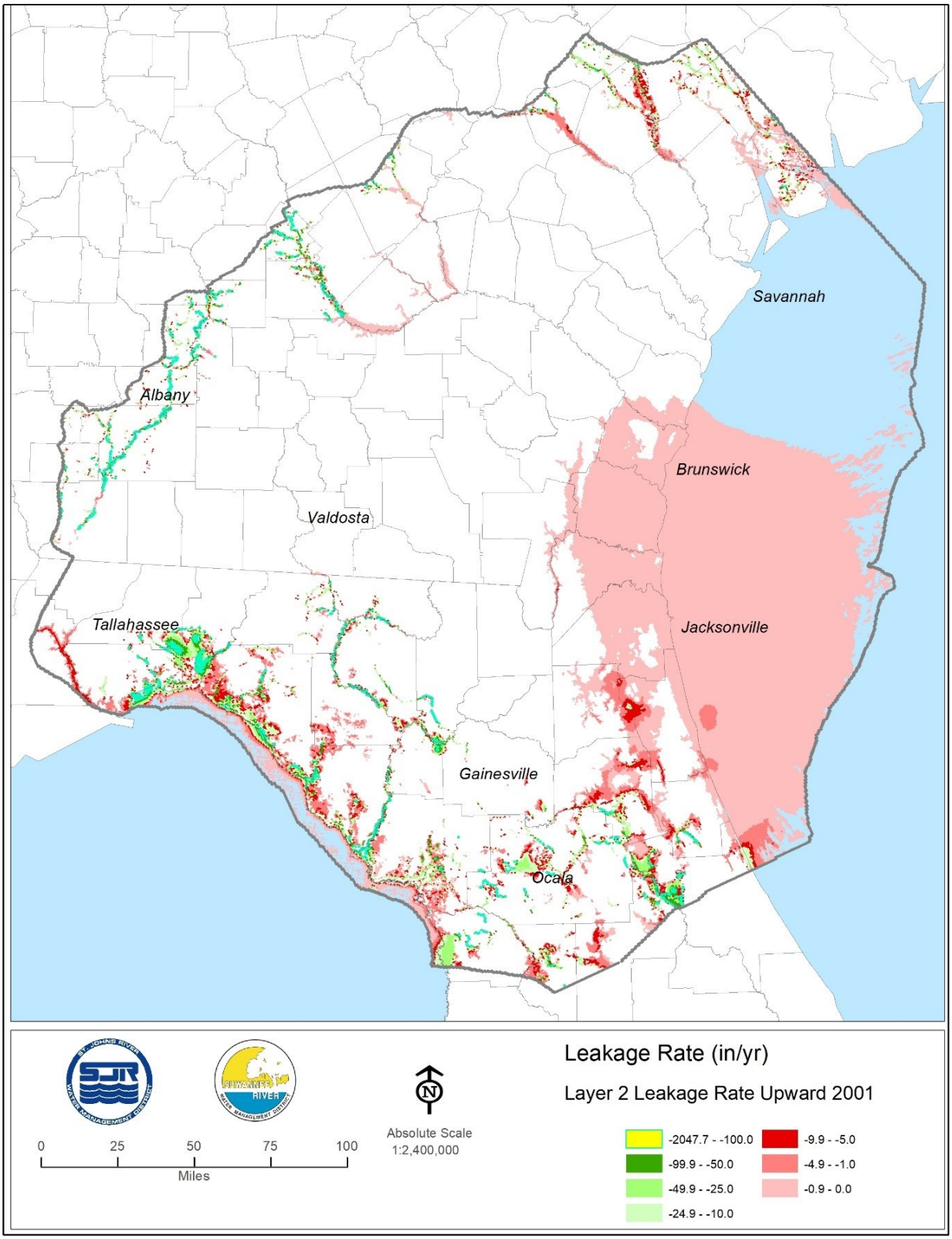

Figure 4-63. Flow through lower face, Layer 2, 2001 (upward leakage rate, Layer 3 to 2, inches/year)

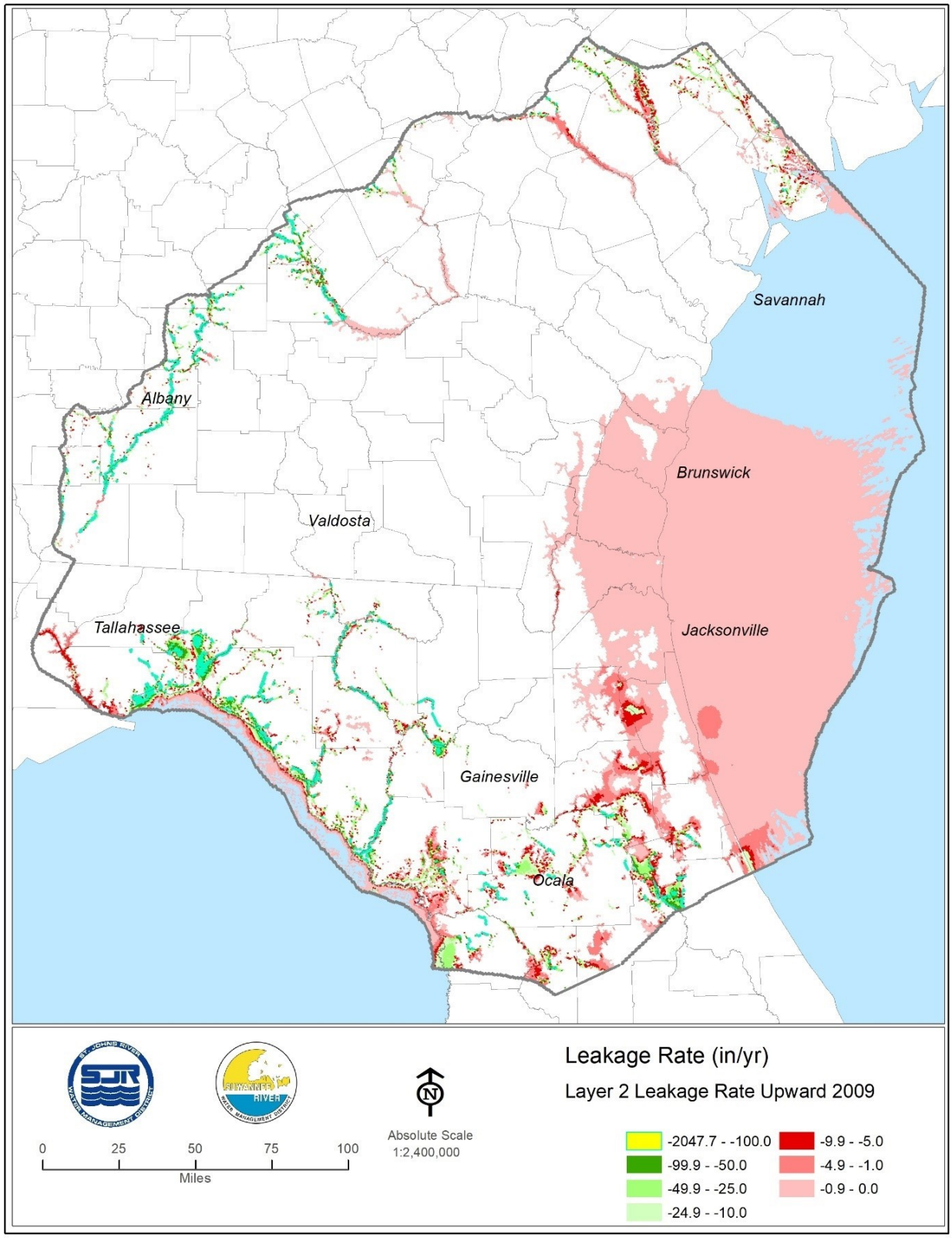

Figure 4-64. Flow through lower face, Layer 2, 2009 (upward leakage rate, Layer 3 to 2, inches/year)

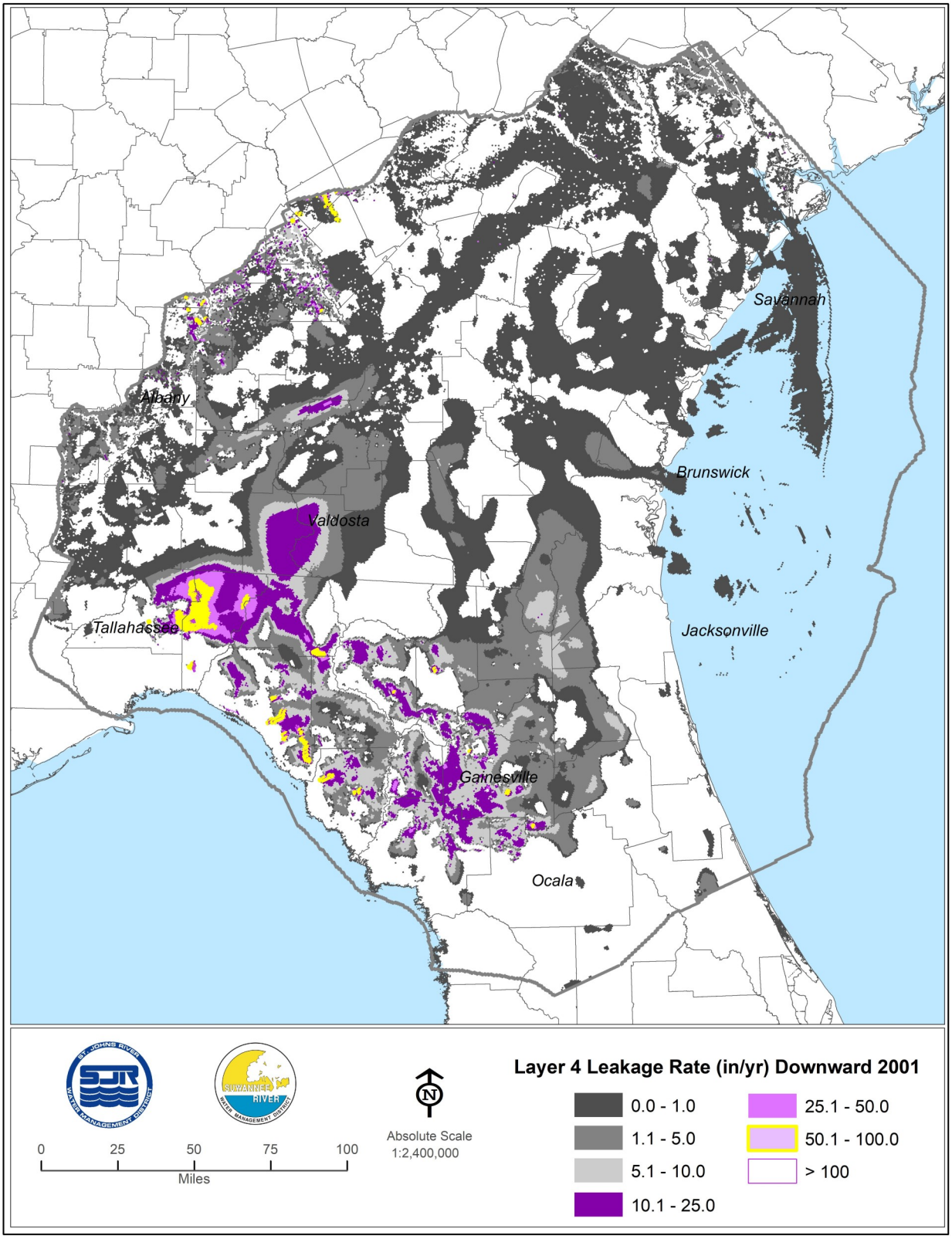

Figure 4-65. Flow through lower face, Layer 4, 2001 (downward leakage rate, Layer 4 to 5, inches/year)

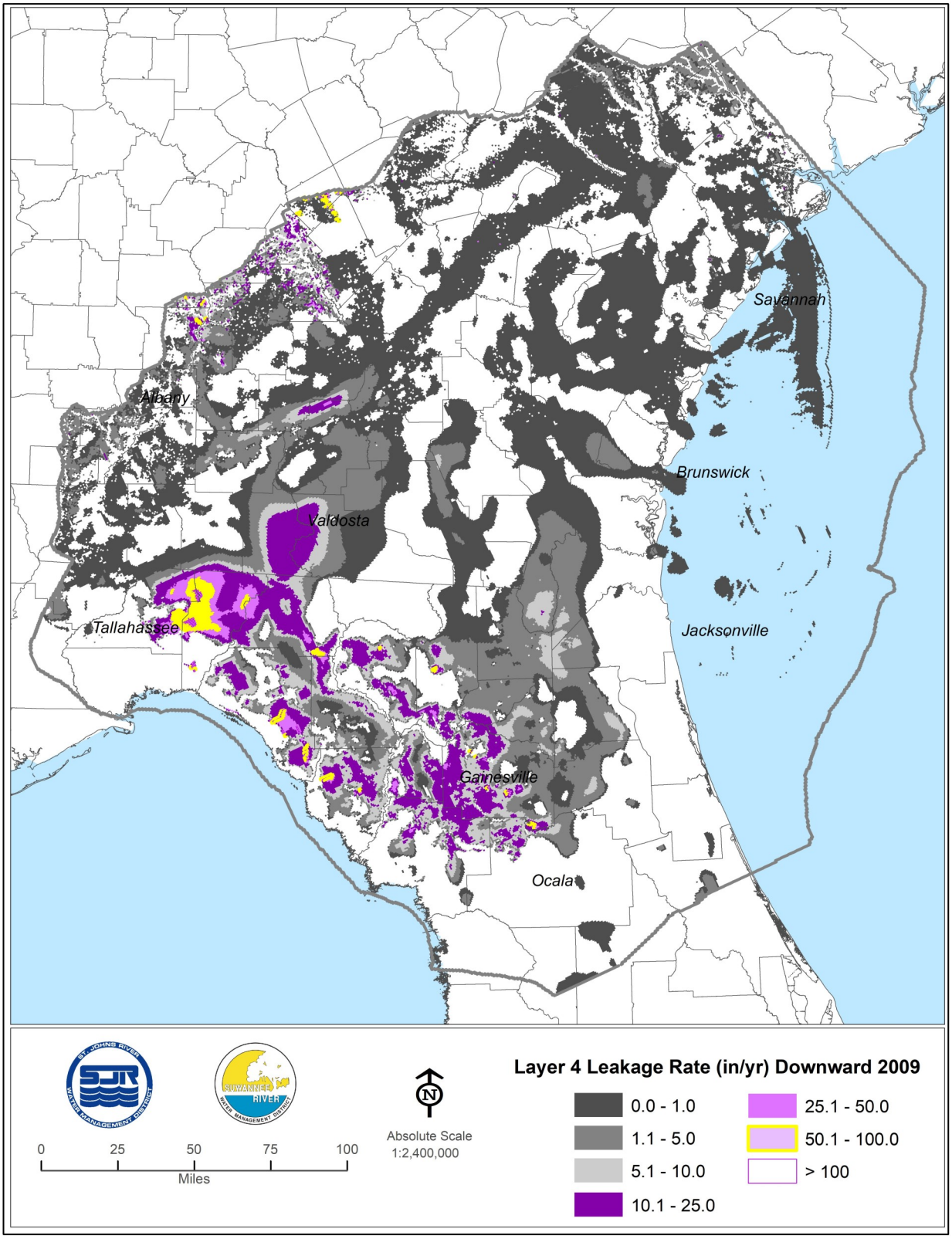

Figure 4-66. Flow through lower face, Layer 4, 2009 (downward leakage rate, Layer 4 to 5, inches/year)

Simulated Upward Leakage Rates of Layer 5 to 4

Maps of simulated upward leakage rates from Layer 5 to 4 for 2001 and 2009 show large areas of upwardly directed leakage from Layer 5 to 4 (Figures 4-67 and 4-68). Leakage rates are highest along the Suwannee River, the coastal regions of the Gulf of Mexico, west-central Marion County, Florida, and the southern extent of the St. Johns River.

Parameters

The CRP group is a set of maps and graphs of calibration derived hydraulic parameters, including horizontal and vertical hydraulic conductivity, aquifer transmissivity, and semiconfining unit leakance. Included in the CRP group is a graphical comparison of calibration derived versus aquifer performance test (APT) derived aquifer transmissivity values and a map of the calibration derived transmissivity of Layer 3. Also included is a map of the sum of the calibration derived transmissivities of Layers 1 through 3 in the unconfined zones of the Floridan aquifer system and of Layer 3 in the confined zones of the Floridan aquifer system. The primary purpose of the map is to show the effects on calibration derived transmissivity estimates of the model layering scheme in unconfined areas.

Horizontal Hydraulic Conductivity of Layer 1

The calibration derived horizontal hydraulic conductivity of Layer 1 is shown on Figure 4-69.

Horizontal Hydraulic Conductivity of Layer 3

The calibration derived horizontal hydraulic conductivity of Layer 3 is shown on Figure 4-70. Examples of areas with low calibration derived horizontal hydraulic conductivity are the general area of the Gulf Trough in Georgia, Mallory Swamp in Lafayette County, Florida, and Waccasassa Flats in Lafayette and Gilchrist counties, Florida. Areas of high calibration derived horizontal hydraulic conductivity include regions with high concentrations of springs, including the Rainbow and Silver springs basins, the Suwannee River corridor, the Santa Fe River Basin, including areas near the Ichetucknee River and High Springs Gap physiographic region. These results are consistent with generally acknowledged hydraulic characteristics of the Upper Floridan aquifer within the respective areas.

Horizontal Hydraulic Conductivity of Layer 5

The horizontal conductivity of Zone 3 (see Chapter 2 for definitions of zones), which is represented by Layer 5, is generally not well known. The calibration results show high horizontal hydraulic conductivity in the Silver and Rainbow springs basins, as generally expected (Figure 4-71). The results also show regions of high horizontal hydraulic conductivity that correspond geospatially to areas of high calibration derived hydraulic conductivity in Layer 3. These areas include parts of the Silver and Rainbow springs basins.

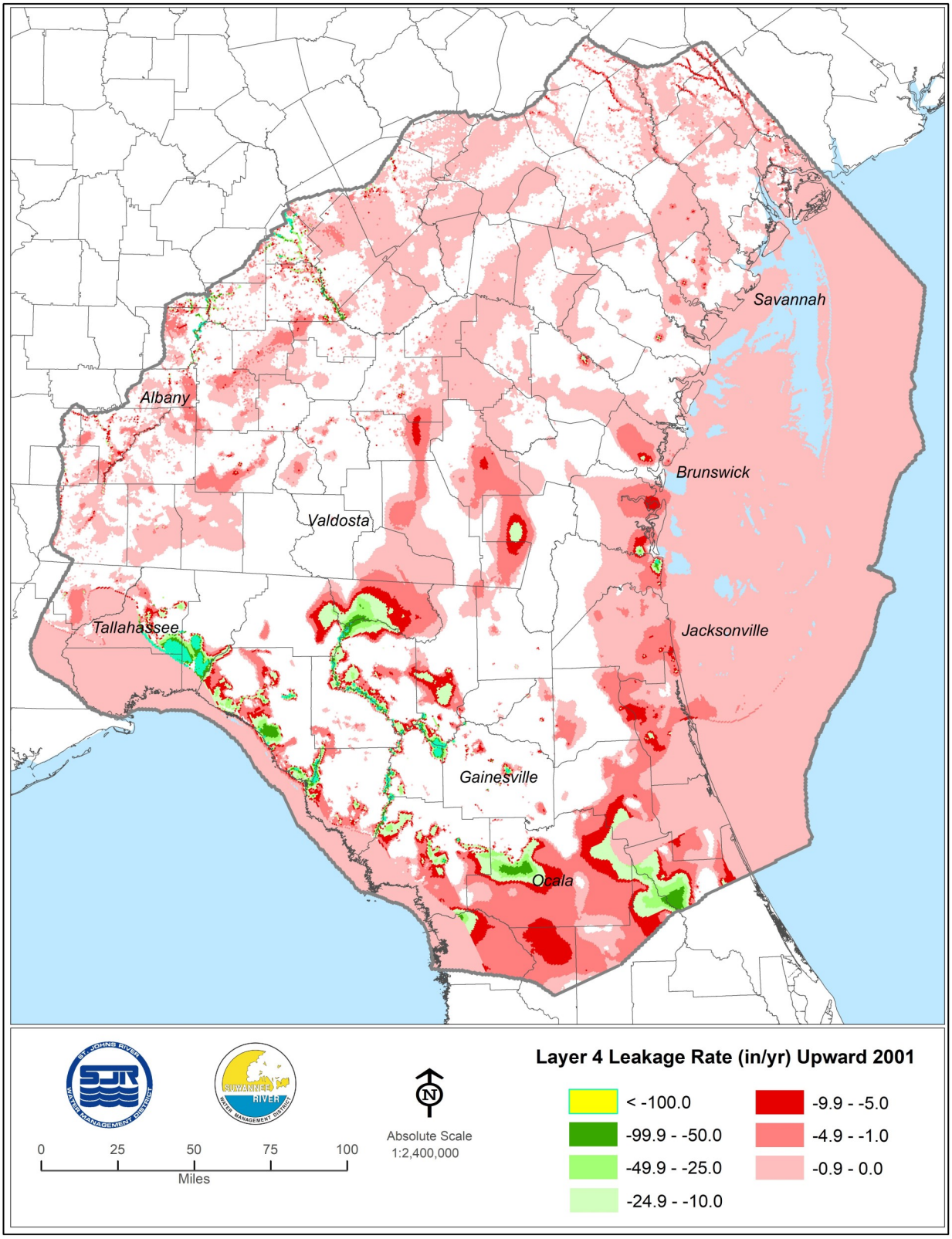

Figure 4-67. Flow through lower face, Layer 4, 2001 (upward leakage rate, Layer 5 to 4, inches/year)

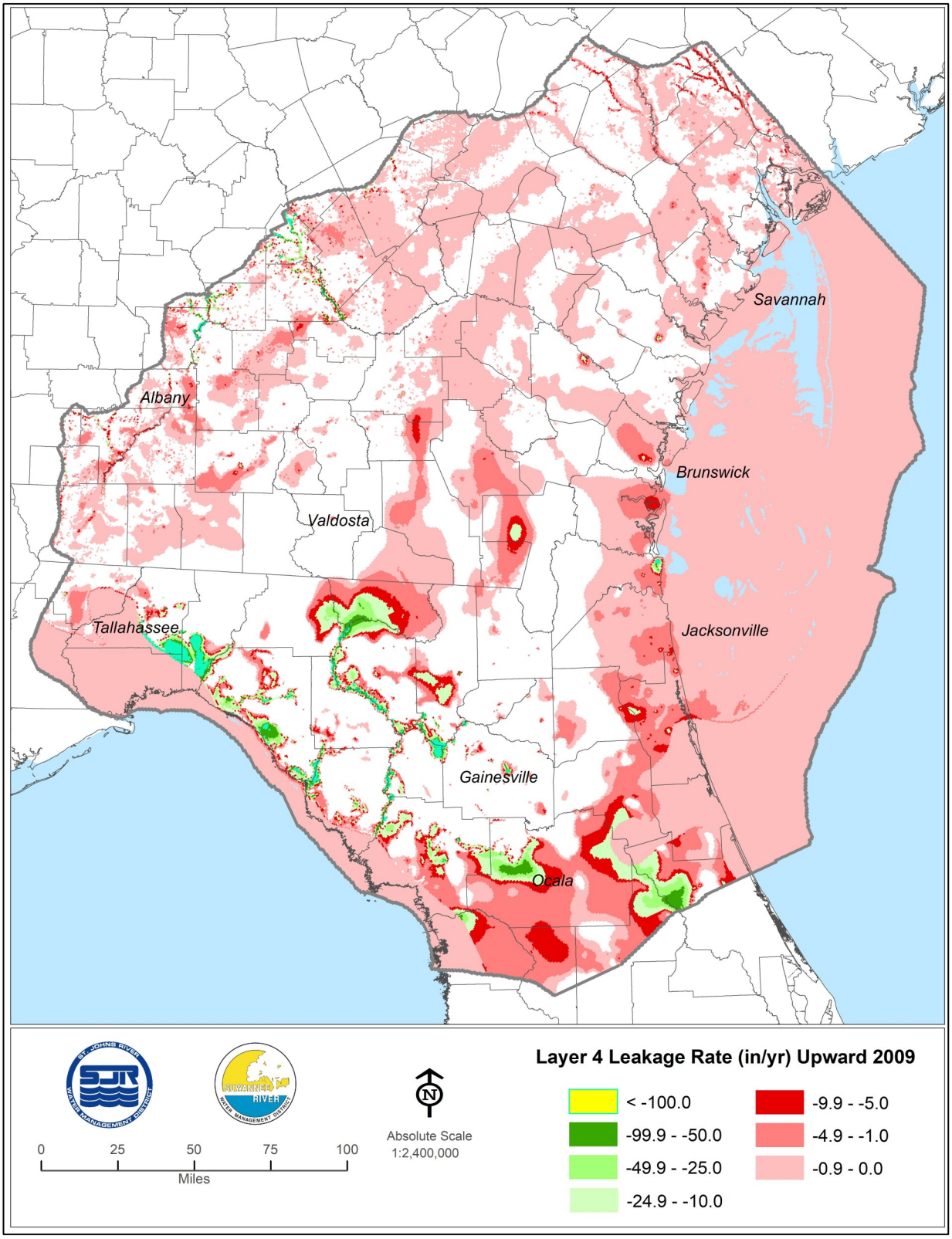

Figure 4-68. Flow through lower face, Layer 4, 2009 (upward leakage rate, Layer 5 to 4, inches/year)

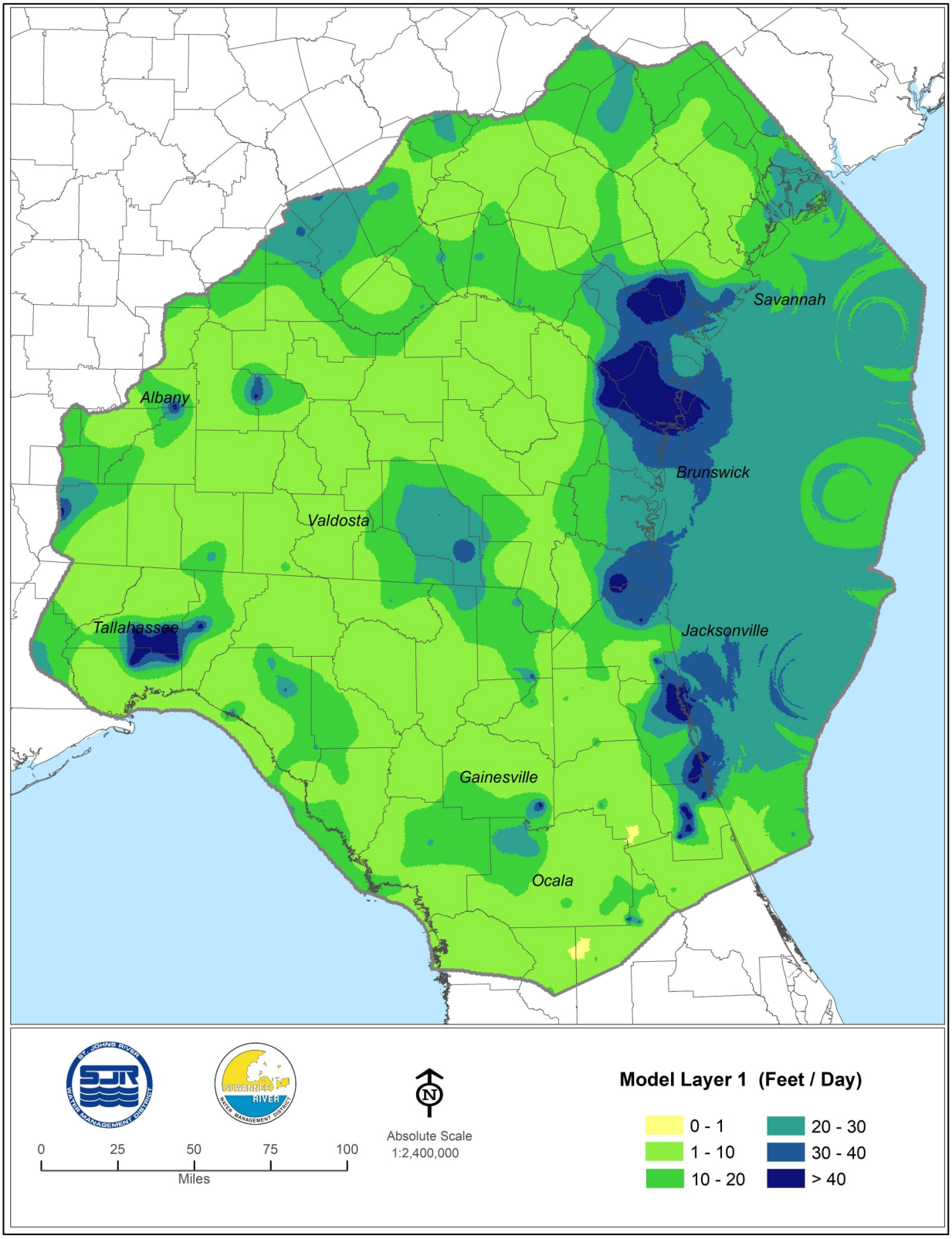

Figure 4-69. Modeled distribution of horizontal hydraulic conductivity (feet/day), model Layer 1

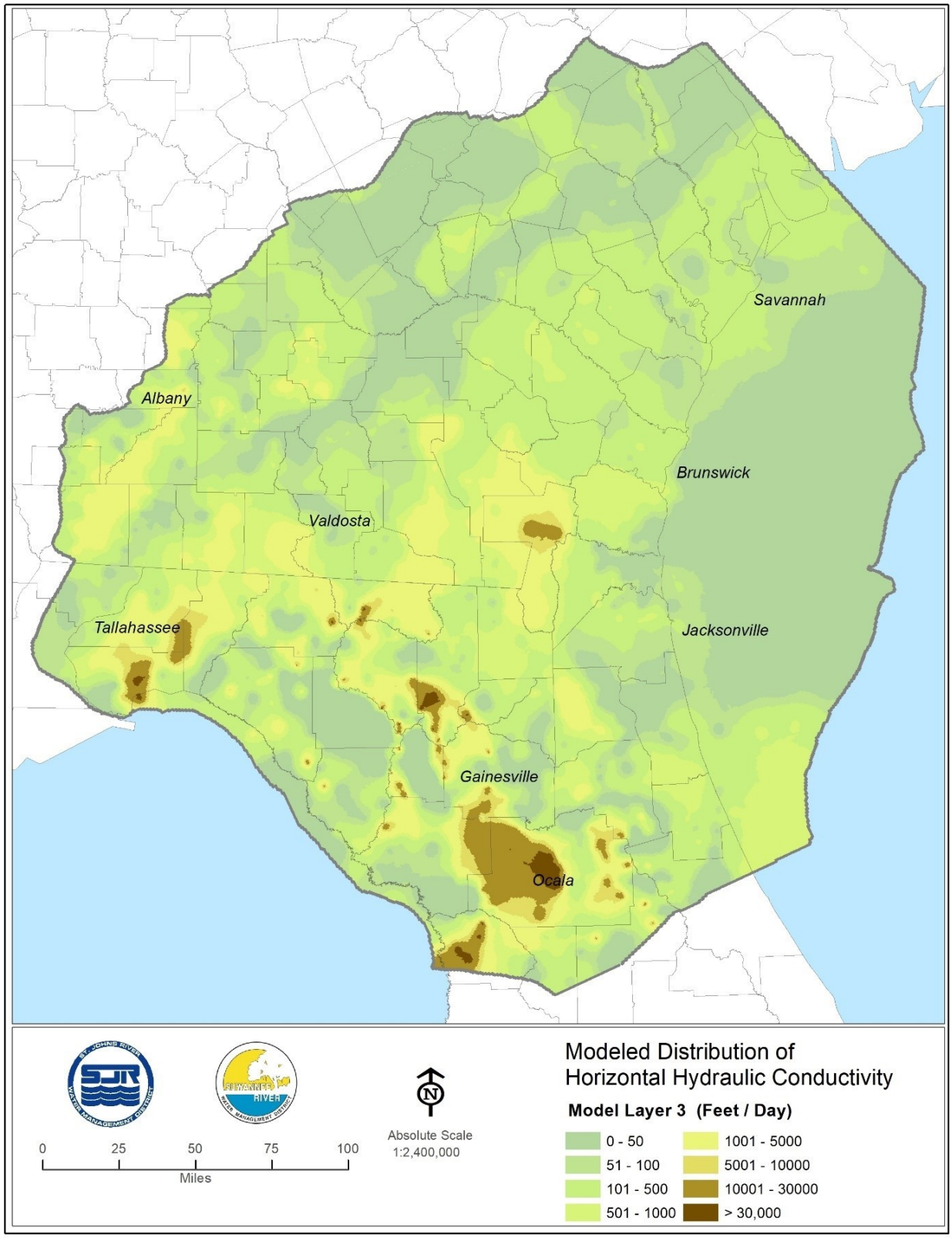

Figure 4-70. Modeled distribution of horizontal hydraulic conductivity (feet/day), model Layer 3

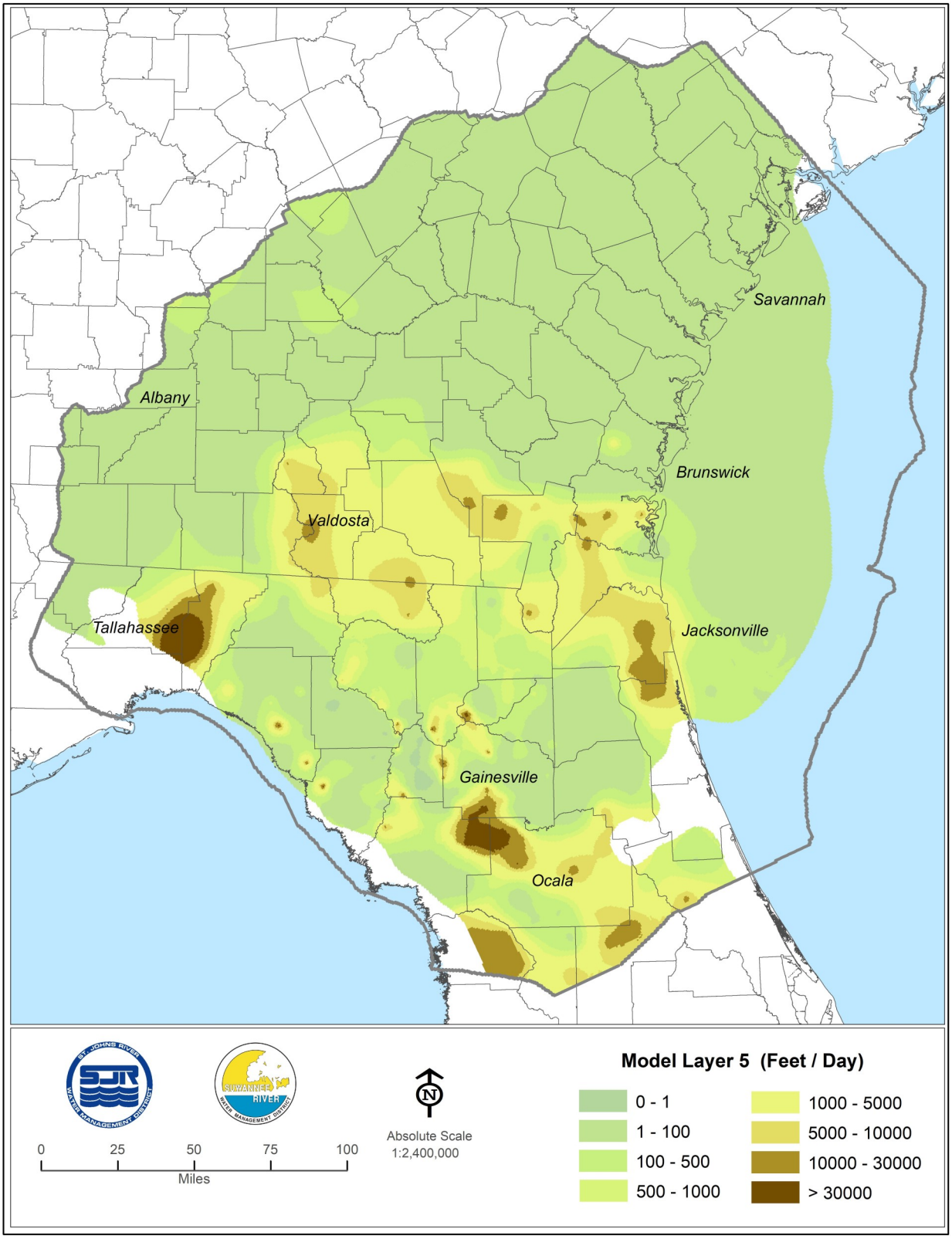

Figure 4-71. Modeled distribution of horizontal hydraulic conductivity (feet/day), model Layer 5

The results also include an area that extends roughly from Valdosta, Georgia, eastward towards the Atlantic Coast and then southward from the Florida Georgia state line between Camden County, Georgia, and Nassau County, Florida, into St. Johns County, Florida. A branch of this zone extends from northeastern Baker County, Florida, and southern Charlton County, Georgia, and intersects with main portion of the zone in south central Nassau and northern Duval counties, Florida. This zone of high hydraulic conductivity connects inland recharge areas to coastal discharge areas.

Another zone of high horizontal hydraulic conductivity extends from the Florida Georgia state line southwest of Valdosta, Georgia, to the general area of southeast Leon and west central Jefferson counties, Florida. This is an area of numerous karstic features, including numerous sinkholes, lying just north of the Woodville Karst Plain.

Areas of relatively low horizontal hydraulic conductivity within Layer 5 include the general area of Mallory Swamp in Lafayette County, Florida, and Waccasassa Flats in Lafayette and Gilchrist counties, Florida. These are areas in which horizontal hydraulic conductivity is generally acknowledged to be relatively low in overlying, shallower zones of the Floridan aquifer system.

Horizontal Hydraulic Conductivity, Layer 7

The horizontal hydraulic conductivity of Layer 7 represents that of the Fernandina permeable zone, which is the lower zone of the Lower Floridan aquifer in northeast Florida and southeast Georgia. The horizontal hydraulic conductivity of this part of the Lower Floridan aquifer is not well defined. Layer 7 horizontal hydraulic conductivities resulting from the calibration range from less than 50 ft/day to more than 100 ft/day (Figure 4-72). Only two groundwater level observation points were available for use in the calibration process for this layer for 2001 and 2009.

Transmissivity of Layer 3

The calibration derived transmissivity distribution of Layer 3 is shown in Figure 4-73.

Transmissivity of Layer 3 in Confined Areas and the Sum of Transmissivities of Layers 1 through 3 in Unconfined Areas

The map of transmissivity of Layer 3 in confined areas and the sum of transmissivities of Layers 1 through 3 in unconfined areas, referred to hereafter as the "composite transmissivity map," shows the effective transmissivity of Layer 1 through 3 in unconfined areas rather than the transmissivity of Layer 3 only (Figure 4-74). The effective transmissivity in unconfined areas is calculated as the sum of the transmissivities of Layer 1, 2 and 3. The map shows Layer 3 transmissivity only in confined areas. The purpose of the map is to show the effects on transmissivity estimates of the model layering scheme in unconfined areas. This map and that of Layer 3 transmissivity are similar in configuration and general ranges, but significant differences occur in highly karstic areas, such as parts of the Silver and Rainbow springs basins (Figure 4-75).

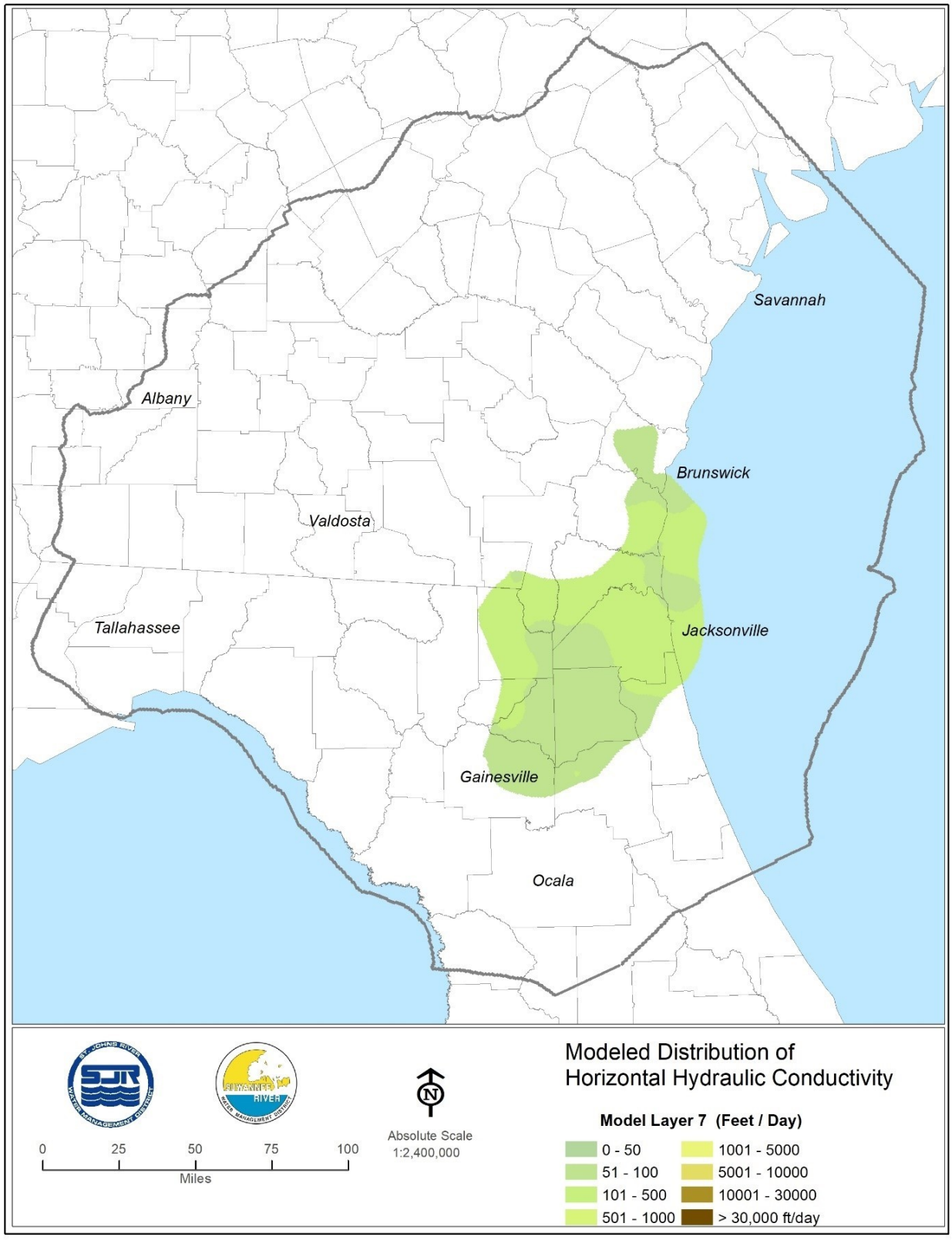

Figure 4-72. Modeled distribution of horizontal hydraulic conductivity (feet/day), model Layer 7

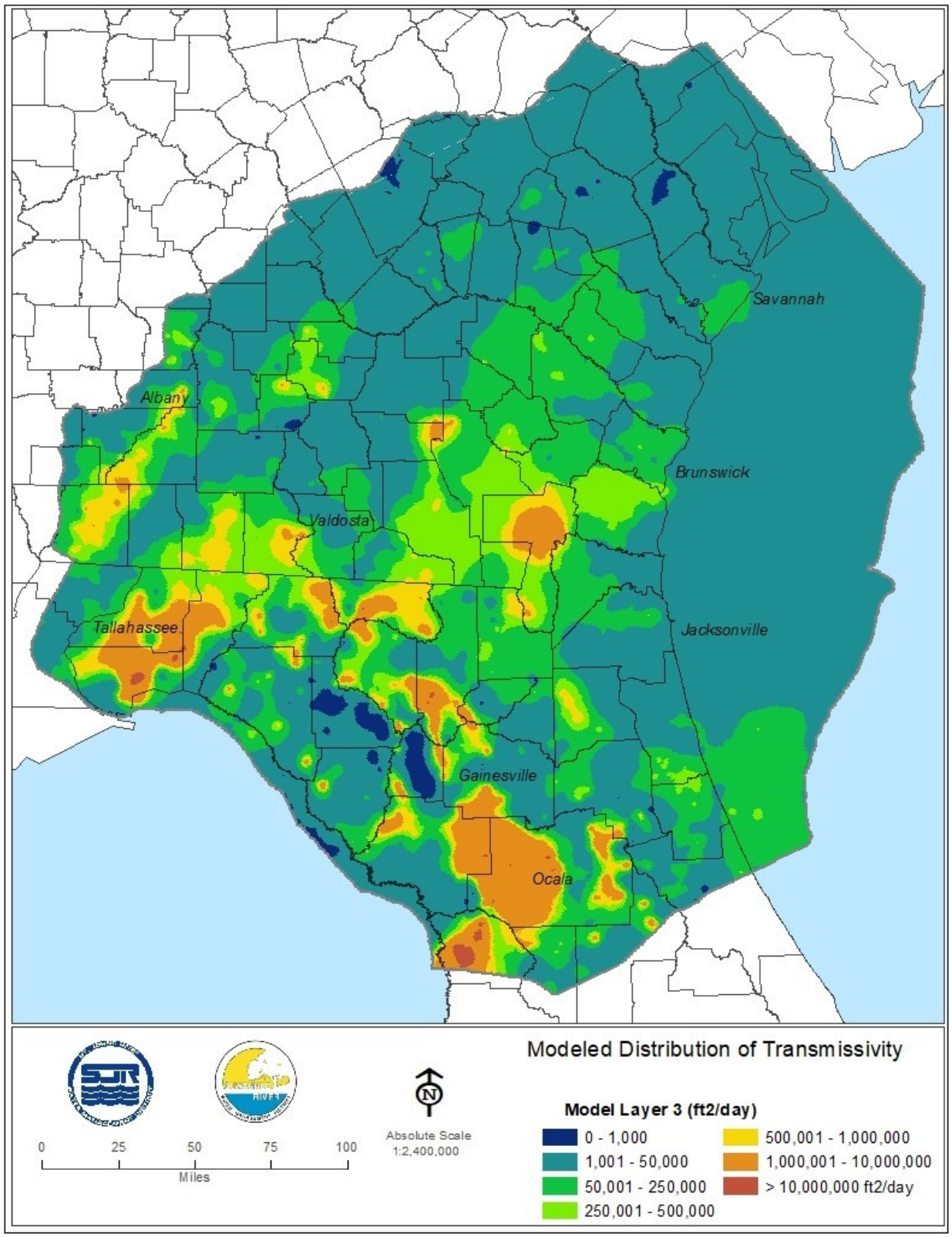

Figure 4-73. Spatial distribution of transmissivity (feet squared/day), model Layer 3

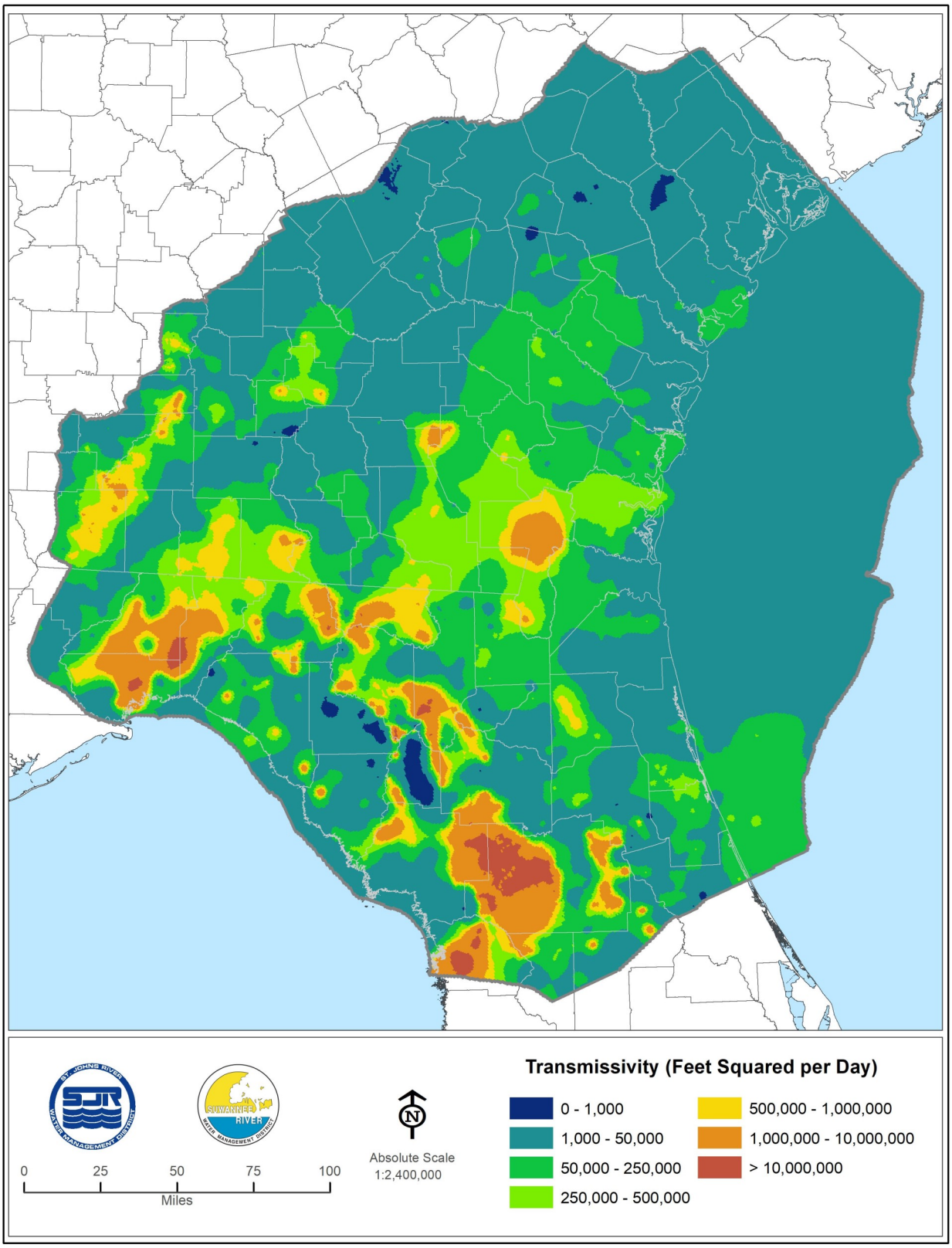

Figure 4-74. Spatial distribution of transmissivity (feet squared/day), upper Floridan aquifer – Layers 1-3 unconfined region, Layer 1 confined region

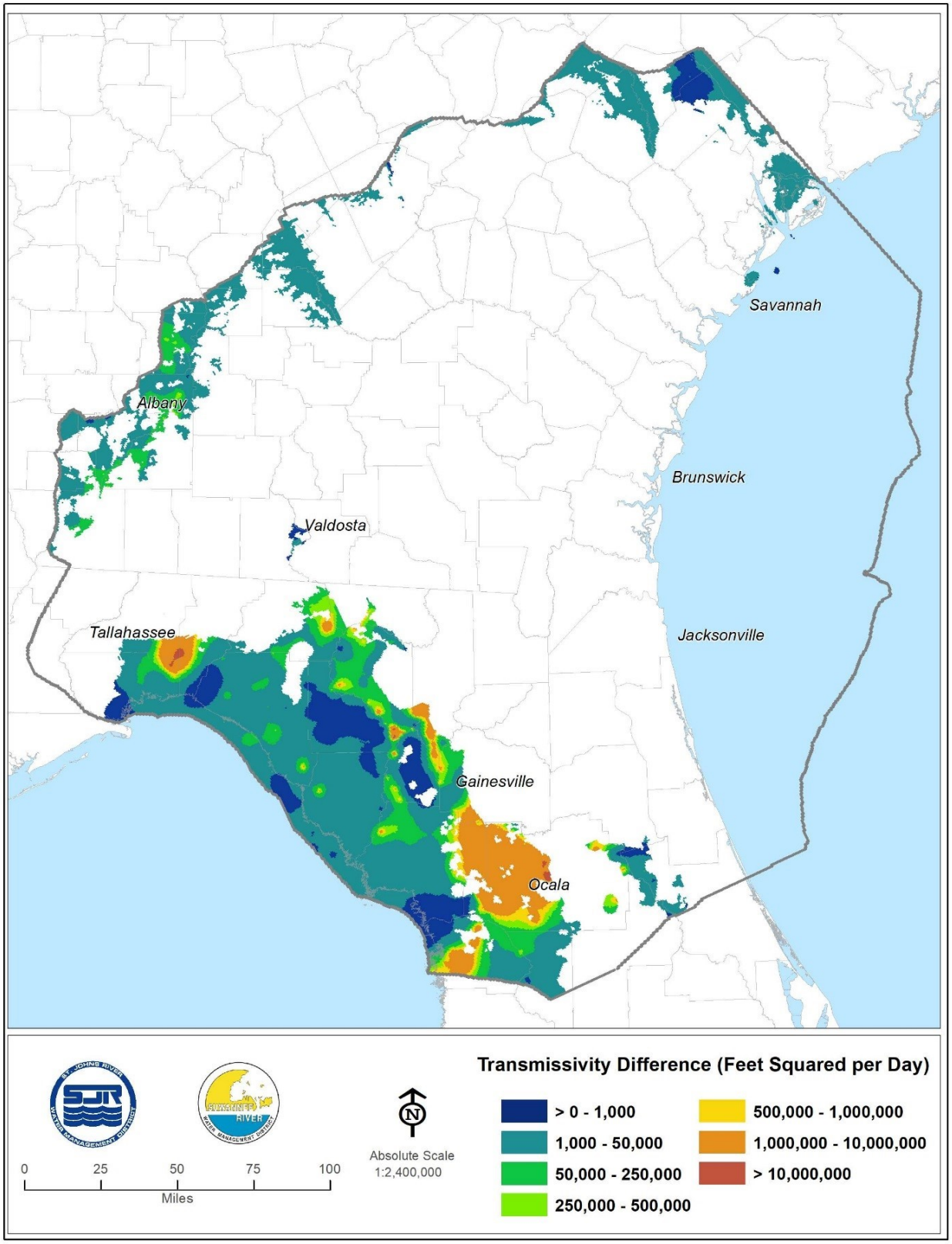

Figure 4-75. Difference in transmissivity of Layer 3 and upper-Floridan-aquifer transmissivity distributions (feet squared per day)

Observed versus Calibration Derived Transmissivity of the Upper Floridan aquifer

The comparison of calibration derived transmissivity of the Upper Floridan aquifer to APT derived is shown in Figure 4-76. APT derived transmissivity values are presented as reported in various reports that document them and as "normalized values," which are the reported values divided by the depth of penetration of the pumped well of the APT and multiplied by the thickness of the aquifer at the APT site. The APT results and comparison to corresponding calibration derived values should be interpreted with a degree of caution. APTs are limited in ability to stress highly transmissive systems, such as the Upper Floridan aquifer. This limits the spatial extent of the stresses, and therefore the extent to which APT derived transmissivities can represent the system. APT results are therefore more localized, and differences should be expected between those results and the calibration results of models such as the NFSEG model with grid cell dimensions that represent larger "samples" of the aquifer.

Transmissivity, Layer 5

The calibration derived Layer 5 transmissivity distribution is shown in Figure 4-77. The transmissivity distribution of Layer 5 exhibits numerous similarities with the spatial patterns of Layer 3, such as higher values in areas with greater spring flows and lower values in areas such as Mallory Swamp and Waccasassa Flats. The results of five APTs performed on the Lower Floridan aquifer are shown on the map of Figure 4-77 also.

Vertical Hydraulic Conductivity of Layer 2

The calibration derived distribution of Layer 2 vertical hydraulic conductivity is shown in Figure 4-78. These values are generally consistent with the degree of confinement provided by the intermediate confining unit, being relatively low where it is thick and high where it is thin or absent, as expected.

Vertical Hydraulic Conductivity of Layer 4

The calibration derived distribution of Layer 4 vertical hydraulic conductivity shows moderate to low values of vertical hydraulic conductivity in areas in which Miller (1986) mapped various middle confining units within the NFSEG model. Values are moderately high to very high outside of those areas (Figure 4-79).

Vertical Hydraulic Conductivity, Layer 6

The calibration derived vertical hydraulic conductivity of Layer 6 shows generally low values of vertical hydraulic conductivity (Figure 4-80).

Leakance of Layer 2

In terms of relative magnitude, the geospatial patterns of the calibration derived Layer 2 leakance distribution resemble the Layer 2 distribution of vertical hydraulic conductivity. Values range from less than 10^{-7} to greater than 1 per day (day^{-1}). Higher values are associated with areas in which the intermediate confining unit is thin or absent and lower values with areas in which it is relatively thick (Figure 4-81).

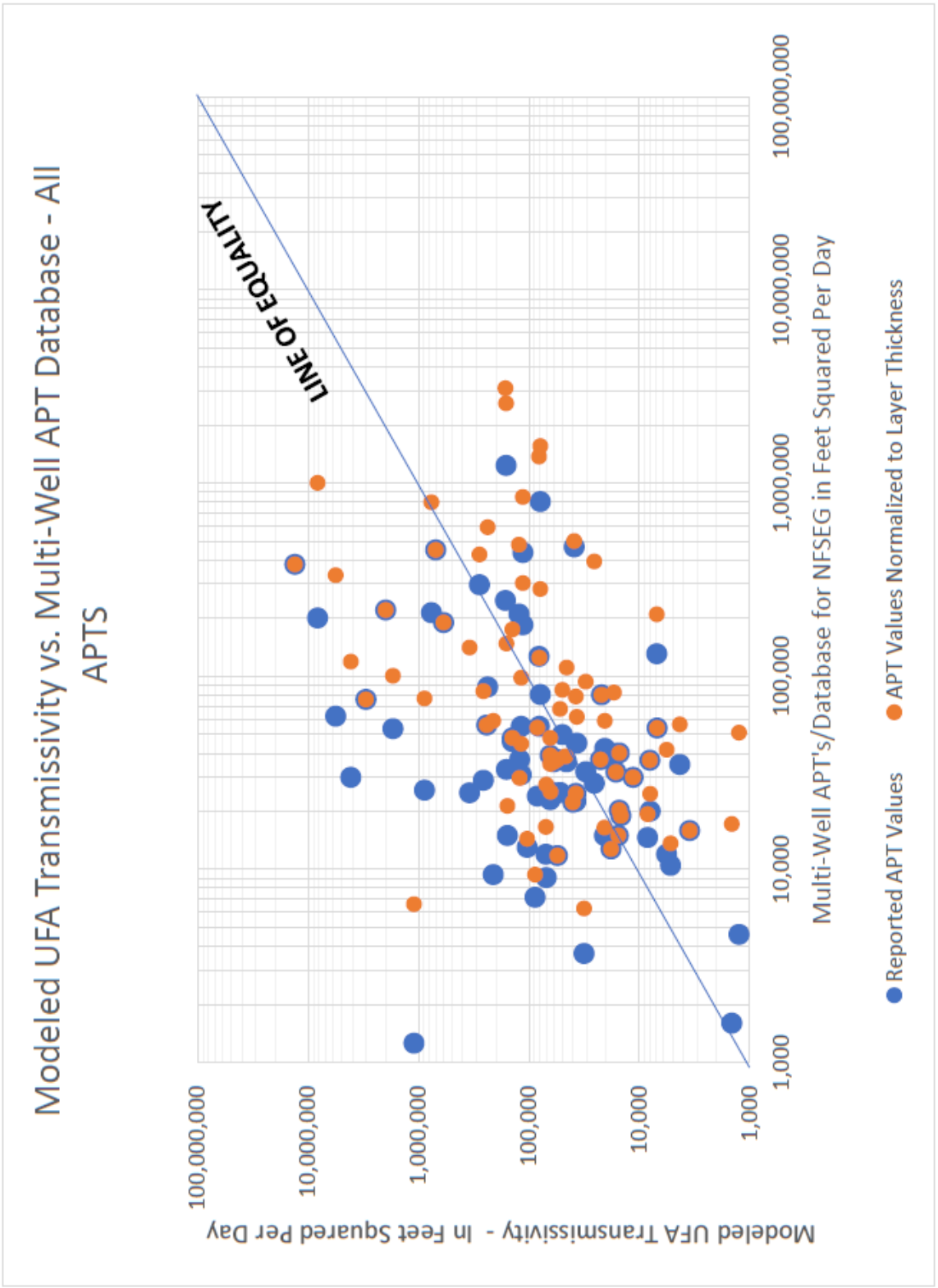

Figure 4-76. Multi-well-APT-derived transmissivity versus calibration-derived transmissivity (feet squared per day), upper Floridan aquifer

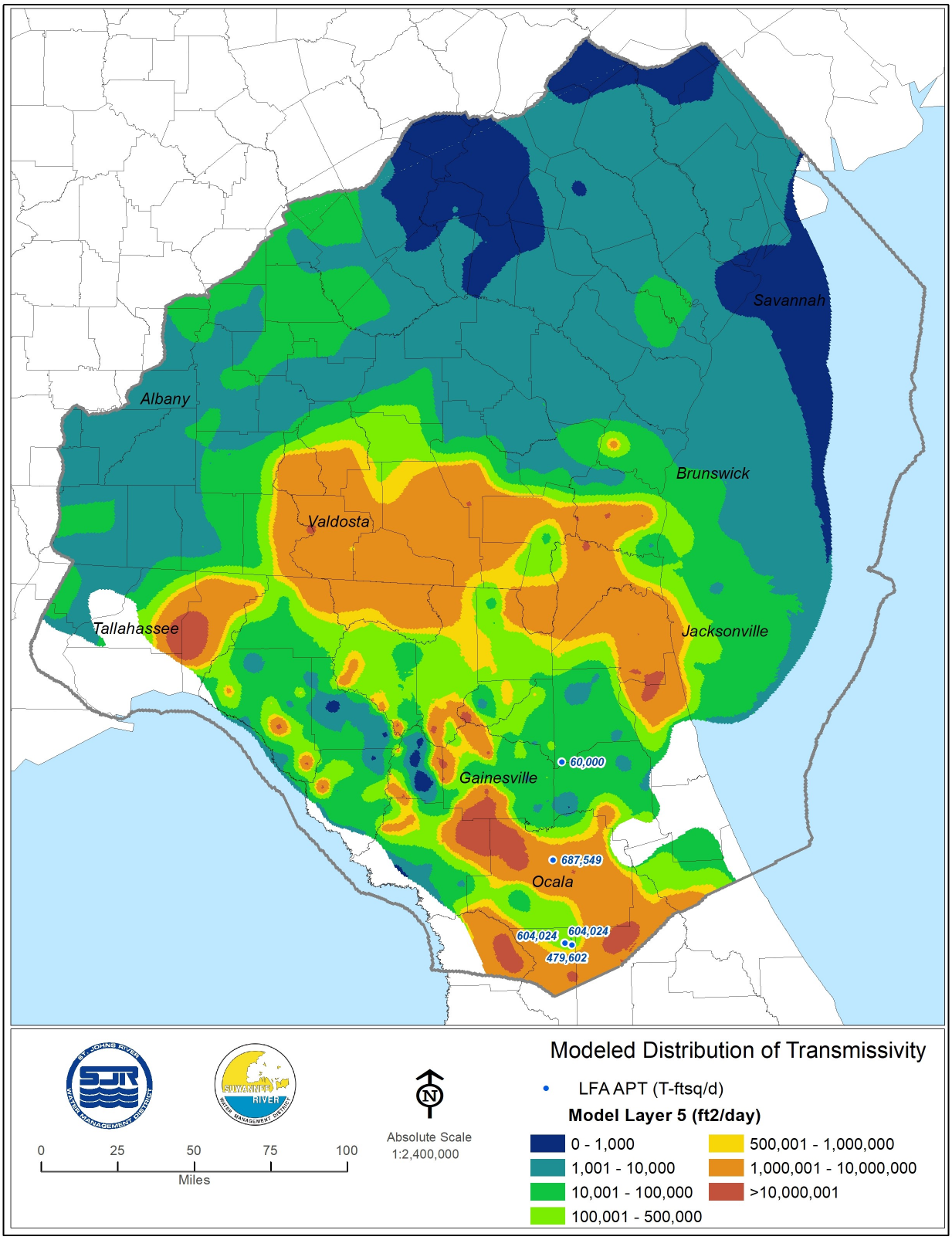

Figure 4-77. Spatial distribution of transmissivity (feet squared/day), model Layer 5. NFSEG v1.1 APT database values super imposed

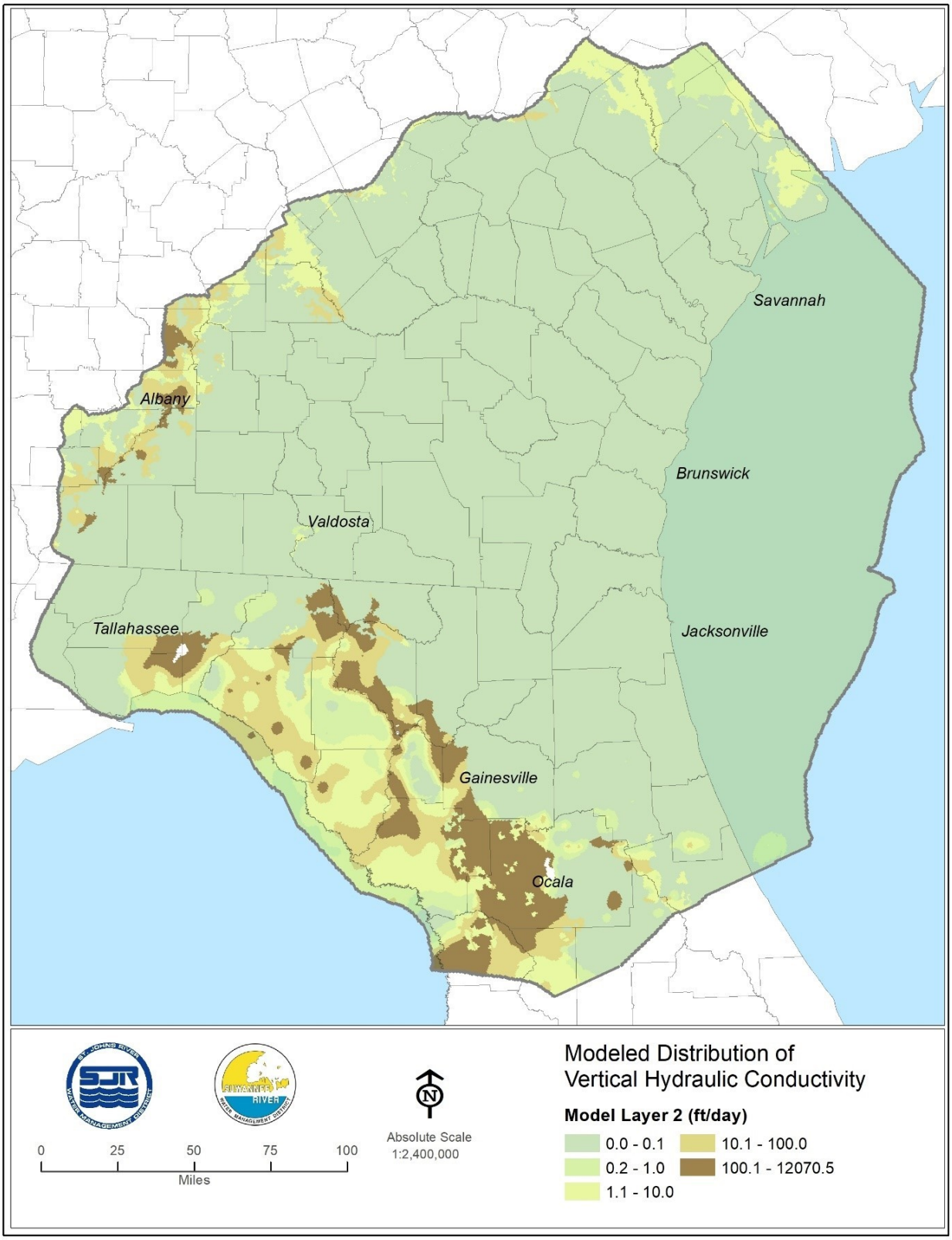

Figure 4-78. Modeled distribution of vertical hydraulic conductivity (feet/day), model Layer 2

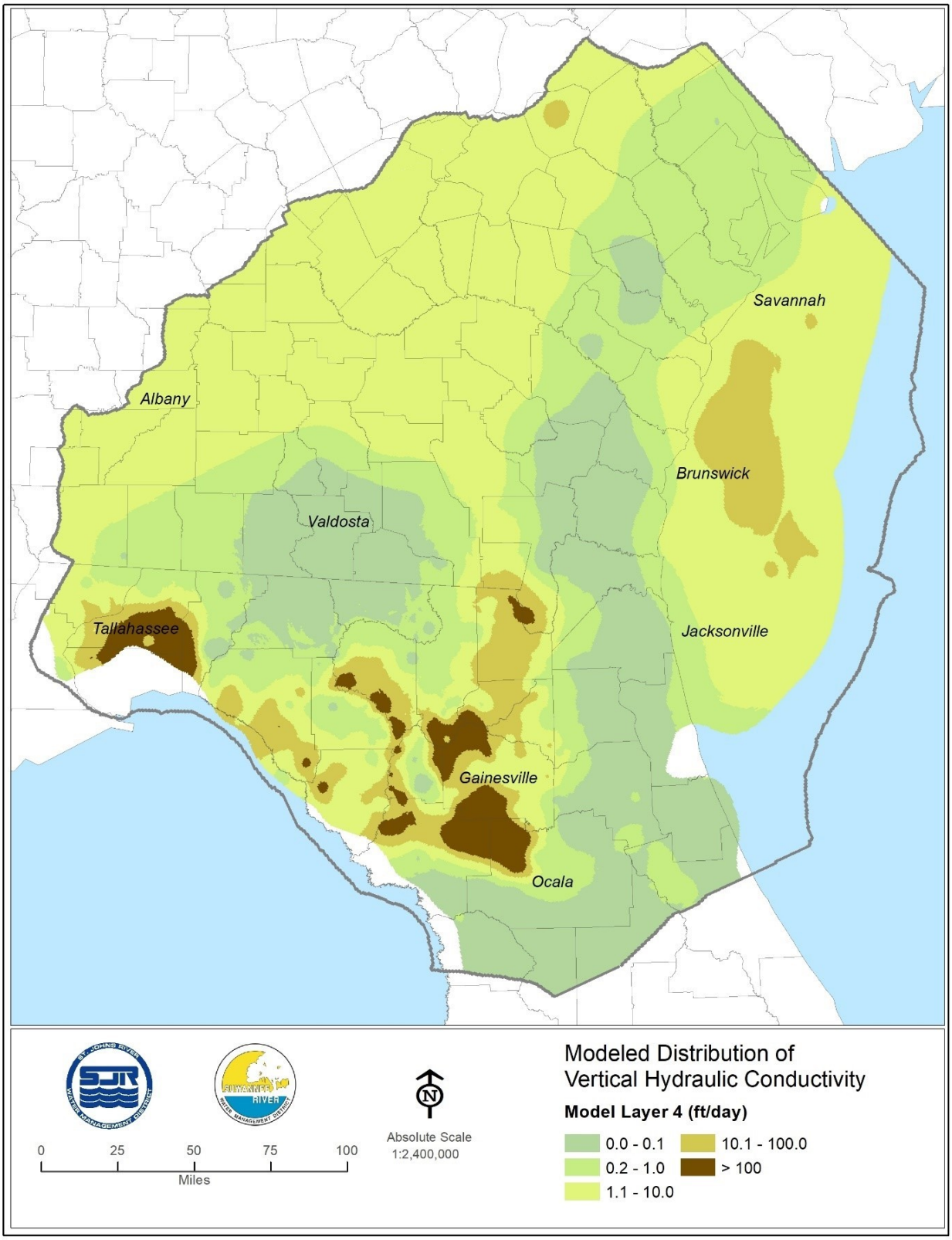

Figure 4-79. Modeled distribution of vertical hydraulic conductivity (feet/day), model Layer 4

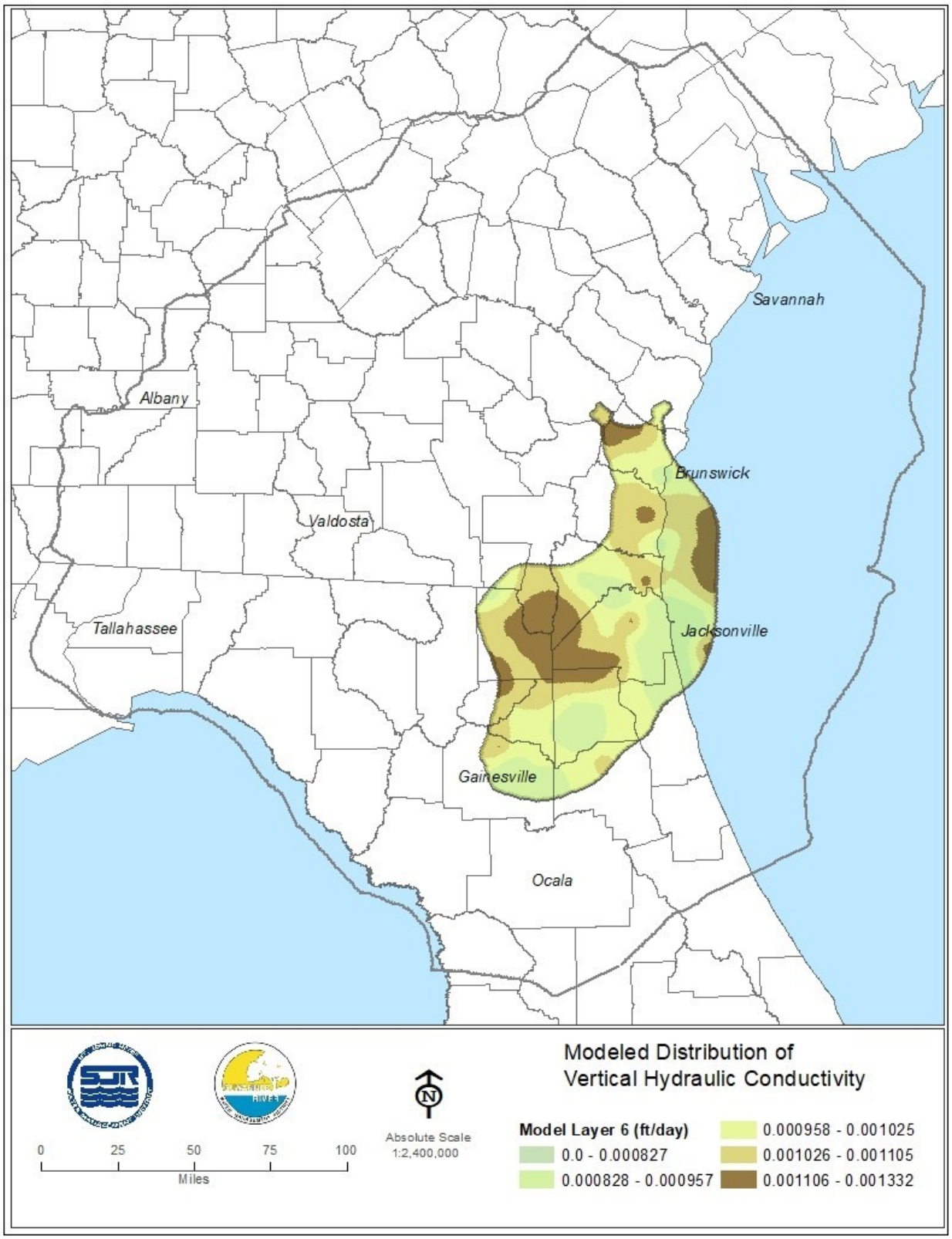

Figure 4-80. Modeled distribution of vertical hydraulic conductivity (feet/day), model Layer 6

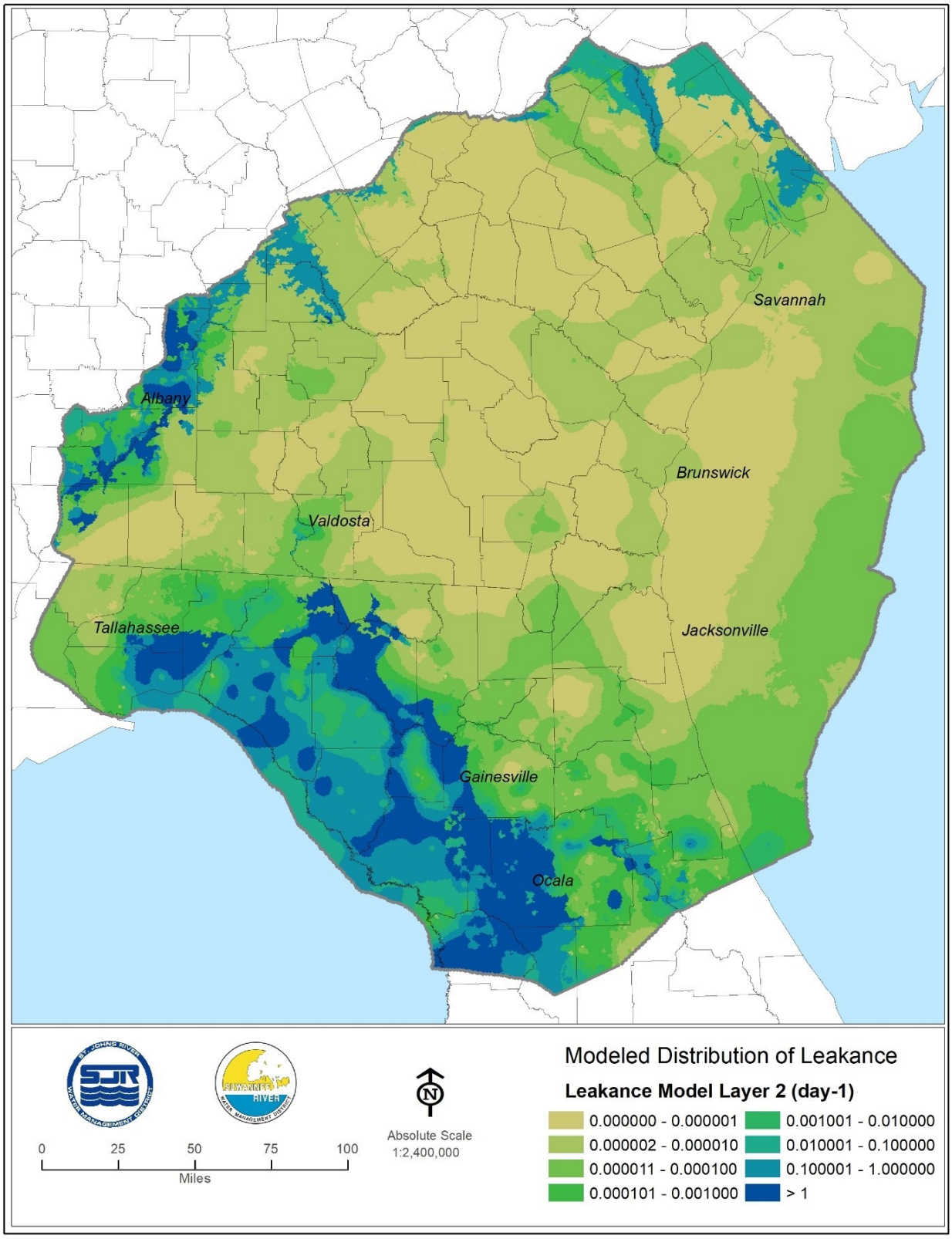

Figure 4-81. Modeled distribution of leakance, model Layer 2

Leakance of Layer 4

Similarly, in terms of relative magnitude, the Layer 4 leakance distribution generally corresponds geospatially to the calibration derived distribution of Layer 4 vertical hydraulic conductivity (Figure 4-82).

ADDITIONAL DISCUSSION

The following discussion provides additional interpretation of calibration results regarding groundwater levels, baseflows, and other items. The specific topics address here are as follows:

- Recharge and maximum saturated ET as potential calibration parameters;
- Baseflow targets and matches;
- Spring Flow Target Uncertainty;
- Statistics of groundwater level residuals of NFSEG v1.1 with comparisons to those of other groundwater models with overlapping domains;
- Statistical and spatial trends in NFSEG v1.1 groundwater level residuals in comparison to other groundwater models;
- Calibration derived transmissivity of the Upper Floridan aquifer of NFSEG v1.1 vs. corresponding APT derived values;
- Procedures used to guide PEST in the NFSEG calibration process such as specification of observation group weights, limiting pilot point ranges, use of synthetic targets, and use of lake leakage estimates used as observations.

Recharge and Maximum Saturated ET as Calibration Parameters

Direct observations of recharge and maximum saturated ET at scales other than site scale are not available. Therefore, recognizing the potentially significant influence of these parameters in the calibration process, as later confirmed by the results of the sensitivity and uncertainty analyses (see Chapter 7 and Appendix L), the Districts undertook the development of more than 50 HSPF models for attainment of reasonable estimates of recharge and maximum saturated ET. The HSPF models are calibration constrained and based on internally consistent mass balances of the surface water and groundwater flow systems (Chapter 9), features that help to enforce realistic estimates of recharge and maximum saturated ET.

Adjusting or refining estimates of recharge and maximum saturated ET through the calibration process can facilitate matching groundwater level and flow targets. However, such an approach must be implemented carefully to prevent unrealistic changes that can negatively impact the representations of other aspects of the flow system, such as groundwater levels or springs flows. This is particularly applicable to the idea of adjusting recharge and/or maximum saturated ET to match baseflow targets, because uncertainty surrounding baseflow targets is generally relatively high. Therefore, the potential exists for sacrificing the model fit to relatively high quality groundwater level or spring flow targets and/or for adjusting recharge and maximum saturated ET estimates to an unreasonable degree to match uncertain baseflow targets.

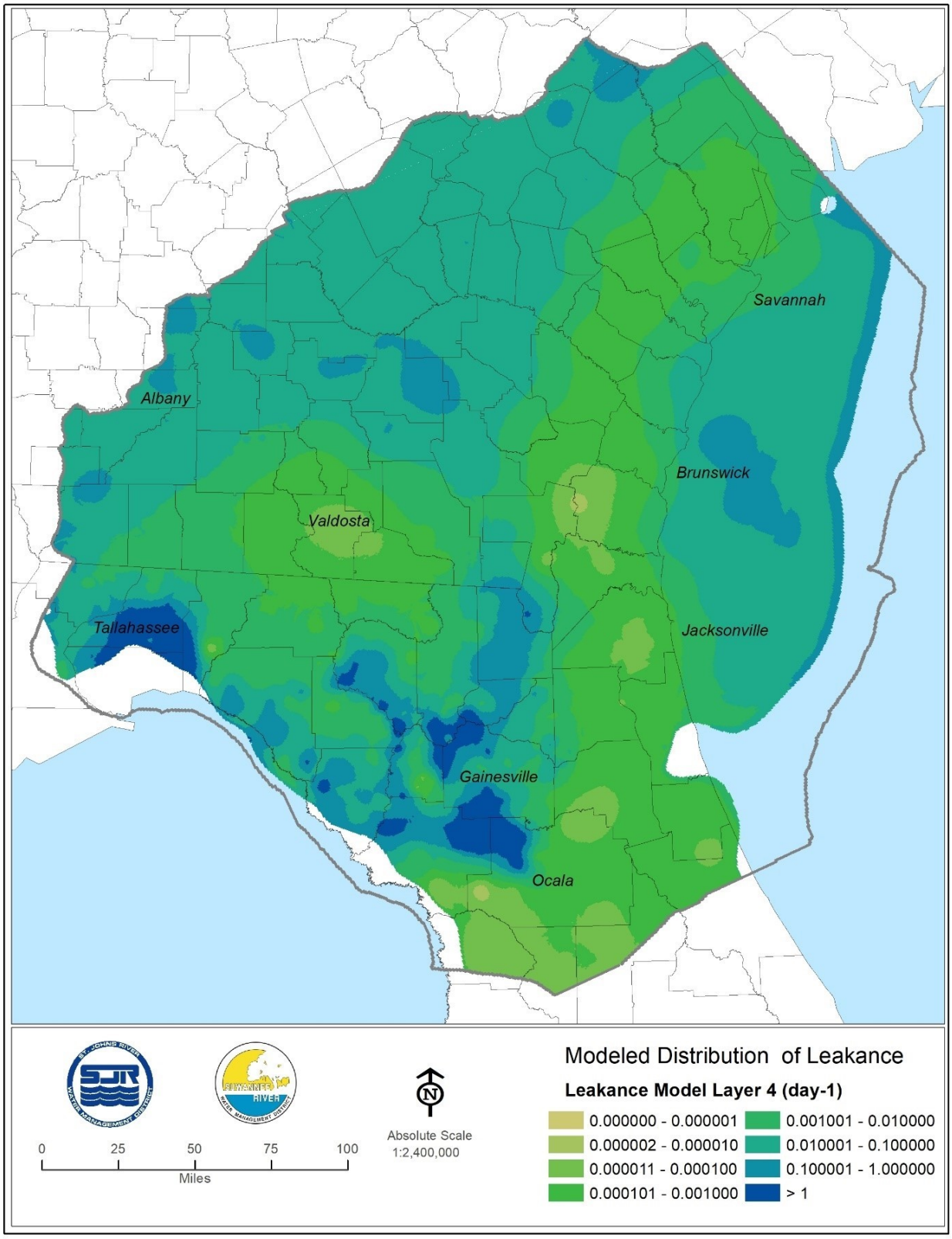

Figure 4-82. Modeled distribution of leakance, model Layer 4

After completion of the NFSEG v1.1 calibration, additional review of the NFSEG v1.1 baseflow targets was performed, resulting in an improved understanding of the factors that contribute to differences between estimated and corresponding simulated baseflows. An important conclusion was that the larger differences frequently reflect uncertainty in the targets, as simulated baseflows are more reasonable than corresponding baseflow targets in many cases. The diversity of observation types and the numbers of each type, as utilized in the NFSEG v1.1 calibration process, compensated for the effects of baseflow targets that were of poor quality. Therefore, in retrospect, the approach implemented in the NFSEG v1.1 calibration process of focusing on adjustments in parameters other than recharge and maximum saturated ET, such as hydraulic conductivity, is still viewed as the best approach.

Future calibration efforts may focus on reducing uncertainty in recharge and maximum saturated ET values through refinement of HSPF models and adjustment of recharge and maximum saturated ET during the calibration process. Recharge and maximum saturated ET can be adjustable parameters during model calibration if an adequate level of confidence can be associated with the baseflow targets (and other targets). Prior to making recharge and maximum saturated ET adjustable in future calibration efforts, baseflow targets will need to undergo additional screening and, where possible, refinement. Once that process is completed, a weight will be applied to each baseflow target in the calibration process, as deemed appropriate, in view of the uncertainty associated with the target. The process will continue to incorporate the HSPF models to enforce reasonable constraints on derived estimates of recharge and maximum saturated ET. Additional details regarding the implementation of this process will be worked out through a careful planning process.

Quality of Baseflow Matches

Variability in the baseflow estimates used in the NFSEG v1.1 calibration was characterized by calculating the difference between minimum and maximum values of the five baseflow separation methods used to calculate baseflow observations for each station (Durden and others, in process). For baseflow observations corresponding to river or stream reaches that were not bounded by an upstream gauge, the difference between the maximum and minimum values obtained from the five baseflow separation methods accounted for the variability in baseflow of the reach.

For baseflow estimates in reaches that had one or more gauges limiting the upstream extent of any reach, the five ‘baseflow pickup’ estimates were first computed for each individual gauge within the reach (one for each of the baseflow separation methods). For each gauge within the reach, the baseflow estimate for any downstream gauge was subtracted by the baseflow estimate of any upstream gauges. For example, in a reach containing gauges A, B and C, in order from upstream to downstream, the baseflow estimate of Gauge A would not be affected by any upstream gauge estimates. The baseflow estimate of Gauge B would be subtracted by the estimate of Gauge A; and the baseflow estimate of Gauge C would be subtracted by the estimates of both Gauges A and B. This method also applies to gauges downstream of branching reaches, whereby the baseflow estimates of any and all gauges within any branch of the reach are subtracted from the estimates of the downstream gauge.

Once these five 'baseflow pickup' estimates were computed for each gauged reach, minimum and maximum values were computed from the five estimates. A gauged reach is defined as a river or stream reach that is bounded by one gauging station at the downstream limit of the reach and zero or more gauges at the upstream limits of the reach. Only gauged reaches with corresponding non zero weighted observations in the calibration dataset were considered in this analysis. The results of these methods for calibration years 2001 and 2009 are shown in Tables 1 and 2 of Appendix O.

Note that in some reaches of the Suwannee River and its major tributaries that are incised into the Upper Floridan aquifer, target baseflow pickup values used in the calibration were typically estimated as the difference in total flow (rather than baseflow). When these target values were less than or greater than the minimum or maximum values, respectively, determined using the five baseflow separation methods, then the minimum and maximum values used in this assessment were decreased or increased to include the target values. It should also be noted that the minimum and maximum values that were calculated using the method described in the previous paragraph are not intended to define the full range of plausible baseflow or baseflow pickup estimates. Rather, they only represent the minimum and maximum values from the small sample of five or six baseflow methods that were employed in this study.

The true plausible range of estimates could be larger because additional baseflow methods or combinations of methods could produce suitable baseflow estimates outside of the range defined by the sample of baseflow estimation methods employed in this study. This is evident in some of the results shown in Tables 1 and 2 of Appendix O, where simulated values are close to their corresponding target values but still fall outside of the range defined by the available sample of baseflow separation methods.

Finally, it should be noted that the target values shown in Tables 1 and 2 do not equal the mean of the five baseflow method cases where an alternative method was used to estimate a target value, such as using changes in total flow to estimate baseflow pickups in karstic areas lacking well developed surface drainage networks.

In calendar year 2001, there were 79 targets with non zero weighted baseflow targets where variability estimates were available (Table 1 of Appendix O). There were four gauged reaches where the flow in the reach represents the combined contribution of discharge from springs along a river. Calibration targets at these gauges were computed as being equal to average annual (total) flow. Therefore, variability could not be computed from a set of baseflow separation results.

Forty-eight of the simulated values associated with these calendar year 2001 targets were within a range defined by the minimum and maximum values. Sixty-nine of the simulated values were within a factor of 2 or less of these minimum and maximum values. In calendar year 2009, there were 52 targets with non zero weighted baseflow targets where variability estimates were available2 (Table 2 of Appendix O). Twenty-seven of the simulated values associated with these calendar year 2009 targets were within their respective minimum and maximum values. Fifty simulated values were within a factor of 2 of these minimum and maximum values.

The results shown in Tables 1 and 2 of Appendix O indicate that some of the baseflow estimates can be quite variable. For example, values of the target qr01_2319500, (baseflow pickup for the Suwannee River at Ellaville gauged reach) produced from the five baseflow separation methods, ranged over almost an order of magnitude (approximately 190 to 1,080 cfs; Table 1 of Appendix O). The simulated value for target qr01_2319500 (baseflow pickup for the Suwannee River at Ellaville gauged reach) was 728 cfs, which was approximately 300 cfs higher than its corresponding target value but within the range in baseflow pickup estimates produced from the five baseflow separation methods (Table 1 of Appendix O). Note that the target value for this gauged reach was different from the mean of the baseflow pickup estimates from the five baseflow separation methods because this gauged reach occurred in an unconfined, highly karstic area where the Suwannee is incised into the Upper Floridan aquifer. The simulated value is actually nearly identical to the baseflow pickup estimate obtained by averaging the results from the five different baseflow separation methods, indicating a very close match using this alternative, but equally viable target estimate.

The use of changes in total flow (rather than baseflow) in unconfined, karstic river reaches in areas lacking channelized surface drainage networks was implemented at the outset of the project because it provided a means of estimating baseflow pickup that did not require baseflow separation analysis. It is possible that baseflow pickup estimates calculated as changes in baseflow (rather than total flow) may actually provide improved estimates of baseflow pickup because baseflow separation 'filters out' high flow values during periods of rapid hydrograph changes, when flow estimates from stage discharge ratings may be less accurate.

There were several gauging stations where baseflow target estimation was affected by issues commonly encountered with hydrologic data, such as periods of missing data, difficulty in estimating daily values because of rating curve uncertainty arising from unstable channel controls or difficult to measure cross sections, complexity of hydrogeologic conditions near a stream gauging station, or by regulation of surface flows. For example, flow estimates at station 02321975, Santa Fe River at US Highway 441 near High Springs, Florida, were most likely underestimated during the calendar years 2001, 2009 and 2010. Measurements made during these years were wading measurements that were made downstream of the two swallets that capture large quantities of river water in 2009 and 2010, and likely in 2001, as well (Tom Mirti, personal communication). Measurements of 83 and 371 cubic feet per second (cfs) of flow captured by the swallets were made in April 2017 and August 2018 under median and higher than normal conditions, respectively.

These captured flows represented 26 percent of the flow in the river upstream of the swallets during the April 2017 measurement and 24 percent of the flow upstream of the swallets during the August 2018 measurement. Increasing the baseflow estimates at this gauge in the two calibration years increases the target values in the reach upstream of this gauge (targets, qr01_2321975 and qr09_2321975) and decreases the target values downstream of this gauge (targets, qr01_2322500 and qr09_2322500). In both the upstream and downstream set of targets, residuals improve, after correcting these targets, by 25 percent of the mean annual flow at gauging station 2321975, in both years (decreasing by approximately 11 cfs in 2001 and 54 cfs in 2009).

Estimation of baseflow target values can also be difficult and less accurate when extremely high flows occur during a period of interest. Variations in flows during extremely high conditions can be more difficult to estimate because the inundated cross section of the river is much greater under these conditions, so small levels of uncertainty in the river stage can be associated with larger levels of flow uncertainty. In addition, under highly unsteady conditions associated with the downstream propagation of a flood wave, river flows often become more difficult to estimate with stage discharge ratings because the water surface slope (and energy gradient) varies with the passage of the flood wave.

Examples of these conditions that can affect the accuracy of flow (and therefore baseflow) estimates occurred during the spring of 2009, when peak flows on the Alapaha and Withlacoochee Rivers were the highest or among the highest recorded. It is also likely that large quantities of river to aquifer leakage occurred from the Alapaha, Withlacoochee, and Suwannee Rivers as the flood wave progressed downstream through these very karstic river reaches. Such conditions would be expected to diminish the degree to which baseflow or baseflow pickup estimates correspond to recharge rates in the contributing areas to the reaches of interest. These conditions frequently occur during the winter and spring flooding season along the Suwannee, but their effect on flow estimation should be greatest as flooding approaches more extreme levels.

Estimation of baseflow target values can also be difficult and less accurate when the change in flow along a gauged reach is small relative to the magnitude of water flowing in to and out of the reach. Examples of such reaches include the shorter gauged reaches on the Suwannee River between the Ellaville and Luraville gauging stations. The changes in total flow in these reaches were less than ten percent of the flow at the downstream end of the reach, indicating that the estimated changes in flow (and therefore baseflow) in these reaches may be small (and therefore of limited significance) relative to uncertainties in estimating flows at the upstream or downstream limits of these gauged reaches.

These problems are compounded during years with extreme flooding conditions, such as those described in the previous paragraph. Another example is the gauged reach upstream from the Suwannee River near Wilcox. The baseflow estimate for this site was only about five percent of the annual mean flow in 2001. In addition, tidal variations in flow at the Wilcox gauge can be quite large, making it difficult to estimate flows because of variable slope conditions, as evidenced by the fact that the accuracy of the flow record in 2001 was described as poor.

Even in the absence of extreme conditions or conditions that pose challenges for estimating flow records, baseflow estimation is commonly subject to high levels of uncertainty. ASTM document, D5981/D5981M-18, (ASTM, 2018) notes that "… baseflow estimates are generally accurate only to within an order of magnitude", so the simulated baseflow values were also evaluated to see if they fell within an order of magnitude of the corresponding target. Model simulated baseflow values were generally well within an order of magnitude of the corresponding target value in both calibration years. Seven simulated values were an order of magnitude beyond the target value, however.

In one of these (corresponding to observation qr01_2324000), the actual baseflow target appears to be too high (and should therefore have been zero weighted) because more than five months of poor quality estimated daily flows occurred during calendar year 2001 at gauge 02324000. The simulated value corresponding to observation qr01_2314500 is associated with the reach upstream of gauge 02314500, Suwannee River at US Highway 441 near Fargo, Georgia. Baseflow estimation at this site may be difficult to estimate because the Okefenokee Swamp constitutes a large proportion of the drainage basin. Low flows at the site are also affected at times by Mixons Ferry Dam (Alhadeff, Jack S., and McCallum, B., 2002).

The remaining simulated values that differed from their corresponding targets by more than an order of magnitude were generally comparable in magnitude to the minimum or maximum estimated baseflow values or the difference between simulated and target values were generally less than about 2 cfs. For example, the simulated value corresponding to observation qr01_2244420 was 2.8 cfs, which was very close to the corresponding minimum baseflow estimate of 3.5 cfs. An exception to this was the simulated value corresponding to observation qr01_2324500 on the Fenholloway River near Foley, Florida), which is very close to a localized, large volume industrial groundwater withdrawal and treated wastewater return.

Spring Flow Target Uncertainty

Uncertainty in the values of spring flow targets is a function of a variety factors. These include uncertainties in field measurements, rating curve estimation error (for spring measurements that are based on 'rating curves' that are fit to field measurements), insufficient numbers of measurements (time sampling errors), and departures from steady state assumptions (in which spring flows used to calibrate a model are generated by significant changes in storage during the calibration period, in addition to average recharge rates during the calibration period). Some studies indicated that the errors in individual flow measurements could range from 2 to 20 percent (Sauer and Meyer 1992).

Continuous spring flows are typically computed from rating curves that are based on relations between field measured spring flows and continuous measurements of stage, velocity, or groundwater level. Therefore, the accuracy of spring flows depends on the accuracy of rating curves and the individual measurements of spring flows. Harmel and others (2006) indicated that cumulative errors associated with rating curves and individual flow measurements could range from 3 to 42 percent (Harmel and others 2006). Some springs also lack well defined 'spring runs' or experience reversing when the stage in receiving water bodies rises, making them difficult to measure and increasing the uncertainty associated with field measurements or continuous flow data.

A small fraction of the springs simulated in the NFSEG have continuous flow estimates, and most of the springs (65 percent) simulated in the NFSEG model have fewer than five measurements available within their period of record, so few of the spring flow targets used to calibrate the NFSEG model were based on a complete set of 365 daily spring flow values within a given calibration year. Therefore, factors in addition to measurement error must be considered when characterizing target uncertainty.

One of these factors is time sampling uncertainty, which is the uncertainty arising from having a limited number of (field or rating curve based) measurements to estimate the spring flow in a given period (including estimating the typical or long term median or average flow). Even in the few instances when a complete set of daily flow values were available within a given year, uncertainty in the targets still exists because of departures from the steady state assumptions and because of measurement error. Therefore, the uncertainty associated with spring flow measurement error will probably be the least important contributor to target uncertainty in most cases.

Standard procedures for establishing acceptable error bounds for spring flow targets (or head, baseflow, or other targets) are not well documented. This is perhaps not surprising because the relative worth of a given target or type of target will likely depend on the nature of a desired prediction (for example prediction type or location) and the consequences (benefits and risks) associated with a given decision. Given the fact that these factors are often not known in advance for a prediction and that errors stemming from sample limitations or departures from steady state assumptions, errors most likely account for much of the uncertainty in spring flow targets. Perhaps the most useful approach to evaluating the model fit to spring flows is to characterize the temporal variability of spring flows.

This flow variability information can then be used to provide a useful and generally applicable context for evaluating the difference between simulated spring flows and their corresponding target values. For example, if a given spring flow residual is negative (underestimates a target spring flow), then the magnitude of that residual could be compared to the expected difference between period of record minimum and median measured spring flow. Similarly, if a given spring flow residual is positive (overestimates a target spring flow), the magnitude of that residual could be compared to the expected difference between maximum and median measured spring flow.

This approach of characterizing uncertainty of spring flow targets based on spring flow variability can be employed with the NFSEG model. As noted above, most springs represented in the NFSEG model only have a few spring flow measurements available. Therefore, assessing spring flow variability was implemented in a multistep process that leveraged data from springs with larger numbers of measurements. The initial steps in this process were as follows: (1) select a subset of NFSEG springs at which 10 or more flow measurements were available from the period of record at that spring, (2) calculate minimum, maximum, and median values for the period of record at these selected springs, (3) calculate the difference between period of record maximum and median values for each spring, and (4) calculate the difference between period of record minimum and median values for each spring. These last two steps resulted in a dataset comprising 114 springs at which differences between period of record minimum and median values and period of record differences between maximum and median values were computed.

These two sets of differences (maximum minus median and median minus minimum) were then ‘scaled’ at each spring by dividing these differences by the respective period of record median flow at each spring. This was done so that the resulting differences for each spring would be normalized by their respective magnitude of flow.

Thereby becoming useful for estimating flow variability at springs spanning a wide range of flows. For discussion purposes, the resulting 'scaled differences' were referred to as normalized minimums (calculated as the quantity, median minus minimum, divided by median) and normalized maximums (calculated as the quantity, maximum minus median, divided by median).

The final step in this process was to compute summary statistics for the set of normalized minimums and normalized maximums that were calculated for the set of 114 springs with ten or more measurements. Among these springs, the median value of the normalized minimum was 0.74, with lower and upper quartiles (25^{th} and 75^{th} percentiles, respectively) equal to 0.45 and 1.0, respectively. Among this same set of springs, the median value of the normalized maximum was 1.2, and the lower and upper quartiles were 0.60 and 2.5, respectively

A description of how the summary statistics described in the previous paragraph might be applied to evaluate spring flow residuals is provided in the following example of a spring that has a hypothetical target value of 15 cfs and a 10 cfs simulated value from the calibration, yielding a residual of -5 cfs. Because this is a negative valued residual (underestimation), a summary statistic that describes the normalized minimums is the basis for our estimate. If the residual had been positively valued, we would have selected a statistic describing the normalized maximums. In this example we'll use the median of the normalized minimums but we could choose the lower (or upper) quartile of the normalized minimums if we wanted a more (or less) restrictive estimate of the range. As described in the previous paragraph, the median value of the normalized minimums from the 114 springs with ten or more measurements was 0.74. The estimate of the minimum value for our target is therefore, 15 – (0.74*15), which equals 15 – 11.1 or 3.9 cfs (a difference of 11.1 cfs from the target value). Recall that our simulated value in this example was 10 cfs and our residual was -5 cfs, so we would note that our simulated and residual values were within a plausible range of variability at this spring.

Comparisons of Groundwater Level Residual Statistics to Other Models

The models selected for the residual statistics comparison include existing regional scale models developed for or by SJRMWD or SRWMD. The models have overlapping domains with NFSEG v1.1 and are used for regulatory and/or water use planning purposes. The models selected are as followed, SRWMD Version 2 of the North Florida model (NF v2; Intera, Inc. 2014), version 2 of the Peninsular Florida model (PF v2; Intera, Inc. 2011), and the following SJRWMD models: version 3 of the Northeast Florida model (NEF v3; Russo 2011), the North Central Florida model (NCF; Motz and Dogan, 2004), the Volusia model (VOL; Williams 2006), and the East Central Florida model (ECF; McGurk and Presley 2002) (Table 4-9). In comparison to NFSEG v1.1, all the aforementioned models have a smaller active area and less groundwater level targets. Save PF v2, all have the same cell size spacing: 2,500 by 2,500 ft (Table 4-9).

Table 4-9. Model calibration and discretization properties

Ground water Model	Number of SAS Targets	Number of UFA Targets	Discretization of Uniform Grid			Active Area (mi^2)
			Column	Rows	Spacing (ft)	
NF v2	118	487	490	380	2,500	26,700
PF v2	343	669	210	300	5,000	57,000
NEF v3	43	131	200	260	2,500	11,700
NCF	82	279	150	168	2,500	5,650
VOL	55	72	100	100	2,500	2,200
ECF	100	208	194	174	2,500	7,600
NFSEG v1.1 (2009)	567	990	704	752	2,500	60,000

The comparisons of surficial aquifer system and Upper Floridan aquifer groundwater level residual statistics for each model to NFSEG v1.1 are explained below and included: 1) domain wide comparisons, 2) model overlap comparisons, and 3) 1-to-1 model overlap comparisons

1) Domain Wide Comparisons: The calibration statistics in Table 4-10 are representative of the entire active extents of the model layers used to represent the SAS and UFA in their respective models. The table shows that NFSEG v1.1 calibration statistics are either comparable or in some cases better than the numerous regional models it was compared against. The statistics shown for comparison models may include groundwater level calibration targets that are outside of the NFSEG v1.1 model domain. For the NFSEG v1.1 2009 calibration year, SAS statistics do not include synthetic targets which are not observations but estimates that were utilized to impart system knowledge to PEST in areas of scarce groundwater level observations.

2) Model Overlap Comparisons: Further analyzing the calibration statistics of NFSEG v1.1 versus those of the existing regional scale models, the data sets used to determine the calibration statistics were limited to groundwater level observations located within the respective areas of domain overlap. This comparison excludes the regions of the respective model domains which are outside the areas of overlap between the domain of NFSEG and the respective regional scale models, thus providing a more direct comparison. For this reason, model

Table 4-10. Domain-wide groundwater-level calibration statistics comparison

Groundwater Model	SAS				UFA			
	Number of Targets	Mean Error (ft)	Abs Mean Error (ft)	RMSE* (ft)	Number of Targets	Mean Error (ft)	Abs Mean Error (ft)	RMSE * (ft)
NF v2	118	-0.77	4.54	7.43	487	-0.83	2.79	4.09
PF v2	343	1.99	8.15	12.24	669	0.12	3.52	4.92
NEF v3	43	1.57	2.63	3.82	131	1.31	2.50	3.26
NCF	82	0.19	4.01	4.84	279	0.01	3.10	3.75
VOL	100	-0.55	3.21	5.01	208	-0.43	2.41	3.07
ECF	55	0.98	3.65	6.44	72	-0.08	2.80	3.63
NFSEG v1.1 (2001)	228	-0.06	4.20	6.23	979	-0.45	3.68	4.98
NFSEG v1.1 (2009)	328	0.10	3.60	5.79	990	-0.91	3.40	4.67

overlap comparisons are more appropriate than the comparisons represented in Table 4-10 that include observations from large areas not common to both models. Statistics for the NFSEG v1.1 2001 and 2009 calibration years show that NFSEG v1.1 is calibrated comparatively with other regional models in the SAS and UFA (Table 4-11).

3) 1-to-1 Model Overlap Comparisons: Observation points were limited to groundwater level targets utilized in the calibration of both models. The 1-to-1 model overlap comparison is the most direct method for comparisons of the groundwater level residuals because it excludes targets from outside the areas of overlap and includes only those targets that were common to both model calibrations. For these reasons, it is the most reliable indicator of the quality of the NFSEG v1.1 2009 calibration relative to those of the existing regional scale models to which it was compared (Table 4-12 a, Table 4-12 b). The results indicate that both the NFSEG v1.1 2001 and 2009 calibrations are at least comparable to the other regional scale models and many cases are arguably better (Table 4-12 a, Table 4-12 b).

Comparisons to PF v2 and NF v2 are perhaps the most instructive, because the respective domains of these two models overlap to the largest extent with the domain of NFSEG v1.1 and more comparable to NFSEG v1.1 in terms of domain extent and the numbers of targets common to their respective calibrations.

Table 4-11. Model overlap groundwater-level calibration statistics comparison

Ground water Model	SAS				UFA			
	Number of Targets	Mean Error (ft)	Abs Mean Error (ft)	RMSE* (ft)	Number of Targets	Mean Error (ft)	Abs Mean Error (ft)	RMSE* (ft)
NF v2	114	-0.35	4.22	6.00	470	-0.84	2.83	4.13
NFSEG v1.1 2001	209	-0.18	4.00	5.77	784	-0.57	3.74	5.10
NFSEG v1.1 2009**	224	0.20	3.52	5.75	790	-0.93	3.37	4.71
PF v2	138	1.28	6.32	8.66	673	0.13	2.53	3.32
NFSEG v1.1 2001	187	-0.42	3.93	5.78	628	-0.25	3.33	4.35
NFSEG v1.1 2009**	203	0.24	3.58	5.94	637	-0.53	3.00	4.11
NEF v3	43	1.57	2.63	3.82	131	1.31	2.50	3.26
NFSEG v1.1 2001	120	0.06	3.98	5.71	298	0.80	3.41	4.39
NFSEG v1.1 2009**	115	0.29	3.65	6.21	289	0.37	2.80	3.94
NCF	75	0.31	4.10	4.95	253	0.02	3.09	3.75
NFSEG v1.1 2001	115	-1.85	4.44	6.53	265	-0.85	3.07	3.95
NFSEG v1.1 2009**	107	-0.26	4.41	7.47	268	0.39	2.63	3.61
VOL	38	0.11	2.81	5.05	47	0.04	2.67	3.46
NFSEG v1.1 2001	45	-1.69	3.62	5.78	53	-1.51	3.22	3.83
NFSEG v1.1 2009**	41	0.66	2.39	3.52	50	0.70	2.97	3.68
ECF	17	-0.92	3.01	5.27	17	-1.49	3.08	4.06
NFSEG v1.1 2001	21	-2.67	3.67	5.34	29	-3.08	4.45	4.96
NFSEG v1.1 2009**	26	-2.62	4.29	6.13	30	0.75	2.69	3.56

*Root mean square of errors
**The NFSEG v1.1 2009 calibration statistics do not include synthetic targets for the SAS.

Table 4-12a. 1-to-1 Model overlap groundwater-level calibration statistics comparison surficial aquifer

Groundwater Model	SAS			
	Number of Targets	Mean Error (ft)	Abs Mean Error (ft.)	RMSE (ft)
NF v2 w/ Common NFSEG v1.1 2001 Targets	79	0.77	3.58	5.33
NFSEG v1.1 2001 w/Common NF v2 Targets	79	0.10	3.92	6.15
NF v2 w/ common NFSEG v1.1 2009 Targets	73	0.84	3.12	4.71
NFSEG v1.1 2009 w/Common NF v2 Targets	73	0.58	3.42	4.68
PF v2 w/ common NFSEG v1.1 2001 Targets	70	-1.93	8.78	13.78
NFSEG v1.1 2001 w/Common PF v2 Targets	70	-0.96	4.65	7.15
PF v2 w/ common NFSEG v1.1 2009 Targets	56	-0.35	8.19	13.64
NFSEG v1.1 2009 w/Common PF v2 Targets	56	0.38	3.93	5.29
NEF v3 w/ common NFSEG v1.1 2001 Targets	37	1.52	2.74	4.02
NFSEG v1.1 2001 w/Common NEF v3 Targets	37	0.93	4.08	6.20
NEF v3 w/ common NFSEG v1.1 2009 Targets	35	1.57	2.85	4.13
NFSEG v1.1 2009 w/Common NEF v3 Targets	35	0.57	3.87	5.29
NCF w/ common NFSEG v1.1 2001 Targets	38	1.84	4.39	5.13
NFSEG v1.1 2001 w/Common NCF Targets	38	-1.54	3.96	5.92
NCF w/ common NFSEG v1.1 2009 Targets	34	1.77	4.60	5.28
NFSEG v1.1 2009 w/Common NCF Targets	34	-0.53	4.33	5.89
VOL w/ common NFSEG v1.1 2001 Targets	31	-0.18	2.97	5.35
NFSEG v1.1 2001 w/Common VOL Targets	31	-1.67	3.44	5.30
VOL w/ common NFSEG v1.1 2009 Targets	27	-0.35	3.20	5.69
NFSEG v1.1 2009 w/Common VOL Targets	27	0.54	2.75	3.98
ECF w/ common NFSEG v1.1 2001 Targets	5	-3.95	4.65	8.47
NFSEG v1.1 2001 w/Common ECF Targets	5	-2.10	2.17	2.80
ECF w/ common NFSEG v1.1 2009 Targets	7	-2.68	3.68	7.20
NFSEG v1.1 2009 w/Common ECF Targets	7	0.67	3.05	3.44

Table 4-12b. 1-to-1 Model overlap groundwater-level calibration statistics comparison upper Floridan aquifer

Groundwater Model	UFA			
	Number of Targets	Mean Error (ft)	Abs Mean Error (ft.)	RMSE (ft)
NF v2 w/ Common NFSEG v1.1 2001 Targets	311	-0.46	2.32	3.51
NFSEG v1.1 2001 w/Common NF v2 Targets	311	-0.35	3.24	4.37
NF v2 w/ common NFSEG v1.1 2009 Targets	304	-0.54	2.40	3.68
NFSEG v1.1 2009 w/Common NF v2 Targets	304	-0.97	3.15	4.57
PF v2 w/ common NFSEG v1.1 2001 Targets	375	-0.40	3.14	4.14
NFSEG v1.1 2001 w/Common PF v2 Targets	375	-0.30	3.40	4.50
PF v2 w/ common NFSEG v1.1 2009 Targets	343	-0.18	3.07	4.06
NFSEG v1.1 2009 w/Common PF v2 Targets	343	-0.46	3.03	4.28
NEF v3 w/ common NFSEG v1.1 2001 Targets	124	1.24	2.43	3.20
NFSEG v1.1 2001 w/Common NEF v3 Targets	124	0.43	3.07	4.21
NEF v3 w/ common NFSEG v1.1 2009 Targets	118	1.36	2.42	3.22
NFSEG v1.1 2009 w/Common NEF v3 Targets	118	0.10	2.39	3.84
NCF w/ common NFSEG v1.1 2001 Targets	163	-0.07	3.01	3.71
NFSEG v1.1 2001 w/Common NCF Targets	163	-1.17	2.59	3.21
NCF w/ common NFSEG v1.1 2009 Targets	160	-0.08	3.02	3.72
NFSEG v1.1 2009 w/Common NCF Targets	160	0.30	2.37	3.06
VOL w/ common NFSEG v1.1 2001 Targets	35	0.00	2.61	3.49
NFSEG v1.1 2001 w/Common VOL Targets	35	-1.52	2.80	3.39
VOL w/ common NFSEG v1.1 2009 Targets	34	0.01	2.80	3.60
NFSEG v1.1 2009 w/Common VOL Targets	34	0.93	2.54	3.20
ECF w/ common NFSEG v1.1 2001 Targets	8	-0.92	3.04	4.62
NFSEG v1.1 2001 w/Common ECF Targets	8	-3.34	3.65	4.19
ECF w/ common NFSEG v1.1 2009 Targets	8	-0.92	3.04	4.62
NFSEG v1.1 2009 w/Common ECF Targets	8	0.58	2.19	2.89

Statistical and Spatial Trends in NFSEG v1.1 Groundwater Level Residuals and Comparison of Trends to Other Groundwater Models

Groundwater level target residuals for the Upper Floridan aquifer were mapped across the NFSEG v1.1 model domain for both the 2001 and 2009 calibration years (Figures 4 -21 and 4-22). It was observed that Upper Floridan aquifer groundwater level residuals in much of Duval, Clay, and St. Johns counties, Florida, and Camden County, Georgia, reflect widespread under simulation by the model. Conversely, in much of Columbia, Hamilton, Suwannee, Madison, and Gilchrist counties, Florida, they reflect widespread over simulation by the model.

NFSEG is like other regional scale models in that certain areas of the model domain are prone to certain types of problems that are local to the areas in question, the result being that over or under simulation prevails within certain parts of the model domain. Examples of existing regional scale models that exhibit similar results include the SJRWMD NEF v3 model, the SRWMD NF v2 model, and the SJRWMD NCF v2 model. These models are all peer reviewed groundwater models that have been utilized in MFL and regulatory evaluations.

Examination of the calibration results of these models shows numerous clusters of either positive or negative groundwater level residuals. Similar clusters appear in the same or similar locations in models that were calibrated to different calibration periods. The underlying causes of such tendencies are difficult to ascertain and eliminate.

A pre dominance of positive or negative groundwater level residuals within a sub region is indicative of "trends" in groundwater level residuals. The trends described above were also identified in previous models used for regulatory and/or MFL purposes that have significant overlap with the NFSEG v1.1 model. This includes the SRWMD NF v2 model (Intera, Inc. 2014) and the PF v2 model (Intera, Inc. 2011). (Figures 4-83 and 4-84). Note that residuals from -5 to +5 were removed from displaying on Figures 4-83 and 4-84 for better representation of trends.

Upper Floridan aquifer groundwater level target residual maps were also prepared for other previous regulatory models such as SJRWMD's NEF v3 model (Russo 2011) and North Central Florida model (NCF; Motz and Dogan, 2004) however they did not have sufficient observations for comparison.

Calibration Derived Transmissivity of the Upper Floridan aquifer of NFSEG v1.1 versus Corresponding APT Derived Values

APT data from the water management districts as well as the USGS APT database used to create the 2010 map titled, *"Transmissivity of the Upper Floridan aquifer in Florida and Parts of Georgia, South Carolina, and Alabama"* (Scientific Investigations Map (SIM) 3204; Kuniansky and others 2012) were compared to NFSEG calibration derived transmissivity values. During the review of the USGS and internal databases performed by SJRWMD, APTs were chosen for comparison to calibration derived values if they contained an observation well in the same zone as the pumping well and a minimum

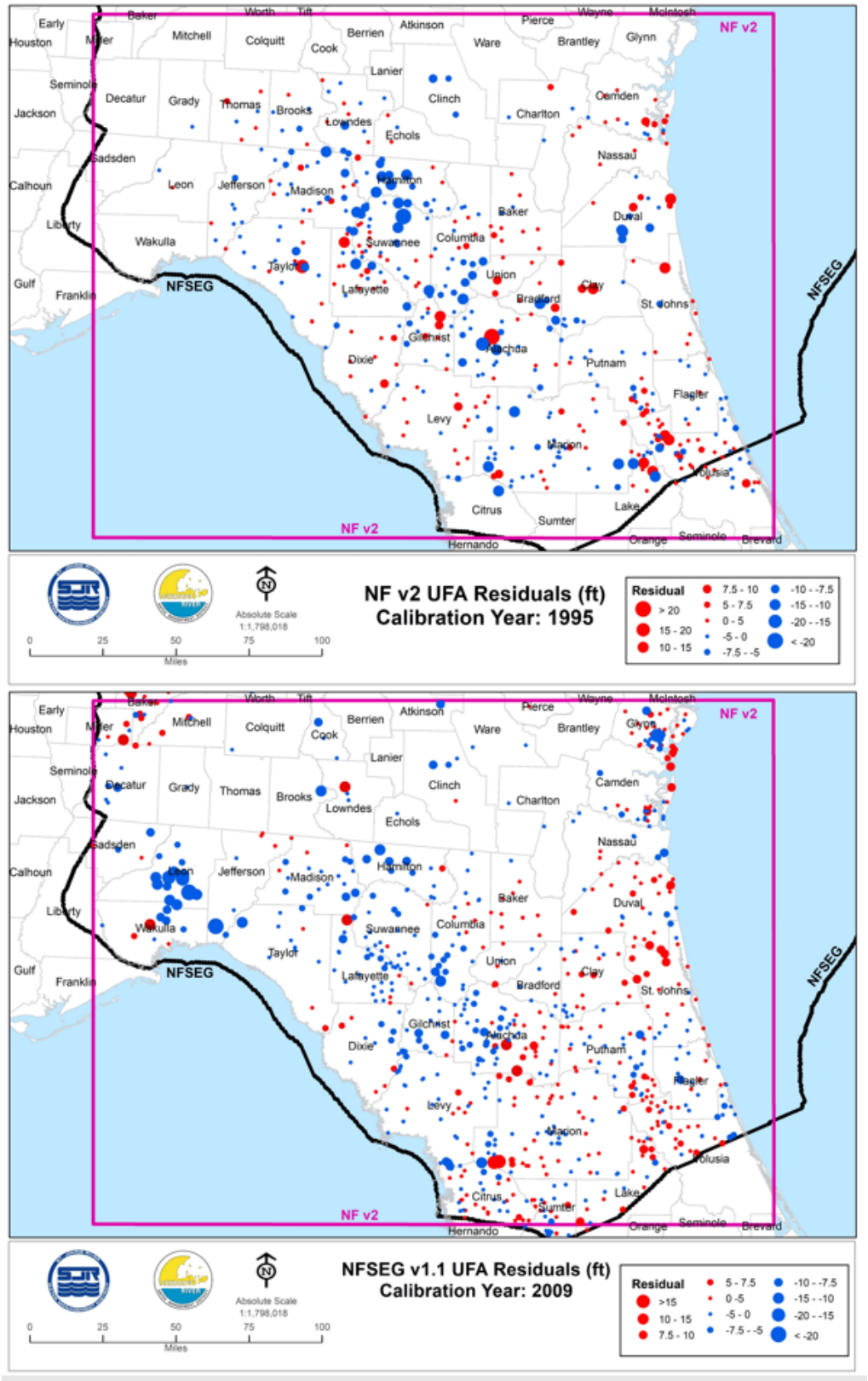

Figure 4-83. Residuals of UFA hydraulic head (feet), North Florida Model Version 2 and NFSEG v1.1 (2009)

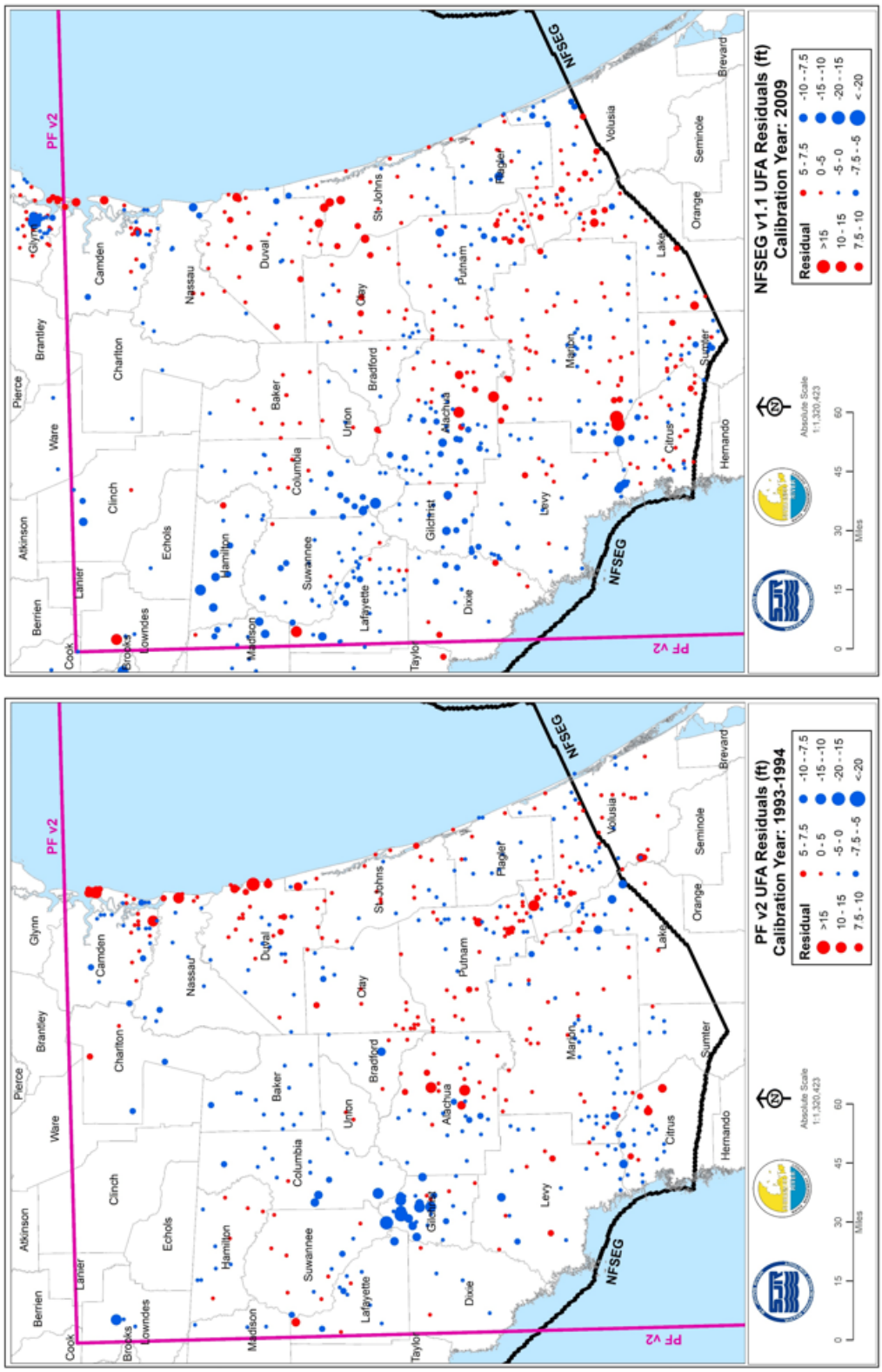

Figure 4-84. Residuals of UFA hydraulic head (feet), Peninsular Florida Model Version 2 and NFSEG v1.1 (2009)

test duration of 12-24 hours. Exceptions were made in areas where limited APT data were available, such as in the SRWMD. A total of 109 APTs were thus selected for comparison to NFSEG calibration derived transmissivity values (Figure 4-92). As part of the analysis, the APT derived transmissivity values were normalized by layer thickness for more accurate comparison.

A comparison of NFSEG v1.1 calibration derived transmissivity values versus APT derived transmissivity values for areas in which the Upper Floridan aquifer is confined is shown in Figure 4-85. The same comparison for unconfined areas is shown in Figure 4-86. Out of the 109 APTs selected for comparisons with the NFSEG v1.1 model, 84 lie within confined regions and 25 within unconfined regions. Review of Figure 4-85 indicates that 90 percent of the points (76 out of 84) are within an order of magnitude of the line of equality in the confined portions of the system. Review of Figure 4-86 shows that 56 percent of the points (14 out of 25) are within one order of magnitude of the line of equality in the unconfined portion of the model domain.

In both cases, the APT/modeled comparison indicates that modeled Upper Floridan aquifer transmissivities generally tend to be somewhat greater than the APT values, with points in the unconfined areas exhibiting more of this tendency. This is perhaps not surprising given the karstic nature of the Upper Floridan aquifer, and the tendency for karst features to be more highly developed in unconfined areas. Aquifer performance tests 'sample' a smaller volume of the aquifer than the resolution of the model grid or the scale with which properties might be inferred through calibration with the available data and parameterization scheme. It can also be difficult to stress the system sufficiently in highly transmissive, karstic areas. Thus, aquifer performance tests may not reflect transmissivity contributions from karst features (and their connections) that may occur over longer spatial scales or may reflect local scale variability in transmissivity.

It is important to note that USGS SIM 3204 was derived from surface interpolation of the APT data points only. As such, although the map shows the spatial distribution of transmissivity within a very large area, the accuracy of the transmissivity values shown on the map should be considered very low in the areas where APT data are not available or sparse. The compilation of the map did not consider Upper Floridan aquifer potentiometric surface gradients, presence or absence of surface drainage networks, or areas of concentrated groundwater discharge from springs, all of which provide useful information for making inferences about the spatial distribution of transmissivity. As a result, changes in transmissivities that might be indicated by such data may not be mapped when interpolating between sparsely spaced points. Therefore, it is expected that there will be differences between SIM 3204 and our modeled Upper Floridan aquifer transmissivity.

Perhaps the most useful approach for comparing transmissivity estimates derived from the NFSEG v1.1 calibration with those derived from APT results is to compare them geographically (Figure 4-87) rather than with scatter plots, such as those shown in Figures 4-85 and 4-86. Such a comparison was performed and indicated a spatial correlation between both sets of estimates. The APT derived values in the core areas of the model domain in northern peninsular Florida are generally within an order of magnitude of the calibration derived values in the same general area.

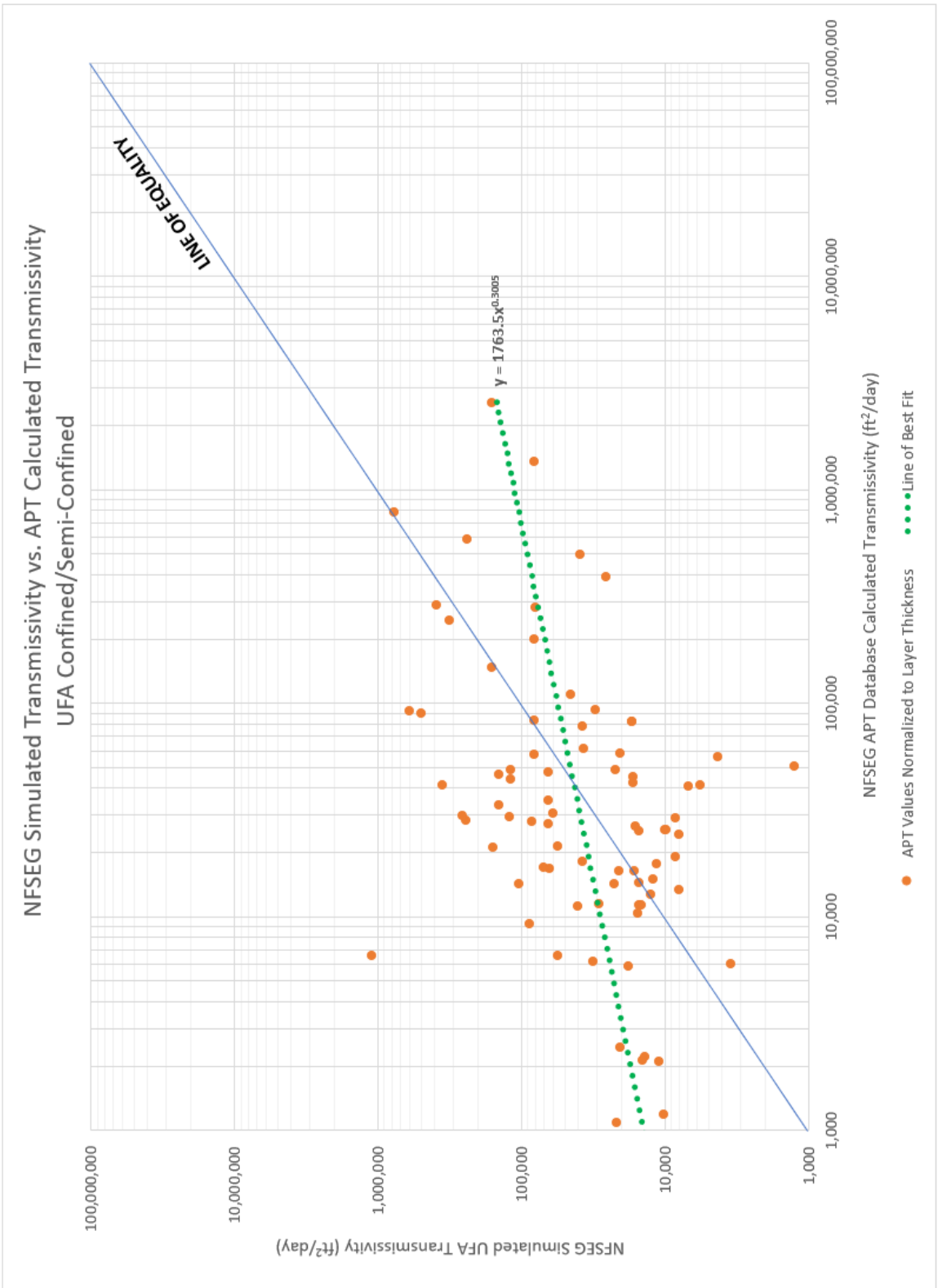

Figure 4-85. Scatter plot of NFSEG v1.1 transmissivity vs. NFSEG APT database, confined region

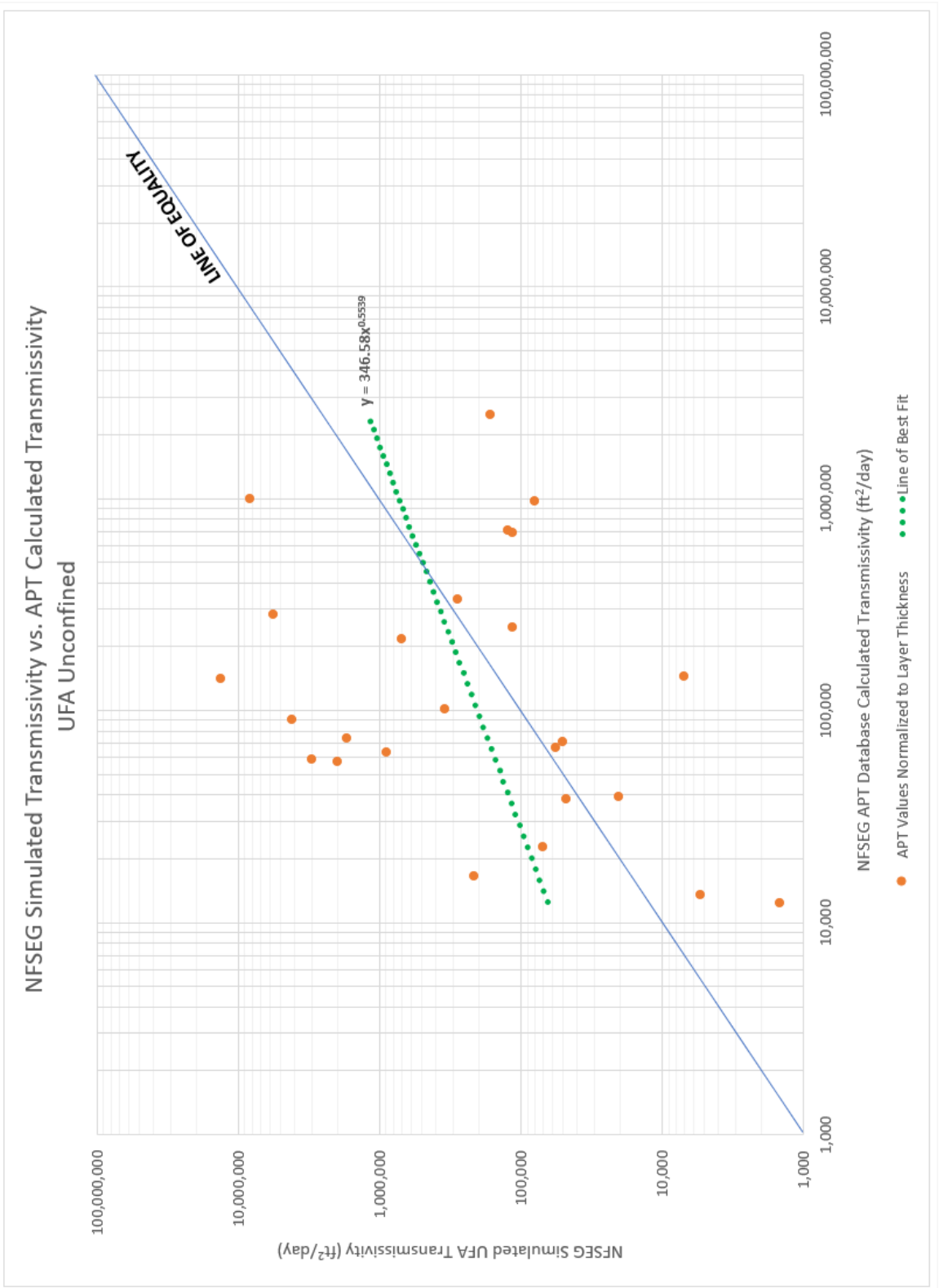

Figure 4-86. Scatter plot of NFSEG v1.1 transmissivity vs. NFSEG APT database, unconfined region

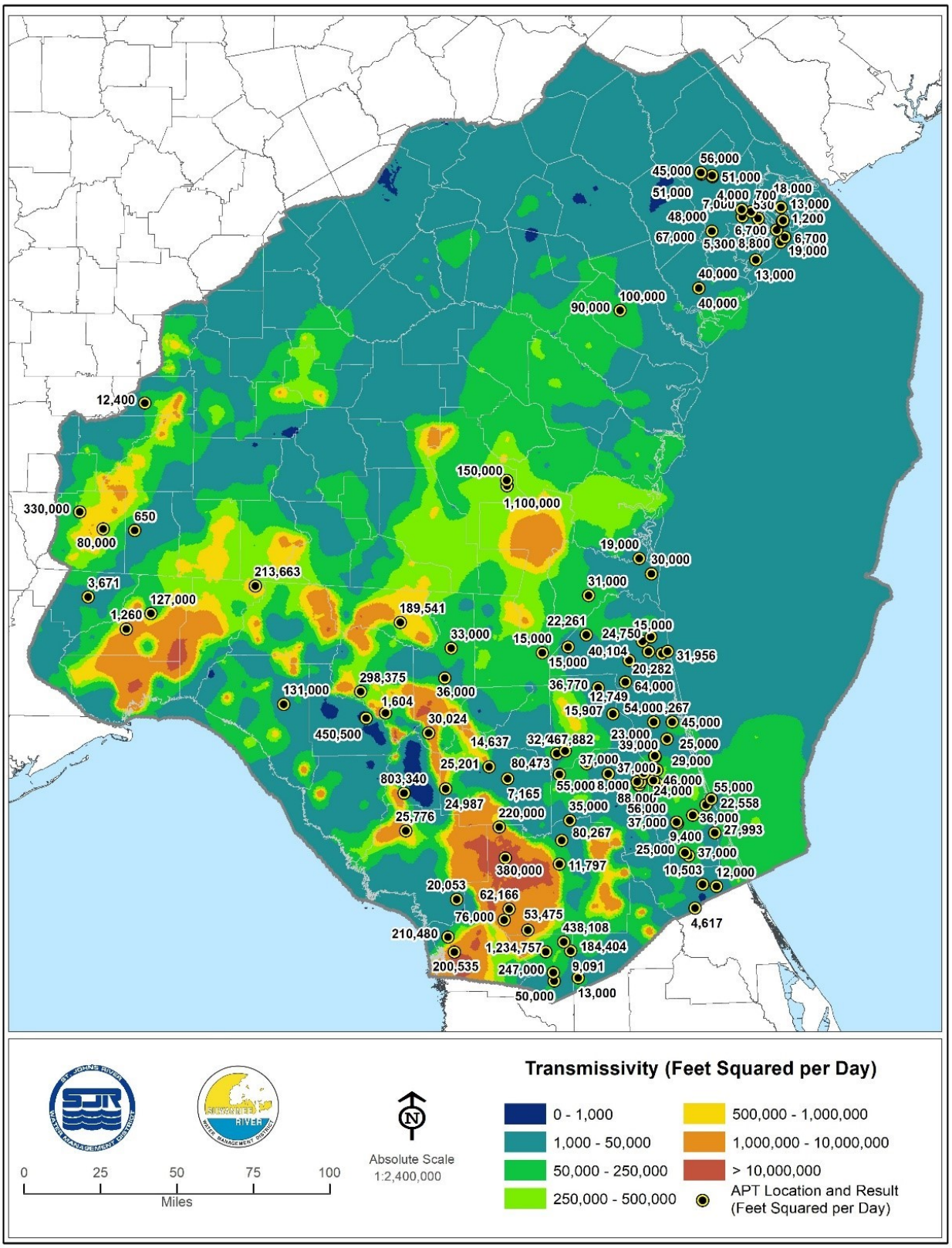

Figure 4-87. Locations and results of APTs used for comparisons to calibration-derived transmissivities

In addition, the geographic comparison indicates that many of the points exhibiting larger differences between APT and calibration derived values occur in locations where there are large changes in transmissivity over short distances. Finally, some of the large discrepancies between APT derived and calibration derived values where transmissivity is likely to be highest, are the highly karstic contributing areas to the Silver and Rainbow rivers in eastern Levy and central and western Marion counties, and in Citrus County (Figure 4-87).

Calibration Derived Transmissivity of the Upper Floridan aquifer in Previous Regional Groundwater Models versus Corresponding APT Derived Values

Comparison plots for calibration derived transmissivity values versus the APT derived transmissivity values were also completed for the NF v2 and PF v2 regional groundwater models. Both models share the significant domain overlap and similar domain size as NFSEG v1.1. The same set of NFSEG v1.1 APT derived transmissivity values were applied in the analysis, except only APTs that fell within each respective model domain were included. APT derived transmissivity values were normalized by layer thickness for a more accurate comparison.

Scatter plots of the NF v2 calibration derived transmissivity values versus the NFSEG v1.1 APT derived transmissivity values include 79 out of the 109 APTs selected for development of NFSEG v1.1. Fifty five of the 79 APTs were performed within confined portions of the groundwater system, and the other 24 were within unconfined areas. Review of Figure 4-88 indicates that in the confined areas, 89 percent of the points (49 out of 55) were within one order of magnitude of the line of equality. Review of Figure 4-89 shows that in unconfined areas 79 percent of the points (19 out of 24) were within one order of magnitude of the line of equality.

Scatter plots of the PF v2 calibration derived transmissivity values versus the NFSEG v1.1 APT derived transmissivity values include 75 out of the 109 APTs selected for development of NFSEG v1.1. Fifty five of the 79 APTs were performed within confined portions of the groundwater system and the other 20 were within unconfined areas. Review of Figure 4-90 indicates that in the confined areas, 98 percent of the points (54 out of 55) were within one order of magnitude of the line of equality. Review of Figure 4-91 shows that in unconfined areas 65 percent of the points (13 out of 20) were within one order of magnitude of the line of equality.

Overall, the comparison plots of APT derived transmissivity values to calibration derived transmissivity values correspond well to the calibration derived NFSEG v1.1 comparisons. The PF v2, NF v2, and NFSEG v1.1 models exhibit similar degrees of variability in confined areas, and each exhibits a higher degree of variability in unconfined regions due to reasons stated previously.

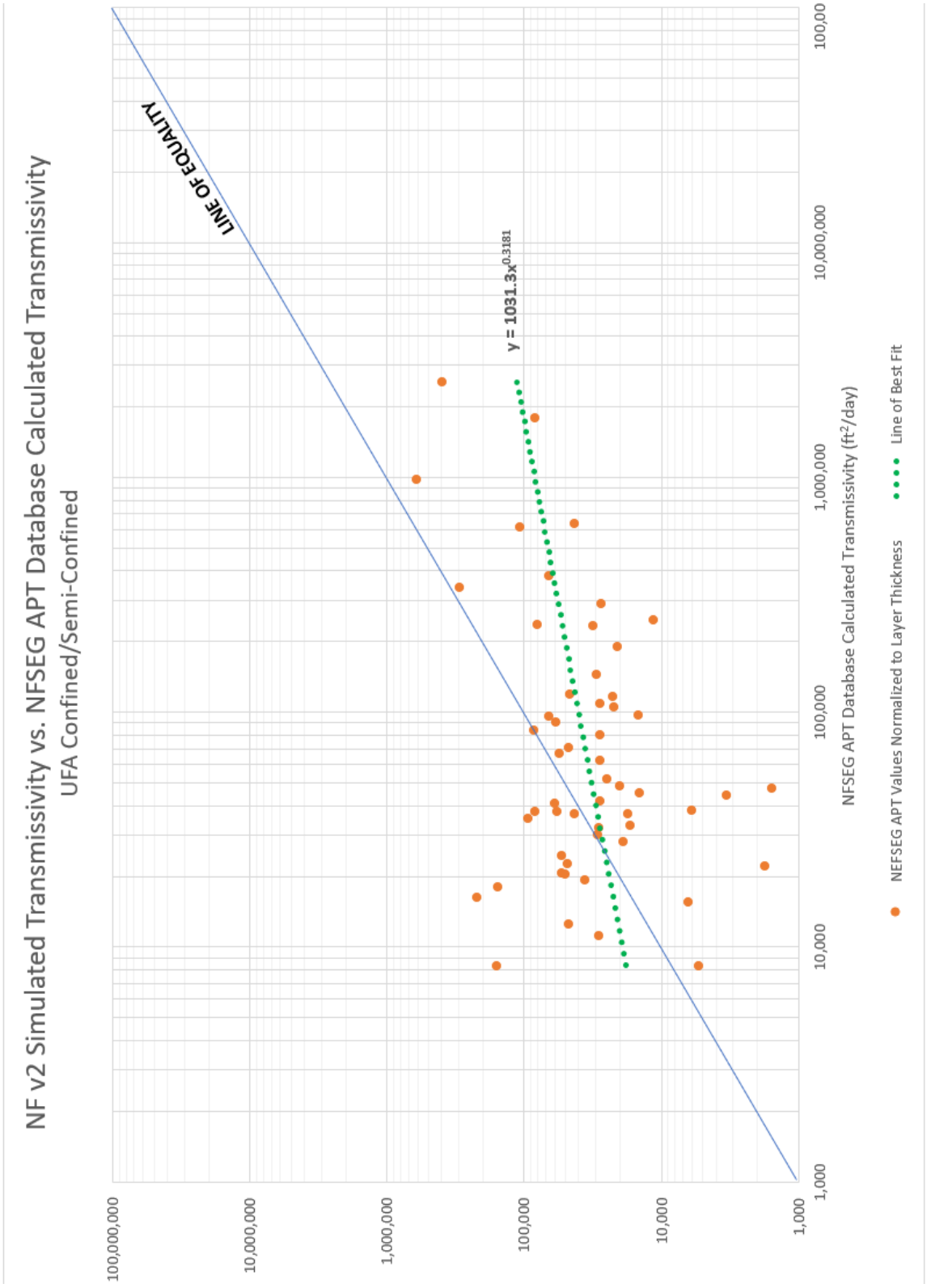

Figure 4-88. Scatter plot of NF v2 UFA transmissivity vs. NFSEG APT database, confined region

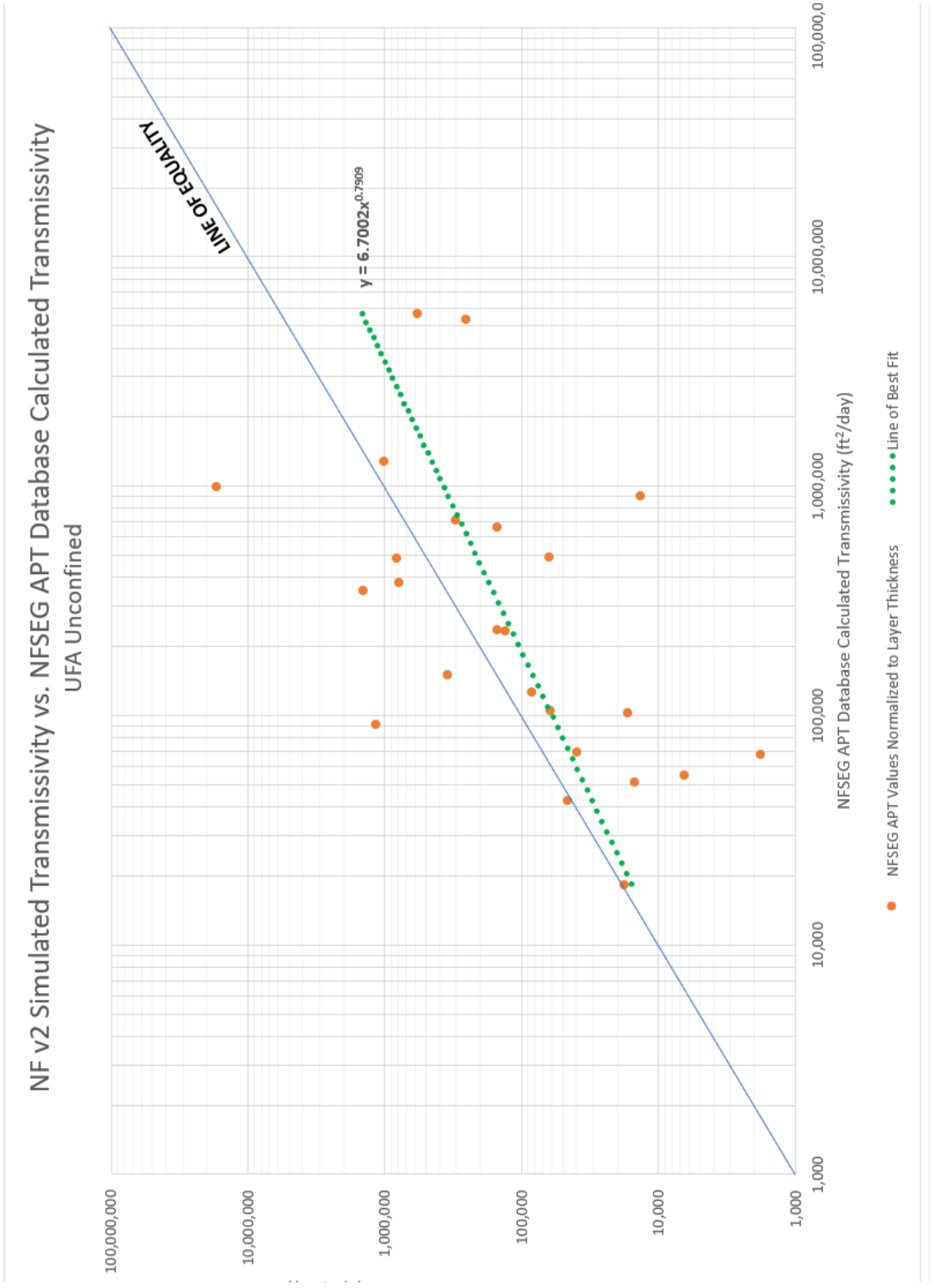

Figure 4-89. Scatter plot of NF v2 UFA transmissivity vs. NFSEG APT database, unconfined region

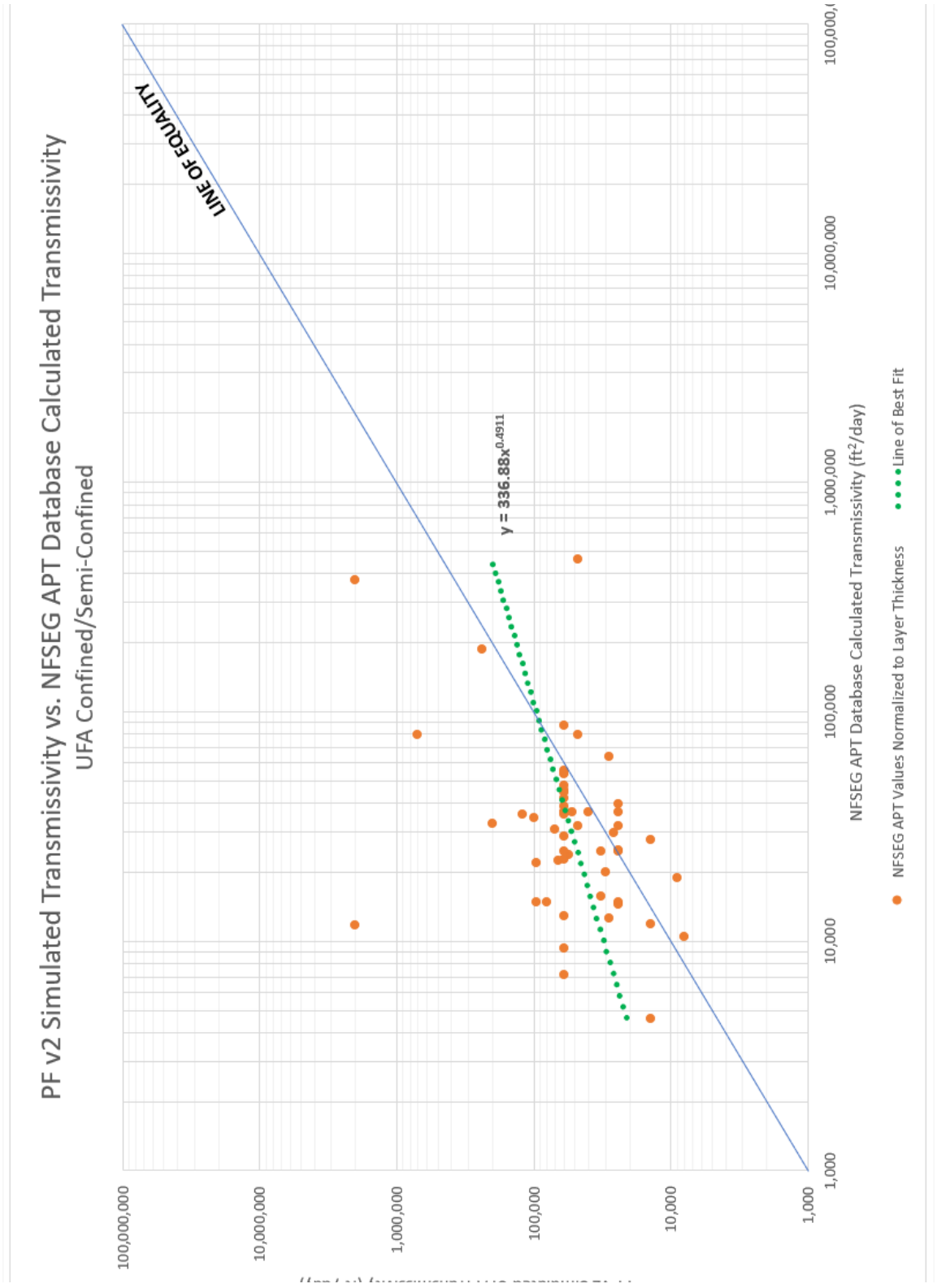

Figure 4-90. Scatter plot of PF v2 UFA transmissivity vs. NFSEG APT Database, confined region

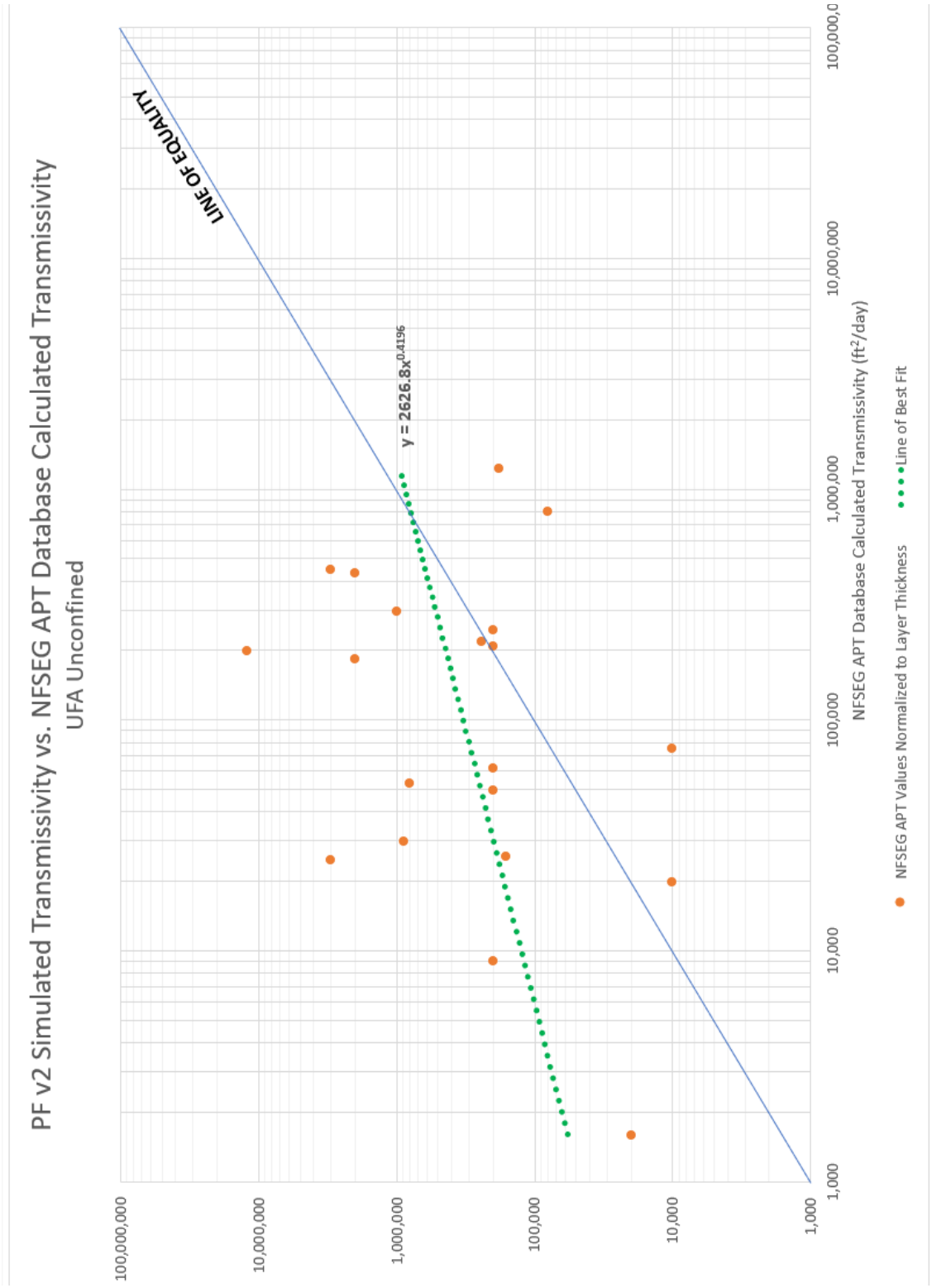

Figure 4-91. Scatter plot of PF v2 UFA transmissivity vs. NFSEG APT database, unconfined region

Comparison of NFSEG v1.1 Calibration Statistics in Portions of Model Domain that correspond to the North Florida Water Supply Planning Areas versus Overall Model Domain

The North Florida Regional Water Supply Partnership was established in 2011 through a formal agreement executed by the Florida Department of Environmental Protection (FDEP), SJRWMD, and SRWMD. The planning area includes 14 counties in north Florida, five within SRWMD ,six within SJRWMD and three within both Districts (Figure 4-92). The purpose of the Partnership is to protect natural resources and water supplies in north Florida. This is being achieved through collaborative planning, scientific tool development and related efforts.

The NFSEG groundwater model has been used, and will be in the future, to evaluate impacts with the planning area, which is why the planning area corresponds in location to the core of the NFSEG model domain (Figure 4-92). The following discussion therefore compares the groundwater level statistics that are representative of the portion of the model domain that corresponds to the planning area of the overall model domain.

Groundwater level calibration statistics were calculated for the entire NFSEG v1.1 model domain and within the North Florida Regional Water Supply Planning Area (NFRWSPA) portion of the model domain and are included in Table 4-13. Layer 1 synthetic targets and Layer 2 targets are not incorporated into the statistics for reasons provided in the discussion of the calibration results. As shown in Table 4-13, the groundwater level calibration statistics are generally better within the NFRWSPA than within the domain as a whole. This is true of Layer 3 calibration statistics as well. Also, 2001 statistics are shown to be better than corresponding statistics of 2009.

Table 4-13. Groundwater-level calibration statistics: overall model domain versus NFRWSPA

Description of Included Water Level Residuals	Mean Error (ft)	Standard Deviation (ft)	Absolute Mean Error (ft)	RMSE (ft)
Whole Active Extent, 2001	-0.3	5.4	3.9	5.4
Whole Active Extent, 2009	-0.7	5.0	3.5	5.0
NFWSPA Active Extent, 2001	0.5	5.1	3.7	5.1
NFWSPA Active Extent, 2009	-0.4	4.7	3.4	4.7
Whole Active Extent, Layer 1, 2001	-0.1	6.2	4.2	6.2
Whole Active Extent, Layer 1, 2009	0.1	5.8	3.6	5.8
NFWSPA Active Extent, Layer 1, 2001	0.6	5.9	4.0	5.9
NFWSPA Active Extent, Layer 1, 2009	0.1	4.6	3.4	4.6
Whole Active Extent, Layer 3, 2001	-0.5	5.0	3.7	5.0
Whole Active Extent, Layer 3, 2009	-0.9	4.6	3.4	4.7
NFWSPA Active Extent, Layer 3, 2001	0.3	4.4	3.4	4.4
NFWSPA Active Extent, Layer 3, 2009	-0.7	4.2	3.1	4.4
Whole Active Extent, Layer 5, 2001	2.6	5.7	5.4	6.1
Whole Active Extent, Layer 5, 2009	1.0	5.2	4.2	5.3
NFWSPA Active Extent, Layer 5, 2001	4.3	4.7	5.3	6.3
NFWSPA Active Extent, Layer 5, 2009	3.4	4.4	4.5	5.4

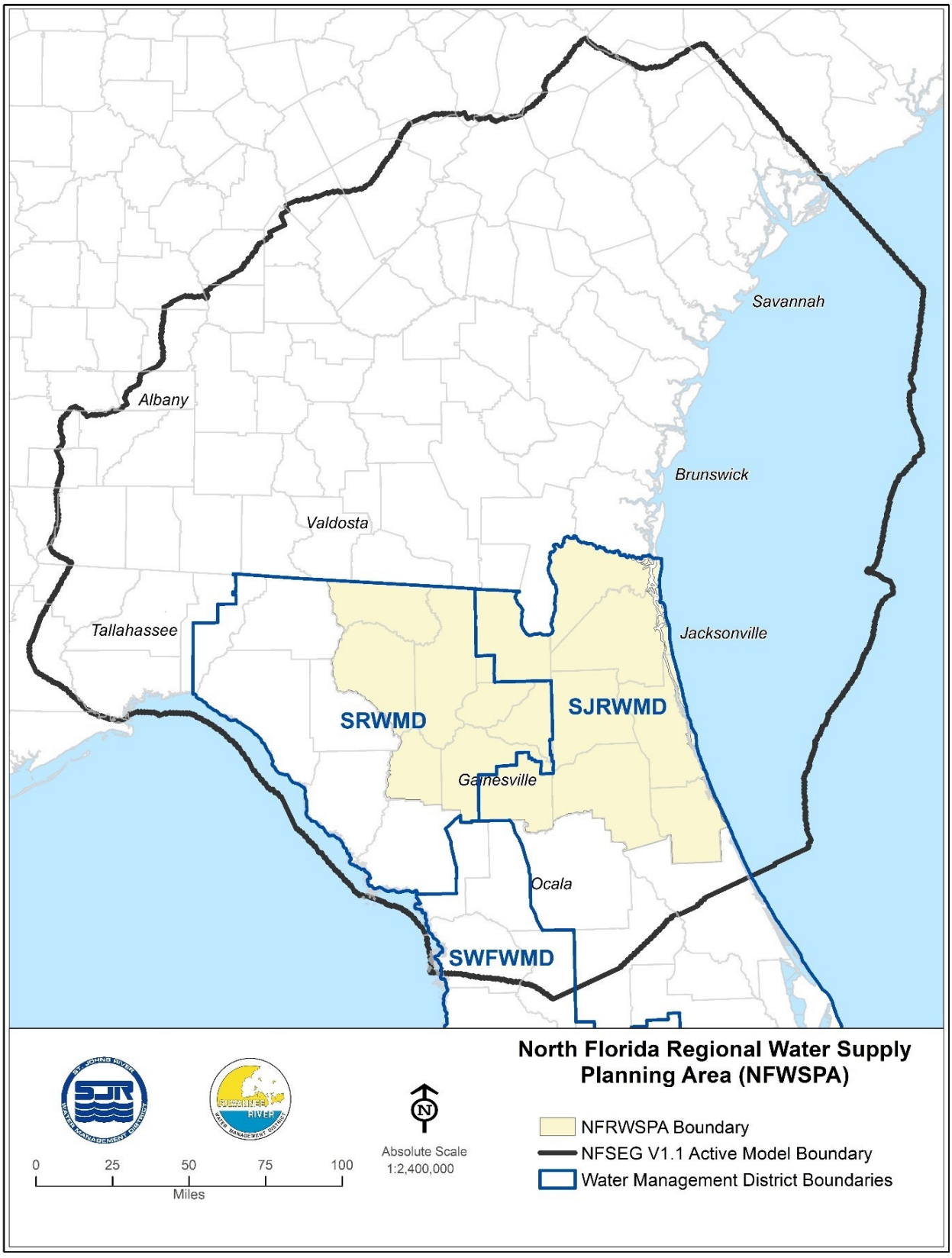

Figure 4-92. Map of North Florida regional water supply planning area

CHAPTER 5. MODEL SIMULATIONS

As part of NFSEG v1.1 model development, a verification simulation and a no-pumping simulation were conducted to assess the performance of the NFSEG model for predicting groundwater levels and flows.

VERIFICATION SIMULATION

For the NFSEG model verification, the year 2010 was selected at an early stage of model development by the NFSEG technical team, composed of the modeling team as well as technical experts assigned by stakeholders. Based on annual average rainfall distribution from NLDAS used in NFSEG model development, the year 2010 does not resemble either of the calibration years (2001 and 2009) which makes it suitable for a verification simulation (Figure 5-1). The year 2009 was generally considered a wet year and the year 2001 was generally considered a dry year throughout most of the model domain. The year 2010, however, was drier than 2001 in some parts of model domain, such as areas along the eastern model boundary covering much of the St. Johns River watershed and eastern parts of Georgia and South Carolina, whereas it could be considered an average rainfall year along the western model boundary in Florida (Figure 5-2). Relative to the year 2009, the year 2010 was drier throughout most of the model domain, except for areas along the southwestern model boundary which includes Marion and Levy counties (Figure 5-2).

To setup the 2010 verification simulation, model input files were developed for the year 2010 based on methods established in the calibration simulations, which are described in detail in the following section. The prediction performance of the NFSEG model was assessed using the 2010 verification results by reviewing the difference between simulated and observed values of groundwater levels, spring flows and baseflows, simulated 2010 potentiometric surface of the UFA and simulated 2010 mass balance for reasonableness.

Model Input Files

The following section includes brief descriptions of the MODFLOW-NWT packages that were updated with 2010 input data for the verification simulation. To maintain consistency and enable comparison with the NFSEG v1.1 calibration simulations, model input files were developed for the year 2010 using the same methods established for the years 2001 and 2009 during model calibration. Chapter 3 of this report includes more detailed information regarding the NFSEG v1.1 model calibration input files and implementation.

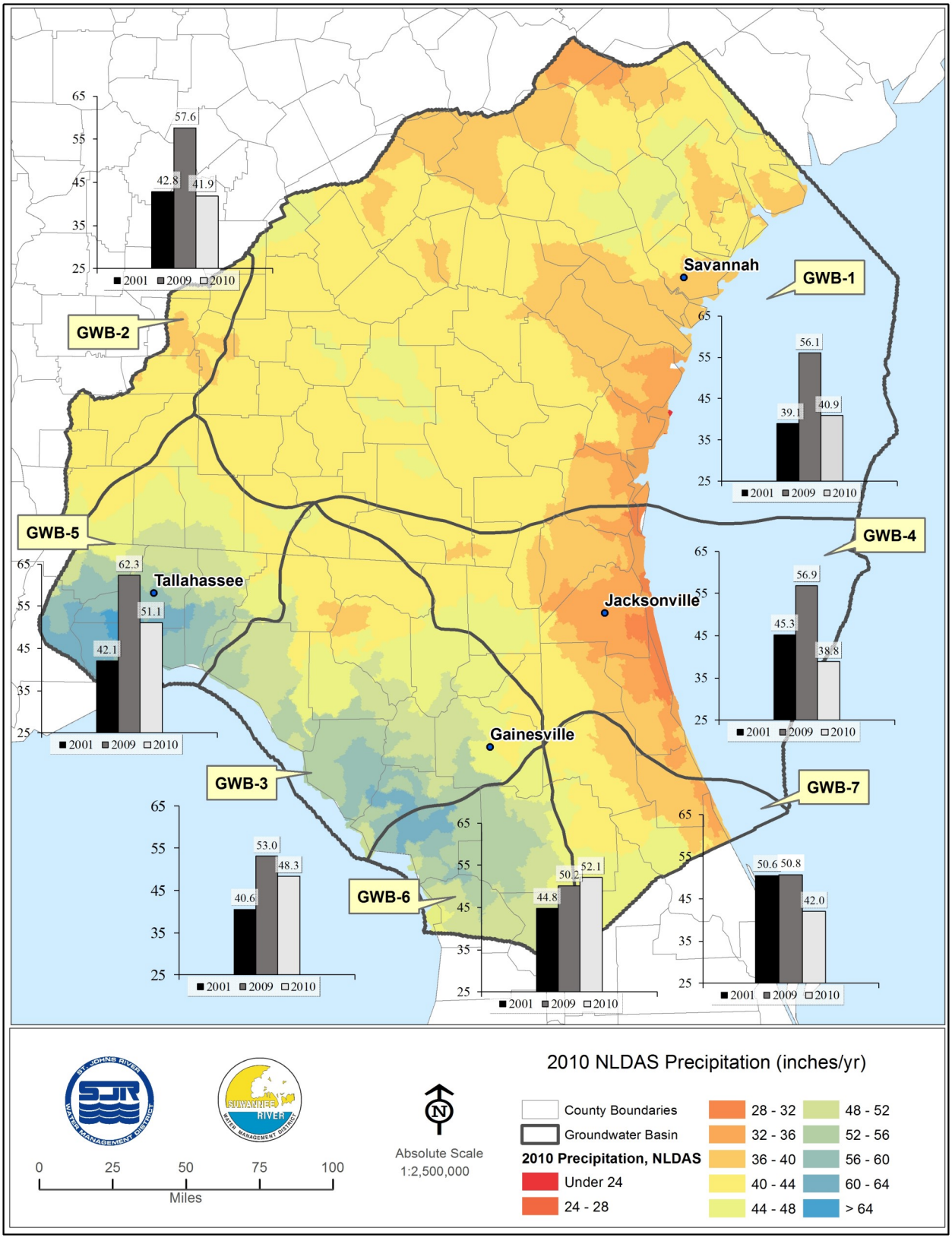

Figure 5-1. Map of annual average precipitation in 2010, and bar charts of 2001, 2009 and 2010 average annual precipitation by groundwater basin

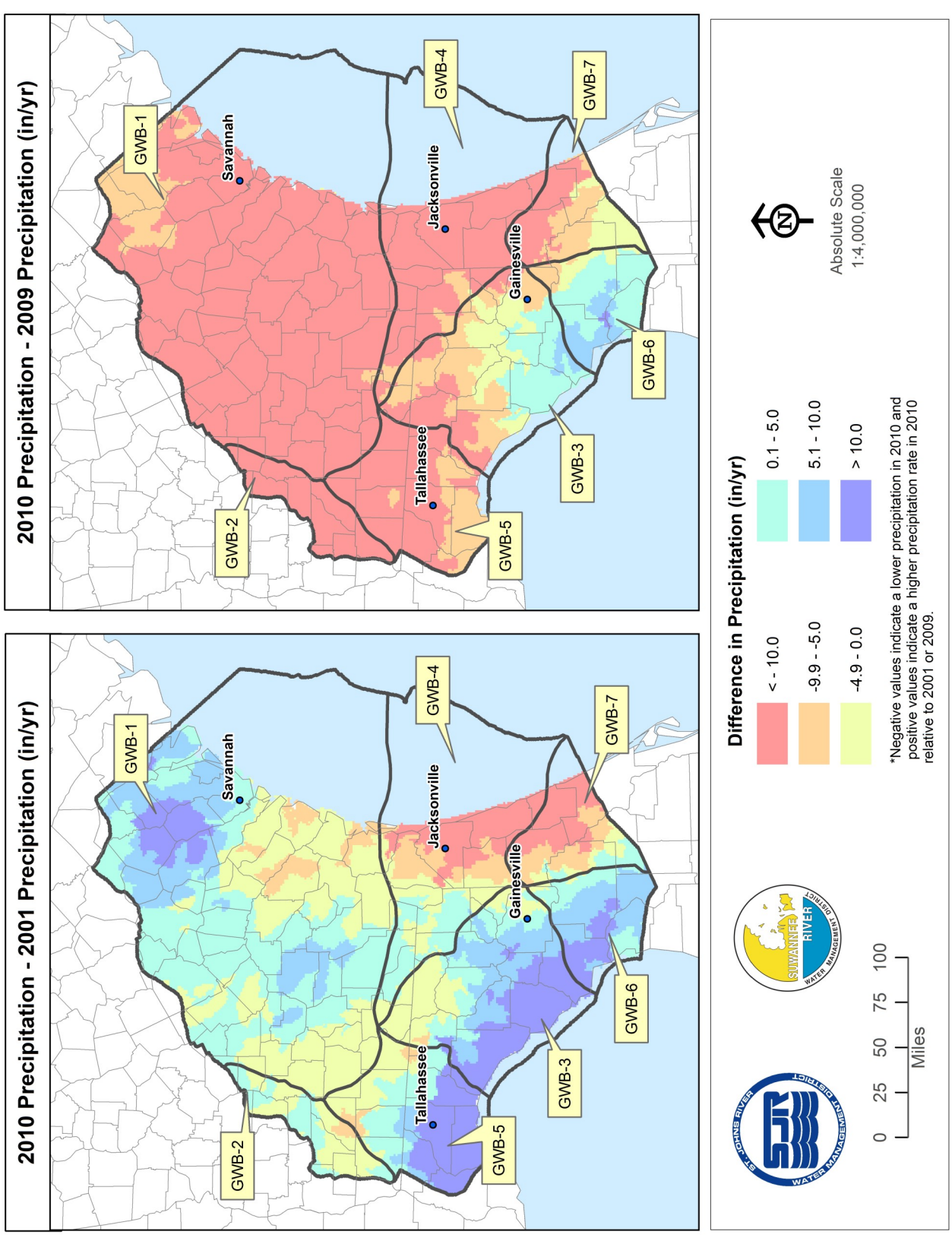

Figure 5-2. Difference in precipitation rate between 2010 and 2001 (left) and 2010 and 2009 (right)

Recharge and Maximum Saturated Evapotranspiration

In the NFSEG model verification simulation, separate external arrays of recharge and maximum saturated evapotranspiration (MSET) rates were developed for 2010 using HSPF models developed for the NFSEG model (see Chapter 9 for more information). Figure 5-3 shows the distribution of the 2010 MSET as well as average annual MSET in 2001, 2009 and 2010 within delineated groundwater basins (GWBs). Figure 5-4 shows the difference between MSET in 2010 relative to the years 2001 and 2009 within delineated groundwater basins (GWBs). Despite similarity in average annual MSET within each GWB among all three years, there is evident spatial variation in MSET in 2010 relative to each calibration year. In the year 2010, MSET was generally lower than 2001 and 2009 along the western model boundary and higher along the eastern model boundary (Figure 5-4).

The applied recharge rate in 2010 and average annual recharge rate for 2001, 2009 and 2010 within each GWB are shown in Figure 5-5. There appears to be greater variation in the average annual recharge rate within each GWB relative to MSET. The spatial variations in the recharge rate in the year 2010 relative to 2001 and 2009 are shown in Figure 5-6. In the year 2010, the recharge rate was higher than in 2001 and 2009 in the southwest portion of the model and generally lower along the eastern model boundary. In parts of southern Georgia, the recharge rate in the year 2010 was generally higher than in the year 2001 but lower than in the year 2009 (Figure 5-6). Like rainfall distribution, geographic variations in MSET and applied recharge rates in 2010 are distinct from those in 2001 and 2009.

Drain and River Package

Stage and bottom elevation estimation for development of the 2010 Drain and River Packages followed the same methodology used for 2001 and 2009. Sources of actual stream and lake stage data for 2010 include the USGS and various water management districts, which provided median water levels for 2010. Where stage data were unavailable, land surface elevation was used to represent stage. In the Suwannee River and some of its tributaries, stages for 2010 were obtained from the SRWMD HEC-RAS surface water models. A hydrodynamic model developed by SJRWMD was the source of stages for the St. Johns River for 2010.

Well and Multi-Node Well Packages

The Well Package was used to represent single aquifer withdrawal wells, while the Multi-Node Well Package was used to represent withdrawal wells open to both the Upper and Lower Floridan aquifers in 2010. All water uses represented in the 2001 and 2009 groundwater withdrawal dataset are included in 2010. Figure 5-7 through Figure 5 -8 show the distribution of groundwater withdrawals by water use type and counties in 2010. Influxes due to rapid infiltration basins (RIBS), natural sinks, drainage wells and injection wells were also simulated with the Well Package (see section 3 for more information). Figure 5-9 includes the multi-aquifer withdrawal wells included in the 2010 simulation. Table 5-1 includes the total groundwater withdrawals and influxes (in mgd) in 2010 compared to those in 2001 and 2009.

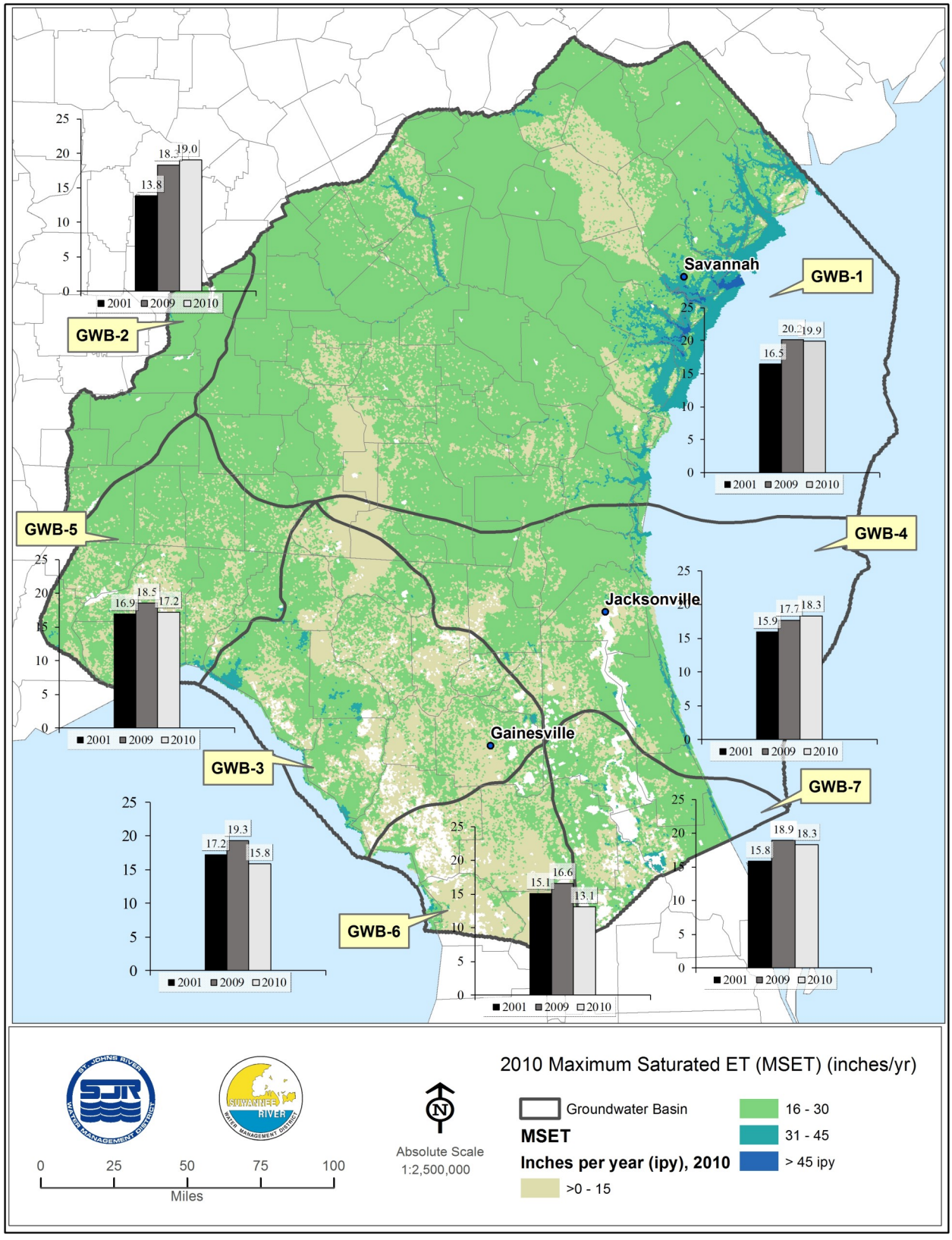

Figure 5-3. Map of annual average MSET in 2010, and bar charts of 2001, 2009 and 2010 average annual MSET by groundwater basin

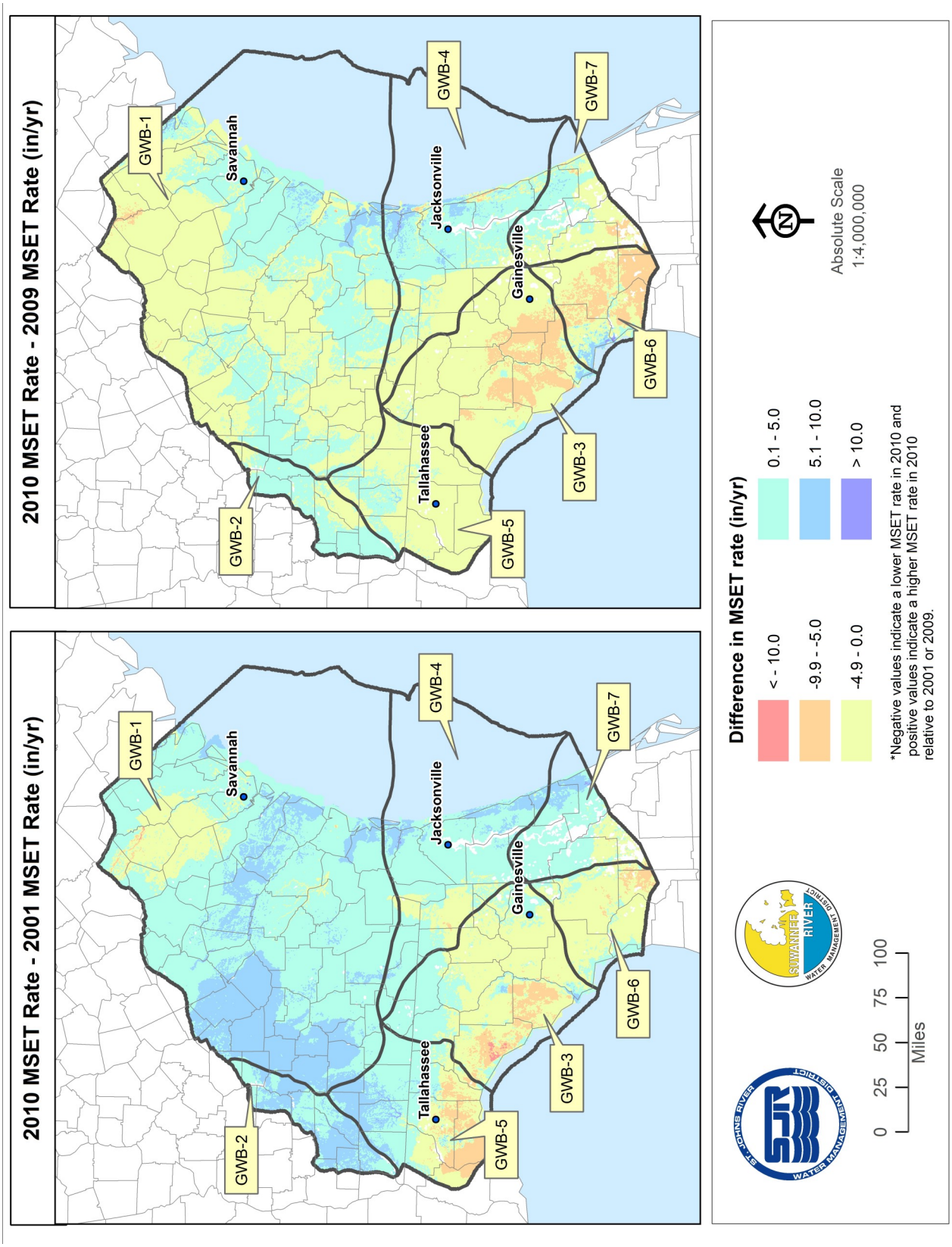

Figure 5-4. Difference in MSET rate between 2010 and 2001 (left) and 2010 and 2009

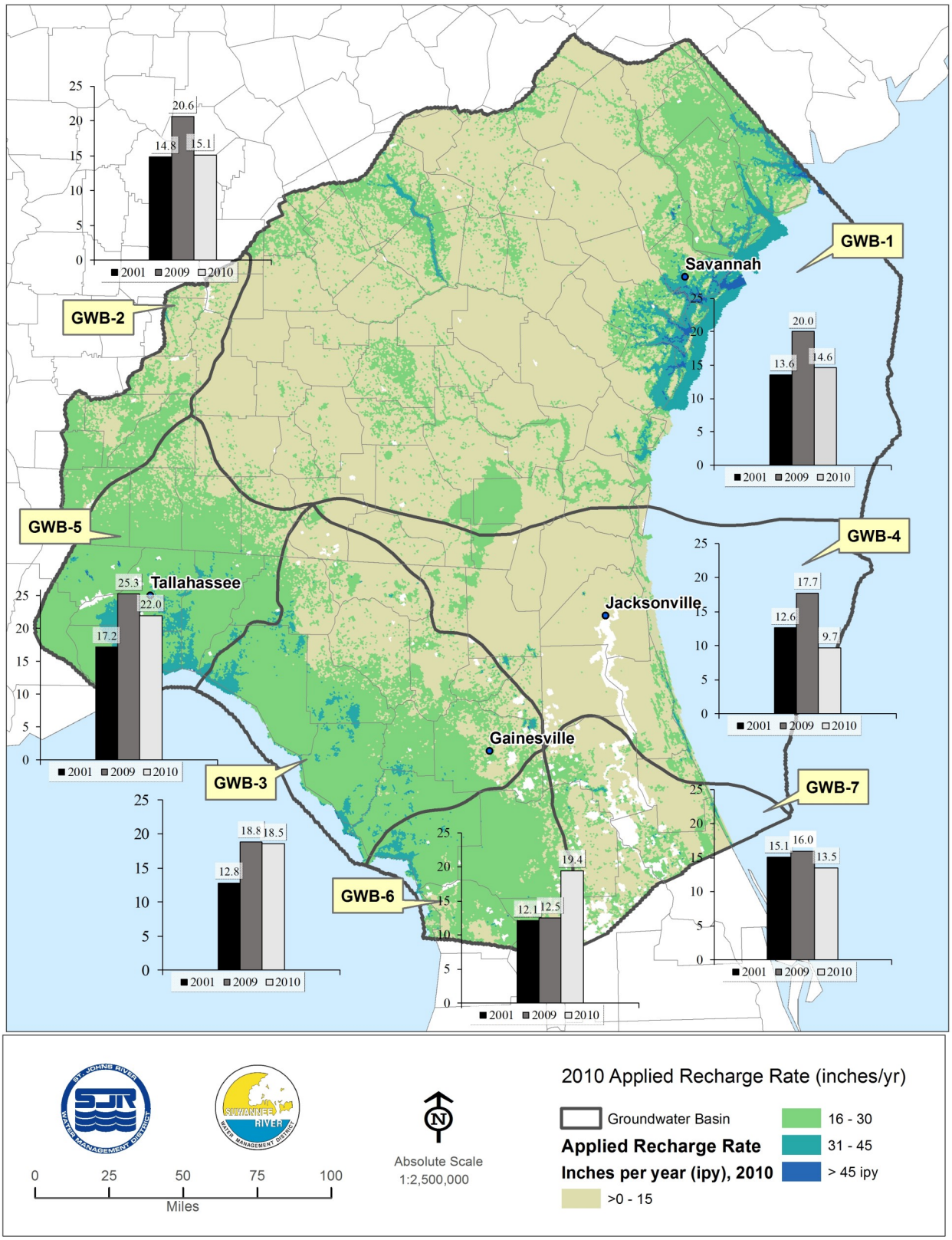

Figure 5-5. Map of annual average recharge rate in 2010, and bar charts of 2001, 2009 and 2010 average annual recharge rate by groundwater basin

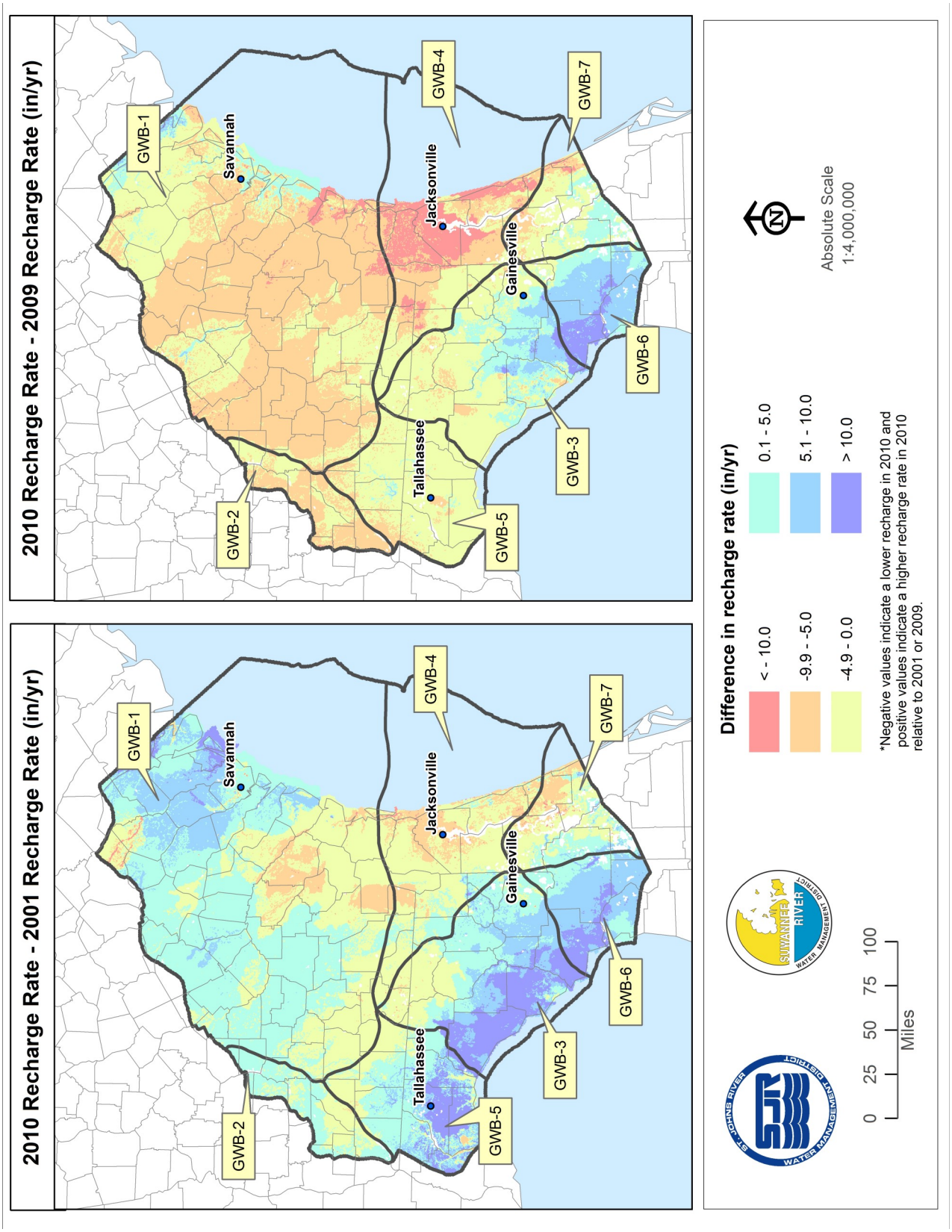

Figure 5-6. Difference in recharge rate between 2010 and 2001 (left) and 2010 and 2009

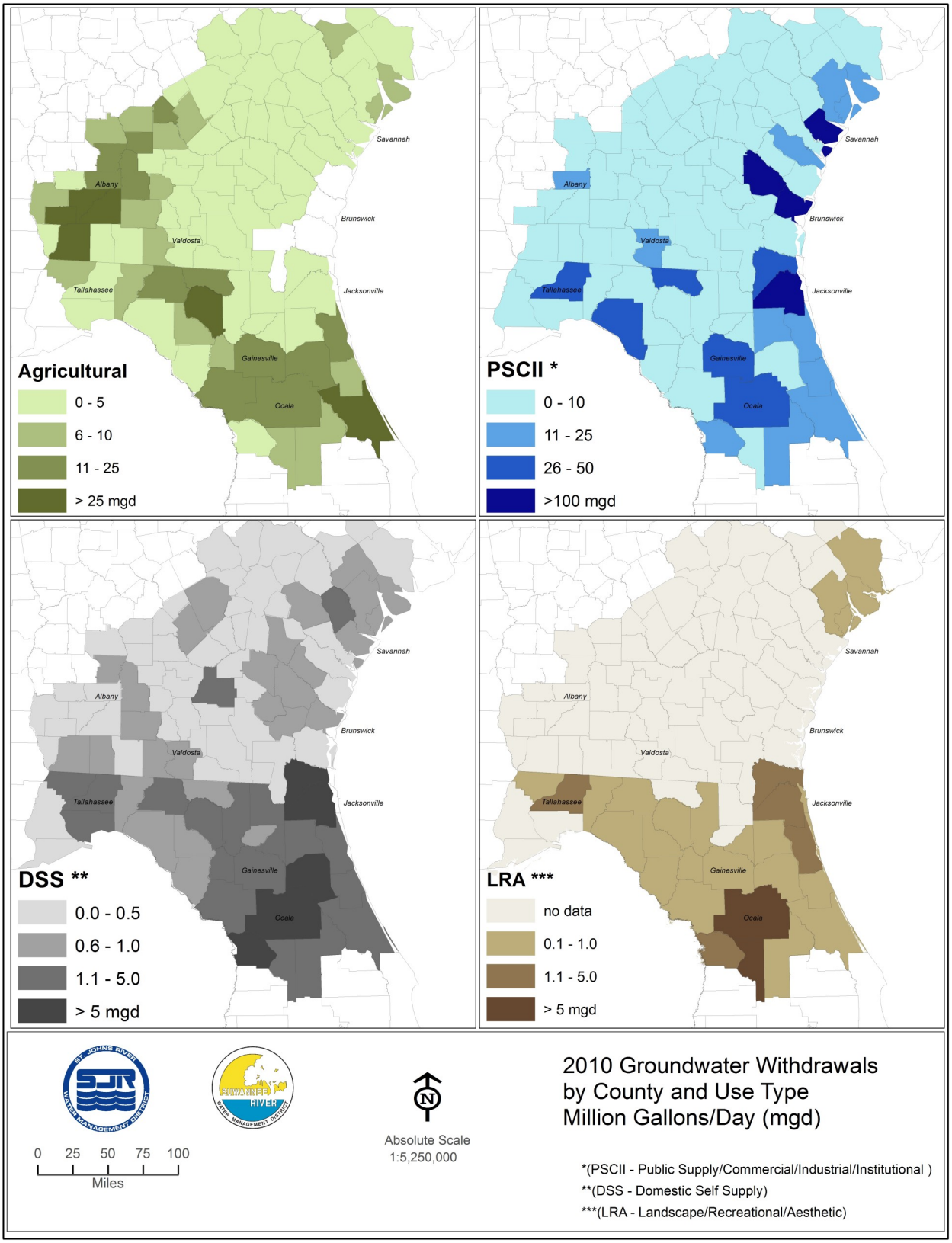

Figure 5-7. Distribution of public-supply, commercial-industrial and institutional withdrawals (MGD), 2010

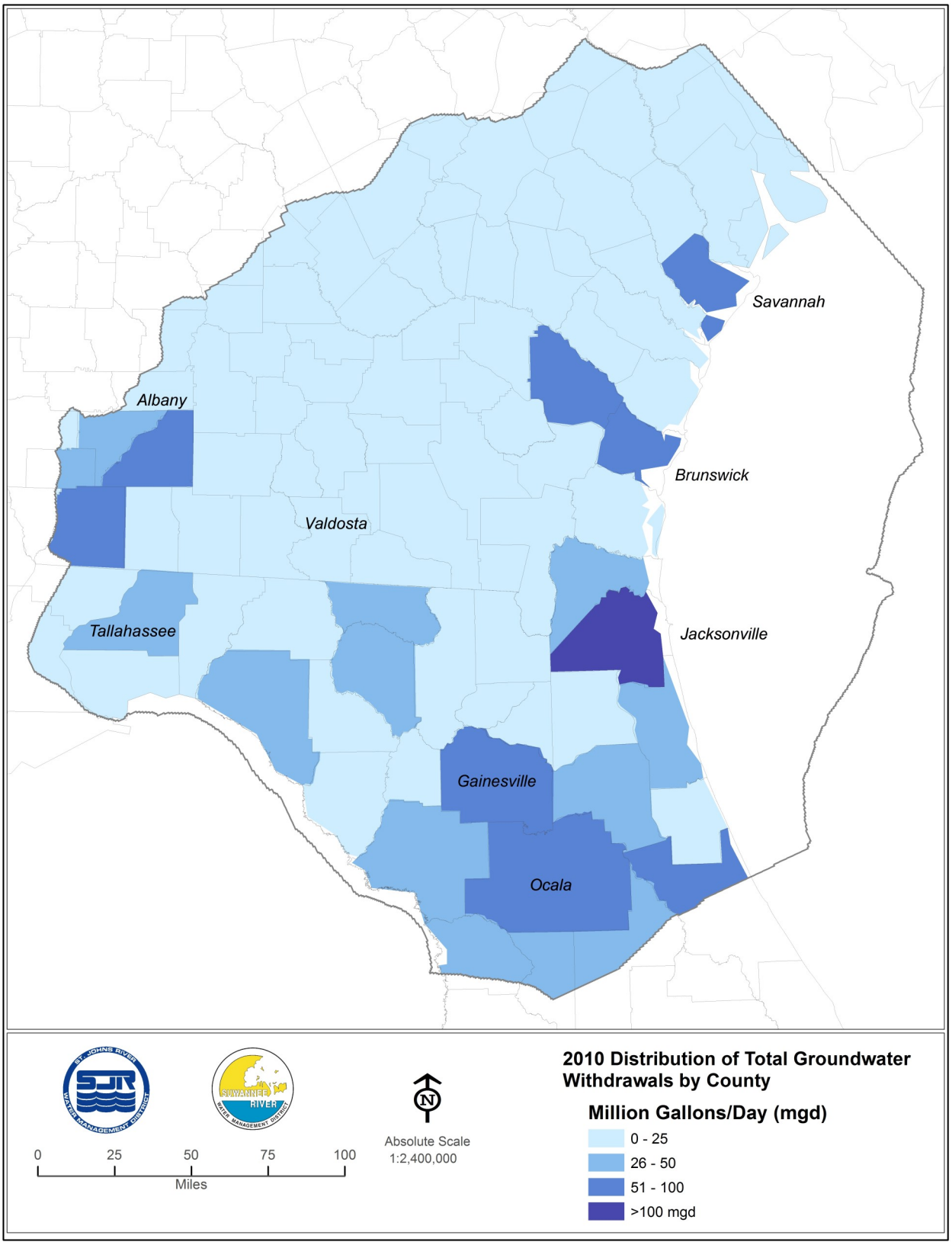

Figure 5-8. Distribution of total groundwater withdrawals by county (MGD), 2010

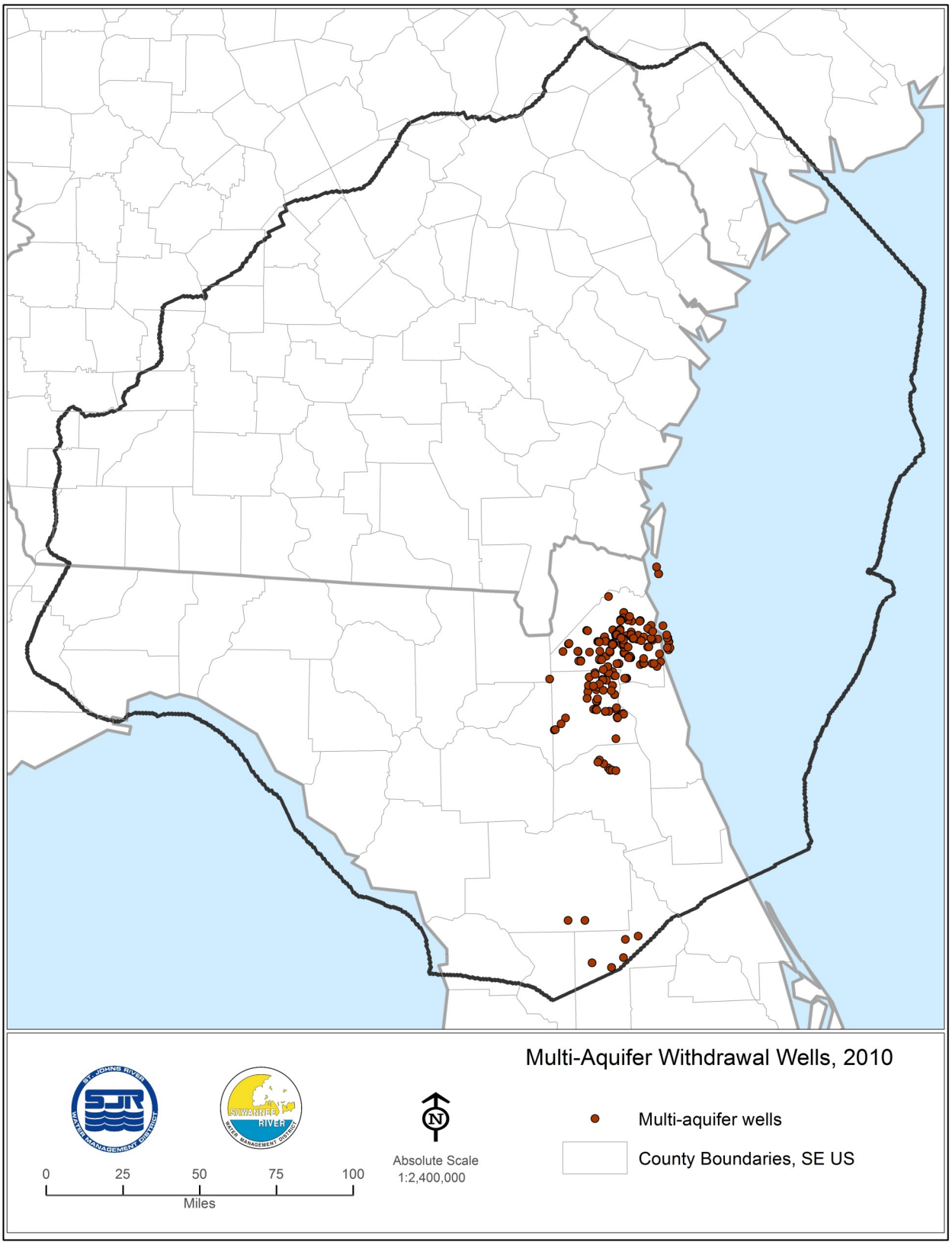

Figure 5-9. Distribution of multi-aquifer wells in 2010

Table 5-1. Summary of groundwater withdrawals and influxes

Groundwater Withdrawals and Influxes	Q 2001 million gallons per day	Q 2009 million gallons per day	Q 2010 million gallons per day
Single aquifer well withdrawals	1,568	1,557	1,487
Multi-aquifer well withdrawals	125	119	120
Influxes (RIBS, injection wells, swallets, drainage wells)	315	392	457

General Head Boundary Package

Lateral Boundaries

For the 2010 verification simulation, lateral boundary conditions types were identical to those used in the 2001 and 2009 calibration, with most of the NFSEG model lateral boundaries assigned no-flow boundaries (See Chapter 3 for more information). For the small portion of the lateral boundaries that were represented with the General Head Boundary (GHB) Package, source heads for model Layer 3 (UFA) were generated using the May-June 2010 potentiometric surface (Kinnaman and Dixon, 2011) and average observed water levels in 2010. Where GHB source heads were assigned for other layers, the values were the same as for the UFA.

Spring Pool Elevations

The GHB package was also used to simulate spring discharges by specifying spring pool elevations for the springs in the NFSEG model domain (Figure 2-1). Spring pool elevations were assigned based on observed median water levels for 2010. In the case where no observed data was available for 2010, if a spring is adjacent to a river, the nearby 2010 river stage was assumed to be the pool elevation. In cases where no observed data were available, or were based on limited observations, and no adjacent river cell was available, the USGS 3DEP 10m DEM elevation was used to set the pool elevations. The assigned spring pool elevations were later compared with the observed 2010 potentiometric surface of the UFA to ensure that the pool elevations were lower than the UFA water levels for a flowing spring.

Observation Datasets

To assess model performance for the year 2010, residual statistics were evaluated for the three types of observation groups: Groundwater levels; Spring discharge rates; and Baseflow rates.

Groundwater levels

The groundwater level observation data were compiled from a variety of sources, including the USGS and water management districts. Observed UFA water levels for 2010 were compared with the May-June 2010 UFA potentiometric surface developed by the USGS to check for significant discrepancies that could be due to measurement error. The May-June 2010 potentiometric surface was selected for comparison because this was the only data available from USGS in the year 2010 in which the UFA potentiometric surface extended into Georgia. As a result, a total of 1329 observation wells with a 2010 median observed water level were used to assess model performance using the results of the 2010 simulation (Figure 5-10). Appendix I includes the observation well water level data for 2010.

Springflows

Spring discharge rates for the year 2010 were developed based on direct observations if available for 2010 or estimates using direct observations from other years if sufficient data was not available. Sources of actual spring discharge included the USGS and water management districts. If sufficient data were not available for a spring, a literature value from the Florida Geological Survey (FGS) Bulletin 66 (Scott and others, 2004) was used as an initial estimate of spring flow. Appendix J includes the 2010 observed/ estimated spring discharge rates in the model domain.

Baseflows

As discussed in detail in section 2, baseflows were estimated for the year 2010 by averaging the results of five baseflow estimation approaches. Although the average of all approaches was used as the initial baseflow estimation for a given gauge, the minimum and maximum estimated baseflow of all techniques was considered for evaluation of simulated baseflows. For gauges within unconfined areas, in which total streamflow is dominated by groundwater discharge, total streamflow was used to estimate changes in baseflow at a given gauge. Two baseflow observation data groups were developed for the year 2010 – the baseflow pickup group, representing the change in baseflow between a downstream and zero or one upstream gauge, and the cumulative group, representing the total baseflow contributions from collections of baseflow pickup reaches to a given gauge. Based on available data, baseflow pickup estimates were developed for 41 USGS gauges and cumulative baseflow estimates were developed for ten USGS gauges in 2010. Appendix K includes the 2010 estimated baseflow pickups and cumulative baseflows as well as the range of flows estimated from the five baseflow separation techniques described in Chapter 2.

Assessment of 2010 Simulation Results

The results of the 2010 verification simulation (modeled minus observed) are included in Appendices I through K. Appendix I includes the 2010 simulated groundwater levels and residuals. Appendix J includes the 2010 simulated spring discharge rates and residuals. Appendix K includes the 2010 simulated baseflow pickups and cumulative

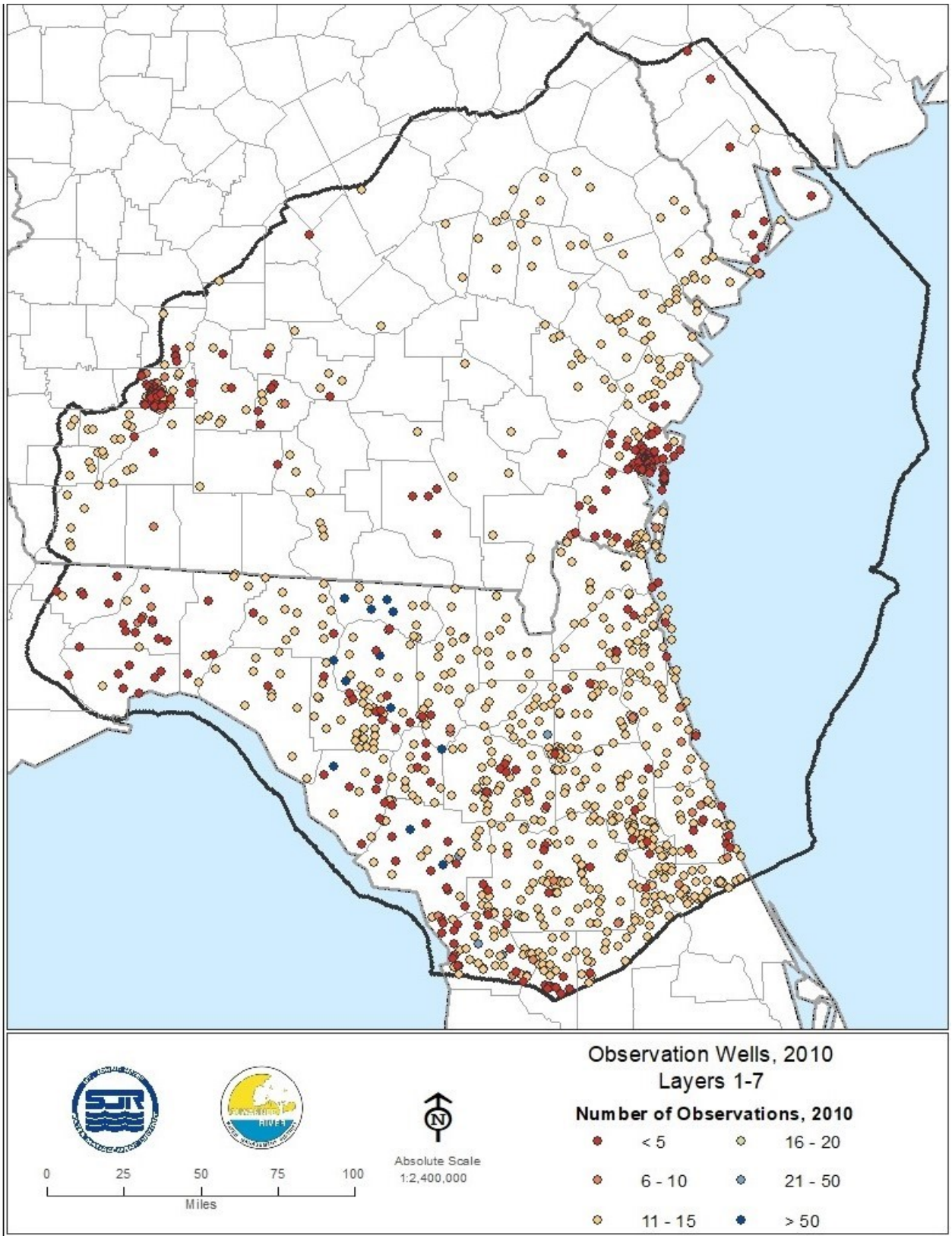

Figure 5-10. Distribution of observation wells, 2010

baseflows and residuals.

The performance of the NFSEG model was assessed using the 2010 verification results as follows:

- Groundwater level, spring flow and baseflow residual statistics from the 2010 simulation were compared with the 2001 and 2009 calibration statistics;
- The spatial distribution of the 2010 UFA level residuals was compared with that of 2001 and 2009 UFA level residuals;
- The simulated 2010 potentiometric surface of the UFA was compared with the observed 2010 potentiometric surface of the UFA; and
- The simulated 2010 mass balance was reviewed for reasonableness.

Residual Statistics

Residual statistics were computed for simulated 2010 groundwater levels, spring discharge rates and baseflow rates and compared with 2001 and 2009 calibration statistics.

Groundwater Levels

The overall distribution of simulated and observed groundwater levels for Layers 1, 3 and 5 are shown in Figures 5-11 through 5-13. The groundwater level residual statistics of the 2010 simulation were compared with the groundwater level residual statistics of the 2001 and 2009 calibration simulations (Figure 5-14). Overall, groundwater level residual statistics in 2010 were similar to those in 2001 and 2009. The 2010 simulation performed slightly better in predicting Layer 1 groundwater levels than in 2009, whereas the 2010 residuals were slightly higher than the 2001 and 2009 residuals in Layers 3 and 5. Appendix I includes the 2010 simulated groundwater levels and residuals for the 1329 observation wells included in the 2010 simulation.

Spring Flows

Figure 5-15 shows the distribution of simulated and observed spring flows in 2010. Spring flow residual statistics in 2010 were compared to those in 2001 and 2009 for individual springs in the NFSEG model (Figure 5-16). Overall, spring flow residual statistics in 2010 were similar to residual statistics in 2001 and 2009. Relative to 2001 and 2009, the 2010 simulation resulted in a higher absolute mean spring flow residual. The 2010 residual mean is lower than 2001 and 2009, but still negative, which suggests an overall slight underestimation of spring flow. The residual standard deviation of 2010 spring flow is higher than the residual standard deviation in 2001, but lower than the residual standard deviation in 2009 (Figure 5-16).

Table 5-2 includes simulated and observed spring flows in 2010 for important first magnitude springs and spring groups. As shown in Table 5-2, the model performed well in matching important spring flows except for Silver Springs group, Rainbow Springs, St. Marks River Rise and Spring Creek Springs Group. This could be due to uncertainties in some of the parameters such as spring pool elevation, flow estimates, recharge and maximum saturated ET (MSET). St. Marks River Rise and Spring Creek

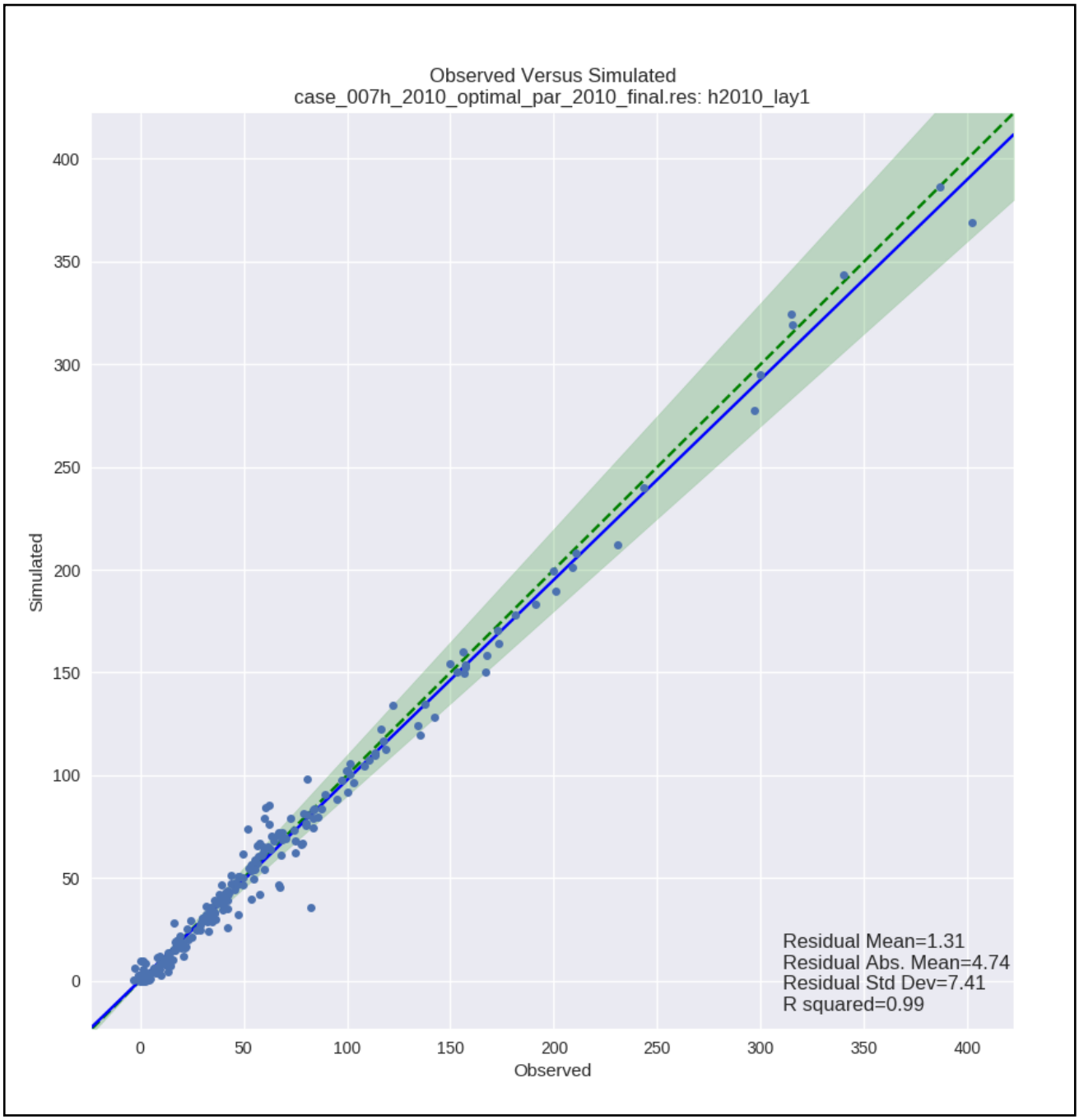

Figure 5-11. Simulated vs. observed groundwater levels (feet NAVD88), Model Layer 1, 2010

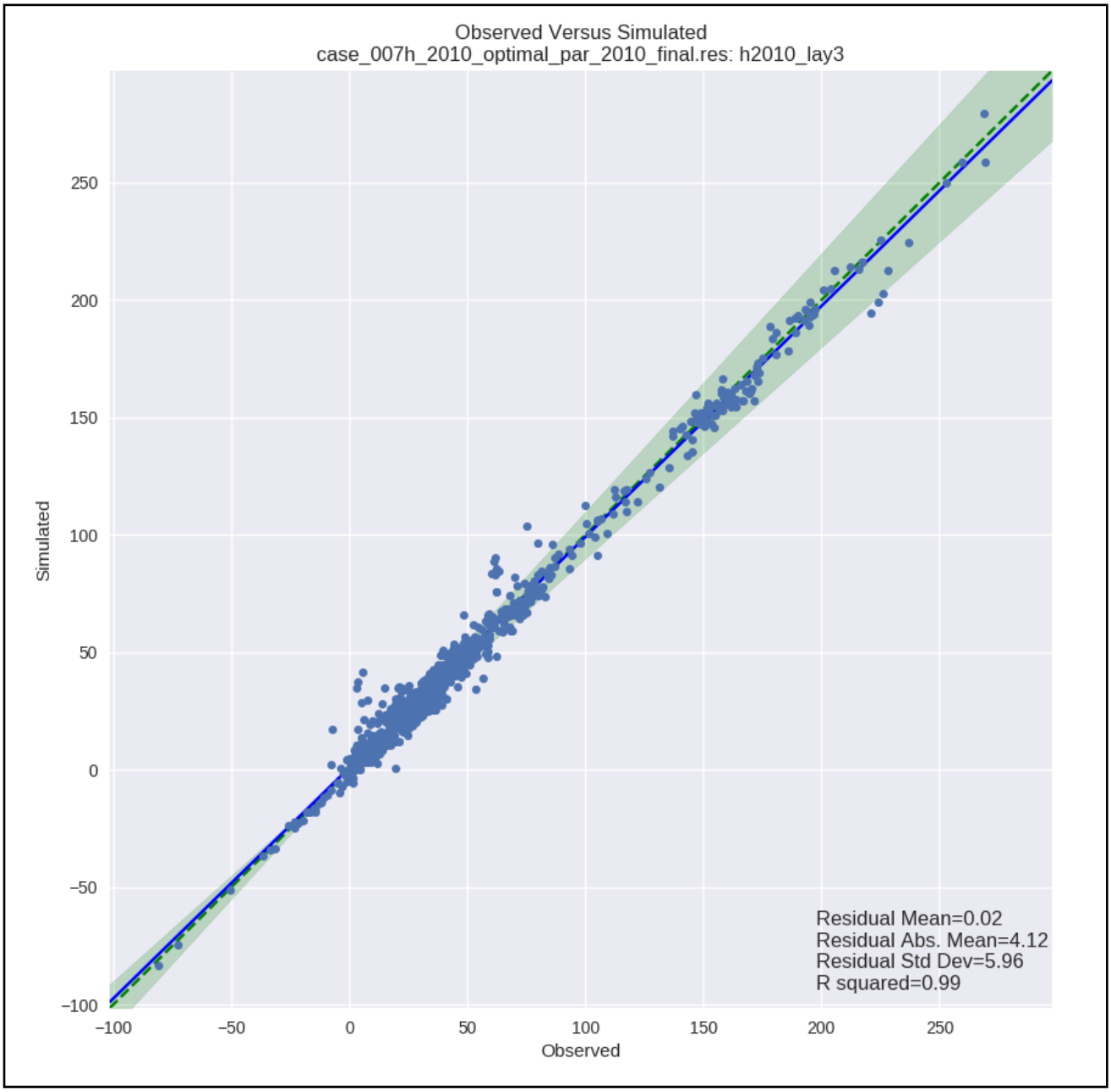

Figure 5-12. Simulated vs. observed groundwater levels (feet NAVD88), Model Layer 3, 2010

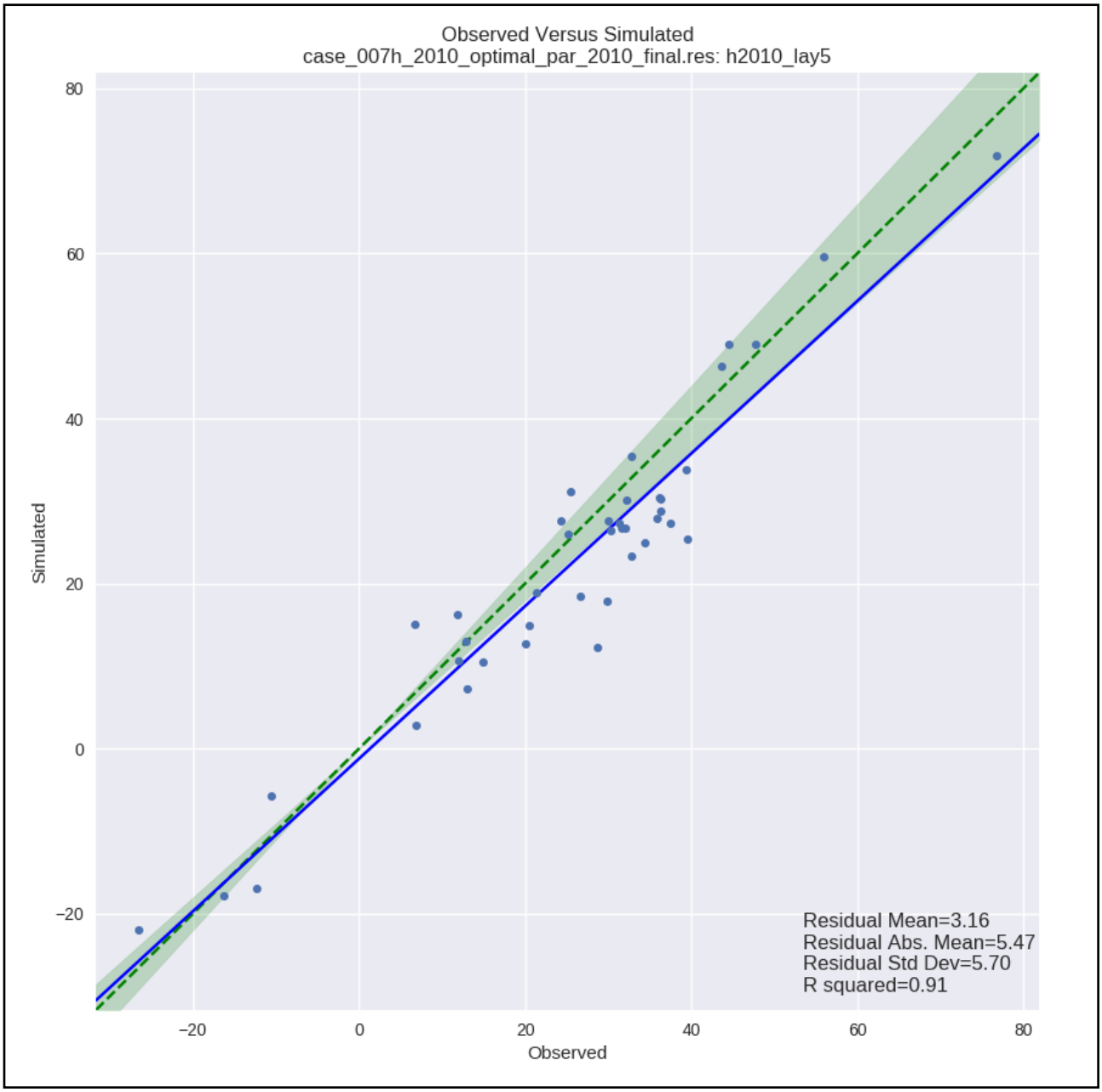

Figure 5-13. Simulated vs. observed groundwater levels (feet NAVD88), Model Layer 5, 2010

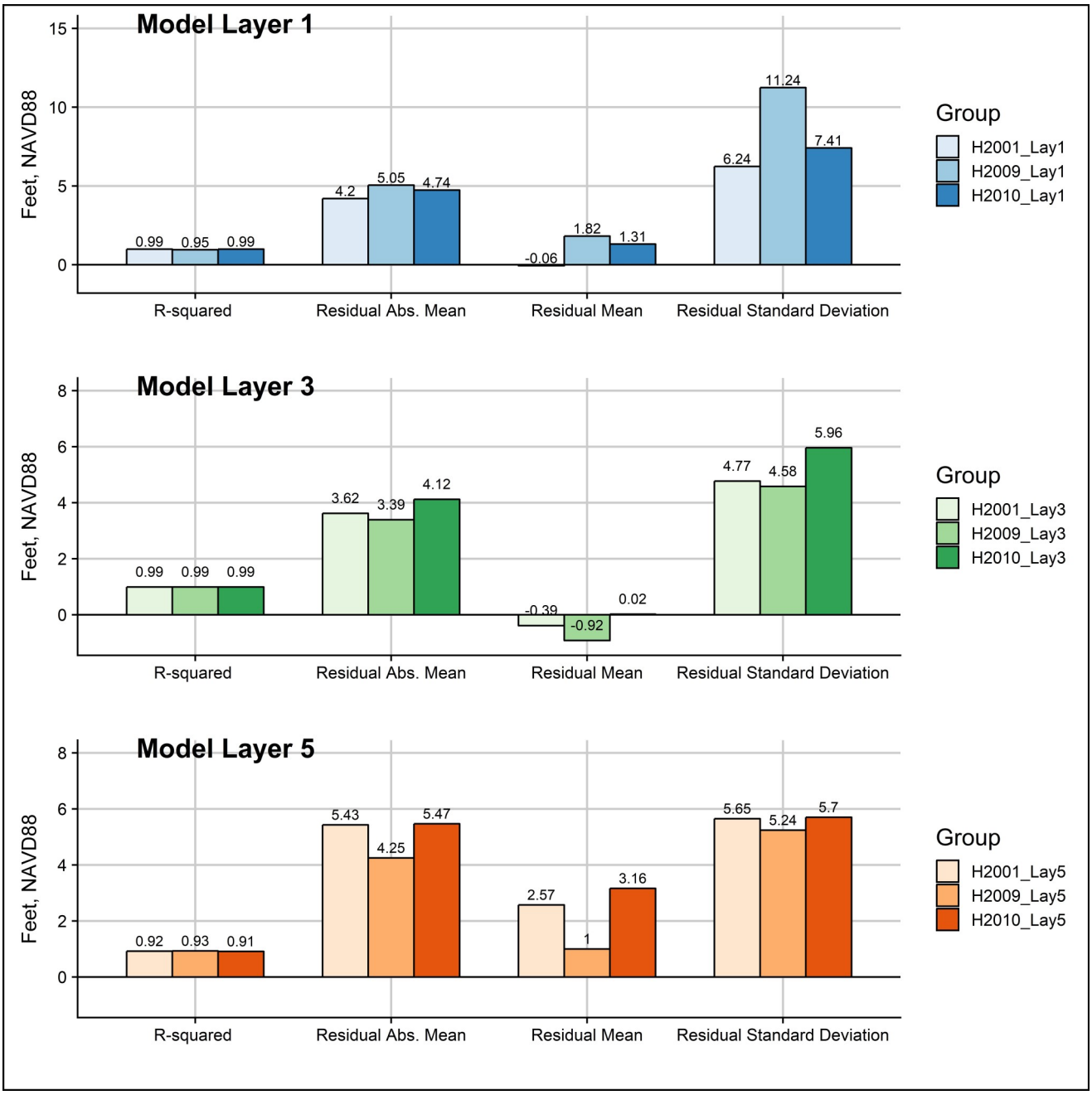

Figure 5-14. Residual groundwater level statistics comparison for model Layers 1, 3 and 5

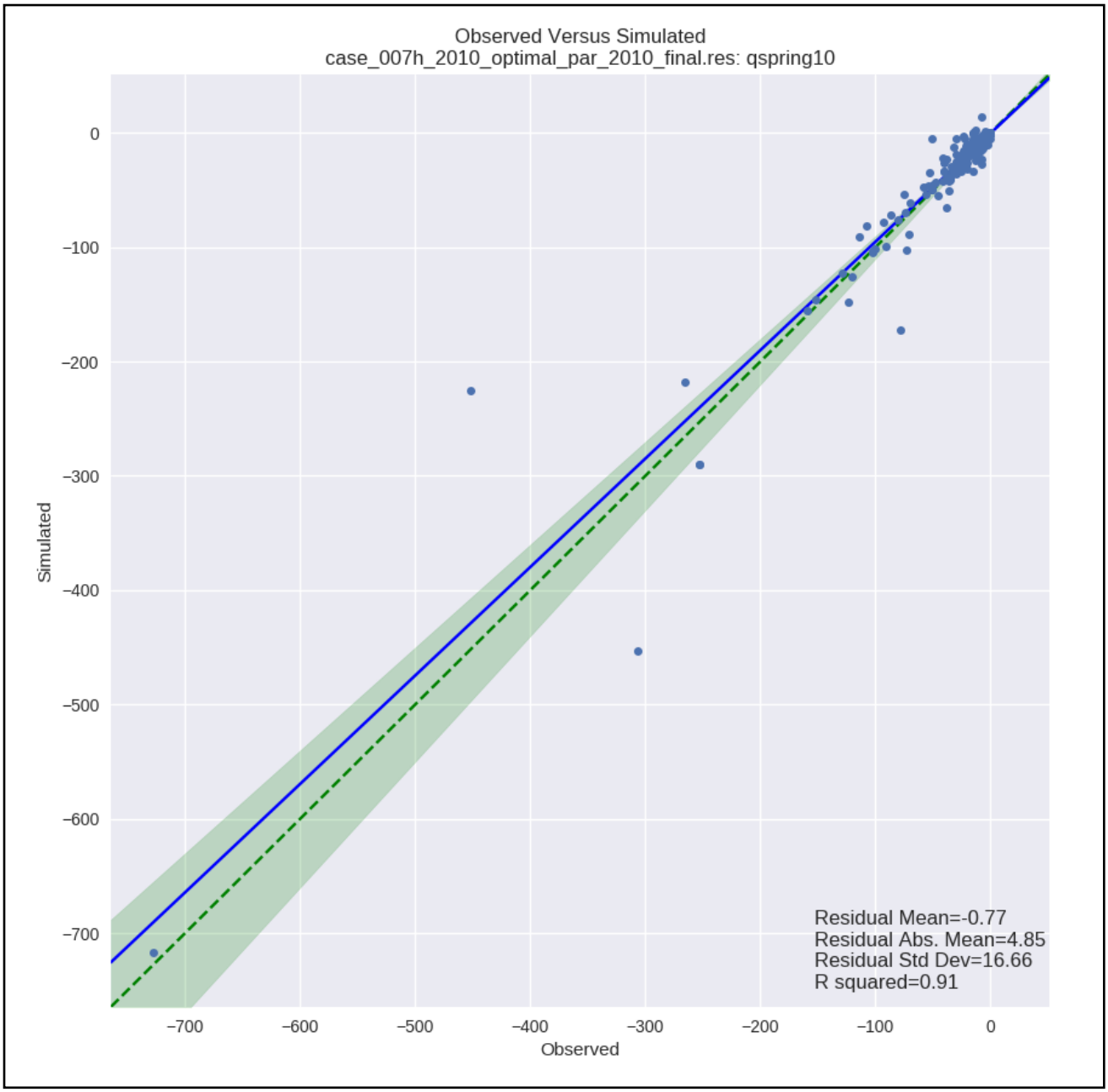

Figure 5-15. Simulated vs. observed spring discharges (cfs), 2010

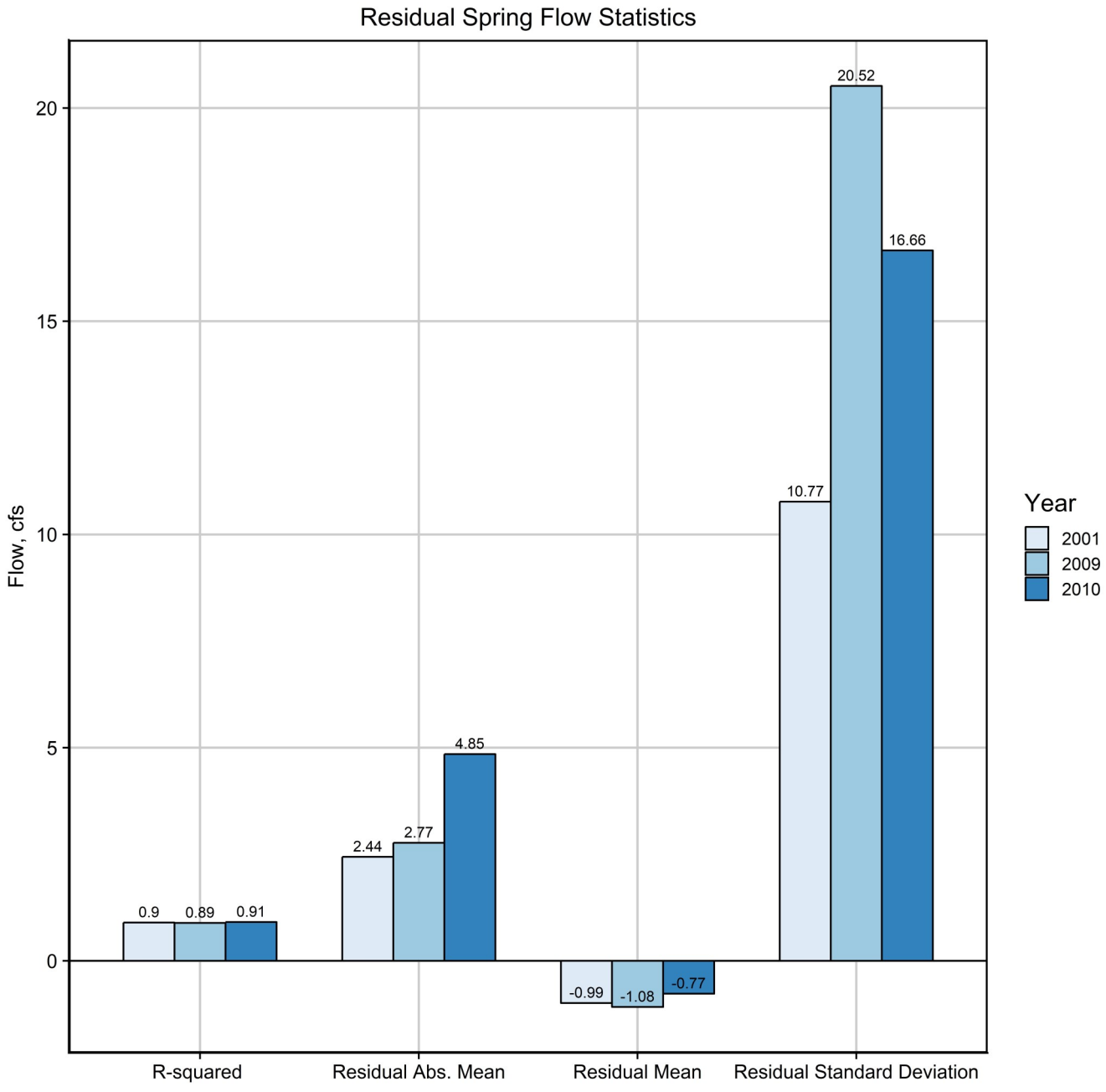

Figure 5-16. Residual spring discharge statistics comparison

Table 5-2. Observed and simulated spring flows

Important first magnitude springs and spring groups	Water Management District	Estimated Discharge, (cfs)	Simulated Discharge, (cfs)	Residual Discharge, (cfs)	Percent Error
Wacissa Springs Group	SR	440	411	29	7%
Ichetucknee Springs Group	SR	287	264	23	8%
Crystal River Springs Group	SWF	473	490	-17	4%
Rainbow Springs	SWF	618	757	-139	22%
Springs on the Santa Fe River between the gauges near Worthington Springs and Fort White	SR	687	721	-34	5%
Silver Springs Group	SJR	588	693	-105	18%
Lower Santa Fe Springs Group	SR	881	916	-35	4%
Wakulla Spring Main Vent	NWF	728	717	11	2%
Wacissa Head Spring	SR	159	155	4	3%
Madison Blue Spring	SR	129	122	7	5%
Alexander Spring	SJR	102	104	-2	2%
Silver Glen Spring	SJR	100	101	-1	1%
St. Marks River Rise	NWF	452	226	226	50%
Spring Creek Springs Group	NWF	307	452	-145	47%

are both located in Northwest Florida, which was an area of less focus for the NFSEG model. The model calibration of this area was relatively poor in 2001 and 2009 simulations, which may be improved in later versions of the model.

Rainbow Springs and Silver Springs are within a groundwater basin with higher annually averaged precipitation and estimated recharge in 2010 than either 2001 or 2009 (GWB-6 in Figures 5-2 and 5-6). Spring flows are highly sensitive to recharge and MSET values which were estimated through surface water models. For example, the estimated recharge in GWB-6 is between 15 and 30 inches per year (Figure 5-5). A potential error of 10 to 15% (which is acceptable in recharge estimates) could easily make up the difference between the simulated and observed flows of Silver and Rainbow springs in 2010.

Examination of available data indicated that flows at Silver and Rainbow Springs are highly sensitive to pool elevation, an estimated input parameter in the model. The observed data show that increases in pool elevations by 0.2 feet at Silver Springs and 0.4 feet at Rainbow Springs correspond to a flow increase of approximately 100 cfs, which is close to what the model is overestimating by in 2010. In addition, according to recently completed minimum flows and levels reports for both springs, there has been significant change in the relationship between pool elevation and spring flows mainly due to increased aquatic vegetation in the river runs since 2000, which would also reduce the model's ability to predict flows for these springs in recent periods. It should also be noted that no pool elevation measurements at Rainbow Springs were available for the simulation year, 2010. Thus, the pool elevation at Rainbow Springs in 2010 had to be estimated based on limited pool elevation measurements at the spring from 2014 through 2017 and downstream stage recorded at USGS gauge 02313100. Appendix J includes the simulated spring flows and residuals for all springs included in the 2010 simulation.

Estimated Baseflows

Figure 5-17 shows the distribution of simulated and estimated baseflow pickups in 2010. The 2010 estimated baseflow pickup residual statistics were compared with the 2001 and 2009 calibration statistics (Figure 5-18). Overall, baseflow pickup residual statistics in 2010 were similar to those in 2001 and 2009. The residual absolute mean and residual standard deviation in the year 2010 were larger than 2001, but smaller than 2009. The residual mean in the year 2010 was negative, which indicates an overall underestimation of baseflow pickups, compared to an overall overestimation of baseflow pickups in 2001 and 2009 (Figure 5-18). Appendix K includes the range of estimated baseflow pickups along with simulated residuals in 2010.

Cumulative baseflow estimates were developed for 10 USGS gauges based on available data. Table 5-3 includes the range of cumulative baseflow estimates, based on five baseflow estimation techniques, along with simulated cumulative baseflows in 2010. These results are also displayed graphically in Figure 5-19. Figure 5-20 includes the cumulative baseflow residual statistics for 2010, compared to 2001 and 2009. The mean residual in 2010 is negative, which suggests an overall underestimation of cumulative baseflow, while 2001 and 2009 both simulated an overall overestimation of cumulative baseflow. The residual standard deviation and residual absolute mean are larg-

Table 5-3. Range of estimated cumulative baseflow and simulated baseflow

USGS Gauge	Gauge Name	Estimated Average Baseflow (cfs)	Estimated Minimum Baseflow (cfs)	Estimated Maximum Baseflow (cfs)	Simulated Baseflow (cfs)
02228000	Satilla River at Atkinson, Ga	-653	-220	-974	-656
02231000	St. Marys River Near Mac-clenny, Fl	-106	-35	-152	-41
02243000	Orange Creek at Orange Springs, Fl	-7	-3	-10	-10
02315500	Suwannee River at White Springs, Fla.	-542	-106	-863	26
02317620	Alapaha River Near Jen-nings Fla	-607	-145	-915	-447
02319000	Withlacoochee River Near Pinetta, Fla.	-607	-151	-892	-365
02319500	Suwannee River at Ellaville, Fla	-3253	-1656	-4332	-1864
02320500	Suwannee River at Bran-ford, Fla.	-4376	-2873	-5708	-2695
02321500	Santa Fe River at Worthington Springs, Fla.	-74	-17	-123	-33
02322500	Santa Fe River Near Fort White, Fla.	-790	-697	-851	-803

*Note: A negative sign indicates flow from the surficial aquifer system to a stream reach. A positive sign indicates reverse flow, from the stream into the surficial aquifer system.

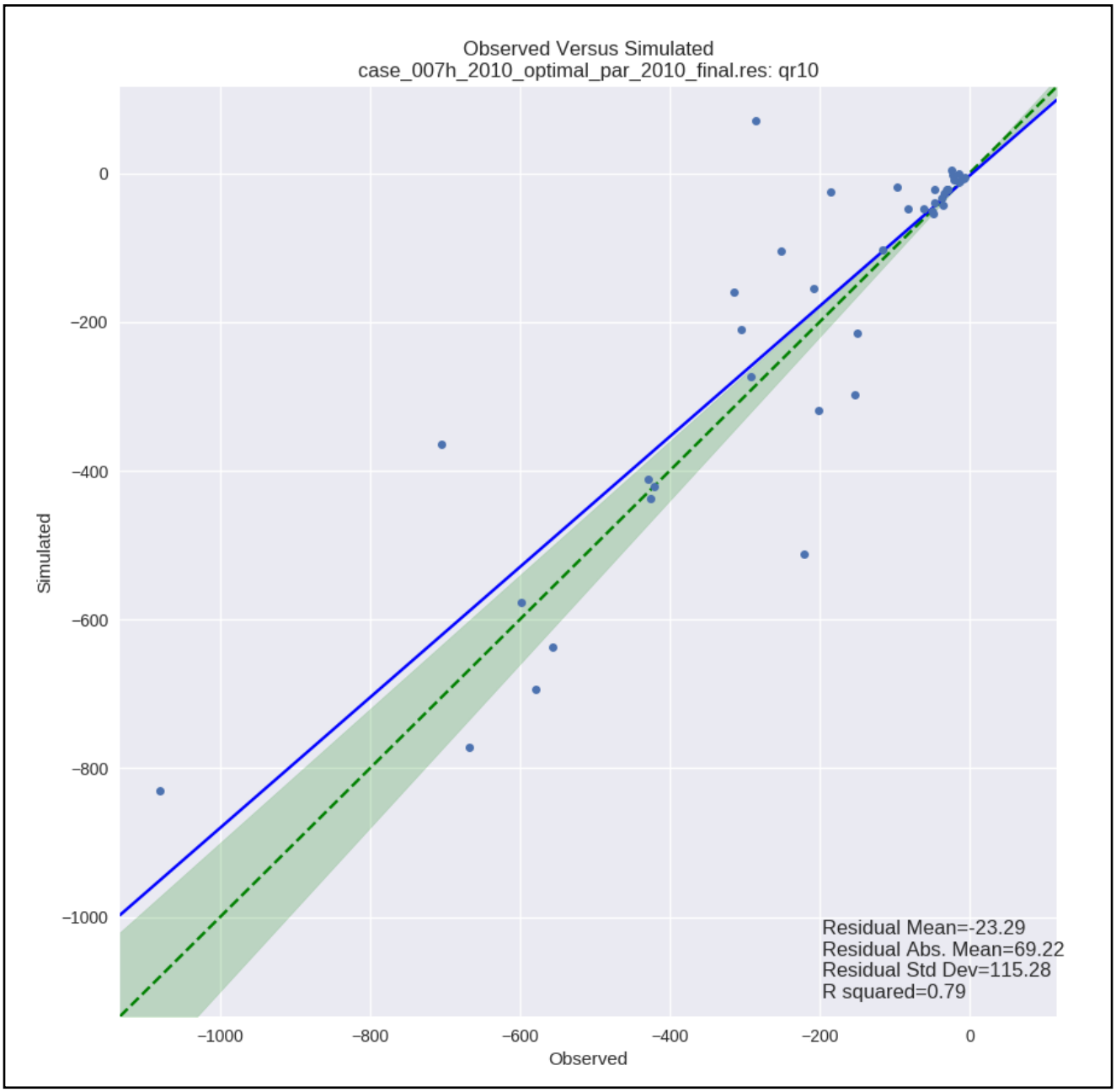

Figure 5-17. Simulated vs. estimated easeflow pickups (cfs), 2010

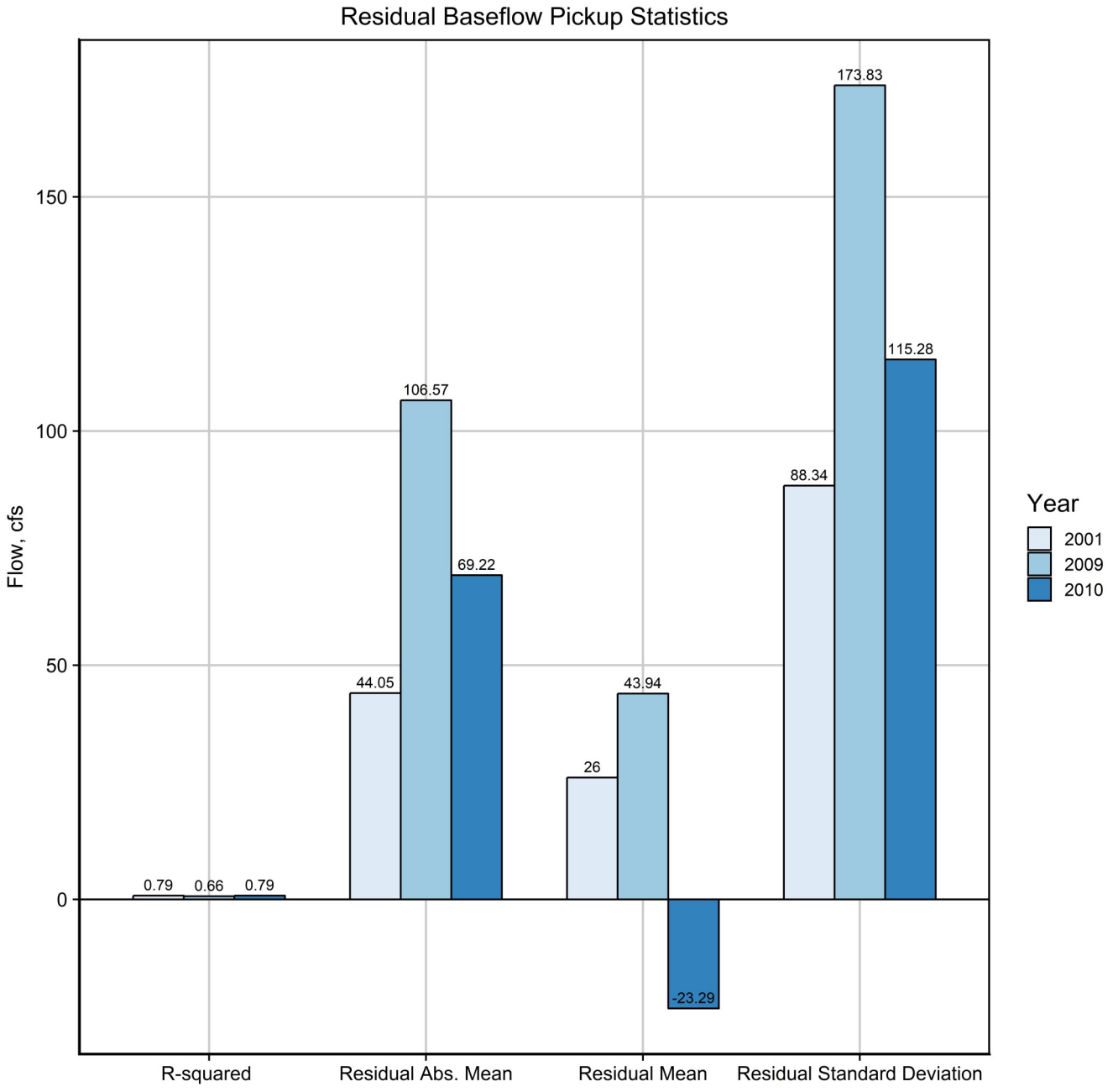

Figure 5-18. Residual baseflow pickup statistics comparison

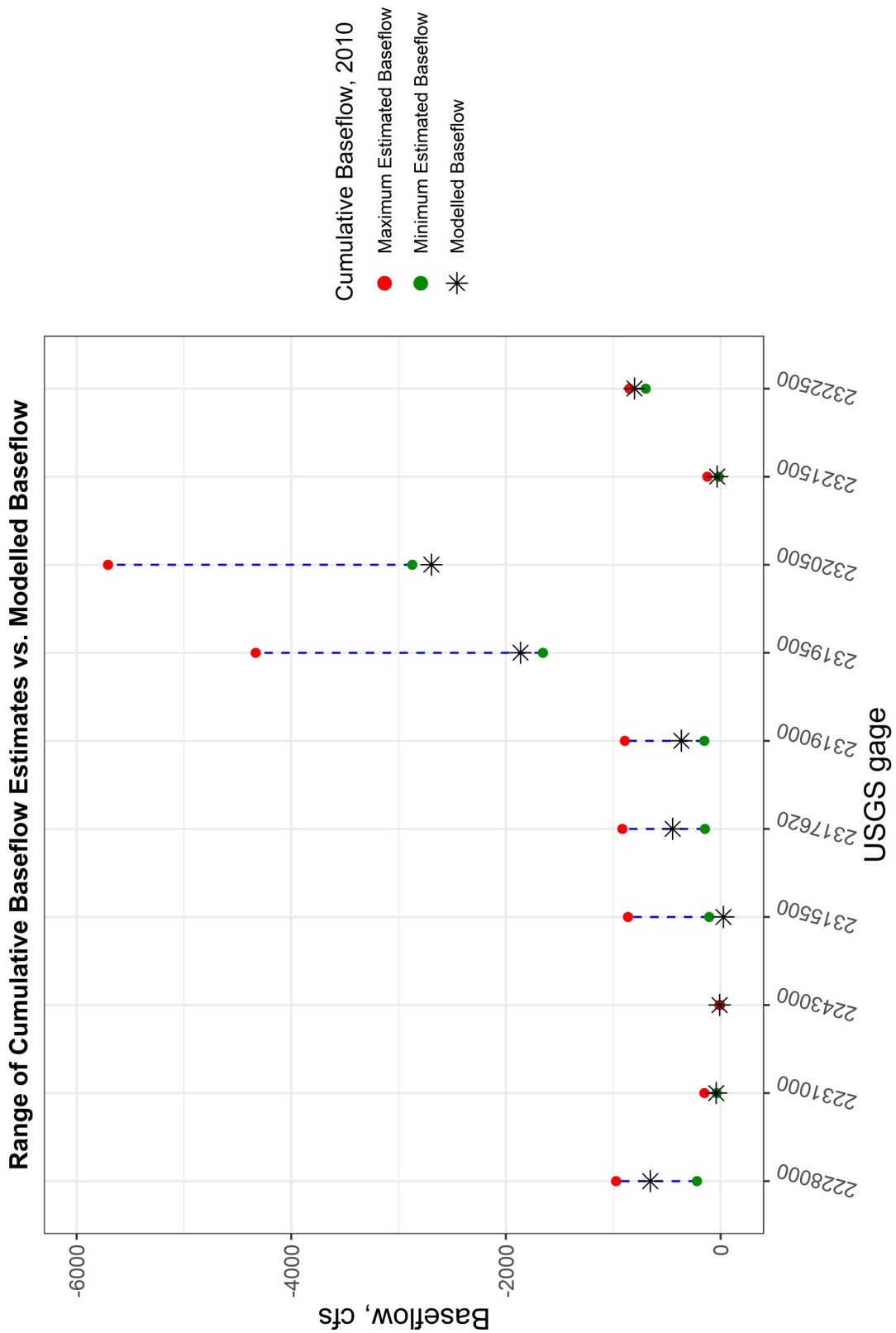

Figure 5-19. Simulated vs. estimated range of cumulative baseflow estimates in 2010

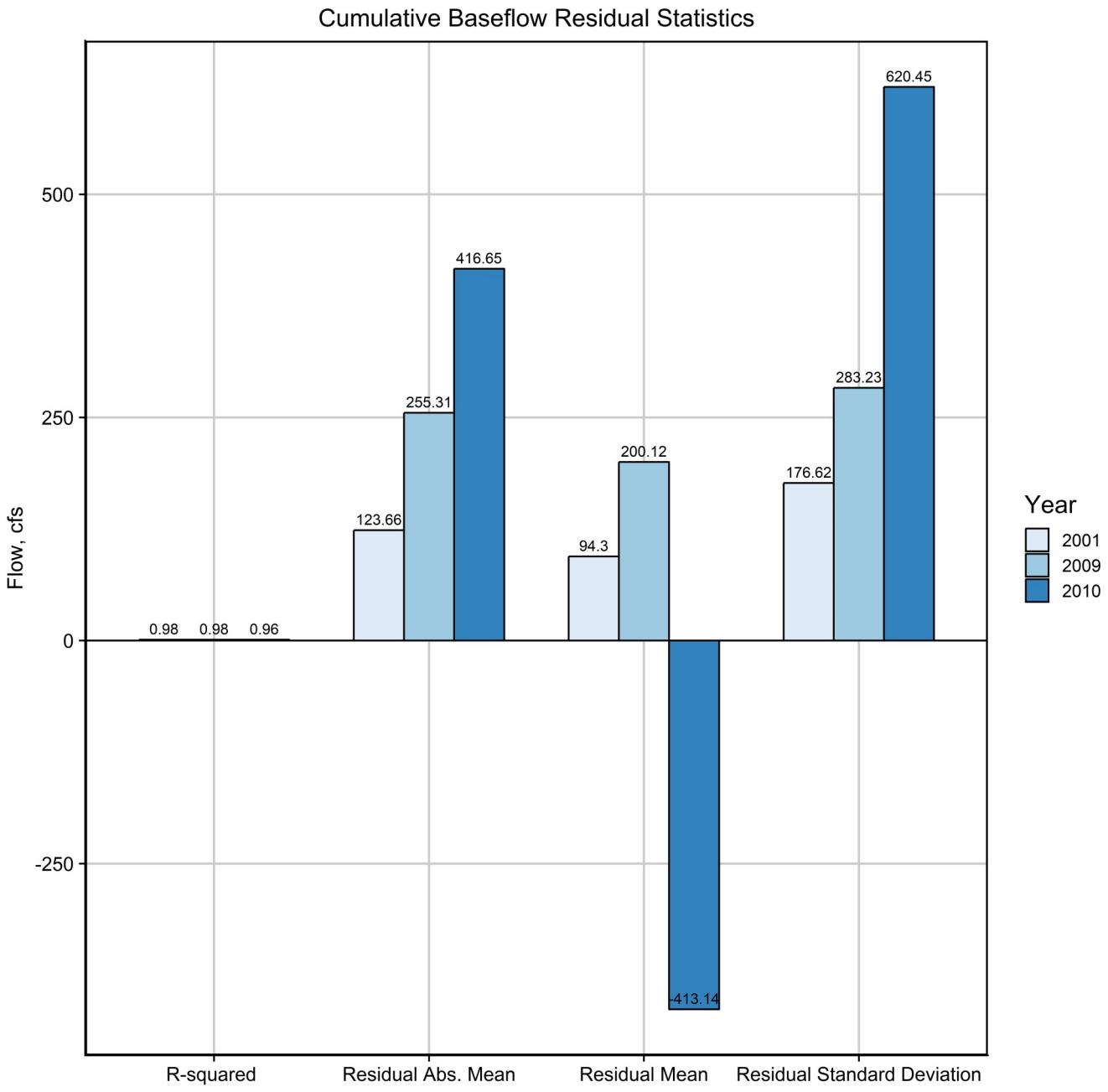

Figure 5-20. Residual cumulative baseflow statistics comparison

er in 2010 relative to 2001 and 2009. It should be noted, however, that these statistics are highly dependent on the estimated baseflow target, which represents the average of five baseflow estimation techniques. When comparing to the range (minimum and maximum) of estimated cumulative baseflows, the 2010 simulation predicted a cumulative baseflow within the estimated range for 8 of the 10 USGS gauges in which a cumulative baseflow was estimated with available data. (Table 5-3). Simulated cumulative baseflow at USGS gauges 02315500 and 02320500 were outside of the estimated cumulative baseflow range, which could be attributed to uncertainty associated with each baseflow estimation technique.

Spatial Distribution of UFA Level Residuals

The spatial distribution of groundwater level residuals in 2010 for Model Layer 1 and Model Layer 3 within delineated GWBs is shown in Figure 5-21 and Figure 5-22, respectively. Of the 1329 total observation wells used as simulation targets in 2010, 238 are in Model Layer 1 and 829 are in Model Layer 3. The predicted water level was within 5 feet of the observed water level for most of the wells located in Model Layer 1 and Model Layer 3. Overall, the 2010 spatial distribution of residuals in Model Layer 1 and Model Layer 3 are similar to the 2001 and 2009 calibration results, suggesting a reasonable prediction of water level in the year 2010.

Groundwater level residuals in 2010 were compared to those in 2001 and 2009 at each 2010 overlapping observation well. With this method, only observations common in all three years were directly compared. Using this approach, 165 wells were directly compared in Model Layer 1 and 829 wells were directly compared in Model Layer 3 for all years. The percentage of wells meeting a statistical criterion of residuals within +/- 5 feet and +/- 2.5 feet were compared for each year within delineated GWBs and model-wide in Model Layer 1 (Table 5-4) and Model Layer 3 (Table 5-5). Model-wide, the percentage of wells in Model Layer 1 with a residual within ±5 feet (70 percent) was slightly lower, but comparable to those of 2001 (72 percent) and 2009 (79 percent). Similarly, the percentage of wells in Model Layer 3 with a residual within ±5 feet (73 percent) was slightly lower, but comparable to those of 2001 (77 percent) and 2009 (78 percent). The percentage of wells in Model Layer 1 with a residual within ±2.5 feet (41 percent) was slightly lower, but comparable to those of 2001 (48 percent) and 2009 (55 percent). The percentage of wells in Model Layer 3 with a residual within ±2.5 feet (43 percent) was also slightly lower, but comparable to those of 2001 (44 percent) and 2009 (50 percent).

Simulated UFA Potentiometric Surface

The simulated 2010 UFA potentiometric surface (Figure 5-23) was compared with the observed 2010 UFA potentiometric surface (Figure 5-24). The observed 2010 UFA potentiometric surface was developed using medians of observed water level data and, in unconfined areas, estimated river stages, which were interpolated and contoured to create a median potentiometric surface map. The comparison between the simulated and observed UFA potentiometric surface suggested that the 2010 simulation closely cap-

Table 5-4. Distribution of water level residuals in model Layer 1 by GWB

Groundwater Basin	-5 feet < Residual < 5 feet % of wells			-2.5 feet < Residual < 2.5 feet % of wells		
	2001	2009	2010	2001	2009	2010
GWB-1 (9 wells)	78	89	89	56	44	44
GWB-2 (6 wells)	33	67	50	0	17	0
GWB-3 (20 wells)	70	90	70	65	50	45
GWB-4 (45 wells)	76	69	58	47	51	38
GWB-5 (3 wells)	67	100	100	0	67	33
GWB-6 (14 wells)	71	71	71	43	64	50
GWB-7 (68 wells)	72	82	76	51	60	44
Model-wide (165 wells)	72	79	70	48	55	41

*Note: Only observations common in all years (2001, 2009 and 2010) were used in this analysis.

Table 5-5. Distribution of water level residuals in model Layer 3 by GWB

Groundwater Basin	-5 feet < Residual < 5 feet % of wells			-2.5 feet < Residual < 2.5 feet % of wells		
	2001	2009	2010	2001	2009	2010
GWB-1 (144 wells)	79	81	83	43	45	52
GWB-2 (94 wells)	70	76	65	32	40	30
GWB-3 (179 wells)	79	74	69	51	41	40
GWB-4 (131 wells)	73	81	70	44	60	34
GWB-5 (39 wells)	46	41	44	23	31	18
GWB-6 (126 wells)	83	83	75	50	63	55
GWB-7 (116 wells)	85	84	85	47	58	53
Model-wide (829 wells)	77	78	73	44	50	43

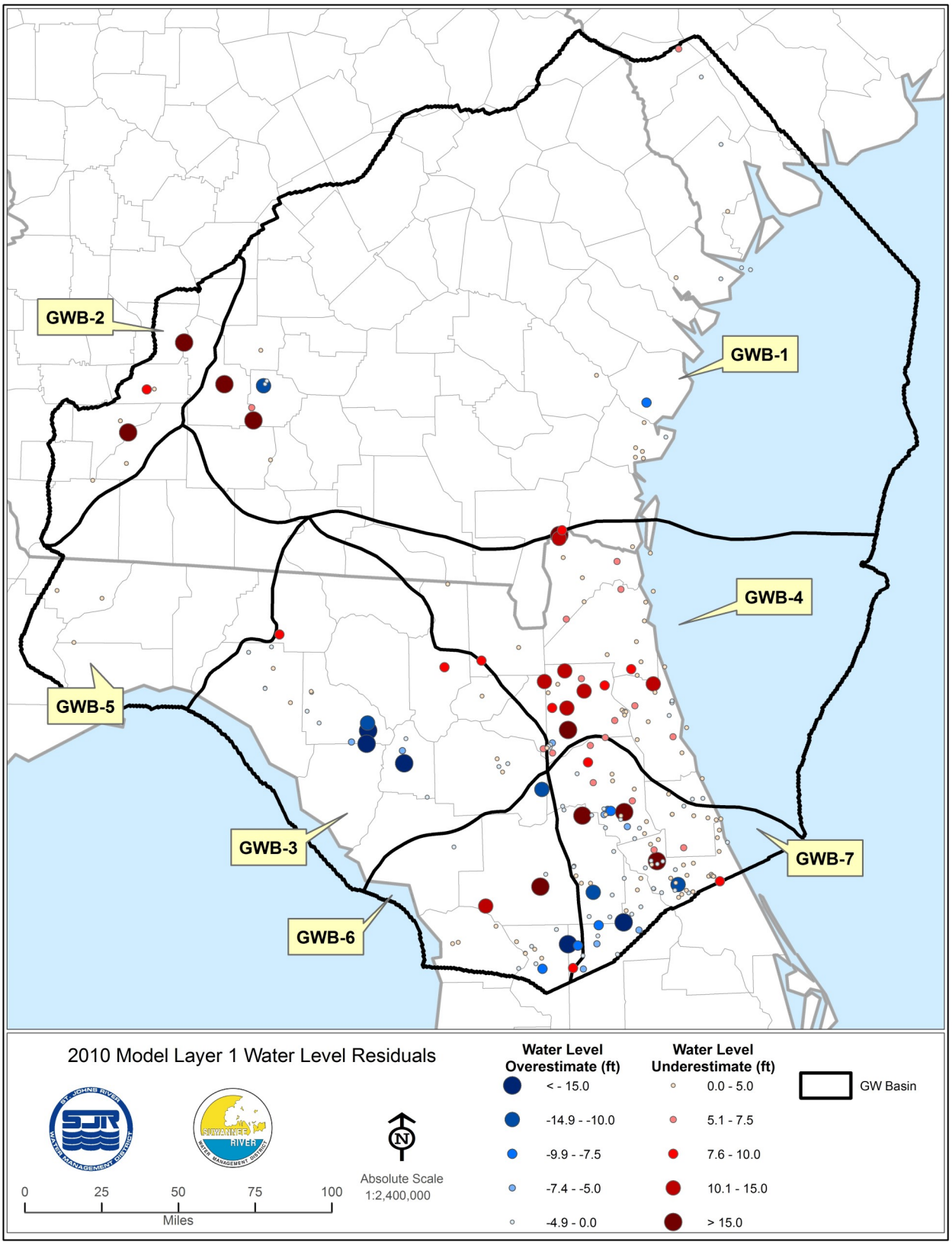

Figure 5-21. 2010 groundwater level residuals, model Layer 1

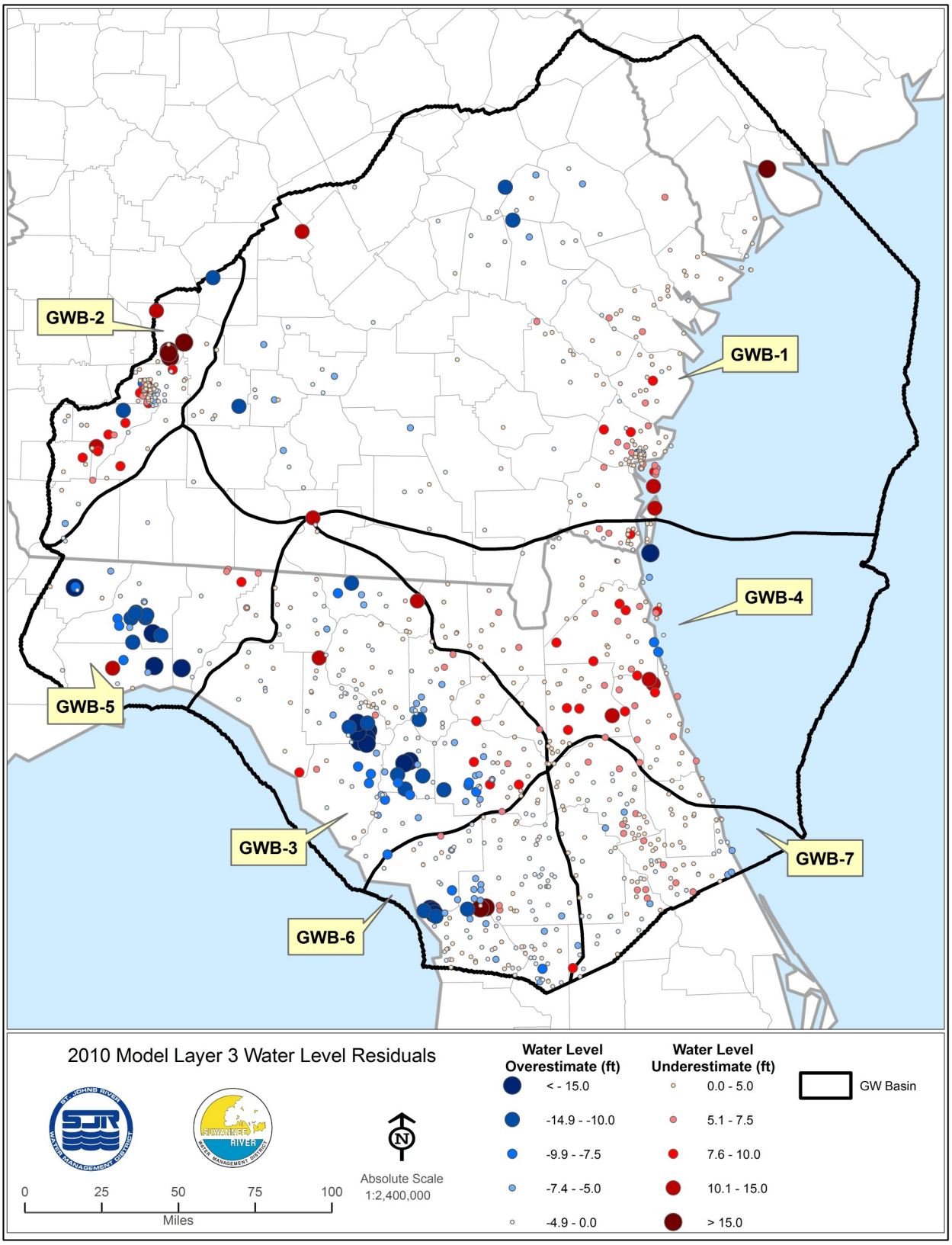

Figure 5-22. 2010 groundwater level residuals, model Layer 3

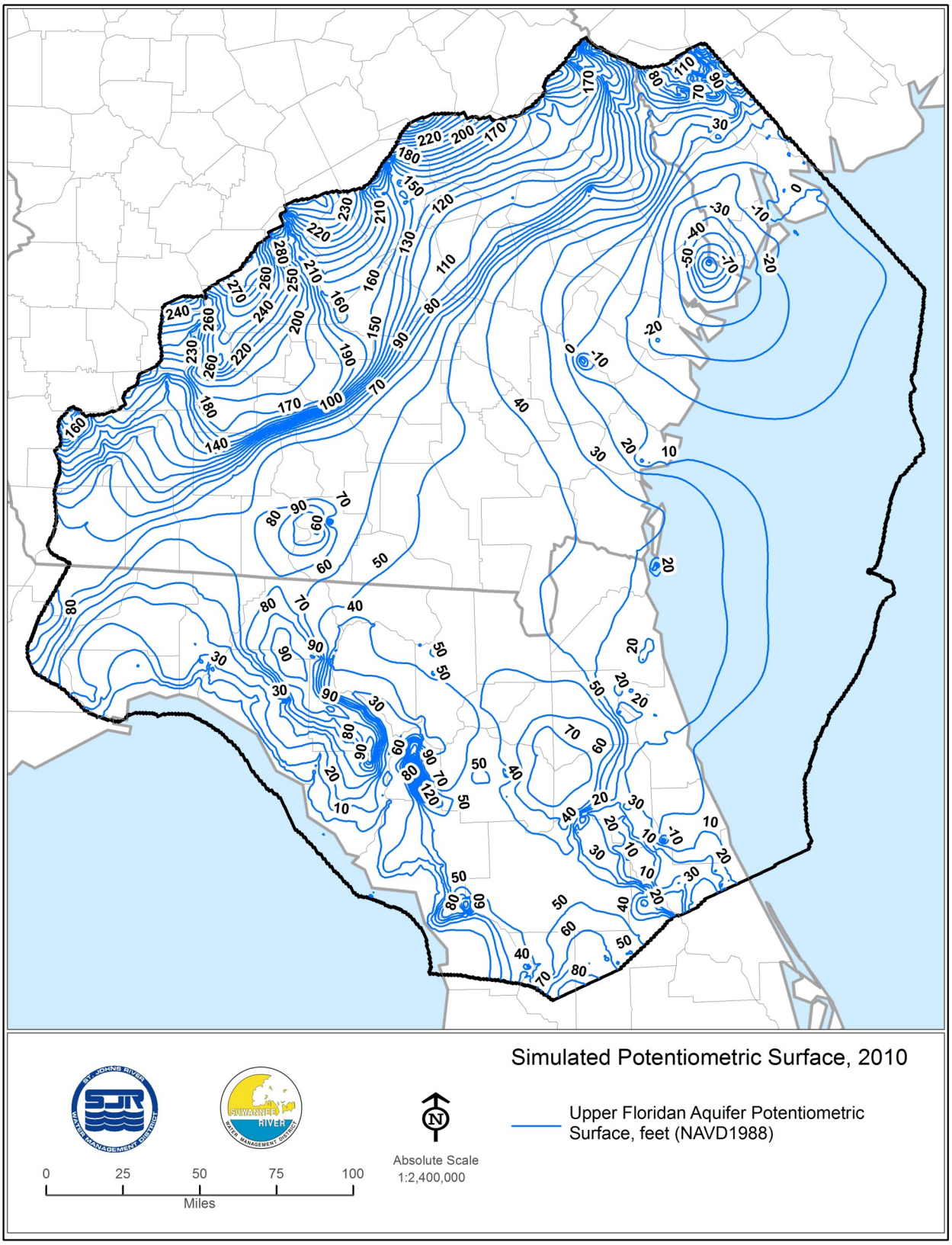

Figure 5-23. Simulated UFA potentiometric surface, 2010

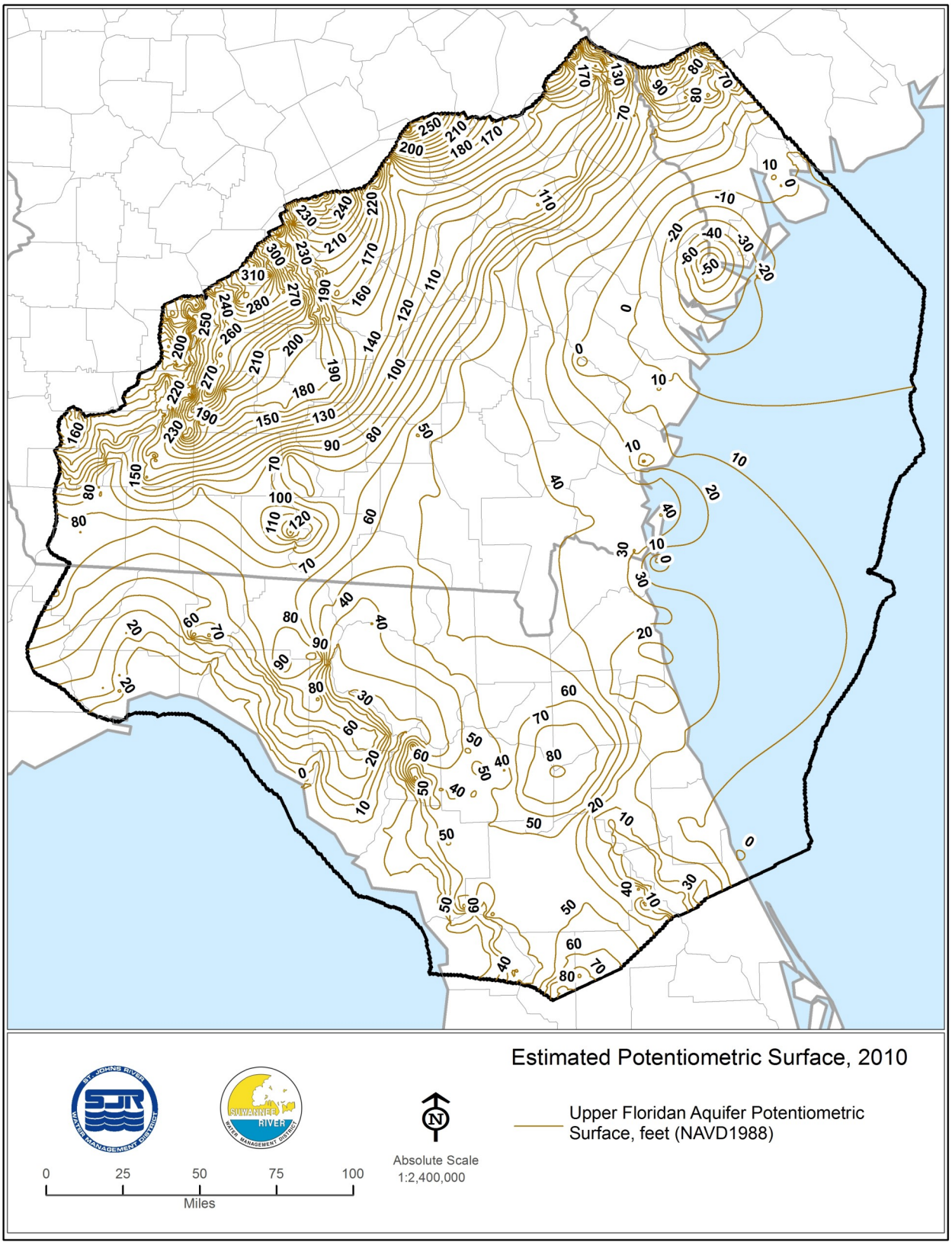

Figure 5-24. Observed UFA potentiometric surface, 2010

tured the general shape of the observed 2010 potentiometric contours including the major features in the potentiometric map, such as the Valdosta potentiometric high, the Keystone Heights potentiometric high, and wellfield drawdown in the Gainesville area.

Simulated Model Fluxes

Section 6 presents a detailed model mass balance summary using simulated flows into and out of each model layer for 2001, 2009 and 2010. Figure 5-25 includes the model-wide mass balance for the year 2010. Table 5-6 presents a summary of simulated net fluxes into the model in 2010, compared to 2001 and 2009. Drain and river flows in 2010 are slightly higher than in 2001, but lower than in 2009 throughout the model. GHB flows out of Layer 3 in 2010 are higher than in 2001 and 2009. However, the portion of GHB flows in Layer 3 represented by spring flows in the year 2010 is higher than in the year 2001, but less than spring flows in 2009. Applied recharge in 2010 is within the range of applied recharge in 2001 and 2009. Similarly, simulated evapotranspiration from groundwater in 2010 is higher than that simulated in 2001, but lower than 2009. Model fluxes into and out of Model Layer 3 in 2010 are comparable to corresponding simulated fluxes in 2001 and 2009.

NO-PUMPING SIMULATION

Predictions of groundwater levels and spring flows under a no-pumping condition are needed to support a variety of water resource decisions. These types of predictions are used to help assess whether minimum flow and level standards (and proxies for these standards) are being met at water bodies of interest. The NFSEG v1.1 model was developed in large part so that no-pumping simulations would not be limited by issues such as lateral boundary proximity that have affected other models.

Staff conducted a historical review of previous regional modeling efforts where groundwater withdrawals were completely removed for a model simulation. There has generally been an evolution through time of approaches with the most early regional groundwater flow models using a specified head surficial aquifer that served as a boundary condition for the simulation. As model complexity, data collection, and computing power increased, the surficial aquifer has been more routinely actively simulated and earlier steady-state approaches have been increasingly replaced by transient simulations. The testing or demonstration of the reasonableness of no-pumping scenarios is also becoming more common.

The most recent example of evaluating a no-pumping condition was for the Integrated Northern Tampa Bay (INTB) model by the University of South Florida (Ross and Trout, 2017). The INTB model is a transient integrated surface and groundwater model encompassing a domain of 4,000 square miles in west-central Florida (Geurink and Basso, 2013). From the USF report:

Comparisons between heads and fluxes were made for pumping and no-pumping scenarios to determine if the differences were reasonable. Because limited data exist to

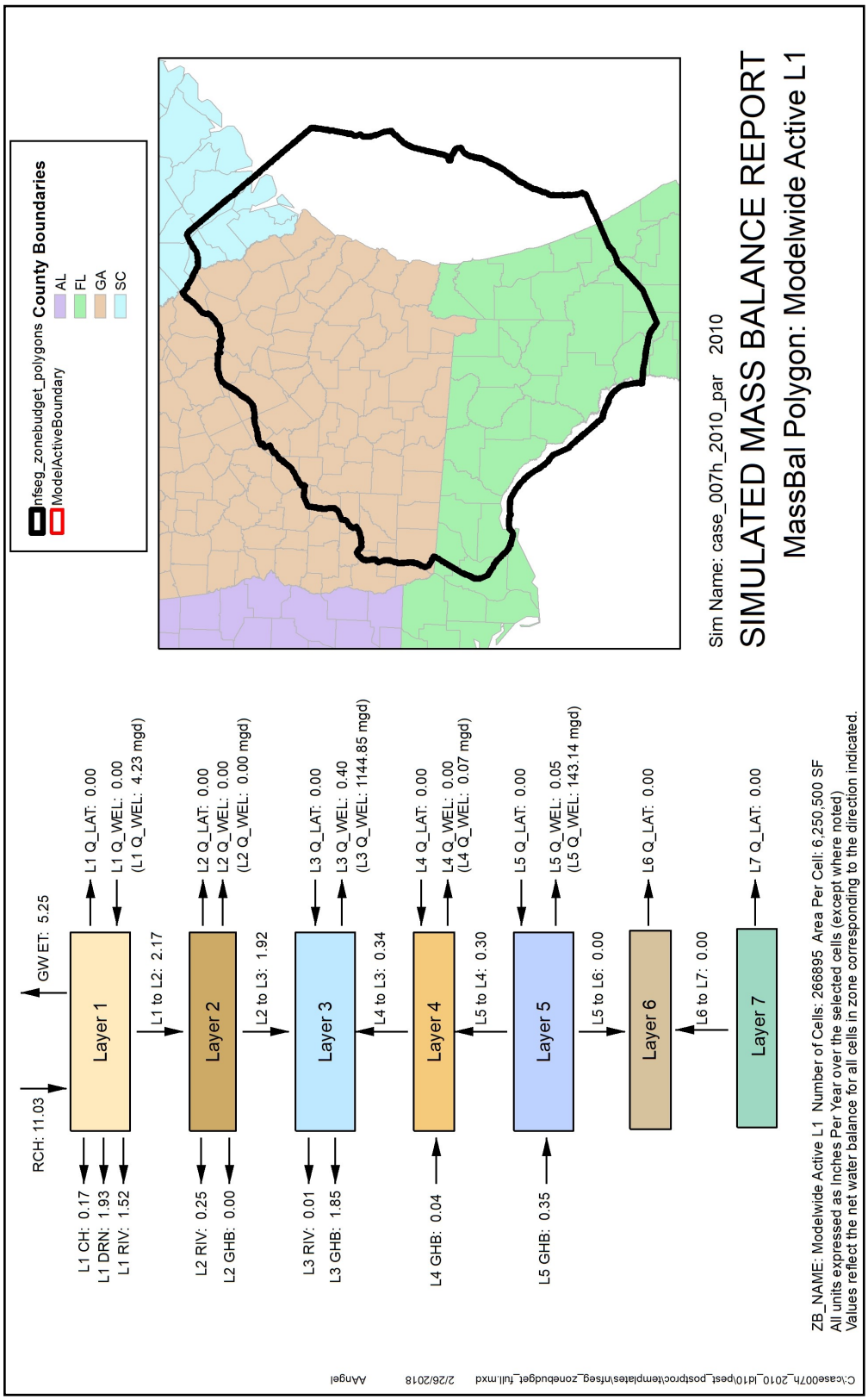

Figure 5-25. Model wide mass balance summary, 2010 (arrows indicate net flow into or out of the layer)

Table 5-6. Comparison of simulated net fluxes to model for 2001, 2009 and 2010 (all flows in/year)

MODEL YEAR	MODEL LAYER	CH	DRN	GHB	GHB SPRING FLOWS	GW ET	LAT, Q_LAT	Q_WEL	RCH	RIV	FLOW TO LOWER LAYER
2001	1	-0.15	-1.66	—	0	-4.74	0	-1.82E-04	9.67	-1.36	-1.76
	2	—	—	0	0	—	0	0	—	-0.26	-1.51
	3	—	—	-0.08	-1.36	—	0	-0.43	—	-0.01	0.37
	4	—	—	0.04	0	—	0	0	—	—	0.33
	5	—	—	0.39	0	—	0	-0.06	—	—	-2.07E-07
	6	—	—	—	—	—	0	—	—	—	1.05E-08
	7	—	—	—	—	—	0	—	—	—	—
2009	1	-0.21	-2.59	0	0	-6.86	0	1.49E-03	13.9	-2.19	-2.07
	2	—	—	0	0	—	0	0	—	-0.29	-1.78
	3	—	—	-0.08	-1.63	—	0	-0.4	—	-0.01	0.35
	4	—	—	0.04	0	—	0	0	—	—	0.31
	5	—	—	0.36	0	—	0	0.05	—	—	-4.12E-07
	6	—	—	—	—	—	0	—	—	—	-1.92E-07
	7	—	—	—	—	—	0	—	—	—	—
2010	1	-0.17	-1.93	—	—	-5.25	0	1.49E-03	11	-1.52	-2.17
	2	—	—	0	0	—	0	0	—	-0.25	-1.92
	3	—	—	-0.37	-1.48	—	0	-0.4	—	-0.01	0.34
	4	—	—	0.04	0	—	0	0	—	—	0.3
	5	—	—	0.35	0	—	0	0.05	—	—	-2.28E-07
	6	—	—	—	—	—	0	—	—	—	2.89E-08
	7	—	—	—	—	—	0	—	—	—	—

*Note: — INDICATES CELL NOT APPLICABLE TO THE LAYER.
POSITIVE NUMBER INDICATES INFLOW FROM THE LAYER, WHILE NEGATIVE INDI-

validate how well the model can predict the effects of the elimination of groundwater pumping across the domain, the approach taken here is mostly to examine the change in various groundwater flow-system components and determine if the overall weight of evidence is consistent with expected results.

Selected elements from the USF review of the INTB model were applied to the NFSEG v1.1 model review to test the reasonableness of the model predictions of simulated withdrawal impacts using the difference between the steady-state no-pumping condition and the 2009 condition. Components examined for this review included groundwater levels, spring discharges, groundwater above land surface and a comparison of the simulated no-pumping UFA potentiometric surface to the USGS predevelopment potentiometric surface.

Groundwater Levels

The USGS compiled a map of the potentiometric surface of the Floridan aquifer system (Figure 5-26), which represents an estimate of that surface prior to significant withdrawals/development (Johnston et al, 1980: Figure 5-26). The map was based on a composite of previously developed maps with modifications where necessary, and potentiometric surface maps where pumping was relatively low. According to Johnston et al. (1980), the purpose of the map was not to show precise water level data at specific sites; rather, to show the best estimate of the configuration of the predevelopment potentiometric surface using the best available data at that time. This data was used to evaluate the reasonableness of simulated groundwater levels when all pumping is removed from the NFSEG v1.1 model.

A comparison of no-pumping simulated groundwater levels for Layer 3 was made to the USGS predevelopment groundwater levels within a sub-region of the NFSEG model domain (Figure 5-27) that includes areas of the upper basin of the Santa Fe River, that are likely to be the focus of future applications of the NFSEG model. It excludes areas that correspond to northern portions of the NFSEG domain that may be unduly influenced by the specified source heads of the GHB conditions used to simulate flux across the northern lateral boundary, as well as other areas where changes in the regional potentiometric surface have been less pronounced. The simulated groundwater levels of Layer 3 were chosen for this comparison because Layer 3 is generally representative of the uppermost vertical extent of the Floridan aquifer system (the Upper Floridan aquifer or Zone 1, as defined in Chapter 2, where the middle confining unit is not present). This is the same vertical extent that encompasses the open intervals of most or all of the observation wells used in the construction of the predevelopment potentiometric surface map.

Several factors may contribute to the differences between the estimated potentiometric surface and the surface from the no-pumping simulation. Some inaccuracies in the USGS map may be present because of limited observations and some approximations, as detailed by Johnston et al (1980). Differences in rainfall amounts between 2009 and the general period that the observations on which the USGS map is based, may explain some differences within the sub-region. The effects of changes to the predevelopment

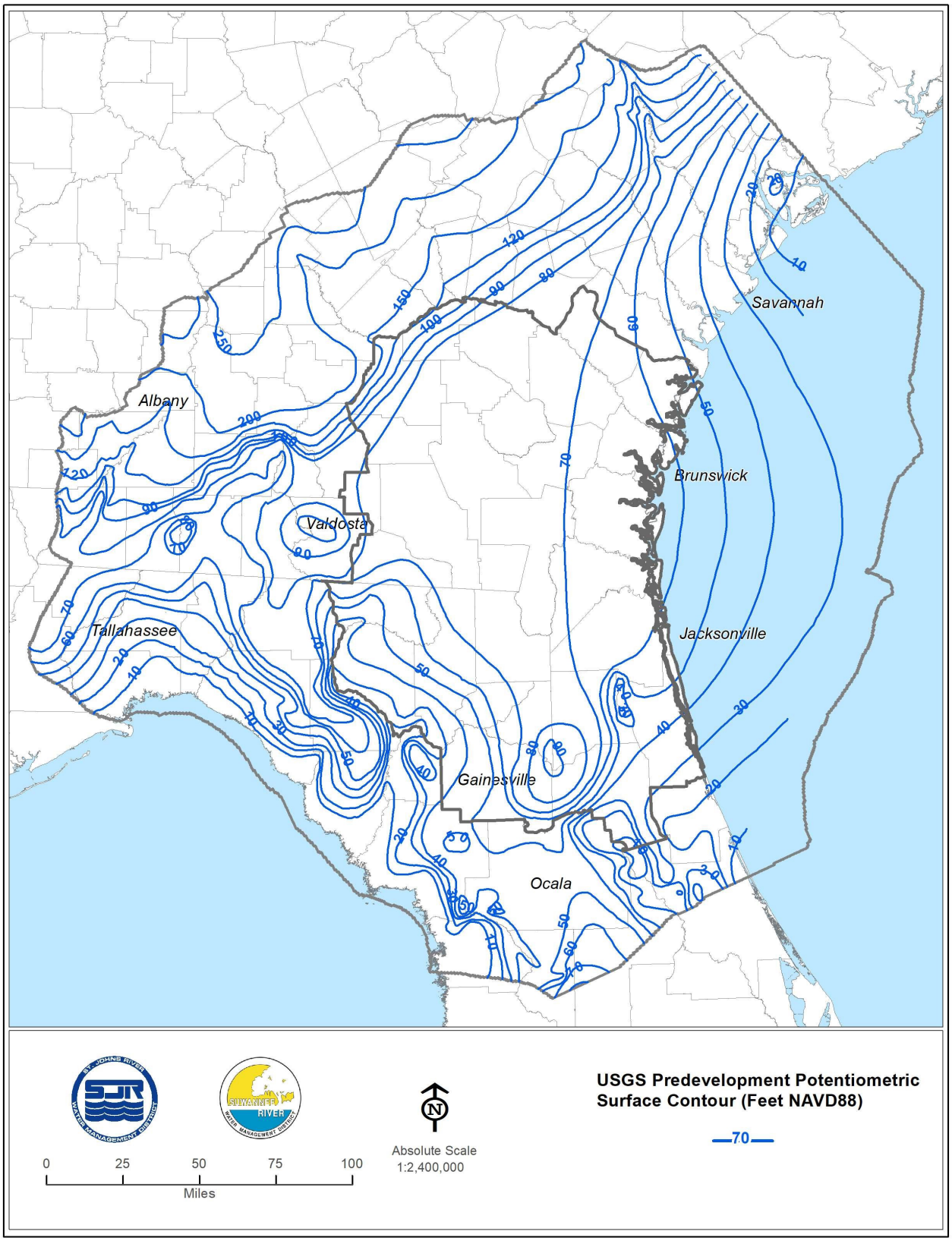

Figure 5-26. USGS estimated predevelopment potentiometric surface of the Floridan aquifer system within the NFSEG domain (after Johnston et al. 1980)

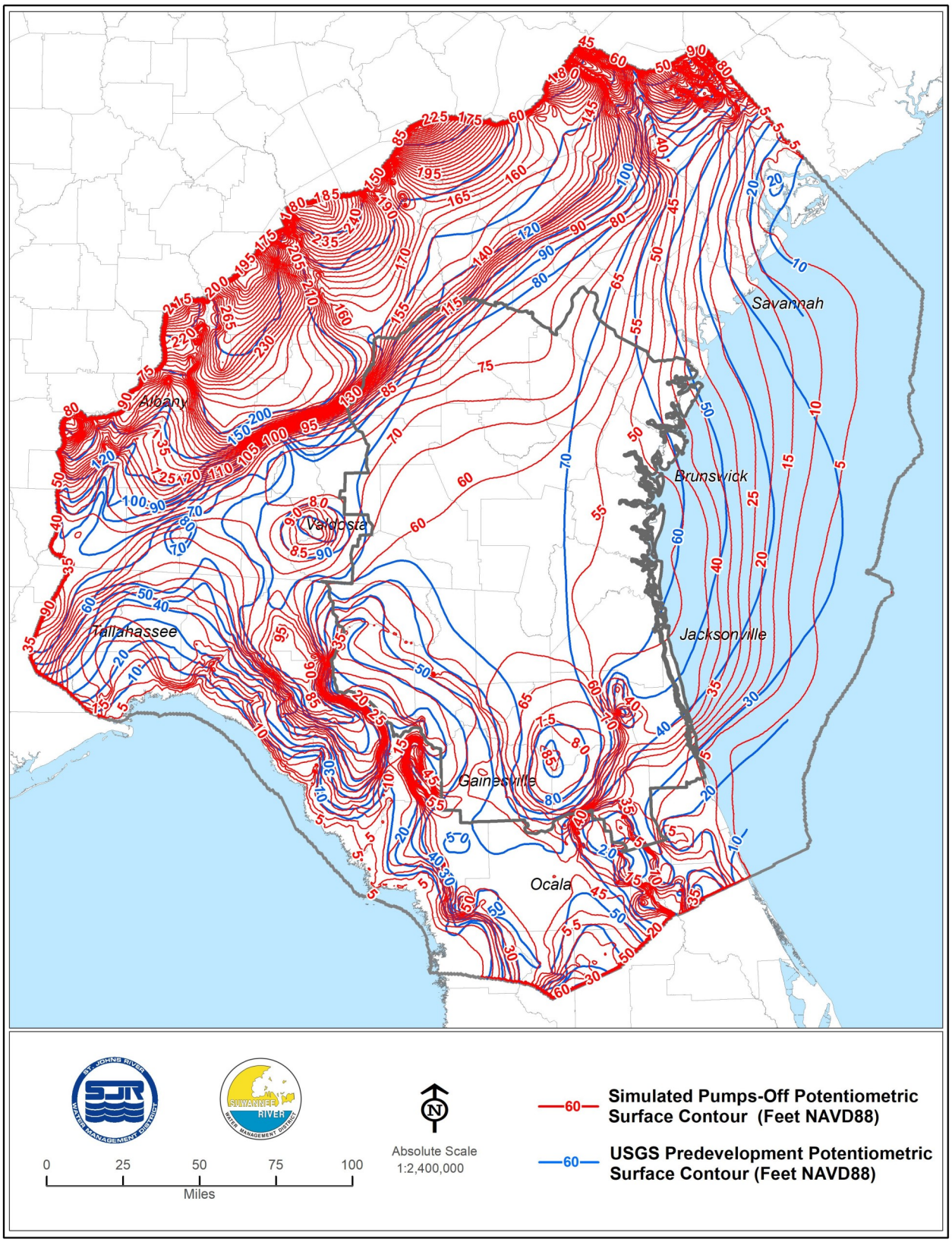

Figure 5-27. NFSEG simulated no-pumping Layer 3 potentiometric surface and USGS estimated predevelopment potentiometric surface of the Floridan aquifer system (after Johnston et al. 1980)

hydrological system other than pumping also play a role. Simulation error is a contributing factor; the no-pumping simulation represents a major departure from the general conditions to which the NFSEG model was calibrated.

In general, the simulated no-pumping surface is about 0 to 15 feet lower than the estimated predevelopment potentiometric surface (Figure 5-28). In most of the areas of the Keystone Heights potentiometric high and of the upper Santa Fe basin (Figures 5-27 and 5-28) simulated no-pumping heads are within 0 to 10 feet of the estimated potentiometric surface. In the central portion of the sub-region, simulated water levels are generally 10 to 15 feet lower than corresponding estimated predevelopment potentiometric surface. This includes areas of intense groundwater withdrawals along the coasts of northeast Florida and southeast Georgia. In a few areas, differences in water levels exceed 15 feet, but these are relatively small in extent.

The comparison shows a reasonable agreement in the configuration of the two surfaces (Figure 5-28), and changes in the configuration from pumps-on to no-pumping conditions are consistent with expected changes associated with removal of pumping stresses. For example, the surface from the no-pumping simulation reproduced the coastwise parallel contour configuration along the Atlantic coastline in southern Georgia and northeastern Florida. In addition, the higher contours near the Keystone Heights potentiometric high in the modern surfaces exhibited an expected migration toward coastal areas to the east and towards the upper Suwannee River to the west.

Spring Discharges

A comparison of simulated no-pumping spring discharges for selected springs to observed values reported by Stringfield (1936) shows simulated no-pumping spring discharges that are generally within the provided range of corresponding observed discharges (Table 5-7). These observations are used for the comparison because they were made in a period in which large-scale pumping impacts had generally not occurred yet and, thus, are the best available data representative of a no-pumping condition.

Given these considerations, along with the fact that the NFSEG v1.1 was not calibrated to the no-pumping condition, the model performance is generally good in matching the spring discharges, apart from White Sulphur Springs (also known as “White Springs”) and Juniper Springs, both of which have been affected by anthropogenic changes. In general, the model is matching minimums of Stringfield’s (1936) observations well. The range of Stringfield’s (1936) observations shows the potential for temporal variation in the discharges of many springs. These variations would presumably have been due largely to variations in rainfall amounts.

The changes made at Juniper Springs included the creation of a swimming area by enclosure of the spring vent within a wall and installation of an outlet control, presumably resulting in the raising of the spring pool (http://springseternalproject.org/springs/jumiper-springs; Rosenau et al. 1977). The work occurred in the mid-1930’s and was conducted by the Civilian Conservation Corps (http://springseternalproject.org/springs/jumiper-springs). This is the probable reason for the reduction in spring flow relative

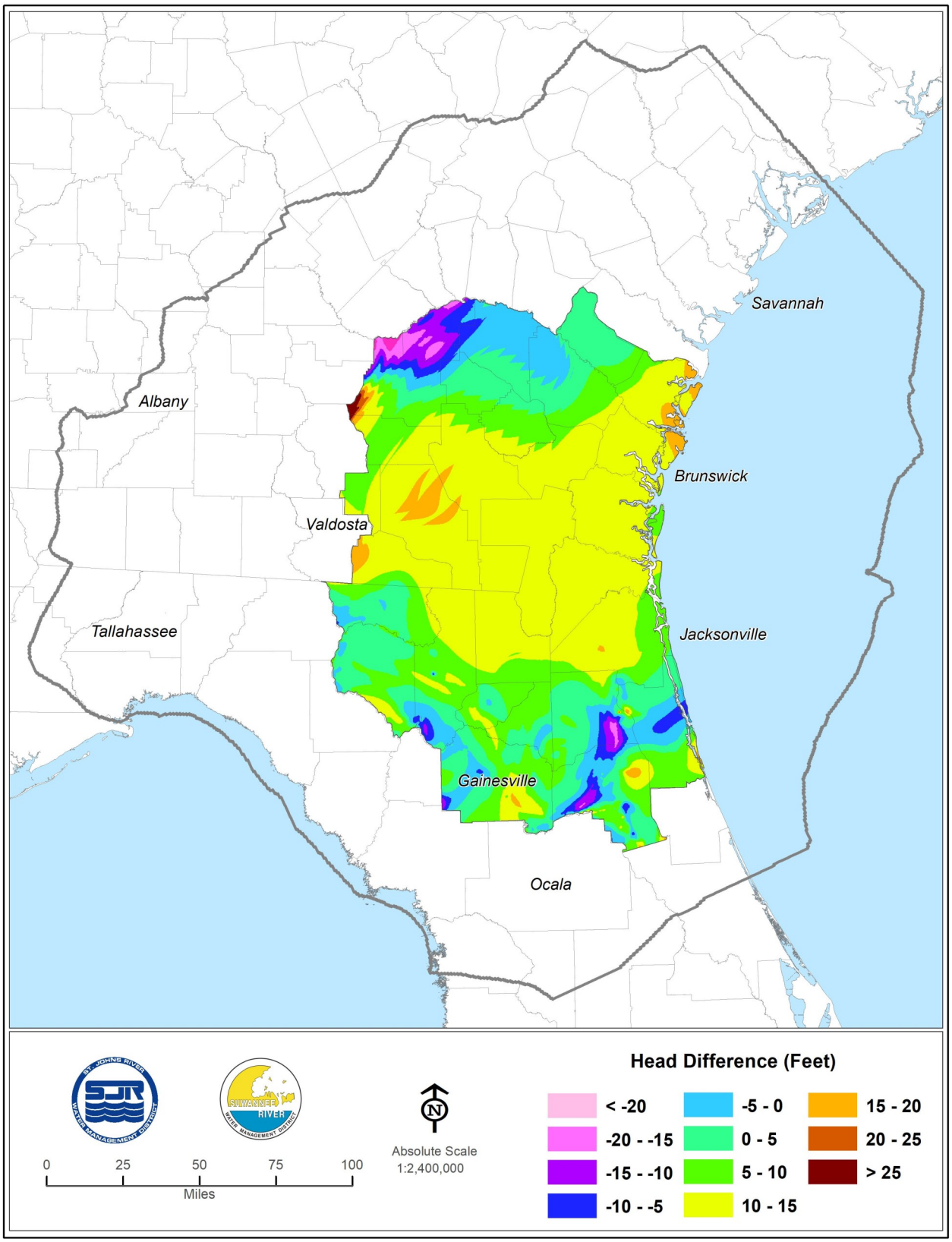

Figure 5-28. Differences between the USGS estimated predevelopment potentiometric surface of the Floridan aquifer system (after Johnston et al. 1980) and the NFSEG simulated no-pumping Layer 3 potentiometric surface within the area of interest

Table 5-7. Simulated 2009 and no-pumping spring discharges and corresponding observations of Stringfield (1936) for selected springs

Spring	2009 Simulated Discharge (cfs)	No-pumping Simulated Discharge (cfs)	Stringfield (1936) Observed Discharges				
			Minimum Discharge (cfs)	Date	Maximum Discharge (cfs)	Date	Mean Discharge (cfs)
Silver	509	532	526	6/6/1933	1240	9/9/1933	808
Rainbow	570	579	487	10/3/1932	910	10/4/1933	652
Itchetucknee	264	279	260	6/4/1932	467	6/30/1930	340
Homosassa	124	124	141	2/14/1933	177	3/15/1932	159
Manatee	129	129	149	3/14/1932	n/a	n/a	149
Silver Glen	101	102	90	2/7/1933	125	3/17/1931	104
Alexander	102	103	112	2/12/1931	124	2/7/1933	68
Juniper	15	15	106	2/7/1933	117	3/3/1932	112
Fanning	68	68	79	3/14/1932	109	10/25/1930	94
Salt	92	92	62	2/7/1933	105	5/5/1931	85
Poe	43	44	31	3/14/1932	87	2/19/1917	59
Madison Blue	104	118	75	3/15/1932	n/a	n/a	75
White	6	2	36	11/4/1931	67	5/8/1927	48
Suwanacoochee	29	32	18	3/16/1932	41	11/6/1931	30
Ponce de Leon	21	22	20	3/7/1932	22	2/11/1929	21

to the observations of Stringfield (1936), which occurred in 1932 and 1933, as noted in Table 5-7. Thus, lowering the specified pool elevation in the model representation of this spring might improve the no-pumping simulated flow of Juniper Springs. Regarding White Sulphur Springs, simulation of spring flow is complicated by interaction with the Suwannee River, the highly karstic nature of the Floridan aquifer in the area of the spring vent, and enclosure of the spring vent by a concrete wall installed in the early 1900's. Therefore, improving simulated spring flows under pumps-on and pumps-off conditions may require representation of the spring vent and surrounding areas with a greater degree of resolution and possibly under transient conditions as well.

Simulated Flooding in Layer 1

An important indication of the ability of the model to simulate the no-pumping condition is the degree to which simulated flooding in Layer 1 increases due to the elimination of simulated groundwater pumping. Limited flooding in Layer 1 occurs in both the 2001 and 2009 version of the model. When simulated groundwater pumping, which is mostly concentrated in Layers 3 and 5, is removed, the resulting increases in groundwater levels of Layer 3 propagate into Layer 1 and cause additional flooding in some areas. Figure 5-29 shows the change in simulated flooding depths between the 2009 and no-pumping simulations. The maximum increase in flooding depth is between 7 and 10 feet, and this occurs over relatively small areas. In most areas, the simulated increase in flooding depth is less than a foot. This result is another indication of the ability of the model to respond reasonably to the removal of pumping stresses.

Baseflow Estimates from 1933 through 1942

Historical baseflows were evaluated for the period of 1933 through 1942 at seven different gauges with long-term streamflow observations based on the HYSEP local minimum, BFI standard, BFI modified, and USF methods (Table 5-8). The following statistics were used to summarize the resulting baseflow estimates: maximum, minimum, 25^{th} (exceedance) percentile, median, and 75^{th} (exceedance) percentile. Simulated baseflows were then extracted from the pumps-off simulation that is based on 2009 hydrologic conditions at the gauges listed in Table 5-8. The simulated pumps-off baseflows at gauges 0223100 and 02315500 were within the range of the median estimated baseflows as derived from the various methods. The simulated pumps-off baseflows at 02319000, 02319500, and 02320500 were between the respective medians and 25^{th} percentiles. The simulated pumps-off baseflow at gauge 02246000 fell between the respective 25^{th} percentiles and the maximums. The simulated pumps-off baseflow at gauge 02322500 was approximately 6 percent lower than minimum estimated baseflow from the USF method (Tables 5-9 through 5-15).

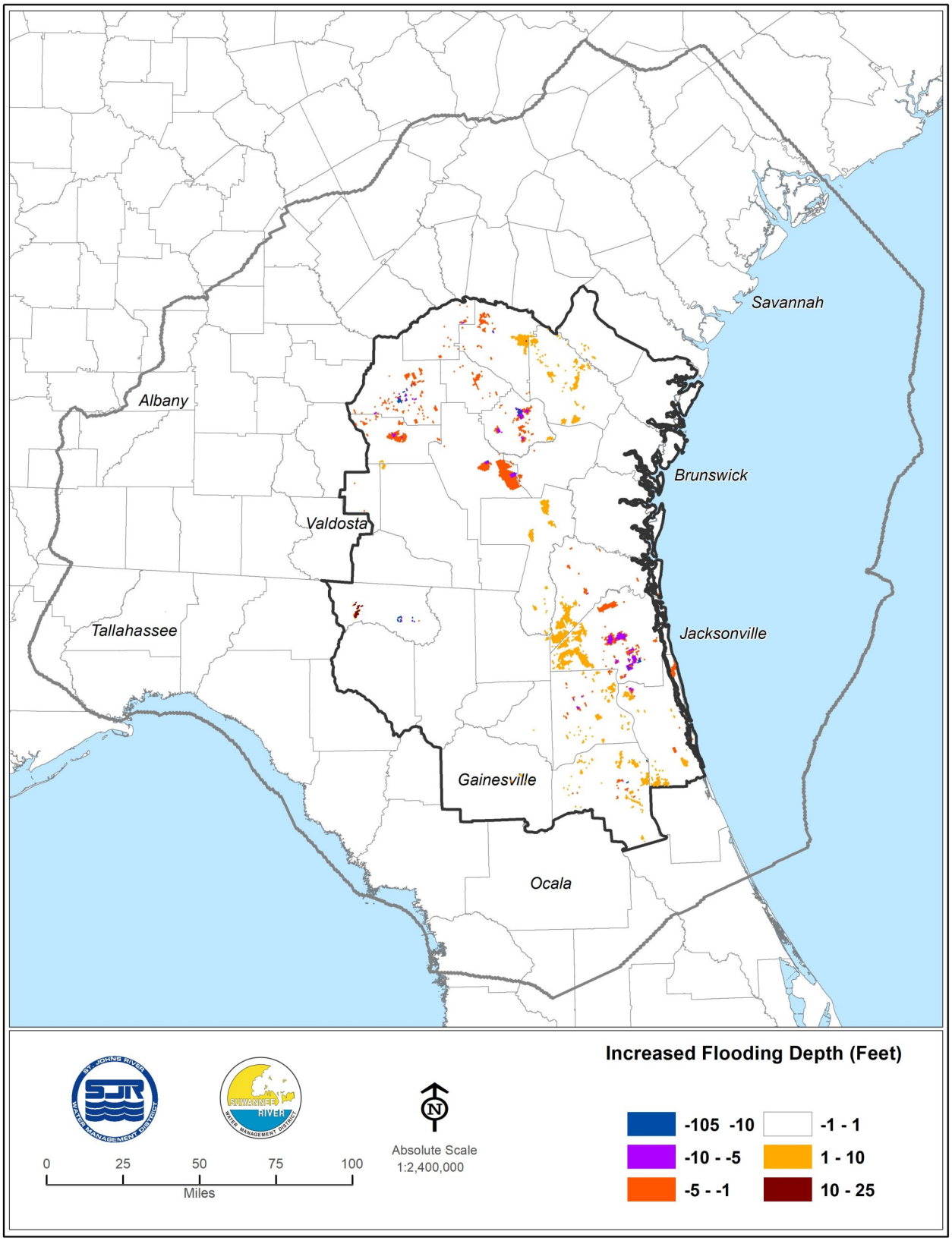

Figure 5-29. Increases in depth of flooding of NFSEG Layer 1 between the NFSEG 2009 and no-pumping simulations within the area of interest

Table 5-8. Key USGS Stream gauging stations with daily discharge data for the period 1933 through 1942

USGS Gauge Number	USGS Gauge Name	No-Pumping Simulated Baseflow (cfs)
2231000	ST. MARYS RIVER NEAR MACCLENNY, FL	92.8
2246000	NORTH FORK BLACK CREEK NEAR MIDDLE-BURG, FL	70.8
2315500	SUWANNEE RIVER AT WHITE SPRINGS, FL	162
2319000	WITHLACOOCHEE RIVER NEAR PINETTA, FL	857
2319500	SUWANNEE RIVER AT ELLAVILLE, FL	3320
2320500	SUWANNEE RIVER AT BRANFORD, FL	4260
2322500	SANTA FE RIVER NEAR FORT WHITE, FL	798

Table 5-9. Summary statistics of annual average flow and annual average baseflows, 1933-1942, for USGS Gauge 0223100, ST. MARYS RIVER NEAR MACCLEN NY, FL

Statistic	Observed Annual Average Flow (cfs)	HYSEP Local Minimum Annual Average Baseflow (cfs)	BFI Standard Annual Average Baseflow (cfs)	BFI Modified Annual Average Baseflow (cfs)	USF Method Annual Average Baseflow (cfs)
25th Percentile	650.0	307.0	266.1	266.5	55.8
Median	466.2	222.8	180.5	179.5	45.7
75th Percentile	350.7	146.8	123.3	122.0	32.8
Minimum	272.3	98.8	98.1	79.4	23.3
Maximum	839.1	567.5	425.7	420.3	84.5

Table 5-10. Summary statistics of annual average flow and annual average baseflows, 1933-1942, for USGS Gauge 0224600, NORTH FORK BLACK CREEK NEAR MIDDLEBURG, FL

Statistic	Observed Annual Average Flow (cfs)	HYSEP Local Minimum Annual Average Baseflow (cfs)	BFI Standard Annual Average Baseflow (cfs)	BFI Modified Annual Average Baseflow (cfs)	USF Method Annual Average Baseflow (cfs)
25th Percentile	181	61	42	42	17
Median	131	50	36	36	14
75th Percentile	109	43	30	29	12
Minimum	93	37	29	28	8
Maximum	221	77	59	59	19

Table 5-11. Summary statistics of annual average flow and annual average baseflows, 1933-1942, for USGS Gauge 02315500, SUWANNEE RIVER AT WHITE SPRINGS, FL

Statistic	Observed Annual Average Flow (cfs)	HYSEP Local Minimum Annual Average Baseflow (cfs)	BFI Standard Annual Average Baseflow (cfs)	BFI Modified Annual Average Baseflow (cfs)	USF Method Annual Average Baseflow (cfs)
25th Percentile	1,620	889	1,112	1,123	192
Median	775	469	520	507	106
75th Percentile	566	320	322	312	57
Minimum	218	99	93	90	22
Maximum	2,283	1,123	1,299	1,370	390

Table 5-12. Summary statistics of annual average flow and annual average baseflows, 1933 -1942, for USGS Gauge 02319000, WITHLACOOCHEE RIVER NEAR PINETTA, FL

Statistic	Observed Annual Average Flow (cfs)	HYSEP Local Minimum Annual Average Baseflow (cfs)	BFI Standard Annual Average Baseflow (cfs)	BFI Modified Annual Average Baseflow (cfs)	USF Method Annual Average Baseflow (cfs)
25th Percentile	1,759	907	932	932	241
Median	1,129	644	512	514	197
75th Percentile	577	400	368	380	145
Minimum	413	225	250	221	109
Maximum	2,212	1,158	1,213	1,215	317

Table 5-13. Summary statistics of annual average flow and annual average baseflows, 1933-1942, for USGS Gauge 02319500, SUWANNEE RIVER AT ELLAVILLE, FL

Statistic	Observed Annual Average Flow (cfs)	HYSEP Local Minimum Annual Average Baseflow (cfs)	BFI Standard Annual Average Baseflow (cfs)	BFI Modified Annual Average Baseflow (cfs)	USF Method Annual Average Baseflow (cfs)
25th Percentile	6,395	3,860	4,796	5,232	2,214
Median	3,945	2,743	3,135	3,068	1,813
75th Percentile	2,649	2,045	2,185	2,172	1,433
Minimum	2,201	1,701	1,906	1,885	1,275
Maximum	7,558	4,588	6,346	6,193	2,960

Table 5-14. Summary statistics of annual average flow and annual average baseflows, 1933-1942, for USGS Gauge 02320500, SUWANNEE RIVER AT BRANFORD, FL

Statistic	Observed Annual Average Flow (cfs)	HYSEP Local Minimum Annual Average Baseflow (cfs)	BFI Standard Annual Average Baseflow (cfs)	BFI Modified Annual Average Baseflow (cfs)	USF Method Annual Average Baseflow (cfs)
25th Percentile	7,273	4,837	6,495	6,497	3,456
Median	4,726	3,787	4,167	4,133	2,755
75th Percentile	3,487	2,867	3,163	3,139	2,286
Minimum	3,139	2,625	2,826	2,826	2,137
Maximum	8,313	5,964	7,262	7,236	4,113

Table 5-15. Summary statistics of annual average Flow and annual average baseflows, 1933-1942, for USGS Gauge 02322500, SANTA FE RIVER NEAR FORT WHITE, FL

Statistic	Observed Annual Average Flow (cfs)	HYSEP Local Minimum Annual Average Baseflow (cfs)	BFI Standard Annual Average Baseflow (cfs)	BFI Modified Annual Average Baseflow (cfs)	USF Method Annual Average Baseflow (cfs)
25th Percentile	1,685	1,447	1,478	1,474	1,069
Median	1,399	1,242	1,271	1,270	1,002
75th Percentile	1,296	1,203	1,226	1,220	933
Minimum	1,188	1,056	1,095	1,087	853
Maximum	2,191	2,095	2,081	2,117	1,548

CHAPTER 6. WATER BUDGET ANALYSIS

To gain insight into the behavior of the groundwater flow system and the NFSEG v1.1 model simulations, water budgets were developed for the overall model domain and for individual groundwater basins. In each of these areas, separate water budgets were developed for the 2001, 2009, 2010 verification and 2009 no-pumping simulations. These water budgets provide information about the relative magnitudes of the various sources, sinks and interlayer exchanges of groundwater in the model.

The model domain was delineated into seven groundwater basins (GWB) based primarily on maps of the estimated and simulated 2009 potentiometric surfaces of the UFA (Figure 6 -1). The configuration of groundwater sub-basins by Bush and Johnston (1988) and the 2010 potentiometric surface of Kinnaman and Dixon (2010) also guided the GWB delineation.

Fluxes accounted for in this analysis include simulated discharges to or from the MODFLOW boundary condition packages that were implemented in NFSEG v1.1 model (GHB, River, Drain, ET, Recharge, Well and Specified Head boundary conditions), as well as vertical transfers between model layers. Each boundary condition type is used to represent one or more aspects of the groundwater flow system. Simulated fluxes across lateral boundaries between groundwater basins occurs in some cases in the GWB analyses. The GWB boundaries were drawn to approximate groundwater streamlines (effectively a type of no-flow boundary). However, some inaccuracy in delineating these boundaries is inevitable and shifts of simulated flux is indicative of a degree of inaccuracy associated with delineation of GWB boundaries since flux across streamlines does not occur in actual flow systems. This type of flux is denoted below as QLat.

The simulated water budgets for the individual basins highlight the differences within the overall groundwater flow system from region to region. Ranges of values or percentages discussed below represent the results from the 2001, 2009 and 2010 stress periods unless otherwise stated. Arrows in referenced figures indicate the direction of net flow (fluxes in minus fluxes out) into or out of a model layer for a given GWB.

MODEL-WIDE SUMMARY

Model-wide simulated flows are generally greater in 2009 than 2001, reflecting the generally drier conditions observed in 2001 and wetter conditions observed in 2009. Simulated 2010 flows corresponded more closely to 2009 than 2001 simulated values. Flows for the 2009 no-pumping simulation are generally similar to the 2009 simulation results. Well package flows are used to represent natural influxes to the Floridan aquifer system via sinks in all simulations. Individual basin flows for 2010 are closer to 2009 individual basin flows in the western GWBs (GWBs 2, 3, 5, 6) and closer to 2001 basin flows in the eastern GWBs (GWBs 1, 4, 7). These results reflect the drier prevailing conditions

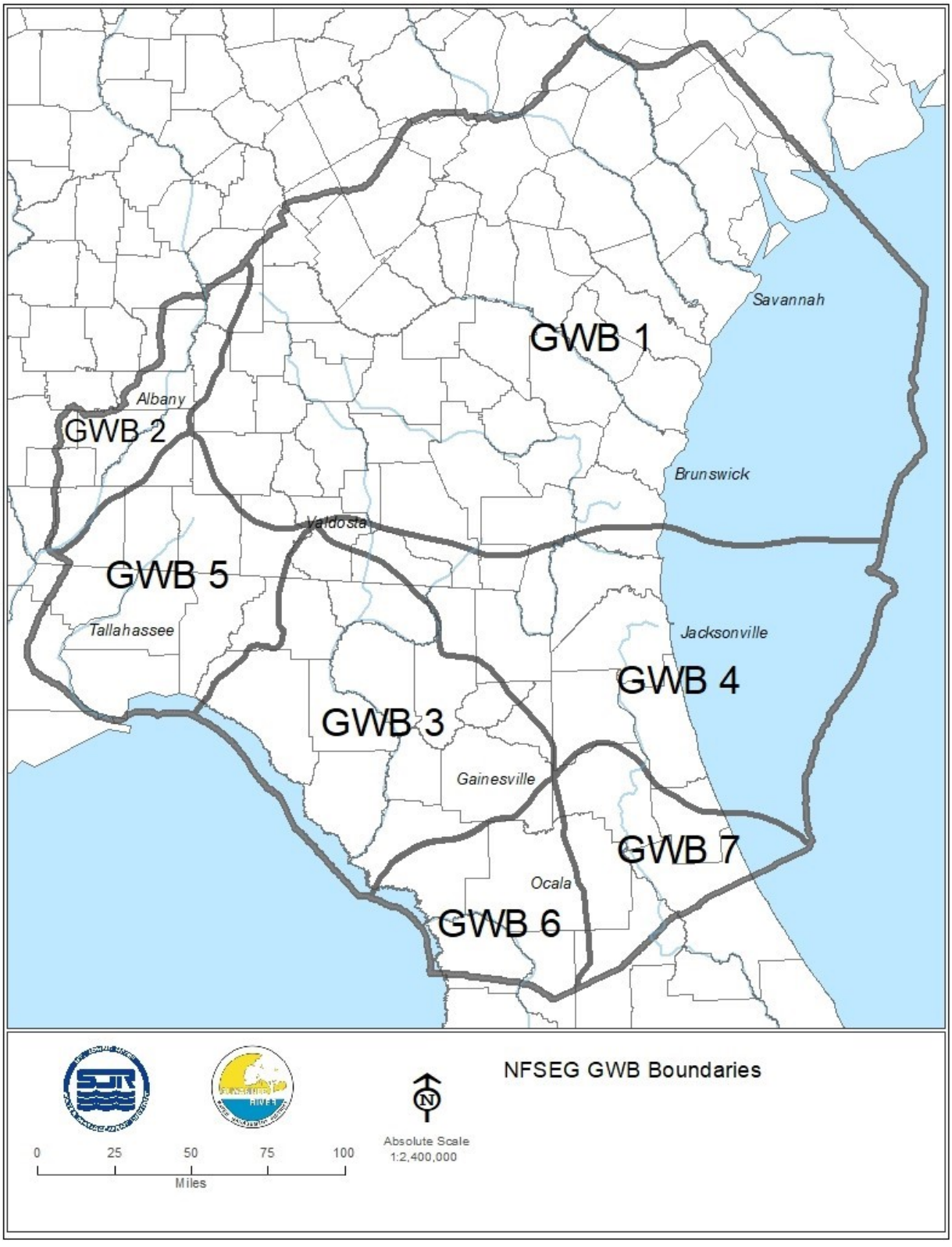

Figure 6-1. Map of all groundwater basins (GWB) within the model boundary

that occurred in 2010 in the eastern area of the model domain and the wetter conditions that occurred in the western area.

Net recharge into Layer 1 (RCH – GW ET) ranges from 4.93 to 7.06 in/yr for 2001, 2009 and 2010 (Figures 6-2 to 6-4). Twenty-nine to thirty seven percent of the net recharge to Layer 1 is transferred to Layer 2, with nearly all the remainder flowing to drains and rivers. Of the vertical flow from Layer 1 to Layer 2, 86-88% is transferred from Layer 2 to Layer 3 and the remainder flows out of Layer 2 to rivers. Flow from Layer 2 comprises 80-85% of flows into Layer 3 and the remaining 15-20% flows upwardly from Layer 4. Discharge to GHBs that represent springs and lateral flux boundaries remove the most water from Layer 3 model wide. Nearly all of this GHB discharge is to features representing springs. Simulated Layer 3 GHB flows representing spring discharge are 1.36, 1.63 and 1.48 in/yr (Tables 6.1-6.3) for 2001, 2009 and 2010, respectively. Simulated Layer 3 GHB flows representing net lateral boundary flux are much smaller: 0.08, 0.08 and 0.37 in/yr, respectively (out of the model domain). Simulated well withdrawals make up 18-23% of discharge from Layer 3. Most of the water transferred from Layer 4 to Layer 3 originates as influx to Layer 5 via GHBs that simulate lateral boundary flux. Influx via these GHBs accounts for 100% of inflow to Layer 5 model wide. Of the total influx to Layer 5, 85-86% is transferred vertically to Layer 4 and the remainder discharges to wells.

For Layer 1, the no-pumping simulation increased constant head outflows by 19%, decreased drainage outflows by 0.38%, increased river outflows by 5.0%, GW ET by 0.29% and decreased vertical flow from Layer 1 to 2 by 21.3%. River outflow from Layer 2 increased by 10.3% and vertical flow from Layer 2 to Layer 3 decreased by 25.8%. Spring boundary outflows from Layer 3 increased by 6.7% and the vertical flow of water from Layer 4 to Layer 3 increased by 8.6%. General head boundary flows into and out of Layer 5 decreased by 2.8% and the vertical flow of water from Layer 5 to Layer 4 increased by 12.9%. The positive inflows to Layer 3 from wells in the no-pumping simulation represent the natural influx to the Floridan aquifer system via sinks. Downward leakage rates from Layers 1 and 2 in the 2009 no-pumping water budget (Figure 6-5) are smaller than corresponding rates for the 2009 (pumps on) water budget. This reduction in leakage is consistent with expected reductions of pumping induced recharge to underlying layers. See Table 6.4 for simulated model wide mass balance for no-pumping.

GROUNDWATER BASINS SUMMARY

Mass balance calculations for individual basins highlight the differences in groundwater flow within the groundwater basins. Flows in GWB 1 are largely affected by UFA pumping, with almost all water contributed to Layer 3 removed via well withdrawal. GWB 2 is a river dominated groundwater basin with most surface recharge contributed to river boundary flows, resulting in less vertical flow to Layer 3. As such, well withdrawal from Layer 3 results in relatively large vertical flows from Layer 4 in GWB 2. GWB 3 is dominated by spring flows, as most water contributed to Layer 3 is discharged by springs. Highly confined layers in GWB 4 result in relatively low vertical flows to the Floridan, which results in high lateral boundary flows that balance Layer 3

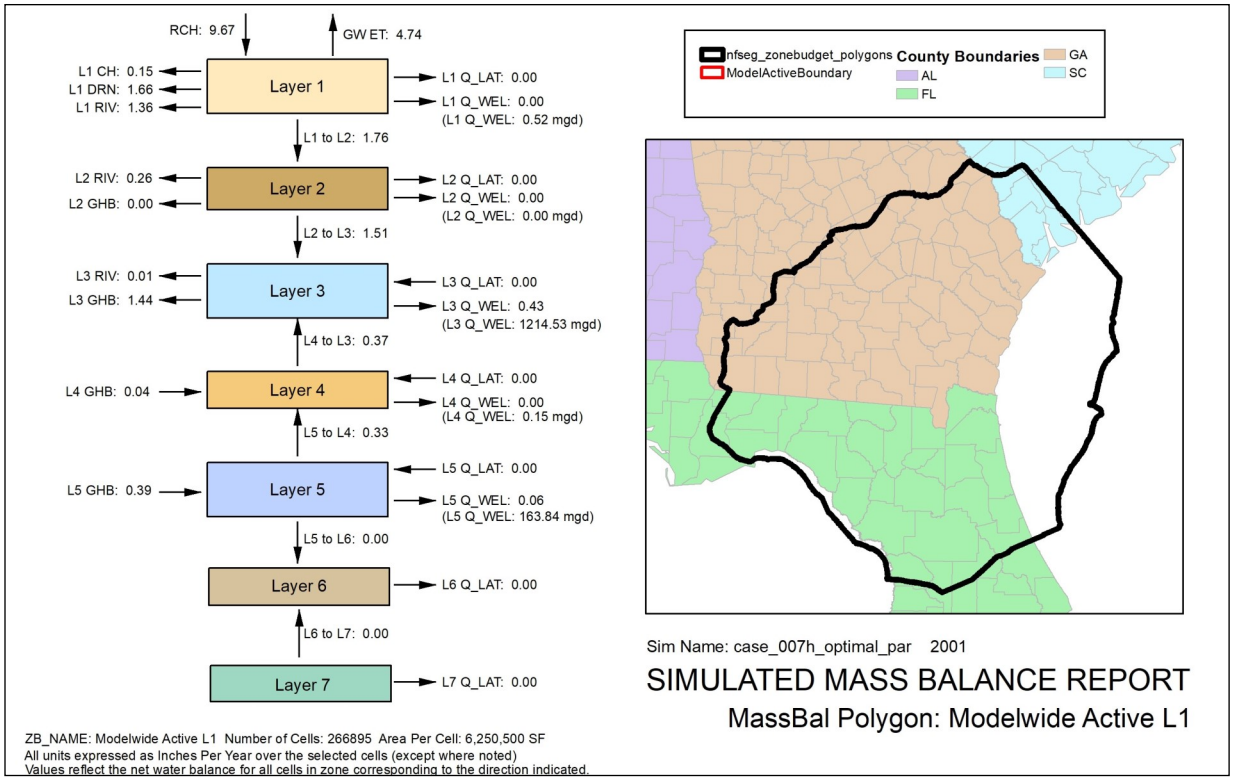

Figure 6-2. Simulated model wide mass balance for 2001
*Arrows indicate net flow (inflows + outflows) into or out of the layer.

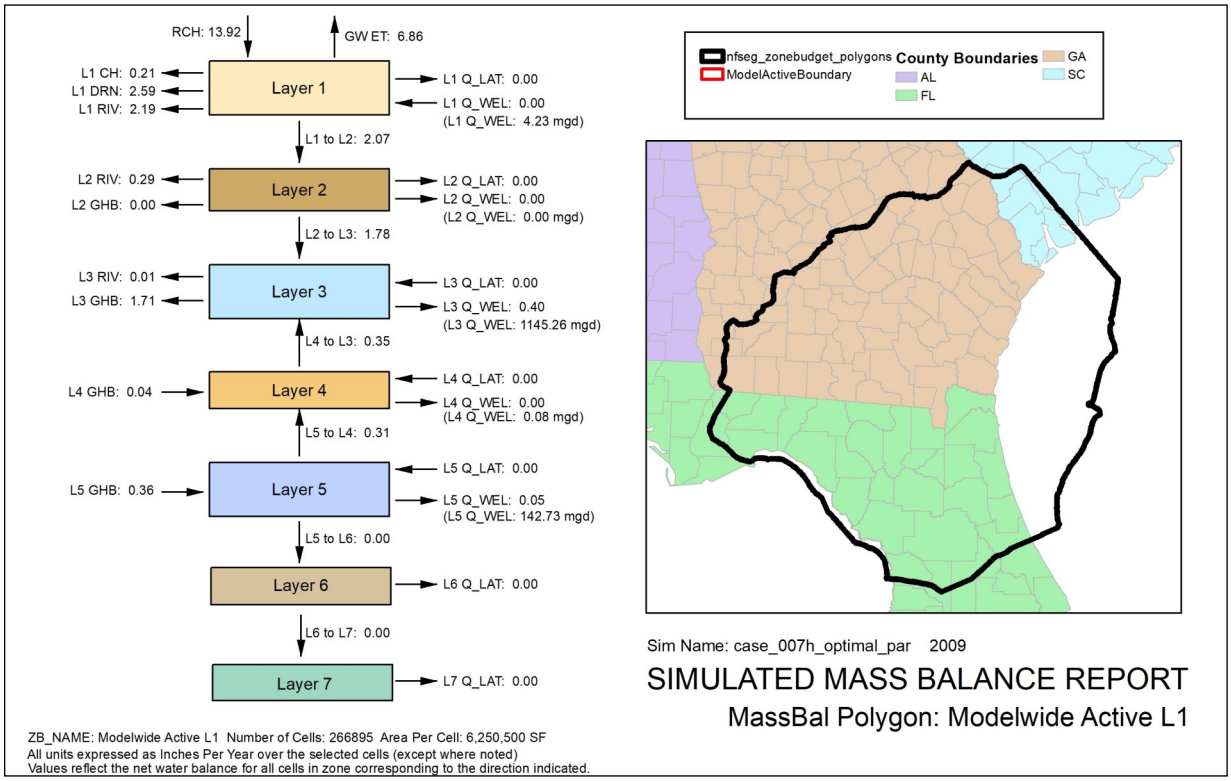

Figure 6-3. Simulated model wide mass balance for 2009
*Arrows indicate net flow (inflows + outflows) into or out of the layer.

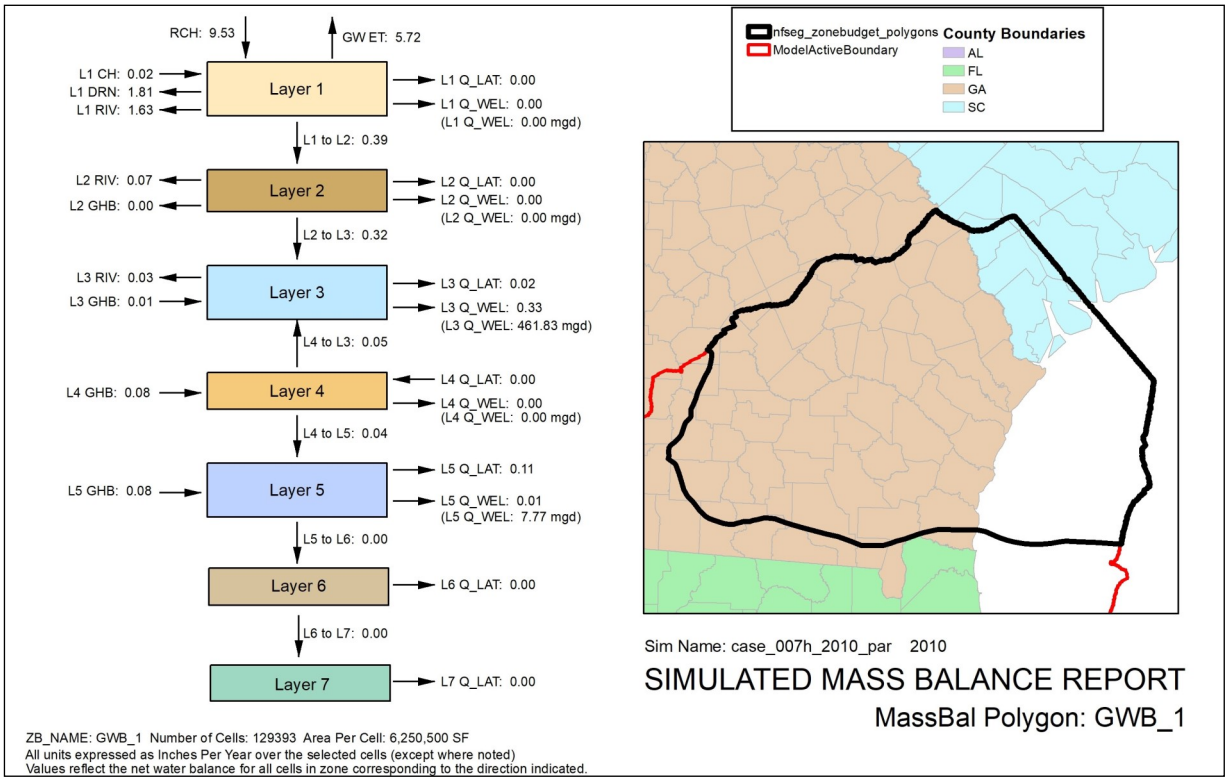

Figure 6-4. Simulated model wide mass balance for 2010
*Arrows indicate net flow (inflows + outflows) into or out of the layer.

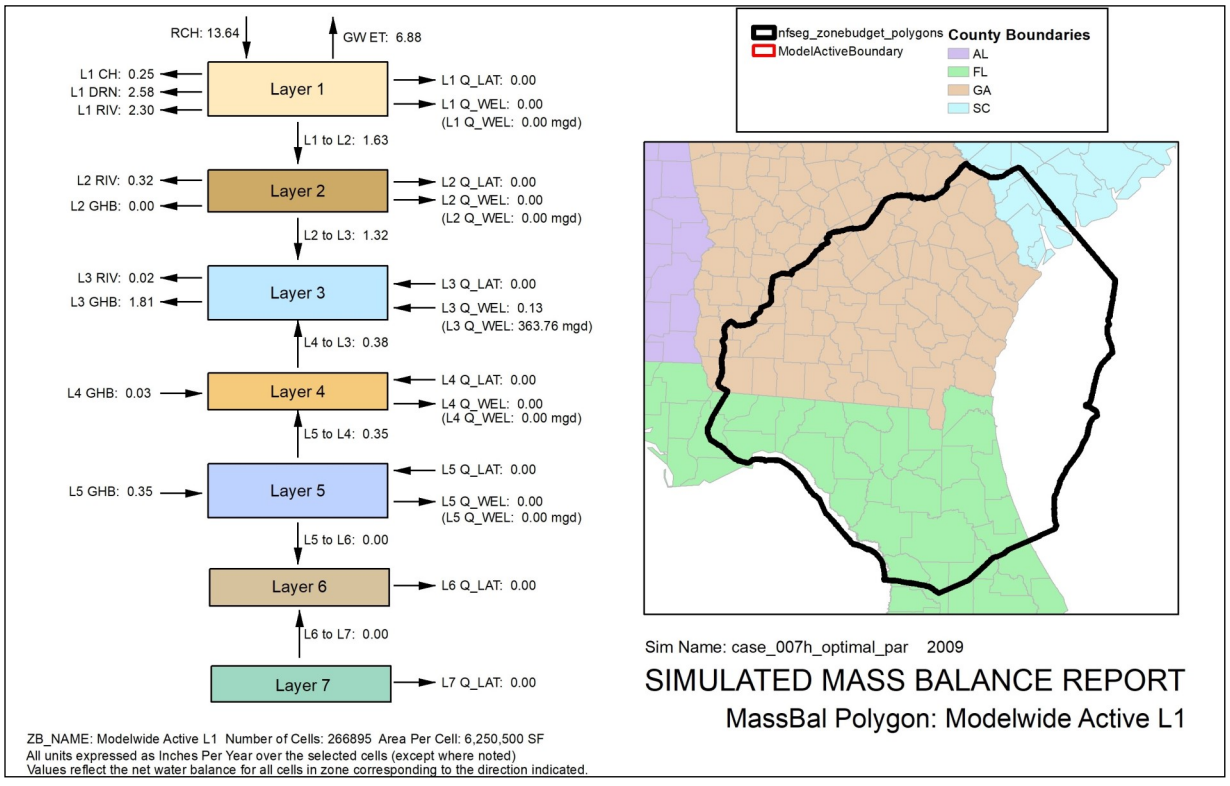

Figure 6-5. Simulated model wide mass balance for no-pumping
*Arrows indicate net flow (inflows + outflows) into or out of the layer.

and Layer 5 well withdrawals. GWB 5 is spring dominated, similar to GWB 3, with contributions from the surface flowing to Layer 3 spring discharge and 100% of all vertical flow to Layer 5 withdrawn from wells. GWB 6 is also spring dominated and less confined than GWB 5, which results in the vertical flows of water from the surface and from Layer 5 to make up spring discharge in Layer 3. GWB 7 is dominated by surface flows, as water from Layer 5 boundary heads flows upward to Layer 3 spring discharges and Layer 1 river and drainage boundaries. Details for each GWB are provided below.

Table 6-1. Simulated model wide mass balance for 2001 (all flows in/yr)

Layer	CH	DRN	GHB	GHB Spring Flows	GW ET	LAT, Q/LAT	Q_WEL	RCH	RIV	Flow to Lower Layer
Layer 1	-0.15	-1.66	0.00	0.00	-4.74	0.00	-1.82E-04	9.67	-1.36	-1.76
Layer 2	0.00	0.00	0.00	-0.00	0.00	0.00	0.00	0.00	-0.26	-1.51
Layer 3	0.00	0.00	-0.08	-1.36	0.00	0.00	-0.43	0.00	-0.01	0.37
Layer 4	0.00	0.00	0.04	0.00	0.00	0.00	0.00	0.00	0.00	0.33
Layer 5	0.00	0.00	0.39	0.00	0.00	0.00	-0.06	0.00	0.00	-2.07E-07
Layer 6	0.00	0.00	0.00	0.00	0.00	0.00	0.00	0.00	0.00	1.05E-08
Layer 7	0.00	0.00	0.00	0.00	0.00	0.00	0.00	0.00	0.00	

Table 6-2. Simulated model wide mass balance for 2009 (all flows in/yr)

Layer	CH	DRN	GHB	GHB Spring Flows	GW ET	LAT, Q/LAT	Q_WEL	RCH	RIV	Flow to Lower Layer
Layer 1	-0.21	-2.59	0.00	0.00	-6.86	0.00	1.49E-03	13.9	-2.19	-2.07
Layer 2	0.00	0.00	0.00	-0.00	0.00	0.00	0.00	0.00	-0.29	-1.78
Layer 3	0.00	0.00	-0.08	-1.63	0.00	0.00	-0.40	0.00	-0.01	0.35
Layer 4	0.00	0.00	0.04	0.00	0.00	0.00	0.00	0.00	0.00	0.31
Layer 5	0.00	0.00	0.36	0.00	0.00	0.00	0.05	0.00	0.00	-4.12E-07
Layer 6	0.00	0.00	0.00	0.00	0.00	0.00	0.00	0.00	0.00	-1.92E-07
Layer 7	0.00	0.00	0.00	0.00	0.00	0.00	0.00	0.00	0.00	

GWB 1

Net recharge into Layer 1 is 3.84, 5.98 and 3.81 in/yr for 2001, 2009 and 2010 respectively (Figures 6-6 to 6-8). Seven to ten percent of the Layer 1 net recharge is transferred to Layer 2 and the remainder discharges from Layer 1 to river and drain boundaries in near equal proportions. Of the water transferred from Layer 1 to Layer 2, 75-82% flows vertically downward to Layer 3, with the remainder flowing out of Layer 2 to river boundaries. Eighty-four to ninety two percent of the inflows to Layer 3 are derived from downward leakage from Layer 2, with other contributions occurring from Layer 4 (5-13%) and from general head boundary flows (2-3%). Well withdrawals from Layer 3 make up 87-90% of all flows out of Layer 3, with flows to river boundaries making up about 8% and lateral boundary flows making up 2-5% of all Layer 3 outward flows. General head boundary flows make up all water flows into Layer 4. In 2001, 62% of Layer 4 outflows were to Layer 3, whereas in 2009 and 2010, 50-71% of

Table 6-3. Simulated model wide mass balance for 2010 (all flows in/yr)

Layer	CH	DRN	GHB	GHB Spring Flows	GW ET	LAT, Q/LAT	Q_WEL	RCH	RIV	Flow to Lower Layer
Layer 1	-0.17	-1.93	0.00	0.00	-5.25	0.00	1.49E-03	11.0	-1.52	-2.17
Layer 2	0.00	0.00	0.00	-0.00	0.00	0.00	0.00	0.00	-0.25	-1.92
Layer 3	0.00	0.00	-0.37	-1.48	0.00	0.00	-0.40	0.00	-0.01	0.34
Layer 4	0.00	0.00	0.04	0.00	0.00	0.00	0.00	0.00	0.00	0.30
Layer 5	0.00	0.00	0.35	0.00	0.00	0.00	0.05	0.00	0.00	-2.28E-07
Layer 6	0.00	0.00	0.00	0.00	0.00	0.00	0.00	0.00	0.00	2.89E-08
Layer 7	0.00	0.00	0.00	0.00	0.00	0.00	0.00	0.00	0.00	

Table 6-4. Simulated model wide mass balance for no-pumping (all flows in/yr)

Layer	CH	DRN	GHB	GHB Spring Flows	GW ET	LAT, Q/LAT	Q_WEL	RCH	RIV	Flow to Lower Layer
Layer 1	-0.25	-2.58	0.00	0.00	-6.88	0.00	0.00	13.6	-2.30	-1.63
Layer 2	0.00	0.00	0.00	-0.00	0.00	0.00	0.00	0.00	-0.32	-1.32
Layer 3	0.00	0.00	-0.07	-1.74	0.00	0.00	0.13	0.00	-0.02	0.38
Layer 4	0.00	0.00	0.03	0.00	0.00	0.00	0.00	0.00	0.00	0.35
Layer 5	0.00	0.00	0.35	0.00	0.00	0.00	0.00	0.00	0.00	-2.52E-07
Layer 6	0.00	0.00	0.00	0.00	0.00	0.00	0.00	0.00	0.00	5.25E-09
Layer 7	0.00	0.00	0.00	0.00	0.00	0.00	0.00	0.00	0.00	

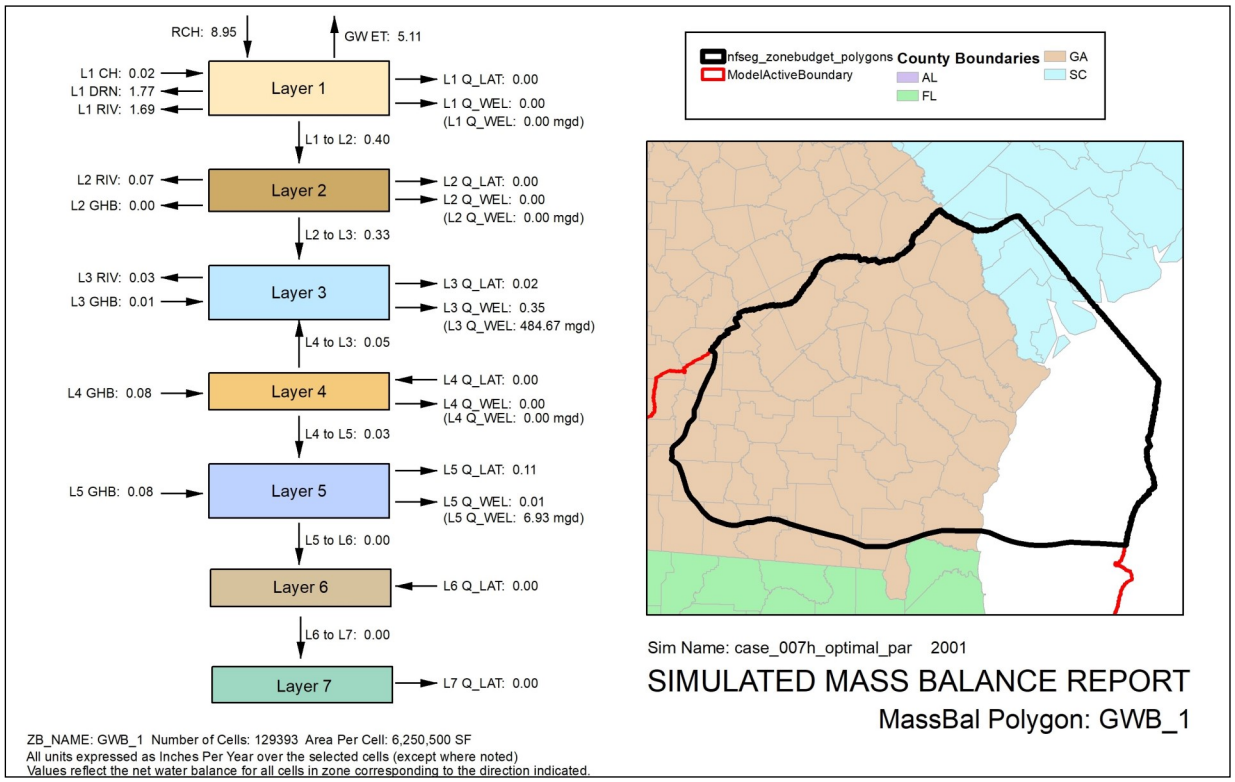

Figure 6-6. Simulated mass balance of GWB 1 for 2001

*Arrows indicate net flow (inflows + outflows) into or out of the layer.

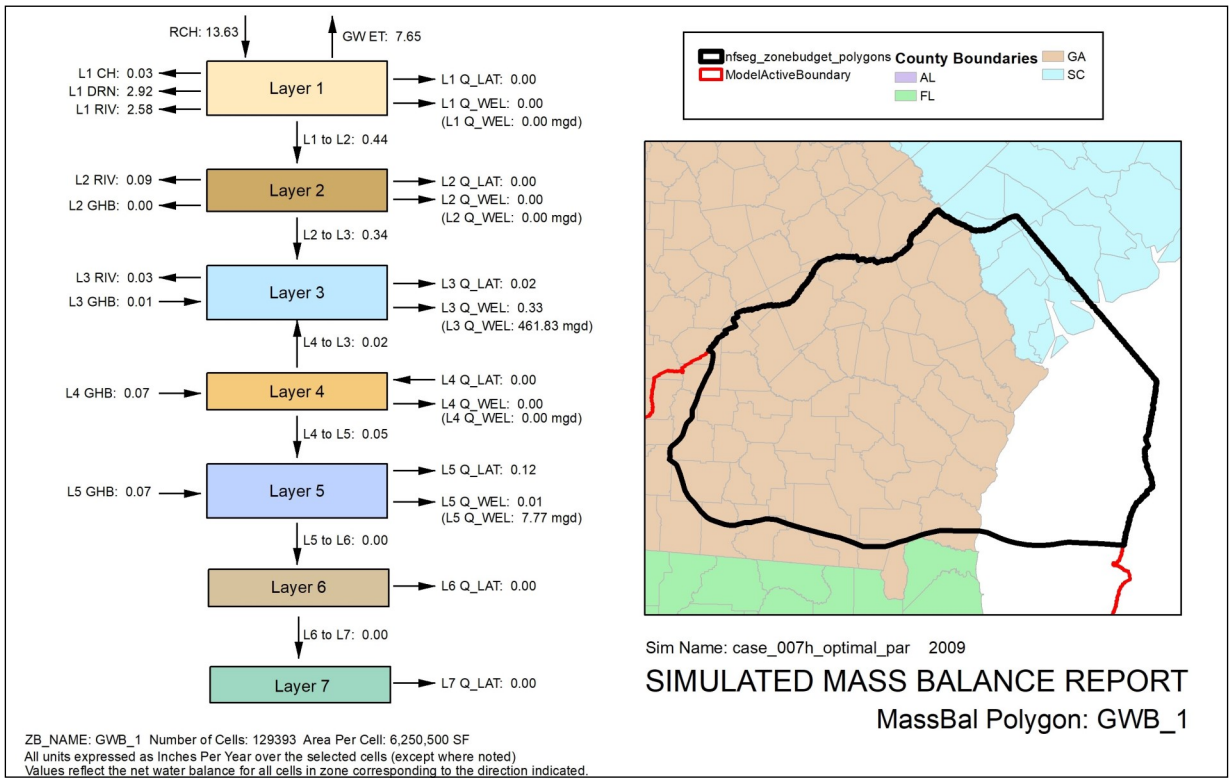

Figure 6-7. Simulated mass balance of GWB 1 for 2009

*Arrows indicate net flow (inflows + outflows) into or out of the layer.

Layer 4 outflows were to Layer 5. Of the water transferred to Layer 5 from Layer 4, 8-9% was discharged to wells and the remainder flowed laterally out of the layer. See Tables 6.5-6.7 for simulated mass balance of GWB1 for 2001, 2009, 2010.

For the 2009 no-pumping simulation, the flows into and out of Layer 1 show an increase in constant head outflows from 0.03 to 0.08 in/yr, 1.0% lower drainage outflows, 1.94% increase in river outflows, 0.13% increase in GW ET and a 51.2% decrease in vertical flow from Layer 1 to Layer 2 (Figure 6-9). River outflow from Layer 2 increased by 11.1% and vertical flow from Layer 2 to Layer 3 decreased by 67.6%. The direction of vertical flow of water between Layer 3 and Layer 4 reversed and increased in magnitude from 0.02 to 0.06 in/yr in the no-pumping scenario. The rate of vertical flow from Layer 5 to Layer 4 increased from 0.05 to 0.13 in/yr. The reduction in downward leakage from Layer 2, reversal in flow direction between Layers 3 and 5 and increase in downward leakage to Layer 5 are also consistent with an expected reduction in pumping induced leakage to Layer 3 and corresponding increase in groundwater flow to down-gradient sinks, such as rivers and springs that are sustained by flows from the Upper Floridan aquifer. General head boundary flows into and out of Layer 5 did not significantly change. See Table 6.8 for simulated mass balance of GWB1 for no-pumping.

GWB 2

Net recharge into Layer 1 is 11.96, 15.78 and 11.67 in/yr for 2001, 2009 and 2010 re-

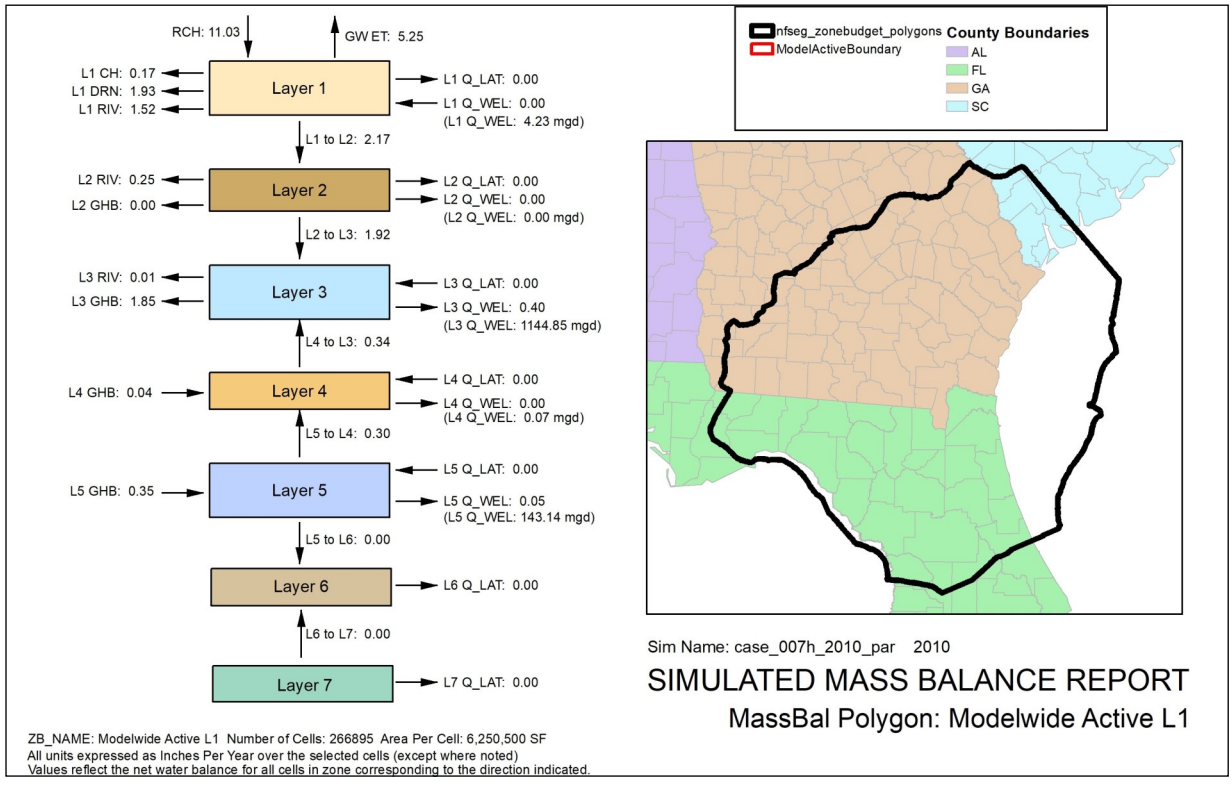

Figure 6-8. Simulated mass balance of GWB 1 for 2010
*Arrows indicate net flow (inflows + outflows) into or out of the layer.

spectively (Figures 6-10 to 6-12). Forty-six to fifty three percent of the Layer 1 net recharge flows to river boundaries, 41-49% flows vertically to Layer 2 and 5-6% is discharged to drainage boundaries. Lateral flows make up less than 1% of all water flows into Layer 2. Rivers make up 64-79% of Layer 2 water outflows, consistent with low confinement in the region and the remainder is transferred vertically to Layer 3. Of the total water entering Layer 3, 52-73% of water flows vertically from Layer 2, 17-31% flows vertically upward from Layer 4 and 6-17% flows laterally from the basin boundary. Almost 100% of all water entering Layer 3 is removed via well withdrawals, with a small amount contributed to river boundary flows. Vertical flow from Layer 5 to Layer 4 makes up 87-92% of all water flow into Layer 4, with the remainder contributed from general and lateral boundary heads. Of all water transferred into Layer 5 via general and lateral heads, 4-7% is withdrawn via wells and the remainder is transferred to Layer 4.

Table 6-5. Simulated mass balance of GWB 1 for 2001 (all flows in/yr)

Layer	CH	DRN	GHB	GHB Spring Flows	GW ET	LAT, Q/LAT	Q_WEL	RCH	RIV	Flow to Lower Layer
Layer 1	0.02	-1.77	0.00	0.00	-5.11	-1.71E-03	0.00	8.95	-1.69	-0.40
Layer 2	0.00	0.00	0.00	0.00	0.00	-5.37E-06	0.00	0.00	-0.07	-0.33
Layer 3	0.00	0.00	0.01	0.00	0.00	-0.02	-0.35	0.00	-0.03	0.05
Layer 4	0.00	0.00	0.08	0.00	0.00	2.02E-03	0.00	0.00	0.00	-0.03
Layer 5	0.00	0.00	0.08	0.00	0.00	-0.11	-0.01	0.00	0.00	-7.94E-05
Layer 6	0.00	0.00	0.00	0.00	0.00	5.42E-09	0.00	0.00	0.00	-7.93E-05
Layer 7	0.00	0.00	0.00	0.00	0.00	-7.93E-05	0.00	0.00	0.00	

Table 6-6. Simulated mass balance of GWB 1 for 2009 (all flows in/yr)

Layer	CH	DRN	GHB	GHB Spring Flows	GW ET	LAT, Q/LAT	Q_WEL	RCH	RIV	Flow to Lower Layer
Layer 1	-0.03	-2.92	0.00	0.00	-7.65	-2.21E-03	0.00	13.6	-2.58	-0.43
Layer 2	0.00	0.00	0.00	0.00	0.00	-5.78E-06	0.00	0.00	-0.09	-0.34
Layer 3	0.00	0.00	0.01	0.00	0.00	-0.02	-0.33	0.00	-0.03	0.02
Layer 4	0.00	0.00	0.07	0.00	0.00	1.67E-03	0.00	0.00	0.00	-0.05
Layer 5	0.00	0.00	0.07	0.00	0.00	-0.12	-0.01	0.00	0.00	-3.41E-05
Layer 6	0.00	0.00	0.00	0.00	0.00	0.00	0.00	0.00	0.00	-3.39E-05
Layer 7	0.00	0.00	0.00	0.00	0.00	-3.39E-05	0.00	0.00	0.00	

See Tables 6.9-6.11 for simulated mass balance of GWB2 for 2001, 2009, 2010.

Compared to the 2009 simulation, the 2009 no-pumping simulation flows into and out of Layer 1 show 3.2% greater drainage outflows, 16.0% increase in river outflows, 1.4% decrease in GW ET and a 47.5% decrease in vertical flow from Layer 1 to Layer 2 (Figure 6-13). River outflow from Layer 2 increased by 7.8% and vertical flow from

Table 6-7. Simulated mass balance of GWB 1 for 2010 (all flows in/yr)

Layer	CH	DRN	GHB	GHB Spring Flows	GW ET	LAT, Q/ LAT	Q_WEL	RCH	RIV	Flow to Lower Layer
Layer 1	0.02	-1.81	0.00	0.00	-5.25	0.00	0.00	9.53	-1.63	-0.39
Layer 2	0.00	0.00	0.00	0.00	0.00	0.00	0.00	0.00	-0.07	-0.32
Layer 3	0.00	0.00	0.01	0.00	0.00	0.02	-0.33	0.00	-0.03	0.05
Layer 4	0.00	0.00	0.08	0.00	0.00	0.00	0.00	0.00	0.00	-0.04
Layer 5	0.00	0.00	0.08	0.00	0.00	0.11	-0.01	0.00	0.00	-2.28E-07
Layer 6	0.00	0.00	0.00	0.00	0.00	0.00	0.00	0.00	0.00	2.89E-08
Layer 7	0.00	0.00	0.00	0.00	0.00	0.00	0.00	0.00	0.00	

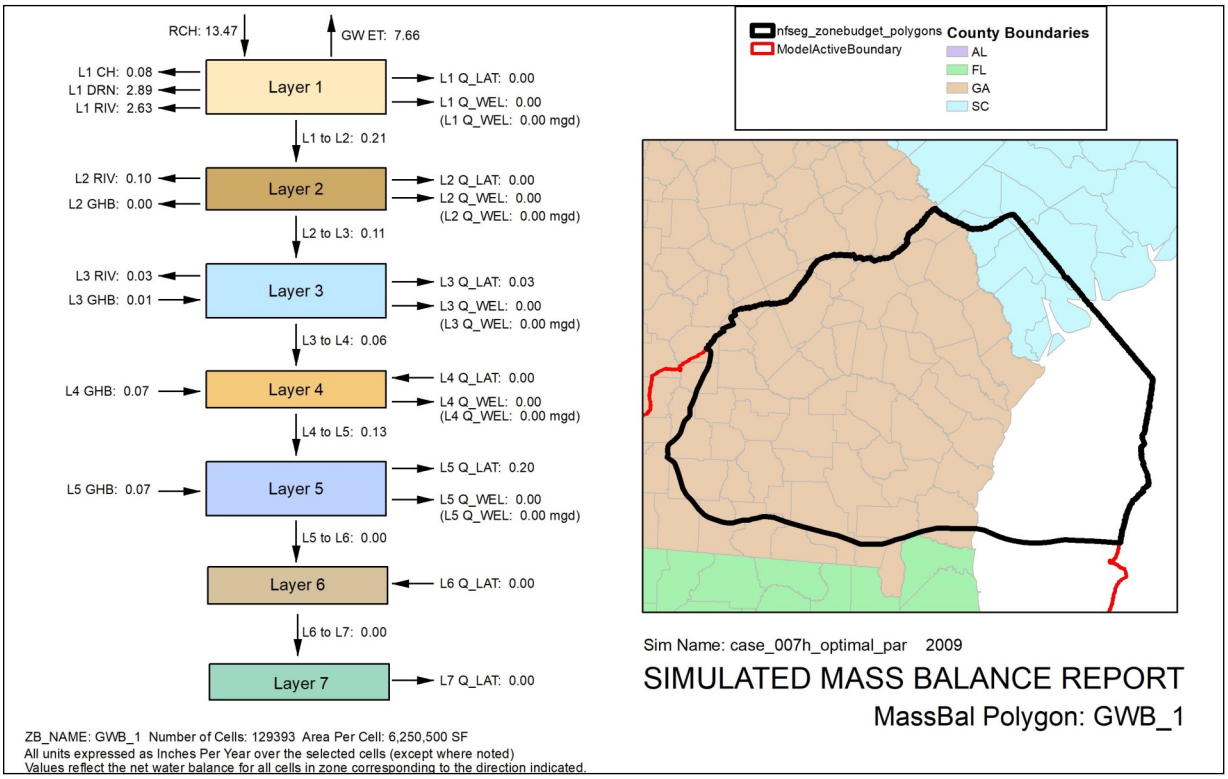

Figure 6-9. Simulated mass balance of GWB 1 for no-pumping
*Arrows indicate net flow (inflows + outflows) into or out of the layer.

Table 6-8. Simulated mass balance of GWB 1 for no-pumping (all flows in/yr)

Layer	CH	DRN	GHB	GHB Spring Flows	GW ET	LAT, Q/LAT	Q_WEL	RCH	RIV	Flow to Lower Layer
Layer 1	-0.08	-2.89	0.00	0.00	-7.66	-2.18E-03	0.00	13.47	-2.63	-0.21
Layer 2	0.00	0.00	0.00	0.00	0.00	-5.58E-06	0.00	0.00	-0.10	-0.11
Layer 3	0.00	0.00	0.01	0.00	0.00	-0.03	0.00	0.00	-0.03	-0.06
Layer 4	0.00	0.00	0.07	0.00	0.00	6.06E-04	0.00	0.00	0.00	-0.13
Layer 5	0.00	0.00	0.07	0.00	0.00	-0.20	0.00	0.00	0.00	-7.61E-05
Layer 6	0.00	0.00	0.00	0.00	0.00	0.00	0.00	0.00	0.00	-7.60E-05
Layer 7	0.00	0.00	0.00	0.00	0.00	-7.60E-05	0.00	0.00	0.00	

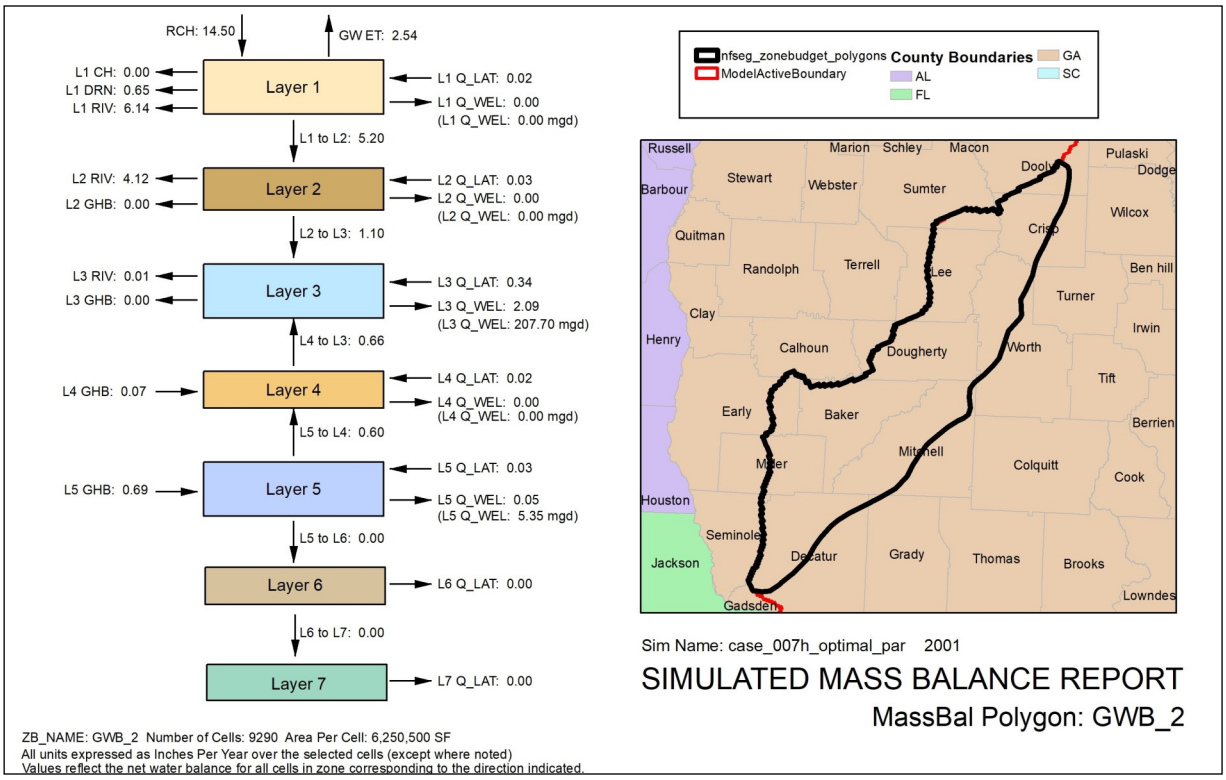

Figure 6-10. Simulated mass balance of GWB 2 for 2001
*Arrows indicate net flow (inflows + outflows) into or out of the layer.

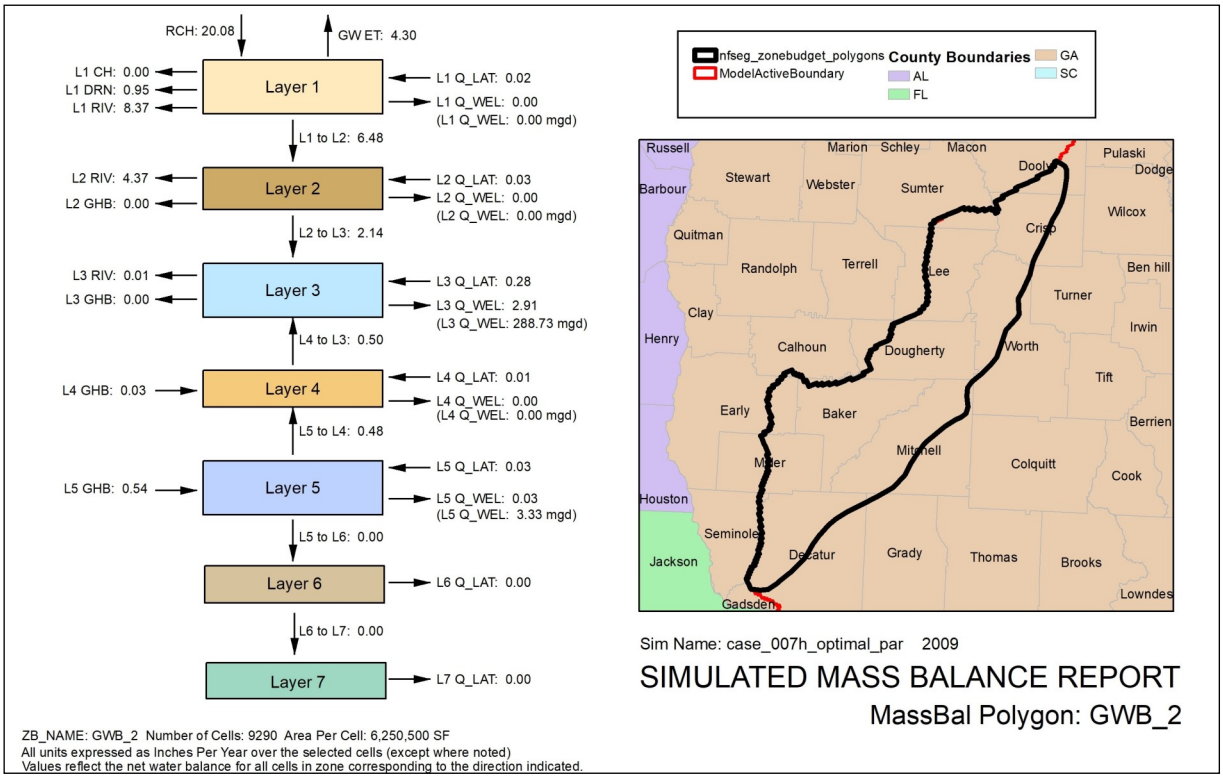

Figure 6.11. Simulated mass balance of GWB 2 for 2009
*Arrows indicate net flow (inflows + outflows) into or out of the layer.

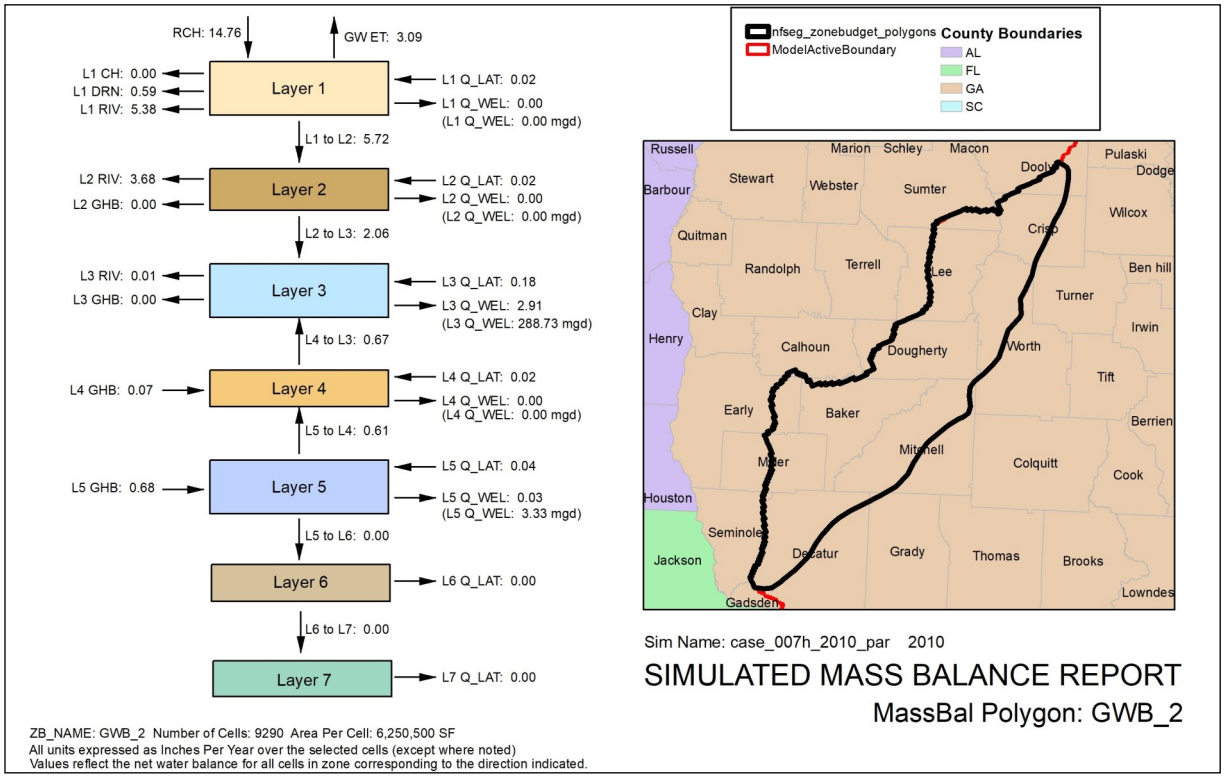

Figure 6-12. Simulated mass balance of GWB 2 for 2010
*Arrows indicate net flow (inflows + outflows) into or out of the layer.

Layer 2 to Layer 3 decreases by 40.6%. The vertical flow of water from Layer 4 to Layer 3 increased by 6% and general head boundary flows into Layer 4 decreased by 33.3%. General head boundary flows into and out of Layer 5 decreased by 5.6% and lateral influxes to Layer 5 decreased by 66%. See Table 6.12 for simulated mass balance of GWB2 for no-pumping.

GWB 3

Net recharge into Layer 1 is 7.02, 9.87 and 10.56 in/yr for 2001, 2009 and 2010 respectively (Figures 6-14 to 6-16). There is 0.06 in/yr of water flows into Layer 1 at river boundaries for 2001 and 1.04 and 1.10 in/yr of water flows out of Layer 1 at river boundaries for 2009 and 2010 respectively. These river outflows represent about 12 to 18 percent of the net recharge to Layer 1. An additional twelve to eighteen percent of the net recharge to Layer 1 is discharged to drain boundaries, but the bulk of the net recharge to Layer 1 (68-84%) is transferred vertically to Layer 2. Most of GWB 3 is unconfined and the simulation results reflect this with downward flow from Layer 1 representing the only water budget component with a net inflow to Layer 2 and approximately 88-90% of the water entering Layer 2 then flowing downward to Layer 3. The remainder of the Layer 2 inflows are transferred to rivers. Vertical flow from Layer 2 to Layer 3 makes up 92-96% of all water entering Layer 3 with the remainder consisting of vertically upward flow from Layer 4 and lateral boundary head flows. Of the total water entering Layer 3, 8% was removed through well withdrawals for 2001 and about 4% was removed for well withdrawals in 2009 and 2010, which is consistent with 2001 being a dry year. The simulated Layer 3 GHB flows consist of 5.17, 6.10 and 4.75 in/yr spring boundary discharge rates and 0.01, 0.21 and 1.65 in/yr rates of lateral outflow rates for 2001, 2009 and 2010 respectively (Tables 6.13-6.15). Vertical flow from Layer 4 to Layer 3 was 84%, 80% and 56% of the vertical flow from Layer 5 into Layer 4 for 2001, 2009 and 2010, respectively. Flow of water into Layer 5 included lateral boundary flows from adjacent GWBs, making up 91-97% of all flows into the layer, with injection well contributions (Q_WEL) making up the remaining flow into the layer.

For the flows into and out of Layer 1, the cessation of well withdrawals results in no change in constant head outflows, 1.3% greater drainage outflows, 11.5% increase in river outflows, 0.15% increase in GW ET and a 7.1% decrease in vertical flow from Layer 1 to Layer 2 (Figure 6-17). River outflow from Layer 2 increased by 13.9% and vertical flow from Layer 2 to Layer 3 decreases by 9.7%. Spring boundary outflows from Layer 3 increased by 13.9% and the vertical flow of water from Layer 4 to Layer 3 increased from 0.33 to 0.86 in/yr. General head boundary flows into and out of Layer 5 did not significantly change. The vertical flow of water from Layer 5 to Layer 4 increased from 0.41 to 0.93 in/yr. Lateral boundary flows into Layer 5 increased from 0.39 to 0.93 in/yr. The positive inflows to Layer 3 from wells in the no-pumping simulation represent the natural influx to the Floridan aquifer system via sinks. Downward leakage rates from Layers 1 and 2 in the 2009 no-pumping water budget are smaller than corresponding rates for the 2009 (pumps on) water budget. As described previously, this reduction is consistent with expected reductions in pumping induced leakage to Layer 3. See Table 6.16 for simulated mass balance of GWB3 for no-pumping.

GWB 4

Net recharge into Layer 1 is 1.81, 2.68 and 1.08 in/yr for 2001, 2009 and 2010 respectively (Figures 6-18 to 6-20). Of the total net recharge, 13-30% flows vertically to Layer 2 and the remainder flows outward to river boundaries, drain boundaries, constant heads and, to a lesser extent, well withdrawals. All leakage from Layer 1 into Layer 2 flows vertically downward to Layer 3. Of that vertical flow into Layer 3, 94-103% of that is removed from Layer 3 via well withdrawals. Lateral flows into Layer 3 make up any potential deficits in the mass balance due to well withdrawal. Flows from Layer 3 to Layer 4 ranged from 0.06 to 0.08 in/yr and 100% of that water continues to flow downward to Layer 5. Well withdrawals are up to 4 times greater than the vertical flow of water into Layer 5. Lateral boundary flows make up any deficits in the mass balance of Layer 5. See Tables 6.17-6.19 for simulated mass balance of GWB4 for 2001, 2009, 2010.

Table 6-9. Simulated mass balance of GWB 2 for 2001 (all flows in/yr)

Layer	CH	DRN	GHB	GHB Spring Flows	GW ET	LAT, Q/LAT	Q_WEL	RCH	RIV	Flow to Lower Layer
Layer 1	0.00	-0.65	0.00	0.00	-2.54	0.02	0.00	14.5	-6.14	-5.20
Layer 2	0.00	0.00	0.00	0.00	0.00	0.03	0.00	0.00	-4.12	-1.10
Layer 3	0.00	0.00	0.00	0.00	0.00	0.34	-2.09	0.00	-0.01	0.66
Layer 4	0.00	0.00	0.07	0.00	0.00	0.02	0.00	0.00	0.00	0.60
Layer 5	0.00	0.00	0.69	0.00	0.00	0.03	-0.05	0.00	0.00	0.00
Layer 6	0.00	0.00	0.00	0.00	0.00	0.00	0.00	0.00	0.00	0.00
Layer 7	0.00	0.00	0.00	0.00	0.00	0.00	0.00	0.00	0.00	

Table 6-10. Simulated mass balance of GWB 2 for 2009 (all flows in/yr)

Layer	CH	DRN	GHB	GHB Spring Flows	GW ET	LAT, Q/ LAT	Q_WEL	RCH	RIV	Flow to Lower Layer
Layer 1	0.00	-0.95	0.00	0.00	-4.30	0.02	0.00	20.1	-8.37	-6.48
Layer 2	0.00	0.00	0.00	0.00	0.00	0.03	0.00	0.00	-4.37	-2.14
Layer 3	0.00	0.00	0.00	0.00	0.00	0.28	-2.91	0.00	-0.01	0.50
Layer 4	0.00	0.00	0.03	0.00	0.00	0.01	0.00	0.00	0.00	0.48
Layer 5	0.00	0.00	0.54	0.00	0.00	0.03	-0.03	0.00	0.00	0.00
Layer 6	0.00	0.00	0.00	0.00	0.00	0.00	0.00	0.00	0.00	0.00
Layer 7	0.00	0.00	0.00	0.00	0.00	0.00	0.00	0.00	0.00	

Table 6-11. Simulated mass balance of GWB 2 for 2010 (all flows in/yr)

Layer	CH	DRN	GHB	GHB Spring Flows	GW ET	LAT, Q/ LAT	Q_WEL	RCH	RIV	Flow to Lower Layer
Layer 1	0.00	-0.59	0.00	0.00	-3.09	0.02	0.00	14.8	-5.38	-5.72
Layer 2	0.00	0.00	0.00	0.00	0.00	0.02	0.00	0.00	-3.68	-2.06
Layer 3	0.00	0.00	0.00	0.00	0.00	0.18	-2.91	0.00	-0.01	0.67
Layer 4	0.00	0.00	0.07	0.00	0.00	0.02	0.00	0.00	0.00	0.61
Layer 5	0.00	0.00	0.68	0.00	0.00	0.04	-0.03	0.00	0.00	0.00
Layer 6	0.00	0.00	0.00	0.00	0.00	0.00	0.00	0.00	0.00	0.00
Layer 7	0.00	0.00	0.00	0.00	0.00	0.00	0.00	0.00	0.00	

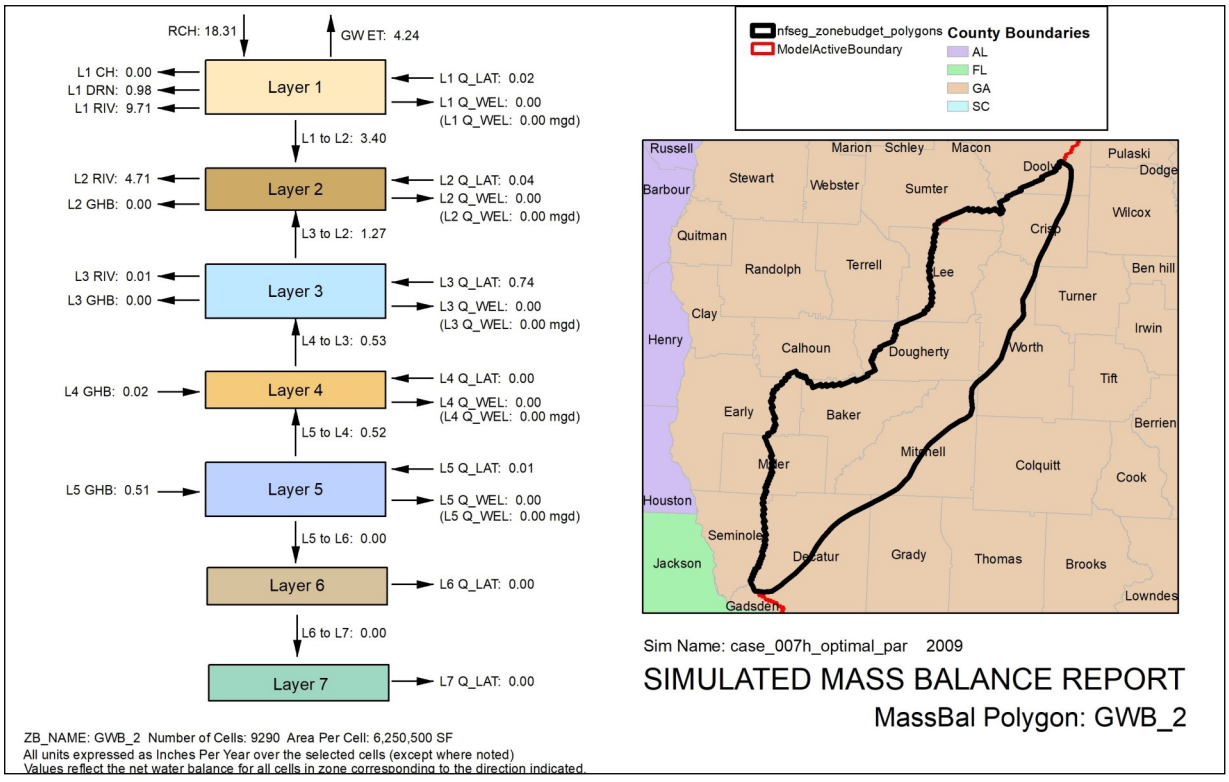

Figure 6-13. Simulated mass balance of GWB 2 for no-pumping
*Arrows indicate net flow (inflows + outflows) into or out of the layer.

Table 6-12. Simulated mass balance of GWB 2 for no-pumping (all flows in/yr)

Layer	CH	DRN	GHB	GHB Spring Flows	GW ET	LAT, Q/LAT	Q_WEL	RCH	RIV	Flow to Lower Layer
Layer 1	0.00	-0.98	0.00	0.00	-4.24	0.02	0.00	18.31	-9.71	-3.40
Layer 2	0.00	0.00	0.00	0.00	0.00	0.04	0.00	0.00	-4.71	1.27
Layer 3	0.00	0.00	0.00	0.00	0.00	0.74	0.00	0.00	-0.01	0.53
Layer 4	0.00	0.00	0.02	0.00	0.00	3.79E-04	0.00	0.00	0.00	0.52
Layer 5	0.00	0.00	0.51	0.00	0.00	0.01	0.00	0.00	0.00	0.00
Layer 6	0.00	0.00	0.00	0.00	0.00	0.00	0.00	0.00	0.00	0.00
Layer 7	0.00	0.00	0.00	0.00	0.00	0.00	0.00	0.00	0.00	

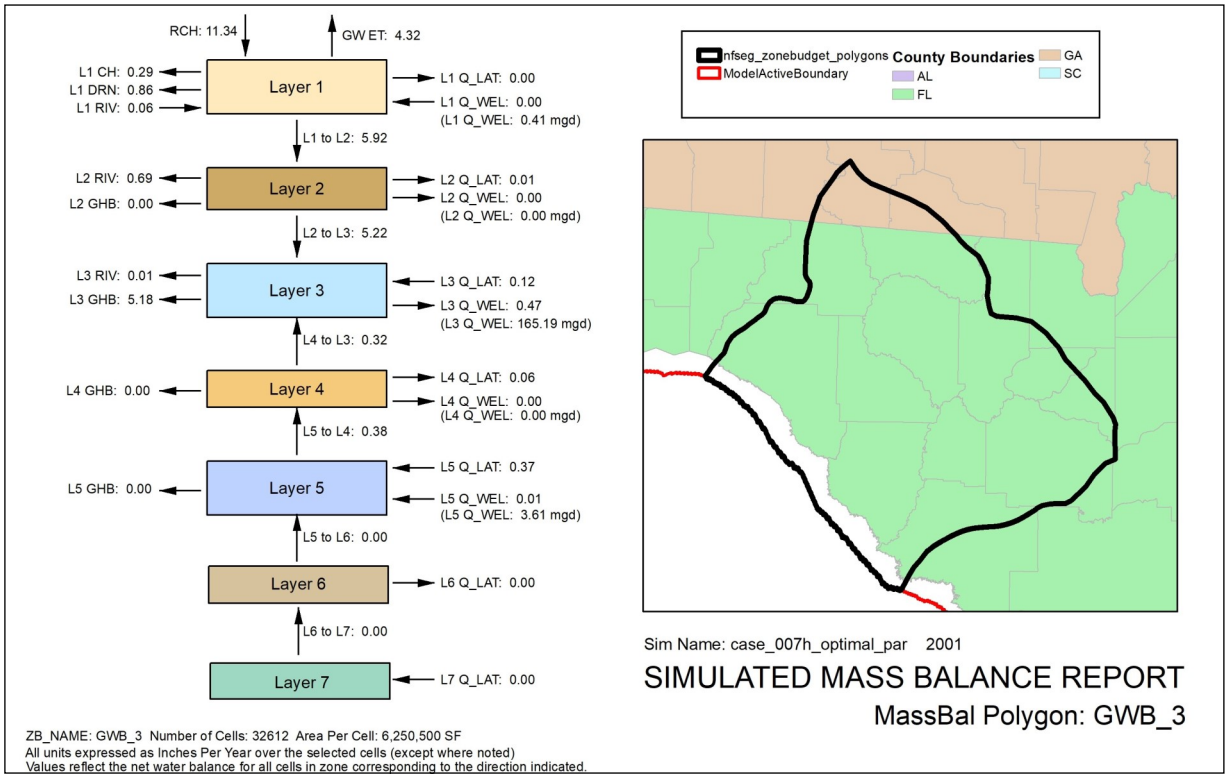

Figure 6-14. Simulated mass balance of GWB 3 for 2001
*Arrows indicate net flow (inflows + outflows) into or out of the layer.

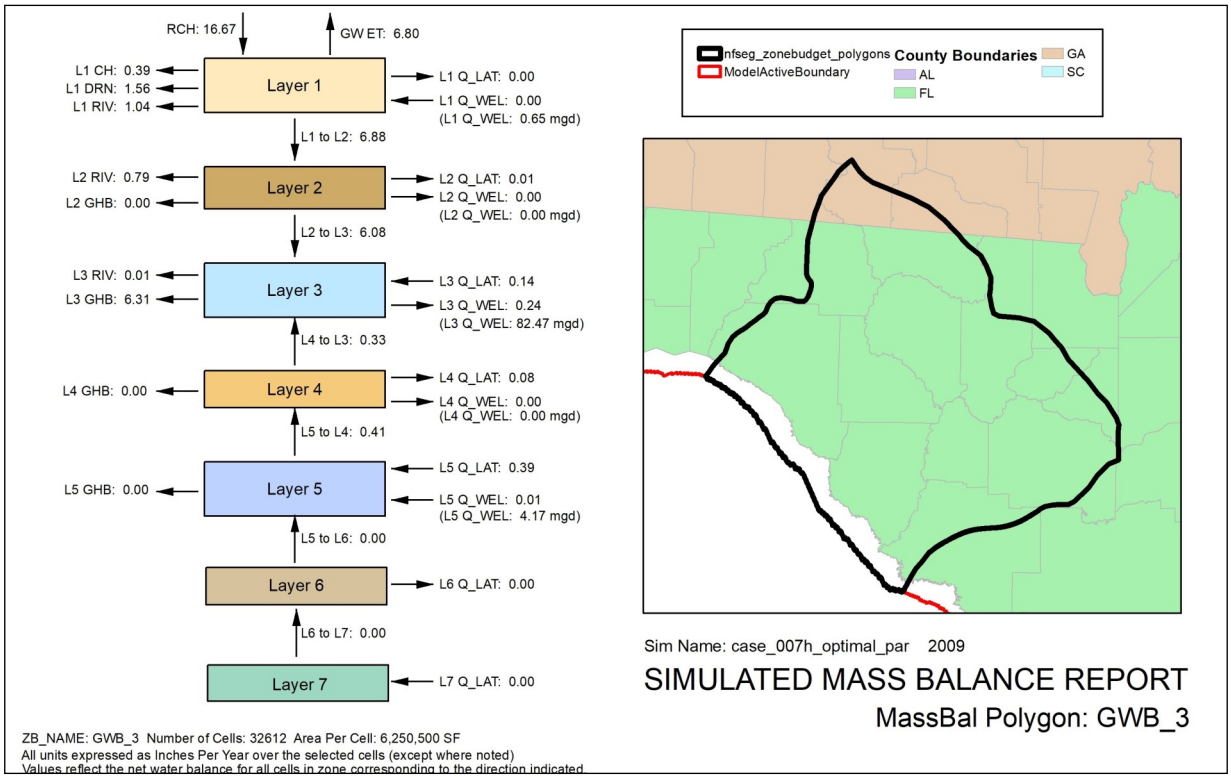

Figure 6-15. Simulated mass balance of GWB 3 for 2009
*Arrows indicate net flow (inflows + outflows) into or out of the layer.

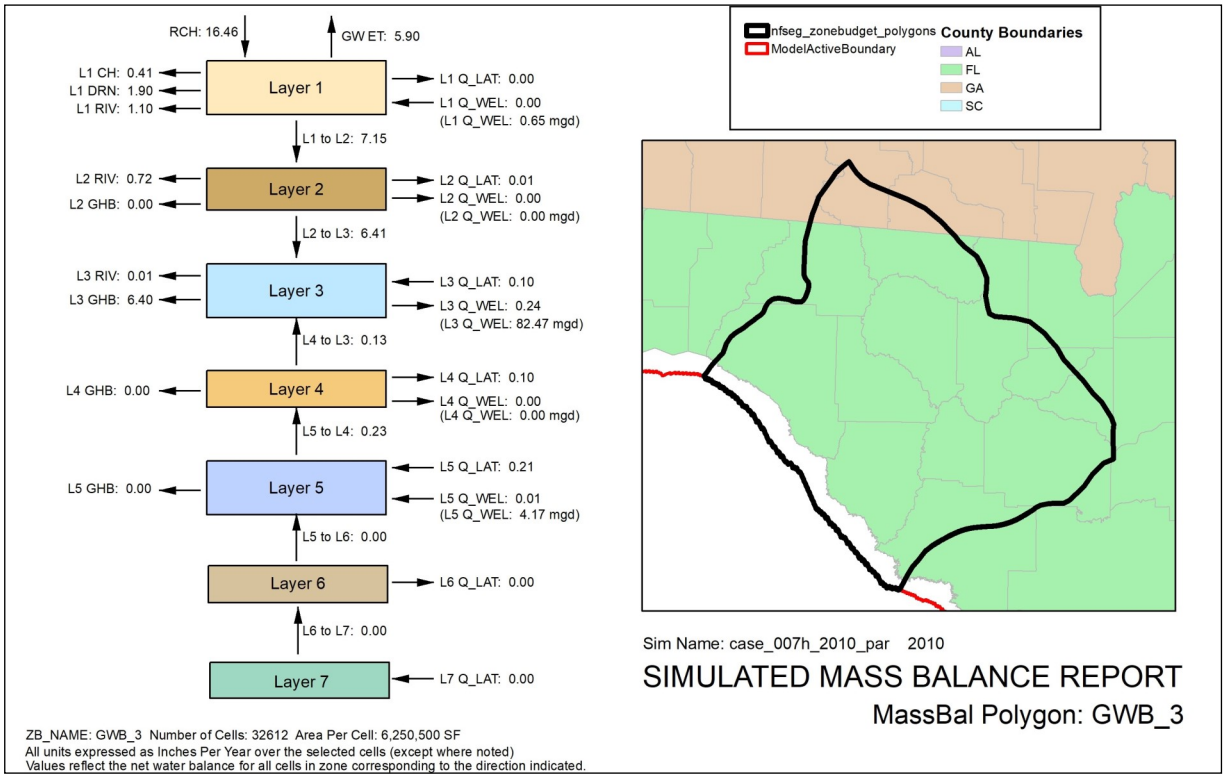

Figure 6-16. Simulated mass balance of GWB 3 for 2010
*Arrows indicate net flow (inflows + outflows) into or out of the layer.

Table 6-13. Simulated mass balance of GWB 3 for 2001 (all flows in/yr)

Layer	CH	DRN	GHB	GHB Spring Flows	GW ET	LAT, Q/LAT	Q_WEL	RCH	RIV	Flow to Lower Layer
Layer 1	-0.29	-0.86	0.00	0.00	-4.32	-4.02E-04	1.19E-03	11.3	0.06	-5.92
Layer 2	0.00	0.00	0.00	-0.00	0.00	-0.01	0.00	0.00	-0.69	-5.22
Layer 3	0.00	0.00	-0.01	-5.17	0.00	0.12	-0.47	0.00	-0.01	0.32
Layer 4	0.00	0.00	0.00	0.00	0.00	-0.06	0.00	0.00	0.00	0.38
Layer 5	0.00	0.00	0.00	0.00	0.00	0.37	0.01	0.00	0.00	1.77E-03
Layer 6	0.00	0.00	0.00	0.00	0.00	-8.59E-08	0.00	0.00	0.00	1.77E-03
Layer 7	0.00	0.00	0.00	0.00	0.00	1.77E-03	0.00	0.00	0.00	

Table 6-14. Simulated mass balance of GWB 3 for 2009 (all flows in/yr)

Layer	CH	DRN	GHB	GHB Spring Flows	GW ET	LAT, Q/LAT	Q_WEL	RCH	RIV	Flow to Lower Layer
Layer 1	-0.39	-1.56	0.00	0.00	-6.80	-7.14E-04	1.86E-03	16.7	-1.04	-6.88
Layer 2	0.00	0.00	0.00	-0.00	0.00	-0.01	0.00	0.00	-0.79	-6.08
Layer 3	0.00	0.00	-0.21	-6.10	0.00	0.14	-0.24	0.00	-0.01	0.33
Layer 4	0.00	0.00	0.00	0.00	0.00	-0.08	0.00	0.00	0.00	0.41
Layer 5	0.00	0.00	0.00	0.00	0.00	0.39	0.01	0.00	0.00	2.04E-03
Layer 6	0.00	0.00	0.00	0.00	0.00	-8.59E-08	0.00	0.00	0.00	2.04E-03
Layer 7	0.00	0.00	0.00	0.00	0.00	2.04E-03	0.00	0.00	0.00	

Table 6-15. Simulated mass balance of GWB 3 for 2010 (all flows in/yr)

Layer	CH	DRN	GHB	GHB Spring Flows	GW ET	LAT, Q/LAT	Q_WEL	RCH	RIV	Flow to Lower Layer
Layer 1	-0.41	-1.90	0.00	0.00	-5.90	-6.89E-04	1.86E-03	16.5	-1.10	-7.15
Layer 2	0.00	0.00	0.00	-0.00	0.00	-0.01	0.00	0.00	-0.72	-6.41
Layer 3	0.00	0.00	-1.65	-4.75	0.00	0.10	-0.24	0.00	-0.01	0.13
Layer 4	0.00	0.00	0.00	0.00	0.00	-0.10	0.00	0.00	0.00	0.23
Layer 5	0.00	0.00	0.00	0.00	0.00	0.21	0.01	0.00	0.00	1.23E-03
Layer 6	0.00	0.00	0.00	0.00	0.00	-8.59E-08	0.00	0.00	0.00	1.23E-03
Layer 7	0.00	0.00	0.00	0.00	0.00	1.23E-03	0.00	0.00	0.00	

Table 6-16. Simulated mass balance of GWB 3 for no-pumping (all flows in/yr)

Layer	CH	DRN	GHB	GHB Spring Flows	GW ET	LAT, Q/LAT	Q_WEL	RCH	RIV	Flow to Lower Layer
Layer 1	-0.39	-1.58	0.00	0.00	-6.81	-6.94E-04	0.00	16.3	-1.16	-6.39
Layer 2	0.00	0.00	0.00	-0.00	0.00	-0.01	0.00	0.00	-0.90	-5.49
Layer 3	0.00	0.00	-0.02	-6.95	0.00	0.20	0.44	0.00	-0.01	0.86
Layer 4	0.00	0.00	0.00	0.00	0.00	-0.07	0.00	0.00	0.00	0.93
Layer 5	0.00	0.00	0.00	0.00	0.00	0.93	0.00	0.00	0.00	2.50E-03
Layer 6	0.00	0.00	0.00	0.00	0.00	-8.59E-08	0.00	0.00	0.00	2.50E-03
Layer 7	0.00	0.00	0.00	0.00	0.00	2.50E-03	0.00	0.00	0.00	

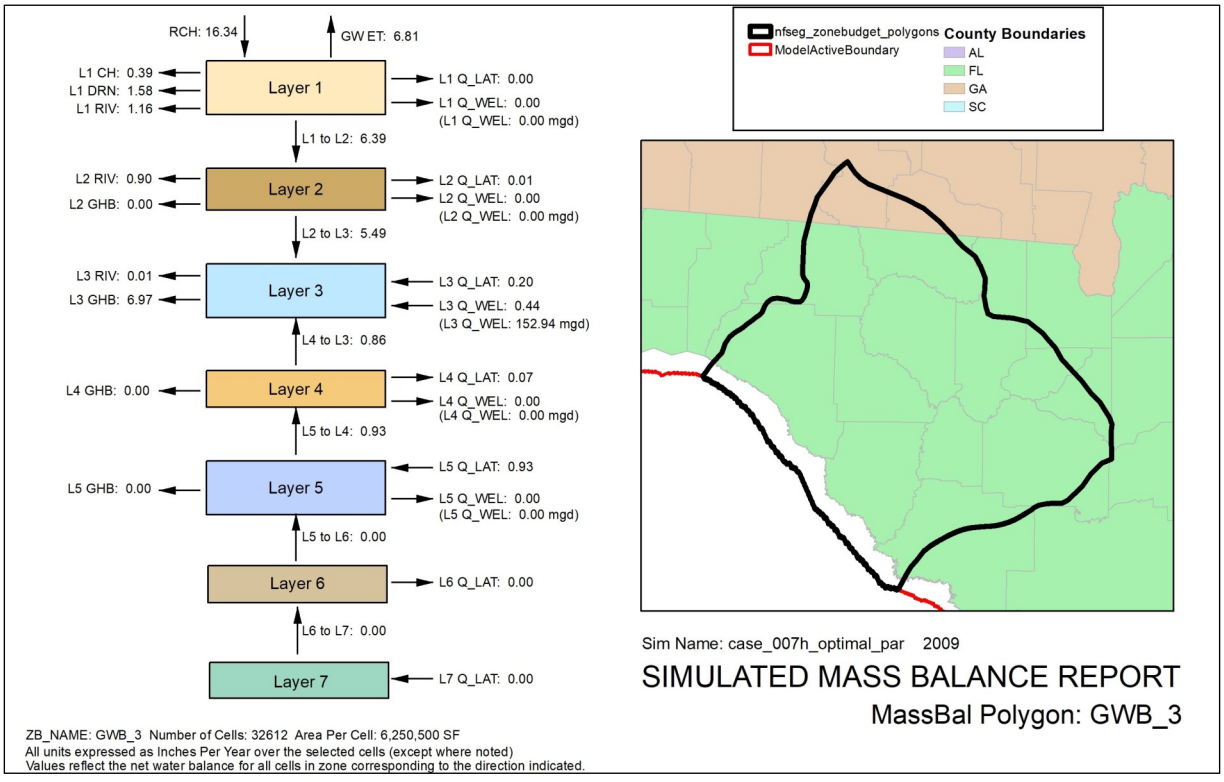

Figure 6-17. Simulated mass balance of GWB 3 for no-pumping
*Arrows indicate net flow (inflows + outflows) into or out of the layer.

For the 2009 no-pumping simulation, the removal of well withdrawals results in 26.3% greater constant head outflows, no significant change in drainage outflows, 4.2% increase in river outflows, 1.1% increase in GW ET and an 86% decrease in vertical flow from Layer 1 to Layer 2 (Figure 6-21). Vertical flow from Layer 2 to Layer 3 similarly decreases by 86%. Reduced well withdrawals from Layer 3 results in a decrease in vertical flow from Layer 3 to Layer 4 from 0.08 to 0.02 in/yr. Vertical flow from Layer 4 to Layer 5 also decreased from 0.08 to 0.02 in/yr. General head boundary flows into and out of Layer 5 did not significantly change. Lateral boundary flows into Layer 5 decreased from 0.18 to 0.02 in/yr. See Table 6.20 for simulated mass balance of GWB4 for no-pumping.

GWB 5

In GWB5, net recharge into Layer 1 is 10.00, 15.42 and 13.77 in/yr for 2001, 2009 and 2010 respectively (Figures 6-22 to 6-24). Of the net recharge into Layer 1, 44-47% is discharged at drain boundaries, 32-36% flows vertically down to Layer 2 and the remainder flows out via constant heads, river boundaries and lateral head boundary flows. Flows from Layer 1 to Layer 2 make up 97-98% of all water flow into Layer 2, with the remainder made up of net inflows from River Package features. Vertical flow from Layer 2 to Layer 3 makes up all of Layer 2 outflows. Of the total water flows into Layer 3, 7-8% comes from well contributions (representing surface to sinkhole flows) and the remainder flows vertically from Layer 2. GHB spring flows make up 83-88% of all water outflow from Layer 3, with the remainder consisting of vertical flow to Layer 4 and, to a lesser extent, lateral boundary flow. The simulated Layer 3 GHB flows consist of 3.88, 4.19 and 5.19 in/yr spring discharge and 0.54, -0.60 (outflow) and 0.57 in/yr inflows across lateral flux boundaries for 2001, 2009 and 2010 respectively (Tables 6.21-6.23). All water flowing from Layer 3 to Layer 4 continues to flow vertically downward to Layer 5. Moreover, downward vertical flow from Layer 4 makes up 100% of the total water inflow to Layer 5. Well withdrawals from Layer 5 are less than 1 MGD for each study period. As such, essentially of all water outflow from Layer 5 consists of lateral boundary flows.

Comparing the water budget for the no-pumping simulation with the corresponding 2009 simulation, indicated that, for Layer 1, the changes in well withdrawals result in less than 1 percent increases in constant head, drainage and change in GW ET flows; a 4.5% change in river outflows and a 7 percent reduction in vertical flow from Layer 1 to Layer 2 (Figure 6-25). Simulated vertical flow from Layer 2 to Layer 3 also fell by 7 percent. Simulated spring outflows from Layer 3 increased by about 2 percent and the vertical flow of water from Layer 3 to Layer 4 decreased by 15 percent. Corresponding reductions in the flows from Layer 4 to 5 and across lateral boundaries of Layer 5 were also simulated. The positive inflows to Layer 3 from wells represent the natural influx to the Floridan aquifer system via sinks. See Table 6.24 for simulated mass balance of GWB5 for no-pumping.

GWB 6

In GWB 6, simulated net recharge into Layer 1 is from 7.80, 8.13 and 13.90 in/yr for 2001, 2009 and 2010 respectively (Figures 6-26 to 6-28). Three to nine percent of the simulated Layer 1 net recharge flows to river boundaries, 67-77% flows vertically to

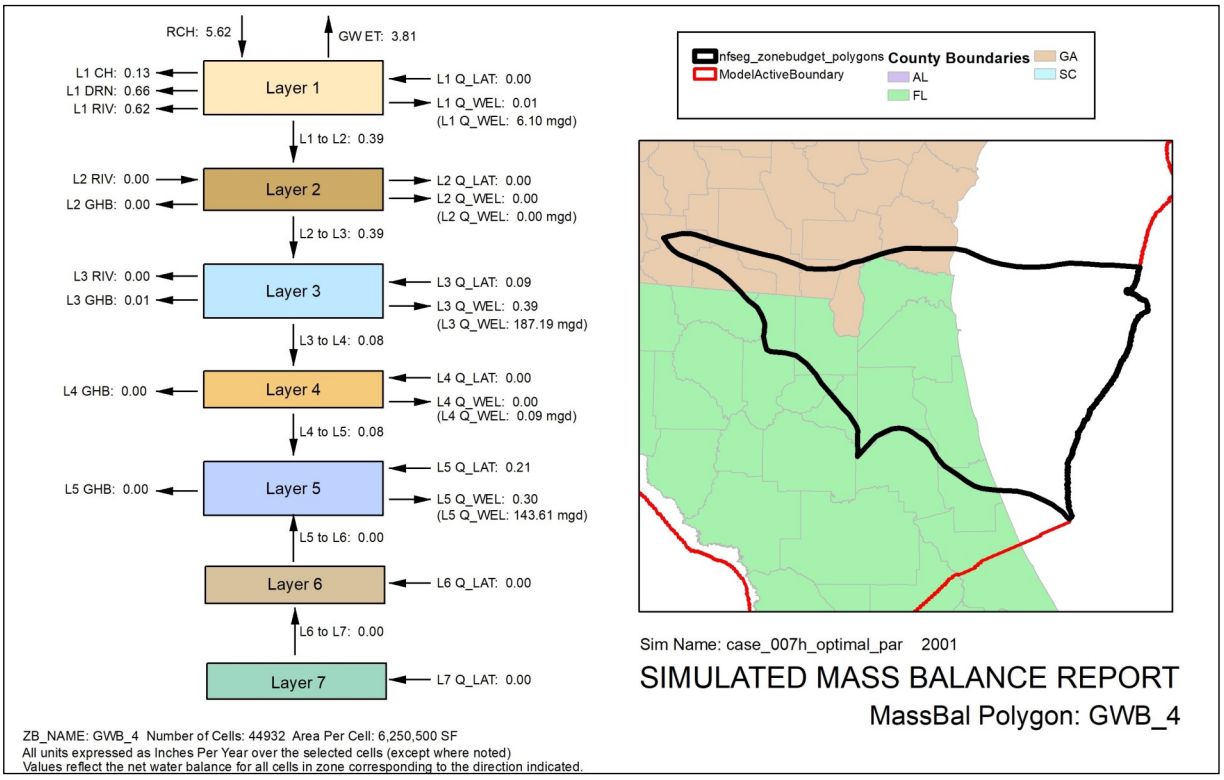

Figure 6.18. Simulated mass balance of GWB 4 for 2001
*Arrows indicate net flow (inflows + outflows) into or out of the layer.

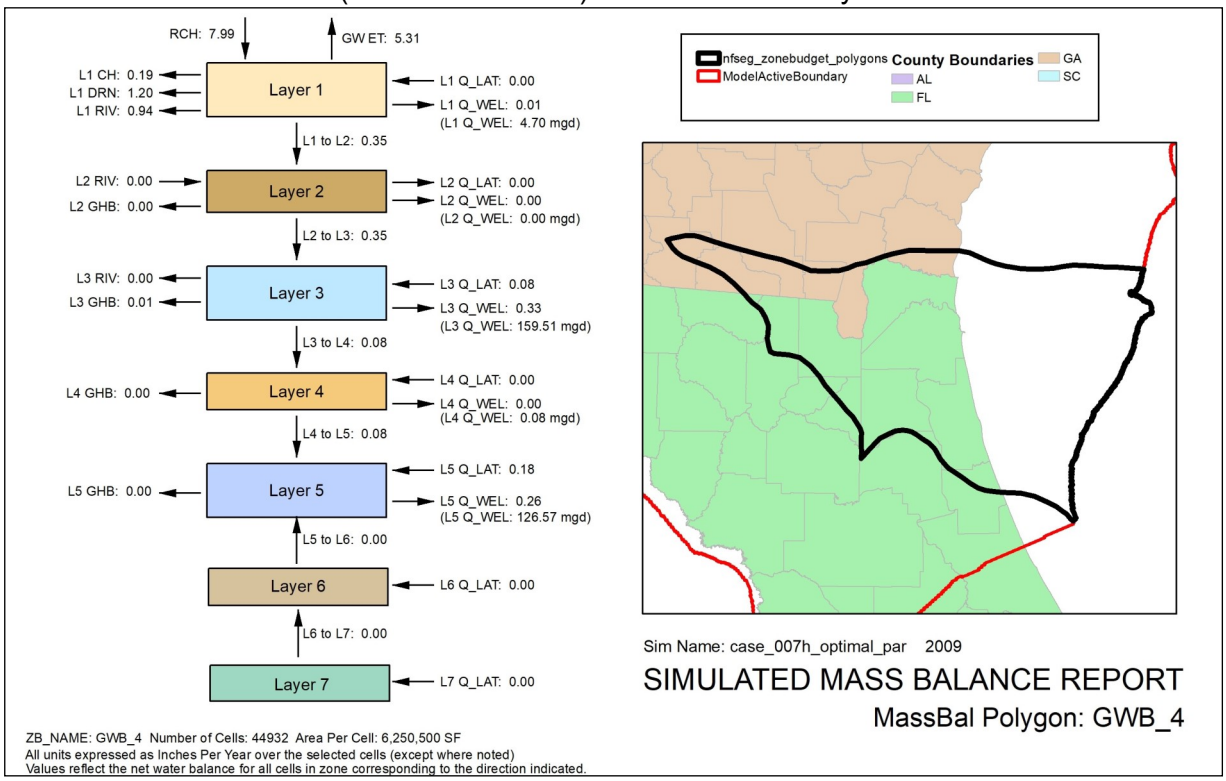

Figure 6-19. Simulated mass balance of GWB 4 for 2009
*Arrows indicate net flow (inflows + outflows) into or out of the layer.

Table 6-17. Simulated mass balance of GWB 4 for 2001 (all flows in/yr)

Layer	CH	DRN	GHB	GHB Spring Flows	GW ET	LAT, Q/LAT	Q_WEL	RCH	RIV	Flow to Lower Layer
Layer 1	-0.13	-0.66	0.00	0.00	-3.81	1.46E-04	-0.01	5.62	-0.62	-0.39
Layer 2	0.00	0.00	0.00	-0.00	0.00	-6.25E-06	0.00	0.00	2.80E-03	-0.39
Layer 3	0.00	0.00	-0.01	-0.00	0.00	0.09	-0.39	0.00	0.00	-0.08
Layer 4	0.00	0.00	0.00	0.00	0.00	2.41E-03	0.00	0.00	0.00	-0.08
Layer 5	0.00	0.00	0.00	0.00	0.00	0.21	-0.30	0.00	0.00	3.50E-03
Layer 6	0.00	0.00	0.00	0.00	0.00	1.72E-07	0.00	0.00	0.00	3.50E-03
Layer 7	0.00	0.00	0.00	0.00	0.00	3.50E-03	0.00	0.00	0.00	

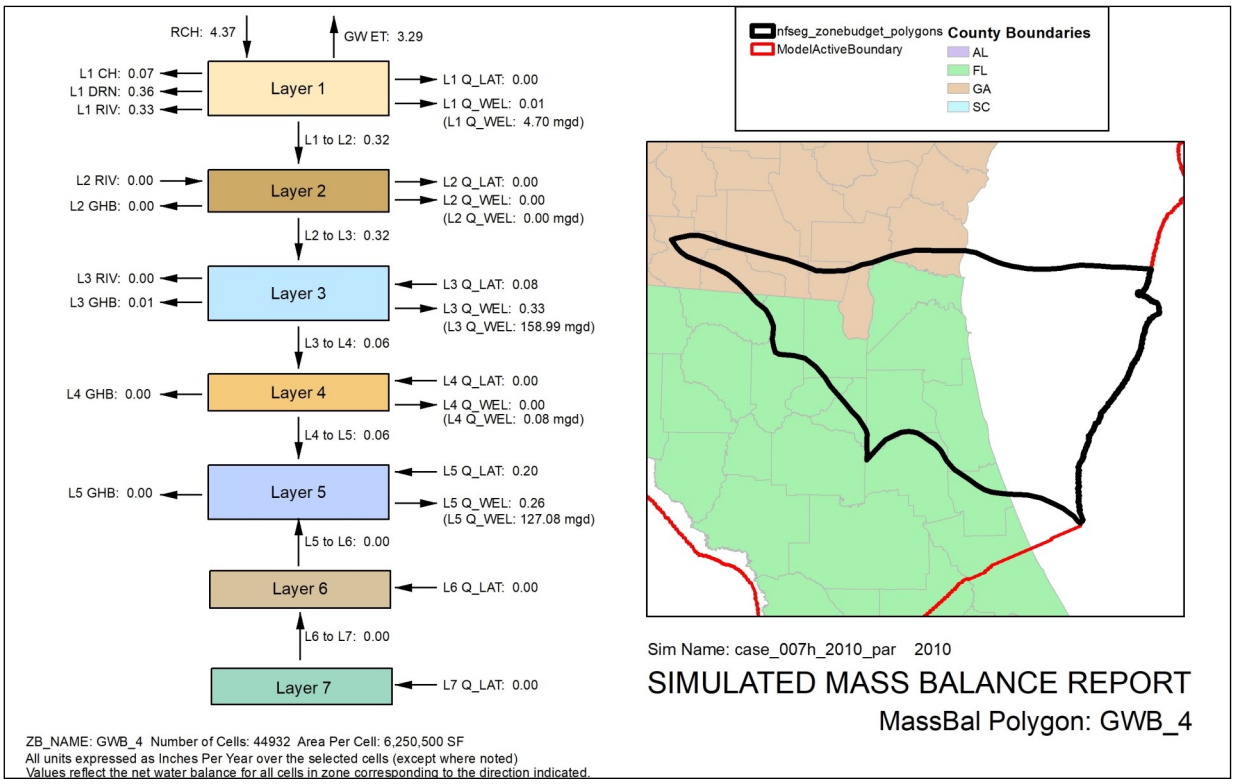

Figure 6-20. Simulated mass balance of GWB 4 for 2010
*Arrows indicate net flow (inflows + outflows) into or out of the layer.

Table 6-18. Simulated mass balance of GWB 4 for 2009 (all flows in/yr)

Layer	CH	DRN	GHB	GHB Spring Flows	GW ET	LAT, Q/LAT	Q_WEL	RCH	RIV	Flow to Lower Layer
Layer 1	-0.19	-1.20	0.00	0.00	-5.31	7.19E-05	-0.01	7.99	-0.94	-0.35
Layer 2	0.00	0.00	0.00	-0.00	0.00	-4.18E-06	0.00	0.00	2.94E-03	-0.35
Layer 3	0.00	0.00	-0.01	-0.00	0.00	0.08	-0.33	0.00	0.00	-0.08
Layer 4	0.00	0.00	0.00	0.00	0.00	1.89E-03	0.00	0.00	0.00	-0.08
Layer 5	0.00	0.00	0.00	0.00	0.00	0.18	-0.26	0.00	0.00	3.29E-03
Layer 6	0.00	0.00	0.00	0.00	0.00	1.87E-07	0.00	0.00	0.00	3.29E-03
Layer 7	0.00	0.00	0.00	0.00	0.00	3.29E-03	0.00	0.00	0.00	

Table 6-19. Simulated mass balance of GWB 4 for 2010 (all flows in/yr)

Layer	CH	DRN	GHB	GHB Spring Flows	GW ET	LAT, Q/LAT	Q_WEL	RCH	RIV	Flow to Lower Layer
Layer 1	-0.07	-0.36	0.00	0.00	-3.29	-6.30E-05	-0.01	4.37	-0.33	-0.32
Layer 2	0.00	0.00	-0.00	0.00	0.00	-7.53E-06	0.00	0.00	3.87E-03	-0.32
Layer 3	0.00	0.00	-0.01	-0.00	0.00	0.08	-0.33	0.00	0.00	-0.06
Layer 4	0.00	0.00	0.00	0.00	0.00	2.61E-03	0.00	0.00	0.00	-0.06
Layer 5	0.00	0.00	0.00	0.00	0.00	0.20	-0.26	0.00	0.00	3.51E-03
Layer 6	0.00	0.00	0.00	0.00	0.00	1.72E-07	0.00	0.00	0.00	3.51E-03
Layer 7	0.00	0.00	0.00	0.00	0.00	3.51E-03	0.00	0.00	0.00	

Table 6-20. Simulated mass balance of GWB 4 for no-pumping (all flows in/yr)

Layer	CH	DRN	GHB	GHB Spring Flows	GW ET	LAT, Q/LAT	Q_WEL	RCH	RIV	Flow to Lower Layer
Layer 1	-0.24	-1.20	0.00	0.00	-5.37	7.77E-05	0.00	7.84	-0.98	-0.05
Layer 2	0.00	0.00	0.00	-0.00	0.00	-4.96E-06	0.00	0.00	1.53E-03	-0.05
Layer 3	0.00	0.00	-0.02	-0.00	0.00	-0.01	0.00	0.00	0.00	-0.02
Layer 4	0.00	0.00	0.00	0.00	0.00	-5.65E-05	0.00	0.00	0.00	-0.02
Layer 5	0.00	0.00	0.00	0.00	0.00	-0.03	0.00	0.00	0.00	2.05E-03
Layer 6	0.00	0.00	0.00	0.00	0.00	1.40E-07	0.00	0.00	0.00	2.05E-03
Layer 7	0.00	0.00	0.00	0.00	0.00	2.05E-03	0.00	0.00	0.00	

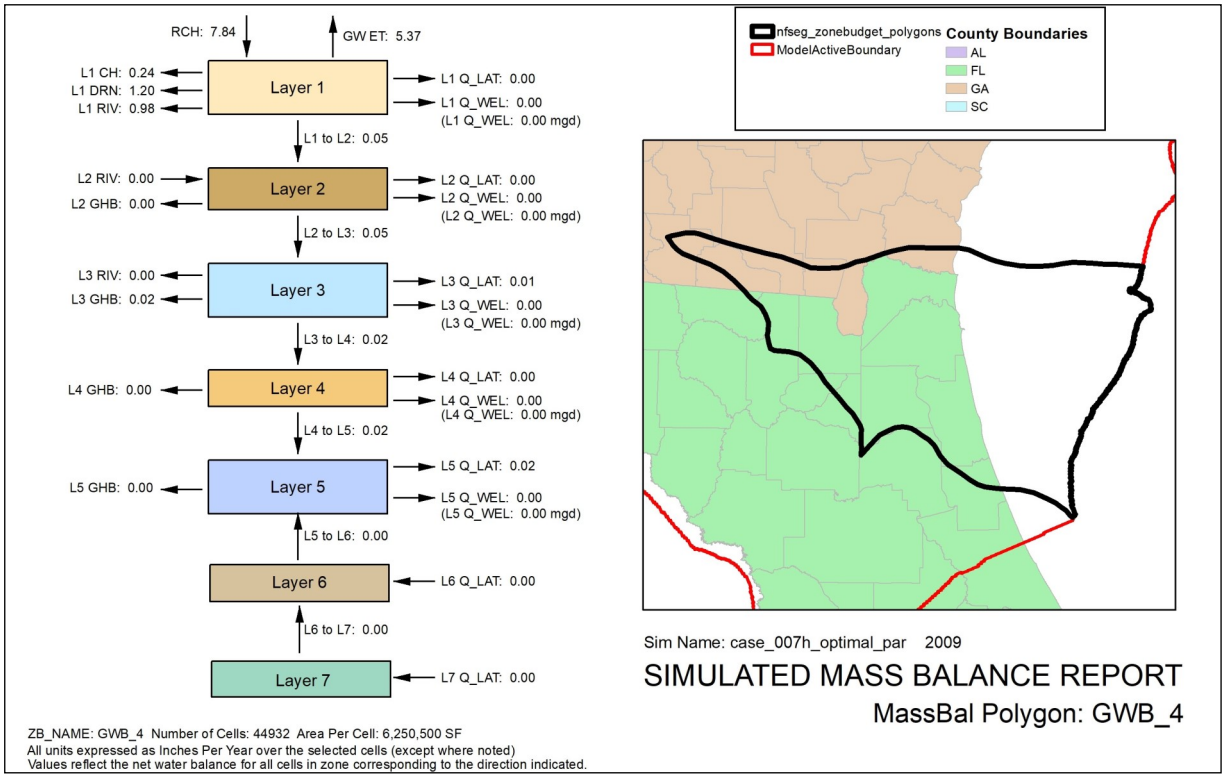

Figure 6-21. Simulated mass balance of GWB 4 for no-pumping
*Arrows indicate net flow (inflows + outflows) into or out of the layer.

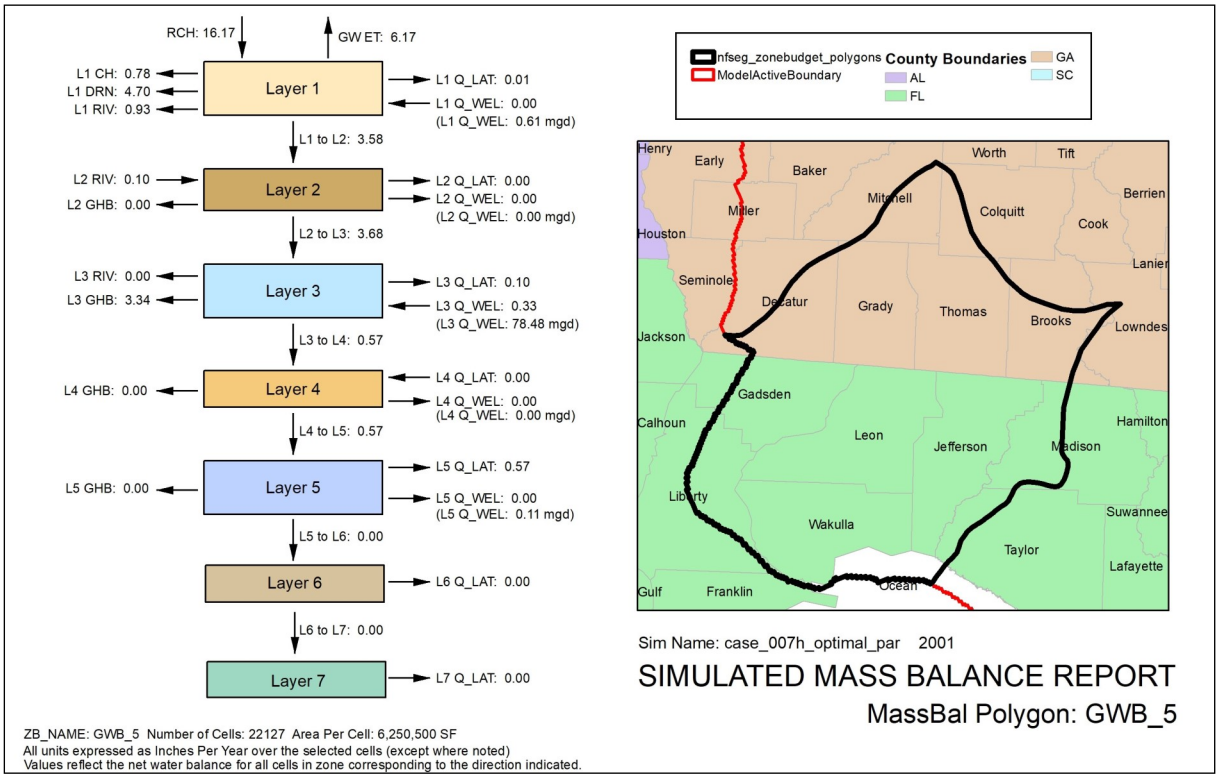

Figure 6-22. Simulated mass balance of GWB 5 for 2001
*Arrows indicate net flow (inflows + outflows) into or out of the layer.

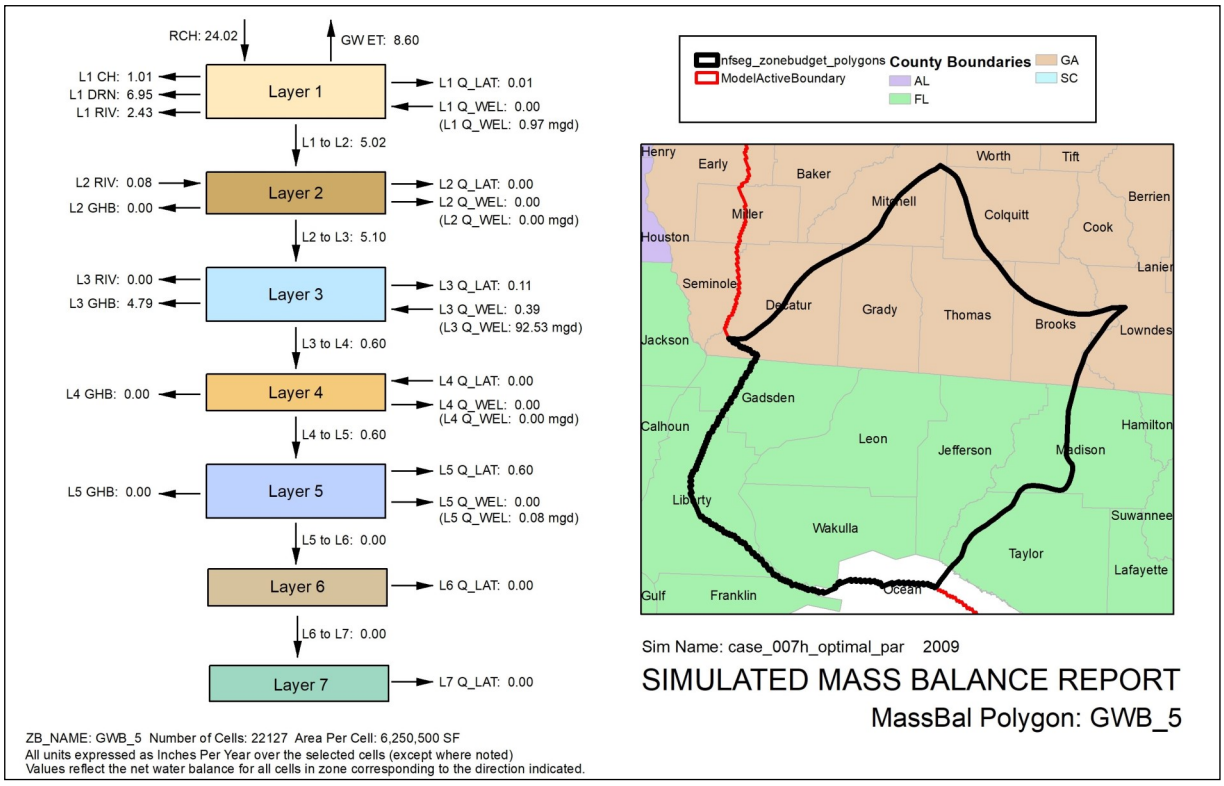

Figure 6-23. Simulated mass balance of GWB 5 for 2009
*Arrows indicate net flow (inflows + outflows) into or out of the layer.

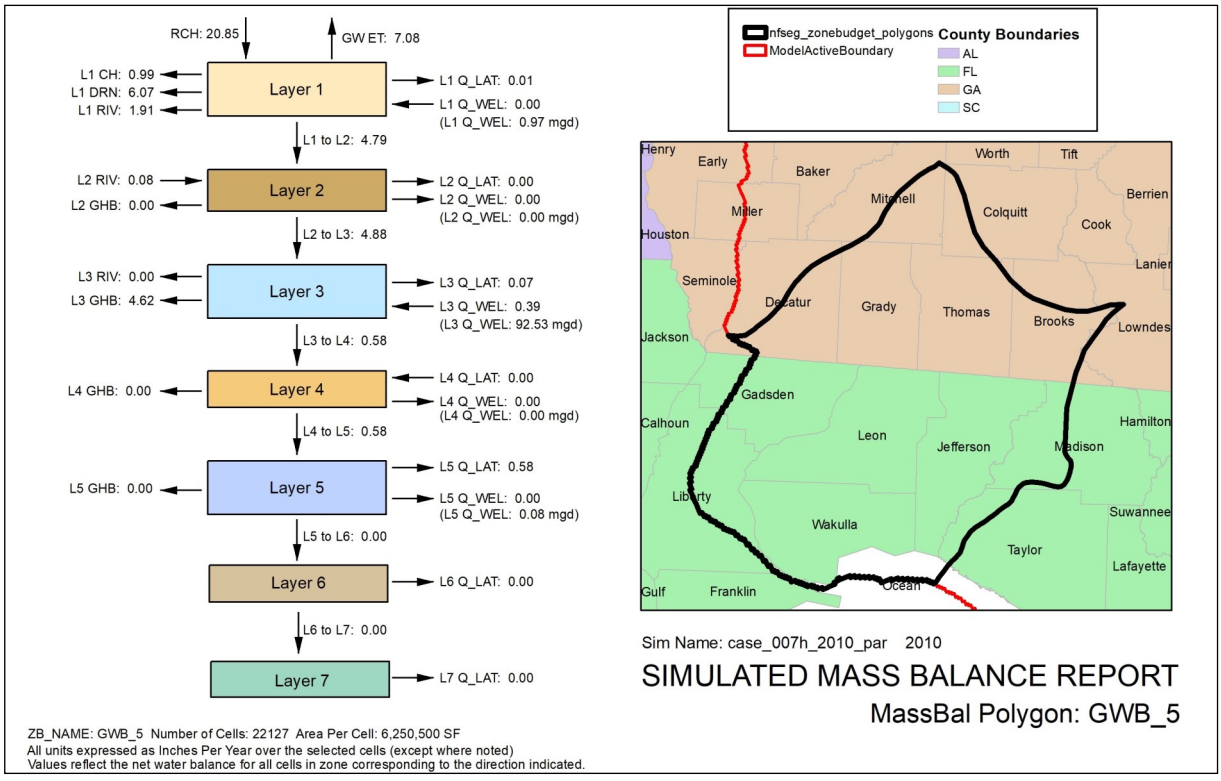

Figure 6-24. Simulated mass balance of GWB 5 for 2010
*Arrows indicate net flow (inflows + outflows) into or out of the layer.

Table 6-21. Simulated mass balance of GWB 5 for 2001 (all flows in/yr)

Layer	CH	DRN	GHB	GHB Spring Flows	GW ET	LAT, Q/LAT	Q_WEL	RCH	RIV	Flow to Lower Layer
Layer 1	-0.78	-4.70	0.00	0.00	-6.17	-6.19E-03	2.60E-03	16.2	-0.93	-3.58
Layer 2	0.00	0.00	0.00	0.00	0.00	-1.32E-03	0.00	0.00	0.10	-3.68
Layer 3	0.00	0.00	0.54	-3.88	0.00	-0.10	0.33	0.00	0.00	-0.57
Layer 4	0.00	0.00	0.00	0.00	0.00	3.24E-04	0.00	0.00	0.00	-0.57
Layer 5	0.00	0.00	0.00	0.00	0.00	-0.57	-4.84E-04	0.00	0.00	0.00
Layer 6	0.00	0.00	0.00	0.00	0.00	0.00	0.00	0.00	0.00	0.00
Layer 7	0.00	0.00	0.00	0.00	0.00	0.00	0.00	0.00	0.00	

Table 6-22. Simulated mass balance of GWB 5 for 2009 (all flows in/yr)

Layer	CH	DRN	GHB	GHB Spring Flows	GW ET	LAT, Q/LAT	Q_WEL	RCH	RIV	Flow to Lower Layer
Layer 1	-0.39	-1.56	0.00	0.00	-6.80	-7.14E-04	1.86E-03	16.7	-1.04	-6.88
Layer 2	0.00	0.00	0.00	-0.00	0.00	-0.01	0.00	0.00	-0.79	-6.08
Layer 3	0.00	0.00	-0.21	-6.10	0.00	0.14	-0.24	0.00	-0.01	0.33
Layer 4	0.00	0.00	0.00	0.00	0.00	-0.08	0.00	0.00	0.00	0.41
Layer 5	0.00	0.00	0.00	0.00	0.00	0.39	0.01	0.00	0.00	2.04E-03
Layer 6	0.00	0.00	0.00	0.00	0.00	-8.59E-08	0.00	0.00	0.00	2.04E-03
Layer 7	0.00	0.00	0.00	0.00	0.00	2.04E-03	0.00	0.00	0.00	

Table 6-23. Simulated mass balance of GWB 5 for 2010 (all flows in/yr)

Layer	CH	DRN	GHB	GHB Spring Flows	GW ET	LAT, Q/LAT	Q_WEL	RCH	RIV	Flow to Lower Layer
Layer 1	-0.99	-6.07	0.00	0.00	-7.08	-7.29E-03	4.11E-03	20.9	-1.91	-4.79
Layer 2	0.00	0.00	0.00	0.00	0.00	-2.48E-03	0.00	0.00	0.08	-4.87
Layer 3	0.00	0.00	0.57	-5.19	0.00	-0.07	0.39	0.00	0.00	-0.58
Layer 4	0.00	0.00	0.00	0.00	0.00	1.04E-03	0.00	0.00	0.00	-0.58
Layer 5	0.00	0.00	0.00	0.00	0.00	-0.58	-3.46E-04	0.00	0.00	0.00
Layer 6	0.00	0.00	0.00	0.00	0.00	0.00	0.00	0.00	0.00	0.00
Layer 7	0.00	0.00	0.00	0.00	0.00	0.00	0.00	0.00	0.00	

Layer 2, 12-18% discharges at drain boundaries and the nearly all of the remainder flows out to constant heads. Lateral flows make up less than 1% of all water flows into Layer 2. River boundary flows make up about 1% of Layer 2 water outflows and most of the remainder is transferred vertically to Layer 3. Of the total water entering Layer 3, 62-73% of water flows vertically from Layer 2, 26-37% flows vertically upward from Layer 4 and less than 1% flows laterally from the basin boundary. Approximately 91-93% of all water entering Layer 3 is removed as GHB springflows and the remainder is removed from Layer 3 through well withdrawals. The simulated Layer 3 GHB flows consist of 6.00, 6.12 and 7.60 in/yr spring discharges and 2.57, 2.72 and 4.19 in/yr lateral boundary outflows for 2001, 2009 and 2010 respectively (Tables 6.25-6.27). Vertical flow from Layer 5 to Layer 4 makes up 92-96% of all water flow into Layer 4, with the remainder contributed from lateral boundary flows. General head boundary flows into Layer 5 make up 85% of all water flows for 2001 and 57-58% for 2009 and 2010, with the remainder consisting of lateral boundary flows. Of all water transferred into Layer 5 via lateral boundary flows, less than 1 percent is withdrawn via wells and the remainder is transferred to Layer 4.

For the 2009 no-pumping simulation, the removal of well withdrawals resulted in 1.8% greater simulated constant head outflows, 1.9% greater drainage outflows, 24.1% increase in river outflows, 1.0% increase in GW ET and a 11.3% decrease in vertical flow from Layer 1 to Layer 2 (Figure 6-29). River outflow from Layer 2 decreases by 65% and vertical flow from Layer 2 to Layer 3 decreases by 11.6%. Spring boundary outflows from Layer 3 increased by 6.9% and the upward vertical flow of water from Layer 4 to Layer 3 decreased by 0.29%. General head boundary flows into and out of Layer 5 decreased by 1.0% and the vertical flow of water from Layer 5 to Layer 4 decreased by 0.31%. See Table 6.28 for simulated mass balance of GWB6 for no-pumping.

GWB 7

In GWB 7, simulated net recharge into Layer 1 is 4.73, 4.49 and 3.82 in/yr for 2001, 2009 and 2010 respectively (Figures 6-30 to 6-32). Net recharge makes up 80-88% of water flow into Layer 1, with vertical upward flow from Layer 2 and, to a lesser extent, well contributions making up the remainder. Flows to river boundaries make up 54-57% of all flows out of Layer 1, discharge at drain boundaries makes up 40-43% and constant heads make up about 3%. Vertical flow from Layer 3 makes up all water inflows to Layer 2 and about 99% of that inflow is transferred vertically upward to Layer 1, with the remainder flowing out at river boundaries. Vertical flow from Layer 4 makes up 98-99% of all water inflow to Layer 3 and the remainder consists of lateral boundary flows. Of the total Layer 3 inflow, 58-60% is transferred out through GHB springflows, 19-23% is withdrawn through wells and the remainder is transferred vertically to Layer 2. The simulated Layer 3 GHB flows consisted of 2.27, 2.31 and 2.00 in/yr spring discharge and 0.04, 0.01 and 0.33 in/yr general boundary outflows for 2001, 2009 and 2010 respectively (Tables 6.29-6.31). One hundred percent of inflow to Layer 4 was vertically transferred from Layer 5 and 100% of that continued to flow upward to Layer 3. Approximately 0.01 in/yr flowed from Layer 5 to Layer 6 and then to Layer 7. Most water inflow into Layer 5 was from general head boundary flows, with a lesser amount contributed from lateral boundary flows. Of the total outflows of water from Layer 5, 1-2% consisted of well withdrawals.

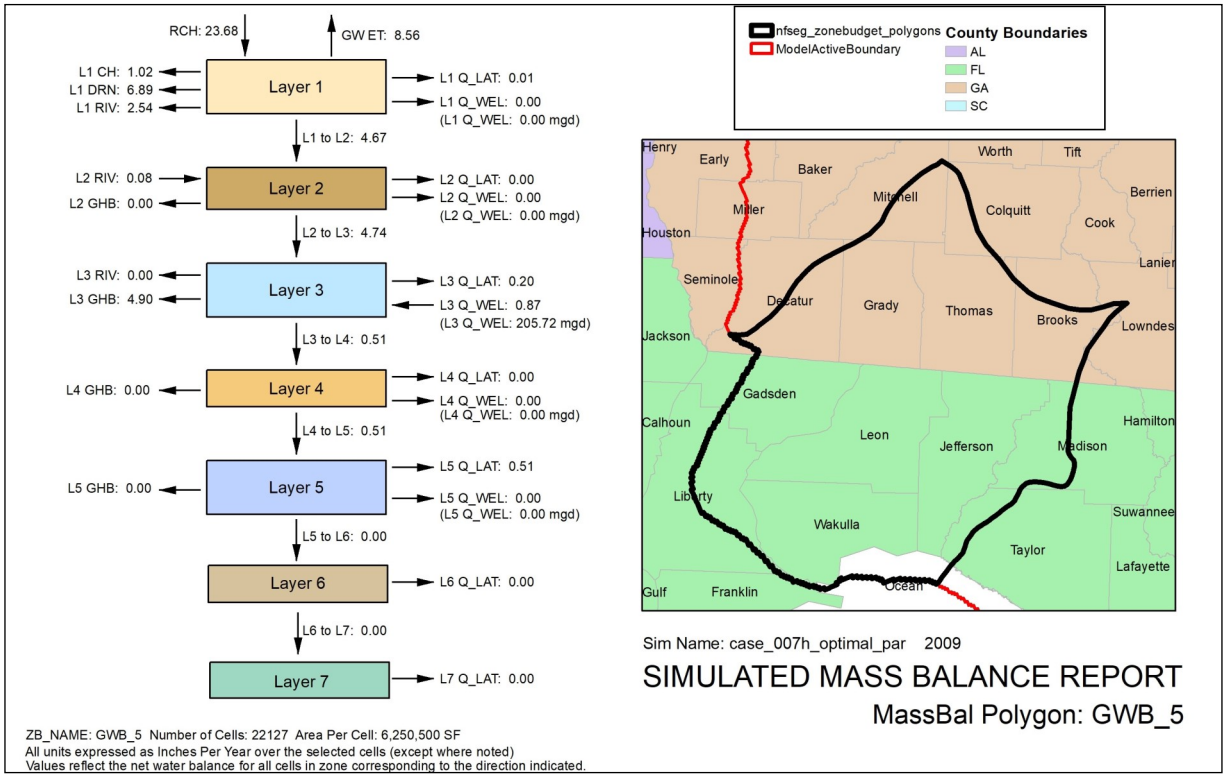

Figure 6-25. Simulated mass balance of GWB 5 for no pumping
*Arrows indicate net flow (inflows + outflows) into or out of the layer.

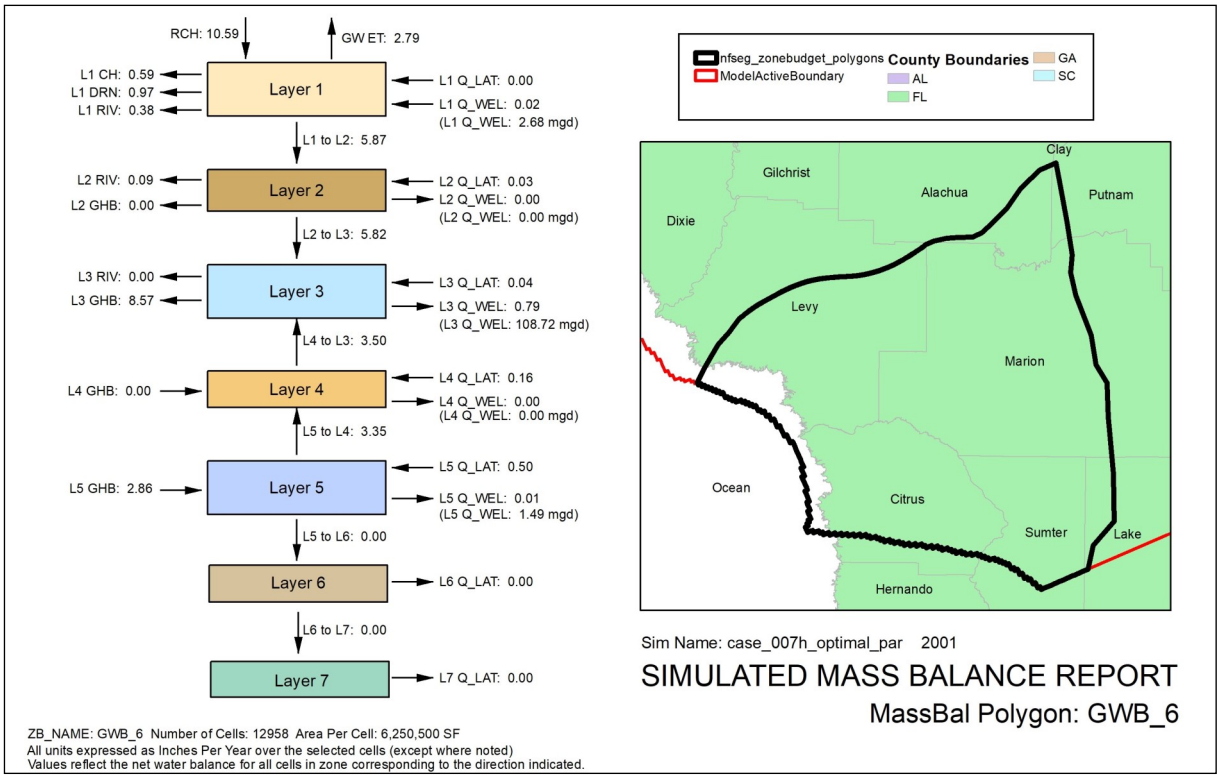

Figure 6-26. Simulated mass balance of GWB 6 for 2001
*Arrows indicate net flow (inflows + outflows) into or out of the layer.

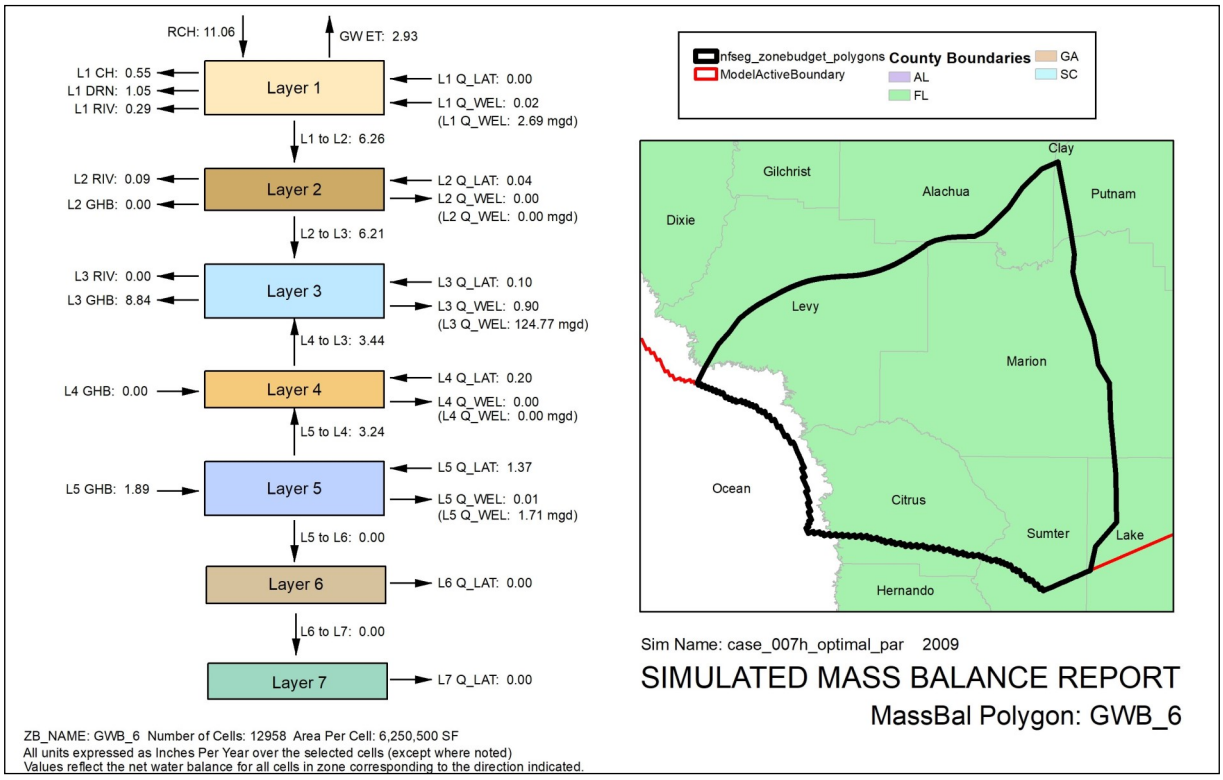

Figure 6-27. Simulated mass balance of GWB 6 for 2009
*Arrows indicate net flow (inflows + outflows) into or out of the layer.

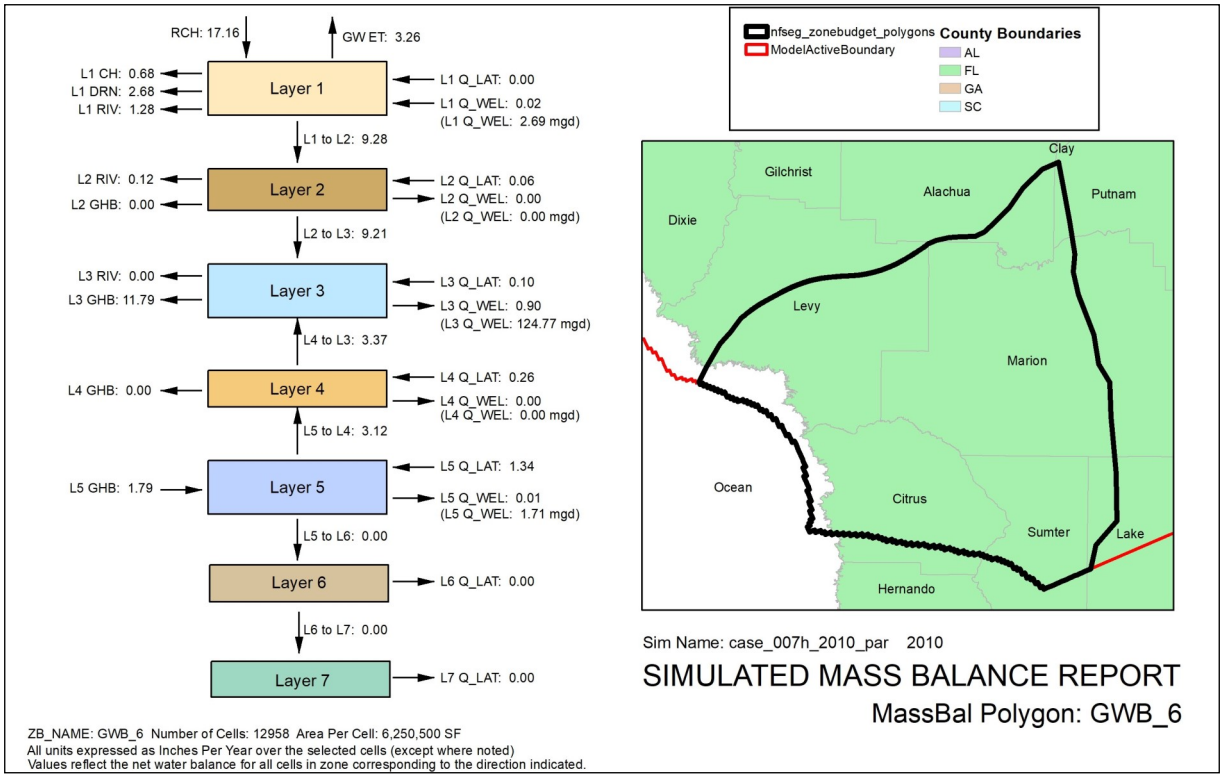

Figure 6-28. Simulated mass balance of GWB 6 for 2010
*Arrows indicate net flow (inflows + outflows) into or out of the layer.

Table 6-24. Simulated mass balance of GWB 5 for no pumping (all flows in/yr)

Layer	CH	DRN	GHB	GHB Spring Flows	GW ET	LAT, Q/LAT	Q_WEL	RCH	RIV	Flow to Lower Layer
Layer 1	-1.02	-6.89	0.00	0.00	-8.56	0.01	0.00	243.6	-2.54	-4.67
Layer 2	0.00	0.00	0.00	0.00	0.00	-3.68E-03	0.00	0.00	0.08	-4.74
Layer 3	0.00	0.00	0.64	-5.54	0.00	-0.20	0.87	0.00	0.00	-0.51
Layer 4	0.00	0.00	0.00	0.00	0.00	-1.72E-04	0.00	0.00	0.00	-0.51
Layer 5	0.00	0.00	0.00	0.00	0.00	-0.51	0.00	0.00	0.00	0.00
Layer 6	0.00	0.00	0.00	0.00	0.00	0.00	0.00	0.00	0.00	0.00
Layer 7	0.00	0.00	0.00	0.00	0.00	0.00	0.00	0.00	0.00	

Table 6-25. Simulated mass balance of GWB 6 for 2001 (all flows in/yr)

Layer	CH	DRN	GHB	GHB Spring Flows	GW ET	LAT, Q/LAT	Q_WEL	RCH	RIV	Flow to Lower Layer
Layer 1	-0.59	-0.97	0.00	0.00	-2.79	1.35E-03	0.02	10.6	-0.38	-5.87
Layer 2	0.00	0.00	0.00	0.00	0.00	0.03	0.00	0.00	-0.09	-5.82
Layer 3	0.00	0.00	-2.57	-6.00	0.00	0.04	-0.79	0.00	0.00	3.50
Layer 4	0.00	0.00	0.00	0.00	0.00	0.16	0.00	0.00	0.00	3.35
Layer 5	0.00	0.00	2.86	0.00	0.00	0.50	-0.01	0.00	0.00	-2.68E-03
Layer 6	0.00	0.00	0.00	0.00	0.00	0.00	0.00	0.00	0.00	-2.68E-03
Layer 7	0.00	0.00	0.00	0.00	0.00	-2.68E-03	0.00	0.00	0.00	

Table 6-26. Simulated mass balance of GWB 6 for 2009 (all flows in/yr)

Layer	CH	DRN	GHB	GHB Spring Flows	GW ET	LAT, Q/LAT	Q_WEL	RCH	RIV	Flow to Lower Layer
Layer 1	-0.55	-1.05	0.00	0.00	-2.93	1.52E-03	0.02	11.1	-0.29	-6.26
Layer 2	0.00	0.00	0.00	0.00	0.00	0.04	0.00	0.00	-0.09	-6.21
Layer 3	0.00	0.00	-2.72	-6.12	0.00	0.10	-0.90	0.00	0.00	3.44
Layer 4	0.00	0.00	0.00	0.00	0.00	0.20	0.00	0.00	0.00	3.24
Layer 5	0.00	0.00	1.89	0.00	0.00	1.37	-0.01	0.00	0.00	-2.37E-03
Layer 6	0.00	0.00	0.00	0.00	0.00	0.00	0.00	0.00	0.00	-2.37E-03
Layer 7	0.00	0.00	0.00	0.00	0.00	-2.37E-03	0.00	0.00	0.00	

Table 6-27. Simulated mass balance of GWB 6 for 2010 (all flows in/yr)

Layer	CH	DRN	GHB	GHB Spring Flows	GW ET	LAT, Q/LAT	Q_WEL	RCH	RIV	Flow to Lower Layer
Layer 1	-0.68	-2.68	0.00	0.00	-3.26	1.55E-03	0.02	17.2	-1.28	-9.28
Layer 2	0.00	0.00	0.00	0.00	0.00	0.06	0.00	0.00	-0.12	-9.21
Layer 3	0.00	0.00	-4.19	-7.60	0.00	0.10	-0.90	0.00	0.00	3.37
Layer 4	0.00	0.00	0.00	0.00	0.00	0.26	0.00	0.00	0.00	3.12
Layer 5	0.00	0.00	1.79	0.00	0.00	1.34	-0.01	0.00	0.00	-2.24E-03
Layer 6	0.00	0.00	0.00	0.00	0.00	0.00	0.00	0.00	0.00	-2.24E-03
Layer 7	0.00	0.00	0.00	0.00	0.00	-2.24E-03	0.00	0.00	0.00	

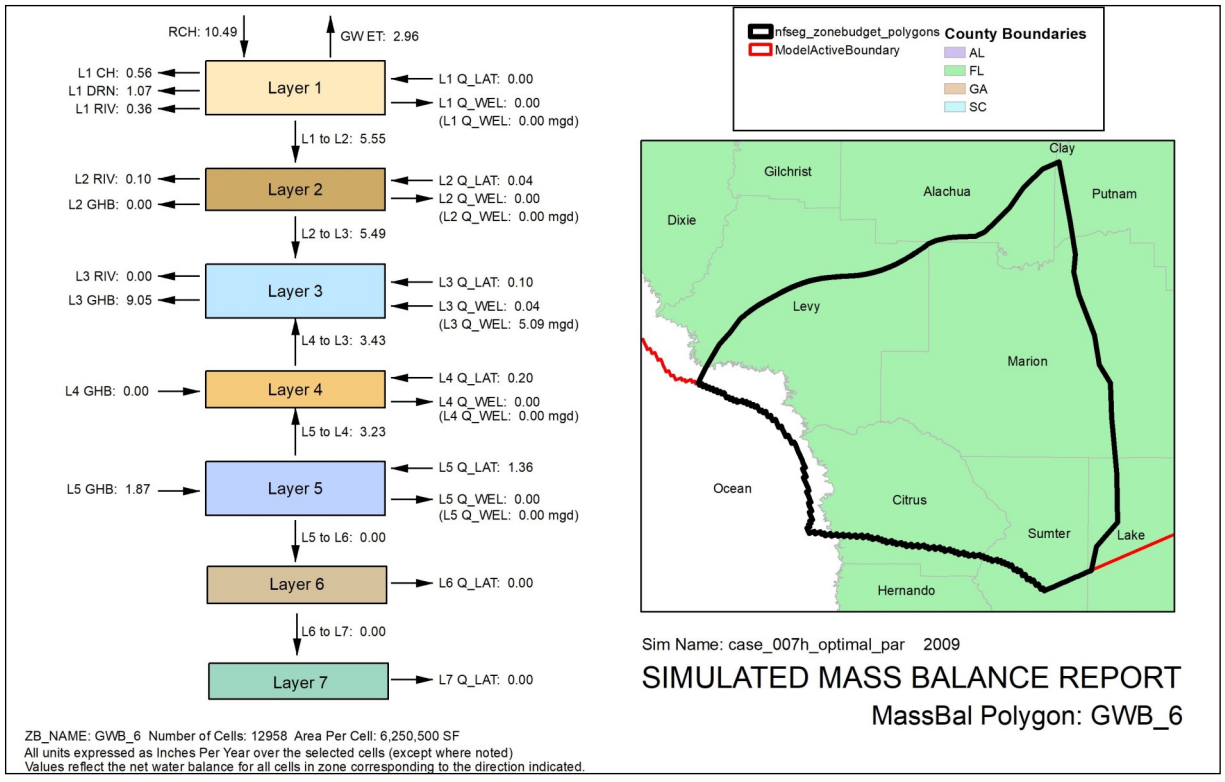

Figure 6-29. Simulated mass balance of GWB 6 for no-pumping
*Arrows indicate net flow (inflows + outflows) into or out of the layer.

For the flows into and out of Layer 1, the changes in well withdrawals for the 2009 no-pumping simulation resulted in 29% greater simulated constant head outflows, 0.90% greater drainage outflows, 5.2% increase in river outflows, 1.9% increase in GW ET and a 97.3% increase in upward vertical flow from Layer 2 to Layer 1 (Figure 6-33). Upward vertical flow from Layer 3 to Layer 2 increased similarly by 97.4%. Spring outflows from Layer 3 increased by 2.2 percent and total general head boundary flows changed from a 0.17 in/yr inflow to a 1.36 in/yr outflow from Layer 3. The vertical flow of water from Layer 4 to Layer 3 decreased by 1.8% and the vertical flow of water from Layer 5 to Layer 4 decreased by the same percentage. General head boundary flows into Layer 5 decreased by 4%. The small (0.01 in/yr) positive inflows to Layer 3 from wells in the no-pumping simulation represented the natural influx to the Floridan aquifer system via sinks. See Table 6.32 for simulated mass balance of GWB7 for no-pumping.

Overall Summary

Figures 6-34 through 6-37 provide a simplified summary of simulated model wide mass balances for years 2001, 2009, 2010 and a no-pumping scenario, respectively. These bar graphs illustrate inflows and outflows from the major model components: recharge, Et, wells, springs, rivers and other drains, constant head and lateral leakage.

Table 6-28. Simulated mass balance of GWB 6 for no pumping (all flows in/yr)

Layer	CH	DRN	GHB	GHB Spring Flows	GW ET	LAT, Q/LAT	Q_WEL	RCH	RIV	Flow to Lower Layer
Layer 1	-0.56	-1.07	0.00	0.00	-2.96	1.53E-03	0.00	10.49	-0.36	-5.55
Layer 2	0.00	0.00	0.00	0.00	0.00	0.04	0.00	0.00	-0.10	-5.49
Layer 3	0.00	0.00	-2.51	-6.54	0.00	0.10	0.04	0.00	0.00	3.43
Layer 4	0.00	0.00	0.00	0.00	0.00	0.20	0.00	0.00	0.00	3.23
Layer 5	0.00	0.00	1.87	0.00	0.00	1.36	0.00	0.00	0.00	-1.98E-03
Layer 6	0.00	0.00	0.00	0.00	0.00	0.00	0.00	0.00	0.00	-1.98E-03
Layer 7	0.00	0.00	0.00	0.00	0.00	-1.98E-03	0.00	0.00	0.00	

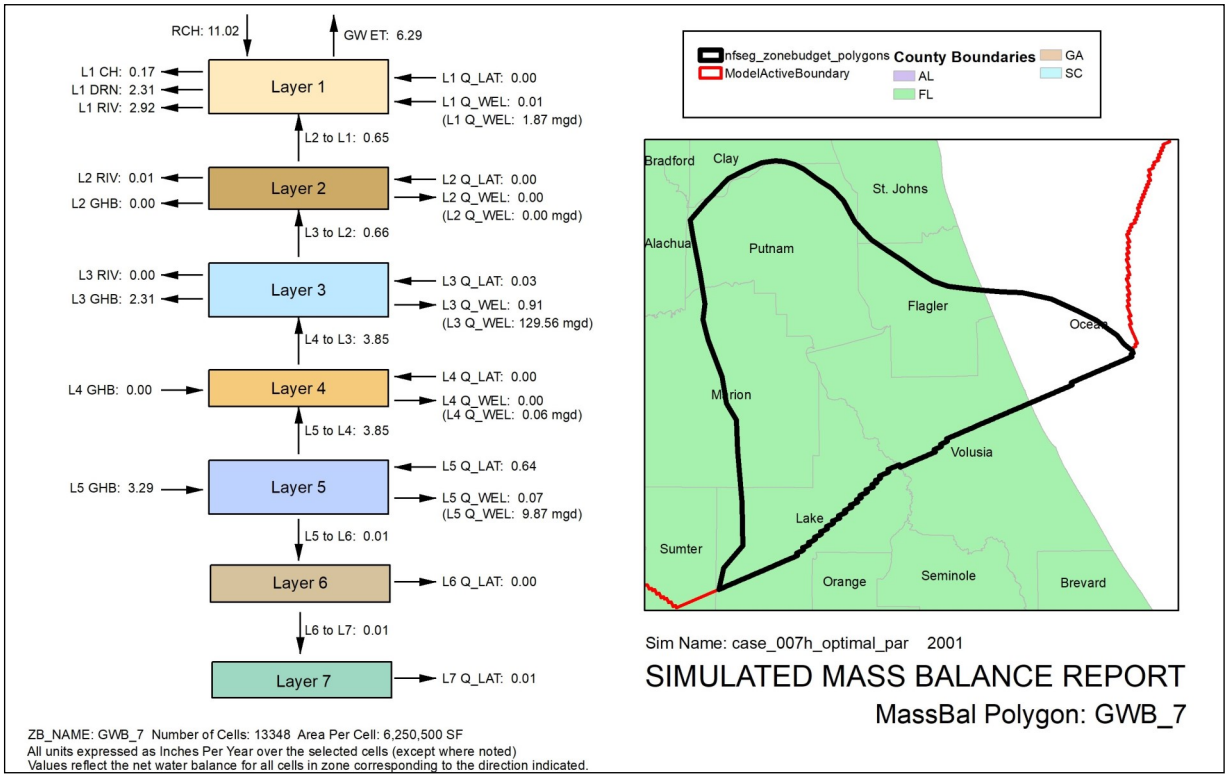

Figure 6-30. Simulated mass balance of GWB 7 for 2001
*Arrows indicate net flow (inflows + outflows) into or out of the layer.

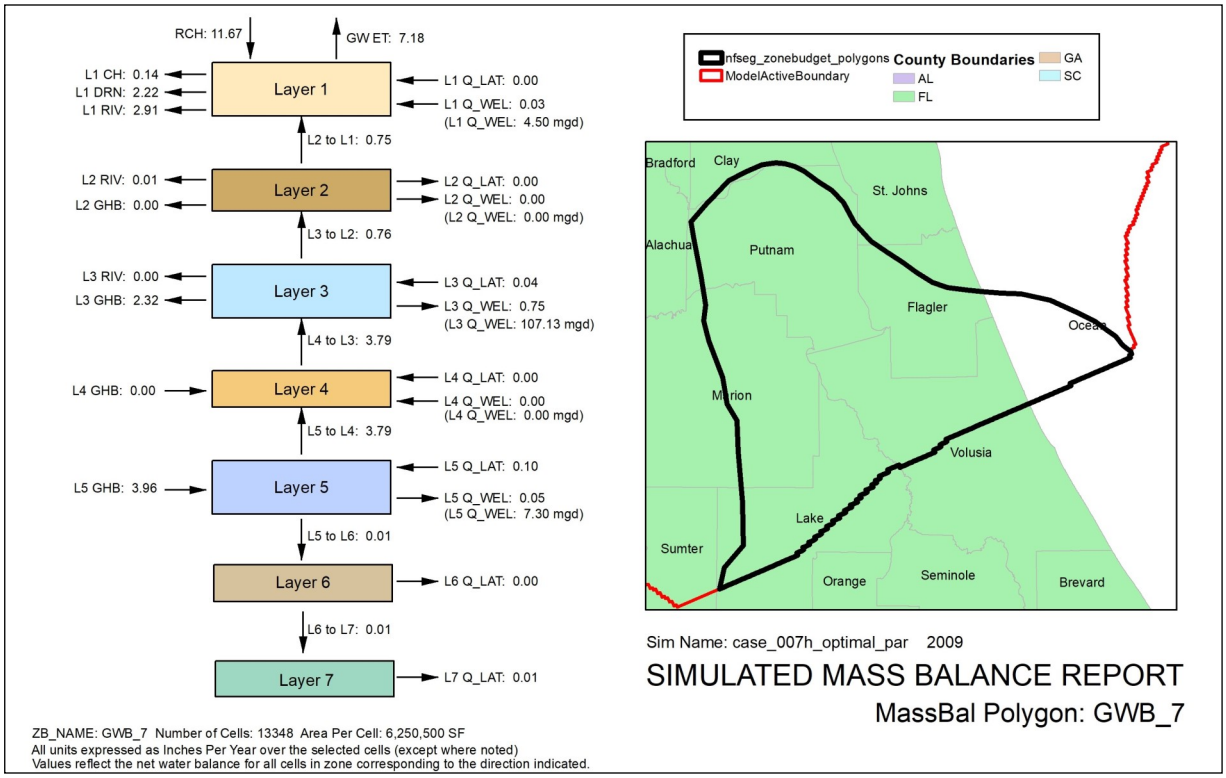

Figure 6-31. Simulated mass balance of GWB 7 for 2009
*Arrows indicate net flow (inflows + outflows) into or out of the layer.

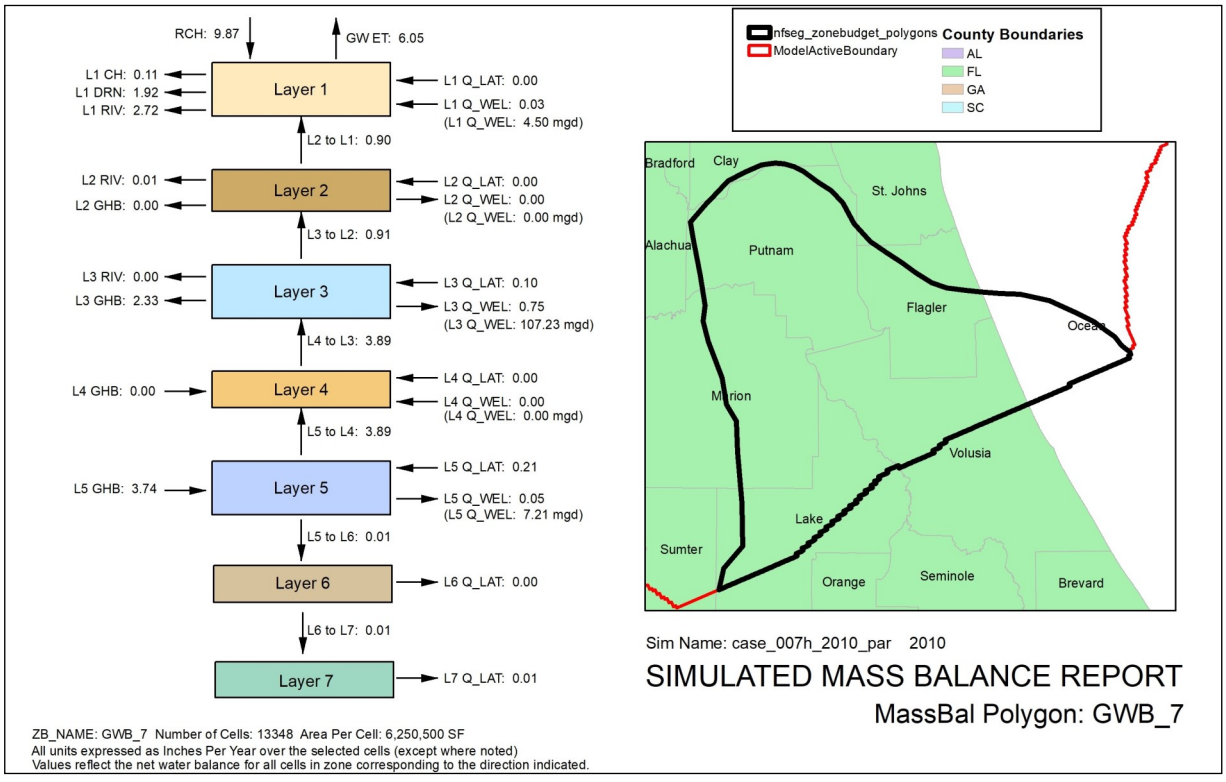

Figure 6-32. Simulated mass balance of GWB 7 for 2010
*Arrows indicate net flow (inflows + outflows) into or out of the layer.

Table 6-29. Simulated mass balance of GWB 7 for 2001 (all flows in/yr)

Layer	CH	DRN	GHB	GHB Spring Flows	GW ET	LAT, Q/LAT	Q_WEL	RCH	RIV	Flow to Lower Layer
Layer 1	-0.17	-2.31	0.00	0.00	-6.29	3.75E-03	0.01	11.0	-2.92	0.65
Layer 2	0.00	0.00	0.00	0.00	0.00	3.10E-05	0.00	0.00	-0.01	0.66
Layer 3	0.00	0.00	-0.04	-2.27	0.00	0.03	-0.91	0.00	0.00	3.85
Layer 4	0.00	0.00	0.00	0.00	0.00	5.92E-04	0.00	0.00	0.00	3.85
Layer 5	0.00	0.00	3.29	0.00	0.00	0.64	-0.07	0.00	0.00	-0.01
Layer 6	0.00	0.00	0.00	0.00	0.00	-5.25E-07	0.00	0.00	0.00	-0.01
Layer 7	0.00	0.00	0.00	0.00	0.00	-0.01	0.00	0.00	0.00	

Table 6-30. Simulated mass balance of GWB 7 for 2009 (all flows in/yr)

Layer	CH	DRN	GHB	GHB Spring Flows	GW ET	LAT, Q/LAT	Q_WEL	RCH	RIV	Flow to Lower Layer
Layer 1	-0.14	-2.22	0.00	0.00	-7.18	3.67E-03	0.03	11.7	-2.91	0.75
Layer 2	0.00	0.00	0.00	0.00	0.00	-3.79E-05	0.00	0.00	-0.01	0.76
Layer 3	0.00	0.00	-0.01	-2.31	0.00	0.04	-0.75	0.00	0.00	3.79
Layer 4	0.00	0.00	0.00	0.00	0.00	4.62E-04	0.00	0.00	0.00	3.79
Layer 5	0.00	0.00	3.96	0.00	0.00	-0.10	-0.05	0.00	0.00	-0.01
Layer 6	0.00	0.00	0.00	0.00	0.00	-6.30E-07	0.00	0.00	0.00	-0.01
Layer 7	0.00	0.00	0.00	0.00	0.00	-0.01	0.00	0.00	0.00	

Table 6-31. Simulated mass balance of GWB 7 for 2010 (all flows in/yr)

Layer	CH	DRN	GHB	GHB Spring Flows	GW ET	LAT, Q/LAT	Q_WEL	RCH	RIV	Flow to Lower Layer
Layer 1	-0.11	-1.92	0.00	0.00	-6.05	3.62E-03	0.03	9.87	-2.72	0.90
Layer 2	0.00	0.00	0.00	0.00	0.00	7.06E-05	0.00	0.00	-0.01	0.91
Layer 3	0.00	0.00	-0.33	-2.00	0.00	0.10	-0.75	0.00	0.00	3.89
Layer 4	0.00	0.00	0.00	0.00	0.00	1.18E-03	0.00	0.00	0.00	3.89
Layer 5	0.00	0.00	3.74	0.00	0.00	0.21	-0.05	0.00	0.00	-0.01
Layer 6	0.00	0.00	0.00	0.00	0.00	-6.30E-07	0.00	0.00	0.00	-0.01
Layer 7	0.00	0.00	0.00	0.00	0.00	-0.01	0.00	0.00	0.00	

Table 6-32. Simulated mass balance of GWB 7 for no-pumping (all flows in/yr)

Layer	CH	DRN	GHB	GHB Spring Flows	GW ET	LAT, Q/LAT	Q_WEL	RCH	RIV	Flow to Lower Layer
Layer 1	-0.18	-2.24	0.00	0.00	-7.32	3.95E-03	0.00	11.31	-3.06	1.48
Layer 2	0.00	0.00	0.00	0.00	0.00	-3.53E-05	0.00	0.00	-0.01	1.50
Layer 3	0.00	0.00	-0.02	-2.36	0.00	0.13	0.00	0.00	0.00	3.72
Layer 4	0.00	0.00	0.00	0.00	0.00	8.36E-04	0.00	0.00	0.00	3.72
Layer 5	0.00	0.00	3.81	0.00	0.00	-0.09	0.00	0.00	0.00	-0.01
Layer 6	0.00	0.00	0.00	0.00	0.00	-4.72E-07	0.00	0.00	0.00	-0.01
Layer 7	0.00	0.00	0.00	0.00	0.00	-0.01	0.00	0.00	0.00	

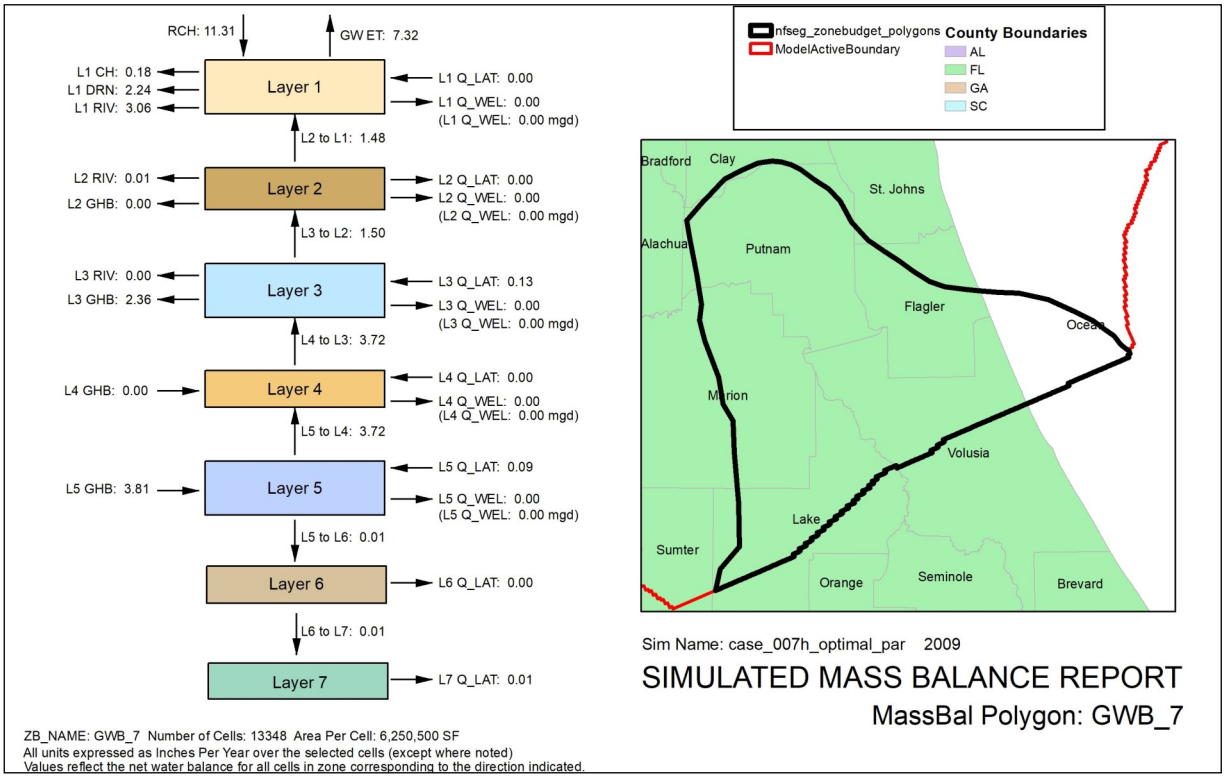

Figure 6-33. Simulated mass balance of GWB 7 for no-pumping
*Arrows indicate net flow (inflows + outflows) into or out of the layer.

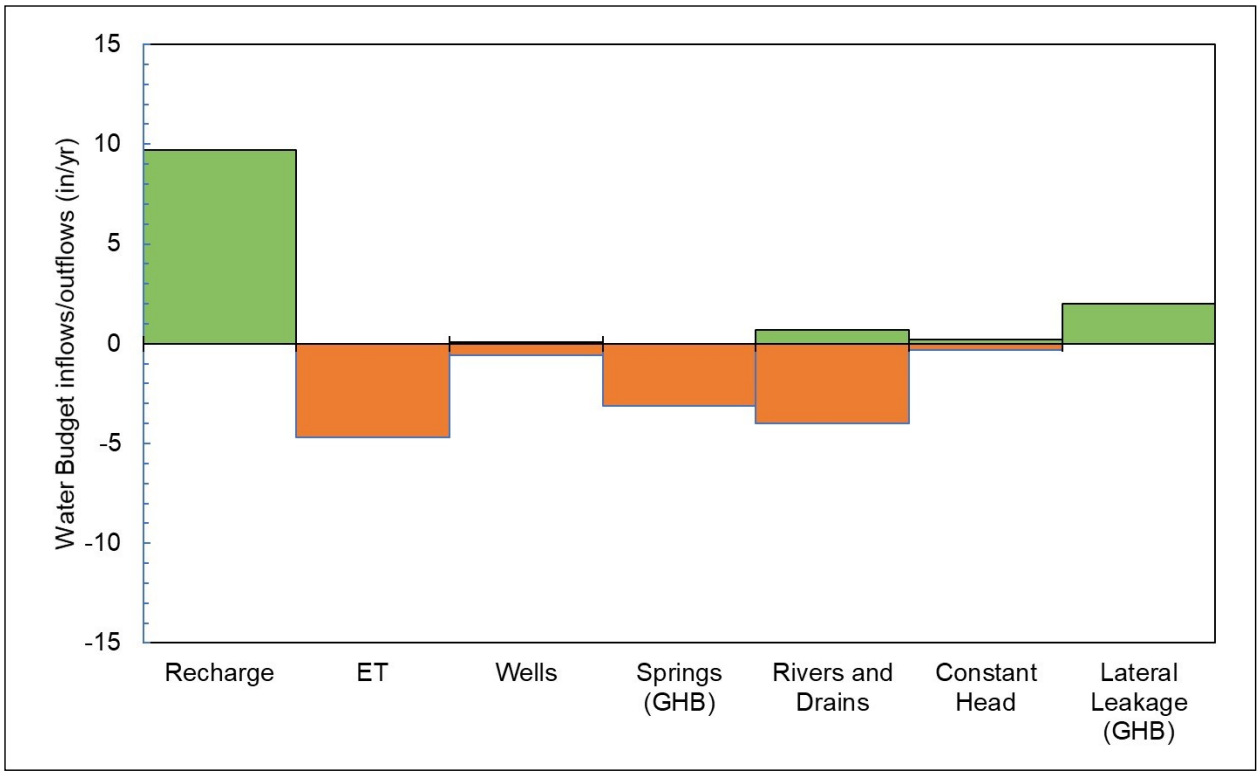

Figure 6-34. Inflows and outflows of simulated model wide mass balance for 2001

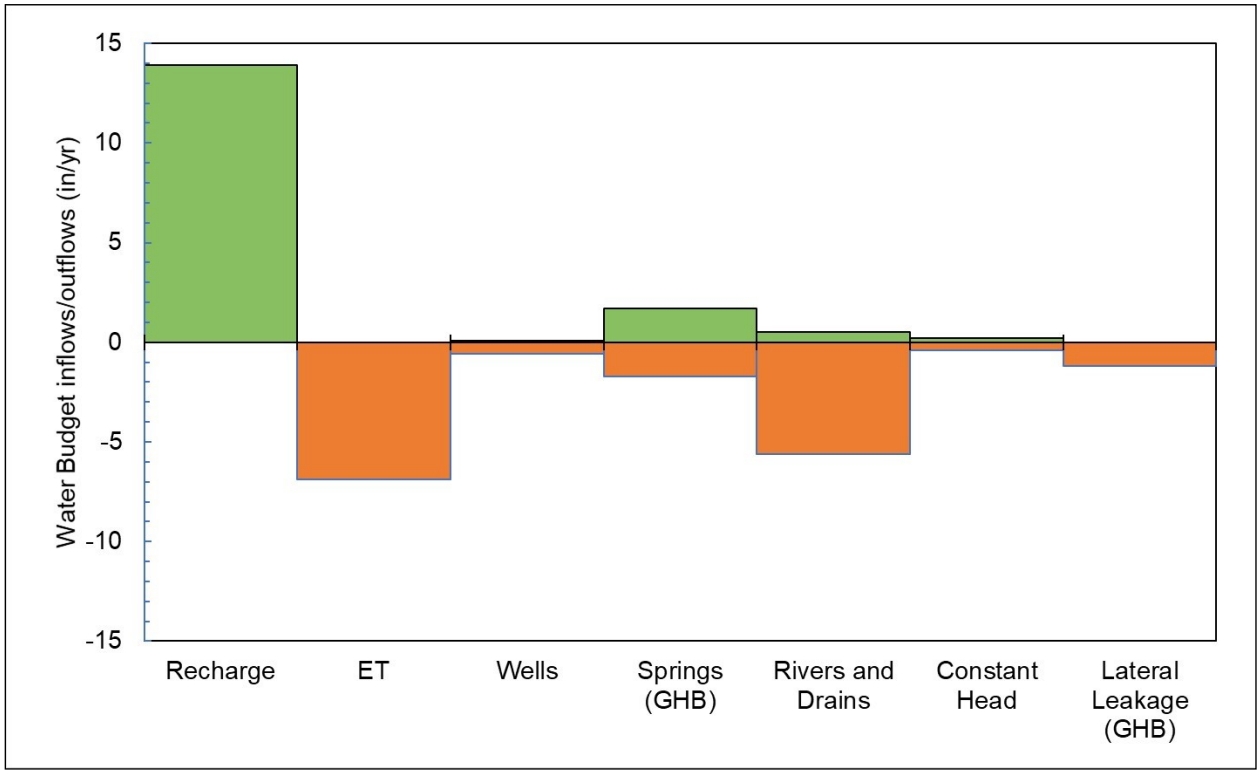

Figure 6-35. Inflows and outflows of simulated model wide mass balance for 2009

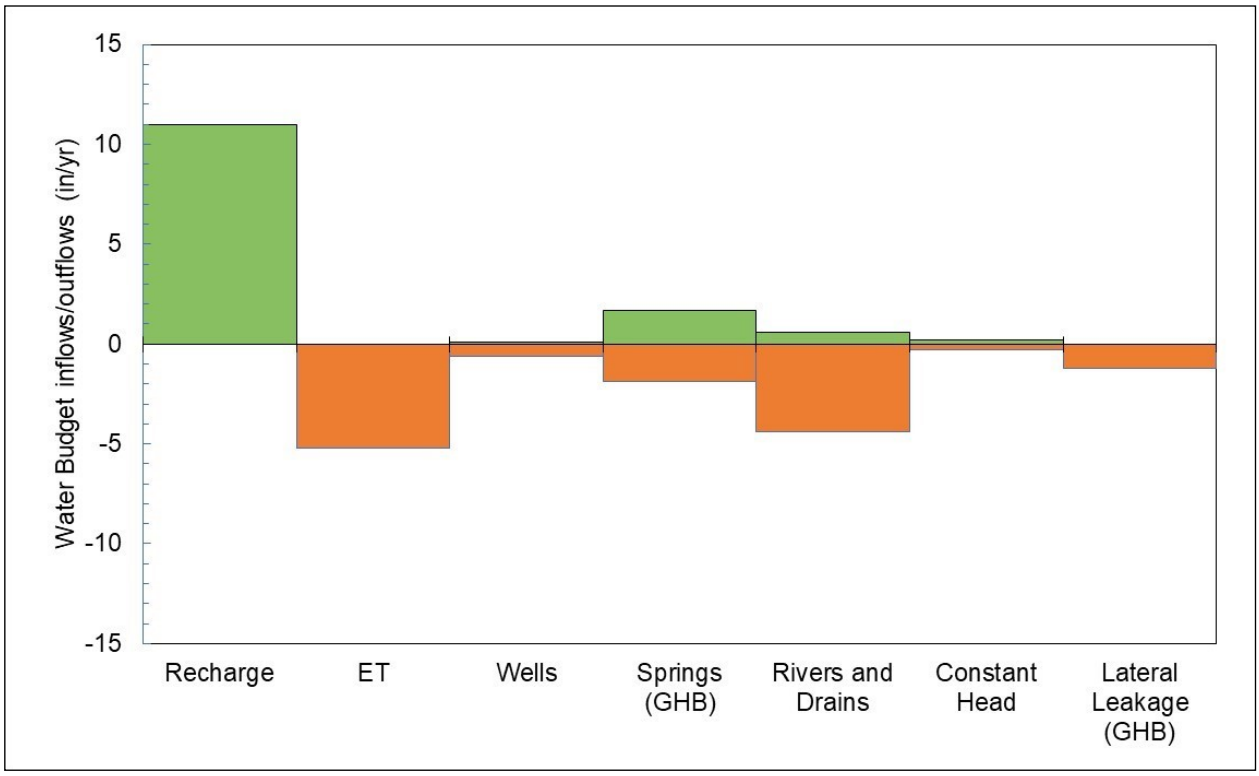

Figure 6-36. Inflows and outflows of simulated model wide mass balance for 2010

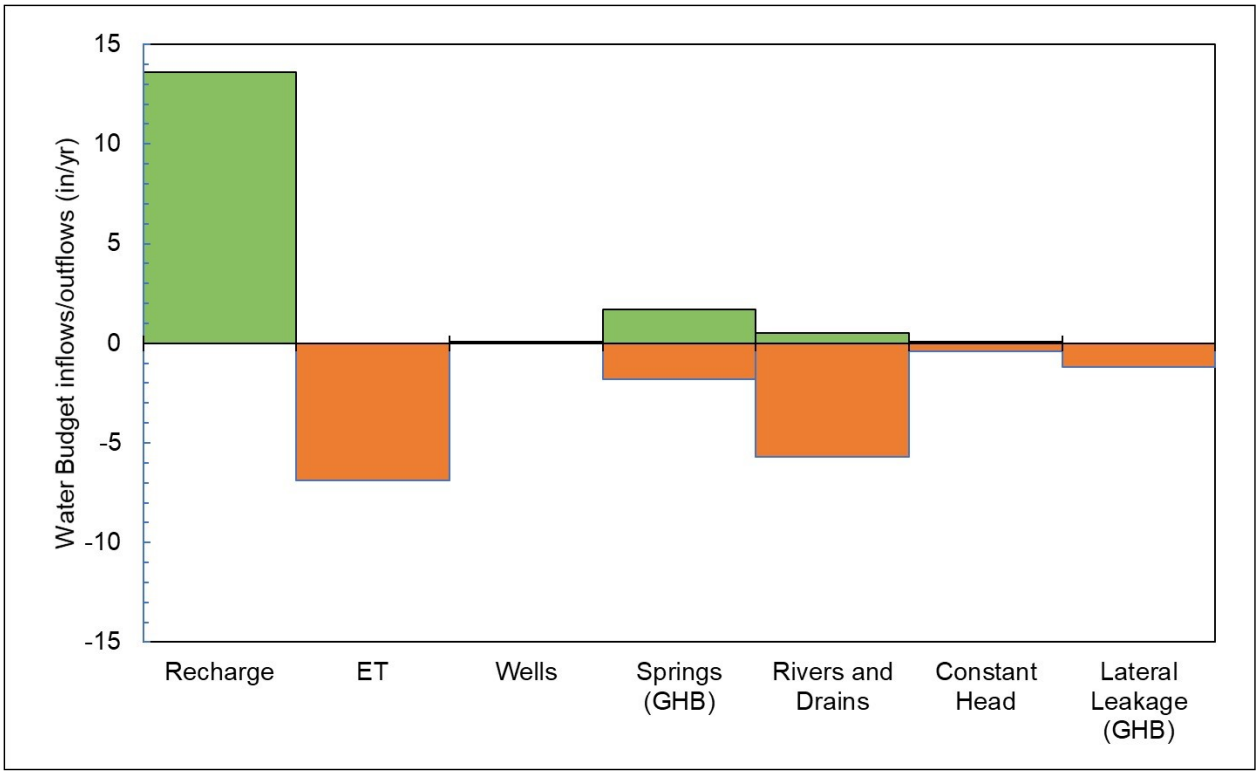

Figure 6-37. Inflows and outflows of simulated model wide mass balance for no-pumping scenario

CHAPTER 7. SENSITIVITY AND UNCERTAINTY ANALYSIS

The NFSEG v1.1 model was designed to be a tool that can be used to evaluate inter-district and inter-state groundwater pumping impacts, in addition to within-district impacts. A primary function of the model is to simulate regional effects of pumping on groundwater levels, stream and river base flows, and spring flows. To further support use of this tool, a parameter sensitivity and uncertainty assessment was conducted to help estimate the uncertainty associated with the model estimated parameters and predictions of future system scenarios. The objectives of these analyses were to evaluate the sensitivity of model parameters used to calibrate the NFSEG v1.1, provide a quantitative assessment of the overall NFSEG v1.1 calibration performance, and provide quantitative estimates of the uncertainty of key model predictions.

The Parameter ESTimation (PEST) software (Doherty, 2010a) used in the model calibration was also used to facilitate aspects of the sensitivity and uncertainty analyses. A PEST defined parameter is any variable used to determine the value of a model input variable. For example, values of horizontal hydraulic conductivity parameters are estimated by PEST at specified points called pilot points. Therefore, horizontal hydraulic conductivity values determined by PEST at two different pilot points are two different parameters even if the two pilot points are assigned to the same model layer. The actual model input values assigned to model grid cells are determined by interpolating between the pilot points. PEST also estimates parameter values without the use of pilot points. For example, there is a unique PEST conductance parameter associated with each spring which is used to directly estimate the corresponding conductance value for that spring in the MODFLOW GHB Package input file.

PEST organizes related sets of parameters into parameter groups. The NFSEG model has nearly 9,000 parameters, most of which are adjustable parameters that are estimated through model calibration. Each of these parameters are assigned to one of 23 PEST parameter groups. For example, the horizontal hydraulic conductivity pilot points in Layer 1 are assigned to the PEST parameter group, ‘k1x’. Similarly, PEST organizes related sets of observations (‘calibration targets’) into observation groups. For example, 2001 groundwater level observations for model Layer 3 are assigned to the PEST observation group ‘h2001-lay3’. This grouping of parameters and observations provided a useful framework for organizing the sensitivity analyses described below.

PARAMETER SENSITIVITY ANALYSIS

The sensitivity of model outputs to individual parameters was evaluated to better understand the importance of various model input parameters to the behavior of simulated

flows and levels. The sensitivity analysis included calculation of "traditional" parameter sensitivities as well as calculation of composite-scaled sensitivities (Hill and Tiedeman, 2007). Each of these analyses is discussed below. It should also be noted that parameter sensitivities are a key component of parameter and prediction uncertainty analysis.

Traditional Sensitivity Analysis

The traditional sensitivity analysis evaluated changes in the average and standard deviation of groundwater level, baseflow and spring flow residuals in response to changes to the parameter groups or sets of parameter groups. These changes were quantified by increasing and decreasing the calibrated parameter values for a given parameter group or set of parameter groups, running the model, and calculating new statistics for the groundwater level, baseflow and spring-flow residuals. Changes in parameter values were limited to their respective upper or lower bounds as specified in the model calibration. To implement the traditional sensitivity analysis, parameters were organized into 'traditional sensitivity analysis parameter sets' (parameter sets). In some cases, these parameter sets represented collections of PEST parameter groups, while in other cases they only contained one PEST parameter group (Table 7-1).

Table 7-1. Traditional Sensitivity Analysis Parameter Sets

Parameter Set ID	Description
kx	Horizontal hydraulic conductivity pilot points in Layers 1, 3, 5, and 7. Includes PEST parameter groups k1x, k3x, k5x, k7x.
kz	Vertical hydraulic conductivity pilot points in Layers 2, 4, and 6. Includes PEST parameter groups k2z, k4z, k6z.
k3xz	Vertical hydraulic conductivity multipliers in Layers 2, 4, and 5 where the middle confining unit of the Floridan aquifer system is assumed to be absent. Includes PEST parameter groups k2zk3z, k4zk3z, k5xk3x.
vanis	Vertical anisotropy for each Layer 1 through 7. Includes PEST parameter groups vanis1 through vanis7.
lcm	Lakebed conductance multipliers.
rcm	Riverbed conductance multipliers.
sc	Spring conductance multipliers for each spring.
rechmul	Recharge multipliers.
evtrmul	Maximum saturated evapotranspiration rate multipliers.
lkzmul	Vertical hydraulic conductivity conductance multipliers beneath lakes.
ghb	GHB source heads.

Parameter sensitivity was evaluated by plotting the standard deviation of residuals for all observation wells and total simulated baseflows and spring flows against the multiplier used for each parameter group. The multiplier range for all parameter sets, except maximum saturated evapotranspiration rate multiplier (evtrmul), varied from 0.2 to 5. To minimize issues associated with model convergence, evtrmul varied over a narrower range of 0.2 to 2. The sensitivity of groundwater levels, baseflows and spring flows to lateral boundary (GHB) water levels was also evaluated by adding 'offset values' to GHB lateral water levels over an interval of ±5 feet. In some instances, the large changes in parameter values prevented the NWT solver from achieving convergence (for example for model runs where the recharge parameter set, rechmul, was scaled with multiplier values of 0.2 and 0.5).

Results from the sensitivity analysis (Figure 7-1 to 7-6) indicated that simulated water levels were most sensitive to recharge, horizontal and vertical hydraulic conductivity, and evapotranspiration multipliers that were less than one (Figure 7-1). Simulated water levels were moderately sensitive to vertical hydraulic conductivity multipliers in Layers 2, 4 and 5 where the middle confining unit of the Floridan aquifer system was assumed to be absent, and to the anisotropy of Layers 1 through 7. Simulated water levels were relatively insensitive to lakebed conductance, riverbed conductance, spring conductance, lake conductance multipliers, evapotranspiration multiplier values greater than 1 (Figure 7-1) and to changes in GHB lateral boundary heads (Figure 7-4).

Simulated baseflows were highly sensitive to changes in recharge, horizontal hydraulic conductivity, evapotranspiration, vertical hydraulic conductivity and conductance multipliers beneath lakes when those multipliers were greater than 1.25 (Figure 7-2). Simulated baseflows were moderately sensitive to changes in vertical anisotropy, spring conductance, river conductance, and conductance multipliers beneath lakes for multiplier values less than one. Baseflows were insensitive to changes in lake conductance (Figure 7-2) and GHB lateral boundary heads (Figure 7-5).

Simulated spring flow was highly sensitive to changes in recharge, horizontal hydraulic conductivity, vertical hydraulic conductivity, and spring conductance. Note that the change in the slope of sensitivity versus multiplier curve for recharge at multiplier values between 0.2 and 0.5 is most likely caused by solver convergence issues. Simulated spring flow was moderately sensitive to changes in evapotranspiration and vertical anisotropy. Total spring flow was insensitive to changes in lakebed conductance, vertical hydraulic conductivity conductance multipliers beneath lakes (Figure 7-3), and GHB lateral boundary heads (Figure 7-6).

Composite-scaled Sensitivity Analysis

Composite-scaled sensitivities (css; Hill and Tiedeman, 2007) were calculated for each PEST parameter by summing the product of the sensitivity of each observation to a given parameter, the observation weight, and the parameter value. See equation below.

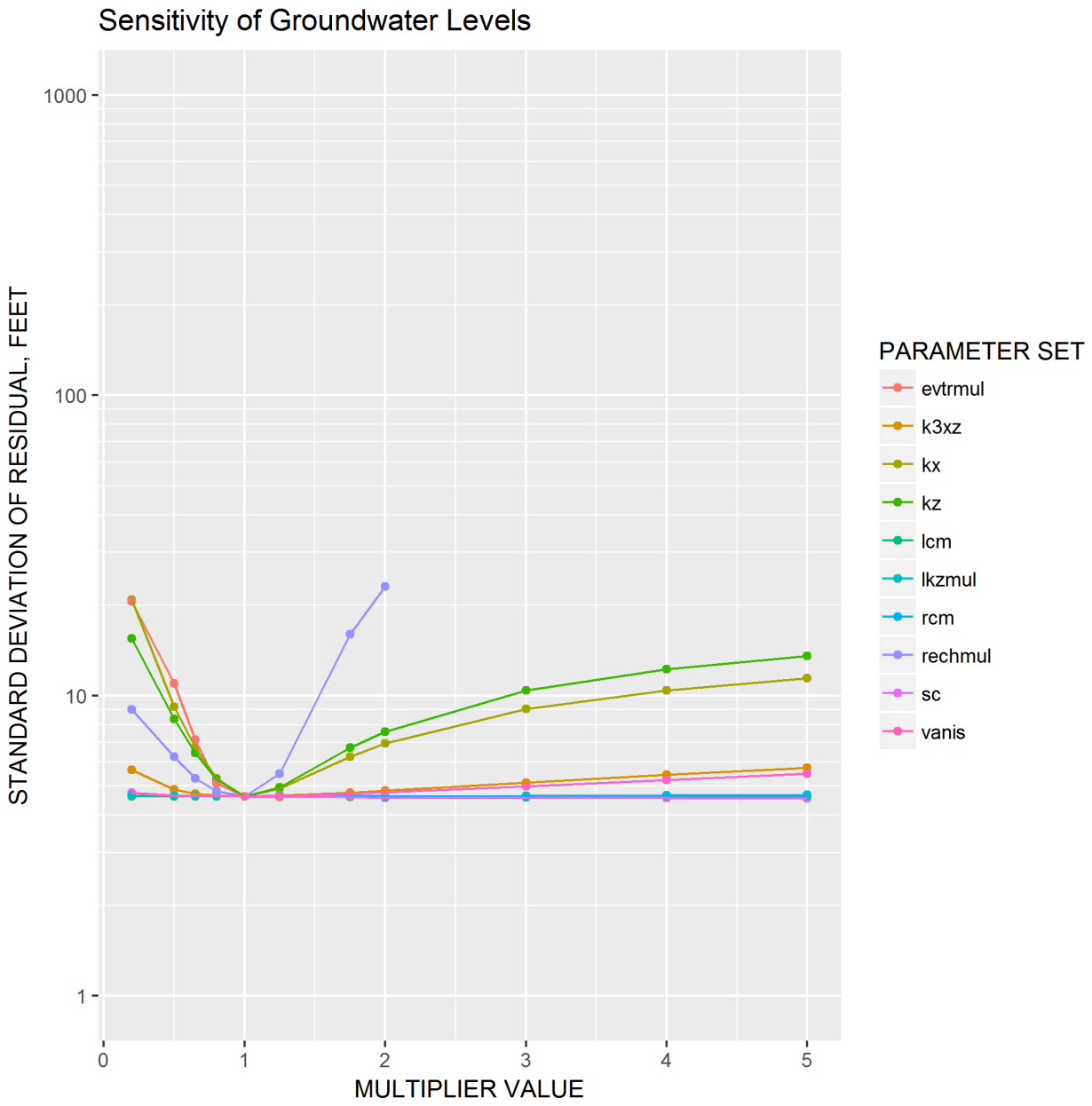

Figure 7-1. Sensitivity of simulated groundwater levels to changes in aquifer parameters and boundary conditions

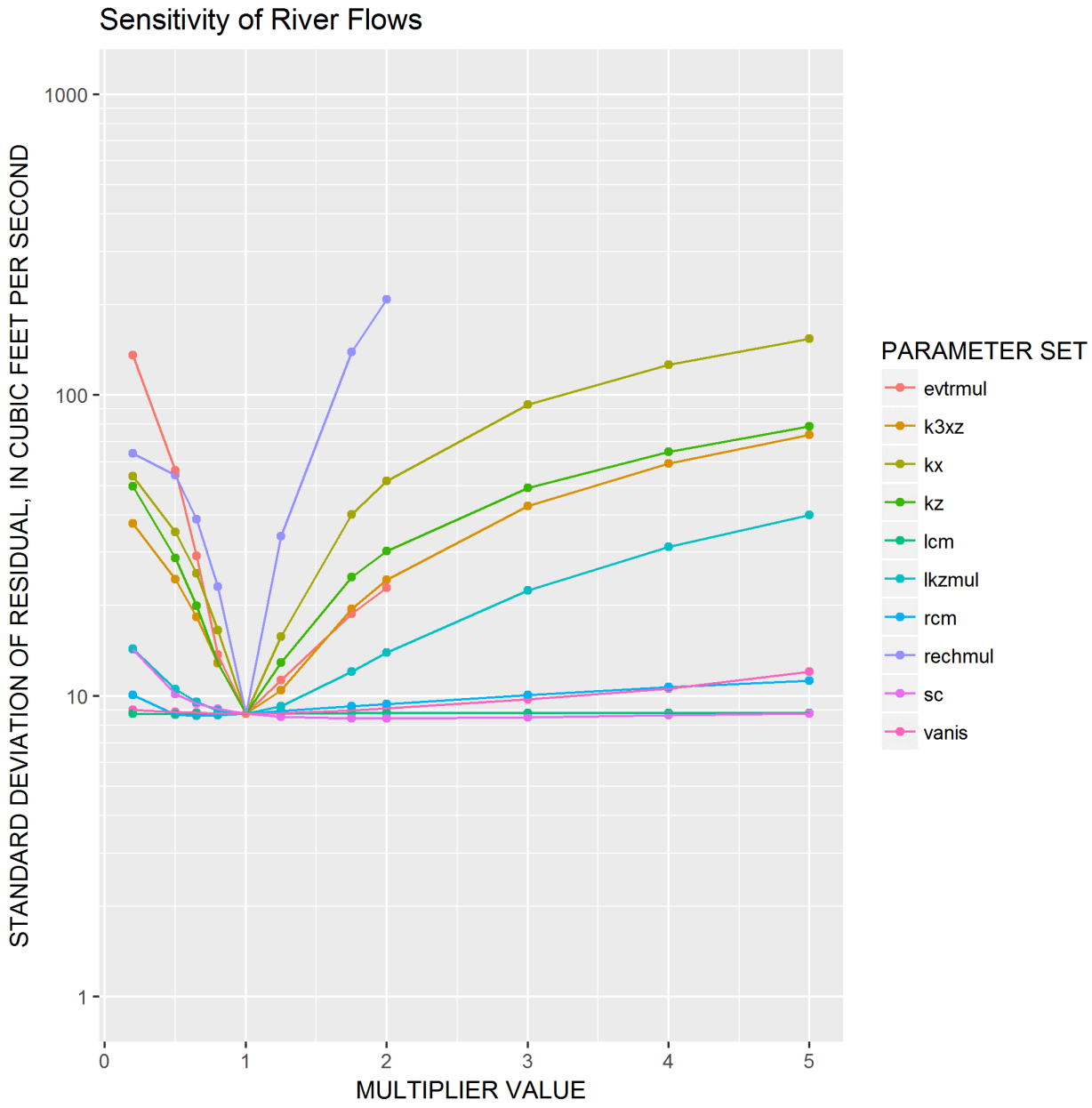

Figure 7-2. Sensitivity of simulated baseflows levels to changes in aquifer parameters and boundary conditions

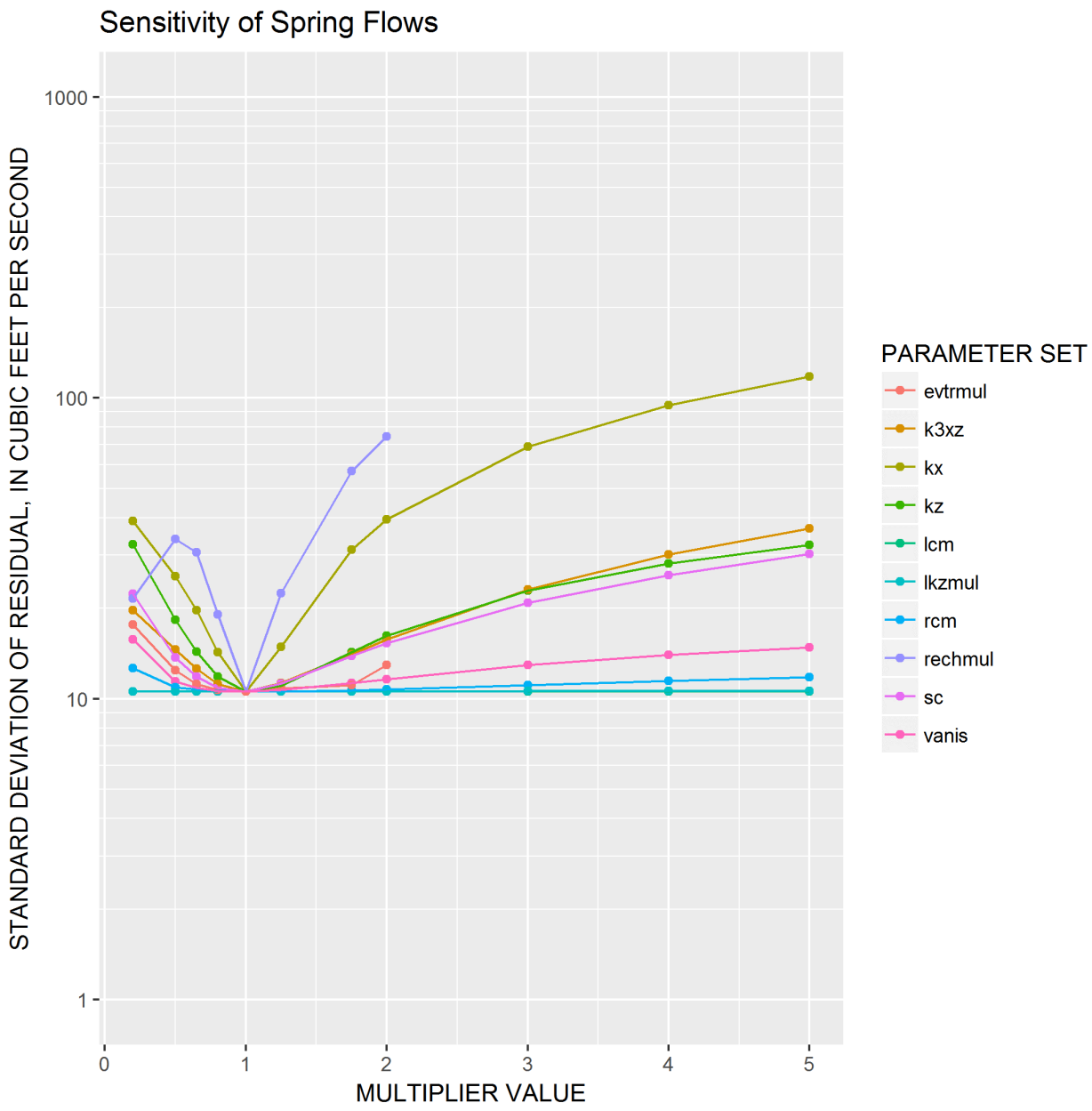

Figure 7-3. Sensitivity of simulated spring flows levels to changes in aquifer parameters and boundary conditions

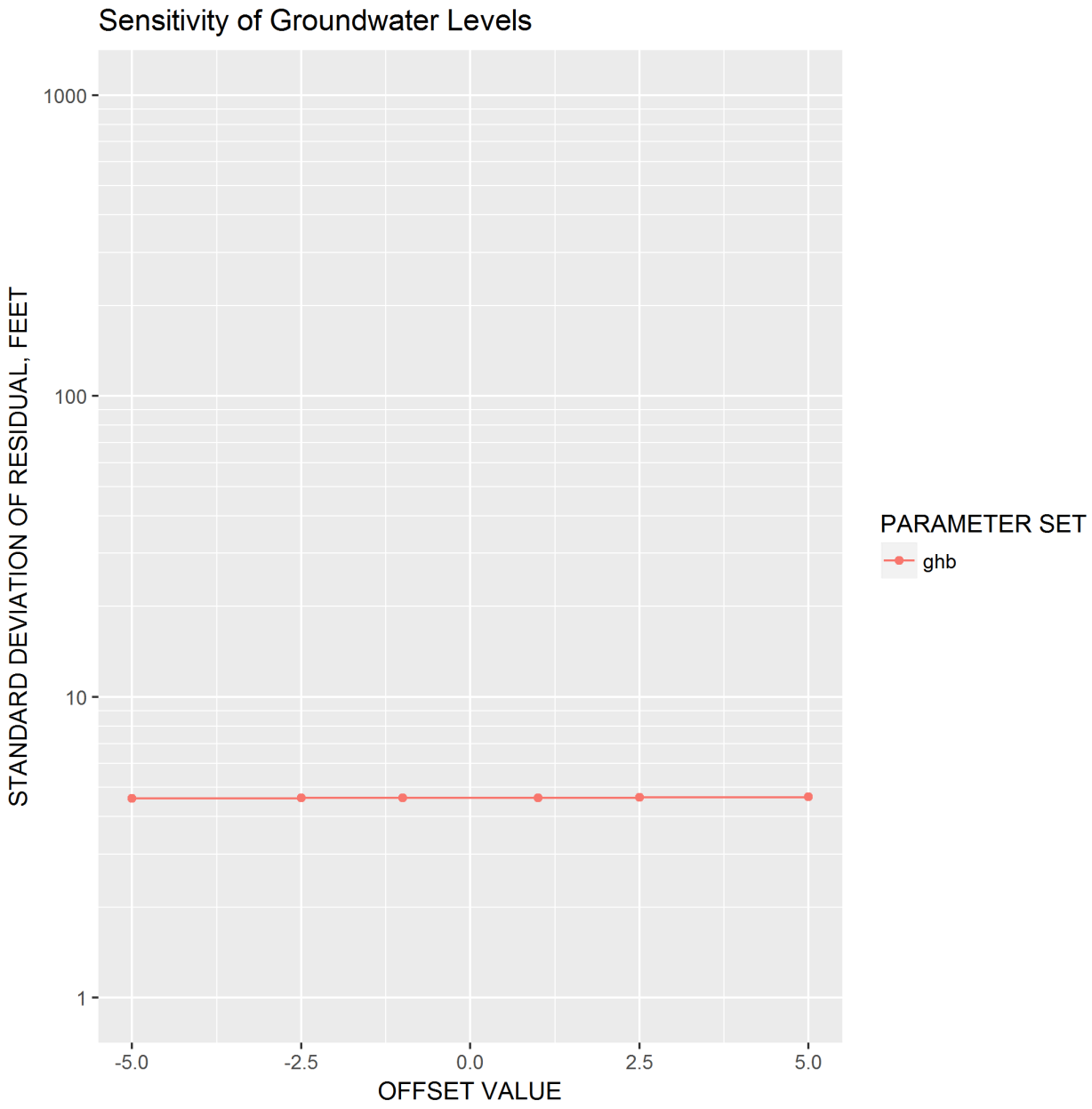

Figure 7-4. Sensitivity of simulated groundwater levels to changes in lateral boundary heads

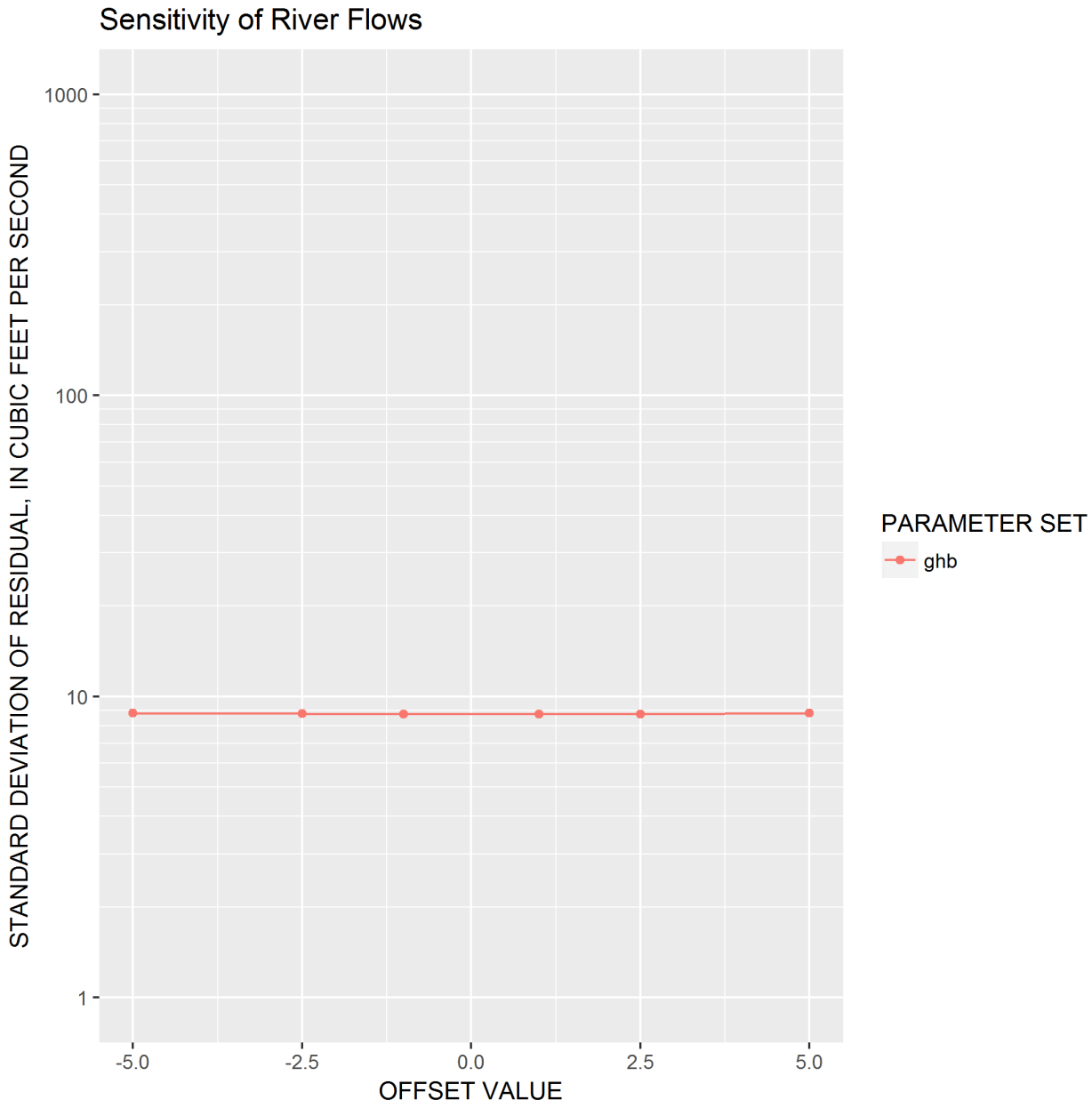

Figure 7-5. Sensitivity of simulated baseflows to changes in lateral boundary heads

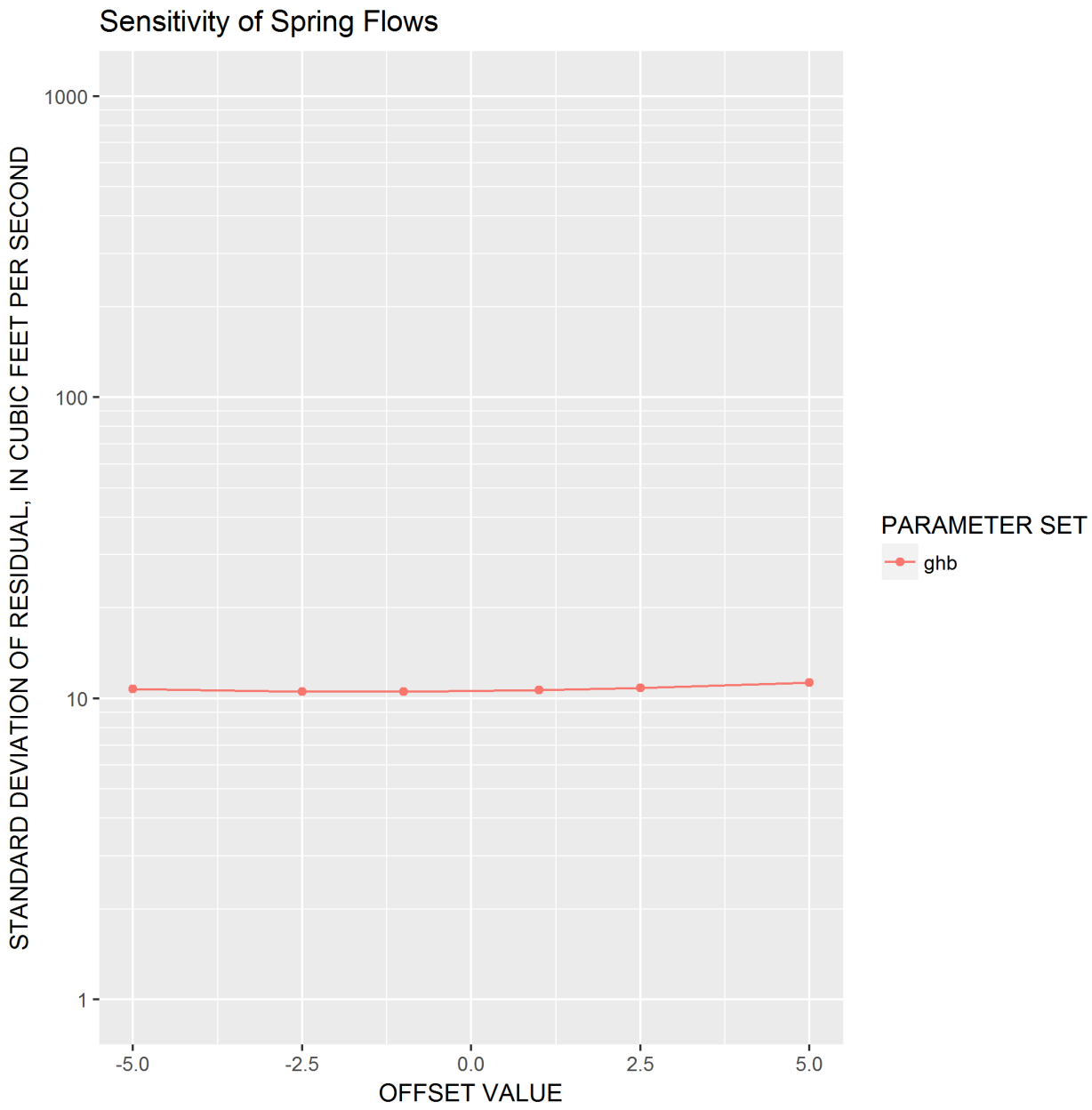

Figure 7-6. Sensitivity of simulated spring flows to changes in lateral boundary heads

$$css_i = \sum_{j=1}^{N} \left| \frac{\partial y_j}{\partial k_i} \right| k_i w_j$$

where:

css_i : composite-scaled sensitivity for PEST parameter, k_i
N : total number of observations,
$\frac{\partial y_j}{\partial k_i}$: sensitivity of observation, y_j, with respect to parameter, k_i,
and
w_j : weight assigned to observation, y_j.

Composite-scaled sensitivities may be further aggregated by summing the *css* values of all members in a PEST parameter group (Sepúlveda and others, 2012). This approach is useful when large numbers of parameters are used during model calibration and was therefore adopted for the analysis of the NFSEG v1.1 model. Thus, the composite-scaled sensitivities in this report represent an aggregate measure of the sensitivities of observations to PEST parameter groups. Parameter groups with large *css* values relative to the other parameters indicate that model simulated equivalents of observations are more sensitive to those parameters.

Parameter group *css* values are presented for four sets of observations:

- Composite scaled sensitivities for all observations combined,
- Composite scaled sensitivities for all groundwater level observations,
- Composite scaled sensitivities for spring flow observations, and
- Composite scaled sensitivities for all river baseflow observations.

The horizontal hydraulic conductivity parameter group k3x was associated with consistently high *css* values across all of sets of observations indicating the high sensitivity of both water level and flow observation types to Layer 3 horizontal hydraulic conductivity pilot point values (Figures 7-7 through 7-10). This sensitivity is reasonable, given the importance of the hydraulic conductivity of the Upper Floridan aquifer in establishing horizontal-head gradients and spatial patterns of groundwater flow within the aquifer and to river reaches, including those sustained by spring discharge. Higher *css* values for the k3x parameter group are expected because of the large number of groundwater level, baseflow, and spring flow observations in Layer 3. When groundwater level, baseflow and spring flow observations are considered together, the k3x and spring-conductance (sc) parameter groups have the highest *css* values (Figure 7-7).

When the analysis of *css* values is limited to groundwater level observations, the k3x parameter group had the largest values (Figure 7-8). The k2z parameter group was also associated with large *css* values. Larger k2z *css* values for this set of observations is consistent with the fact that vertical hydraulic conductivity of the intermediate confining unit affects groundwater levels in the surficial and Floridan aquifer system through its role in mediating recharge rates to the Floridan aquifer in confined areas.

The k3x parameter group was also associated with the largest *css* values when the analysis was restricted to baseflow observations (Figure 7-9). This association is consistent with the fact that spatial variability in the horizontal hydraulic conductivity of the Upper Floridan aquifer is one of the most critical factors affecting patterns of groundwater flow within the aquifer, including the disposition of recharge entering the aquifer. The k2z parameter group *css* values were the second largest among the various parameter groups, a result that is expected given the importance of the intermediate confining unit vertical hydraulic conductivity in determining recharge rates to the Upper Floridan aquifer in confined areas.

The sc parameter group was associated with the largest *css* values when the analysis was restricted to spring flow observations (Figure 7-10). Simulated spring discharge is directly proportional to spring conductance. The differences in spring conductance values among springs in a given area can also influence discharge rates to the springs relative to one another. Larger *css* values are consistent with an expectedly influential role of this parameter group. The *css* value of the k3x parameter group was nearly as large as that of the sc group, which again illustrates the importance of this parameter group in determining spatial patterns of groundwater flow within the Floridan aquifer system.

UNCERTAINTY ANALYSIS

A parameter and predictive uncertainty analysis was conducted to quantify the uncertainty of calibrated model parameters and simulated key model predictions. Although the sensitivity analysis was useful to assess the influence of observations and parameters on each other, additional analyses are required to estimate the uncertainties of the parameter estimates obtained from the model calibration and the model predictions made from model simulations.

The overall approach for the uncertainty analysis included a nonlinear uncertainty analysis, like that described in Sepulveda and Doherty (2015), in which a set of random, calibration-constrained parameter datasets (called realizations) were generated and used to estimate uncertainty of parameters and predictions of interest. The analysis consisted of two main components; an initial linear analysis and a nonlinear analysis for estimating the uncertainty of parameters and model predictions.

The initial linear analysis was performed to generate estimates of pre-calibration parameter and prediction uncertainty and initial estimates of post-calibration parameter and prediction uncertainty. This helped assess the improvement in the predictive capabilities and original parameter estimates. The objective of the nonlinear analysis was to estimate the uncertainty of model parameters and a set of key model predictions by

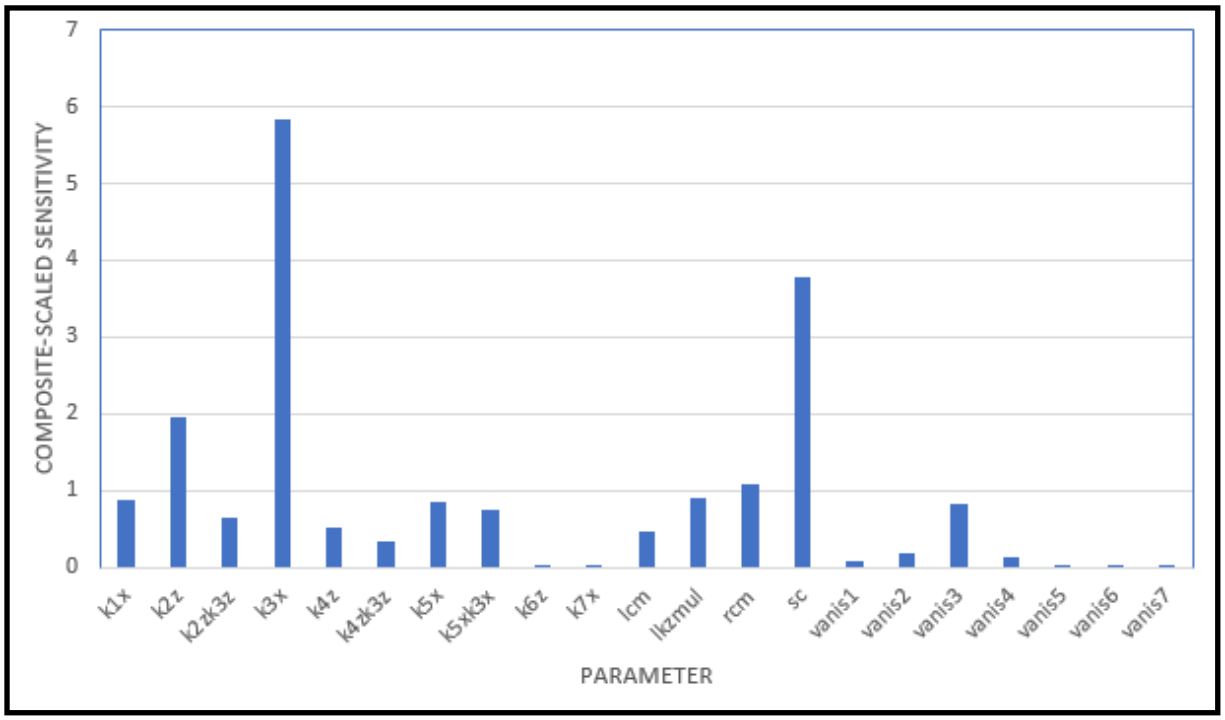

Figure 7-7. Composite-scaled sensitivities for all observations. Parameter group IDs are defined in Table 7-1.

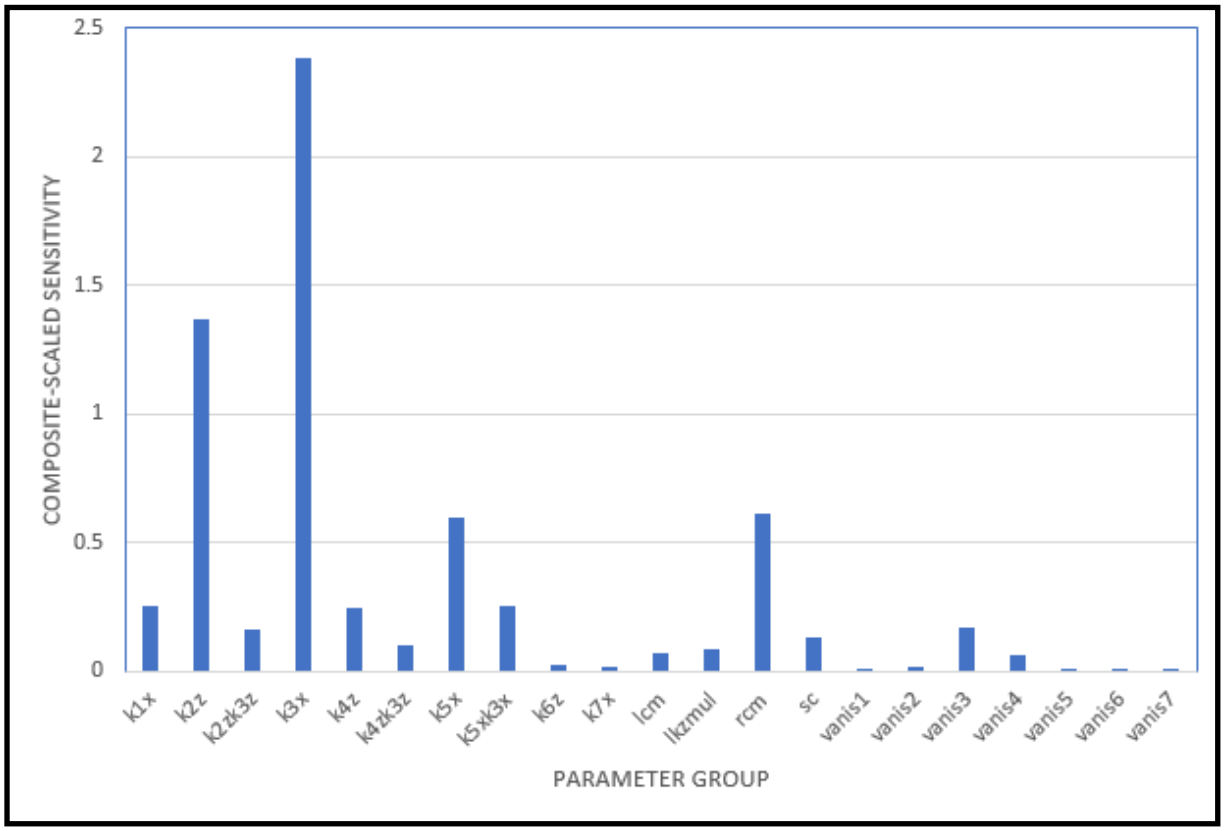

Figure 7-8. Composite-scaled sensitivities for groundwater-level observations. Parameter group IDs are defined in Table 7-1.

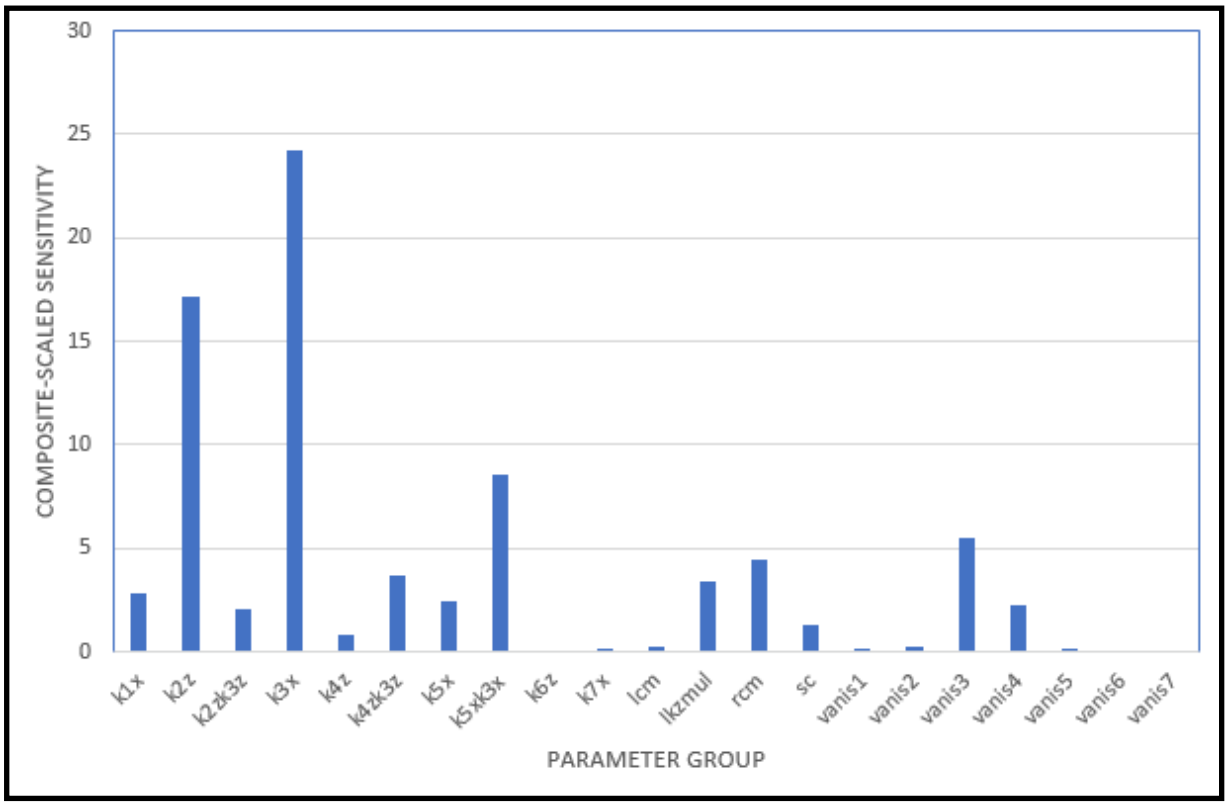

Figure 7-9. Composite-scaled sensitivities for baseflow observations. Parameter group IDs are defined in Table 7-1.

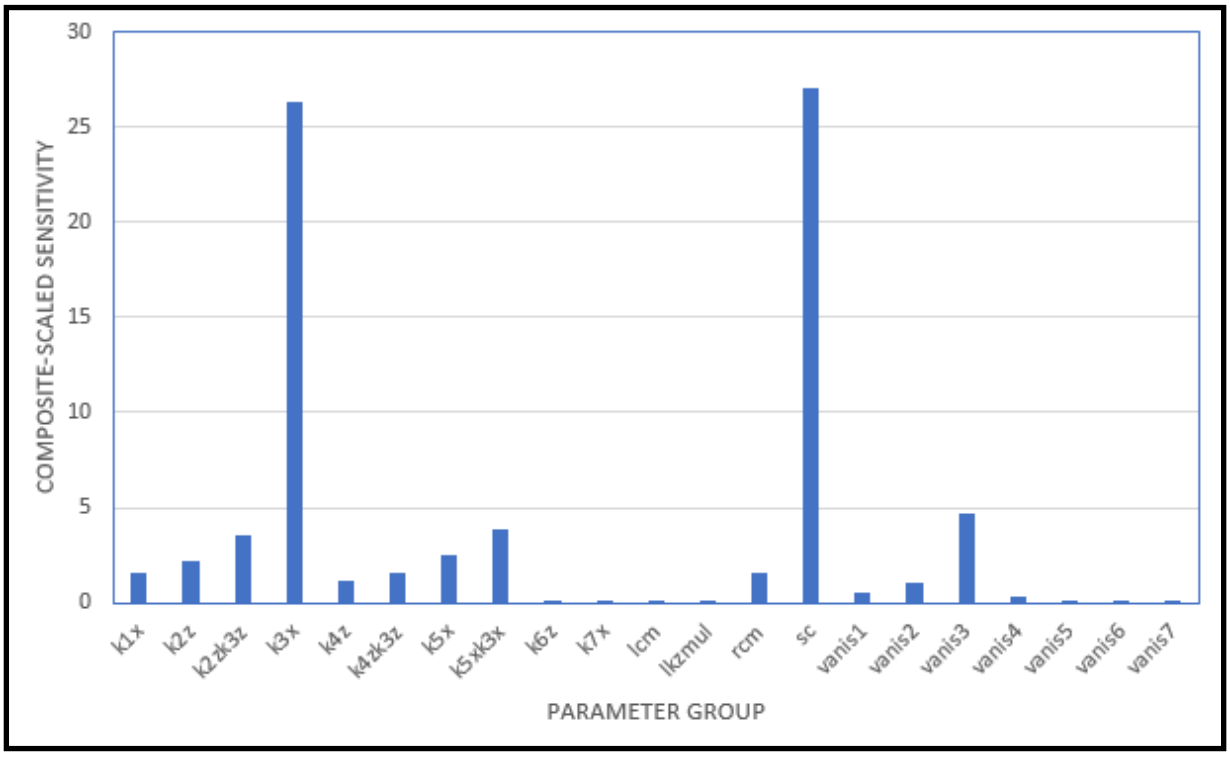

Figure 7-10. Composite-scaled sensitivities for groundwater-level observations. Parameter group IDs are defined in Table 7-1.

generating many different calibration-constrained model parameter datasets.

The analysis used an approach that does not depend exclusively on an assumption of model linearity. The analysis employed a process to generate calibration-constrained parameter sets and included: (1) random generation of parameter datasets by sampling the post-calibration parameter distribution estimated from the initial linear analysis; and (2) retaining parameter datasets that produced calibration statistics like those from calibrated parameters. The results of the uncertainty analyses subtasks are described below with additional details presented in Appendix L.

Parameter Uncertainty Analysis Results

A total of 522 reasonable sets of parameters were generated as part of the NFSEG uncertainty analysis, each of which fit the observation dataset used in the calibration almost as well as the calibrated model did. Therefore, they represent other possible versions of the NFSEG model which could be developed through model calibration. The uncertainties of model parameters were estimated by calculating the standard deviation of the parameter values from these 522 parameter sets. Parameter uncertainties can also be expressed using histograms and estimated probability distributions and with maps of standard deviations or related variables. Examples of these are presented in Appendix L, which provides a detailed description of the methods and results of the uncertainty analysis.

Although not always explicitly recognized in most modeling studies, model defects stemming from factors unrelated to measurement (target value) uncertainties are an inherent component of environmental models. These defects arise from incorrect specification of boundary conditions, insufficient numbers of parameters to represent the heterogeneity of system properties or stresses, spatial or temporal discretization or other issues (Doherty, 2015). These defects are a source of 'structural error' in the simulated system response and contribute to the uncertainty associated with parameter estimates inferred through model calibration, as well as predictions that are a function of those parameter estimates. Unfortunately, "… the nature and extent of model defects is normally unknown and cannot be quantified" (Doherty, 2015). Therefore, the magnitude and spatial (or temporal) distribution of the structural errors arising from these defects generally cannot be quantified, although their effect on model predictions is reduced for predictions of head or flow changes in response to changes in system stresses. As noted in Appendix L, the presence of structural noise is a feature of all groundwater models, including the NFSEG model, and therefore the uncertainty estimates presented in this report "… should be viewed as representing lower bounds on the uncertainties of predictions of management interest rather than their true uncertainties" (Doherty, 2015).

To facilitate comparison of parameter uncertainty across model layers and among different parameter types, coefficients of variation were used to illustrate the range of parameter uncertainty within and between parameter groups (Figure 7-11). Among the vertical anisotropy parameters (vanis), only the Layer 3 vertical anisotropy parameter was included because that is the only vertical anisotropy parameter spatially varying

within the model domain. Coefficient of variation is a measure of uncertainty and is calculated here by dividing the parameter standard deviation by the estimated mean parameter value. Model parameters with high coefficients of variation relative to the other parameters indicate the uncertainty (as a fraction of the estimated mean parameter value) is higher for that parameter. The range of coefficient of variation values for each parameter group is shown using boxplots, which summarize the 25th percentile, median, 75th percentile, as well as values occurring beyond the 25th and 75th percentiles.

When compared across model layers, as shown in Figure 7-11, the coefficient of variation boxplots indicated that uncertainty is generally similar for hydraulic conductivity values of Layers 1 through 3. The uncertainty is highest for hydraulic conductivity values for Layers 6 and 7. This is not unexpected because there were not many observations available for calibration of model parameters in these layers. The median coefficient of variation for Layer 5 hydraulic conductivity is larger than values for Layers 1 through 4, but smaller than Layers 6 and 7. The number of observations in Layer 5 available for model calibration was more than those in Layers 6 and 7 but less than those in Layers 1 and 3. The lake conductance parameter group had the highest uncertainty. Recharge and maximum saturated ET multipliers appear to be the parameters with the lowest uncertainty.

The length of the boxplot is equal to the interquartile range and longer boxplots indicate more variability in the uncertainty within the parameter group. Thus, the lkzmul parameters that were used to adjust the vertical hydraulic conductivity of Layer 2 underneath the lakes appear to have the largest variability in uncertainty.

Predictive Uncertainty Analysis Results

The objective of the nonlinear uncertainty analysis was to assess the uncertainty of predicted values of groundwater levels and flows for a hypothetical 2035 pumping scenario, as well as the predicted change in groundwater flows and levels (differences) from 2009 to 2035 at a representative set of locations (Figure 7-12). At each location, a predicted value was generated for each of the 522 sets of parameters described previously. The uncertainty of each prediction was summarized by plotting histograms and computing standard deviations from the set of predictive values generated by simulating 2035 withdrawal conditions with the 522 sets of parameters.

Figure 7-13 shows the range of predicted drawdown in the Upper Floridan aquifer level near Lake Brooklyn resulting from the simulations performed using 522 different sets of parameters. As shown in the figure, when the same 2009 and 2035 pumping conditions were simulated using 522 different sets of parameters, the predicted UFA drawdown near Lake Brooklyn due to change in pumping from 2009 to 2035 was generally between 1.7 and 1.95 feet. The uncertainty (expressed as standard deviation) for this prediction was estimated at 0.05 feet.

Figure 7-14 shows the range of predicted flow reductions from 2009 to 2035 in the Santa Fe River near Fort White resulting from the simulations performed using 522 different sets of parameters. As shown in the figure, when the same 2009 and 2035 pumping conditions were simulated using 522 different sets of parameters, the predicted flow

reduction in the Santa Fe River near Forth White due to change in pumping from 2009 to 2035 was generally between 14.5 and 17 cfs. The uncertainty (expressed as standard deviation) for this prediction was estimated at 0.77 cfs.

Appendix L includes the uncertainty estimates at all 48 selected prediction locations. The uncertainty estimates of the predicted differences (drawdown and flow reduction) are much smaller than the uncertainty estimate of absolute values of predicted groundwater levels and spring and river flows. This is consistent with the expectation that the model performs better at predicting the differences than absolute values of groundwater levels and flows. As discussed in Appendix L in detail, predictive errors potentially resulting from model approximation of the real system will tend to cancel when predictive differences are computed. It should also be noted that NFSEG v1.1 will mostly be used to predict differences rather than absolute values.

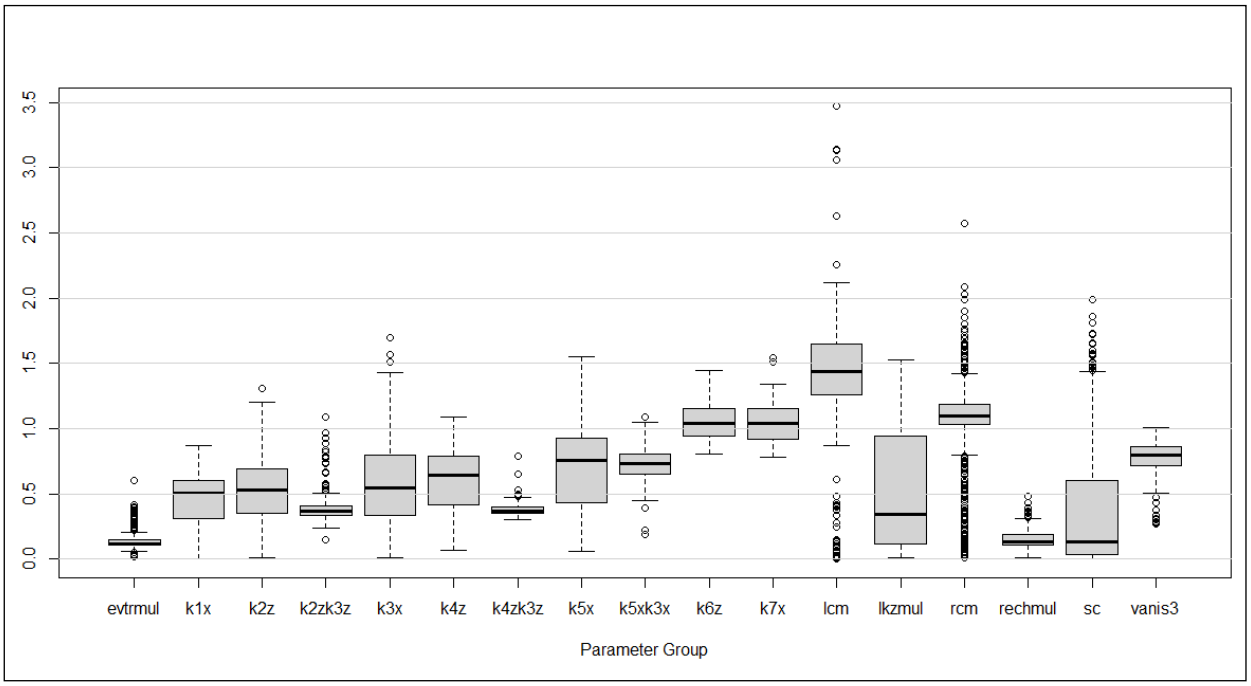

Figure 7-11. Coefficient of Variations for all parameter groups. Parameter group IDs are defined in Table 7-1.

Figure 7-12. Locations evaluated in the prediction uncertainty analysis.

*Points shown as orange are locations of simulated Upper Floridan aquifer groundwater levels. Points shown as green are springs. Black triangles represent the downstream limits of simulated river reaches.

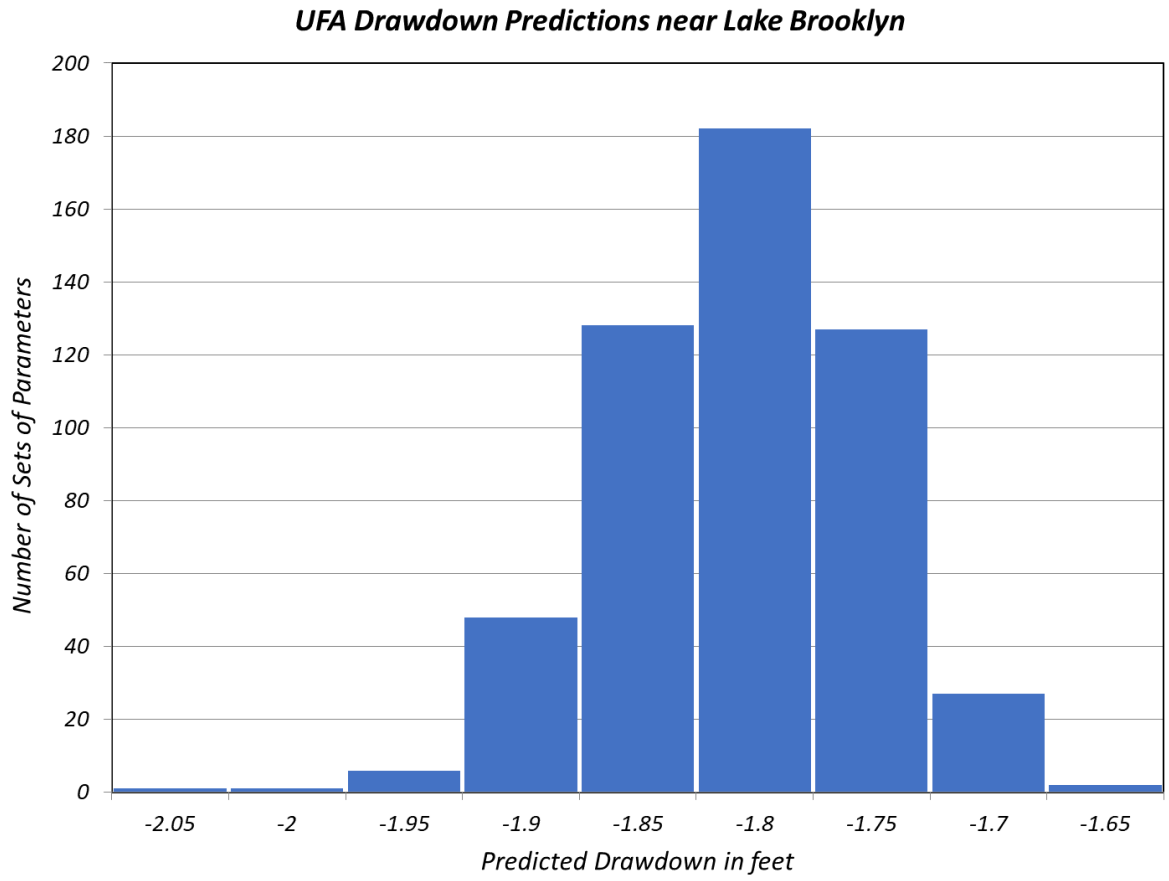

Figure 7-13. Histogram for the predicted change in flow in the Upper Floridan aquifer groundwater level near Lake Brooklyn from 2009 to the 2035 hypothetical withdrawal scenario based on 522 sets of parameters.

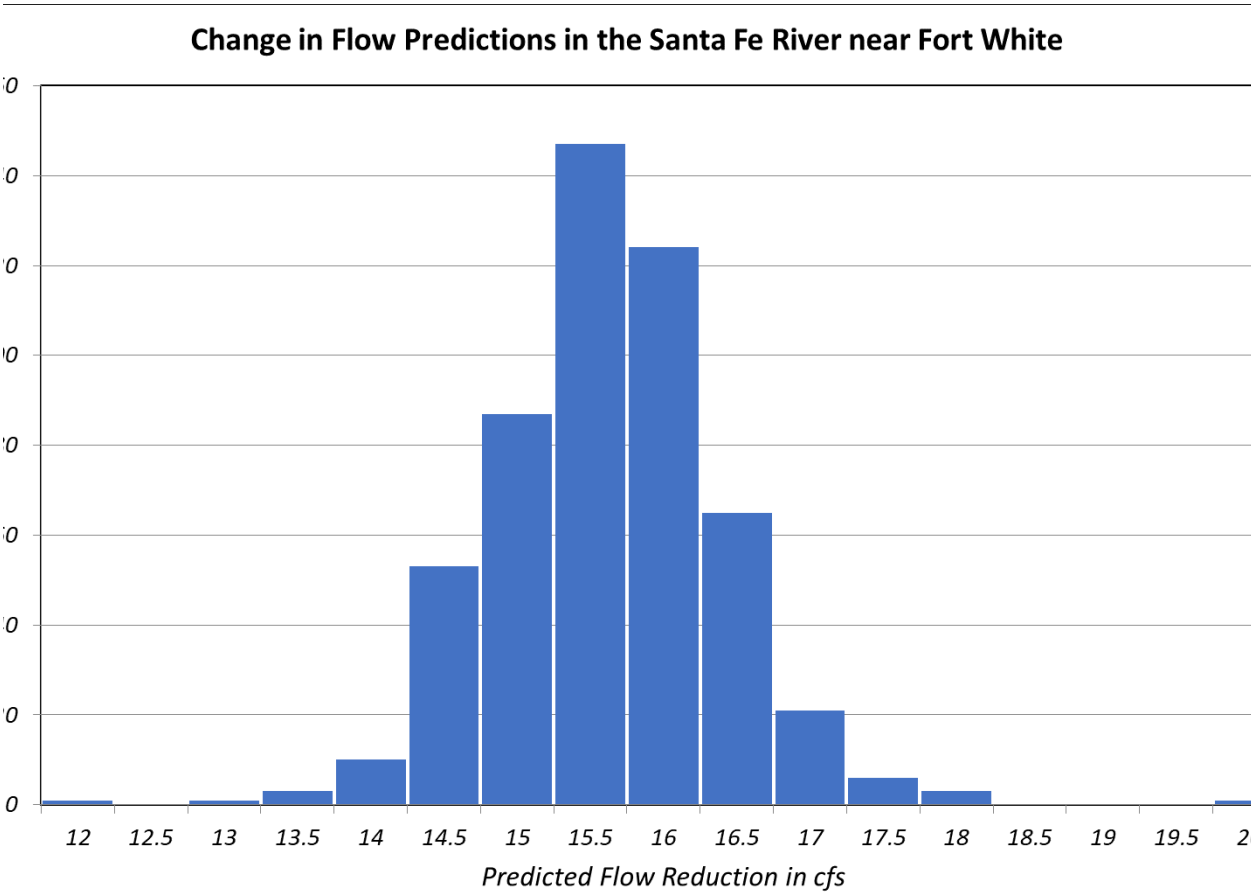

Figure 7-14. Histogram for the predicted flow reduction in the Santa Fe River near Fort White from 2009 to the 2035 hypothetical withdrawal scenario based on 522 sets of parameters

CHAPTER 8. MODEL LIMITATIONS

The NFSEG model was designed to evaluate inter- and intra-district and interstate changes in groundwater levels, spring flows, and river baseflows in the surficial and Floridan aquifer systems resulting from groundwater use within the model domain. Towards that goal, the model development included a wide variety of observation types, including groundwater levels, differences in groundwater levels between adjacent points within Zone 1 (i.e., horizontal-head differences within Layer 3), differences in groundwater levels across the intermediate confining unit and Zone 2 (i.e., vertical-head differences across Layers 2 and 4), spring flows, and river baseflows.

Limitations of the NFSEG v1.1 model are like those of other regional groundwater flow models and are typically related to approximations or simplifications that are necessary for development of large regional groundwater models. Generalizations of the groundwater hydrology system and approximations due to data availability or quality are examples of simplifications. These approximations or simplifications do not prevent the application of the NFSEG v1.1 model for its intended uses. A description of limitations that should be considered during application of the model are described below.

One limitation that is inherent to all regional groundwater models is grid-cell size. Grid-cell size limits the degree of resolution in the representation of simulated groundwater-level and drawdown distributions, as only one value is determined per grid cell. It also limits the degree to which fine-scale geometries of features like rivers can be represented, which could be a limitation if the effects of local-scale geometries of such features on the hydraulic-head head field are of interest. In such cases, finer scale resolution can be introduced through local-grid refinement approaches. This type of limitation should also be considered when simulating groundwater levels in areas with significant variability in the water table of the surficial aquifer system or potentiometric surface of the Floridan aquifer system over distances smaller than those of individual grid cells. Caution should also be exercised when using the model to simulate drawdown at scales approaching or less than a single model grid cell. Grid-cell size also limits the degree of resolution of input parameters such as horizontal hydraulic conductivity, as only one value can be assigned per grid cell. For flow simulations, these limitations should generally diminish as the size of the groundwater contributing area associated with a given water body increases.

It should be noted that the NFSEG individual grid cells are relatively small (0.224 square miles) given the 60,000 square miles area of the model domain; and their size is comparable to or better than other existing groundwater models. As stated in Chapter 3 in the section entitled “NFSEG Grid,” precedent for uniform grids comprised of grid cells with dimensions of 2,500 feet by 2,500 feet is well established within the domain

of NFSEG and in nearby areas, extending back decades. Examples of existing regional-scale groundwater models with uniform grids comprised of grid cells of 2,500 feet by 2,500 feet include the NF v2 (Intera, Inc. 2014), NEF v3 (Russo 2011), the NCF v2 (Motz and Dogan 2004), the Volusia (Williams 2006), and ECF (McGurk and Presley 2002) regional groundwater flow models. There is no regional-scale groundwater flow model that has been or is being utilized by the Districts for regulatory and/or planning applications and that shares significant domain overlap with NFSEG that does not have a uniform grid of 2,500 feet by 2,500 feet, with the possible exception of the PF v2 (Intera, Inc. 2011) model, which has a uniform grid of 5,000 feet by 5,000 feet. For this reason, the precision and accuracy of NFSEG simulation results are not impaired by grid-cell size to any greater extent than for any of the other regional-scale models with which it shares significant domain overlap. Furthermore, the much larger extent of the NFSEG active model domain greatly enhances the potential for accurate evaluation of regional-scale pumping effects relative to the other previously mentioned regional-scale models.

As in all environmental models, the parameter estimates obtained from the calibration of the NFSEG model are nonunique, and many possible combinations of alternate parameter values could achieve a similar level of fit to the target values used in the calibration. This lack of uniqueness was recognized in the formative stages of the NFSEG development effort, in which a calibration approach that employed the PEST calibration and uncertainty estimation software was chosen to allow for an exploration of many possible combination of parameter values, evaluation of areal extent of the middle confining unit, and to ultimately facilitate an analysis of the uncertainty of model parameters and predictions. The results of this analysis were described in Chapter 7 and Appendix L.

The NFSEG model simulates a single groundwater level representing a vertical average of the units that constitute the surficial aquifer system, rather than a vertical distribution of groundwater levels. Representation of the surficial aquifer system as a single layer may be an additional model limitation because this assumes that groundwater levels within the surficial aquifer system do not vary vertically. It is not common to represent the surficial aquifer system with this level of detail in regional models and the hydrogeologic information necessary for delineation of vertical differences is typically not available except at local scales. This should be considered when applying the model to evaluate more local surficial aquifer level changes.

A similar generalization is utilized in the simulation of the intermediate confining unit, which is represented in the NFSEG model as a single layer (Layer 2). A single groundwater level that represents a vertical average across the vertical extent of the intermediate confining unit is simulated rather than a vertical distribution of groundwater levels, which means local aquifers that may exist within the intermediate confining unit/aquifer system are not represented explicitly in the NFSEG groundwater model. Therefore, the NFSEG model is not intended to evaluate the effects of pumping from intermediate aquifers.

The NFSEG model represents the groundwater system as steady state, whereas in the

actual groundwater system, levels and flows fluctuate continuously with time. The assumption of steady state conditions may affect the calibration, as changes in storage are assumed to be negligible. For this reason, the calibration years, 2001 and 2009, were selected with consideration of groundwater level stability. As a result. no storage parameters were estimated through calibration. Therefore, the NFSEG model is intended to be used primarily for steady state evaluation of changes in groundwater levels, spring flows, and river baseflows in the surficial and Floridan aquifer systems. The model should not be used for transient phenomenon, such as short-term climatic events, replication of aquifer performance tests, etc.

The representation of the groundwater flow system is limited to that of the freshwater groundwater flow system in the NFSEG model. The model assumes the location of freshwater boundaries are fixed, and it is not intended to simulate variable density flow.

As noted in Kuniansky, 2016, properly conceptualized single-continuum porous-equivalent (SCPE) models are adequate for simulation of the Floridan aquifer system to address water-supply problems involving monthly or annual conditions, even in regions with well-defined conduit networks, such as in the Woodville Karst Plain/Wakulla Springs region. More complex models incorporating conduit systems are required for shorter term simulations, such as replicating spring discharge from a single storm event. Being an SCPE model, solution features such as conduits that occur near springs that discharge from the Floridan aquifer system are not explicitly represented in the NFSEG model. This may limit the use of the NFSEG model in determining travel times of solutes in karstic areas of the Floridan aquifer system. This limitation may not be as influential in confined areas of the Floridan aquifer system, where solution features may be less prevalent.

The effects of lateral boundaries may limit the accuracy of model results near lateral boundaries. In the case of no-flow lateral boundaries that do not represent physical boundaries, simulated changes in groundwater levels in response to increases in groundwater withdrawals may be overestimated near these boundaries. In the case of GHB lateral boundaries, simulated changes in groundwater levels in response to increases in groundwater withdrawals may be underestimated near these boundaries. Lateral-boundary effects occur in all groundwater models, i.e., they are not unique to NFSEG. In the case of NFSEG, great efforts were made to minimize these effects (see the discussion of lateral boundaries in Chapter 3), and the effectiveness of the utilized approaches was corroborated by the results of the NFSEG sensitivity analysis, which showed virtually no sensitivity to simulated groundwater levels, spring flows, and baseflows to lateral general-head boundary conditions (see the discussion of the sensitivity analysis of Chapter 7). Defining an area in which such limitations apply is not possible because the relative importance of lateral boundary effects depends not only on the locations of hypothetical changes in stress but on their magnitudes as well. The nature of a given proposed evaluation also plays a critical role in determining the level of acceptability of possible lateral boundary effects. Thus, considerations of lateral boundary effects must be evaluated on case-by-case basis and included in the planning process of any proposed application of any groundwater model.

CHAPTER 9. DEVELOPMENT AND CALIBRATION OF SURFACE WATER MODELS TO ESTABLISH GROUNDWATER MODEL BOUNDARY CONDITIONS

INTRODUCTION

To improve estimates of recharge and maximum saturated evapotranspiration (MSET) for groundwater model input, surface water hydrology for all the surface water basins within the groundwater model boundary were simulated using the Hydrological Simulation Program—FORTRAN (HSPF) software (Bicknell et al. 2001). HSPF is a comprehensive, rainfall runoff water quality model. Calibration of HSPF models to observed surface water flows represents a significant improvement in estimation of recharge and MSET over the previous Soil Conservation Service (SCS) curve number model and approach. The SCS model does not track evaporation and infiltration, which are important components of the surface water balance.

The model conceptualization, input datasets, calibration approach and calibration results for the 55 HSPF models used in the NFSEG v1.1 are described in this chapter.

HYDROLOGICAL SIMULATION PROGRAM – FORTRAN (HSPF)

The Hydrological Simulation Program – FORTRAN (HSPF) is a comprehensive hydrology and water quality modeling system. Currently HSPF is part of the USEPA Better Assessment Science Integrating point & Non-point Sources (BASINS) modeling environment. HSPF is highly regarded as a complete and defensible watershed model for the simulation of hydrology and water quality. The HSPF model has been applied in climatic regimes around the world. HSPF continues to undergo refinement and enhancement of its component simulation capabilities along with user support and code.

The watershed is conceptually represented in HSPF by a series of storage compartments (e.g. surface depression, soil zone, ground water zone, river segment). Based on the principal of mass conservation, HSPF performs continuous budget analysis of water quantity and quality for these storage compartments. Given the inputs of meteorological time series and the parameter values related to watershed characteristics, HSPF generates time series of runoff, stream flow, loading rates and concentrations of various in-stream water quality constituents.

While most parameters of HSPF can be specified by spatial and physical watershed data, such as land use, topography, stream characteristics, and soil property; a few parame-

ters, such as those related to infiltration, evaporation and instream kinetics, need to be determined through the calibration process. Model calibration is the process of adjusting values of model parameters to accurately reproduce the observed flow and water quality data. Once calibrated, the HSPF model is considered able to accurately represent the hydrologic and water quality processes in the watershed and can be utilized for scenario analysis.

A watershed and its stream network are characterized in HSPF by various pervious land segments (PERLND), impervious land segments (IMPLND) and reach segments (RCHRES) based on sub-watershed delineation, land uses and the ratio of perviousness and imperviousness for each land use. The pervious portion of a land use in a sub-watershed is represented as a PERLND, and the impervious portion of a land use in a sub-watershed is represented as an IMPLND. For modeling purposes, the stream network in a sub-watershed is grouped together and represented as a RCHRES. The geometric and hydraulic properties of a RCHRES are represented in HSPF by an FTABLE, which describes the relationships between stage, surface area, volume and discharge for the reach segment. Detailed description of these submodules can be found in Bicknell et al. (2001).

Major Water Budget Components of HSPF

Some understanding of how HSPF views the world is necessary to establish where MODFLOW and HSPF overlap in the overall water balance. Figure 9-2 and Figure 9-3 illustrate the water storages and flows through the HSPF system for PERLND and IMPLND. The legend for the model simulation graphics in Figure 9-2, Figure 9-3 and Figure 9-4 is provided in Figure 9-1. The simulated hydrologic processes for a PERLND include interception, infiltration, evapotranspiration, runoff and deep percolation. The simulated processes for an IMPLND are like those for a PERLND, except there are no infiltration and subsequent subsurface processes.

The RCHRES is the HSPF representation of storage and flow within the local stream reach. In the models, the RCHRES is also the source for water use that comes from surface water. A diagram of a RCHRES is presented as Figure 9-4.

HSPF and MODFLOW approach water balance and sometimes term definitions from different perspectives. Coordination between the two models and the derivation of the recharge and maximum saturated ET equations are presented in Appendix Q. Table 9-1 lists the overlapping parts of the MODFLOW and HSPF water balances and the uses within each.

Inactive Groundwater Inflow (IGWI) is defined in the HSPF environment as the saturated groundwater component of the water balance that does not contribute to baseflow. It is always a loss out of the ‘bottom’ of the HSPF water balance. IGWI in terms of a representation in MODFLOW would be analogous to recharge from the surficial to the next lower aquifer through a confining layer.

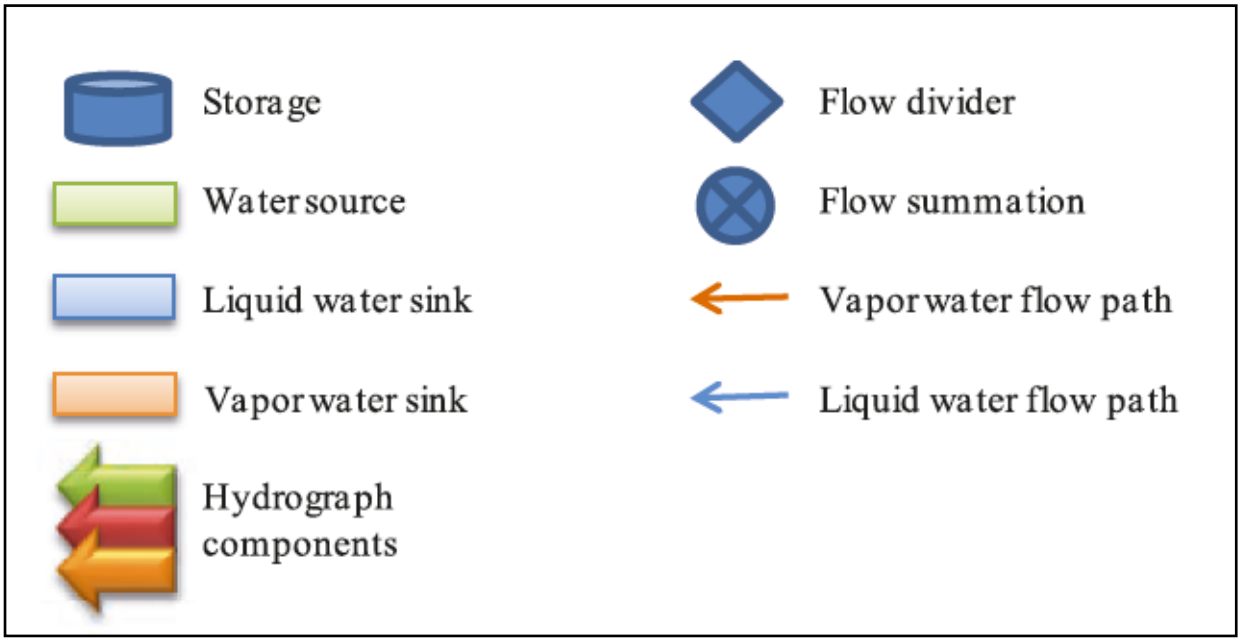

Figure 9-1. Legend for HSPF model simulation graphics in Figure 2 and Figure 3

Table 9-1. Overlapping water balance components between MODFLOW and HSPF.

MODFLOW	HSPF Variables (variable definitions are in Figure 2)	Purpose
Recharge to water table	IGWI + AGWI + SURET	MODFLOW input
Recharge from surficial to next lower confined aquifer. If MODFLOW or data indicate discharge to surficial, then IGWI should be near zero.	IGWI	Comparison/calibration
Baseflow	AGWO	Comparison/calibration
Maximum Saturated ET	Potential ET – CEPE – UZET – LZET	MODFLOW/ET package input
Saturated ET	AGWET + BASET	Comparison/calibration

INPUT DATA

The model input data are collected from various sources and reformatted to form a consistent framework for the model to use. The input data can be split into three categories; meteorology (Table 9-2), consumptive use (Table 9-3) and the input data that defines the watershed (Table 9-4).

Meteorology

The precipitation and potential evaporation time-series define the primary hydrologic drivers for HSPF. For HSPF, potential evaporation is defined as the evaporation from a shallow body of water subject to full exposure to sun and wind.

Both precipitation and the core evaporation datasets came from the National Land Data Assimilation Systems (NLDAS). The NLDAS is a quality controlled, meteorological dataset developed to be spatially and temporarily consistent across the contiguous United States (Xia, et al., 2012).

NLDAS has core project support from the NOAA Climate Program Office's Modeling, Analysis, Predictions, and Projections (MAPP) program. It is a collaboration project among the following groups:

- NOAA/NCEP's Environmental Modeling Center (EMC)
- NASA's Goddard Space Flight Center (GSFC)
- Princeton University
- University of Washington
- NOAA/NWS Office of Hydrological Development (OHD)
- NOAA/NCEP Climate Prediction Center (CPC)

The NLDAS project also includes four different hydrology models, with the precipitation data as part of the forcing dataset. Table 9-5 lists all the variables in the forcing dataset.

Table 9-2. HSPF meteorological boundary conditions

Data	Data Source
Precipitation	National Land Data Assimilation System (NLDAS)
Evaporation	National Land Data Assimilation System (NLDAS) and USGS Evapotranspiration project in Florida

Precipitation

NLDAS combines daily and hourly rain gauge data, NEXRAD Stage II, satellite estimates and model estimates of precipitation. The data is combined spatially and disaggregated or filled as needed to create a consistent dataset. There are several quality control checks throughout the process. See Table 9-6 for the datasets used and for what purpose.

Table 9-3. Water use data for HSPF

Data	Data Source
Agricultural irrigation time series	External time-series and polygon layer based on FSAID 1 and tensioned to practice using agricultural use data from SJRWMD, SRWMD, SWFWMD, NWFWMD and USGS
Agricultural surface water withdrawals	
Agricultural groundwater withdrawals	
Agricultural irrigated acreage	Irrigated acreage in Florida based on FSAID 1 for Florida and USGS outside Florida
Urban irrigation demand	SJRWMD Water Supply Planning and Georgia EPD

Table 9-4. Spatial data

Data	Data Source
Watershed and subwatershed boundaries HUC8 watershed boundaries: used to establish spatial extent of the models HUC12 subwatershed boundaries: used for establishing closed, flat, and frontal basins to improve subwatershed delineation	NHDPlus version 2
Elevation (for delineation)	1/8 arcsecond gridded dataset from the 3 Digital Elevation Program (3DEP)
Location of USGS flow observation stations (for delineation)	USGS
Land cover	National Land Cover Database, 2001

NLDAS Data Integration and Availability

NLDAS data is available through two platforms and several Internet applications:

- Platform
  - BASINS: Seamless integration into Better Assessment Science Integrating Point and Nonpoint Sources (BASINS) as a meteorological data source for development of HSPF models.
  - HydroDesktop: NLDAS is one of the datasets included in the Consortium of Universities for the Advancement of Hydrologic Science, Inc. (CUAHSI) HydroDesktop application.
- Internet
  - The "tsgettoolbox" tool available for installation within any modern, scientific Python distribution supplies command line and Python library access to NLDAS and other time-series data.
  - The main web site to download NLDAS data is: https://disc.gsfc.nasa.gov/datasets/NLDAS_FORA0125_H_V002/summary?keywords=NLDAS
  - Mirador is an earth science data search tool. It has a drastically simplified, clean interface and employs the Google mini appliance for metadata keyword searches. Other features include quick response, spatial and parameter sub-setting, data file hit estimator, Gazetteer (geographic search by feature name capability), and an interactive shopping cart. http://mirador.gsfc.nasa.gov/

Table 9-5. NLDAS parameters in forcing file "A"

NLDAS Parameter	Units	Notes
U wind component	m/s	at 10 meters height
V wind component	m/s	at 10 meters height
air temperature	K	at 2 meters height
specific humidity	kg/kg	at 2 meters height
surface pressure	Pa	
surface downward longwave radiation	W/m^2	
surface downward shortwave radiation	W/m^2	bias corrected using GOES observations
precipitation hourly total	kg/m^2 equates to mm	
precipitation fraction that is convective	unitless	NARR weather model
CAPE: Convective Available Potential Energy	J/kg	NARR weather model
potential evaporation	kg/m^2 equates to mm	NARR weather model

- Giovanni is a Web-based application developed by the GES DISC NASA that provides a simple and intuitive way to visualize, analyze and access vast amounts of Earth science remote sensing data without having to download the data. http://disc.sci.gsfc.nasa.gov/giovanni
- SSW is a Simple Subset Wizard that provides a simple interface for parameter and spatial sub-setting and format conversion.
- USGS has adopted the NLDAS datasets and made them available through the USGS Geo Data Portal (GDP). The GDP has the ability to process data in various ways for you and when finished, sends you a link to download the results. http://cida.usgs.gov/gdp/
- With the USGS Geo Data Portal you can also write a Python program using the pyGDP library to pull data directly from GDP into your Python program.

Table 9-6. List of datasets used to develop the NLDAS precipitation dataset

Dataset	Years	CONUS	Advantages	Disadvantages
CPC daily rain gauge analysis (unified) (Daly et al. 1994) (Higgins et al. 2000)	1979 - 2011	1/8th-degree PRISM adjusted analysis	less bias than radar estimates; improved station density; improved QC checks; least squares distance analysis	coarse temporal resolution; overly smooth spatial analysis scheme
CPC daily rain gauge analysis (operational) Chen et al. (2008)	2012 - present	1/8th-degree PRISM adjusted analysis	less bias than radar estimates; optimal interpolation method	coarse temporal resolution
Stage II Doppler hourly 4-km radar data	1996 - present	1st choice to temporally disaggregate	hourly, 4 km	errors in radar-based magnitude; gaps from equipment downtime and topography
CMORPH Satellite retrieved half-hourly 8-km analysis	2002 - present	2nd choice to temporally disaggregate		
CPC HPD 2x2.5-degree hourly gauge analysis	1979 - present	3rd choice to temporally disaggregate		
NARR/R-CDAS 3-hourly 32-km model simulated precipitation	1979 - present	4th choice to temporally disaggregate	Able to fill in all spatial and temporal gaps	

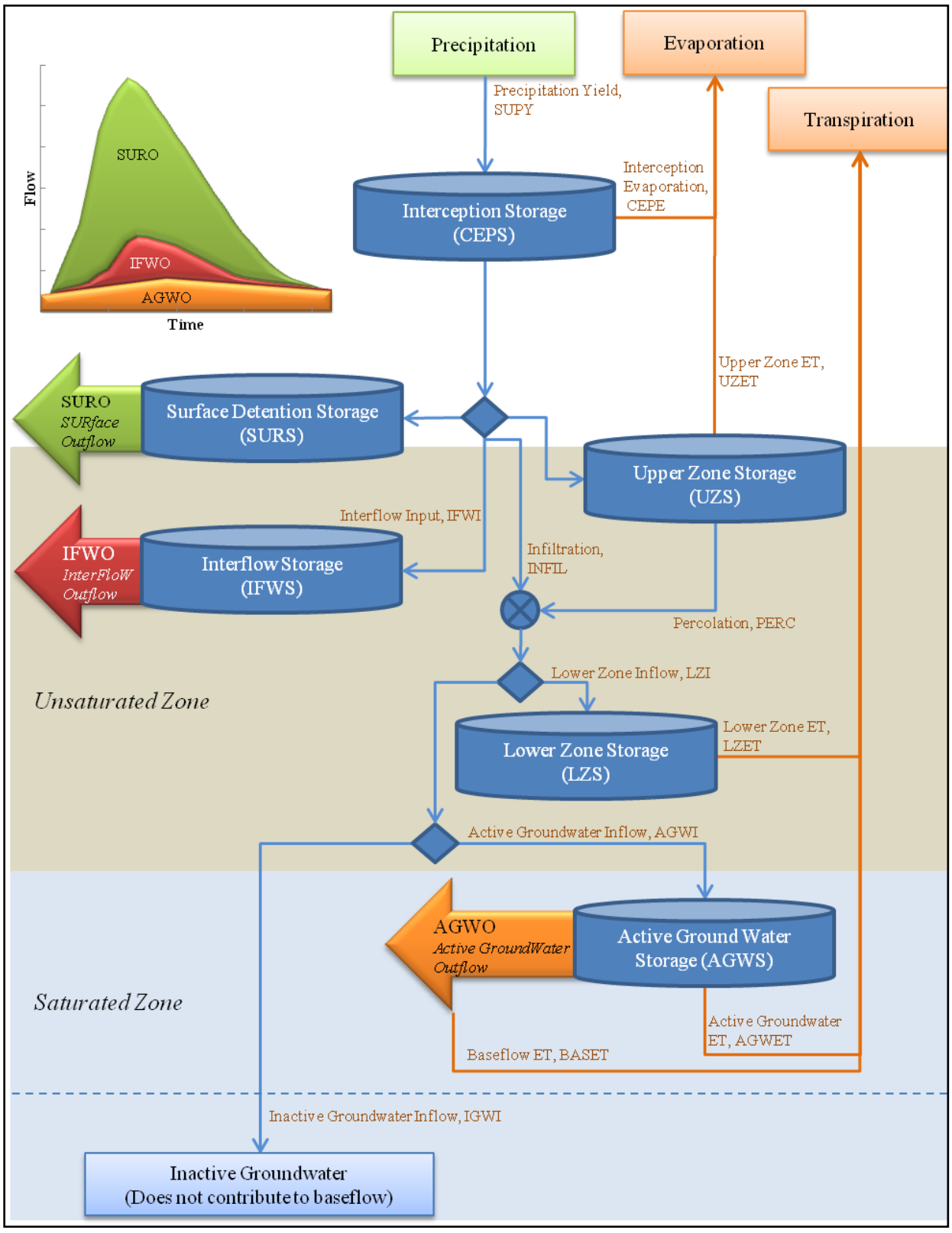

Figure 9-2. Illustration of water storage and movement in HSPF PERvious LaND (PERLND)

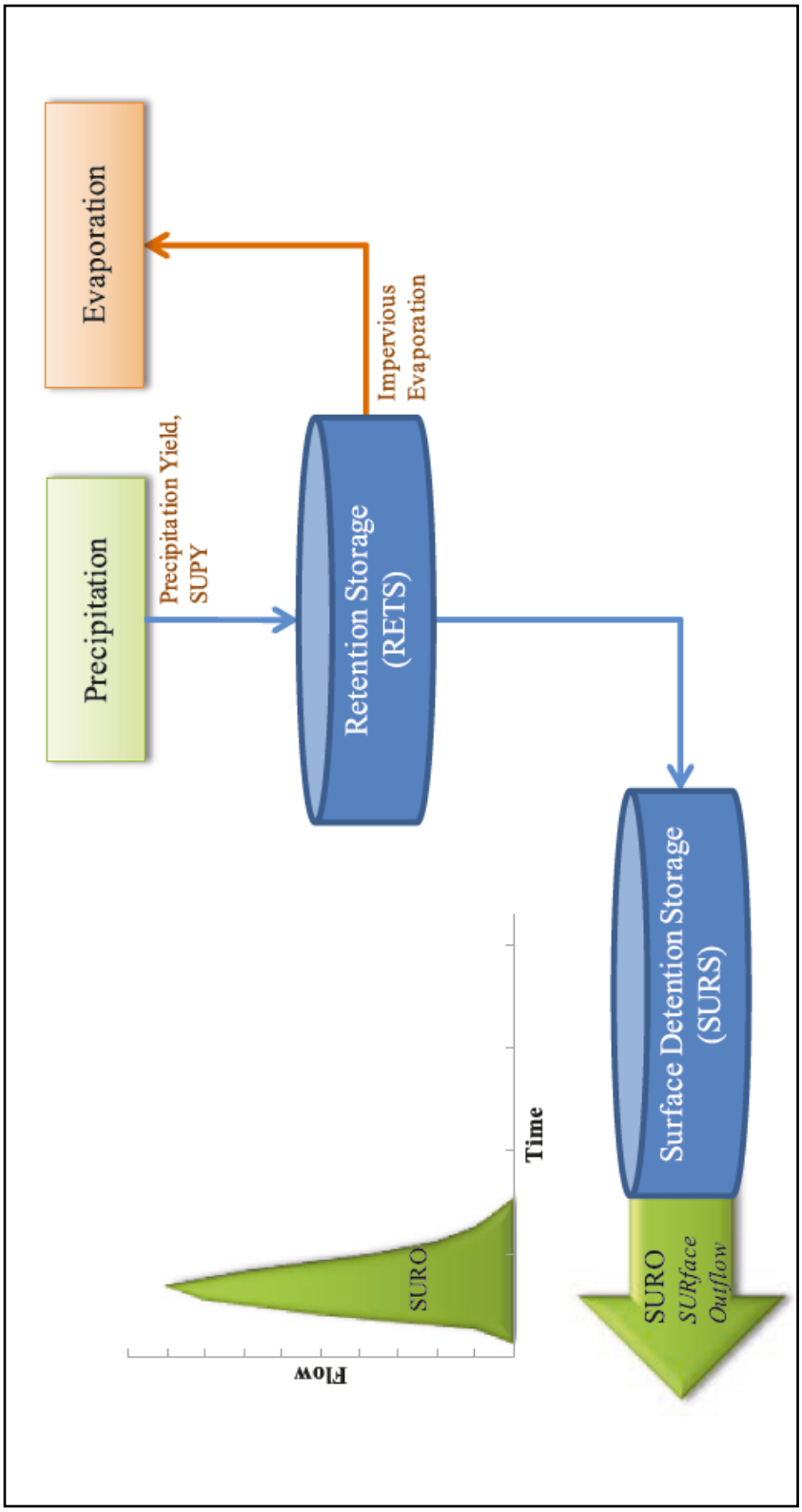

Figure 9-3. Illustration of water storage and movement in the HSPF model impervious land element (IMPLND)

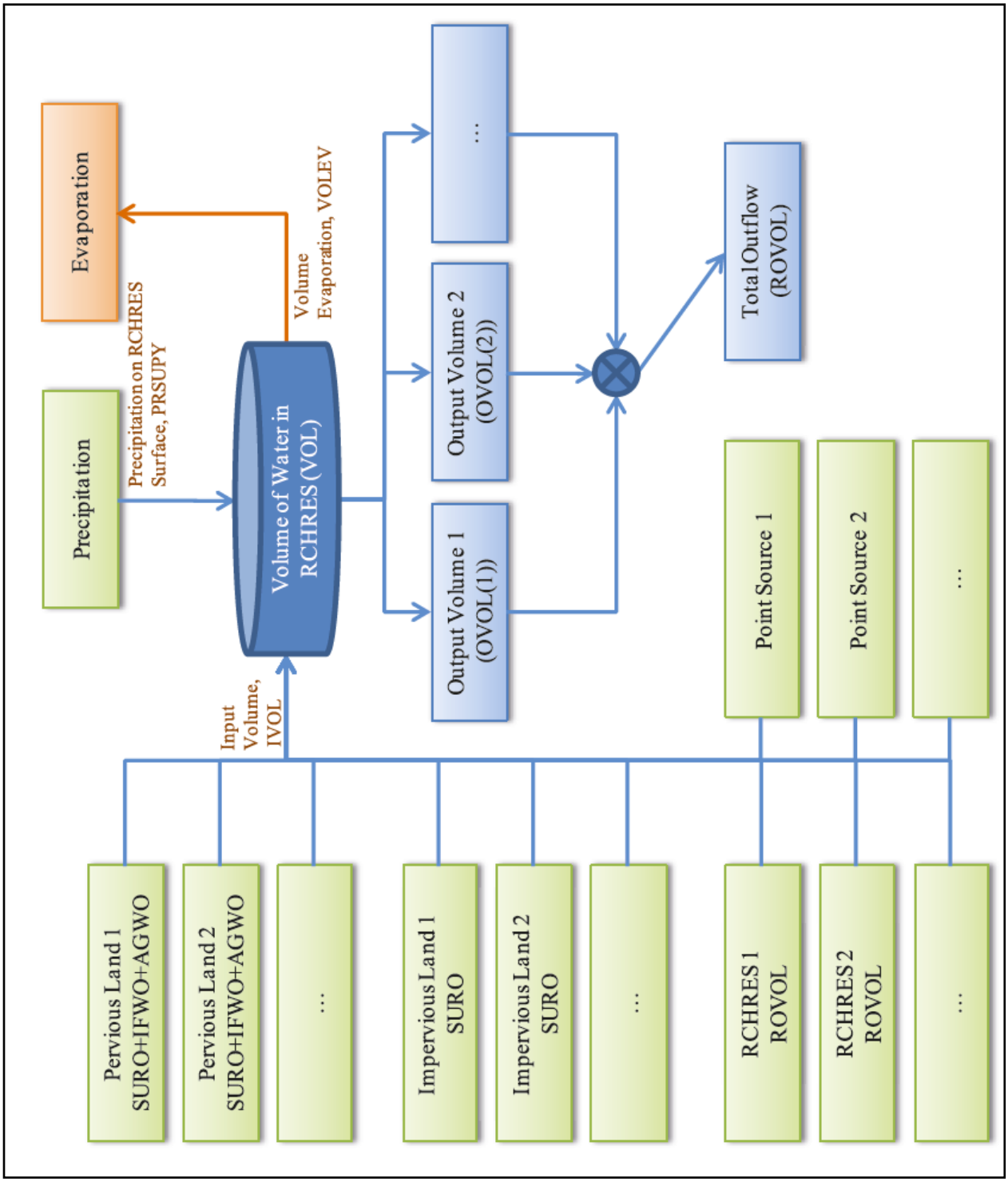

Figure 9-4. Water collection and movement in a HSPF reach/reservoir element (RCHRES)

COMPARISON AGAINST NEXRAD AND RAIN GAUGES

Raw NEXRAD rainfall estimates are very poor at capturing accurate volumes though they can represent the spatial characteristics of rainfall. Rain gauges are very good at getting good volumes but have poor spatial representation. The District NEXRAD vendors combined these datasets by adjusting the NEXRAD surface so that the average volumes calculated by NEXRAD would match the average volume from the rain gauges. Over long periods of time you would expect close agreement. Table 9-7 compares the processing and available data from the three systems.

A map of the average annual differences (NEXRAD - NLDAS) is shown in Figure 9-5. Figure 9-5 is created by first developing a NEXRAD dataset that can be compared to the NLDAS by calculating an area-weighted average of the NEXRAD grids that lie within each NLDAS grid cell. Included in Figure 9-5 is an indication of the influence of each of the main NEXRAD radar installations that cover the SJRWMD. The figure shows that most of the precipitation estimates are within plus or minus 10% (approximately plus or minus 5 inches) of each other.

NLDAS was chosen since it covered Georgia, South Carolina and Alabama, and it supplied the hourly intervals needed by HSPF. The NLDAS precipitation dataset has been very nice to work with in the calibration of the HSPF models.

Table 9-7. Comparison of available data from NLDAS, NEXRAD and rain gauges

	NLDAS	SJRWMD NEXRAD Precipitation	SJRWMD Rain Gauges
Spatial Type	Gridded	Gridded	Irregularly spaced
Spatial Aggregation	Average over grid cell	Average over grid cell	Sample from 8 inch diameter rain gauge
Spatial Domain	Continental United States	SJRWMD plus buffer[1]	SJRWMD
Spatial Interval	⅛ degree x ⅛ degree approx. 12x12 km	2x2 km	If there are approx. 100 gauges then would average 20 km between gauges
Time Domain	1979-continuing	2007-continuing[2]	Early 1970s-continuing
Time Interval	1 hour	1 hour	Time stamp for each 0.01 inch tip, typically summed to an hour

1. What is currently available to SJRWMD staff, though all of Florida is processed by the current contractor (Vieux and Associates).
2. Hourly data is no longer available before 2007 due to problems with the data.

Nigro et al. (2010) compared the performance of NLDAS, Stage IV NEXRAD (4x4 km) and rain gauges in HSPF models of the Chesapeake Bay watershed. They found significant improvements of using the NLDAS or NEXRAD precipitation compared to point rain gauges. They saw little difference in the performance between NLDAS and Stage IV NEXRAD precipitation; "There is no demonstrable advantage for using the Stage IV data over the NLDAS 1/8th degree data based on our results."

NLDAS annual precipitation is mapped in Figure 9-6, Figure 9-7 and Figure 9-8, for years 2001, 2009 and 2010, respectively.

Potential Evaporation

The NLDAS potential evaporation, instead of being a data assimilation product like precipitation (there are very few evaporation data sources available to assimilate), is taken unchanged from the North American Regional Reanalysis weather model without any corrections or modifications. After an initial evaluation of the utility, it was shown too high to be used directly. A monthly correction factor was developed by comparing the NLDAS potential evaporation to data from the USGS Florida Evaporation project (http://fl.water.usgs.gov/et/).

The monthly factors shown in Figure 9-9 represent a spatial coherence at the locations scattered throughout the SJRWMD.

From this analysis to tension the NLDAS data to the USGS data, the monthly factors in Table 9-8 were applied to the NLDAS potential evaporation data.

The annual potential evaporation, tensioned to USGS potential evaporation, for 2001, 2009 and 2010 are shown in Figure 9-10, Figure 9-11 and Figure 9-12, respectively.

WATER USE

The consumptive water use throughout the NFSEG domain is documented in detail by others that have worked on the development of the datasets. The description in this document addresses only how the dataset was included in the HSPF models.

Agricultural Irrigation

The agricultural irrigation time-series were developed as part of FSAID 1. The overall process was to run the Agricultural Field-Scale Irrigation Requirements Simulation (AFSIRS) model to establish demand based irrigation requirements and then tension those volumes to match actual practice. The AFSIRS model used the same NLDAS precipitation as the HSPF models and a reference evapotranspiration dataset derived from the other meteorological data in the NLDAS suite. The reference evapotranspiration development was performed by Intera under contract with the SJRWMD.

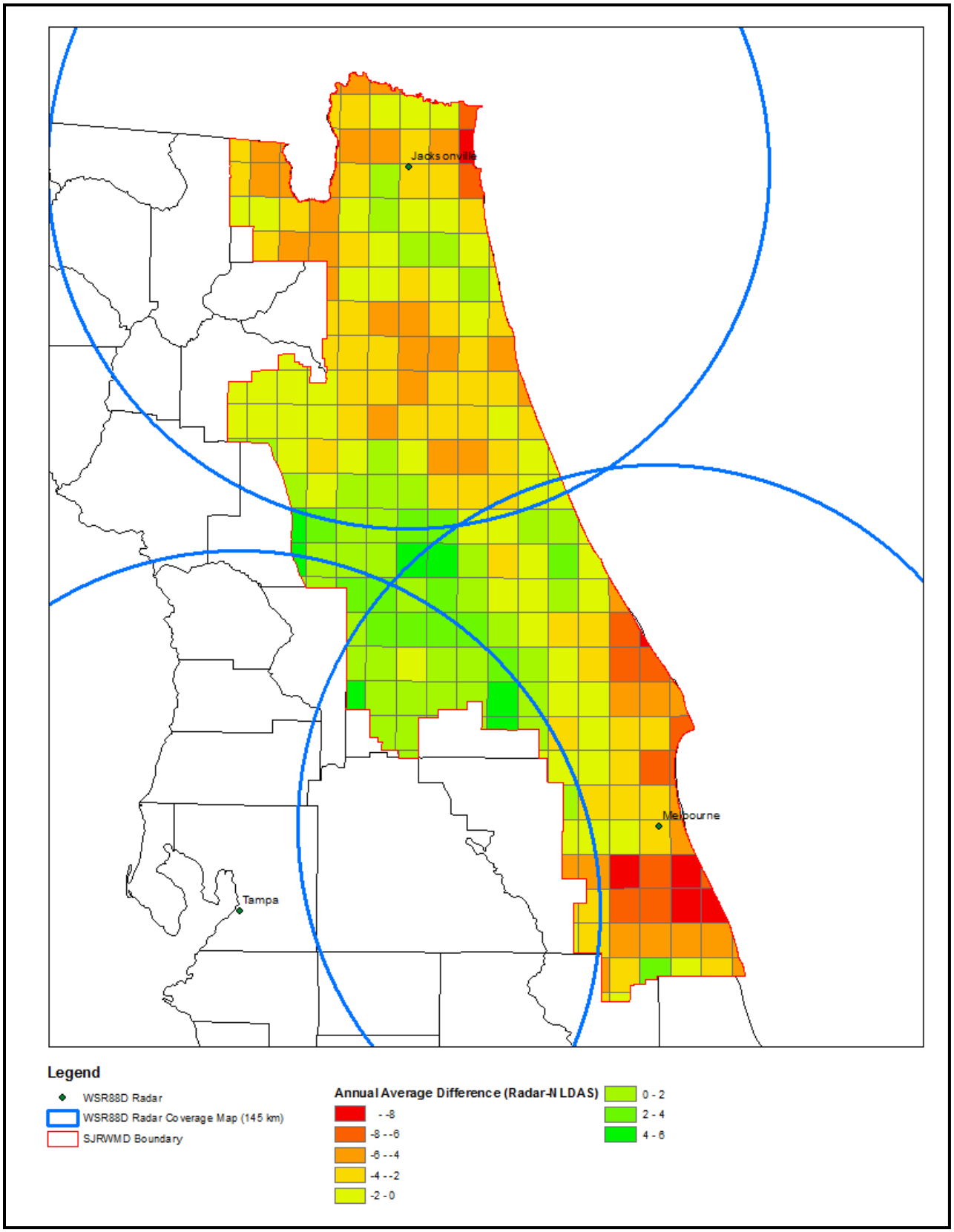

Figure 9-5. Average annual difference between NEXRAD and NLDAS precipitation

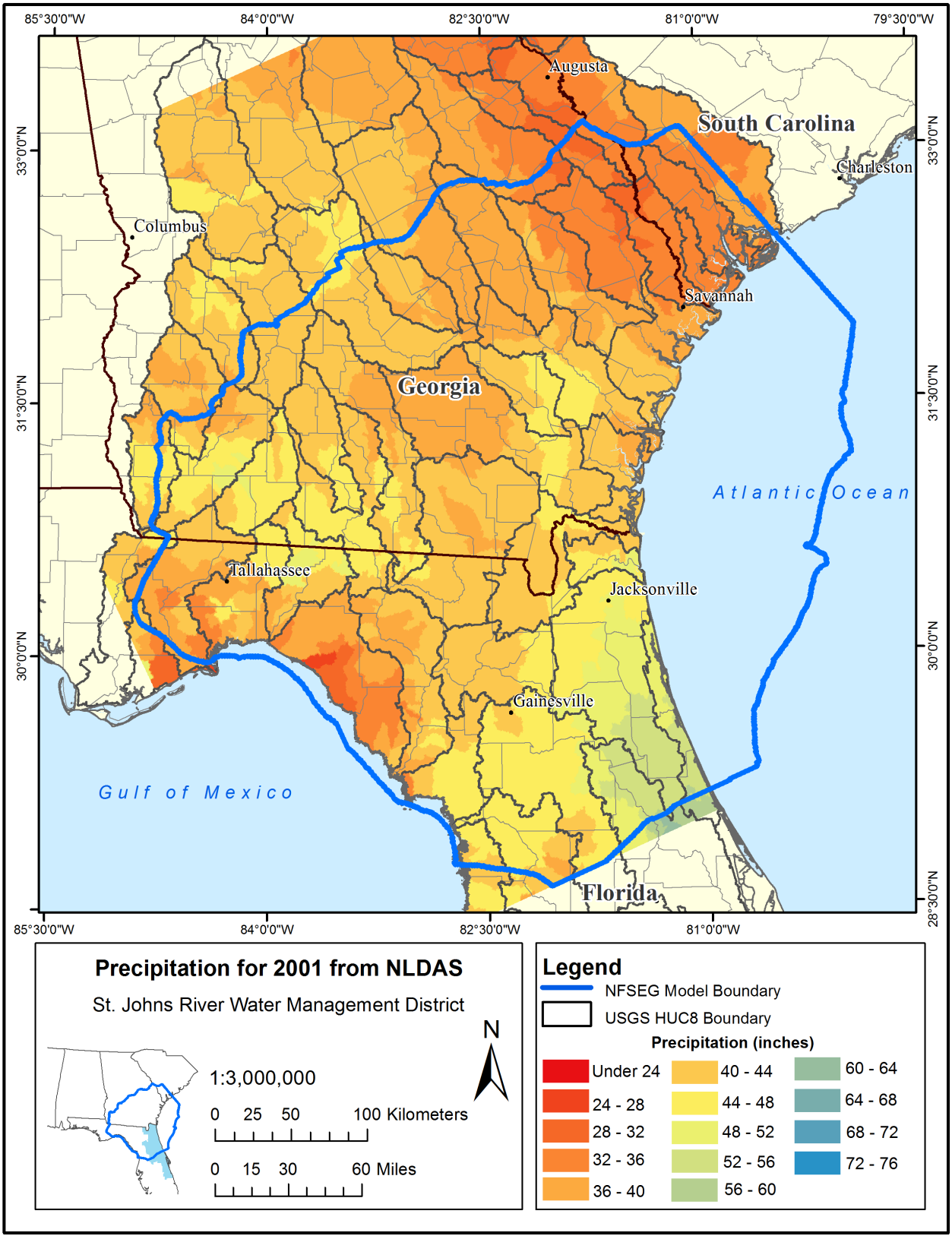

Figure 9-6. NLDAS annual precipitation for 2001 in inches

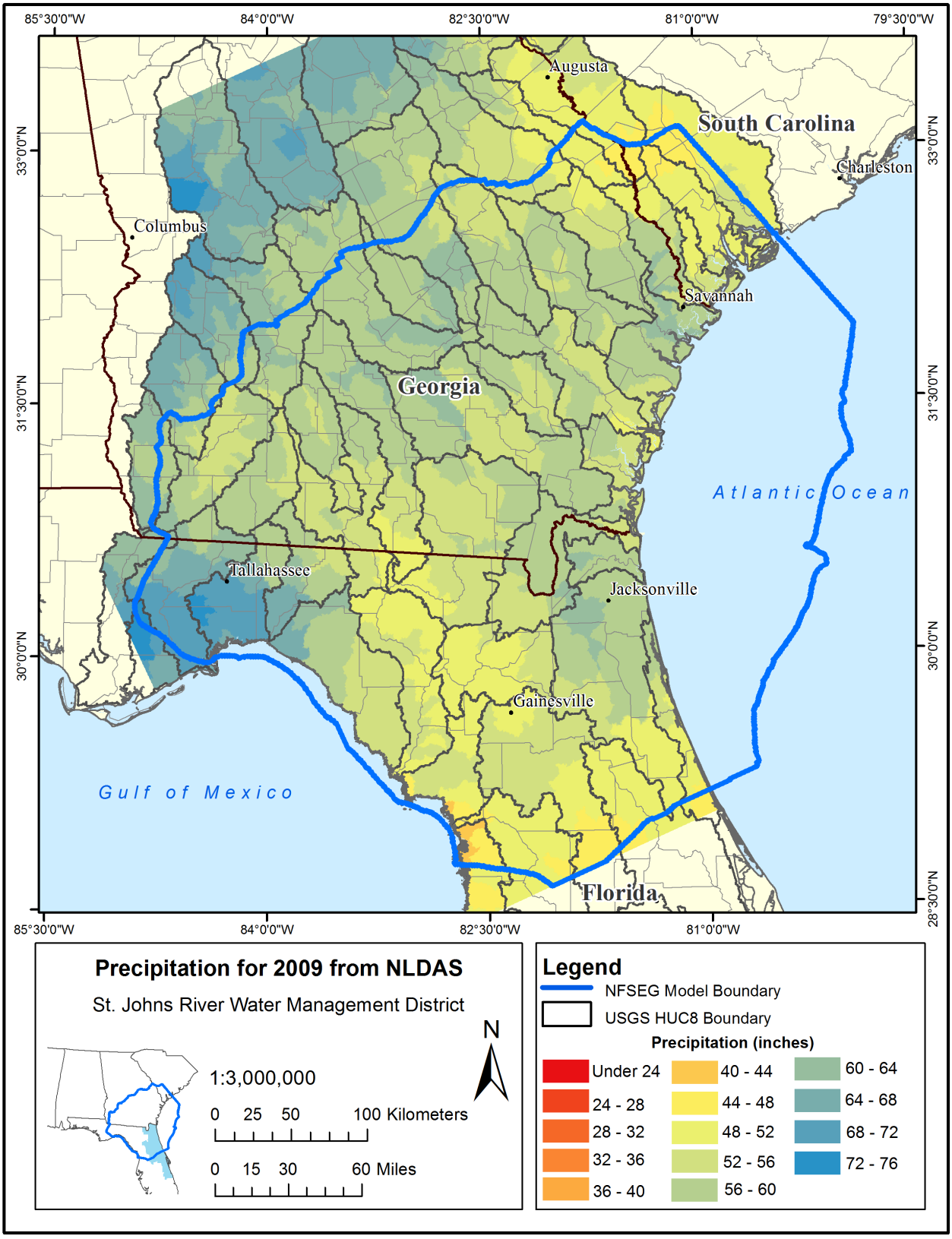

Figure 9-7. NLDAS annual precipitation for 2009 in inches

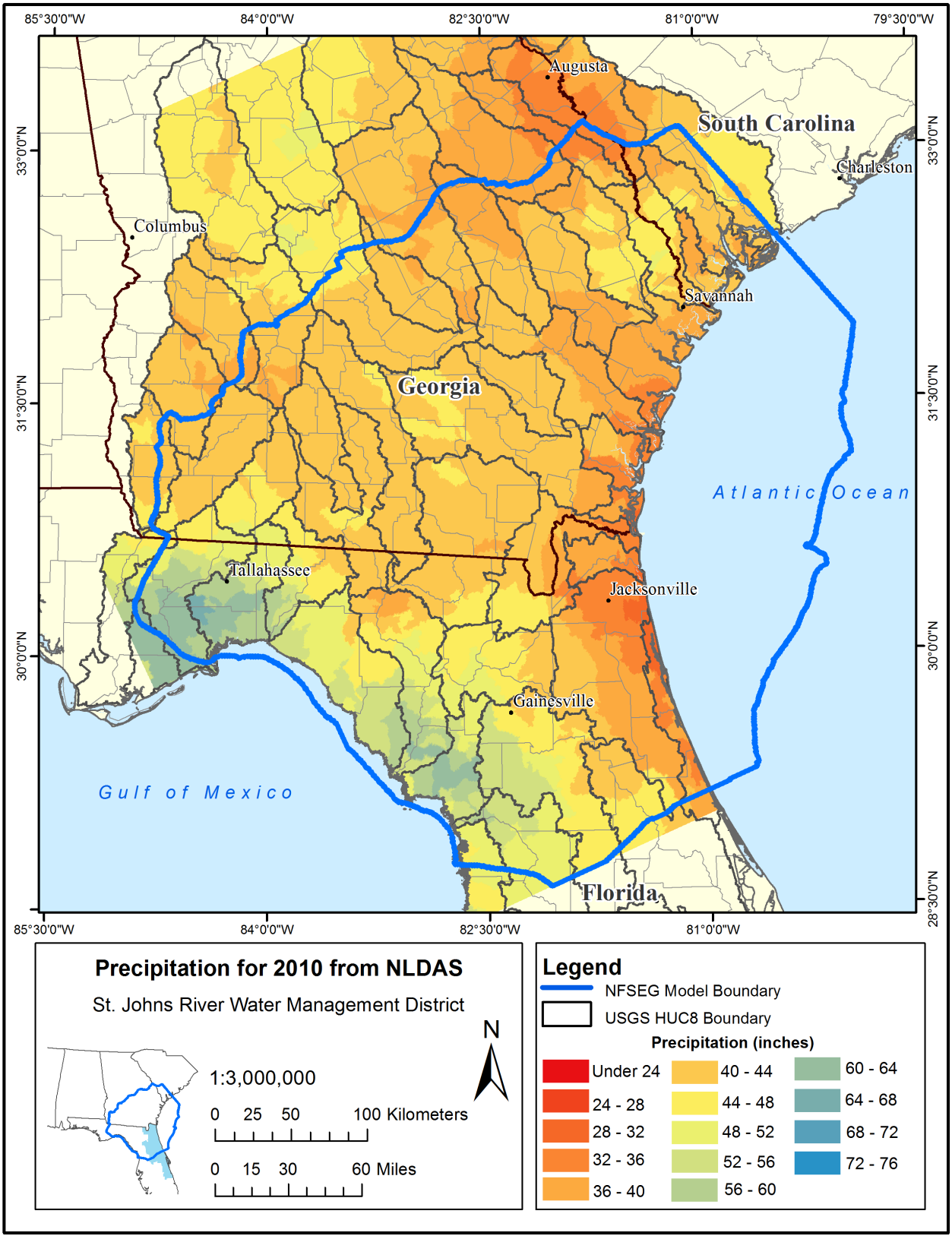

Figure 9-8. NLDAS annual precipitation for 2010 in inches

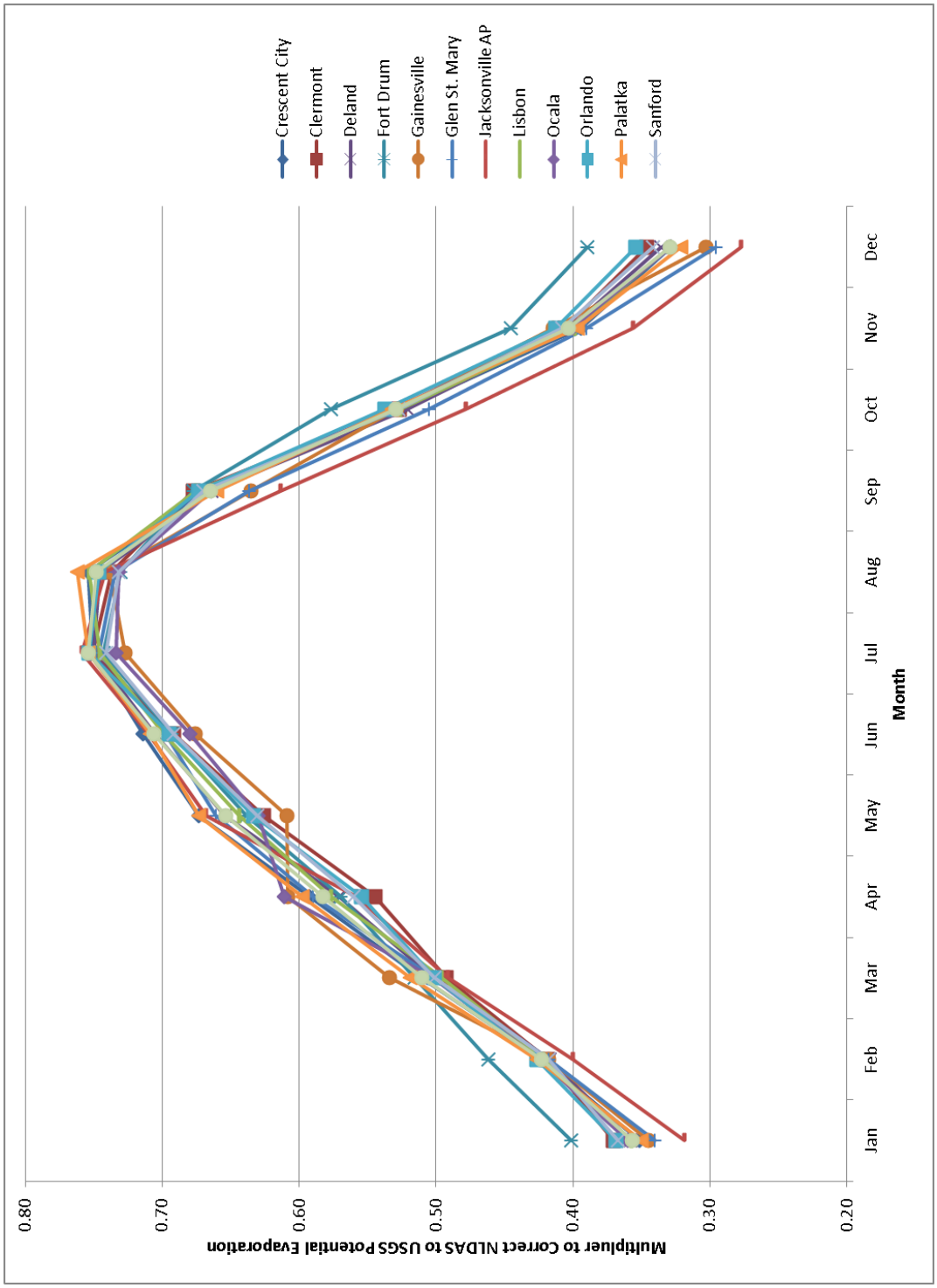

Figure 9-9. Comparison of NLDAS potential evaporation to USGS potential evaporation at several locations

Irrigation in HSPF can be included in two ways, imposed as an external time-series (analogous to adding additional precipitation), or using a crop demand algorithm based on the AFSIRS model. The irrigation demand time-series was established by the SJRWMD Water Supply Planning group based on a separate run of AFSIRS, then tensioned to practice. Since the tensioning to practice could not be done easily within HSPF, a time-series of irrigation per polygon was developed that is imposed as an external source into HSPF.

Which dataset was used for tensioning to practice was based on availability of data. For SJRWMD and SWFWMD, actual metered data was used. For SRWMD, Georgia, Alabama and South Carolina the USGS county wide estimates were used.

The daily time-series was disaggregated to hourly and applied between the hours of 6 and 10 in the morning.

The irrigation types used to put the water into the correct part of the HSPF water balance are shown in Table 9-9.

Two time-series were developed for each irrigated polygon, one for irrigation supplied by groundwater and the other for irrigation supplied by surface water. The time-series that represented the irrigation supplied by surface water was also used to take the same amount of water from the local reach.

Additional detail about the development of the tensioned FSAID 1 project is provided in the documentation of the water use component of the NFSEG project.

Table 9-8. Monthly tensioning factors for NLDAS potential evaporation

Month	Factor
January	0.36
February	0.42
March	0.51
April	0.58
May	0.65
June	0.71
July	0.75
August	0.75
September	0.66
October	0.53
November	0.40
December	0.33

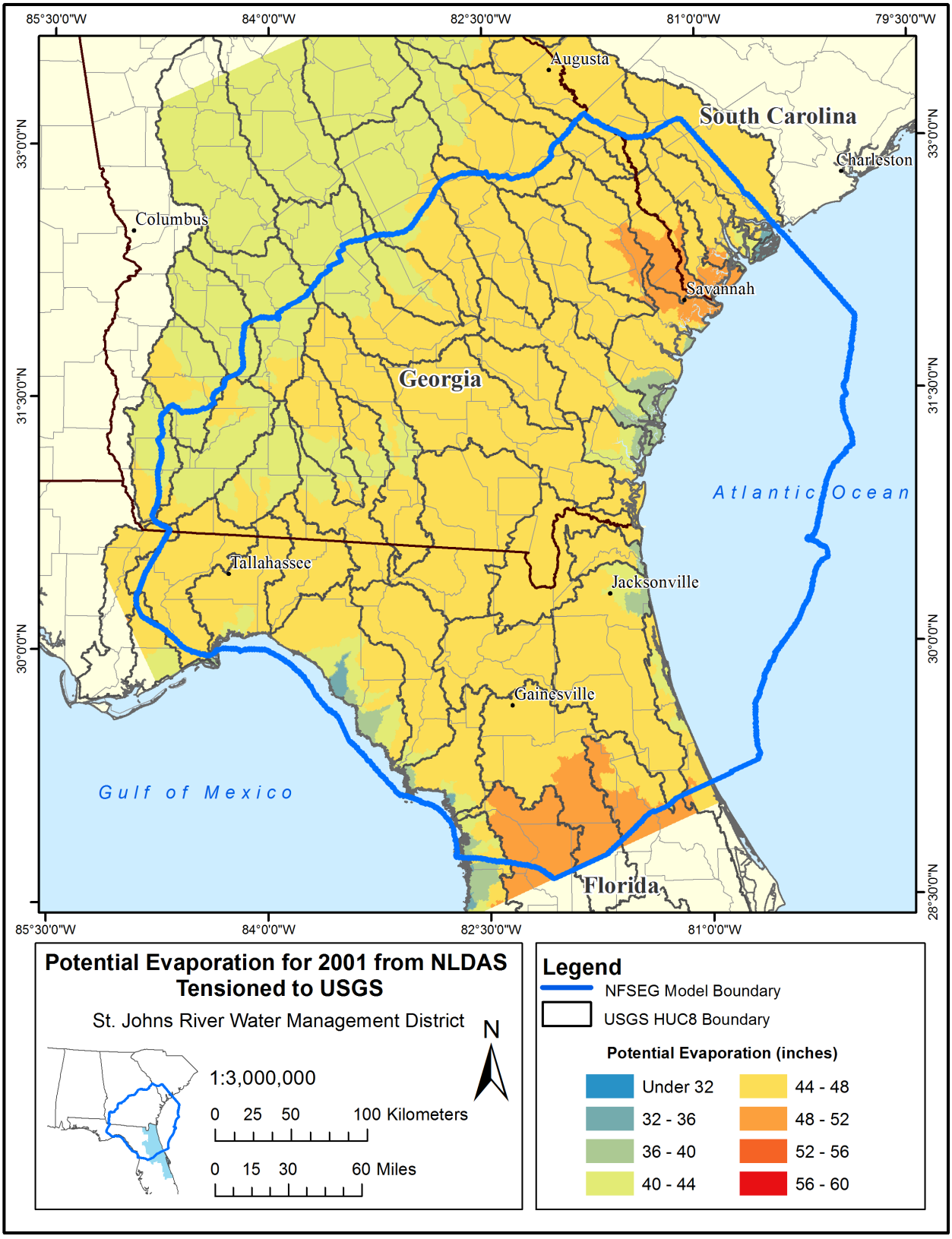

Figure 9-10. Potential evaporation for 2001 from NLDAS tensioned to USGS

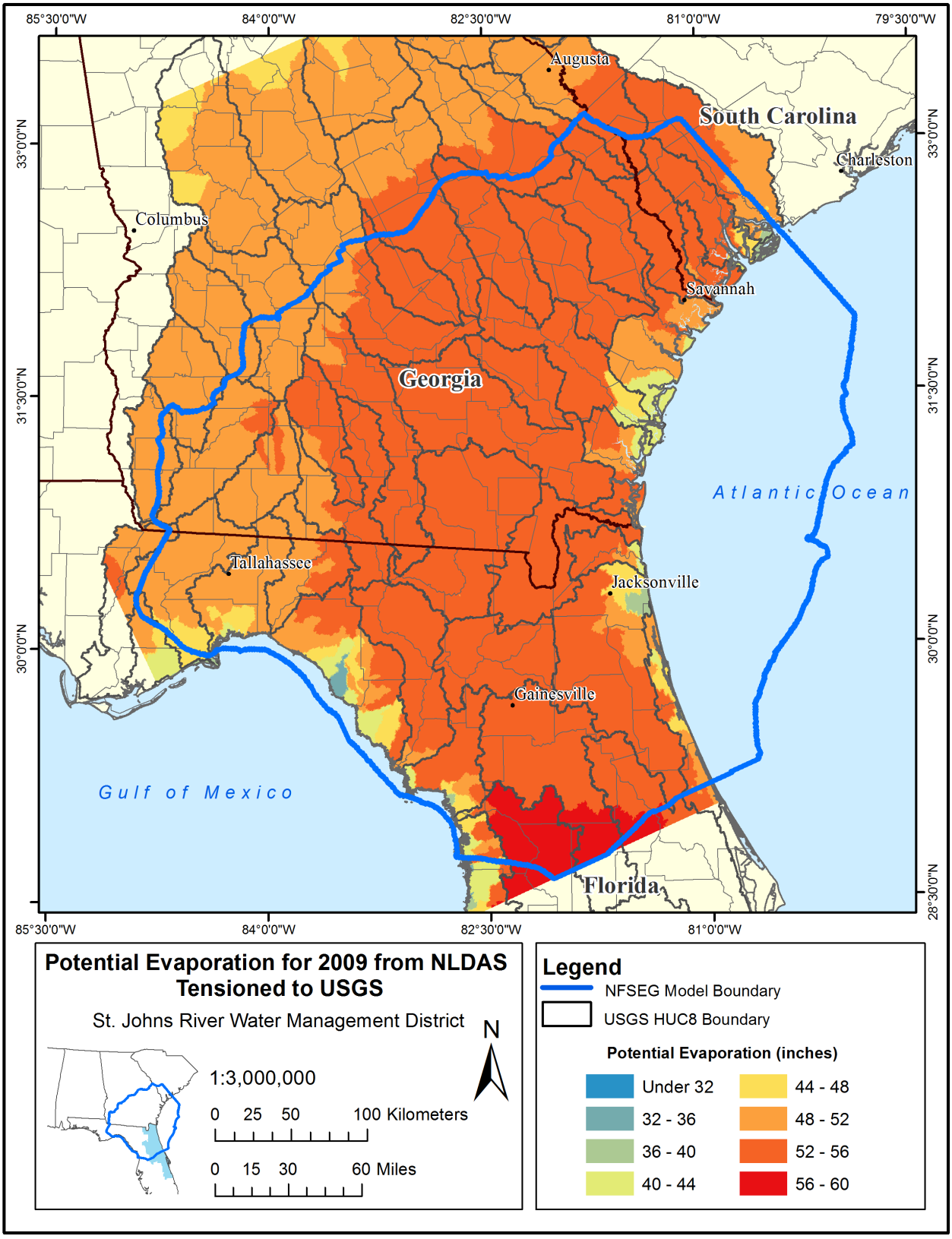

Figure 9-11. Potential evaporation for 2009 from NLDAS tensioned to USGS

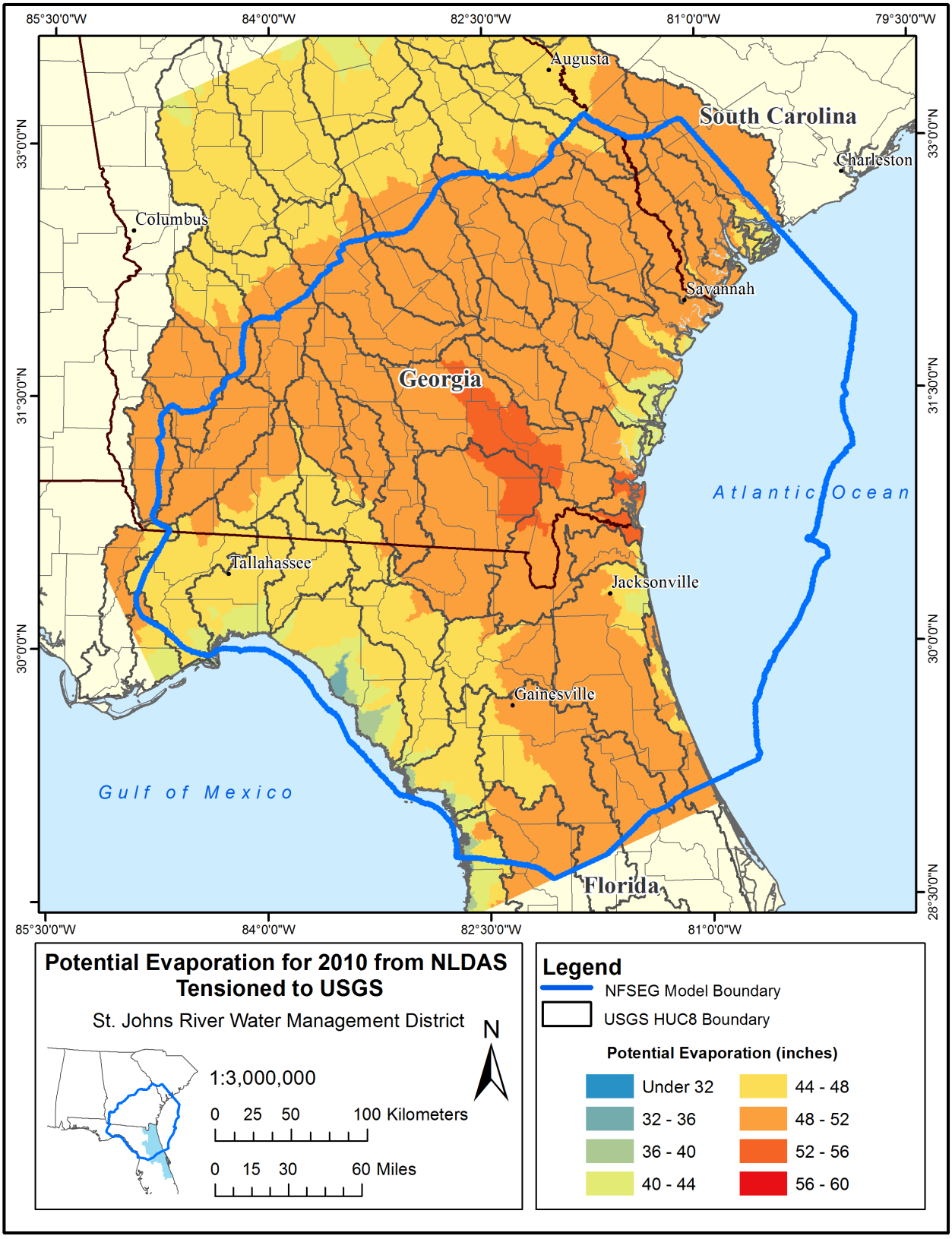

Figure 9-12. Potential evaporation for 2010 from NLDAS tensioned to USGS

Urban Irrigation and Septic Fields

A monthly time-series for indoor, outdoor, and indoor that would go to septic was developed for each sub-watershed. This effort started with utility records compared to parcel records then extended to account for domestic self-supply and areas in Florida and Georgia where there were no utility records. Additional detail about the development of this dataset is provided in the documentation of the urban water use component of the NFSEG project.

The irrigation and septic volumes were applied uniformly within each month and uniformly across all urban land uses. Since this uniformity implied a low application rate, the irrigation was applied as Surface Lateral Inflow (SURLI) to avoid interception losses that would occur if applied as precipitation. Volume from septic fields was applied to Lower Zone Lateral Inflow (LZLI). All water for urban irrigation and septic field contribution was considered to come from groundwater.

Golf Courses

Golf course irrigation use was established based on the best available data for the region. Where available, permitted or measured values were used. Otherwise, USGS estimates were used. Additional detail is available in other NFSEG documentation.

Monthly time-series of golf course volumes were established per irrigated area. The volumes were imposed into HSPF as SURLI and, from an evaluation of sourcing data in SJRWMD, an estimated split of 50/50 was established between surface water and groundwater. The volume to supply the surface water component is taken from the local reach within HSPF.

Table 9-9. Irrigation type matched to appropriate part of HSPF water balance

Irrigation System	Application to HSPF Water Balance
Micro Drip	SURLI: Surface Storage Lateral Inflow
Container Nursery	SURLI: Surface Storage Lateral Inflow
Crown Flooding	LZLI: Lower Zone Lateral Inflow
Low Volume	SURLI: Surface Storage Lateral Inflow
Micro Spray	SURLI: Surface Storage Lateral Inflow
Overhead	SURLI: Surface Storage Lateral Inflow
Seepage (Pipeline, Linear Pipeline)	LZLI: Lower Zone Lateral Inflow
All other types	Applied as precipitation (PREC)

Reuse

Reuse data came from FDEP as part of the WAFR database. Since sourcing and volumes for agricultural irrigation, urban irrigation and septic, and golf course irrigation were already established in other ways, the inclusion of those reuse components would double count the reuse volumes. The WAFR database does not include the actual polygon area for spray fields or other aerial applications, there is only a point. Therefore, all aerial discharges were applied to developed open space within the subwatershed. The point discharges were sent to the local reach. Additional detail is available in other documentation of the development of NFSEG water use datasets.

SPATIAL DATA

Most of the framework describing the subwatersheds within the HSPF models is developed from spatial data.

Watershed and Sub-Watershed Boundaries

The model boundaries were set to the USGS HUC8 watershed boundaries (Figure 9-13). There are 55 models within or contributing to the NFSEG groundwater model. Watershed boundaries are established by the USGS at several levels identifies by a series of digits as part of the Watershed Boundary Dataset (WBD). The HUC4 boundaries form very large watersheds, with the HUC8 boundaries as subwatersheds of HUC4, and HUC12 are subwatersheds of the HUC8 boundaries. There are some regions that also have HUC16 subwatersheds but these are outside of the southeast. The HUC4 is labeled with 4 digits, the HUC8 with 8 digits, and the HUC12 with 12 digits. All of the HUC8 subwatersheds in a HUC4 have the same 4 digits at the beginning and all HUC12 subwatersheds in a HUC8 share the same 8 digits at the beginning.

Elevation

Elevation data is used to delineate the subwatersheds so that boundaries are set to calibration points. The elevation dataset chosen for this work is the National Elevation Dataset (NED). This dataset is a gridded 1/3 x 1/3 arc-second (approximately 10x10 meter) Digital Elevation Model (DEM). All elevation data managed by the USGS has been collected under the umbrella of a new program called 3D Elevation Program (3DEP). The 3DEP has adopted the NED as the gridded dataset component of their suite of datasets. The NED elevation data for the NFSEG domain is mapped in Figure 9-14.

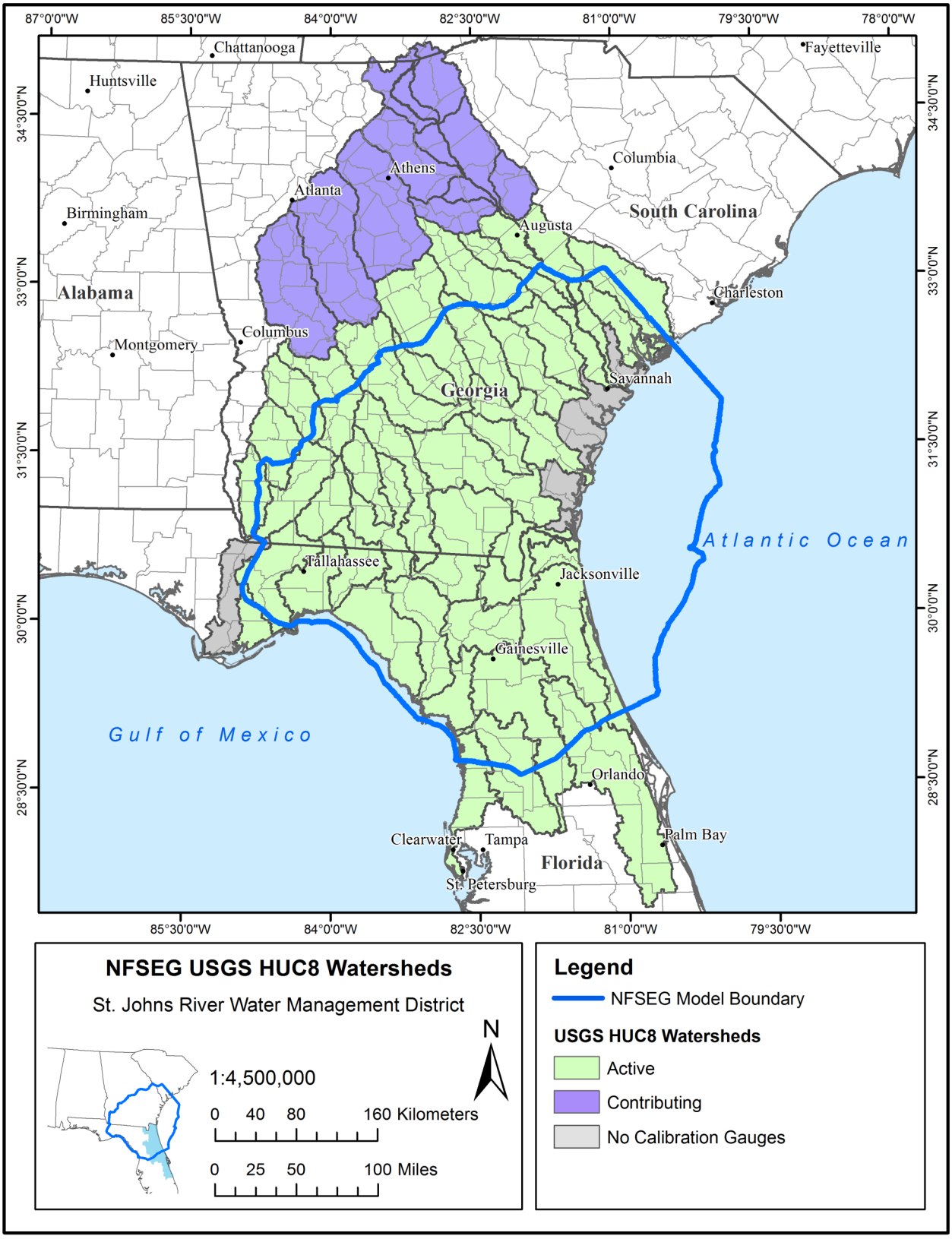

Figure 9-13. USGS HUC8 watersheds

Land Cover

The National Land Cover Database (NLCD) land use coverage is a convenient, consistent, nationwide land use coverage. It consists of the groups identified in the first column of Table 9-10. The initial parameter ranges used in the first cut model will be taken from previous models developed by SJRWMD. Figure 9-15 is a map of the NLCD land cover categories.

Impervious areas include all surface areas that prevent water from infiltrating into the ground. Typical impervious areas are roofs, roads and parking lots. These impervious areas can be classified into two categories: directly connected impervious area (DCIA) and non directly connected impervious area (NDCIA). DCIAs are the impervious areas that directly connect to the drainage network with no opportunity for infiltration. NDCIAs are the impervious areas that drain to pervious areas. In this study, only DCIAs are modeled as IMPLND, and NDCIAs are lumped to PERLND.

Among 12 consolidated land uses, four urban land groups consisting of the Low, Medium, and High Density Residential, and Industrial, which also includes commercial, (LDR, MDR, HDR, IND respectively) are assumed to have DCIA. The remaining land uses are taken as consisting of only pervious land elements. Estimation of the percent DCIA focus on matching the observed flows during small storm events because most runoff during small storms is generated from DCIA. Impacts of changing imperviousness percentages on total mass balance and seasonal flow distribution are also considered.

Table 9-11 lists the percentages of DCIA determined from this analysis and used in this study.

Calibration Data

Two main datasets were used for calibration. The flow observations from USGS stations and estimates of total evapotranspiration from literature.

USGS Flow Observation

All available daily flow data from all USGS flow observation stations within the NFSEG domain was downloaded from USGS and the locations are shown in Figure 9-16. Figure 9-16 also identifies those observation stations that were used for calibration. There are several reasons why a station may not have beeen used for calibration, including short period of record, wrong location to be included in the delineation process, tidally influenced, or indications that the data was of very poor quality.

There are inherent difficulties in flow measurement in Florida due to shallow slopes, poorly defined cross sections, interaction with groundwater (springs and swallets), tailwater, man-made structural controls, and tidal influences. The USGS rating curve model also has errors associated with the estimated flow.

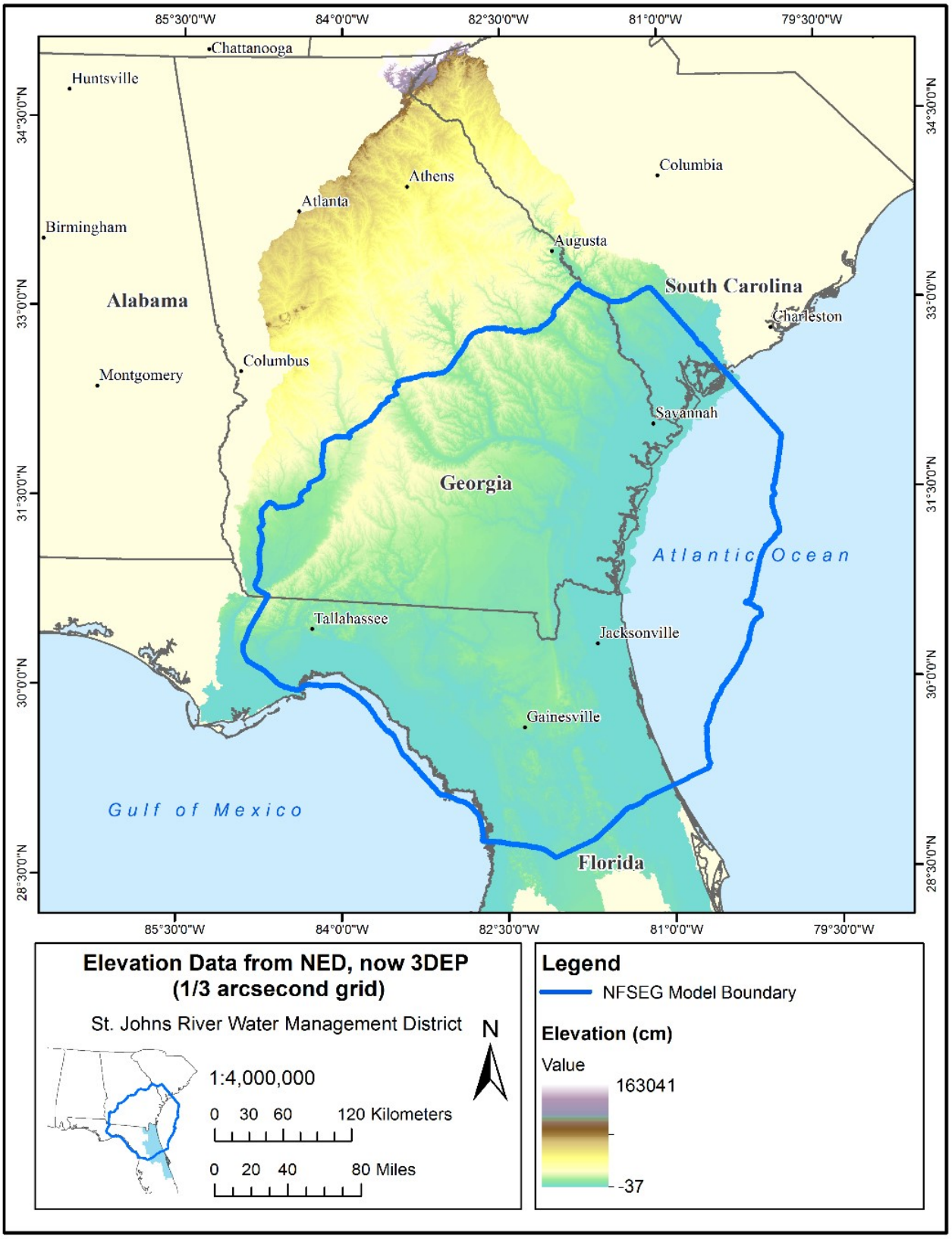

Figure 9-14. Elevation from the National Elevation Dataset (NED), now 3DEP

Table 9-10. NLCD and HSPF land cover classifications

NLCD Land Use	NLCD Code	HSPF Land Cover Group Assignment	Approximate Percentage of NFSEG Domain
Water			
Water-Open	11: areas of open water, generally with less than 25% cover of vegetation or soil.	1: Water	3.3
Ice/Snow-Perennial	12: areas characterized by a perennial cover of ice and/or snow, generally greater than 25% of total cover.	(not applicable)	0.0
Developed			
Developed-Open Space	21: areas with a mixture of some constructed materials, but mostly vegetation in the form of lawn grasses. Impervious surfaces account for less than 20% of total cover. These areas most commonly include large-lot single-family housing units, parks, golf courses, and vegetation planted in developed settings for recreation, erosion control, or aesthetic purposes.	2: Developed Open Space	5.8
Developed-Low Intensity	22: areas with a mixture of constructed materials and vegetation. Impervious surfaces account for 20% to 49% percent of total cover. These areas most commonly include single-family housing units.	3: Developed Low Intensity	2.3
Developed-Medium Intensity	23: areas with a mixture of constructed materials and vegetation. Impervious surfaces account for 50% to 79% of the total cover. These areas most commonly include single-family housing units.	4: Developed Medium Intensity	0.6
Developed-High Intensity	24: areas of bedrock, desert pavement, scarps, talus, slides, volcanic material, glacial debris, sand dunes, strip mines, gravel pits and other accumulations of earthen material. Generally, vegetation accounts for less than 15% of total cover.	5: Developed High Intensity	0.2
Barren			
Barren Land	31: areas of bedrock, desert pavement, scarps, talus, slides, volcanic material, glacial debris, sand dunes, strip mines, gravel pits and other accumulations of earthen material. Generally, vegetation accounts for less than 15% of total cover.	6: Open and barren land	0.4

Table 9-10 -- *Continued*

NLCD Land Use	NLCD Code	HSPF Land Cover Group Assignment	Approximate Percentage of NFSEG Domain
Forest			
Forest-Deciduous	41: areas dominated by trees generally greater than 5 meters tall, and greater than 20% of total vegetation cover. More than 75% of the tree species shed foliage simultaneously in response to seasonal change.	7: Forest	8.9
Forest-Evergreen	42: areas dominated by trees generally greater than 5 meters tall, and greater than 20% of total vegetation cover. More than 75% of the tree species maintain their leaves all year. Canopy is never without green foliage.	7: Forest	24.9
Forest-Mixed	43: areas dominated by trees generally greater than 5 meters tall, and greater than 20% of total vegetation cover. Neither deciduous nor evergreen species are greater than 75% of total tree cover.	7: Forest	2.6
Shrubland			
Scrub-Dwarf	51: Alaska only areas dominated by shrubs less than 20 centimeters tall with shrub canopy typically greater than 20% of total vegetation. This type is often co-associated with grasses, sedges, herbs, and non-vascular vegetation.	(not applicable)	0.0
Scrub-Scrub	52: areas dominated by shrubs; less than 5 meters tall with shrub canopy typically greater than 20% of total vegetation. This class includes true shrubs, young trees in an early successional stage or trees stunted from environmental conditions.	8: Shrub	5.9
Herbaceous			
Grassland	71: areas dominated by gramanoid or herbaceous vegetation, generally greater than 80% of total vegetation. These areas are not subject to intensive management such as tilling, but can be utilized for grazing.	9: Rangeland	5.6
Sedge	72: Alaska only	(not applicable)	0.0

Table 9-10 -- *Continued*

NLCD Land Use	NLCD Code	HSPF Land Cover Group Assignment	Approximate Percentage of NFSEG
Herbaceous			
Lichens	73: Alaska only	(NA)	0.0
Moss	74: Alaska only vegetation.	(NA)	0.0
Cultivated			
Agriculture-Pasture	81: areas of grasses, legumes, or grass-legume mixtures planted for livestock grazing or the production of seed or hay crops, typically on a perennial cycle. Pasture/hay vegetation accounts for greater than 20% of total vegetation.	10: Pasture	8.1
Agriculture-Cultivated Crops	82: areas used for the production of annual crops, such as corn, soybeans, vegetables, tobacco, and cotton, and also perennial woody crops such as orchards and vineyards. Crop vegetation accounts for greater than 20% of total vegetation. This class also includes all land being actively tilled.	11: Agricultural general	8.4
Wetlands			
Wetlands-Woody	90: areas where forest or shrubland vegetation accounts for greater than 20% of vegetative cover and the soil or substrate is periodically saturated with or covered with water.	12: Wetlands	18.9
Wetlands-Emergent Herbaceous	95: Areas where perennial herbaceous vegetation accounts for greater than 80% of vegetative cover and the soil or substrate is periodically saturated with or covered with water.	12: Wetlands	4.0
Irrigated			
Golf Courses	Uses parameters from “Developed Open Space”	15: Golf Courses	
Agriculture-Pasture: Irrigated	Uses parameters from “Agriculture-Pasture”	17: Pasture: Irrigated	
Agriculture-Cultivated Crops: Irrigated	Uses parameters from “Agriculture-Cultivated Crops”	18: Agricultural -general: Irrigated	

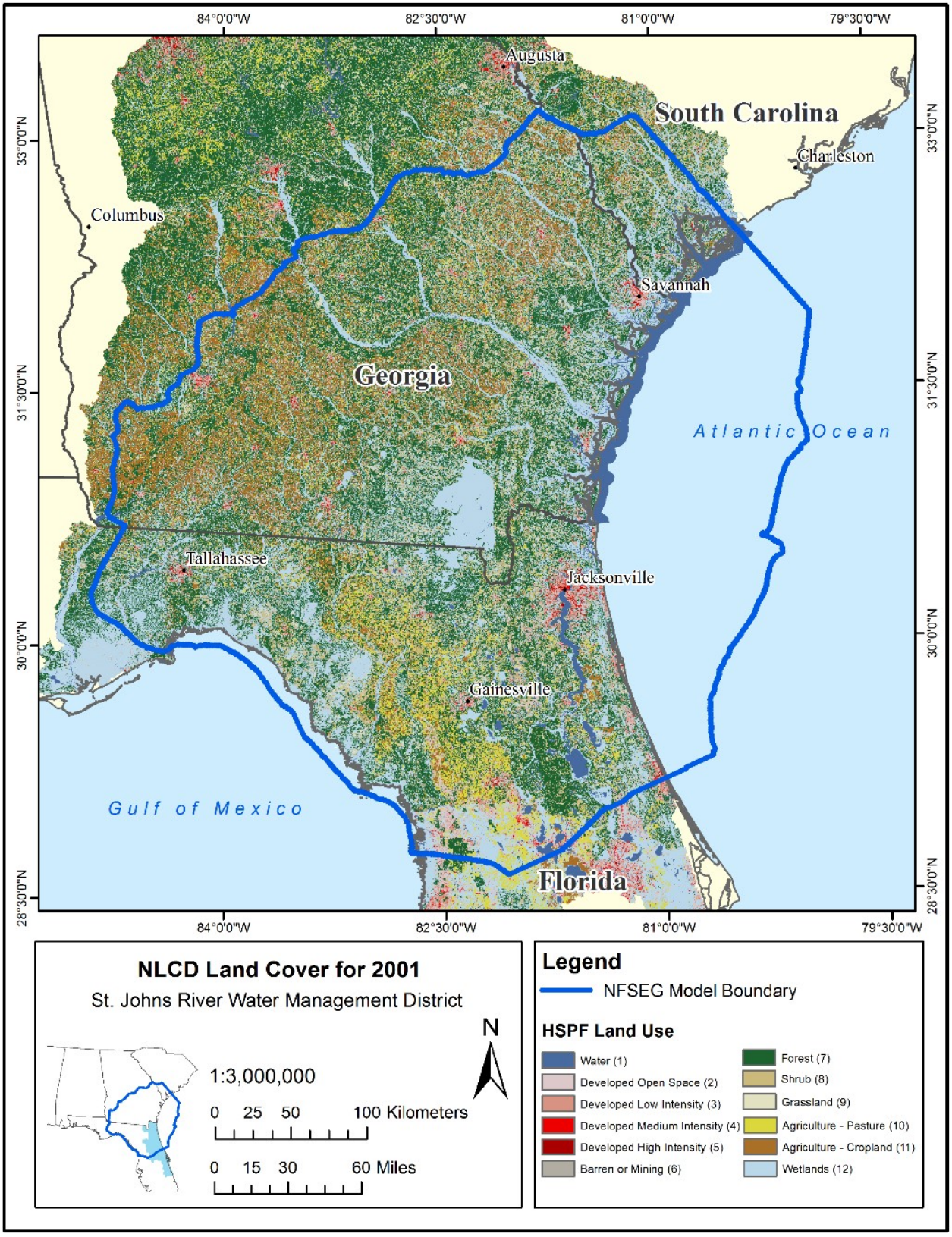

Figure 9-15. National Land Cover database, land cover for 2001

Even though there are several ways to estimate the rating curve error (Dymond and Christian 1982), the USGS has established a subjective estimate of annual flow data quality established by a review of measured data, datum shifts, and other characteristics of the flow measurement station. Table 9-12 describes the USGS system of data quality estimation (Kennedy 1983). The USGS system provides a general site-specific estimate of error and there may be significantly more error where there are few flow measurements in the rating curve, for example at high and low flows. However, the USGS gives a single quality category for each water year of record.

Most USGS flow measurement stations in Florida are rated 'Fair'. An 'Excellent' rating for a station in Florida is very rare. A map illustrating the USGS assigned data quality for flow observations in water year 2009 is presented in Figure 9-17. For 2009 there isn't an 'Excellent' rated gauge in any of the HSPF models.

Literature Total Evapotranspiration Estimates

Evapotranspiration in HSPF is calculated for each of the land cover segments in each subwatershed. A literature review collected estimates of evapotranspiration ranges for the land cover classes included in the HSPF model.

Evapotranspiration values found in the literature review were used as reference values in the HSPF calibration process using PEST. This was performed in order to have adequate estimation for evapotranspiration in the model water budget. Table 9-13 presents the evapotranspiration values and their reference source.

HSPF Model Development

The first step in development of a surface water model is to delineate the subwatersheds so that the calibration points represent outflow from a subwatershed. The delineation process at the same time establishes the stream network. The next step is to establish the areas of all the land cover PERLNDs, and IMPLNDs within each subwatershed.

Table 9-11. Percentage pervious land cover of directly connected impervious area

Land Uses	% Imperviousness
Low Density Residential (LDR)	5
Medium Density Residential (MDR)	10
High Density Residential (HDR)	20
Industrial and Commercial (IND)	50

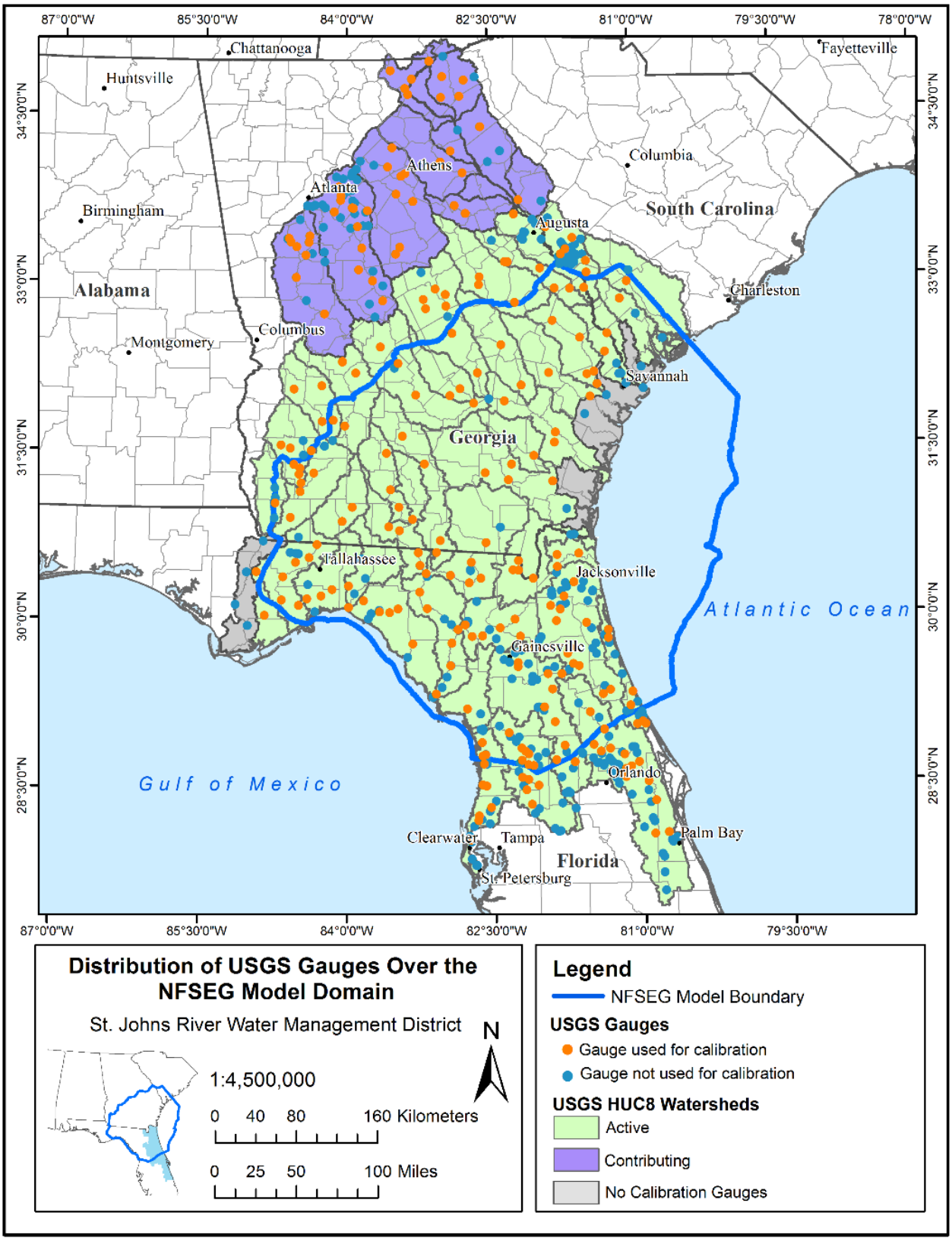

Figure 9-16. USGS Flow Observation Gauges

Sub-Watershed Delineation

To calibrate against data at the USGS gauge stations, the sub-watersheds need to be created to have their exits correspond with the location of the gauges. This process is called delineation and the TauDEM software was used for this project. The TauDEM software is a suite of programs used to analyze Digital Elevation Models (DEM) to determine sub-watersheds and corresponding stream reaches.

Conventional TauDEM processing would entail use of the following TauDEM commands:

1. pitremove: The DEM grid is used to create the pit filled DEM grid. Filling of pits is required for the remaining steps to function reliably. A pit is considered a mistake in the DEM and the elevation in pits is increased until there is a continuous downslope to the stream.
2. d8flowdir: The pit filled DEM grid is used to calculate a flow direction grid. The flow direction for each elevation grid point is determined as the direction that has the greatest difference in elevation.
3. aread8: The flow direction grid is used to calculate the flow accumulation grid. An accumulation count is developed for each grid which is the count of all grid cells that flow into that grid.
4. threshold: The flow accumulation grid is used to calculate the stream network. A value is set to establish the accumulation count where a stream would develop.
5. streamnet: The pit remove grid, the flow direction grid, the accumulation grid, the threshold grid, and location of USGS gauges are used by "streamnet" to create the delineated sub-watersheds and stream network.

Closed, Flat, and Frontal Sub-Watersheds

The project area has several unique features that affect surface water hydrology and the delineation process. One of these is closed basins which are surface watersheds that have no observable stream flow drainage. The precipitation that falls on a closed basin either must infiltrate or evaporate. The USGS has identified closed basins at the HUC12 level of detail throughout the United States.

Table 9-12. USGS flow data quality categories (Kennedy 1983)

Quality Category	Description
Excellent	95% of daily discharges within 5% of ‘true’
Good	95% of daily discharges within 10% of ‘true’
Fair	95% of daily discharges within 15% of ‘true’
Poor	Daily discharges have less than ‘fair’ accuracy

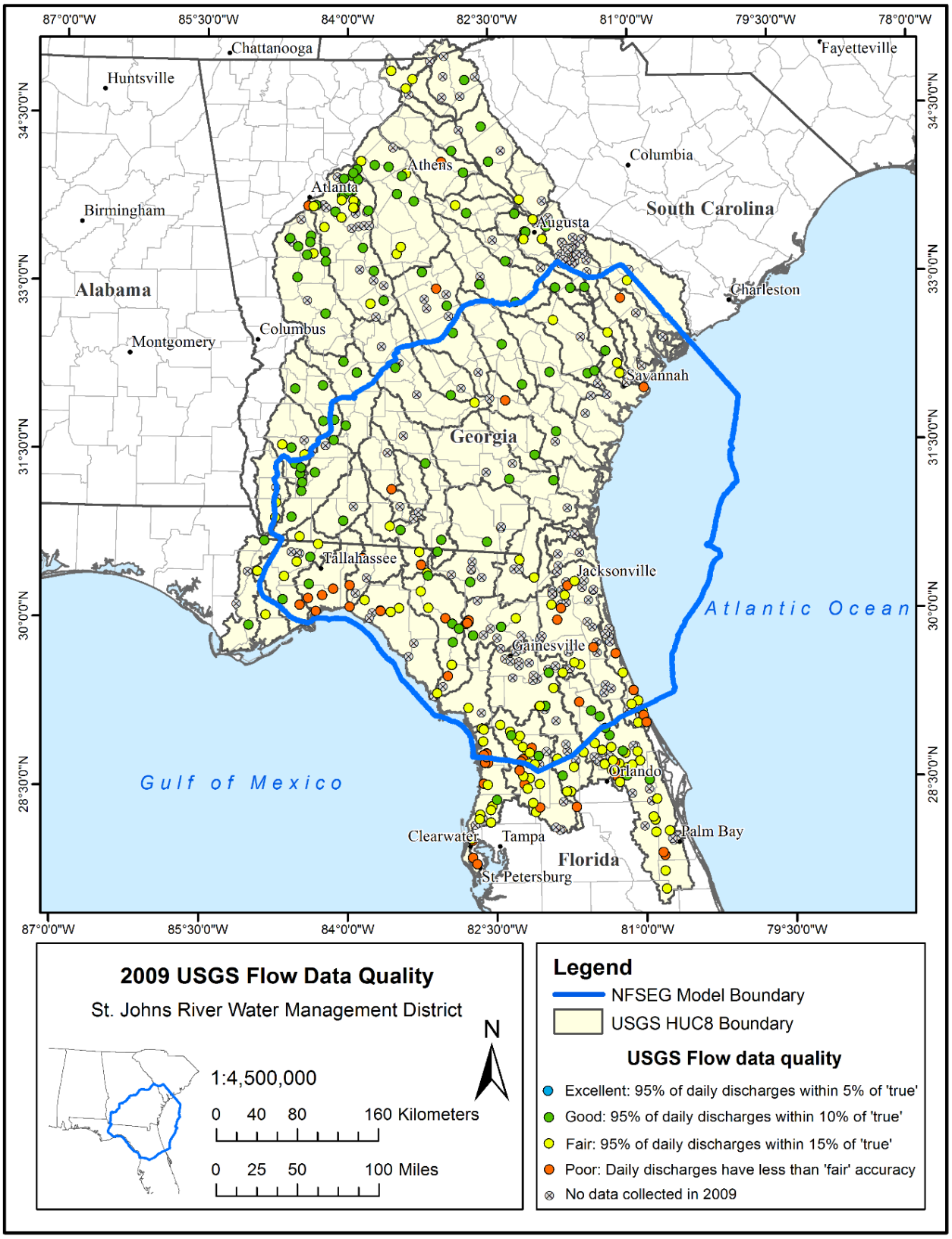

Figure 9-17. USGS quality assessment of flow data for water year 2009

Table 9-13. Literature total evapotranspiration by land cover

HSPF Land Use Code	Land Cover Name	Min mm/d winter	Max mm/d summer	Annually Averaged mm/d	Area	Reference
1	Water	2.8	5.3	4.18	Reedy Lake, FL	Douglas et al. (2009)
		3.5	5.2	4.45	Indian River Lagoon, FL	
2	Developed Open Space			2.13	Oklahoma	Liu et al. (2010)
3	Developed Low Intensity			1.96	Oklahoma	Liu et al. (2010)
4	Developed Medium Intensity			1.88	Oklahoma	Liu et al. (2010)
5	Developed High Intensity			1.79	Oklahoma	Liu et al. (2010)
6	Barren or Mining					
7	Forest			2.82	Havana, FL	Lu et al. (2003)
				2.78	Bradford, FL	
				2.51 to 2.93	Volusia County, FL	Sumner (2001)
		1.3	4.2	3.08	Alachua County, FL	Douglas et al. (2009)
				3.2	Blue spring Tract, FL	
				2.35	Oklahoma	Liu et al. (2010)

Table 9-13 -- *Continued*

HSPF Land Use Code	Land Cover Name	Min mm/d winter	Max mm/d summer	Annually Averaged mm/d	Area	Reference
8	Shrub	0.2	5	1.86	Orange County, FL	Sumner (1996)
				2.21	Oklahoma	Liu et al. (2010)
9	Grass Land			2.2	Oklahoma	Liu et al. (2010)
10	Agriculture - Pasture	0.8	2.9	1.58	Ferris Farm, FL	Douglas et al. (2009)
		1.8	4.3	3.06	Duda Farm, FL	
		0.67	4.72	2.16	Floral City, FL	Sumner and Jacobs (2005)
11	Agriculture - Cropland			2.18	Oklahoma	Liu et al. (2010)
	Citrus	1.4	4.1	3.03	Belle View Farm, FL	Douglas et al. (2009)
		1.9	4.8	3.48	Carlton Ranch Farm, FL	
12	Wetlands			2.36	Withla-coochee State For-est, FL	Ewel and Smith (1992)
		2.04	6.18	-	Alachua County, FL	Jacobs et al. (2002)
		1.42	4.72	3.25	Indian Riv-er County, FL	Mao et al. (2002)
		2.13	4.95	3.66		
		1.5	6.4	3.53		
		2.4	4.8	3.98	Blue Cy-press, FL	Douglas et al. (2009)
		2.9	4.4	3.86	Ever-glades, FL	
				2.39	Oklahoma	Liu et al. (2010)

Figure 9-18 shows the closed basins identified by USGS as well as the closed basins identified by local knowledge. Closed basins are rare with the USGS classifying only 1,189 of the 100,591 HUC12 subwatersheds in the United States as closed basins. The typical approach in surface water models is that closed basins are ignored since there is no surface flow, they are relatively rare and are not part of usual questions asked of surface water models. However, for establishing recharge estimates for a groundwater model, an approach needed to be developed. Within the NFSEG domain there are 35 closed basins identified by the USGS and an additional 32 HUC12 subwatersheds that are known to be closed, though not identified as such by the USGS.

TauDEM processing had to be adapted to handle the special situations that occur in this project. From the conventional TauDEM approach, each closed basin is a pit in the DEM that needs to be filled. Also, TauDEM does a poor job with flat areas. For this project, we handled the closed and flat areas separately from the tributary areas so that known subwatershed boundaries were honored by TauDEM.

Closed Basin Representation

Figure 9-19 illustrates a conventional tributary subwatershed in HSPF where the flow out of the reach to downstream is greater than zero.

Figure 9-20 illustrates the approach taken to represent closed basins for this project. The simple approach would be to simply increase IGWI until there is no flow out of the reach. This would distort all the other model parameters, flows and storages. The parameter adjusted to increase IGWI is called DEEPFR and has a recommended maximum of 0.5 in EPA Technical Note 6. But to have zero flow from the reach, DEEPFR needs to be set at 0.9 or greater.

It was noted that the closed basins had at least one sink that accepted surface water flows (Figure 9-21). To keep the parameters in line for a closed basin, the parameters are taken from a nearby tributary basin and a feature was added to the reach where high flows would be directed to a virtual sink, representing all sinks within the basin. This is a significant improvement because the parameters that affect evaporation and recharge are from a calibrated system and aren't distorted by unusual changes to adapt to the closed basin. This virtual sink was parameterized with an invert, a maximum flow, and a depth above the invert when maximum flow starts. The virtual sink flows for each subwatershed were then divided among the known sink or drainage well features within the subwatershed. Locations of sinks and drainage wells related to closed basins are shown in Figure 9-21.

Since the virtual sink parameters can represent several sinks and dozens of drainage wells in a closed basin, that have very few or no physical measurements or flow observations, PEST was allowed to adjust these parameters within reasonable ranges. Even in closed basins, PEST was given evapotranspiration targets, which would constrain, along with recharge parameters from adjacent basins, the flow down the virtual sink. The virtual sink parameters attempt to represent the depth/flow relationship that would be expected from a single drainage well, but those parameters are not taken from obser-

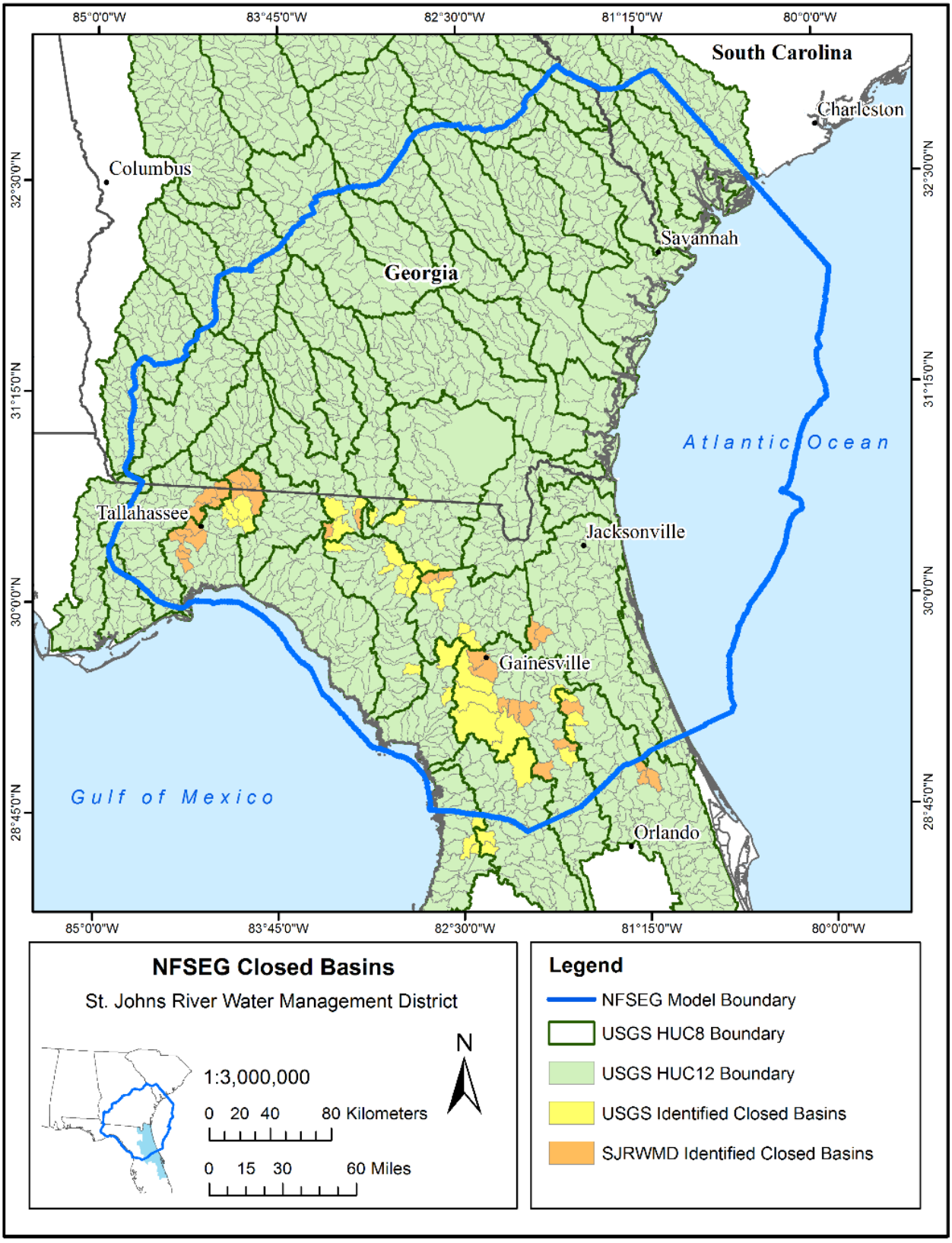

Figure 9-18. Map of closed basins within the NFSEG model

vations. As such, there isn't a way to verify these parameters except in that they are bounded in a reasonable range and the estimated flows are reasonable within the overall surface water budget.

Representation of Springs to Improve HSPF Calibration

Typically, IGWI is a loss term that moves out of the surface water balance simulated by HSPF to deep groundwater and springs are represented as new water imposed directly into the surface water reach. The time-series of imposed spring flow is developed based upon observed data.

Because of very limited, reliable spring flow data, the conventional approach of imposing spring flow into the HSPF models was problematic. Instead, a simple underground reservoir was established in HSPF to collect IGWI within a springshed. This underground reservoir was then used as a source for spring flow. This approach is illustrated in Figure 9-22.

The springsheds were delineated by referencing the Upper Floridan aquifer (UFA) potentiometric surface map as illustrated in Figure 9-23.

The surface subwatershed boundaries did not match the springshed boundaries. The decision about which subwatershed belonged to which springshed was done manually based on which springshed contained the most area of the subwatershed. The assignment of subwatershed to springshed is shown in Figure 9-24. Also, shown in Figure 9-24 is the target reach that receives the accumulated Inactive Groundwater Outflow (IGWO).

Calibration Process

The modeled time-period is dependent on the question that needs to be answered. Flood control analysis is calibrated using a single storm event, a design storm or multiple storm events. Water supply, MFLs and certain environmental analysis require long-term continuous modeling simulations. The land use/cover is set for a point in time and historical rainfall records are selected, which will match the length of rain needed for the simulation. Using the historic rainfall record, it is assumed that the rain in the future will approximate the amount and patterns of the past. These are pseudo-random events and if the period of record used is long enough, there should not be a discernable bias in the data.

The calibration period selected for these hydrologic models is from 1992 to 2015. This period was selected for three reasons.

1. The overall project of the HSPF models was intended to be used for other transient groundwater models that began in 1995.

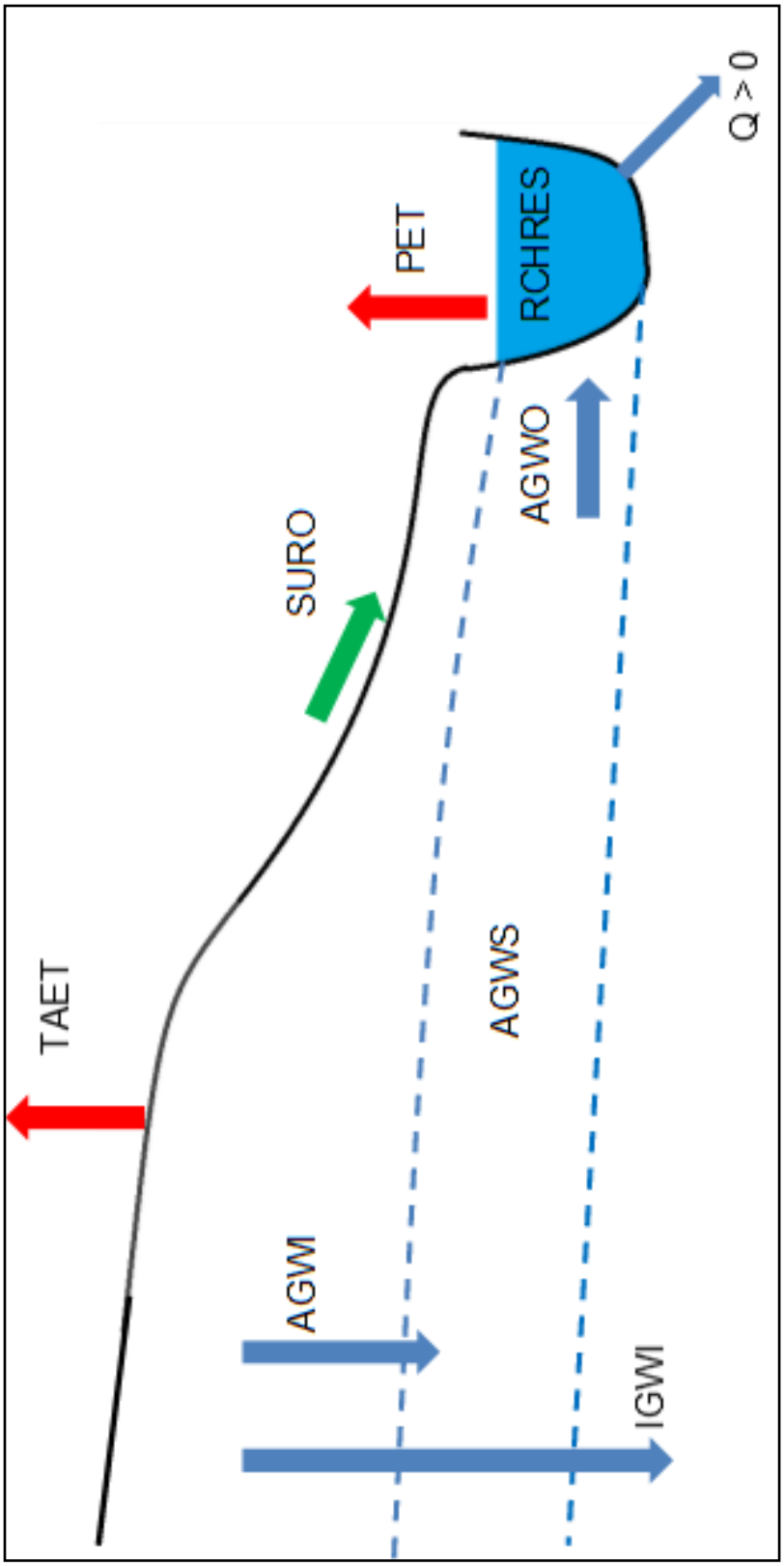

Figure 9-19. Conventional representation of a subwatershed for a tributary basin

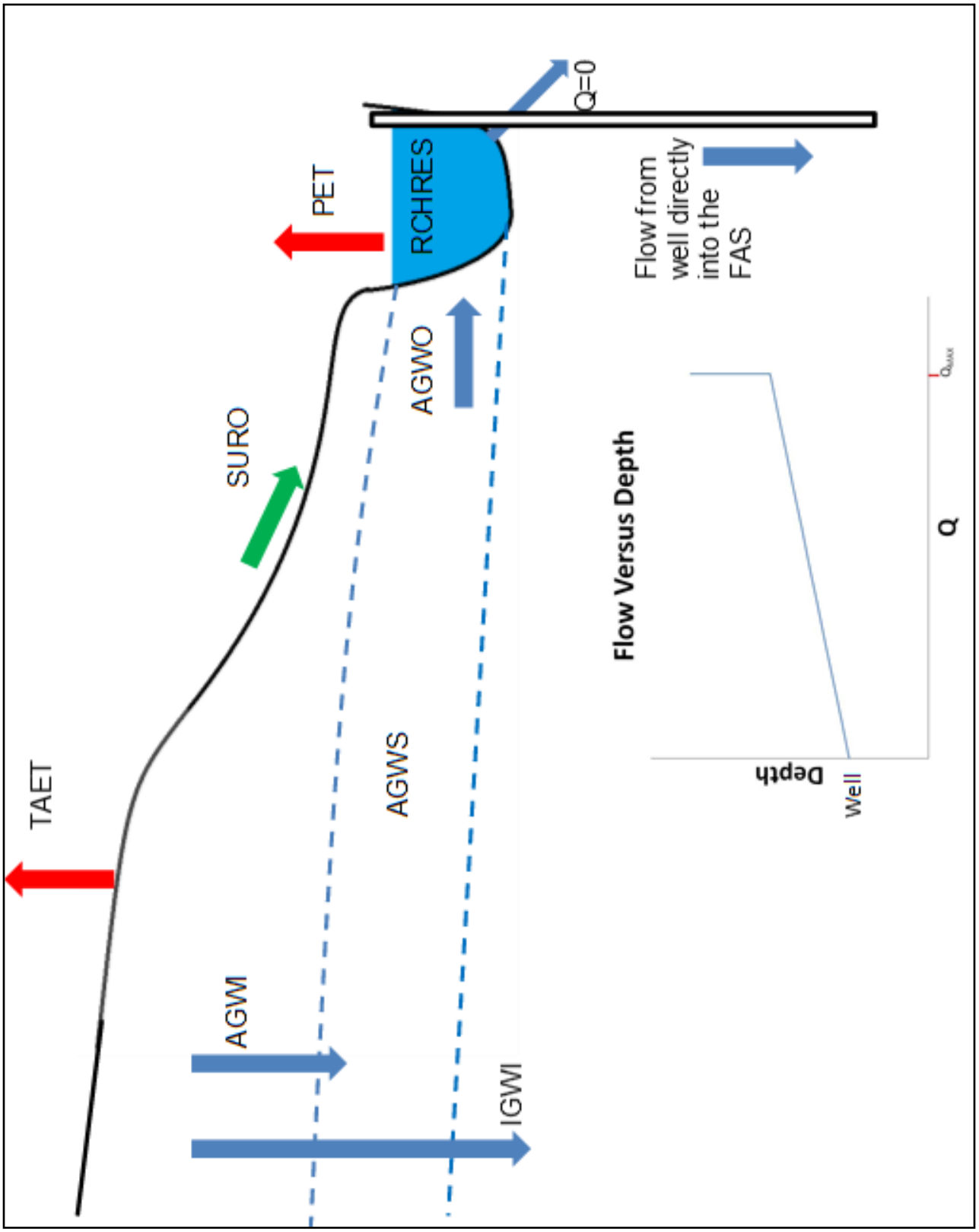

Figure 9-20. Closed basin representation of a sink to replace outflow, where surface flow Q = 0

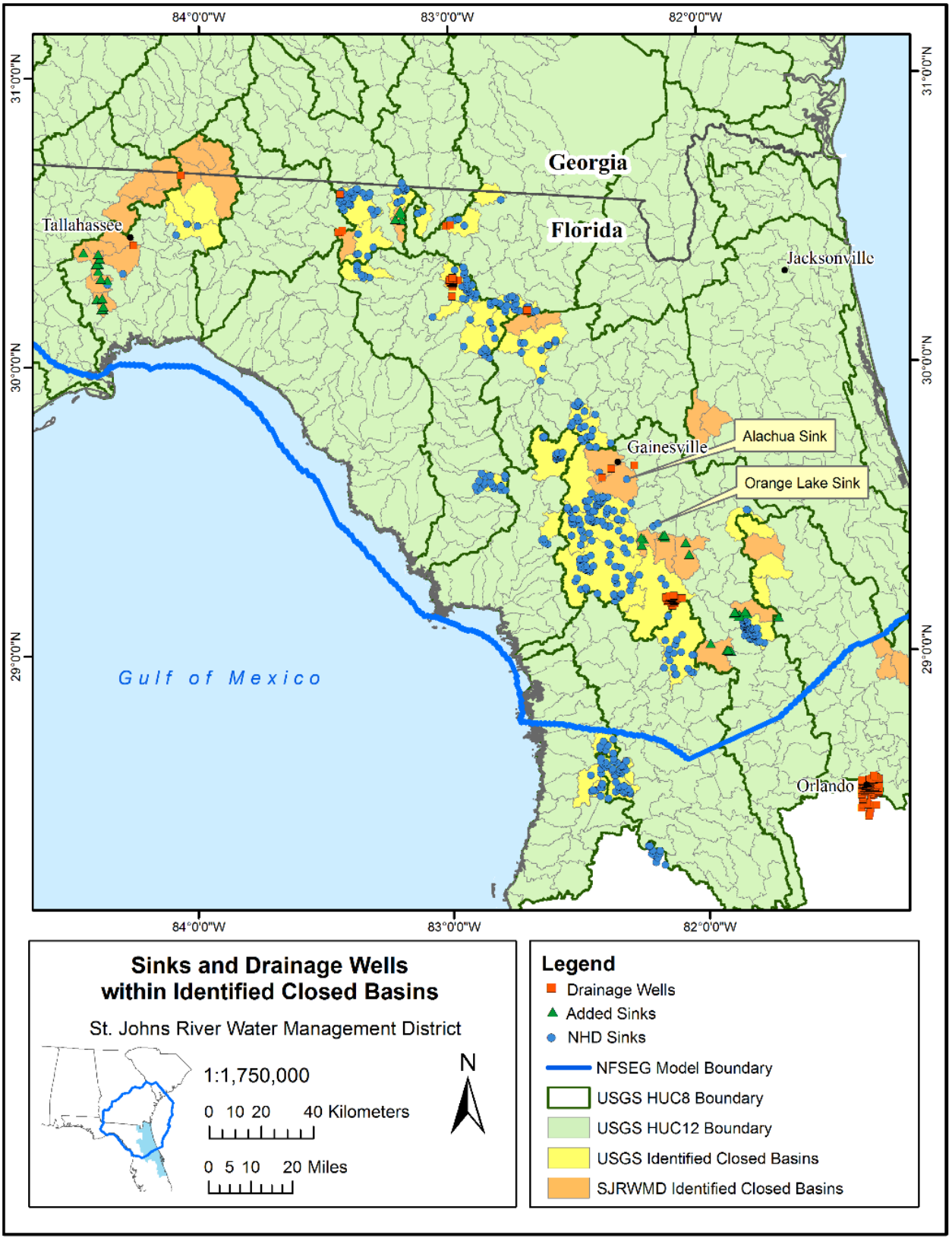

Figure 9-21. Sink and drainage wells within NFSEG domain

2. The longer the time period available for calibration, the less chance of bias in the model due to calibration against a short period of record.
3. It encompasses the planned time frame of 2000-2012 for the transient groundwater model.

The actual time-period of meteorological data and land and stream gauge data is used as input data for the HSPF models. The calibration period of the individual models is within the 1992 to 2015 time-period, depending length of data available for calibration. The calibration performance of the models is described in detail in the Calibration Results section and in the model specific appendices.

The calibration process is illustrated in Figure 9-25. Something to note is that neither the input data to the model nor the calibration data is the "Real World". It is instead a small part of what we imperfectly observe.

MODEL INPUT PARAMETERS

Common Logic

The changes to the model concerning land-use, precipitation and evaporation require a complete examination of the model parameters. Originally, modelers at the District modeled watersheds with HSPF for various purposes and developed model parameters that were characteristic of the individual watersheds. The District has now developed a common logic (Appendix P), which sets reasonable parameter value ranges for all HSPF models in the District. This common logic was an evaluation of the possible range of model parameters given the unique hydrology of Florida, extensive District HSPF experience and the ranges common in other parts of the world (USEPA 2000).

Variability of Parameters Across an HSPF Model

Unless there was information that indicated differently, each model had the same parameters for all subwatersheds. Only when it was obvious that some area of the model was hydrologically different was that area modeled with a separate parameter set. This data driven approach is better than making a parameter set for each subwatershed and means that better flow observations within the model become more important to the calibration than poorer observations. This was proven true after evaluation of the calibration performance (see Calibration Results section).

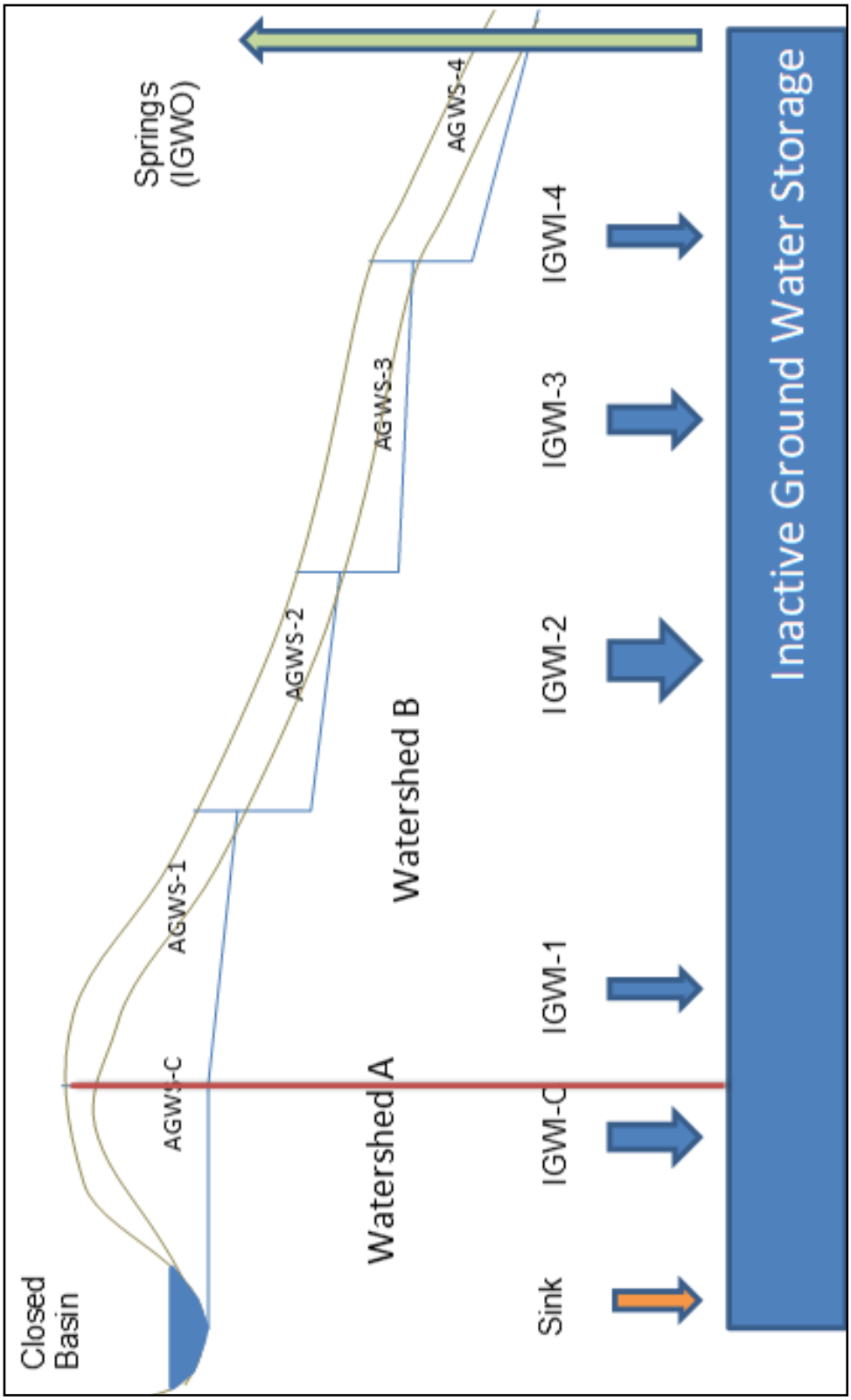

Figure 9-22. Conceptual framework for the IGWO representation of springs

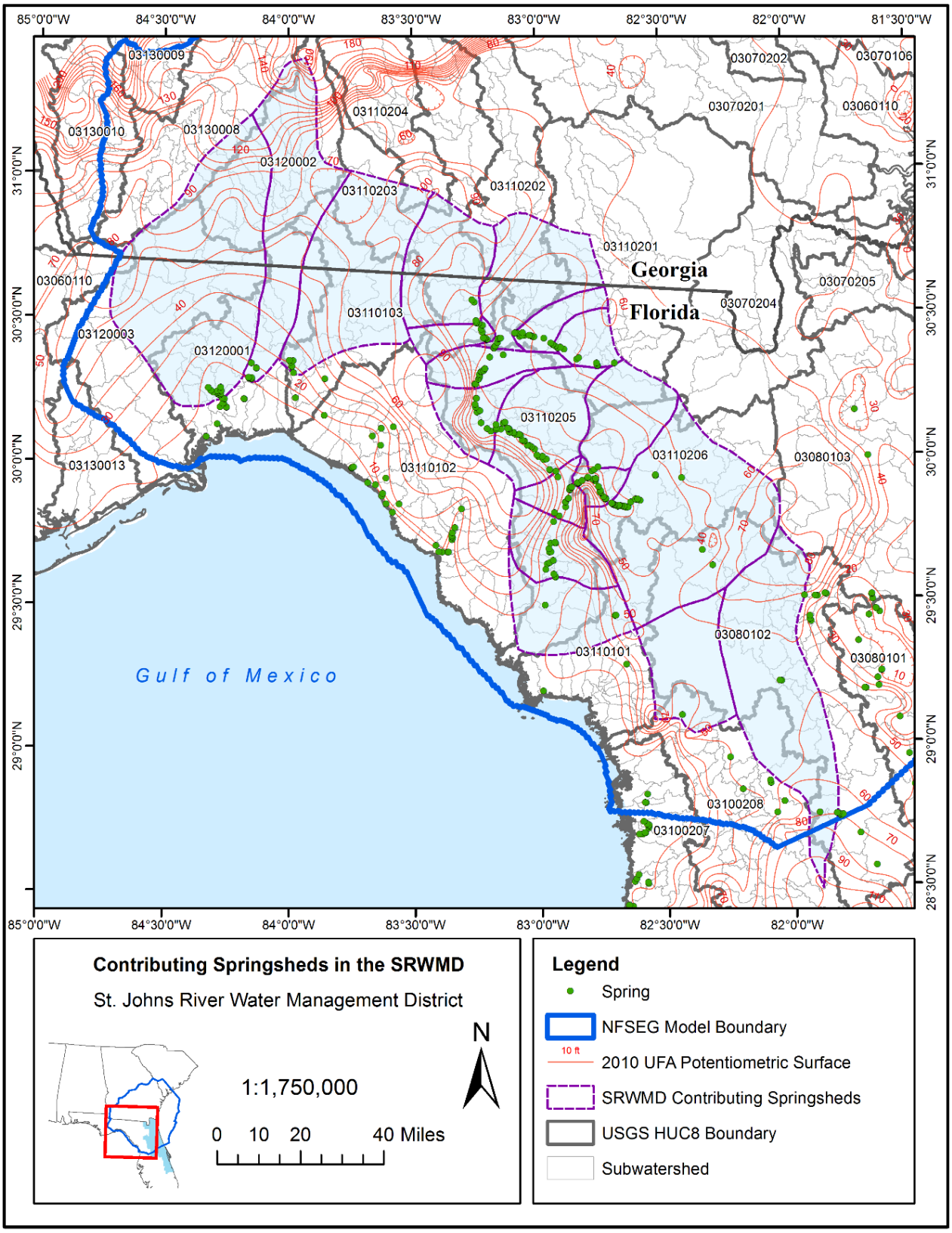

Figure 9-23. UFA Potentiometric surface and springsheds in the Suwannee River Basin

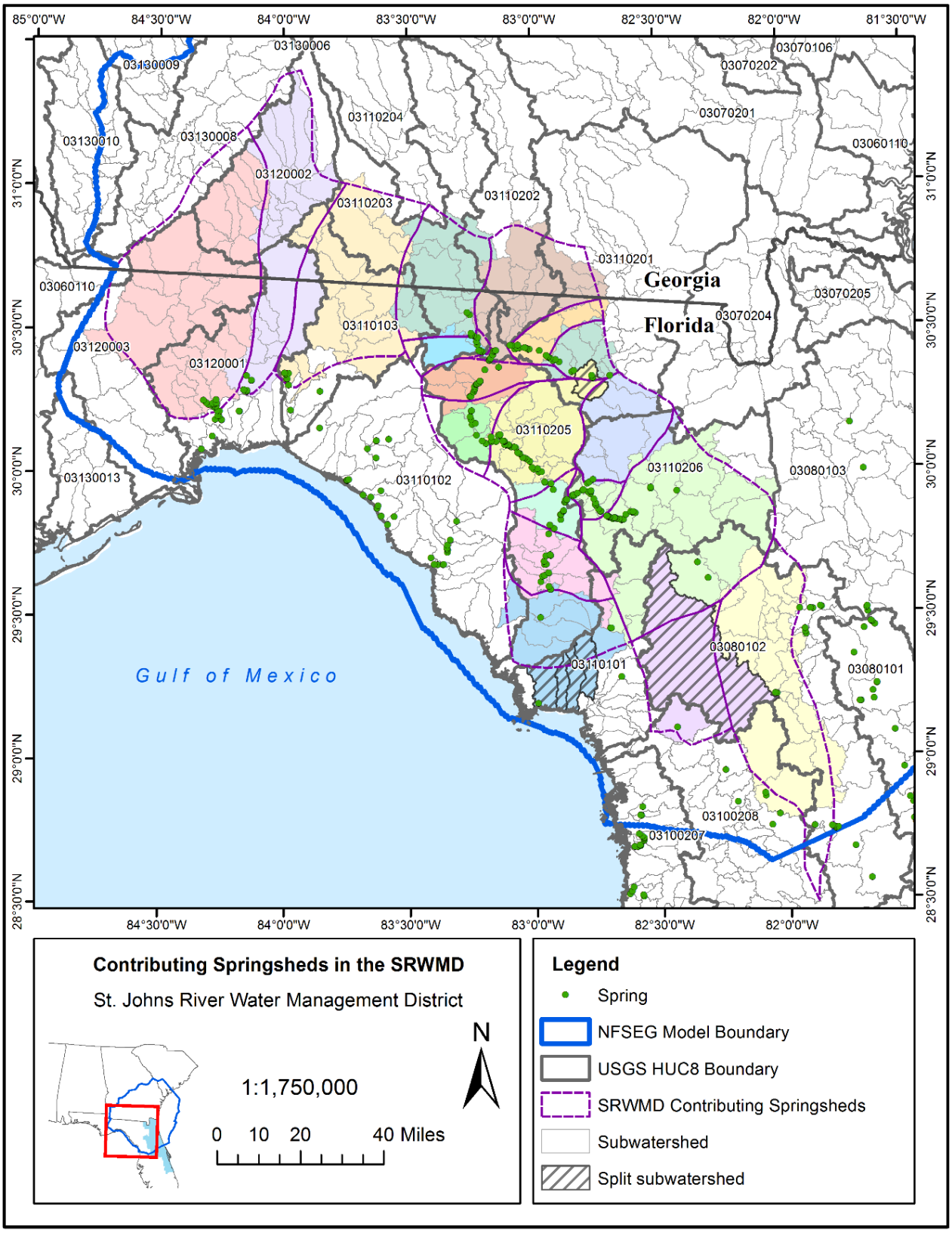

Figure 9-24. Identified subwatersheds that were used as springshed outlets

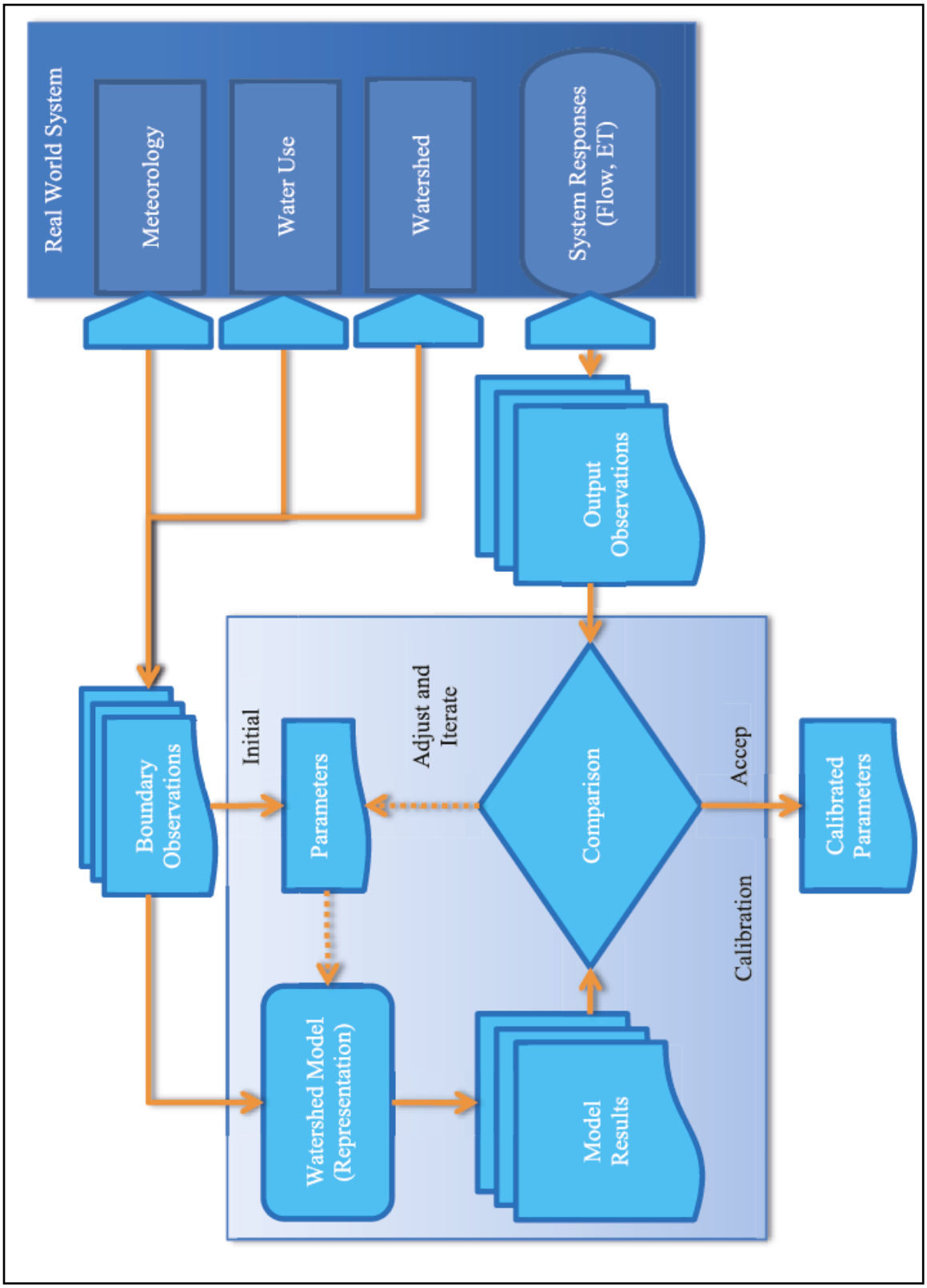

Figure 9-25. Overview of calibration process

Development of FTABLEs for the Stream Network

In HSPF, the stream network in a subwatershed is grouped together and represented as a reach segment, which could be either a free-flowing stream or a mixed lake. The FTABLEs for stream reaches are developed based on the Manning's equation. Channel cross-section characteristics are based on survey data, field visits, USGS quad maps, etc. For example, the stream reaches in the urbanized Lake Jesup watershed are modeled as streams with uniform trapezoidal cross-sections. Stream length, slope and elevation are estimated based on the stream network and digital elevation map available at SJRWMD. Manning's "n" coefficients for these streams are estimated by comparing the calculated stage-discharge relationships with the measured relationships at several USGS flow gauge sites.

For the Ocklawaha basin (03080102), FTABLEs were taken from earlier very detailed models used for the Water Supply Impact Study (Lowe et al. 2012) and the development of Upper Ocklawaha MFLs. For the Suwanee River (03110201 and 03110205), a HEC-RAS model was used to develop FTABLEs. For all other sub-watersheds, the regional approach in BASINS was used.

PARAMETER ESTIMATION WITH PEST

Calibration of HSPF is an iterative process of changing parameters, running simulations, checking results, and repeating until a calibrated model is achieved. When manually performed, this can be a time-consuming endeavor. In addition, it can be difficult to maintain a consistent approach of parameter adjustments to produce calibrated models among a group of HSPF modelers with various levels of experience and expertise. For this reason, Parameter ESTimation (PEST) was used to assist in model calibration.

PEST is a nonlinear parameter estimator that will adjust model parameters to minimize the discrepancies between the pertinent model-generated numbers and the corresponding measurements. It does this by running the model as many times as is necessary to optimize a least-squares objective function. The objective function (represented by the Greek letter, "phi" Φ) is the summation of the weighted, squared, model to measurement differences. PEST evaluates parameter changes based on minimizing the objective function and decides whether to undertake another optimization until no more improvement in the objective function is achieved.

$$\Phi = \sum_{i=1}^{n} (w_i(o_i - s_i))^2$$

Where: Φ is the objective function
n is the number of observations
w_i is the assigned weight for the ith observation
o_i is the ith observation
s_i is the ith simulated value corresponding with the ith observation

The modeler must define the observations that are included in the objective function. The objective function takes the form of matching, as best as possible ,simulated to gauge values for the observations and statistics shown in Table 9-14 and Table 9-15.

Since Φ is a function of the number of observations and the overall magnitude of the values, the assigned weight is an important part of using PEST since it can make observations more or less visible in the calibration process. Because the assignment of weights can be so tedious, there is a utility in the PEST suite to help with this called "PWTADJ1". The initial weighting was established using "PWTADJ1". This utility equalizes the contribution to Φ from each observation group. After the contribution to Φ is equalized, the weighting was increased for a couple observations groups by multiplying by a weight factor, as shown in Table 9-14 and Table 9-15.

PEST was used to optimize the parameters LZSN, LZEPT, INFILT, UZSN, AGWRC, INTFW, IRC, DEEPFR, and the water/wetland surface runoff FTABLE storage-runoff relationship. Relative values of parameters were established by the modelers between land uses to produce expected relative runoff amounts. Urban land, including impervious area, produces the most runoff, agriculture produces the next largest runoff, open land and rangeland produce less, and forest and wetland produce the least runoff. PEST allows parameters to be "tied" to a "parent" parameter. In this way, all the tied parameters are adjusted equally among the various land uses. In general, LZSN, LZEPT, INFILT, and UZSN parameters are tied together between land uses. The exception to this is wetland. Wetland parameters give emphasis to larger upper zone storage and lower infiltration rates. For this reason, wetland parameter sets are not comparable to other land uses and are adjusted independent of the other land uses. The parameters AGWRC and DEEPFR are applied to the entire watershed. In addition, PEST allows parameters to be "fixed" and not adjusted. For example, in many cases of INTFW and IRC (see the Common Logic for INTFW in Appendix P), if these parameters are not given a restricted range close to zero, the parameters are fixed to zero or a very small number.

Regularization of parameters between models using PEST is not planned, but a manual review and adjustment of parameter ranges was made to ensure that adjacent watersheds have similar parameter values.

HSPF Special Actions

HSPF permits the user to perform certain "Special Actions" during a run. A special action instruction specifies the following:

- The operation on which the action is to be performed (e.g., PERLND 10)
- The date/time or condition at which the action is to be taken.
- The variable name and element (if the variable is an array) to be updated.
- The action to be performed. The most common actions are to reset the variable to a specified value and to increment the variable by a specified value, but a variety of mathematical functions are available.

Table 9-14. Observations and statistics used in the PEST objective function for each USGS station used in the calibration

	Number of Observations Within Group	Weight Factor After Equalizing Contribution to Φ
Daily mean	*8767	1
Monthly minimum, maximum,	*288	1
Yearly minimum, maximum, and mean	*24	1
Differences between successive daily terms	*8766	1
Daily flow duration table	59	1.5
Daily time exceedance table	84	1.5
Monthly time exceedance table	84	2
Period of record minimum, maximum, mean, standard deviation, and median	5	1
Baseflow using USGS fixed window with a window of 31 days	*8736	1
Monthly mean of fixed window baseflow	*287	1
Yearly mean of fixed window baseflow	*24	1
Baseflow using USGS sliding window with a window of 31 days	*8736	1
Monthly mean of sliding window baseflow	*287	1
Yearly mean of sliding window baseflow	*24	1
Baseflow using USGS local minima with a window of 31 days	8736	1
Monthly mean of local minima baseflow	*287	1
Yearly mean of local minimum baseflow	*24	1

Table 9-14 -- *Continued*

	Number of Observations Within Group	**Weight Factor After Equalizing Contribution to Φ**
CV, all daily flows CV, log of all daily flows Mean daily flow / median daily flow Ratio, Q10 / Q90 for all daily flows Ratio, Q20 / Q80 for all daily flows Ratio, Q25 / Q75 for all daily flows (Q10 - Q90) / median daily flow (Q20 - Q80) / median daily flow (Q25 - Q75) / median daily flow Mean monthly flow, January… December	21	3
Mean minimum monthly flow, January…December CV of minimum monthly flows Mean minimum daily flow / mean median annual flow Mean minimum annual flow / mean annual flow Median minimum annual flow / median annual flow Ratio of baseflow volume to total flow volume CV of annual minimum flows Mean annual minimum flow divided by catchment area	19	3

* Actual number depends on period of record.

The special action facility is used to accommodate unique characteristics of a watershed, such as:

- Human intervention in a watershed. Events such as plowing, cultivation, fertilizer and pesticide application, and harvesting are simulated in this way.
- Changes to parameters. For example, a user may wish to alter the value of a parameter for which 12 monthly values cannot be supplied. This can be done by specifying a special action for that variable. The parameter could be reset to its original value by specifying another special action, to be taken later.

For this project, special actions were used to create the virtual sink/drainage well in closed basins and basins that have drainage wells.

Table 9-15. Total Actual ET (TAET) observation groups in the objective function.

Observation Group	Number of Observations Within Group	Weight Factor After Equalizing Contribution to Φ
Yearly average total ET for water	24	2
Yearly average total ET for developed open space	24	2
Yearly average total ET for developed low intensity	24	2
Yearly average total ET for developed medium intensity	24	2
Yearly average total ET for developed high intensity	24	2
Yearly average total ET for barren or mining	24	2
Yearly average total ET for forest	24	2
Yearly average total ET for shrub	24	2
Yearly average total ET for grass land	24	2
Yearly average total ET for pasture	24	2
Yearly average total ET for crops	24	2
Yearly average total ET for wetlands	24	2
Yearly maximum total ET for water	24	2
Yearly maximum total ET for forest	24	2
Yearly maximum total ET for shrub	24	2
Yearly maximum total ET for pasture	24	2
Yearly maximum total ET for wetlands	24	2

Surface FTABLEs

Water and wetlands tend to allow limited downward movement of water. Instead, water is stored at or near the surface. One result of this is that water and wetland areas have a larger potential for evapotranspiration. HSPF provides the option to use the FTABLES block to define surface outflow as a function of surface detention depth. This feature allows improved representation of the surface storage and attenuated surface runoff typical of wetlands.

This surface water storage option has been in HSPF for decades. However, it was only available along with a different view and interpretation of the standard HSPF hydrology. For the Water Supply Impact Study (WSIS), District staff added the option to use the surface water storage feature to standard HSPF hydrology. This change has been accepted and vetted by the developer of HSPF, RESPEC, and is available from RESPEC in easy to install Windows packages.

A surface FTABLE was developed for each water and wetland PERLND. Development of the storage-outflow relationship begins with the general function:

$$Q = ay^m$$

Where

Q = fraction of storage that runs off per hour

y = normalized depth above the invert

a, m = general coefficient and exponent

PEST is used to optimize the water and wetland storage-outflow relation by adjusting the depth of incipient flow and equation parameters.

CALIBRATION RESULTS

An important and underappreciated aspect of almost all published stream flow data is that stream flow data are not measured directly but calculated from a rating curve, which serves essentially as a model. Water stages are measured and flow rates corresponding to these stage readings are found using rating curves. When developing rating curves, results of individual flow measurements are plotted with their corresponding stages and stage-discharge relation curves are then developed. From these curves, rating tables are prepared that indicate the approximate discharge for any stage within the range of the measurements. For flows outside the range of the flow measurements, the curves are extrapolated using logarithmic plotting, velocity-area studies, and results of indirect measurements or peak discharge, such as slope area or contracted opening measurements.

If the stage discharge relationship is subject to change because of changes in the physical features that affect the gauge site, discharge is determined by the shifting-control method. In this method, correction factors based on individual discharge measurements and notes of personnel making the measurements are used when applying gauge heights to the rating tables. This method is also used if the stage discharge relationship is changed temporarily due to aquatic growth or debris on the control. Downstream flow obstructions may produce backwater effects that reach the gauge. Upstream obstructions may change the cross-sectional area.

Since there where many parts of the calibration fit in the objective function covering daily, monthly, annual and statistical features of flow, along with estimates of total evaporation, the overall problem with unmodeled hydrologic features is that the calibration will appear poor. If the long-term volumes match, the recharge and maximum saturated evapotranspiration estimates should be robust.

A very common measure of the performance of a hydrologic model is the Nash-Sutcliffe statistic (Moriasi et al. 2007). A Nash-Sutcliffe statistic equal to one is a perfect match between simulated and observed. A zero would mean that the average of the observations is a better model. Negative Nash-Sutcliffe values are possible, though they do not have a meaning. The Nash-Sutcliffe model performance categories are listed in Table 9-16. The spatial distribution of Nash-Sutcliffe values is show in Figure 9-26.

The calibration performance results for the watersheds are presented in Table 9-17. A total of 243 gauges within 50 HUC8 watersheds were used for calibration. Five HUC8 watersheds were ungauged and parameters were used from adjacent models to run them.

Figure 9-27 and Figure 9-28 compare measures of model performance against data quality. Note from the figures that the USGS has not identified any gauge as “Excellent” for 2009. The figures show that measures of model performance, like the Nash-Sutcliffe or percent bias, should not be the only way model performance is evaluated since these measures are also dependent on data quality. It can reasonably be asserted from Figure 9-27 and Figure 9-28 that the simulation is better than the data at representing the system because the simulation is constrained by mass balance, other gauges in the model and target evaporation values from literature.

Calibration plots and statistics are provided as appendices for all 243 gauges. These appendices are organized by model and named “Appendix T-XXXXXXXX” where “XXXXXXXX” is the HUC8 number of the model.

Table 9-16. Grading model calibration performance. Adapted from Moriasi et al. (2007)

Performance Rating	Percent Bias (Monthly)	Nash-Sutcliffe (Monthly)
Very good	< ±10	0.75 < NSE < 1.00
Good	±10 < PEM < ±15	0.65 < NSE < 0.75
Satisfactory	±15 < PEM < ±25	0.50 < NSE < 0.65
Unsatisfactory	> ±25	< 0.50

Table 9-17. Observed and simulated mean monthly flows, percent differences in flows, and Nash-Sutcliffe coefficients for monthly data. All flow values are in cubic feet per second (cfs). Contributing basins that are not in the active cells of the NFSEG MODFLOW model domain are indicated by an asterisk. Monthly Percent Bias and Monthly Nash-Sutcliffe Coefficient shading as used in Table 9-16

Model (HUC8)	HSPF Model Reach	Calibration Gauge	USGS Data Quality Water Year 2009*	Observed Mean Monthly (cfs)	Simulated Mean Monthly (cfs)	Monthly Percent Bias (%)	Monthly Nash-Sutcliffe
03050207	10	02175500	fair	280	282	-1	0.74
03050208	7	02176500	poor	123	109	11	0.76
03060101*	23	02185200		171	179	-5	0.83
	3	02186000	good	174	166	5	0.85
	7	02186645		115	114	1	0.92
	5	02186699	good	55	52	5	0.84
03060102*	1	02176930		208	161	22	0.75
	22	02177000	good	637	576	10	0.85
	18	02178400	good	178	142	20	0.70
	24	02181580	fair	58	293	-403	-25.55
				This gauge does not represent the entire flow from the upstream subwatersheds. It is located ABOVE the powerhouse discharge from Tallulah Falls Lake reservoir. Model flows should be significantly larger than gauge flows.			
	9	02182000		52	68	-30	0.68
				There is a diversion 2 miles upstream of gauge for the City of Toccoa water supply which isn't represented in the model. Model flows should be larger than gauge flows.			
03060103*	16	02187910	good	121	125	-3	0.82
	8	02188600	good	73	55	25	0.73
03060104*	16	02191300	fair	825	828	0	0.89
	5	02191743		163	177	-9	0.85
	21	02192000	good	1571	1506	4	0.92
03060105*	4	02193340	good	24	25	-1	0.82
	20	02193500	good	209	218	-4	0.85

Table 9-17 -- *Continued*

Model (HUC8)	HSPF Model Reach	Calibration Gauge	USGS Data Quality Water Year 2009*	Observed Mean Monthly (cfs)	Simulated Mean Monthly (cfs)	Monthly Percent Bias (%)	Monthly Nash-Sutcliffe
03060106	18	00219730B		134	126	6	0.11
				Very short period of record with less than 30 monthly values which impacts accurate calculation of fit statistics.			
	17	02195320	good	58	53	8	0.86
	20	02196690	good	167	151	9	0.68
	7	02197300		101	109	-7	-1.06
				Long term volumes are pretty good as indicated by the low monthly percent bias. The poor monthly Nash-Sutcliffe is caused by a mismatch to peaks.			
	23	02197310		218	215	2	0.54
	24	02197315		235	236	-1	0.47
				Long term volumes are pretty good, as indicated by the low monthly percent bias. The poor monthly Nash-Sutcliffe is caused by a mismatch to peaks.			
	13	02197400		70	64	8	0.37
	22	02197415		115	148	-29	0.78
				The fit and timing look good, however peaks are missed.			
	38	02197500	fair	9289	3210	65	-0.45
				Flow regulated by Thurmond Lake and other powerplants above gauge that are not explicitly included in the model.			
03060107*	15	02196000	good	305	322	-5	0.86
03060108	8	02197598	good	12	14	-23	0.24
	10	02197600		25	25	0	0.68
	19	02197830		422	382	10	0.87
	20	02198000	good	509	476	6	0.90
	9	02198100	good	25	18	28	0.52

Table 9-17 -- *Continued*

Model (HUC8)	HSPF Model Reach	Calibration Gauge	USGS Data Quality Water Year 2009*	Observed Mean Monthly (cfs)	Simulated Mean Monthly (cfs)	Monthly Percent Bias (%)	Monthly Nash-Sutcliffe
03070102	18	02223056	fair	2206	2482	-13	0.86
	14	02223110		268	272	-1	0.92
	5	02223190		159	68	57	0.45
	22	02223248	good	3478	3487	0	0.96
	7	02223360		103	78	24	0.82
	25	02223500	good	3973	3801	4	0.92
	28	02224500		4238	3804	10	0.90
03070103*	38	02204070	good	315	276	12	0.86
	1	02206500		256	230	10	0.85
	16	02207120	good	265	236	11	0.84
	19	02207220	good	345	316	8	0.81
	20	02207335	good	403	357	12	0.82
	2	02207448	fair	92	99	-7	0.83
	22	02208000		507	509	0	0.97
	39	02208450	good	232	200	14	0.89
	27	02210500	fair	1885	1655	12	0.89
	7	02211800		258	278	-8	0.90
	31	02212735		2042	2006	2	0.96
	33	02213000	good	2602	2371	9	0.89
03070104	6	02214590		127	151	-19	0.80
	19	02215000		3259	3122	4	0.92
	24	02215260		4377	4207	4	0.90
	28	02215500	good	5085	4896	4	0.86
03070105	1	02215900		221	215	3	0.90
	5	02216180	good	45	45	1	0.82

Table 9-17 -- *Continued*

Model (HUC8)	HSPF Model Reach	Calibration Gauge	USGS Data Quality Water Year 2009*	Observed Mean Monthly (cfs)	Simulated Mean Monthly (cfs)	Monthly Percent Bias (%)	Monthly Nash-Sutcliffe
03070106	3	02225000	good	10756	10024	7	0.89
	16	02226000	good	12439	11877	5	0.89
	11	02226100		166	166	0	0.83
03070107	7	02225270		481	370	23	0.82
	12	02225500	good	988	998	-1	0.93
03070201	13	02226362		402	402	0	0.91
	15	02226500	good	931	880	5	0.91
	10	02227270		208	120	42	0.65
	21	02228000	good	2009	1980	1	0.86
03070202	12	02227500	good	473	478	-1	0.83
03070204	4	02228500		112	114	-2	0.79
	6	02229000		95	63	34	0.58
				Includes part of watershed in Okefenokee Swamp, of which the area contribution to this subwatershed is indeterminate.			
	10	02229250		119	79	34	0.69
				Includes part of watershed in Okefenokee Swamp, of which the area contribution to this subwatershed is indeterminate.			
	14	02231000	good	534	484	9	0.86
03070205	4	02231268		15	18	-21	0.80
	7	02231280		38	35	7	0.78
	13	02231289		1087	306	72	-0.30
				Tidally influenced gauge with significant negative flows. HSPF can only simulate positive flow.			

Table 9-17 -- *Continued*

Model (HUC8)	HSPF Model Reach	Calibration Gauge	USGS Data Quality Water Year 2009*	Observed Mean Monthly (cfs)	Simulated Mean Monthly (cfs)	Monthly Percent Bias (%)	Monthly Nash-Sutcliffe
03080101	21	02231600	fair	189	250	-32	0.63
				Since April 1990, flow regulated to some extent by flood control lift gates (S161A), approximately 1.5 mi upstream from the gauge.			
	25	02232000	good	726	632	13	0.70
	29	02232400	fair	1087	958	12	0.71
	31	02232500	good	1314	1220	7	0.72
	11	02233104		103	90	13	0.58
	17	02233484	fair	298	235	21	0.74
	24	02233500	fair	329	256	22	0.69
	35	02234000	fair	1940	1705	12	0.77
	9	02234435	fair	167	180	-8	-0.27
				Affected by tide and wind driven currents on Lake Jesup.			
	39	02234500	fair	2214	2136	4	0.69
	7	02235000	fair	289	291	-1	0.66
	3	02235200	poor	57	80	-40	0.36
	42	02236000	good	2931	2924	0	0.67
	45	02236125	fair	3169	3323	-5	0.63

Table 9-17 -- *Continued*

Model (HUC8)	HSPF Model Reach	Calibration Gauge	USGS Data Quality Water Year 2009*	Observed Mean Monthly (cfs)	Simulated Mean Monthly (cfs)	Monthly Percent Bias (%)	Monthly Nash-Sutcliffe
03080102	25	02237293	fair	31	47	-51	0.61
				Managed water control system upstream of the gauge not represented in the HSPF model. Discharge computed from relation between discharge, head and spillway gate openings.			
	27	02237700	fair	53	56	-7	0.40
				Managed water control system upstream of the gauge not represented in the HSPF model. Discharge computed from relation between discharge, head and gate openings. Starting March 2, 2009, flow regulated by Nutrient Reduction Facility (NURF) which bypasses the lock and dam structure. Discharge is computed by the index velocity and stage in the NURF outlet channel and added to any structure discharge.			
	28	02238000	fair	142	133	6	0.66
	7	02238500	fair	152	153	-1	0.64
	4	02239501		591	612	-4	0.30
				Volume matches very well. Spring flow representation in HSPF is coarse and the timing suffers, as shown by the low Nash-Sutcliffe.			
	10	02240000	good	812	797	2	0.76
	13	02240500	fair	885	851	4	0.80
	31	02240902		51	29	43	0.59
				Since Dec. 23, 1956, flow regulated at station by manipulation of gates in spillway. Discharge computed from relation between discharge, head, gate openings and lockages.			

Table 9-17 -- *Continued*

Model (HUC8)	HSPF Model Reach	Calibration Gauge	USGS Data Quality Water Year 2009*	Observed Mean Monthly (cfs)	Simulated Mean Monthly (cfs)	Monthly Percent Bias (%)	Monthly Nash-Sutcliffe
03080102	31	02240902		51	29	43	0.59
				Since Dec. 23, 1956, flow regulated at station by manipulation of gates in spillway. Discharge computed from relation between discharge, head, gate openings and lockages.			
	32	02241000		23	30	-31	0.51
				Since Dec. 23, 1956, flow regulated at station by manipulation of gates in spillway. Discharge computed from relation between discharge, head, gate openings and lockages.			
	41	02243000	fair	46	52	-14	0.80
	47	02243960	fair	1051	1005	4	0.78
03080103	13	02244040	fair	4652	4638	0	0.59
	40	02244320		75	71	6	0.65
	41	02244420		81	108	-33	0.46
				Discharge represents net of much larger up-stream and downstream discharges.			
	46	02244440	fair	494	582	-18	0.36
				Affected by tide. Discharge represents net of much larger upstream and downstream discharg-es.			
	12	02244473		43	45	-5	0.70
	11	02245050		70	149	-114	-4.23
	9	02245140		56	43	22	0.67
	7	02245328		157	73	53	0.39
				Affected by tides.			
	19	02245500	good	128	130	-1	0.54
	21	02246000	good	174	176	-1	0.84
	25	02246025	fair	456	449	2	0.63
	2	02246318	fair	51	54	-7	0.71

Table 9-17 -- *Continued*

Model (HUC8)	HSPF Model Reach	Calibration Gauge	USGS Data Quality Water Year 2009*	Observed Mean Monthly (cfs)	Simulated Mean Monthly (cfs)	Monthly Percent Bias (%)	Monthly Nash-Sutcliffe
03080103	33	02246500	fair	7969	6909	13	0.16
				Affected by tide. Discharge represents net of much larger upstream and downstream discharg-es.			
03080201	23	02246895		319	20	94	-2.62
				Flow affected by tides.			
	26	02247015		34	34	2	0.39
				Flow affected by tides.			
	5	02247510	fair	50	55	-10	0.66
	15	02247598	poor	129	125	3	0.27
				Flow affected by tides.			
	9	02248000	fair	29	11	62	0.21
	12	02248053	poor	85	85	0	0.61
	8	02248060	poor	38	19	51	0.24
				Discharge not published some days due to bad velocity record. Flow affected by tides.			
03100207	29	02309421	fair	9	3	67	-0.35
	32	02309425	good	16	20	-24	0.24
	27	02310000	fair	58	53	9	0.65
	40	02310280	fair	5	14	-211	-4.76
	41	02310300	fair	21	38	-86	0.23
	18	02310525	fair	156	161	-3	0.52
	19	02310545	fair	173	170	2	0.55
	12	02310663	fair	100	150	-50	0.02
				Affected by tide.			
	7	02310688		59	61	-2	0.72

Table 9-17 -- *Continued*

Model (HUC8)	HSPF Model Reach	Calibration Gauge	USGS Data Quality Water Year 2009*	Observed Mean Monthly (cfs)	Simulated Mean Monthly (cfs)	Monthly Percent Bias (%)	Monthly Nash-Sutcliffe
03100207	9	02310700	poor	202	88	57	-2.70
				Affected by tide.			
	3	02310747	fair	463	34	93	-4.13
				Affected by tide.			
03100208	22	02311500	fair	154	152	1	0.57
	26	02312000	fair	238	214	10	0.63
	9	02312180	fair	39	22	43	0.45
	19	02312200	fair	61	46	24	0.59
	28	02312500	fair	300	282	6	0.68
	32	02312600	fair	300	312	-4	0.56
	6	02312640	fair	11	10	12	0.38
				Flow affected by mining operation upstream that is not represented in the HSPF model. The monthly percent bias is within allowable range, but the low Nash-Sutcliffe indicated poor match in timing caused by the mining operations. Expect little impact on the estimation of yearly recharge.			
	14	02312645		9	13	-45	-4.49
	23	02312700	fair	127	113	11	0.45
				Flow affected at times by backwater from Withlacoochee River. Expect little impact on the estimation of yearly recharge.			
	36	02312720	fair	455	488	-7	0.57
	37	02312722	poor	260	372	-43	-1.05
	41	02313000	fair	646	659	-2	0.65

Table 9-17 -- *Continued*

Model (HUC8)	HSPF Model Reach	Calibration Gauge	USGS Data Quality Water Year 2009*	Observed Mean Monthly (cfs)	Simulated Mean Monthly (cfs)	Monthly Percent Bias (%)	Monthly Nash-Sutcliffe
03100208	1	02313100	fair	622	688	-11	-3.61
				Discharge computed from relation between artesian pressure at Rainbow Springs well and discharge at measuring site. Representation of springs in HSPF is coarse.			
03110101	15	02313700	poor	183	207	-13	0.58
03110102	7	02324000		245	211	14	0.71
	18	02324400	fair	35	64	-82	0.05
				Natural flow affected by large groundwater withdrawals by cellulose plant.			
	19	02324500	fair	117	109	7	0.38
				Natural flow of stream affected by large groundwater withdrawals and subsequent discharge to the Fenholloway River by cellulose plant about 2.4 mi upstream.			
	20	02325000	fair	165	115	30	0.33
				Natural flow of stream affected by large groundwater withdrawals and subsequent discharge to the Fenholloway River by cellulose plant about 10 mi upstream. Flow affected by backwater from Spring Creek at times. Neither the withdrawal nor the backwater are represented in the HSPF model.			
	11	02326000	good	129	130	-1	0.76
03110103	9	02326526	poor	437	468	-7	-0.87
	20	02326550	poor	938	1045	-11	0.20
				Flow affected by tide, which HSPF cannot directly model. Monthly and longer frequency should match better as indicated by the acceptable monthly bias.			
03110201	44	00231427S		136	135	1	0.72
	45	02314500	fair	784	625	20	0.83

Table 9-17 -- *Continued*

Model (HUC8)	HSPF Model Reach	Calibration Gauge	USGS Data Quality Water Year 2009*	Observed Mean Monthly (cfs)	Simulated Mean Monthly (cfs)	Monthly Percent Bias (%)	Monthly Nash-Sutcliffe
03110201	24	02315000		1201	1163	3	0.90
	13	02315200		70	63	9	0.76
	31	02315500	fair	1469	1422	3	0.90
	34	02315550		1982	1997	-1	0.88
	0	02319500	good	5560	5143	8	0.88
03110202	27	02315920		294	290	1	0.85
	30	02316000	good	450	453	-1	0.87
	34	02317500	good	1072	1002	6	0.88
	36	02317620		975	903	7	0.84
03110203	15	00231774A		458	270	41	0.65
	16	02317755		241	173	28	0.76
				Short period of record.			
	18	02318500	good	1237	1086	12	0.83
	13	02318700	poor	233	161	31	0.73
	21	02319000	fair	1758	1546	12	0.82
	22	02319300	fair	1457	1487	-2	0.78
	23	02319394	fair	1982	1777	10	0.79
	44	02319500	good	5560	5131	8	0.88
03110204	1	02317797		101	84	16	0.87
	11	02318000	fair	492	470	5	0.90
	13	02318380		570	545	4	0.91
03110205	14	02319800	good	4803	4832	-1	0.87
	16	02320000	good	5115	4960	3	0.86
	21	02320500	good	6319	6185	2	0.82
	22	02323000	good	6930	7039	-2	0.75

Table 9-17 -- *Continued*

Model (HUC8)	HSPF Model Reach	Calibration Gauge	USGS Data Quality Water Year 2009*	Observed Mean Monthly (cfs)	Simulated Mean Monthly (cfs)	Monthly Percent Bias (%)	Monthly Nash-Sutcliffe
03110205	26	02323500	fair	8157	8485	-4	0.76
	29	02323592	fair	7407	7568	-2	0.74
03110206	7	02320700		32	32	-1	0.32
				Diversions occur at high stages to Lockloosa Creek that are not represented in the HSPF model. At high stages, HSPF simulated higher flows than the observations.			
	11	02321000	fair	136	115	15	0.73
	15	02321500	good	325	299	8	0.79
	17	02321975		772	784	-1	0.74
	18	02322500	fair	1170	1138	3	0.75
	5	02322700	poor	298	297	1	0.60
	21	02322800	fair	1510	1681	-11	0.69
03120001	5	02326900	poor	698	684	2	0.68
	26	02327022	poor	635	588	7	0.06
				Records affected by tide. HSPF should match monthly and longer frequency as indicated by the good match on percent bias. Suspect problems with the precipitation data from 1998 to 2005. Because of good matches outside that time period, recharge estimates are still good. Just model to observation statistics are poor.			
	8	02327033		117	66	44	0.25
				Suspect problems with the precipitation data from 1998 to 2005. Because of good matches outside that time period, recharge estimates are still good Just model to observation statistics are poor.			
03120002	23	02327355		186	180	3	0.94
	27	02327500	fair	525	519	1	0.91

Table 9-17 -- *Continued*

Model (HUC8)	HSPF Model Reach	Calibration Gauge	USGS Data Quality Water Year 2009*	Observed Mean Monthly (cfs)	Simulated Mean Monthly (cfs)	Monthly Percent Bias (%)	Monthly Nash-Sutcliffe
03110205	26	02323500	fair	8157	8485	-4	0.76
	29	02323592	fair	7407	7568	-2	0.74
03110206	7	02320700		32	32	-1	0.32
				Diversions occur at high stages to Lockloosa Creek that are not represented in the HSPF model. At high stages HSPF simulated higher flows than the observations.			
	11	02321000	fair	136	115	15	0.73
	15	02321500	good	325	299	8	0.79
	17	02321975		772	784	-1	0.74
	18	02322500	fair	1170	1138	3	0.75
	5	02322700	poor	298	297	1	0.60
	21	02322800	fair	1510	1681	-11	0.69
03120001	5	02326900	poor	698	684	2	0.68
	26	02327022	poor	635	588	7	0.06
				Records affected by tide. HSPF should match monthly and longer frequency, as indicated by the good match on percent bias. Suspect problems with the precipitation data from 1998 to 2005. Because of good matches outside that time period, recharge estimates are still good. Just model to observation statistics are poor.			
	8	02327033		117	66	44	0.25
				Suspect problems with the precipitation data from 1998 to 2005. Because of good matches outside that time period, recharge estimates are still good. Just model to observation statistics are poor.			
03120002	23	02327355		186	180	3	0.94
	27	02327500	fair	525	519	1	0.91

Table 9-17 -- *Continued*

Model (HUC8)	HSPF Model Reach	Calibration Gauge	USGS Data Quality Water Year 2009*	Observed Mean Monthly (cfs)	Simulated Mean Monthly (cfs)	Monthly Percent Bias (%)	Monthly Nash-Sutcliffe
03120003	4	02327100	fair	174	108	38	0.34
				One of multiple streams that drain a large wetland in the Apalachicola National Forest. Suspect problems with the precipitation data from 1998 to 2005. Because of good matches outside that time period, recharge estimates are still good. Just model to observation statistics are poor.			
	15	02328522	fair	826	842	-2	0.87
	16	02329000	good	1002	1112	-11	0.82
	6	02329600	fair	353	333	6	0.82
	8	02330000	fair	1573	1704	-8	0.83
	3	02330100	good	194	152	22	0.73
	10	02330150	fair	1797	1854	-3	0.80
03130005*	24	02344350	good	181	164	10	0.87
	27	02344396	good	181	174	4	0.94
	33	02344500	good	306	310	-1	0.85
	4	02344605		42	33	21	0.81
	22	02344630		40	43	-6	0.71
	23	02344700	good	121	107	11	0.77
	36	02344872	good	738	762	-3	0.92
	44	02347500	good	1925	1877	3	0.86
03130006	29	02349500		3306	2932	11	0.72
	31	02349605	good	3069	2864	7	0.77
	7	02349900	good	41	43	-6	0.78
	43	02350512	good	4114	3782	8	0.81

Table 9-17 -- *Continued*

Model (HUC8)	HSPF Model Reach	Calibration Gauge	USGS Data Quality Water Year 2009*	Observed Mean Monthly (cfs)	Simulated Mean Monthly (cfs)	Monthly Percent Bias (%)	Monthly Nash-Sutcliffe
03130007	17	02350600	good	193	174	10	0.80
	26	02350900	good	522	508	3	0.84
	18	02351500	good	132	135	-2	0.78
	25	02351890	good	382	371	3	0.77
03130008	23	02353000	good	5815	5704	2	0.81
	24	02355662	good	6375	6717	-5	0.86
	29	02356000	good	6577	7186	-9	0.84
03130009	27	02353265	good	278	281	-1	0.90
	22	02353400	good	220	180	18	0.67
	32	02353500	good	664	646	3	0.85
	10	02354440		67	71	-7	0.83
	28	02354500	good	254	290	-14	0.85
	34	02354800	good	890	940	-6	0.92
	35	02355350	good	856	898	-5	0.88
03130010	18	02357000	good	491	489	0	0.87
03130013	6	02330400	fair	260	222	15	0.63

* Blank cells in the “USGS Data Quality Water Year 2009” column do not have any data collected in water year 2009

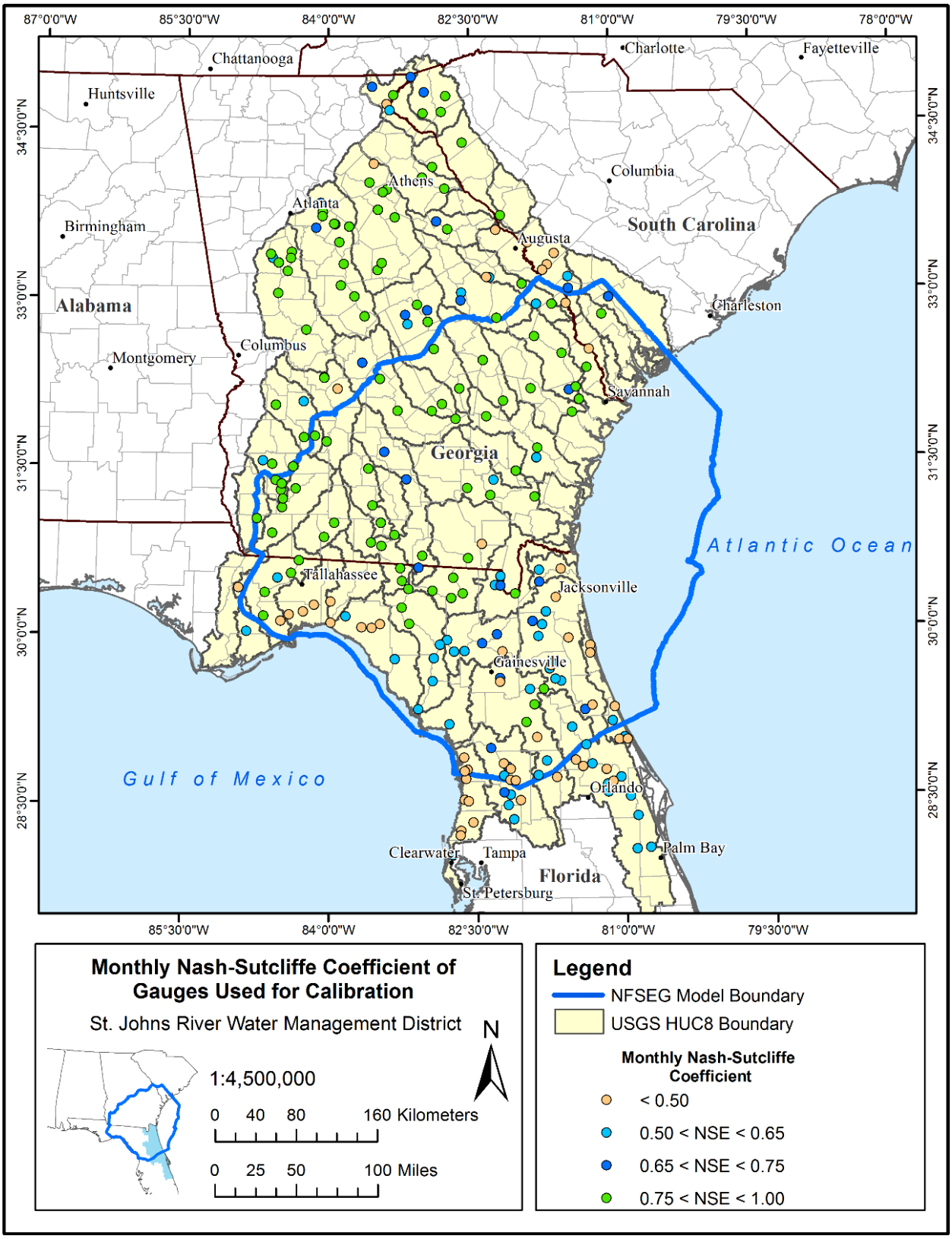

Figure 9-26. Map showing Nash-Sutcliffe values for model calibrations at individual gauges over the NFSEG model domain

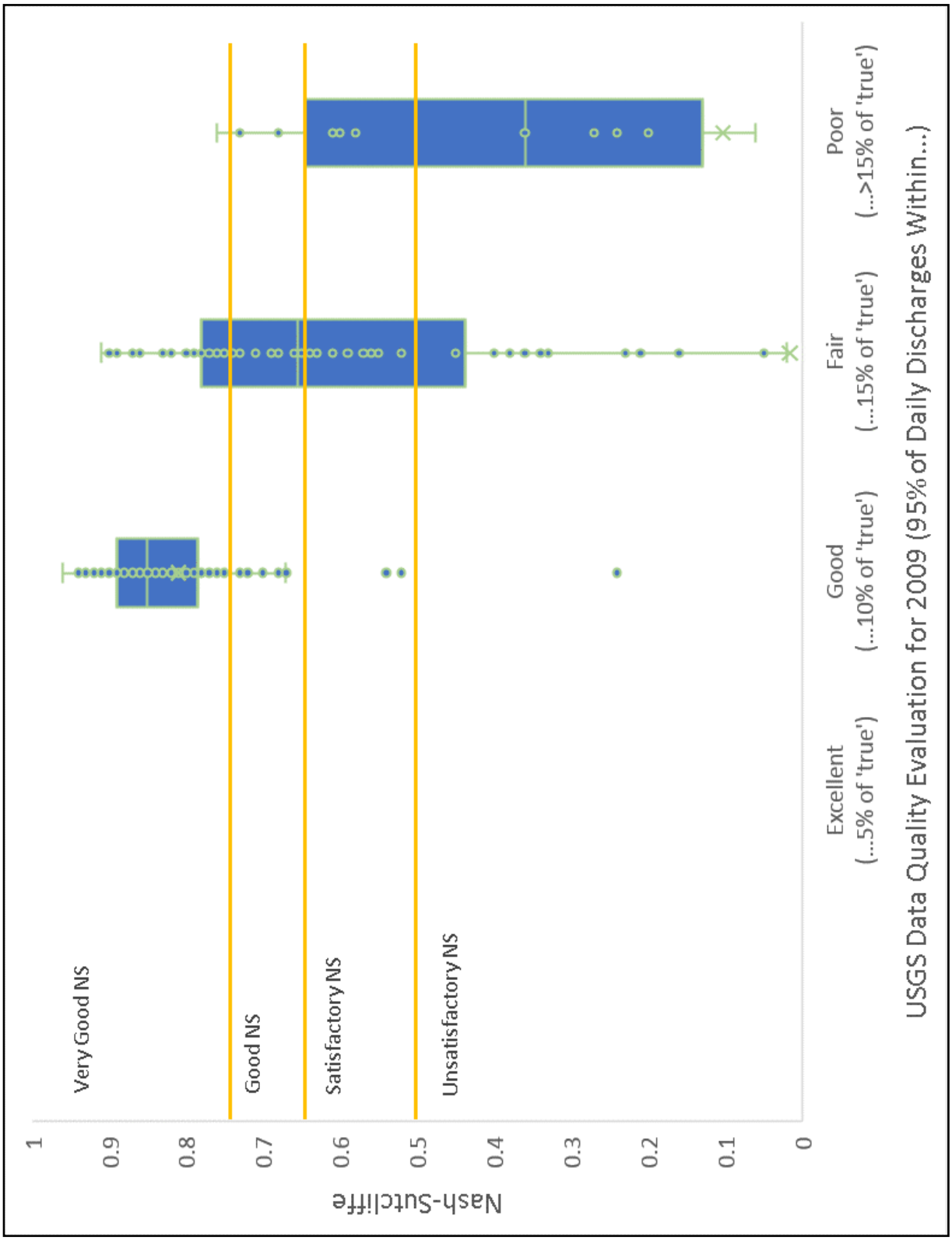

Figure 9-27. Nash-Sutcliffe efficiency values plotted against USGS data quality evaluation

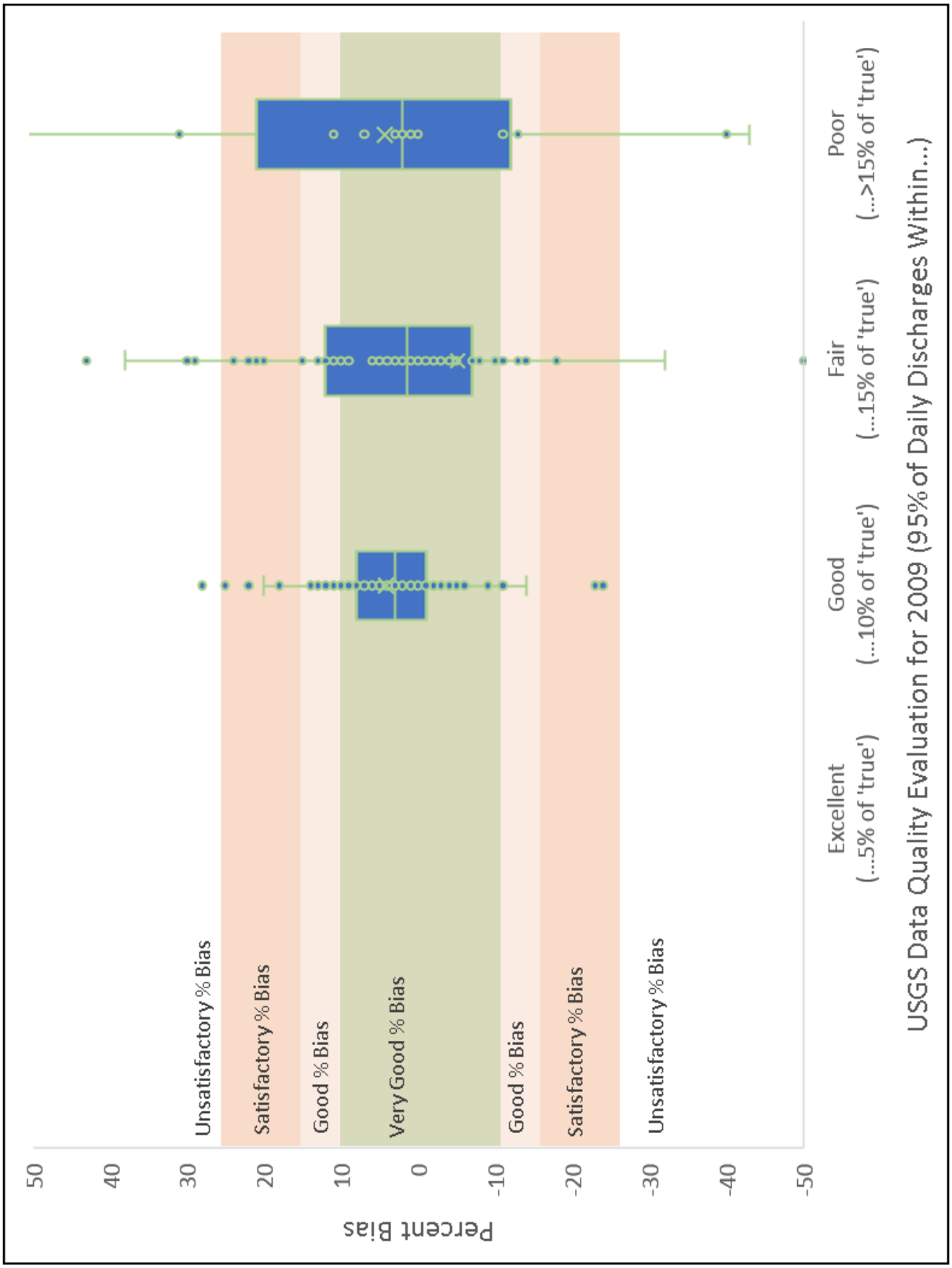

Figure 9-28. Percent bias chart plotted against USGS data quality evaluation

CHAPTER 10. SUMMARY AND CONCLUSIONS

The NFSEG model was developed through a collaborative effort over several years among a technical team of experts from SJRWMD, SRWMD, SWFWMD, and stakeholders from water utilities, private industry, governmental organizations, and environmental groups. The technical team's directive was to ensure appropriate science was applied to the modeling and data analysis to support decision making, and that the work completed was defensible, understood by the team, and collaboratively developed, as described in the Partnership's charter, which is available at northfloridawater.com. The model was designed to be a tool that can be used to evaluate inter-district and inter-state groundwater pumping effects, as well as effects within an individual district. A primary function of the model is to simulate the regional effects of pumping on groundwater levels, stream base flows, and spring flows. Intended applications of the model include evaluations of proposed consumptive use permits, support of analyses of minimum flows and levels, and water supply planning.

The NFSEG model covers about 60,000 square miles, encompassing a large area of the Floridan aquifer system in north Florida, Georgia, and South Carolina (Figure 1-1). Land surface elevations range from sea level to more than 450 feet, NAVD88 in northern Georgia. The area includes hundreds of streams, rivers, lakes and more than 300 springs. NFSEG v1.1 is a three-dimensional, steady state model. The model was calibrated to 2001 and 2009 hydrologic conditions and successfully validated using 2010 conditions. The model consists of seven aquifer layers that represent, from top to bottom, the surficial aquifer system, the intermediate confining unit, the Upper Floridan aquifer, the middle semi-confining unit, the upper zone of the Lower Floridan aquifer, the lower semi-confining unit, and the Fernandina Permeable zone of the Lower Floridan aquifer, where these hydrogeologic units are present.

The model development process included delineation of the model domain, a listing of necessary data, a plan for attainment of the data, a plan for the model configuration, including an approach to model layering, lateral boundary conditions, internal boundary conditions, selection of calibration periods and the calibration process. Two of the more important water budget components are recharge and maximum saturated evapotranspiration (MSET). To improve estimates of recharge and MSET for groundwater model input, surface water hydrology for all the surface water basins within the groundwater model boundary were simulated using the Hydrological Simulation Program - FORTRAN (HSPF) software (Bicknell et al. 2001). HSPF is a comprehensive, rainfall-runoff water quality model. Calibration of HSPF models to observed surface water flows represents a significant improvement in estimation of recharge and MSET over the previous Soil Conservation Service (SCS) curve number model and approach. The SCS model does not track evaporation and infiltration, which are important components

of the surface water balance. Based on the nonlinear uncertainty analysis, recharge and maximum saturated ET multipliers appeared to be the parameters with the lowest uncertainty. This could be because both recharge and maximum saturated ET values were obtained from HSPF models, which were also calibrated using many observations.

The NFSEG model encompasses all or parts of seven large and diverse groundwater basins. The hydrogeology of much of the area is extremely complex because of its karstic nature. For example, the area contains numerous closed basins, direct stream to sink discharges, as well as more than 300 springs, which are a major source of groundwater discharge in key areas of the model domain. Observed groundwater levels in the surficial and Floridan aquifer system ranged from -50 ft to more than 350 ft NAVD88 in 2009. Areas of groundwater levels that are below sea level occur on the Atlantic coast (near Fernandina Beach, Florida, and Brunswick and Savannah, Georgia). These areas are characterized by unusually large horizontal gradients of the potentiometric surface of the Upper Floridan aquifer.

The model was calibrated using Parameter ESTimation (PEST), a program widely used to facilitate model calibration. The PEST calibration process involved minimizing differences between various types of observations and their model simulated equivalents through adjustment of specified model parameters within defined ranges. Observation types included groundwater levels, differences in vertical and horizontal groundwater levels, spring flows and baseflows. Formal consultation and interactions with the NFSEG technical team, stakeholders, and peer-review panel were conducted throughout the model development process to avoid potential oversights and inappropriate approaches.

Emphasis of numerous types of calibration targets and goals, in addition to groundwater levels, supported a more realistic simulation of many different aspects of the groundwater flow system, as over-reliance on groundwater level targets can result in unrealistic estimates of model hydraulic parameters. Inclusion of many observation types serve to lower the uncertainty of parameters to which they are sensitive. Because predictions of interest are also sensitive to these parameters whose uncertainties were reduced by these observations, their uncertainties would have been correspondingly reduced. This was likely partially responsible for the relatively low uncertainties that were associated with most of the predictions (particularly those associated with predictive differences) made by the NFSEG model, as quantified by the nonlinear uncertainty analysis.

The 2001 and 2009 steady state simulations yielded reasonable head and springflow residuals. Although some of the calibration goals were not fully met, the percentages of the groundwater level residuals within 2.5 and 5 feet, generally indicate a good match between observed and corresponding simulated values. It is important to note that the calibration goals were not intended as absolute requirements but as ambitious goals, as stated in the model conceptualization report.

Geographic patterns in the transmissivity of Layer 3, which represents the Upper Floridan aquifer in areas in which the middle confining unit is present, and upper zone of the Upper Floridan aquifer elsewhere, were consistent with expected patterns based on the hydrology and hydrogeology of the model domain. For example, model calibrated values of transmissivity were low in areas with expected low transmissivity in the general

area of the Gulf Trough in Georgia, Mallory Swamp in Lafayette County, Florida, and Waccasassa Flats in Gilchrist and Levy counties, Florida. Similarly, model calibrated values of transmissivity were high in areas where high transmissivity values are expected, including the Rainbow and Silver springs basins, the Suwannee River corridor, the Santa Fe River Basin, including areas near the Ichetucknee River and High Springs Gap physiographic region and the Woodville Karst Plain. Comparisons to the results of aquifer performance tests (APTs) were generally within an order of magnitude in confined areas of the Floridan aquifer system. In unconfined areas of the Floridan aquifer system, the comparison was somewhat less favorable, but this may be due, at least partially, to complications associated with the karstic nature of the flow system in these areas (e.g., APTs may considerably underestimate hydraulic conductivity values if the pumping well does not penetrate a conduit system). The leakance of Layer 2, which represents the intermediate confining unit where it is present, was generally high in areas in which the intermediate confining unit is thin or absent and relatively low where it is present, as expected. Therefore, the results of the calibration, with respect to the transmissivity distribution of the Upper Floridan aquifer and leakance of the intermediate confining unit, were determined to be reasonable.

The simulation of groundwater flow for the year 2010 was conducted as a verification run, as the model was not calibrated to 2010 conditions. Comparisons of simulated and observed groundwater levels and flows indicated a reasonable correspondence between observed groundwater levels and spring flows. The general configuration of the 2010 simulated potentiometric surface of the Upper Floridan aquifer compared well to that of the observed 2010 potentiometric surface. As stated in Chapter 5 of this report, the results of the 2010 verification simulation are an additional indication of the quality of the model calibration.

The pumps off simulation, described in Chapter 5, represents another test of the ability of the model to simulate a condition to which it was not calibrated, to a much greater extent than the 2010 result. The results indicated a reasonable comparison to the configuration of the USGS estimated predevelopment potentiometric surface of the Upper Floridan aquifer and to the flows of major springs observed in the early 1930s, a period that preceded widespread development of the Floridan aquifer system in the area. The simulated groundwater levels of the Upper Floridan aquifer were generally lower than the corresponding groundwater levels, as shown on the USGS predevelopment potentiometric surface, within about 10 feet in many areas but up to 15 feet in some. According to Johnson et al. (1980), the purpose of the USGS map was not to show precise water level data at specific sites; rather, to show the best estimate of the configuration of the predevelopment potentiometric surface using the best available data at that time. Thus, the results of the pumps-off simulation indicated a reasonable simulation of the change in the configuration of the potentiometric surface in response to the removal of pumping stresses, a condition that represents a major departure from the general conditions to which the model was calibrated.

The model was calibrated and configured in a manner that was consistent with generally accepted standards to enable reliable fulfillment of its intended uses. In particular, a wide variety of observation types were employed in the development of the model, including observations that are directly and indirectly related to the head and flow

predictions of interest. In addition, predictive uncertainty analyses indicated that the model is capable of simulating changes in flows and groundwater levels with an accuracy that is comparable to or better than models currently used for planning or regulatory purposes. The uncertainty analyses also indicated that the model performed better at predicting the differences than absolute values of groundwater levels and flows. This could be mainly because predictive errors potentially resulting from model approximation of real system tend to cancel when predictive differences are computed. It should also be noted that NFSEG v1.1 will mostly be used to predict differences rather than absolute values.

LITERATURE CITED

Annable, M. D., L. H. Motz, D. S. Knapp, G. D. Sousa, and W. D. Beddow II. 1996. *Investigation of Lake and Surficial Aquifer Interaction in the Upper Etonia Creek Basin.* SJRWMD Special Publication SJ96-SP15. Palatka, Fla.: St. Johns River Water Management District.

Barker, R. A., and M. Pernik. 1994. *Regional Hydrology and Simulation of Deep Ground-Water Flow in the Southeastern Coastal Plain Aquifer System in Mississippi, Alabama, Georgia, and South Carolina.* Report 1410–C. U. S. Geological Survey.

Barlow, P. M., W. L. Cunningham, T. Zhai, and M. Gray. 2015. *U.S. Geological Survey groundwater toolbox, a graphical and mapping interface for analysis of hydrologic data (version 1.0): user guide for estimation of base flow, runoff, and groundwater recharge from streamflow data,* p.40. Technical Report 3-B10. Reston, Va.: U. S. Geological Survey.

Bellino, J. C. 2011. Albers Equal Area Map Custom Projection Specifications. U.S. Geological Survey, Lutz, Fla.

Bicknell, B. R., J. C. Imhoff, J. L. Kittle Jr., T. H. Jobes, and A. S. Donigan Jr. 2001. *Hydrological Simulation Program– Fortran (HSPF): User's manual for release 12.* U.S. Environmental Protection Agency: Athens, Ga.

Brooks, R., J. S. Clarke, and R. E. Faye. 1985. *Hydrogeology of the Gordon Aquifer System of East-Central Georgia*. Geologic Survey Information Circular 75. Atlanta, Ga.: Department of Natural Resources, Environmental Protection Division, Georgia Geologic Survey.

Bush, P. W., and R. H. Johnston. 1988. *Ground-water hydraulics, regional flow, and ground-water development of the Floridan aquifer system in Florida and in parts of Georgia, South Carolina, and Alabama.* Report 1403–C. U.S. Geological Survey.

[CDM] Camp Dresser and McKee Inc. 2017. Aquifer performance test report (unpublished).

Chen, M., W. Shi, P. Xie, V. B. S. Silva, V. E. Kousky, R. Wayne Higgins, and J. E. Janowiak. 2008. Assessing objective techniques for gauge-based analyses of global daily precipitation. *Journal of Geophysical Research: Atmospheres* 113(D4).

Clark, W. E., R. H. Musgrove, C. G. Menke, and J. W. Cagle, Jr. 1963. *Hydrology of Brooklyn Lake near Keystone Heights, Florida.* Investigation 33. Tallahassee, Fla.: Florida Geological Survey.

Clarke, J. S., C. M. Hacke, and M. F. Peck. 1990. *Geology and Ground-Water Resources of the Coastal Area of Georgia.* Bulletin 113. Department of Natural Resources Environmental Protection Division, Georgia Geologic Survey.

Clarke, J. S., D. C. Leeth, D. Taylor-Harris, J. A. Painter, and J. L. Labowski. 2004. *Summary of Hydraulic Properties of the Floridan Aquifer System in Coastal Georgia and Adjacent Parts of South Carolina and Florida.* Scientific Investigations Report 2004–5264. Reston, Va.: U.S. Geological Survey.

Connect Consulting Inc. 2009. Aquifer performance test report (unpublished).

Daly, C., R. P. Neilson, and D. L. Phillips. 1994. A Statistical-Topographic Model for Mapping Climatological Precipitation over Mountainous Terrain. *Journal of Applied Meteorology* 33(2): 140-158.

Davis, H. 1996. *Hydrogeologic Investigation and Simulation of Ground-Water Flow in the Upper Floridan Aquifer of North-Central Florida and Southwestern Georgia and Delineation of Contributing Areas for Selected City of Tallahassee, Florida, Water-Supply Wells*, p.56. Report 95–4296. Tallahassee, Fla.: U.S. Geological Survey.

Davis, J. N.d. Hydrostratigrahic markers of the Florida Aquifer System. St. Johns River Water Management District, Palatka, Fla.

Davis, J., and D. Boniol. N.d. GIS Hydrogeologic Horizons of the Floridan Aquifer System (Draft).

Davis, J. H., and B. G. Katz. 2007. *Hydrologic Investigation, Water Chemistry Analysis, and Model Delineation of Contributing Areas for City of Tallahassee Public-Supply Wells, Tallahassee, Florida.* Scientific Investigations Report 2007–5070. Reston, Va.: U.S. Geological Survey.

Davis, J. H., B. G. Katz, and D. W. Griffin. 2010. *Nitrate-N Movement in Groundwater from the Land Application of Treated Municipal Wastewater and Other Sources in the Wakulla Springs Springshed, Leon and Wakulla Counties, Florida, 1966-2018*, p.104. Scientific Report 2010–5099. Reston, Va.: U.S. Geological Survey.

Deevey, E. S. 1988. Estimation of downward leakage from Florida lakes. *Limnology and Oceanography* 33(6):1308–1320.

Desmarais, T. 2016. October 16 2016 NFSEG v1.1 RIV/DRN Program: 201612_nfseg_RIVDRNmerge. Unpublished program. St. Johns River Water Management District, Palatka, Fla.

Doherty, J. 2010a. *PEST, Model-independent parameter estimation User Manual, 5th Edition.* User Manual (with slight additions). Brisbane, Australia: Watermark Numerical Computing.

———. 2010b. *PEST, Model-independent parameter estimation--User Manual, 5th Edition.* User Manual. Brisbane, Australia: Watermark Numerical Computing.

———. 2016. *PLPROC A Parameter List Processor* Australia: Watermark Numerical Computing and National Centre for Groundwater Research and Training.

———. 2015. *Calibration and Uncertainty Analysis for Complex Environmental Models PEST: complete theory and what it means for modelling the real world.* Brisbane, Australia: Watermark Numerical Computing.

———. 2016a. *PEST Model-Independent Parameter Estimation User Manual Part I: PEST, SENSAN and Global Optimisers* User Manual a. Watermark Numerical Computing.

———. 2016b. *PEST Model-Independent Parameter Estimation User Manual Part II: PEST Utility Support Software* User Manual b. Watermark Numerical Computing.

Doherty, J., and D. Welter. 2010. A short exploration of structural noise. *Water Resource Research* 46(W05525): 1-14.

Douglas, E. M., J. M. Jacobs, D. M. Sumner, and R. L. Ray. 2009. A comparison of models for estimating potential evapotranspiration for Florida land cover types. *Journal of Hydrology* 373(3-4): 366-376.

Durden, D. 2012. *Data Availability for Development of the North Floridan Southeast Georgia (NFSEG) Regional Groundwater Flow Model in the Area of Its Potential Domain.* Report to NFSEG Technical Team Palatka, Fla.: St. Johns River Water Management District.

Durden, D., T. Cera, and N. Johnson. 2013a. *North Florida Southeast Georgia (NFSEG) Groundwater Flow Model Conceptualization.* Report to NFSEG Technical Team. Palatka, Fla.: St. Johns River Water Management District.

———. 2013b. *North Florida Southeast Georgia (NFSEG) Groundwater Flow Model Conceptualization.* Report to NFSEG Technical Team Palatka, Fla.: St. Johns River Water Management District.

Dykehouse, T. L. 1998. *Water Budget and Vertically Averaged Vertical Conductance for Lake Geneva.* Master's thesis. Gainesville: University of Florida

Dymond, J. R., and R. Christian. 1982. Accuracy of discharge determined from a rating curve. *Hydrological Sciences Journal* 27(4): 493-504.

Ewel, K. C., and J. E. Smith. 1992. Evapotranspiration From Florida Pond Cypress Swamps. *Water Resources Bulletin* 28(2): 299-304.

Falls, W. F., L. G. Harrelson, and M. D. Petkewich. 2005. *Hydrogeology, Water Quality, and Water-Supply Potential of the Lower Floridan Aquifer, Coastal Georgia, 1999-2002.* Scientific Investigations Report 2005–5124. Reston, Va.: U.S. Geological Survey.

Faulkner, G. L. 1973. *Geohydrology of the cross-Florida barge canal area, with special reference to the Ocala vicinity.* WRI-73-1. U.S. Geological Survey.

Fenneman, N. M., and D. W. Johnson. 1946. *Physical Divisions of the United States.* Map

Reston, VA: U.S. Geological Survey.

Florida Geological Survey (previously Southeastern Geological Society). 1986. *Hydrogeological units of Florida.* State of Florida Department of Natural Resources Report 28. Tallahassee, Fla.: Florida Geological Survey.

Geurink, J., and B. Ross. 2013. *Development, Calibration, and Evaluation of the Integrated Northern Tampa Bay Hydrologic Model*, p.916. Technical Publication Brooksville, Fla.: Southwest Florida Water Management District.

Gordu, F., D. Durden, and T. Grubbs. 2016. Development and Calibration of the North Florida Southeast Georgia Groundwater Model (NFSEG V1.0) (Draft). Palatka, Fla.: St. Johns River Water Management District.

Graham, W., and L. Staal. 2010. *District Water Supply Plan 2010; SJRWMD/SRWMD Northeast Florida Water Supply Planning Area.* Summary Report Gainesville, Fla.: University of Florida, Water Institute.

Harbaugh, A. W. 2005. MODFLOW-2005: the U.S. Geological Survey modular groundwater model--the ground-water flow process. *Techniques and Methods*: 6-A16: p. various.

Harmel, R.D., R.J. Cooper, R.M. Slade, R.L. Haney, and J.G. Arnold. 2006. Cumulative uncertainty in measured streamflow and water quality data for small watersheds. *Transactions of the ASABE* 49(3): 689-701.

Hayes, E. C. 1981. *The surficial aquifer in east-central St Johns County, Florida.* Water-Resources Investigations 81–14. Tallahassee, Fla.: U.S. Geological Survey.

Higgins, R. W., W. Shi, E. Yarosh, and R. Joyce. 2000. *Improved United States precipitation quality control system and analysis.* NCEP/Climate Prediction Center Atlas No. 7. Camp Springs, Md.: National Oceanic and Atmospheric Administration, National Weather Service.

Hill, M. C., and C. R. Tiedeman. 2007. *Effective Groundwater Model Calibration: With Analysis of Data, Sensitivities, Predictions, and Uncertainty.* New York: John Wiley & Sons, Inc.

Hirsch, J. D., and A. F. Randazzo. 2000. *Hydraulic Seepage Within an Astatic Karst lake, North-Central Florida,* p. 159–164. Proceedings of The IAH Congress on Groundwater.

Institute of Hydrology. 1980. *Low Flow Studies Report No. 1.* Wallingford, GB: Institute of Hydrology.

Intera, Inc. 2011. *Adaptation of the USGS MegaModel for the Prediction of 2030 Groundwater Impacts.* Special Publ. SJ2012-SP9. Palatka, Fla.: St. Johns River Water Management District.

——— 2014. *Updates and Re-Calibration of the North Florida Groundwater Model*. Live Oak, Fla.: Suwannee River Water Management District.

Jacobs, J. M., S. L. Mergelsberg, A. F. Lopera, and D. A. Myers. 2002. Evapotranspiration from a wet prairie wetland under drought conditions: Paynes Prairie Preserve, Florida, USA. *Wetlands* 22(2): 374-385.

Johnston, R. H., and P. W. Bush. 1988. *Summary of the hydrology of the Floridan aquifer system in Florida and in parts of Georgia, South Carolina, and Alabama.* Professional Paper 1403-H. Washington, D.C.: U.S. Geological Survey.

Johnston, R. H., R.E. Krause, F.W. Meyer, P.D. Ryder, C.H. Tibbals, and J.D. Hunn. 1980. *Estimated potentiometric surface for the Tertiary limestone aquifer system, southeastern United States, prior to development.* Open-File Report Numbered Series 80-406 (Map). U.S. Geological Survey.

Kellam, M. F., and L. L. Gorday. 1990. *Hydrogeology of the Gulf Trough-Apalachicola Embayment Area, Georgia.* Bulletin 94. Atlanta: Georgia Department of Natural Resources Environmental Protection Division, Georgia Geologic Survey.

Kennedy, E. J. 1983. *Computation of Continuous Records of Streamflow*. In Techniques of Water Resource Investigations, Book 3, Chapter A13. U.S. Geological Survey.

Kinnaman, S. L., and J. F. Dixon. 2009. *Potentiometric Surface of the Upper Floridan Aquifer in the St. Johns River Water Management District and Vicinity, Florida.* USGS Scientific Investigations Map 3091. Orlando, Fla.: U.S. Geological Survey.

———. 2011. *Potentiometric Surface of the Upper Floridan Aquifer in Florida and parts of Georgia, South Carolina, and Alabama, May – June 2010*. Scientific Investigations Map 3182. Fla.: U.S. Geological Survey.

Kleinfelder Consulting Inc. 2017. Aquifer performance test report (unpublished).

Knowles, Jr., L. 1996. *Estimation of evapotranspiration in the Rainbow Springs and Silver Springs basins in North-Central Florida*. Water-Resources Investigations 96–4024. Tallahassee, Fla.: U.S. Geological Survey.

———, L., Jr., 2001, *Potentiometric surface of the Upper Floridan aquifer in the St. Johns River Water Management District and vicinity, Florida, May 2001.* Open File Report 01-313, prepared in cooperation with St Johns River Water Management District, South Florida water Management District, Southwest Florida Water Management District. Fla.: U.S. Geological Survey.

Knowles, Jr., L., and S. L. Kinnaman. 2001, September. *Potentiometric Surface of the Upper Floridan Aquifer in the St. Johns River Water Management District and Vicinity, Florida*. Map 02-182. Fla.: U.S. Geological Survey.

Knowles, Jr., L., A. M. O'Reilly, and J. C. Adamski. 2002. *Hydrogeology and simulated effects of ground-water withdrawals from the Floridan aquifer system in Lake County*

and in the Ocala National Forest and vicinity, north-central Florida. Water-Resources Investigations Report 2002-4207. Fla.: U.S. Geological Survey.

Krause, R. E. 1979. *Geohydrology of Brooks, Lowndes, Western Echols Counties, Georgia.* Water-Resources Investigations Report 78–117. Doraville, Ga.: U.S. Geological Survey.

Krause, R. E., and R. B. Randolph. 1989. *Hydrology of the Floridan Aquifer System in Southeast Georgia and Adjacent Parts of Florida and South Carolina.* Professional Paper 1403-D. U.S. Geological Survey.

Kuniansky, E. L., J. C. Bellino, and J. F. Dixon. 2012. *Transmissivity of the Upper Floridan aquifer in Florida and parts of Georgia, South Carolina, and Alabama*. Scientific Investigations Map 3204. Tampa, Fla.: U.S. Geological Survey.

Kuniansky, E. L. 2016. *Simulating Groundwater Flow in Karst Aquifers with Distributed Parameter Models— Comparison of Porous-Equivalent Media and Hybrid Flow Approaches.* Scientific Investigations Report 2016–5116. Reston, Va.: U.S. Geological Survey.

Lane, E. (Edward). 2001. *The Spring Creek Submarine Springs Group, Wakulla County, Florida*. Special publication 47. Tallahassee, Fla.: Florida Geological Survey.

Lee, T.M., and A. Swancar. 1997. Influence of evaporation, ground water, and uncertainty in the hydrologic budget of Lake Lucerne, a seepage lake in Polk County, Florida. *U.S. Geological Survey Water Supply Paper*. 2439: 1-57.

Lin, Z. 2011. Estimating Water Budgets and Vertical Leakages for Karst Lakes in North-Central Florida (United States) Via Hydrological Modeling. *Journal of the American Water Resources Association* 47(2):287-302.

Liu, W., Y. Hong, S. I. Khan, M. Huang, B. Vieux, S. Caliskan, and T. Grout. 2010. Actual evapotranspiration estimation for different land use and land cover in urban regions using Landsat 5 data. *Journal of Applied Remote Sensing* 4(1): 041873.

Long, A. F. 1989. *Hydrologeology of the Clayton and Claiborne Aquifer Systems.* Hydrologic Atlas 19. Atlanta, Ga.: Georgia Department of Natural Resources, Environmental Protection Division, Georgia Geologic Survey.

Lowe, E. F., L. E. Battoe, H. Wilkening, M. Cullum, and T. Bartol. 2012. *St. Johns River Water Supply Impact Study*. Technical Publication SJ2012-1. Palatka, Fla.: St. Johns River Water Management District.

Lu, J., G. Sun, S. G. McNulty, and D. M. Amatya. 2003. Modeling actual evapotranspiration from forested watersheds across the Southeastern United States. *Journal of the American Water Resources Association (JAWRA)*39(4): 887-896.

Mao, L. M., M. J. Bergman, and C. C. Tai. 2002. Evapotranspiration measurement and estimation of three wetland environments in the Upper St Johns River. *Journal of the*

*American Water Resources Association (JAWRA)*38(5): 1271-1285.

McFadden, S. S., and P. D. Perriello. 1983. *Hydrogeology of the Clayton and Claiborne Aquifers in Southwestern Georgia.* Information Circular 55. Atlanta, Ga.: Department of Natural Resources Environmental Protection Division, Georgia Geologic Survey.

McGurk, B., P. F. Preseley. 2002. *Simulation of Effects of Groundwater Withdrawals from the Floridan Aquifer System in East-Central Florida: Model Expansion and Revision.* Technical Publ. SJ2002-3. Palatka, Fla.: St. Johns River Water Management District.

McKay, L., T. Bondelid, T. Dewald, C. Johnston, R. Moore, and A. Rea,. 2013. *NHDPlus Version 2: User Guide (Data Model Version 2.1)*. United States Department of Environmental Protection and U. S. Geological Survey.

Merritt, M. L. 2001. *Simulation of the Interaction Karstic Lakes Magnolia and Brooklyn with the Upper Floridan Aquifer, Southwestern Clay County, Florida.* Water-Resources Investigations Report 00–4204. Tallahassee, Fla.: U.S. Geological Survey.

Miller, J. A. 1986. *Hydrogeologic Framework of the Floridan Aquifer System in Florida and in Parts of Georgia, South Carolina, and Alabama.* Professional Paper 1403-B. Washington D.C.: U.S. Geological Survey.

———. J. A. 1990. Segment 6 Alabama, Florida, Georgia, and South Carolina. In *Ground Water Atlas of the United States,* Hydrologic Investigations Chapter 730-G. Reston,Va.: U. S. Geological Survey.

———. J. A. 1991. Top of the lower semiconfining unit, thickness of the lower semiconfining unit. Personal Communication. U. S. Geological Survey.

Milliman, J. D. 1972. *Atlantic continental shelf and slope of the United States; petrology of the sand fraction of sediments, northern New Jersey to southern Florida.* Numbered Series 529-J. Washington, D.C.: U. S. Geological Survey.

Moore, K. 2007. *BASINS Technical Note 2: Two Automated Methods for Creating Hydraulic Function Tables (FTABLES).* EPA BASINS Technical Note 2. United States Environmental Protection Agency, Office of Water.

Moriasi, D. N., J. G. Arnold, M. W. Van Liew, R. L. Bingner, R. D. Harmel, and T. L. Veith. 2007. Model evaluation guidelines for systematic quantification of accuracy in watershed simulations. *Transactions of the ASABE* 50(3): 885-900.

Motz, L.H., and A. Dogan. 2004. *North-Central Florida Active Water-Table Regional Groundwater Flow Model, p. 141*. Special Publications SJ2005-SP16. Palatka, Fla.: St. Johns River Water Management District.

Motz, L. H., J. P. Heaney, W. K. Denton, M. S. Fowler, and G. Leiter. 1994. *Upper Etonia Creek Hydrologic Study; Phase II: Final Report (Revised).* Special Publication SJ92-SP18. Palatka, Fla.: St. Johns River Water Management District.

Motz, L. H., J. P. Heaney, W. K. Denton, and G. Leiter. 1991. *Upper Etonia Creek Hydro-*

logic Study; Phase I Final Report. St. Johns River Water Management District Special Publication SJ 91-SP5. Palatka, Fla.: St. Johns River Water Management District.

Nigro, J., D. Toll, E. Partington, W. Ni-Meister, S. Lee, A. Gutierrez-Magness, T. Engman, and K. Arsenault. 2010. NASA-Modified Precipitation Products to Improve USEPA Nonpoint Source Water Quality Modeling for the Chesapeake Bay. *Journal of Environmental Quali*ty 39(4): 1388-1401.

Niswonger, R. G., S. Panday, , and M. Ibaraki. 2011. *MODFLOW-NWT, A Newton Formulation for MODFLOW-2005, p. 44.* Techniques and Methods Report 6-A37. Reston, Va.: U.S. Geological Survey.

Payne, D. F., M. A. Rumman, and J. S. Clarke. 2005. *Simulation of Ground-Water Flow in Coastal Georgia and Adjacent Parts of South Carolina and Florida-Predevelopment, 1980, and 2000.* Scientific Investigations Report 2005–5089. U.S. Geological Survey, South Atlantic Water Science Center.

Perry, R. G. 1995. *Regional Assessment of Land Use Nitrogen Loading of Unconfined Aquifers.* Ph.D. Dissertation. Tampa: University of South Florida.

Phelps, G. G. 1990. *Geology, Hydrology, and Water Quality of the Surficial Aquifer System in Volusia County, Florida.* Water-Resources Investigations 90–4069. U.S. Geological Survey.

Renken, R. A. 1996. *Hydrogeology of the Southeastern Coastal Plain aquifer system in Mississippi, Alabama, Georgia, and South Carolina.* U.S. Geological Survey Professional Paper 1410-B. Washington, D.C.: United States Government Publishing Office..

Rosenau, J. C., G. L. Faulkner, C. W. Hendry, and R. W. Hull. 1977. *Springs of Florida*. Bulletin 31 (Revised). Tallahassee, Fla.: U.S. Geological Survey and Florida Department of Natural Resources.

Ross, M., and K. Trout. 2017. *Assessment of the integrated northern Tampa Bay model no groundwater pumping scenarios.* Tampa: University of South Florida.

Rupert, F. R. 1988. *The Geology of Wakulla Springs.* Open-File Report 22. Tallahassee, Fla.: Florida Geological Survey.

Russo, V. 2011. Northeast Florida Regional Groundwater Flow Model -- Version 3. (Unpublished report). St. Johns River Water Management District, Palatka, Fla.

Rutledge, A. T. 1998. *Computer Programs for Describing the Recession of Ground-Water Discharge and for Estimating Mean Ground-Water Recharge and Discharge from Streamflow Records—Update.* Water-Resources Investigations Report 98–4148. Reston, Va.: U.S. Geological Survey.

Sauer, V. B., and R. W. Meyer. 1992. *Determination of error in individual discharge measurements*. Open File Report 92-144. Washington, D.C.: U.S. Geological Survey.

Scott, T. M., R. P. Meegan, S. B. Upchurch D, R. C. Means, G. H. Means, R. E. Copeland, J. Jones, T. Roberts, and A. Willet. 2004. *Springs of Florida*, p.677. Bulletin 66. Tallahassee, Fla.: Florida Geological Society.

Sepulveda, N., and J. Doherty. 2015. Uncertainty Analysis of a Groundwater Flow Model in East-Central Florida. *Groundwater* 53:464–474.

Sepulveda, N., C. Tiedeman, A. M. O'Reilly, J. B. Davis, and P. Burger. 2012. *Groundwater flow and water budget in the surficial and Floridan aquifer systems in east-central Florida.* USGS Numbered Series 2012–5161. Reston, VA: U.S. Geological Survey.

Shah, N., M. Nachabe, and M. Ross. 2007. Extinction Depth and Evapotranspiration from Ground Water under Selected Land Covers. *Ground Water* 40(3):329–338.

Shoemaker, W. B., E. L. Kuniansky, S. Birk, S. Bauer, and E. D. Swain. 2008. *Documentation of a Conduit Flow Process (CFP) for MODFLOW-2005.* Reference Manual A24. Reston, Va.: U.S. Geological Survey.

Sloto, R., and M. Crouse. 1996. *Hysep: a computer program for streamflow hydrograph separation and analysis.* Water-Resources Investigations Report 96–4040. Lemoyne, Pa.: U.S. Geological Survey.

Spechler, R. M., and P. S. Hampson. 1984. *Ground-Water Resources of St. Johns County, Florida.* Water-Resources Investigations 83–4187. Tallahassee, Fla.: U.S. Geological Survey.

Steele, W. M., and R. J. McDowell. 1998. *Permeable Thickness of the Miocene Upper and Lower Brunswick Aquifers, Coastal Area, Georgia.* Georgia Geological Survey Information Circular 103. Atlanta, Ga.: Department of Natural Resources, Environmental Protection Division, Georgia Geological Survey.

Stokes, J. and P. Finer. 2014. Digital communication ArcGIS implementation of estimating ET extinction depths. St. Johns River Water Management District, Palatka, Fla.

Stringfield, V. T. 1936. *Artesian water in the Florida peninsula*, p.115–195. Report 773–C.
Washington D.C.: U. S. Geological Survey.

Stricker, V. A. 1983. *South Carolina, Georgia, Alabama, and Mississippi*, p.20. Water-Resources Investigations Report 83–4106. Atlanta: U.S. Geological Survey.

Suscy, P., E. Carter, D. Christian, M. Cullum, K. Park, J. Stewart, and Y. Zhang. 2012. *St. Johns River Water Supply Impact Study; Chapter 5, River Hydrodynamics Calibration.* St. Johns River Water Management District Technical Publication SJ2012-1. Palatka, Fla.: St. Johns River Water Management District.

Sumner, D. M. 1996. *Evapotranspiration from successional vegetation in a deforested area of the Lake Wales Ridge, Florida*. Water-Resources Investigations Report 96-4244. U.S. Geological Society.

———, D. M. 2001. *Evapotranspiration from a Cypress and Pine Forest Subjected to natural Fires in Volusia County, Florida 1998-99*. Water-Resources Investigations Report 01-4245. Tallahassee, Fla.: U. S. Geological Survey.

Sumner, D. M., and J. M. Jacobs. 2005. Utility of Penman–Monteith, Priestley–Taylor, reference evapotranspiration, and pan evaporation methods to estimate pasture evapotranspiration. *Journal of Hydrology* 308(1-4): 81-104.

U.S. Department of the Interior, Floridan Aquifer System Groundwater Availability Study, Numerical Model. N.d. Accessed on the U.S. Geological Survey website at *https://fl.water.usgs.gov/floridan/numerical-model.html*.

[USEPA] United States Environmental Protection Agency. 2000. *BASINS Technical Note 6: Estimating Hydrology and Hydraulic Parameters for HSPF*. Washington, D.C.: Office of Water.

Wikipedia, Climate of Florida. 2012, June 18. Accessed June 1, 2011 at http://en.wikipedia.org/wiki/Climate_of_Florida.

———, Climate of Georgia (U.S. state). 2012. Accessed June 18, 2011, on Wikipedia. at http://en.wikipedia.org/wiki/Climate_of_Georgia_(U.S._state).

Williams, L. J., and E. L. Kuniansky. 2015. *Revised Hydrogeologic Framework of the Floridan Aquifer System in Florida and Parts of Georgia, Alabama, and South Carolina.* Professional Paper 1807. Reston, Va.: U.S. Geological Survey.

Williams, S. 2012. Top of Ground Saline Water. St. Johns River Water Management District, Palatka, Fla.

———, S. 2013. Freshwater extent of the top of the Fernandina permeable zone. St. Johns River Water Management District, Palatka, Fla.

———,, S. A. 2006. *Simulation of the Effects of Groundwater Withdrawals from the Floridan Aquifer System in Volusia County and Vicinity.* Technical Publ. SJ2006-4. Palatka, Fla.: St. Johns River Water Management District.

Xia Y., K. Mitchell, M. Ek, J. Sheffield, B. Cosgrove, E. Wood, L. Luo, C. Alonge, H. Wei, J. Meng, Livneh B., Lettenmaier D., Koren V., Duan Q., K. Mo, Y. Fan, and D. Mocko D. 2012. Continental-scale water and energy flux analysis and validation for the North American Land Data Assimilation System project phase 2 (NLDAS-2): 1. Intercomparison and application of model products. *Journal of Geophysical Research* 117 (D03109) 1-27.